THE UNIVERSITY
of EDINBURGH

MORPHOLOGICAL PROPERTIES OF ARTICULAR CHONDROCYTES IN VARIOUS EXPERIMENTAL AND CLINICAL CONDITIONS

ASIMA KARIM

Submitted for the Degree of Doctor of Philosophy

University of Edinburgh

April 2015

DECLARATION

I hereby declare that the work presented in this Ph.D. thesis was carried out by me at the Centre for Integrative Physiology, School of Biomedical Sciences, University of Edinburgh. The work has not been submitted for any other degree or professional qualification.

Asima Karim

Edinburgh

March 2015

PREFACE

The dissertation consists of experimental work carried out at the Centre for integrative Physiology (Hugh Robson Building, George Square, Edinburgh), University of Edinburgh. The research presented herein was conducted under the supervision of Dr. Andrew Hall during the period August 2011 to August 2014. This dissertation contains less than 100,000 words.

ACKNOWLEDGEMENTS

I would like to thank Dr. Andrew Hall, Dr. Sutherland Maciver and Prof. Mike Shipston for their supervision, enthusiasm, support and advice in this research project. I would especially extend my gratitude to my supervisor Dr. Andrew Hall for being a tremendous mentor to me. His constant encouragement, intellectual guidance and helpful criticism throughout the project enabled me to learn methods of research and science.

I would like to say thanks to Dr. Anish Amin, consultant trauma and orthopaedic surgeon at Royal Infirmary of Edinburgh for providing human femoral heads and other clinical samples.

I would like to say special thanks to Dr. Trudi Gillespie, IMPACT facility, Centre for Integrative Physiology, University of Edinburgh for her expert training on the use of confocal laser scanning microscope. My special appreciations are for Vivian Allison and Louise Dunn, Technical officers in histology lab, Centre for Integrative Physiology, University of Edinburgh, for their assistance in histological techniques utilised in this project.

I would like to extend my thanks to Dr. Noha Eltawil, postdoctoral research assistant at Centre of Integrative Physiology for assisting me in learning immunohistochemical techniques utilised in this project.

I must thank all my colleagues in Dr. Andrew Hall's research group especially Mr. Scott Paterson and Dr. Innes Smith for making my time memorable. I also want to

thank all the staff at Scotbeef Ltd., Bridge of Allan, for their aid in providing bovine feet.

My sincere thanks are to my family for their love, encouragement and trust in me. The accomplishment of this research project and especially thesis writing would not have been possible without their support.

Finally, I would like to thank the College of Medicine and Veterinary Medicine, University of Edinburgh, for a Global Overseas Research Scholarship and Charles Darwin Scholarship, and also University of Health Sciences, Lahore and Higher Education Commission, Pakistan for support.

DEDICATION

To my parents, Ch. Abdul Karim (Late) and Mrs. Nasira Karim for educating me

To my husband, Dr. Muhammad Rehan for always being patient and supportive

To my lovely daughters, Adeena and Aleena for being my inspiration

ABSTRACT

Previous work has suggested that there exists a relationship between chondrocyte morphology and matrix metabolism. Changes to chondrocyte morphology have been reported in human cartilage however it is unclear if these are involved in the degenerative process associated with osteoarthritis (OA). In this work, the morphology of human and bovine chondrocytes has been characterised under a range of conditions. Bovine chondrocytes have been utilised in these experiments as bovine cartilage is non-degenerate and the chondrocytes have 'normal' morphology. However, if human cartilage have been used instead then there is possibility of having chondrocytes of mixed shapes i.e. both 'normal' and 'abnormal' cells. The thesis aimed at experimentally inducing morphological changes to chondrocytes to determine whether these changes resemble those observed in human cartilage. The ultimate aim is to model these changes to clarify the link between morphology and matrix metabolism by determining how morphological changes influence matrix metabolism.

A classification system was developed for chondrocyte morphology allowing the quantification of chondrocyte shapes under different conditions permitting statistical comparisons. The different conditions utilised were (1) non-degenerate and mildly-degenerate human articular cartilage and (2) two *in vitro* models (a) weak 3D agarose gels to study the effect of gel strength and increasing concentrations of foetal calf serum (FCS) on morphology of bovine chondrocytes and (b) scalpel induced mechanically-injured bovine cartilage model to study *in situ* chondrocyte viability and morphology at the injured site in various culture conditions. Additionally, the

effect of raised medium osmolarity on the response of chondrocytes to injury was studied to determine if the abnormal morphology could be reversed.

Using fluorescence-mode confocal laser scanning microscopy (CLSM), chondrocyte viability, volume and morphology were determined and quantified by using Volocity™ 3D image analysis software. Histological evaluation of matrix by using Haematoxylin and eosin, Alcian blue and Masson's trichrome staining of matrix produced by chondrocytes cultured in strong or weak agarose gels and in injured cartilage was determined. Additionally, immunohistochemical evaluation of matrix (collagen Types I & II) produced by chondrocytes was also performed.

Results demonstrated that in non-degenerate human femoral head cartilage, ~83% chondrocytes were normal in morphology and 17±2% chondrocytes had cytoplasmic processes as compared to mildly-degenerate cartilage where 35±5% abnormal chondrocytes with cytoplasmic processes were present. In non-degenerate cartilage, 11±3% chondrocytes formed small sized clusters however clustering was quite evident in the superficial zone of mildly-degenerate human femoral head cartilage where 43±16% chondrocytes had formed large clusters. In mildly-degenerate cartilage the number of abnormal chondrocytes with processes, length of processes and number of processes per cell were greater in the superficial as compared to mid and deep zones.

A model was developed to study the effect of external supporting agarose gel on chondrocyte morphology and also to determine the influence of FCS. Bovine chondrocytes cultured in weak gels after 7 days developed similar morphological changes as those observed in degenerate human cartilage. However, in the strong

gels only few chondrocytes with morphological changes were present i.e. similar to non-degenerate cartilage. These morphological changes (development of clusters and processes) occurred more rapidly with increasing concentrations of FCS. Histology revealed less Alcian blue staining intensity around chondrocytes cultured in weak gels as compared to strong gels suggesting altered matrix produced by abnormal chondrocytes. FCS and gel strength were therefore proposed as related factors in regulating chondrocyte morphology.

In the bovine injured cartilage explant model, after 14 days chondrocytes at the injury in the presence of FCS or synovial fluid (SF) produced morphological changes. These changes comprised cell enlargement, flattening, elongation and production of cytoplasmic processes. In the absence of FCS or SF, chondrocytes at the injury remained unaffected and were morphologically 'normal'. Throughout the cartilage and even in the absence of subchondral bone, chondrocytes displayed morphological abnormalities in the presence of FCS or SF. These findings suggested that this is not the property of chondrocytes in the superficial layers alone rather it is due to the extent of penetration of the 'factors' into the matrix and there is no possibility of interference of injured site with osteocytes or bone factors. Histology revealed that these abnormal chondrocytes showed less staining with Alcian blue at the injury suggesting that these morphological changes might play a role in the changes to matrix metabolism. By raising the osmolarity of the culture medium these changes were inhibited and chondrocytes maintained their normal morphology.

The results suggest that morphogenic/proliferative factors in FCS or SF and strength/damage to the matrix may be inter-related and act as potent controllers of chondrocyte morphology. Raised osmolarity was found to inhibit the morphological

changes suggesting the possibly that hyperosmolarity can antagonise the effects of these factors. The key conclusions from the thesis were (a) in non-degenerate human femoral cartilage a large percentage of chondrocytes ~83% were normal in morphology and the rest were abnormal however in mildly-degenerate cartilage 35±5% abnormal chondrocytes with processes were present (b) the changes to chondrocyte morphology (development of clusters and processes) were exacerbated with cartilage degeneration (c) chondrocytes cultured in the weak gels produced morphological changes as compared to strong gels (d) chondrocytes at the injury displayed marked morphological changes in the presence of FCS or SF (e) by raising the medium osmolarity these morphological changes to chondrocytes at the injury were inhibited. These results show that chondrocyte morphology is complex and strongly dependent on the environmental settings. Experimental conditions were therefore identified which showed increased chondrocyte volume, abnormal morphology with cytoplasmic processes, enhanced proliferation/cluster formation and matrix changes. These changes to volume and morphology of chondrocytes in the models studied in this work had certain similarities to the changes observed in human cartilage suggesting that these shape changes may play a role in the changes to matrix metabolism occurring in OA.

These findings may be of translational relevance in clinical and experimental research into cartilage injury and degeneration by providing new insights in understanding the role played by chondrocyte morphology in cartilage degeneration and injury.

TABLE OF CONTENTS

LIST OF FIGURES

LIST OF TABLES

ABBREVIATIONS

AC	Articular cartilage
ECM	Extracellular matrix
PGs	Proteoglycans
GAG	Glycosaminoglycan
SLRP	Small leucine rich proteoglycan
PCM	Pericellular matrix
SZ	Superficial zone
MZ	Middle zone
DZ	Deep zone
OA	Osteoarthritis
COMP	Cartilage oligomeric matrix protein
TSP	Thrombospondins
GNP	Gross national product
PTOA	Post traumatic osteoarthritis
BMI	Body mass index
TKA	Total knee arthroplasty
MMPs	Matrix metalloproteinases
CPCs	Chondrogenic progenitor cells
ADAMs	A disintegrin and metalloproteinases
TUNEL	Terminal dUTP nick end labelling

RUNX-2	Runt related transcription factor-2
ERK	Extracellular signal regulated kinase
TEM	Transmission electron microscopy
ELISA	Enzyme-linked immunosorbent assay
PCR	Polymerase chain reaction
RT	Real time
ATM	Atomic force microscopy
CLSM	Confocal laser scanning microscopy
IL1ß	Interleukin 1- ß
OCD	Osteochondritis dissecans
IL-6	Interleukin-6
TNFα	Tumour necrosis factor alpha
PDGF	Platelet derived growth factor
IGF-1	Insulin like growth factor 1
FCS	Foetal calf serum
CMFDA	5-chloromethylfluorescein diacetate
PBS	Phosphate-buffered saline
LMP	Low melting point
DMEM	Dulbecco's Modified Eagle's Medium
SF	Synovial fluid
PI	Propidium iodide

DRAQ5	1, 5-bis 2-di-methylamino-ethyl-amino-4, 8-dihydroxyanthracene-9, 10-dione
DMSO	Dimethyl sulphoxide
D/W	Distilled water
AVN	Avascular necrosis
IL-15	Interleukin 15
IL-17	Interleukin 17
IL-18	Interleukin 18
IL-4	Interleukin 4
IL-10	Interleukin 10
IL-13	Interleukin 13
TGFß	Transforming growth factor beta
ERI	Edinburgh Royal Infirmary
PFA	Paraformaldehyde
TKR	Total knee replacement
FD	Full depth
DW	Dipping water
ROI	Region of interest
H&E	Haematoxylin and eosin
OCT	Optimal cutting temperature
SOX9	Sry-related HMG-box gene 9
STWS	Scott's tap water substitute

DPX	Distyrene plasticizer xylene
BF	Bright field
3-D	Three dimensional
2-D	Two dimensional
PCD	Percentage cell death
NA	Numerical aperture
IHC	Immunohistochemistry
EDTA	Ethylenediaminetetra-acetic acid
FGF-2	Fibroblast growth factor-2
RVD	Regulatory volume decrease
RVI	Regulatory volume increase

CHAPTER 1: INTRODUCTION

1.1 Articular cartilage (AC)

1.1.1 Structure and functions

AC is a form of hyaline cartilage, smooth and glassy material covering the ends of bones within synovial joints. AC is an aneural, avascular, alymphatic but highly resilient structure. It is designed with a remarkable property of load bearing, distributing the load across the joint by preventing localised/focused loading and reducing friction at movement of articulating joint surfaces (Buckwalter and Mankin, 1997b). The cell density, thickness, composition and properties of AC vary within the same joint, between different joints and between species (Athanasiou et al., 1991). However, the basic structural and functional properties of the tissue remain the same. AC is an avascular tissue (Jackson and Gu, 2009, Milner et al., 2012). It is nourished by diffusion through the synovial fluid and subchondral bone with synovial fluid being the predominant source (Wang et al., 2013b). The mechanical properties of AC and functional responses of chondrocytes are maintained by the structure and biochemical composition of various components of extracellular matrix (ECM) (Jeffery et al., 1991, Kuettner et al., 1991) and via the complex interactions (such as mechanotransduction by which mechanical loading is transduced into intracellular signals) between chondrocytes and ECM (Loeser, 2002).

1.1.2 Composition

AC is composed of chondrocytes entrenched within highly organised structure of ECM comprising of interstitial fluid and macromolecular framework containing collagens, proteoglycans (PGs) and non-collagenous proteins (Huber et al., 2000). The composition of matrix provides mechanical properties to the tissue and

chondrocytes are responsible for matrix remodelling. A detailed account of various components of AC is given in the following sections.

1.1.2.1 *ECM*

It is comprised of two components: tissue fluid and the framework of macromolecules (Fig. 1.1).

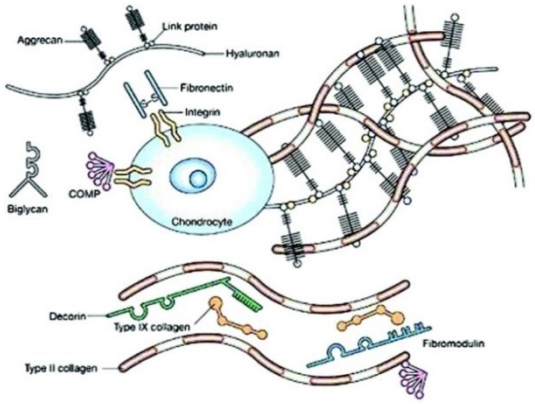

Figure 1.1: Extracellular matrix of articular cartilage.
Two major macromolecules are present in articular cartilage: collagens (mainly, type II) and PGs (notably, aggrecan). Smaller molecules, such as non-collagenous proteins and smaller PGs, are present in smaller amounts. The interaction between the highly negatively charged cartilage PGs and type II collagen provides the compressive and tensile strength of the tissue. (Chen et al., 2006)**.**

It is the interaction between these two components which gives AC its unique mechanical properties and the resilience (Fox et al., 2009). In healthy cartilage 65%-80% of the total weight of cartilage is tissue fluid contributing to the wet weight and the remainder is responsible for the dry weight of cartilage (Fox et al., 2009). Water constitutes 80% of the total weight of cartilage and the hydration status of cartilage is maintained through interactions of water and large aggregating PGs (Maroudas and Schneiderman, 1987). The macromolecular framework consists of three classes: collagens, PGs and non-collagenous proteins (Huber et al., 2000). Out of the total dry

weight of cartilage, 60% is contributed by collagens, 20%-25% by PGs and 15%-20% non-collagenous proteins.

1.1.2.1.1 PGs

PGs have a protein core with one or more glycosaminoglycan (GAG) chains attached to it having at least one negatively charged carboxylate or sulphate group. AC contains two varieties of PGs: large aggrecans and small PGs [(i.e. decorin, biglycan and fibromodulin (Table 1.1)] (Roughley and Lee, 1994).

PG variety	Class	GAG type	number of GAG chains	% in cartilage	Functions
Aggrecans	Large aggregating PG	chondroitin sulphate and keratin sulphate chains	>100	90%	Chondrocyte-matrix interactions and ability to withstand compressive load
Large non-aggregating				10% or less	
Decorin	Small leucine-rich proteoglycan (SLRP) family	dermatan sulphate / chondroitin sulphate	1	3%	Binds with type II collagen and stabilizes it
Biglycan	SLRP	dermatan sulphate / chondroitin sulphate	2		Concentrated in pericellular matrix (PCM) and interacts with type VI collagen
Fibromodulin	SLRP	keratin sulphate	4		Binds with type II collagen and stabilizes collagen meshwork

Table 1.1: Properties of PGs in the cartilage.
Different classes of PGs exist in variable quantities, composition and functions in the AC. (Roughley and Lee, 1994, Buckwalter and Mankin, 1997b).

PGs are highly negatively charged molecules responsible for holding water molecules and they attract cations and repel anions, thereby, creating high osmotic pressure in the cartilage via Gibb's-Donnan equilibrium conditions (Urban, 1994, Hopewell and Urban, 2003). The osmolarity of extracellular fluid ranges from 350 mOsm to 480 mOsm depending on zone of cartilage (Maroudas, 1975, Hopewell and Urban, 2003). Extracellular osmolarity varies between the cartilage zones depending upon the concentration of PGs, being lowest in the superficial zone (SZ), highest in middle zone (MZ) and lower in the deep zone (DZ) with osmolarity around 350 mOsm in the SZ and around 450 mOsm in the MZ (Urban et al., 1993). These high osmotic pressure levels inside cartilage as compared to the surrounding tissues such as plasma with osmotic pressure of 280 mOsm (Bhalla et al., 2000) and synovial fluid with osmolarity of 400 mOsm (Bertram and Krawetz, 2012) increases the tendency of water movement into the cartilage. The movement of water into the cartilage is restricted by the collagen network which resists the Donnan osmotic pressure (Maroudas, 1976, Lai et al., 1991, Buckwalter et al., 2005). During dynamic loading of cartilage plasma membrane is deformed, the physico-chemical environment of the cartilage is altered because the hydrostatic pressure increases and the fluid flows out/fluid loss resulting in changes to ionic content (Urban, 1994). In osteoarthritis (OA), the PG content is reduced and the fluid fraction in the cartilage increases (Maroudas and Venn, 1977, Stockwell, 1991) leading to cartilage swelling. The possible explanation for this apparent paradox is weakened collagen structure and loss of elastic restraint of collagen network causing swelling of PGs (Maroudas et al., 1973, Maroudas, 1976, Bank et al., 2000). In the swollen cartilage the

extracellular osmolarity decreases and chondrocyte volume increases (Urban et al., 1993, Bush and Hall, 2003).

1.1.2.1.2 Collagen

Multiple types of collagen are present in AC especially type II, VI, IX, X and XI arranged in the form of bands of fibrils. The most abundant collagen present is type II which constitutes 90%-95% of the whole collagen content and is responsible for providing tensile strength to the cartilage (Eyre, 2002). The fibres of collagen extend out into the territorial matrix and further in the interterritorial matrix. Embedded in the meshwork of collagen are large aggregating PGs (aggrecans) which provide stiffness and resilience to the tissue (Dudhia, 2005). Collagen type IX and XI are presumably responsible for the reinforcement of the fibrillar meshwork established primarily by collagen type II (Kuettner et al., 1991, Buckwalter and Mankin, 1998, Eyre, 2004). Collagen type VI is present in the immediate vicinity of chondrocytes in the PCM and provides attachment of chondrocytes to the matrix (Guilak et al., 2006). Collagen type X is present in the calcified zone close to tidemark in normal cartilage (Rucklidge et al., 1996).

1.1.2.1.3 Non-collagenous proteins

In normal cartilage in addition to PGs and collagens, the ECM also contains a variety of non-collagenous proteins and glycoproteins but details of only few of them are so far studied in detail (Roughley, 2001). They appear to have structural and regulatory importance in cartilage integrity (Roughley, 2001, Buckwalter et al., 2005) including matrix metabolism, matrix assembly and cell-matrix interactions. The only well

described non-collagenous proteins are Anchorin CII, Cartilage oligomeric matrix protein (COMP), tenascin and fibronectin. Anchorin CII, a surface protein present in the membranes of chondrocytes, is considered to bind chondrocytes to the collagen fibrils in the matrix (Mollenhauer et al., 1984). COMP belongs to the family of Thrombospondins (TSP) and termed as TSP-5 and thought to be associated to collagen type IX (Roughley, 2001). COMP is present within territorial matrix (DiCesare et al., 1994) interacting with other proteins in ECM thus playing an important role in structural integrity of cartilage (Acharya et al., 2014). In early OA, COMP is up-regulated and hence considered a potential biomarker for cartilage degeneration (Salminen et al., 2000). Tenascin and fibronectin are important for interactions between chondrocytes and the matrix (Buckwalter and Mankin, 1998). Tenascin is a glycoprotein present in very small quantities in the ECM of normal cartilage (pericellular areas) in all the zones. It interacts with fibronectin and thus influences connections of chondrocytes with PCM and its expression increases in OA (Chevalier et al., 1994). Fibronectin is also present in small quantities in normal cartilage with a potential role in maintaining chondrocyte phenotype and its levels have been observed to increase in OA (Chevalier, 1993).

1.1.2.1.4 Chondrocytes

Chondrocytes present in human AC constitute only 10% of the total volume of the tissue (Stockwell, 1979). Chondrocytes are normally rounded in morphology except at the tissue surface where they are flattened (Archer and Francis-West, 2003). Chondrocytes residing in various zones of cartilage differ in size, shape and function (Stockwell, 1979, Aydelotte et al., 1988, Mort and Billington, 2001, Goldring, 2012).

The key function of chondrocytes is matrix turnover i.e. synthesis and degradation of macromolecules constituting the framework of cartilage especially PGs and collagens (Muir, 1995, Archer and Francis-West, 2003, Bhosale and Richardson, 2008). The cartilage is an avascular tissue and chondrocytes receive nutrients and oxygen by diffusion (Ge et al., 2006). Therefore chondrocytes obtain principal supply of ATP from substrate-level phosphorylation in glycolysis (Lee and Urban, 1997) and only 10% from oxidative phosphorylation (Otte, 1991). The rate of glycolysis in chondrocytes is comparable with other tissues but overall metabolic activity of the tissue is low because of lower cell density (Buckwalter and Mankin, 1997b). Normal chondrocytic phenotype is characterised by spheroidal shape, Type II collagen synthesis (Eyre, 2002) and production of aggrecans (large aggregating PGs) (Dudhia, 2005). Chondrocytes have various properties for example, they have to withstand high compressive forces *in vivo*, have high matrix to cell volume ratio, do not divide after skeletal maturity unless there is a pathological condition, obtain nutrition by diffusion and survive in low oxygen tension environment (Muir, 1995, Archer and Francis-West, 2003, Bhosale and Richardson, 2008).

1.1.3 Zones of AC

Various researchers have agreed at dividing the AC into four discrete zones (Fig. 1.2): superficial, intermediate/transitional/mid, deep/radial and calcified zones (Buckwalter et al., 1988, James and Uhl, 2001, Bhosale and Richardson, 2008, Fox et al., 2009). However, this division into various zones is arbitrary and there exists no definite demarcation between the various zones of cartilage. The division is typically based upon the morphology and arrangement of chondrocytes and arrangement of collagen fibrils. It is difficult to define the intermediate and deep zones of cartilage

because the arrangement of chondrocytes and collagen fibres is quite similar in these two zones. However, SZ and calcified zones are easily distinguishable because the morphology of chondrocytes in the SZ is typical (ellipsoid) and the calcified zone lies behind the tide line.

Chondrocyte morphology and density varies across the different zones of AC (Siczkowski and Watt, 1990). Additionally, the matrix composition and properties also differ across the various zones (Aydelotte et al., 1988, Wong et al., 1996 , Mort and Billington, 2001, Darling et al., 2006). In human cartilage the water content decreases from superficial to the deep zones of the tissue and is lowest in the DZ (Pearle et al., 2005). The packing and arrangement of collagen fibres changes from superficial to deep zones of cartilage from thin tangential orientation to thick radial ones (Ghadially et al., 1978, Poole et al., 1982, Siczkowski and Watt, 1990). The varied orientation of collagen fibres in various zones of cartilage has a functional significance. The tangential arrangement of collagen fibrils in SZ protects the deeper zones from shear stress and is designed to resist tensile and compressive forces of articulation, in the transitional/mid zone deeper to the SZ collagen fibrils are arranged obliquely and functionally provide first line of defence against the compressive forces transmitted from the surface, in the DZ collagen fibrils are thick and radial in disposition arranged perpendicular to the articular surface (Fig. 1.2B) providing greatest resistance to compressive forces (Fox et al., 2009).

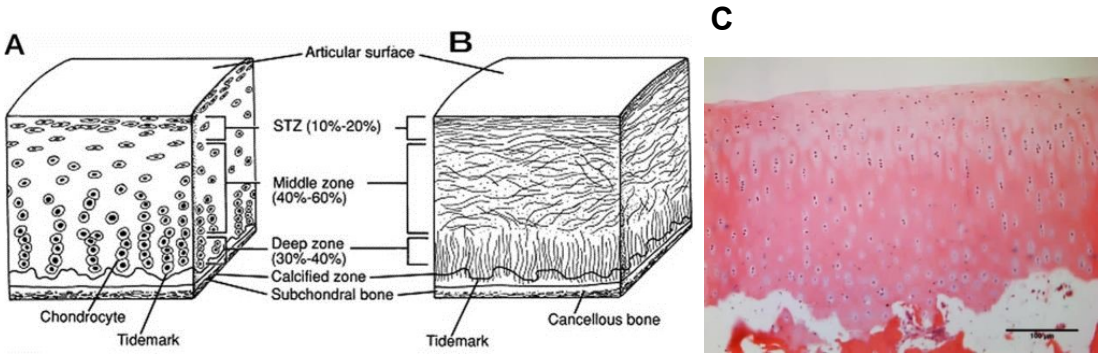

Figure 1.2: Schematic, cross-sectional diagram of healthy articular cartilage. A, cellular organization in the zones of articular cartilage; B, collagen fiber architecture (Fox et al., 2009). Reprinted from the *Journal of the American Academy of Orthopaedic Surgeons*, 1994; 2:192-201. C, Haematoxylin & Eosin stained 10 µm thick histology section from bovine metacarpal-phalangeal joint (author's results). Scale bar = 100 µm.

The concentration of PGs in human cartilage differs across the various zones of cartilage being highest in the MZ, lower in the DZ and lowest in the SZ (Huber et al., 2000). The demarcation of various zones and morphology of chondrocytes in various zones of human cartilage has been described (Humbree et al., 2007). In human cartilage SZ is a thin zone of elongated/ellipsoid chondrocytes comprising 10%-20% of the cartilage volume. The MZ constitutes 40%-60% of cartilage volume and comprises of rounded chondrocytes. The DZ comprises 30% of cartilage volume and contains rounded chondrocytes mostly arranged in vertical columns and biggest in size as compared to chondrocytes in SZ and MZ. Underneath the DZ lies a demarcation, tidemark marking the separation of underlying calcified zone from SZ, MZ and DZ of cartilage. The calcified zone helps in securing the cartilage to the

underlying subchondral bone through the attachment of collagen fibrils and this zone contains hypertrophied chondrocytes (Fox et al., 2009).

The histological evaluation revealed that human and bovine cartilage samples differ in the overall cartilage thickness, average zonal thickness, diameter of chondrocytes and cell density (Pedersen et al., 2013). In the study by Pedersen et al, cartilage was divided into four zones superficial zone (SZ), transitional zone (TZ), radial zone (RZ) and deep zone (DZ) and various parameters of cartilage were studied. Various properties of cartilage and chondrocytes in these cartilage zones are given in Table 1.2 based upon the previous study (Pedersen et al., 2013). The interspecies differences should be taken into account while interpreting observations from bovine model to the humans.

Species	**Cartilage thickness (mm)**	**Zonal cartilage thickness (% of depth)**				**Zonal cell densities (Cells/mm^2)**				**Diameter of chondrocytes (microns)**	
		SZ	TZ	RZ	DZ	SZ	TZ	RZ	DZ	SZ	DZ
Human	2.2-2.8mm	8-10	34-38	38-42	11-16	117-271	63-108	66-83	70-91	16.9	19.7
Bovine	1.9mm	6.5	25	41	26	321	212	225	184	16.9	19.7

Table 1.2: Comparison of properties of human and bovine cartilage.
Full cartilage thickness, cartilage zone ratios, zonal cell densities and diameter of chondrocytes in human and bovine joints (Pedersen et al., 2013).

1.2 OA

It is a painful joint disorder accompanied by joint dysfunction and physical disability at later stages (Buckwalter and Mankin, 1997a). It is the commonest type of arthritis and the worldwide estimates state that 9.6% of men and 18% of women aged >60

yrs. suffer from OA asymptomatically (Murray and Lopez, 1996). In the United States and European population the radiographic observations showed the highest rate of knee OA at the age ≥45 yrs., 14.1% for men and 22.8% for women (Woolf and Pfleger, 2003). Since the incidence increases with age, longer life expectancy will increase the incidence of OA in future according to WHO (Woolf and Pfleger, 2003). OA can affect any synovial joint of the body but its prevalence has been reported to be greatest (85%) in the knee joint (Buckwalter and Brown, 2004). The physical disability caused by OA has a negative effect on self-esteem of patients and they suffer from anxiety, depression, feelings of helplessness and being a burden on society and family (Murphy et al., 2012). As the incidence of OA is increasing it has a high negative impact on UK economy and the total cost has been determined to be 1% of the gross national product (GNP) (March and Bachmeier, 1997). OA is broadly divided into two types: primary OA (idiopathic) and secondary OA/post traumatic OA (PTOA).

1.2.1 Primary OA

The aetiology of primary OA is unknown but is most likely a multifactorial disease (Wieland et al., 2005). In a very recent study several risk factors have been identified to be responsible for causing OA (Apold et al., 2014) and these include age (Li et al., 2013), ethnicity (Felson et al., 2002), genetics (Spector et al., 1996), gender (Srikanth et al., 2005), injury, physical activity, smoking (Toivanen et al., 2010), malalignment (Felson et al., 2013), and overweight/body mass index (BMI) (Martin et al., 2013). Most of the risk factors associated with the development of OA such as ethnicity, genetics, gender, smoking, physical activity and malalignment have conflicting

results in the literature. These risk factors have been reported to be either associated or not associated with OA disease progression and have been reviewed previously (Chaganti and Lane, 2011). However, age, knee injury and obesity have been consistently identified to be associated with radiographic knee OA (Wieland et al., 2005, Chaganti and Lane, 2011). The paradigm of OA is that it is the disease of the whole joint which involves structures of the entire joint including AC, membrane, joint capsule, ligament, muscle and the bone (Wieland et al., 2005). The characteristics of the disease include cartilage degeneration, active bone remodelling and synovitis leading to failure of joint function (Aaron and Racine, 2013). When the cartilage is degenerated and lost, the joint spaces are narrowed down (Lohmander, 2000). The loss of cartilage causes bone to rub on bone which is exceedingly painful as subchondral bone contains pain receptors (Sofat et al., 2011). Changes in the joint structure cause stiffening of the capsule and various symptoms as joint pain, crepitus and restricted movements render the joint non-functional (Buckwalter and Mankin, 1997a). Various pharmacological, non-pharmacological approaches and surgical interventions have been devised with the aim of improving symptoms of OA, but the problem of OA has not been solved as no effective treatment targets the cause of the disease (Buckwalter and Martin, 2006). After the exhaustion of non-operative management for OA, total knee arthroplasty (TKA) is considered to be highly beneficial (Caracciolo and Giaquinto, 2005) and cost effective treatment strategy (Lavernia et al., 1997). Although, TKA is an effective treatment for end stage OA, this technique is accompanied with several post-operative complications including femoropatellar problems, infections and stiffness of the joint (Ronn et al., 2011). The pre-operative condition of the patient affects the outcomes of TKA, patients with

poor health status and severe pain have worse outcomes of this surgery (Lingard et al., 2004).

1.2.1.1 *Matrix degradation in OA*

In healthy cartilage, chondrocytes remain quiescent and are responsible for the maintenance/turn-over of matrix through their metabolic activities (Aigner et al., 2007). However, in OA chondrocytes become 'activated' with rapid proliferation, cluster formation and enhanced production of matrix and degradative enzymes (Aigner et al., 1992, Sandell and Aigner, 2001, Pearle et al., 2005, Goldring and Marcu, 2009, Goldring, 2012). However, these activated chondrocytes are unable to produce ECM with the same characteristics as those of healthy matrix synthesized during cartilage development (Goldring, 2012). The genetic analysis of intact and OA cartilage revealed several mutations in genes encoding for ECM in OA (Loughlin, 2011). The role of various growth factors in stimulating the proliferative ability of chondrocytes in this phase has also been established (Fortier et al., 2011). However, this short-lived phase is soon followed by the destructive phase characterised by enhanced production of cytokines and degrading enzymes involved in the pathogenesis of OA (Goldring, 2000a). Chondrocytes in normal cartilage are known to produce many matrix metalloproteinases (MMPs) (Yoshihara et al., 2000) various serine and cysteine proteases (Mort and Billington, 2001). These are produced during normal matrix turnover in healthy cartilage in response to varying mechanical load. In OA the activities of these enzymes are increased (Dean et al., 1989) leading to the greater breakdown of matrix collagens and proteoglycans over their production. The levels of various MMPs including membrane-type I MMP

(Imai et al., 1997), MMP-7 (Ohta et al., 1998), MMP-8 (Shlopov et al., 1997), aggrecanase (Lohmander et al., 1993), ADAM-10 (Chubinskaya et al., 1998) and ADAM-15 (Böhm et al., 1999) and recently MMP-2 and MMP-9 (Galasso et al., 2012) have been known to increase in OA causing matrix destruction.

In normal conditions many cytokines and growth factors are produced but at low levels to maintain homeostasis of the cartilage (Goldring, 2000b, Sandell and Aigner, 2001). However, in OA it has been suggested that there is an imbalance between the various types of cytokines leading to cartilage degeneration as catabolism overrides anabolism (Martel-Pelletier et al., 1999, Fernandes et al., 2002). These earlier signs of cartilage catabolism are associated with enhanced breakdown of PGs and collagen disruption predominantly at the surface of the cartilage (Stockwell et al., 1983, Guilak et al., 1994, Billinghurst et al., 1997, Stoop et al., 2001). With the progression of disease, proteolytic enzymes cause degradation of PGs (Lark et al., 1997), causing matrix weakening (Aigner and McKenna, 2002), increased permeability of the matrix and increased hydration/swelling of the cartilage (Lai et al., 1991, Wang et al., 2010, Wang et al., 2013a) and decreased tensile stiffness (Maroudas, 1976). Additionally, there is enhanced destruction of collagen type II due to the catabolic effect of degradative enzymes (Poole et al., 2003). The degenerative processes appear to occur predominantly in the SZ of cartilage and around the chondrocytes residing in this zone (Guilak et al., 1994).

Aging leads to certain changes in cartilage matrix causing a decrease in tensile strength thus leaving the tissue inflexible/brittle and susceptible to fatigue failure (Bank et al., 1998). The macromolecules of cartilage matrix i.e. collagen and PGs (aggrecan) show certain changes in relation to the aging process such as collagen

cross linking and shortening of aggrecan molecules (Hugle et al., 2012). Although certain age-related changes in cartilage have been known as critical factors in OA and might play a role in the development of the disease, all OA is not due to aging (Li et al., 2013, Loeser, 2013).

1.2.1.2 *Chondrocyte clusters in OA*

A relatively late event in the pathogenesis of OA and a hallmark of this disease is the presence of clusters of chondrocytes (Weiss and Mirow, 1972, Rothwell and Bentley, 1973, Mitchell et al., 1992, Kouri et al., 1996b, Pfander et al., 2001) suggesting proliferative activity of chondrocytes in OA (Mankin et al., 1971, Hulth et al., 1972, Rothwell and Bentley, 1973). In comparison to OA cartilage, in healthy cartilage chondrocytes rarely divide and their proliferative activity is almost zero (Mankin, 1964). Chondrocyte proliferation by active mitosis has been seen in human OA cartilage leading to cluster formation (Hulth et al., 1972). The clusters of chondrocytes are often seen near fissures/fibrillations of the superficial cartilage layer (Lotz et al., 2010). The presence of these clusters of chondrocytes in the superficial layers of cartilage may be explained due to enhanced admittance of proliferative factors from the damaged collagen matrix in the superficial layers of cartilage (Meachim and Collins, 1962, Hollander et al., 1995). Additionally, these clusters of chondrocytes present in the superficial layers do not appear to increase the anabolism of cartilage (Aigner et al., 1997). This may be because in addition to cluster formation, cell death is also a key player in cartilage degeneration as evidenced by the presence of areas of hypo-cellularity and with increasing severity of disease, cell density decreases (Mistry et al., 2004). This can possibly be the reason

that even chondrocytes proliferate and form clusters during cartilage degeneration but they are unable to compensate for and maintain metabolic homeostasis.

1.2.1.3 *Cell death in OA*

Another characteristic histological finding of OA cartilage is the presence of empty lacunae (Stockwell, 1971) suggesting cell death involved in the pathogenesis of the disease (Blanco et al., 1998, Sharif et al., 2004). The exact mode of cell death in OA is unclear and still controversial with several possible mechanisms proposed such as necrosis, apoptosis, chondroptosis or a combination of these types (Kim et al., 2000, Roach et al., 2004, Wei et al., 2006, Thomas et al., 2007, Almonte-Becerril et al., 2010). Two major types of cell death in OA are characterised as necrosis and apoptosis but it is unclear which type of cell death predominates (Wei et al., 2006). It is suggested that there is an overlap between the two forms of cell death; the apoptosis can lead to necrosis (Carlo and Loeser, 2008). Various studies conducted on animals (Thomas et al., 2007, Carames et al., 2010) and humans (Kim et al., 2000, Sharif et al., 2004) to study the pathogenesis of OA showed a significant correlation between the disease severity and levels of chondrocyte death by apoptosis. Apoptosis is a physiological process which encompasses programmed cell death required for the normal cell turn-over during development and removal of damaged and cancerous cells (Kerr et al., 1972). Apoptosis is measured by the TUNEL method, a specific type of immunohistochemistry that causes staining of 3′-OH ends of DNA present in the apoptotic bodies as described earlier (Gavrieli et al., 1992) is considered a specific method for detecting apoptotic chondrocytes as utilised in a recent study (Zamli et al., 2013). However, whether apoptosis is a mode of cell death

in OA is controversial. A variant of apoptosis called chondroptosis was coined as an alternative mechanism of cell death in OA cartilage (Roach et al., 2004). Chondroptosis differs from standard apoptosis in the morphological features especially in terms of cytoplasmic changes with increased rough endoplasmic reticulum and Golgi apparatus, presence of vacuoles, expulsion of cellular material and final fragmentation of cell (Roach et al., 2004).

1.2.1.4 *Chondrocytes hypertrophy-like changes in OA*

The role of chondrocyte hypertrophy-like changes has been observed in the initiation and progression of OA (Dreier, 2010, van der Krann and van den Berg, 2012) and considered one of the characteristics of this disease (Tchetina et al., 2007) (Fig.1.3).

Morphometric analysis of chondrocyte hypertrophy revealed an increase in the volume of cells and organelles (Buckwalter et al., 1986). There are several markers of hypertrophied chondrocytes in OA cartilage but the classical ones are collagen type X (von der Mark et al., 1992) and MMP-13 (Shlopov et al., 1997). Additionally, an increase in chondrocyte volume was observed in degenerated human cartilage suggesting the possible role of this increase in volume to the altered chondrocyte metabolism in OA (Bush and Hall, 2003).

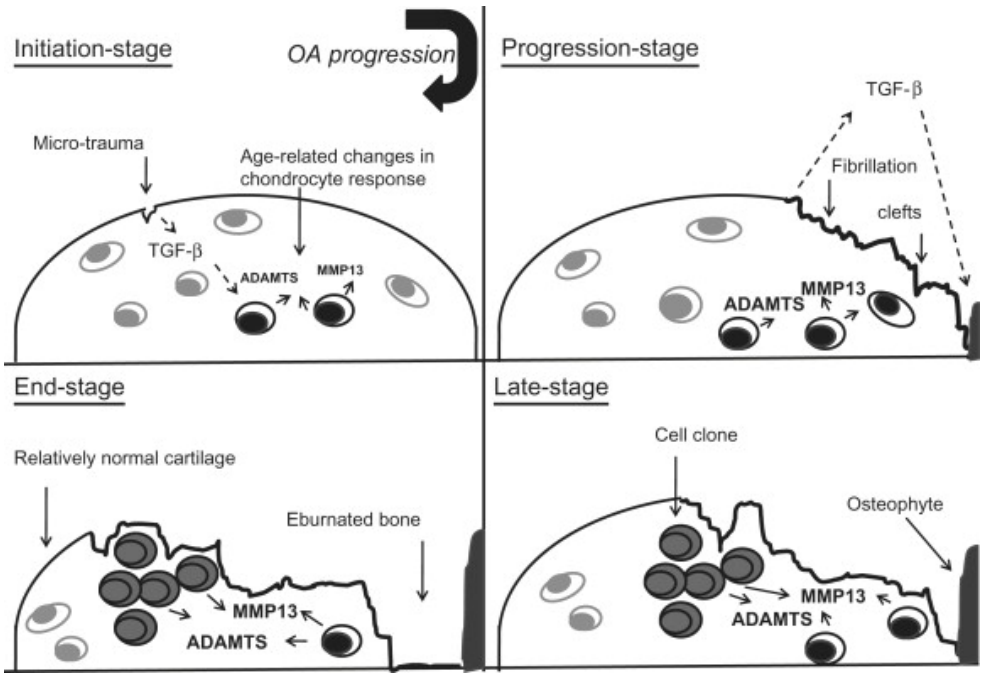

Figure 1.3: Chondrocyte hypertrophy-like changes in a conceptual model of human primary OA.
Cells that have acquired a "hypertrophy-like" phenotype **(**black**)** play an essential role in cartilage breakdown by synthesis of MMP13 and ADAMTS4 and 5. Of note, besides TGF-β numerous other signaling molecules, enzymes and matrix molecules are involved in the OA disease process. (Adapted from van der Krann and van den Berg, 2012).

1.2.1.5 *Changes to chondrocyte phenotype in OA*

Chondrocytes are phenotypically unstable cells (Darling and Athanasiou, 2005) and changes to chondrocyte phenotype have been observed in OA (Kouri et al., 1996a, Miosge et al., 1998, Wang et al., 2003, Yagi et al., 2005). Phenotype switching was observed in chondrocytes which dedifferentiated into flattened fibroblast cells after culture on plastic surface (von der Mark et al., 1977). However, when chondrocytes were cultured in 3D environment using alginate (Bonaventure et al., 1994) or agarose culture conditions they regained their chondrocytic phenotype with the production of mechanically functional matrix macromolecules (Benya and Shaffer, 1982). Normal

chondrocytic phenotype of rabbit cartilage has been characterised by spheroidal shape of the cell with the production of normal cartilaginous matrix (mainly collagen type II and large aggregating PGs i.e. aggrecan) (Benya and Shaffer, 1982). In addition to changes in chondrocyte metabolism and synthetic activity, another important characteristic of OA is phenotypic switching of chondrocytes (Benya et al., 1978, Tesche and Miosge, 2005). There are several studies on human AC which have reported changes to chondrocyte phenotype in OA as reported in a study the presence of fibro-cartilaginous tissue with high content of fibrillar matrix (Miosge et al., 1998, Poole, 1999). In other studies, fibroblast-like chondrocytes were also observed in deep zones of AC with the production of collagen type I and III especially in the advanced stages of disease (Miosge et al., 1998, Sandell and Aigner, 2001, Tesche and Miosge, 2005). Additionally, chondrocytes with abnormal (irregular) morphology were identified as elongated cells and named as secretory type 2 cells (Kouri et al., 1996b). Chondrocytes were studied in OA and compared for the expression of specific markers used for identification of phenotype. In OA cartilage, mostly in the middle zone activated chondrocytes expressing aggrecan and collagen type II were present (Sandell and Aigner, 2001). These cells also produced collagen type IIA thereby, indicating the presence of chondrogenic progenitor cells in the middle layers of OA cartilage (Sandell and Aigner, 2001). However, cells in the deeper layers of OA cartilage showed presence of type X collagen indicating hypertrophied chondrocytes in this zone (Dreier, 2010).

1.2.1.6 *Chondrogenic progenitor cells (CPCs) in OA*

Chondrocytes have been long considered the only cell type present in AC (Stockwell, 1978, Buckwalter and Mankin, 1997b). However, for the first time in 2003 in a culture modified by growth factors, a cell population with multilineage differentiation potential was observed among the de-differentiated adult human articular chondrocytes (Barbero et al., 2003). Later population of cells called CPCs was observed in the SZ of cartilage (Dowthwaite et al., 2004). In several other studies the presence of mesenchymal progenitor cells in normal cartilage and an increase during OA was reported (Alsalameh et al., 2004, Fickert et al., 2004, Hiraoka et al., 2006, Grogan et al., 2009). CPCs have migratory potential and have been seen to migrate to the site of blunt impact or scratch injury in cartilage (Seol et al., 2012). In cartilage injuries the implantation of these CPCs have shown encouraging results in terms of cartilage regeneration (Jiang et al., 2012). These migratory cells were obtained from the late stages of OA cartilage tissue and they possessed the ability of differentiation especially towards chondrogenesis and the properties of progenitor cells (Koelling et al., 2009). The chondrogenic differentiation properties of these cells are regulated by two transcription factors: RUNX-2 and SOX9 being osteogenic and chondrogenic transcription factors respectively. Moreover, enhanced expression of SOX9 was observed in the CPCs when RUNX-2 was down regulated leading to an increase in the expression of type II collagen and aggrecan. The discovery of these migratory progenitor cells from the diseased tissue and having high chondrogenic potential opens new possibilities for devising improved treatment strategies for OA (Koelling et al., 2009).

1.2.1.7 *Chondrocyte-matrix interactions*

Chondrocytes are responsible for maintaining the homeostasis of the cartilage by keeping a balance between the anabolic and catabolic activities (Sandell and Aigner, 2001). The cell-matrix interactions are very important key players in regulating chondrocyte functions (Lee and Loeser, 1998). A family of ECM receptors present on chondrocyte surface is the integrin family of receptors responsible for cell-matrix interactions in cartilage (Loeser, 2014). It is the interaction of ligands from ECM and activation of integrin receptors via these ligands that chondrocytes receive chemical signals from the matrix and transmit mechanical signals to the cell interior. There are several key functions of chondrocytes including cell proliferation, survival, differentiation, morphogenesis and remodelling of cartilage matrix which are regulated by integrin mediated signalling by chondrocytes (Adams and Watt, 1993, Gumbiner, 1996, Giancotti, 2000). There are dual components of integrin mediated signalling in chondrocytes, firstly the organisation of the cytoskeletal elements internally (Wolfenson et al., 2013) and secondly interaction with the growth factors and cytokines externally (Danen and Yamada, 2001, Legate et al., 2009). In normal articular cartilage, several types of integrin receptors are present (Camper et al., 1998). In OA, the expression of several integrin receptors is increased as compared to normal cartilage (Loeser et al., 1995). Of special interest is the increased expression of α1ß1 in OA which has the capability to bind to collagen type II and collagen type VI (present in PCM) in comparison to healthy cartilage (Loeser et al., 1995, Parekh et al., 2014). Additionally, appearance of three types of integrin receptors namely α2ß1, α4ß1 and may be α6ß1 were noticed to be expressed on OA chondrocytes which are not normally present on healthy chondrocytes (Lapadula et

al., 1997, Ostergaard et al., 1998, Loeser, 2014). In OA, fibronectin fragments are produced which signal through integrin α5ß1 and lead to activation of inflammatory and catabolic responses which will eventually lead to cartilage degradation (Loeser, 2014). Chondrocytes when kept in monolayer cultures, de-differentiate and it has been suggested that integrin receptors αVß5 play a role in this phenotype switching through ERK signalling pathway (Fukui et al., 2011). Several integrin receptors for binding with fibronectin, laminin and collagen are expressed by chondrocytes (Loeser, 2000, Loeser, 2002, Egerbacher and Haeusler, 2003). ß1 chain is a component of most of these integrin receptors. Inactivation of cartilage specific ß1 chain in knock out mice resulted in chondrodysplasia, shown by abnormal growth plate with distorted proliferative columns and abnormal shapes of cells (Aszodi et al., 2003). This suggested that integrin receptors play a vital role in regulation of chondrocyte phenotype.

1.2.1.8 *Heterogeneity to chondrocyte morphology in OA*

In OA, phenotypic modulation of chondrocytes in terms of their biosynthetic activity has been observed by various researchers (Table 1.3).

Reference	Source of specimen	Technique	Key findings
(Stockwell, 1978)	Human femoral condylar cartilage	Electron microscopy	Projecting cell processes several micrometres long may extend beyond the lacuna
(Cancedda et al., 1995)	Chick chondrocytes	Electron microscopy	Chondrocytes differentiate
(Kouri et al., 1996a)	Human knee OA AC	Light and TEM	Variability in the chondrocyte phenotype
(Kouri et al., 1996b)	Human knee OA AC	Electron microscopy	Chondrocytes with variable morphologic phenotype coined as Type 2b secretory cells
(Poole, 1997) [Review]	Canine		Remodelling of chondrons at the initiation and progression of OA and migration of progenitor chondrocytes within the microenvironment of chondrons undergoing remodelling
(Miosge et al., 1998)	Human AC	*In situ* hybridization at the light and electron microscopic level	In the late stage OA, in the deep layers irregular shaped secretory chondrocytes were seen which resembled type 2b secretory cells defined by Kouri *et al* (Kouri et al., 1996b)
(Kouri et al., 1998)	Human OA AC	Electron and confocal microscopy	Heterogeneity to chondrocyte morphology was observed
(Lee and Loeser, 1998)	Human OA AC	Confocal microscopy	Chondrocyte in 3D alginate cultures produced processes through the PCM
(Sandell and Aigner, 2001) [Review]			Several factors induce 'de-differentiation' of chondrocyte phenotype to fibroblast-like phenotype in OA.
(Goldring, 2002) [Perspective article]			Chondrocyte phenotype is modulated in OA
(Kouri and Abbud-Lozoya, 2002)	Rat Osteoarthrosis induced model	Electron microscopy	Chondrocyte shape changes along with cytoplasmic projections were observed after 45 days of osteoarthrosis induction
(Aigner and McKenna, 2002) [Review article]			In OA chondrocytes react by changing their cellular phenotype
(Wang et al., 2003)	Human AC	Flow cytometry	In OA tissue cartilage superficial layers were partly lost and replaced by new chondrocyte population with different phenotype
(Bush and Hall, 2003)	Human AC	Confocal microscopy	Chondrocytes exhibited cytoplasmic processes in non-degenerate and degenerate human AC
(Holloway et al., 2004)	Human AC	Epi-fluorescence and confocal microscopy	In non-OA and OA samples cells with multiple elongated processes upto 30µm extending into ECM, fewer in non-OA as compared to OA.
(Tesche and Miosge, 2004)	Human AC	Light and electron microscopy	In OA irregular shaped chondrocytes with numerous filopodia were seen
(Tchetina et al., 2005)	Human AC	ELISA, RT-PCR	Very early changes in OA are accompanied with chondrocyte terminal differentiation and matrix degradation
(Yagi et al., 2005)	Human AC	Quantitative RT-PCR	Loss of chondrocyte phenotype in OA was observed
(Tesche and Miosge, 2005) [Review article]			In late stages of OA fibroblast-like cells are present
(Kouri and Lavalle, 2006)[Review article]			Variability of chondrocyte phenotype was found in rat and human OA cartilage
(Ross et al., 2006)	AC from tibial plateaux of adult dogs	Confocal microscopy	Presence of cytoplasmic cell processes 2-5µm long extending into the surrounding matrix were seen
(Gonzalez et al., 2007)	Human AC	ATM and TEM	In normal human AC in the SZ chondrocytes had cytoplasmic processes
(Lyman et al., 2012)	Human AC	Confocal and TEM	Chondrocytes showed morphological changes as cell flattening and produced cytoplasmic processes in response to injury

Table 1.3: Historical perspective of heterogeneity to chondrocyte morphology in OA.
TEM - Transmission electron microscopy, ELISA–Enzyme-linked immunosorbent assay, PCR - Polymerase chain reaction, RT-Real time, ATM-Atomic force microscopy.

Although chondrocyte ultrastructure and biochemical changes during OA have been studied in detail, chondrocyte morphology has received less attention. The main reason could be that in majority of these studies classical histological techniques were used and they rendered it difficult to visualise the fine morphological details of chondrocytes caused by shrinkage due to tissue fixation techniques (Buckwalter et al., 1986) and single slice observations. By using confocal laser scanning microscopy (CLSM) 3D images of chondrocytes can be obtained and fine details of morphology can be studied in thick samples and even in fixed tissue without much disturbance to the tissue architecture (Brakenhoff et al., 1990).

CLSM with the use of intracellular fluorescent dyes is a very powerful technique for obtaining several optical sections permitting visualisation of 3D morphology and volume calculation of living in situ chondrocytes without much disruption to ECM (Guilak et al., 1995, Errington et al., 1997, Kouri et al., 1998, Bush and Hall, 2001a, Bush and Hall, 2001b). CLSM also rendered it possible to study the morphological details of chondrocytes and thus altered chondrocyte morphology with the presence of cytoplasmic processes in non-degenerate and degenerate tibial plateau cartilage was reported (Bush and Hall, 2003). Furthermore two possible (a) passive and (b) active theories of the existence of these processes were proposed by the scientists in this study. The passive theory stated that possibly the damage to the PCM would provide a pathway for production of processes. The active theory suggested that production of degradative enzymes by altered chondrocyte metabolism would cause local matrix weakening and production of processes. Later in another study on osteoarthritic human femoral head pannus tissue by using CLSM chondrocytes with multiple elongated processes were observed (Holloway et al., 2004). It is unlikely for

these cytoplasmic processes to be cilia because of two main reasons: (1) bovine primary cilia are much smaller (~1.5µm) than these processes (McGlashan et al., 2008) and (2) cilia cannot be visualised with CLSM unless labelled specifically.

The relation between abnormal morphology and altered metabolism was reported in a study conducted on non-degenerate and degenerate human tibial plateau cartilage which stated that abnormal chondrocytes with cytoplasmic processes displayed increased levels if IL1ß and loss of collagen type VI in the PCM (Murray et al., 2010) (Fig. 1.4).

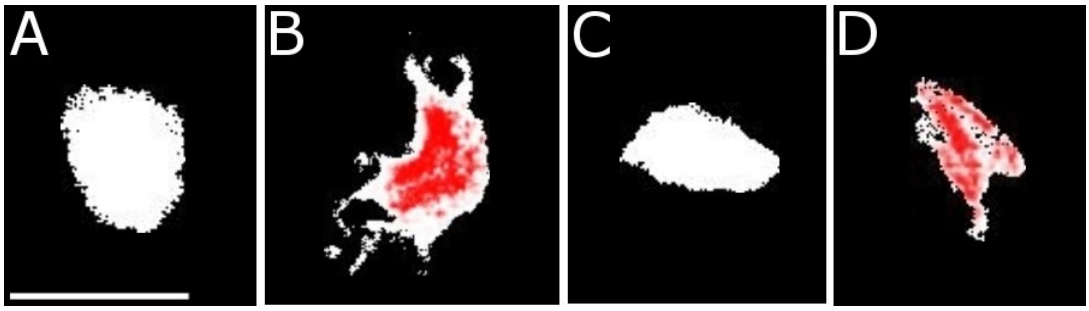

Figure 1.4: Cell morphology and quantification of cell-associated IL-1ß fluorescence.
Examples of IL-1ß fluorescence immuno-histochemistry in cells with varying morphology are shown (images (A–D); bar for all =10µm). In image (A), a normal SZ chondrocyte is shown, with negligible levels of cell-associated IL-1ß immuno-fluorescence, whereas the SZ cell shown in (B) was abnormal and demonstrated marked IL-1 ß labelling. A normal DZ chondrocyte is also shown with no detectable IL-1ß labelling (image (C)), and image (D) illustrates an abnormal DZ chondrocyte with a cytoplasmic process and clear IL-1ß labelling. (Adapted from Murray et al., 2010).

1.2.2 PTOA/Secondary OA

1.2.2.1 *Incidence, causes and treatment strategies for PTOA*

Secondary OA develops as a consequence of joint injury/trauma, characterised by pain and disability (Brown et al., 2006). It can be differentiated from primary OA on the basis of the fact that there is an underlying cause whereas primary OA is mostly idiopathic (Buckwalter and Mankin, 1997a). Mechanical traumas/acute joint injuries lead to progressive cartilage degeneration, remodelling of bone and changes in the soft tissues thereby, causing PTOA. These types of injuries include joint dislocations, tears of joint structures, intra articular fractures and direct blunt injuries (Buckwalter et al., 2013). Of the overall burden of primary and secondary OA, 12% is approximately as a consequence of joint injuries (Brown et al., 2006). The pharmacological and surgical treatment strategies devised so far had been unsuccessful in preventing the progression of PTOA (Anderson et al., 2011). In comparison to primary OA which occurs mainly in old age PTOA progresses slowly and affects specific joints like knee, hip etc. PTOA occurs in young age mostly, quickly progresses and depends upon the extent of injury to the joint (Thambyah, 2005). However, it is difficult to differentiate between the process of degeneration in young adults with an identifiable cause and in old aged people with no known causative factor (Buckwalter and Martin, 2006). Articular cartilage possesses limited capacity for regeneration/repair ("repair" see foot note[1]) of the damaged tissue. Although there are numerous studies conducted on the regeneration of this tissue but

[1] Cartilage repair implies to the regeneration of damaged cartilage by synthesis of mechanically functional matrix. However, repair here suggests the response of chondrocytes towards damage in an effort to heal the defect and does not imply to the restoration of the normal mechanical properties of cartilage.

there is only minimal evidence that this tissue actually repairs itself (Buckwalter and Brown, 2004, Nishida et al., 2004). The treatment strategies employed to prevent and cure PTOA are both conservative and surgical procedures. The conservative treatment plans consist of some non-surgical procedures and medications to reduce the symptoms and are usually employed to patients where injury is minor. These non-operative procedures are done according to the severity of cartilage lesion (Farnworth, 2000).

The surgical procedures are mostly done for the prevention of PTOA after injury, including fracture reduction, arthroscopic debridement, micro fracture, subchondral drilling, repair and reconstruction surgeries, osteochondral grafting, stabilisation procedures, autologous chondrocyte implantation, tissue engineered cartilage implantation and osteotomies (Buckwalter and Martin, 2006). The outcomes of these procedures are variable in different patients in preventing development of PTOA. Therefore, while selecting the best treatment for a patient one should consider the type of injury, potential for healing and effects of treatment on joint repair (Buckwalter, 1998, Marsh et al., 2002).

1.2.2.2 *Pathogenesis of PTOA*

The pathogenic mechanisms involved in the development and progression of PTOA can be categorised roughly into three main phases, immediate events after trauma/injury, acute phase and a chronic phase (Lotz, 2010). The immediate events include collagen rupture, loss of GAGs, haemarthrosis and chondrocyte necrotic death (Szczodry et al., 2009).

The acute phase consists of decreased lubricant properties of synovial fluid, additional cell death due to apoptosis, decreased synthesis of matrix macromolecules (collagen and PGs) and enhanced expression of degrading enzymes and mediators of inflammation (DiMicco et al., 2004, Lee et al., 2005). The chronic phase of PTOA progresses slowly from asymptomatic to symptomatic phase involving inflammation and joint remodelling, eventually causing joint pain and dysfunction (Lotz, 2010).

Osteochondritis dissecans (OCD) is a joint disorder which leads to changes in subchondral bone and overlying cartilage with the progression from cartilage loosening to complete separation of osteochondral fragment called loose body (Paget, 1870). The exact aetiology of the disease is not known however trauma, vascular insults for example ischemia/necrosis and hereditary causes are considered the most frequent causes of OCD development (Andrew et al., 1981, Uozumi et al., 2009). Trauma whether occurring once or several micro traumas are considered to be the most frequent cause of development of this disease as it was noticed that its incidence was highest amongst athletes (Cahill, 1995). The histological examination of OCD samples showed variable results in terms of necrosis of the subchondral bone (Chiroff and Cooke, 1975, Yonetani et al., 2010). The articular cartilage of the OCD samples also depicted a variable picture regarding the presence or absence of degeneration (Linden and Telhag, 1977, Koch et al., 1997, Yonetani et al., 2010). The treatment of OCD can be either preservative or restorative treatment where preservative is to preserve the cartilage by drilling or fixation of the fragment and restorative includes either chondrocyte implantation or osteochondral grafting to substitute the damaged cartilage with hyaline/hyaline-like tissue (Pascual-Garrido et al., 2009). This OCD tissue can be obtained at surgery and is a useful source for

studying the viability and morphology of chondrocytes in diseased cartilage. It is a valuable tissue source to be studied in the context of this thesis because the main aim of the thesis was to study the changes to chondrocyte morphology in various experimental and clinical conditions. Amongst the clinical conditions OCD is a common joint disease and the tissue is easily accessible after surgery. Determining chondrocyte morphology in OCD will provide insight into whether abnormal morphology is a feature of degenerating cartilage in OA alone or these changes also occur in other clinical conditions.

1.2.2.3 *Chondrocyte cell death in PTOA*

Cell death following injury to cartilage has been studied in various *in vivo* and *in vitro* studies (D'Lima et al., 2001b, Kim et al., 2002, Bush et al., 2005, Kurz et al., 2005, Milentijevic et al., 2005). Cartilage cell death is considered the key event in the pathogenesis of development of PTOA (Kuhn et al., 2004). The mechanisms of cell death after traumatic impact to cartilage has given rise to considerable controversy. However, a general consensus is that it can occur in two phases, an immediate phase of necrotic cell death and a later phase comprising of cell death due to apoptosis (Quinn et al., 1998, D'Lima et al., 2001a, Duda et al., 2001). The author agrees to this general concept of initial necrotic and later apoptotic cell death associated with cartilage trauma. The compressive loading of cartilage leads to apoptosis (Chen et al., 2001, D'Lima et al., 2001a) around the injured matrix and the intensity of cell death has a linear relationship with the intensity of injury (Jeffrey et al., 1995). The surface zone chondrocytes are more susceptible to cell death (Torzilli et al., 1999). Matrix degradation is a consequence of chondrocyte death because the

remaining viable chondrocytes are unable to repair the injury effectively (D'Lima et al., 2001b). Moreover, cell death after injury has been found to be associated with loss of GAGs (D'Lima et al., 2001b).

1.2.2.4 *Role of inflammatory cytokines in development of PTOA*

The inflammatory cytokines are involved in the pathogenesis of PTOA and their levels are raised after joint injury (Abramson et al., 2001). IL-1, IL-6 and TNFα are the main cytokines involved in the development of PTOA (Lee et al., 2009). The inflammatory cytokines are responsible for the loss of PGs through an enhanced catabolic activity and decreased anabolic activity (Guilak et al., 2004).

1.2.2.5 *Degradative enzymes in the pathogenesis of PTOA*

The damage to the cartilage after trauma is significantly through the release of extracellular matrix degrading enzymes by the chondrocytes that survive injury (Kurz et al., 2005). These degrading enzymes breakdown the matrix components and produce fragments of collagen and fibronectin which will initiate a positive feedback cycle causing further production of degrading enzymes (Guo et al., 2009). Increased levels of MMP-1, MMP-2, MMP-3, MMP-8, MMP-9, MMP-13, MMP-14 and ADAM-TS5 have been noticed in the cartilage explants after trauma and play a significant role in cartilage degradation and development of PTOA (Lotz, 2010, Kramer et al., 2011).

1.2.2.6 *CPCs in cartilage repair*

CPCs were first reported in the literature as a heterogeneous population of cells present in human AC having the properties of mesenchymal progenitor cells such as

self-renewal capacity and differentiation potential (Barbero et al., 2003). CPCs are capable of migration through the matrix and possess the potential for repair both in the injured and the OA cartilage (Koelling et al., 2009, Seol et al., 2012). The response of chondrocytes to mechanical injury has been reported in a study where chondrocytes produced cytoplasmic processes in reaction to the injury (Lyman et al., 2012). Additionally, after a blunt trauma to the cartilage CPCs appeared at the site of injury after 7-14 days and possessed the migratory ability (Seol et al., 2012). Furthermore, it has been observed that cartilage insult caused by enzymatic degradation led to the migration of CPCs in cultured explants (Seol et al., 2014). The chemotactic factors released by the dead chondrocytes after injury are thought to recruit CPCs at the site of injury (Seol et al., 2012). There are several factors known to increase the chemotactic activity of chondrocytes such as platelet derived growth factor (PDGF) and insulin like growth factor 1 (IGF-1) (Joos et al., 2013). When the cartilage explants were exposed to low intensity ultrasound, the migration of CPCs was enhanced (Jang et al., 2014). In another study it has been proposed that calcium oscillations in CPCs are driven by autocrine/paracrine purinergic mechanism which might influence their differentiation potential (Matta et al., 2015). The role of CPCs in cartilage repair after injury is still unknown; however they are proliferative in nature but phenotypically different from chondrocytes.

1.2.2.7 *Chondroprotective role of hyperosmolarity in cartilage injury*

Chondrocytes are osmotically sensitive cells and react to changes in the osmolarity of ECM with corresponding changes in volume (Bush and Hall, 2001a). The detrimental effect of mechanical trauma has been observed to be accelerated by decrease in extracellular osmolarity (Bush et al., 2005, Amin et al., 2008b, Amin et

al., 2010, Amin et al., 2011). However, increasing the osmolarity of the ECM has a chondroprotective role with a significant reduction in cell death following cartilage trauma (Bush et al., 2005, Amin et al., 2008b). Additionally, in an *in vivo* study hyperosmotic saline has been reported to be related to reduced chondrocyte death and better repair outcomes following sharp scalpel injury (Eltawil et al., 2014). It has also been reported in a study that increasing the osmolarity of joint irrigation solution markedly reduced chondrocyte death during cartilage drilling (Farhan-Alanie and Hall, 2014). The chondroprotective effect of hyperosmolarity on injured cartilage in terms of chondrocyte viability has been studied extensively but the morphology of chondrocytes in response to injury in the presence of hyperosmolar environment has attained less attention. As there exists a close relationship between chondrocyte morphology and metabolism (Murray et al., 2010) therefore studying morphology of chondrocytes in response to hyperosmolarity will provide insight as to whether their metabolism is normal or altered. Thus whether exposing the cartilage to hyperosmolar environment following trauma helps chondrocytes to retain their normal morphology is an important research question which needs to be investigated.

1.3 Chondrocytes in agarose gel culture

Cellular morphology and cell-matrix connections are dissimilar in 2D as compared to 3D environment (Cukierman et al., 2001). 3D culture conditions are more appropriate for culturing cells as they resemble the *in vivo* conditions. De-differentiated chondrocytes restore their differentiated phenotype when cultured in 3D hydrogel cultures (Benya and Shaffer, 1982, Adolphe and Demignot, 2000). Additionally the de-differentiated chondrocytes in agarose culture re-expressed collagen and PG levels similar to primary chondrocytes (Benya and Shaffer, 1982).

3D agarose gel cultures have been reported to be suitable for culturing chondrocytes as they produce mechanically functional matrix (Buschmann et al., 1992). Agarose does not directly affect phenotype and chondrocytes have been kept in agarose culture for 47 days without any obvious change in phenotype (Benya and Shaffer, 1982, Buschmann et al., 1995). In the work by Buschmann et al & Benya and Shaffer the agarose gels with strengths of 2% and 0.5% were used respectively to culture chondrocytes successfully. In the work presented here agarose gel with 2% (strong) and 0.2% (weak) strengths have been utilised to culture chondrocytes. Therefore, the gel strengths used in this thesis to culture chondrocytes are in good agreement with the previously published work. Agarose culture system has been utilised successfully in various studies and is considered quite compatible to chondrocytes, inert in nature and its mechanical properties can be regulated/altered (Mauck et al., 2000, Balgude et al., 2001, Ahearne et al., 2005). In a recent study the effect of matrix elasticity was studied on the phenotype, proliferative ability and ECM expressed by chondrocytes cultured in agarose gels of various strengths (Schuh et al., 2012b). In this previous study by Schuh et al (2012b) it has been reported that chondrocytes cultured in weak gels proliferate and produce more ECM as compared to stiff gels. There are several differences between the previous work and the study presented here and they are (a) in the previous work the minimum gel strength used was 0.75% however, in the present study the minimum strength of agarose gel used is 0.2% (b) in the previous study the main focus was to determine chondrocyte behaviour in gel cultures whereas in the present study the main focus is on the chondrocyte morphology (c) in the previous study the effect of serum was not studied but in the present study the effect of increasing concentrations of serum on chondrocyte morphology is studied.

Therefore, by studying the effect of foetal calf serum (FCS) concentration and gel strength on chondrocyte morphology when cultured in agarose gels will build up on the previous work by Schuh et al (2012b).

Although agarose gel model has been extensively utilised to study various aspects of chondrocytes yet the morphology has not been studied comprehensively. Therefore strong and weak agarose gel models can possibly be utilised to model healthy and degenerate/weakened matrix respectively. We have already highlighted the importance of chondrocyte morphology in OA (section 1.2.1.8) and agarose gels can possibly be the model to study some of the morphological changes in early OA.

1.4 Confocal laser scanning microscopy (CLSM)

In the classical histological procedures currently used to study in situ chondrocytes, the unquantified shrinkage of the chondrocytes may occur with histological fixation techniques (Buckwalter et al., 1986). These alterations may lead to inaccurate estimates of volume/morphology and thus obscuring the fine morphological details. Therefore, histological techniques limit the true examination of the tissue in unaltered physiological conditions and render it difficult to record the response of viable cells to various stimuli. Moreover, physical tissue sectioning involved in the conventional histological procedures is a big hurdle in providing 3D information regarding morphology of chondrocytes. However, CLSM is a type of fluorescence microscopy which allows the acquisition of high resolution 3D images from thick tissues in a relatively unperturbed environment (Brakenhoff et al., 1979). This relatively less destructive imaging technique enables the researchers to obtain morphological information which may possibly be comparable to *in vivo* conditions.

In this thesis the importance of CLSM as a research tool cannot be denied because of its ability to enable acquisition of 3D data on chondrocyte volume/morphology of chondrocytes in an unperturbed microenvironment. The main investigation of the research presented in this thesis involved determination of chondrocyte viability, volume and the cytoplasmic processes. In order to determine chondrocyte viability and morphological characteristics in the aetiological investigation of OA, detailed information regarding the fine morphological details of chondrocytes in an undisturbed microstructure of AC is important. The hypotheses investigated in this thesis involve CLSM as the major research tool and the basic principle of this technique is detailed in the following sections.

1.4.1 Overview of CLSM

Minsky (1988) defined the principle of CLSM in order to improve the resolution of imaging in comparison to the conventional ones (Minsky, 1988). However, Minsky could not utilise this method of imaging because the images were short-lived and couldn't be captured or saved (Jones et al., 2005). Later on the idea of CLSM was reviewed and computers were used to display images. Advancements in computer processors now allow 3D image reconstruction, de-convolution and morphological analysis. CLSM provides several improved imaging properties in comparison to traditional microscopy. The most important of these is the improved resolution which determines image quality in any microscope system. A key characteristic of CLSM is to reject out-of-focus light above and below the focal plane thus creating a sharp image. A series of properly focussed images called optical sections are obtained at precisely defined increments in z-axis. These optical sections are then combined using software to create a 3D reconstruction of the imaged sample.

However, there are certain limitations and few imaging problems associated with this technique just as associated with other research techniques. These are basically the image artefacts associated with this technique. These artefacts can either result from weakening of the signal as the depth of imaging increases or image misrepresentation can occur due to refractive index discrepancy of the sample (Jones et al., 2005). However, it is unlikely that these artefacts can make cells to produce processes as these processes are the cytoplasmic extensions of cells with 5-chloromethylfluorescein diacetate (CMFDA) labelling as strong as observed in the cell body. The other possible artefacts associated with CLSM fluorescent-mode imaging technique is the photo toxicity to the live cells caused by laser excitation of the tissue (Frigault et al., 2009). However, laser induced photo toxicity cannot be an issue for this study as the chondrocytes had been fixed after fluorescent labelling prior to imaging.

1.4.2 Principle of CLSM

In CLSM a laser source launches a laser beam which focusses light through the objective of the microscope on a single point on to the specimen (Fig. 1.5). Following this principle the scattering of light is less and thus a sharp image is created. This laser beam excites the fluorophores incorporated in the specimen and fluorescence is emitted. The fluorescent radiation is again received by the objective and directed towards the photo detector through the dichroic beam splitter. Additionally, the light coming from the specimen passes through a pinhole aperture which rejects unfocussed light. The beam of light passes through two band pass filters i.e. low pass and high pass band filters allowing only a narrow bandwidth of light before hitting the photo detector. The light is then focussed through a pinhole

aperture in front of the detector and out of focus light is eradicated before being registered by the detector. The light from above and below the focal plane does not pass through the pinhole and thus does not contribute in image formation. This light pathway focusses at a single point on the specimen, however a set of motorised rotatory mirrors allow laser to scan the whole specimen. This allows the acquisition of a series of optical sections along the z-axis.

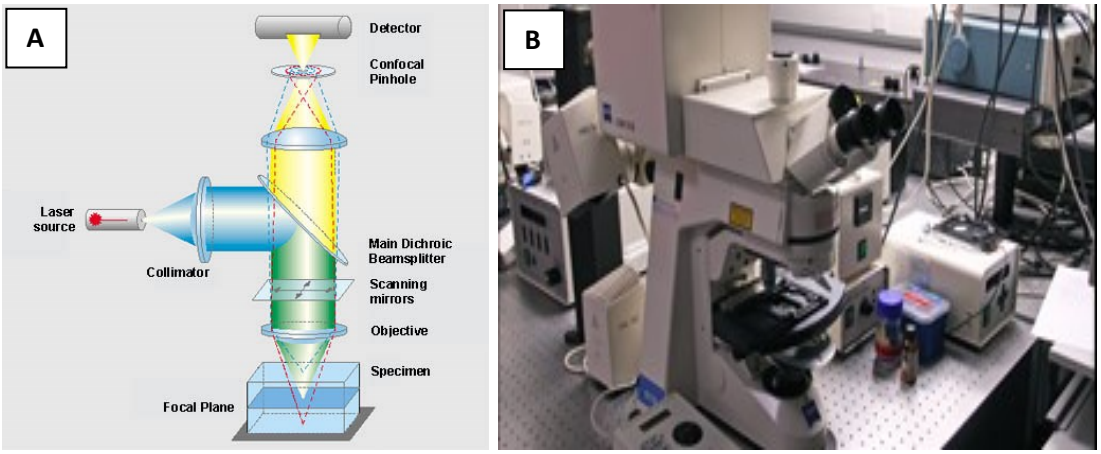

Figure 1.5: System set-up of CLSM.
(A) Simplified diagram showing ray path in CLSM, broken lines indicate out of focus light above (green broken) and below (red broken) the focal plane (www.zeiss.de) (B) A photograph of the Zeiss LSM 510 Axioskop in the laboratory.

1.4.3 CLSM in cartilage research

Confocal microscopy with fluorescence has gained much importance in studying cartilage biology because of its advantage to image chondrocytes *in situ* as compared to the destructive histological conventional techniques (Jones et al., 2005). CLSM has been utilised in studying the structure of cartilage with chondrocytes arranged in columns (Hedlund et al., 1994) and under different loading conditions (He et al., 2014). This technique has been successfully utilised to study the morphological

characteristics of non-degenerate and degenerate AC (Bush and Hall, 2003, Holloway et al., 2004), ECM disruption associated with morphologically abnormal chondrocytes (Murray et al., 2010) and ECM components such as collagen (Poole et al., 1992). In various studies conducted on AC, live and dead cells have been labelled with fluorescent dyes and imaged with CLSM to determine chondrocyte death in mechanically injured AC (Bush et al., 2005, Amin et al., 2008b, Amin et al., 2011). By using CLSM the ultrastructure of human cartilage (Hunziker, 2001), shape and volume analysis of chondrocytes in relation to tissue deformation/loading was studied (Guilak et al., 1995). The effect of physiological loading on the biosynthetic response of chondrocytes has also been extensively studied by using CLSM (Kim et al., 1994, Clark et al., 2003). There are several algorithms used to determine volume of chondrocytes by CLSM, a comparison of these techniques was done in a study (Lucas et al., 1996). Additionally CLSM was used to study chondron structure (Poole, 1997) and immediate microenvironment of chondrons such as type VI collagen (Poole et al., 1992). The ECM components of cartilage have been studied using this tool (Wu et al., 2004). CLSM has been widely used to study the efficacy of various strategies employed in cartilage repair such as chondrocyte implantation (Manolopoulos et al., 1999), cell coating method (Dennis et al., 2004) and osteochondral allografts (Gole et al., 2004).

In the work presented in this thesis, CLSM with fluorescence has been used as a key technique to study cell viability and volume/morphology of chondrocytes under various conditions in bovine, human cartilage samples and cultured chondrocytes.

1.5 Rationale and aims of the thesis

The rationale of this work is based on determining chondrocyte morphology in non-degenerate and mildly-degenerate human cartilage and then utilisation of *in vitro* models to induce morphological changes to chondrocytes. The studies, conducted in the scope of this thesis, hereby, cover the different possible scenarios of weak matrix i.e. mildly-degenerate cartilage, 3D gels with low concentration of agarose and injured cartilage for determining the morphological characteristics of human and bovine chondrocytes. Postulating a single hypothesis is complicated because the methodology involved in various studies presented in this thesis is different however, various aims are summarised below:

1. To determine chondrocyte morphology in grade-0 and grade-1 human femoral head AC.
2. To develop an *in vitro* model of weak matrix by altering agarose concentration to study its effects on chondrocyte morphology. To histologically evaluate alterations in ECM produced by abnormal chondrocytes in weak gels.
3. To develop an *in vitro* partial thickness mechanical injury bovine AC model as a method for demonstrating a weak matrix with enhanced accessibility of FCS to chondrocytes. To evaluate alterations in ECM produced by abnormal chondrocytes at the injury.
4. To utilise this injured bovine AC model as a mode to determine morphology of chondrocytes in response to hyperosmolar environment.

1.6 Outline of the chapters

Chapter 2 – Materials and Methods

In this chapter the generalised biochemicals used in this work and methods for preparing standard and varied culture media and methodology involved in varying medium osmolarity have been detailed. Additionally, the fluorescent probes used to label chondrocytes for CLSM have also been mentioned. This chapter also includes the details of data presentation and statistical analyses of the results presented in this thesis.

Chapters 3-8 comprise the main results section covering all the aims and objectives of the thesis. The specific materials and methods utilised in obtaining these results have been given in detail in the respective chapters.

Chapter 3 - Morphological characteristics of chondrocytes in human articular cartilage

- Non-degenerate (grade-0) and mildly-degenerate (grade-1) human femoral head articular cartilage
- Articular cartilage in various clinical conditions

Chapter 4 - Morphological characteristics of bovine chondrocytes cultured in 3D agarose gels

- Effect of varying gel strength
- Effect of increasing concentrations of FCS

Chapter 5 - Evaluation of matrix produced by chondrocytes cultured in strong or weak agarose gels

Chapter 6 - Morphological characteristics of chondrocytes in injured cartilage cultured under various conditions

- Effect of varying culture media

Chapter 7 - Evaluation of ECM produced by chondrocytes in response to injury cultured under various conditions

Chapter 8 - Effects of short-term and long-term exposure to varying medium osmolarity on chondrocyte morphology in injured cartilage cultured under various conditions

This thesis is concluded by **Chapter 9** where the merits and limitations of the work presented in this thesis have been discussed in general. The clinical and experimental relevance of the work and the potential benefits in the field of cartilage biology have been highlighted.

Finally, the appendix includes the list of published abstracts, oral and poster presentations relating to this work.

CHAPTER 2: GENERAL MATERIALS AND METHODS

2.1 Biochemicals

Biochemicals were obtained from Invitrogen Ltd. (Paisley, UK) or Sigma-Aldrich Co. Ltd. (Poole, UK) unless stated otherwise. Phosphate-buffered saline (PBS) was used to wash osteochondral samples and store them after fixation for microscopy. Formaldehyde solution (PFA; 4% v/v in saline; pH7.3) was used for fixation (Fisher Scientific, Leicestershire, UK). Other biochemicals used for cell isolation and culture were collagenase Type I, 255 units/mg and ultra-pure low melting point (LMP) agarose powder (Sigma-Aldrich Co. Ltd., Poole, UK).

2.1.1 Standard and varied culture media

The standard culture medium used was Dulbecco's Modified Eagle's Medium [standard-DMEM; cat # 41966; 343±2.6mOsm (N=3); 37°C; 5%CO_2; pH7.4] containing penicillin and streptomycin (50U/ml and 50µg/ml respectively) filtered through 0.2 µm pore size syringe filters. For experiments on bovine cartilage explants, standard-DMEM was modified with the addition of 10% foetal calf serum (FCS-DMEM; 339±2.6mOsm; cat # 16010-159, Invitrogen, Paisley, UK) or 10% bovine synovial fluid (SF-DMEM; 334±1.4mOsm). SF was taken aseptically from healthy bovine metacarpophalangeal joints using a sterile syringe at the beginning of dissection, centrifuged (Hettich Zentrifugen Universal 32R) at 21°C, 1500rpm for 10 min. The supernatant SF was pipetted carefully and the remaining cell pellet was discarded, kept in aliquots and stored at -20°C until required. Tissue culture medium used for the culture of isolated chondrocytes in agarose gels was standard-DMEM with NaCl added to increase osmolarity to 383.6±0.8mOsm (380mOsm; N=3); within the range of osmolarity of chondrocytes *in situ* (Hopewell and Urban, 2003),

10% FCS and 50µg/ml ascorbic acid. The osmolarities of culture media were measured with freezing point osmometer (Advanced Micro Osmometer, Model 3300, Vitech Scientific Ltd, West Sussex) after adding antibiotics/FCS/SF/NaCl to the culture media.

2.1.1.1 *Varying medium osmolarity*

Medium osmolarity was measured using a freezing point osmometer. Three measurements were taken and mean osmolarity of these was calculated. For experiments on the response of injured cartilage to osmolarity, medium osmolarity was increased by adding sucrose to the solutions. Sucrose was used as it does not get metabolised by chondrocytes (Fell and Dingle, 1969). The osmolarity of the prepared solutions was varied between 300 to 600 mOsm. In the osmolarity experiments serum-free and serum-rich culture media with varied osmolarities were used as (a) standard-DMEM; 343±2.6 mOsm (DMEM-343) (b) FCS-DMEM; 339±2.6 mOsm (FCS-339) (c) standard-DMEM; 609±1.4 mOsm (DMEM-609) and (d) FCS-DMEM; 606±0.8 mOsm (FCS-606) abbreviated as standard-DMEM, standard-FCS, hyperosmolar-DMEM and hyperosmolar-FCS respectively.

2.1.2 Fluorescent probes

CMFDA (chloromethylfluorescein diacetate) is highly membrane permeable and once inside cells, esterases convert it into 5-chloromethylfluorescein (an impermeable fluorescent compound) which then reacts with thiols of proteins and peptides and thus forms fixable conjugates which uniformly label the cytoplasm of living cells green (De Crombrugghe et al., 2000, Stoddart et al., 2006). Propidium iodide (PI), being impermeable to the intact membrane, penetrates dead cells only

and binds to their DNA emitting light at the red end of the spectrum following laser excitation (Chen et al., 2003). CMFDA labels living cells green and PI labels nuclei of dead cells red and it was reported in a recent study that the dead PI-labelled chondrocytes are incapable of green labelling and cannot recover viability even after 16 days of culture (Smith et al., 2013). Therefore living cells are labelled green with CMFDA and dead cell nuclei labelled red with PI in the present work.

DRAQ5 *1, 5-bis 2-di-methylamino-ethyl-amino-4, 8-dihydroxyanthracene-9, 10-dione* **(**Biostatus, UK), far-red DNA dye was used to fluorescently label the nuclei of living chondrocytes. PI was used to label nuclei of dead cells whereas DRAQ5 was used to label nuclei of live cells in gel culture experiments. The main purpose of using DRAQ5 was to enable counting of cells in a cluster by counting number of nuclei. For the detailed analysis of clusters formed it was not possible to count number of cells involved in forming a cluster instead, nuclei labelled with DRAQ5 were counted. CMFDA was prepared in dimethyl sulphoxide (DMSO) as a 1mM stock solution obtained from the manufacturer (Invitrogen, Paisley, UK) and PI was prepared as an aqueous 1mM stock solution. DRAQ5 (DNA probe) was obtained from manufacturer as 5mM stock solution and was diluted 1:50 in distilled water (D/W). DRAQ5 and PI both can bind to DNA but they differ in their ability to label nuclei such that PI is membrane impermeable and can bind to nuclei of dead cells only whereas DRAQ5 is membrane permeable and can rapidly stain nuclei of both live and fixed cells. The two dyes PI and DRAQ5 were therefore used for determining cell death and counting of chondrocytes in the clusters respectively.

A series of pilot experiments were performed in order to find out suitable concentrations and incubation time for appropriate labelling of isolated

chondrocytes, bovine chondrocytes *in situ* and human chondrocytes *in situ*. The concentration and incubation time found appropriate for chondrocyte labelling in various experimental conditions have been detailed in the specific Materials and Methods sections of respective chapters.

2.2 Data presentation and statistical analyses of results

Data are presented as mean±SEM with *N* representing the number of different animals or patients, *n* the total number of explants and *n′* the total number of cells analysed for each experimental condition. The values for *N, n & n′* are detailed in the results section of each chapter. Statistical tests applied and graphs generated were by using Graph Pad Prism 6 (GraphPad software, Inc., CA, USA). Unpaired, two-tailed, Student's t-tests were used to compare means within groups and indicated by the symbol *. One way analysis of variance (one-way ANOVA) followed by post-hoc Tukey's multiple comparison test was used to compare data between groups and indicated by the symbol #. In the human cartilage experiments, + showed a significant difference between grade-0 and grade-1 cartilage explants according to Student's t-test. In the experiments performed on the bovine injured cartilage explants followed by culture in various conditions data obtained at and distant from the injury was compared using Student's t-test and the significant difference indicated by the symbol ^. In the results obtained from the experiments performed to see the response of injured cartilage to osmolarity, significant difference between the two osmolarities was indicated by the symbol £. A significant difference was accepted when $P<0.05$. The single, double and triple symbols showed the level of significance for $P<0.05$, 0.01 and 0.001 respectively.

CHAPTER 3: RESULTS

MORPHOLOGICAL CHARACTERISTICS OF CHONDROCYTES IN NON-DEGENERATE (GRADE-0) AND MILDLY-DEGENERATE (GRADE-1) HUMAN ARTICULAR CARTILAGE AND IN VARIOUS CLINICAL CONDITIONS

3.1 CHAPTER SUMMARY

The main hypothesis of the work presented in this chapter is that in grade-0 human femoral head AC, chondrocytes show mild perturbation in morphology which exacerbates in grade-1 cartilage. The rationale of this chapter was to study chondrocyte viability and morphological characteristics within grade-0 and grade-1 human femoral head and cartilage obtained from other joints in various clinical conditions. Using CLSM, *in situ* chondrocyte volume was quantified in various zones of grade-0 human femoral articular cartilage. Additionally, quantitative data regarding morphology of chondrocytes (clusters/cytoplasmic processes) were obtained and compared in grade-0 and grade-1 articular cartilage. In grade-0 cartilage there was marked heterogeneity in chondrocyte volume across all the zones. The average volume of chondrocytes in the mid zone (MZ) was significantly greater than volume of superficial zone (SZ) and deep zone (DZ) chondrocytes ($P<0.001$ and $P<0.01$ respectively). In grade-1 cartilage, topographical arrangement of chondrocytes was disorganised, there were more PI-labelled chondrocytes in the SZ and MZ and marked areas of hypo-cellularity were observed. A significantly higher percentage of chondrocytes formed large sized clusters in the SZ of grade-1 (43±16%) as compared to grade-0 cartilage (11±3%; $P=0.008$). A significantly higher percentage of chondrocytes had cytoplasmic processes throughout the whole thickness of grade-1 cartilage (35±5%) as compared to grade-0 cartilage (17±2%; $P=0.0007$). A detailed zone-wise analysis of these cytoplasmic processes revealed that in grade-0 cartilage, fine processes with an average length of ~5µm were present within cells of SZ/MZ and in the DZ the length of processes was only ~3µm. In comparison to this in the grade-1 cartilage, the average length of processes was

15.6±2 μm in the SZ, 6±0.5 μm in the MZ and 4±0.5 μm in the DZ. Regarding the presence of cytoplasmic processes there existed a general trend in grade-1 but no trend observed in grade-0. In grade-1 cartilage, cytoplasmic processes were seen mostly in the SZ, less in the MZ and least in the DZ. Similarly, the length of these processes and the number of processes per cell also decreased with cartilage depth from SZ to DZ. Moreover, in the cartilage samples obtained from joints with various pathological conditions such as osteochondritis dissecans (OCD) and avascular necrosis (AVN) of the joint there were numerous PI-labelled chondrocytes and the chondrocytes exhibited abnormal morphological characteristics in terms of cluster formation and the presence of cytoplasmic processes. These data suggested that in the grade-0 human femoral articular cartilage topographically chondrocytes were arranged in a regular manner, 17±2% chondrocytes had fewer fine cytoplasmic processes and only few cells were present in the form of clusters. However, in grade-1 cartilage the arrangement of chondrocytes was disturbed, clustering was more evident and 35±5% abnormal chondrocytes with numerous long cytoplasmic processes were present. These morphological changes (clusters/processes) were greater in the SZ as compared to the MZ and DZ. These results strongly support the hypothesis that mild morphological changes present (cytoplasmic processes) in grade-0 cartilage are exacerbated in grade-1 cartilage.

3.2 INTRODUCTION

OA is a disease of the whole joint which involves all the structures of the joint such as cartilage, membrane, ligament, capsule, muscle and the bone (Wieland et al., 2005). The main pathological features of the disease are cartilage degeneration, bone

remodelling and synovitis leading to joint failure ultimately (Aaron and Racine, 2013). In OA there is progressive cartilage erosion as a consequence of imbalance between the anabolic and catabolic activities of chondrocytes (Goldring and Goldring, 2004). The changes to chondrocyte matrix metabolism are accompanied by collagen disruption and degradation of PGs (Malemud, 1991, Stoop et al., 2001). With the progression of the disease the matrix is weakened/loosened (Aigner and McKenna, 2002), increased permeability of the matrix, increased hydration and swelling of cartilage because the fluid fraction of the cartilage increases (Maroudas, 1976, Stockwell, 1991, Wang et al., 2013a). This degradation process is manifested in the SZ of cartilage and becomes visible in the form of fissures and fibrillations of cartilage (Hollander et al., 1995, Kleemann et al., 2005). OA is regarded as the disease of the whole joint and the reaction pattern of chondrocytes to the destructive changes in the matrix is an important component in the pathophysiology of OA. However, the immediate response/reaction of chondrocytes is dependent upon the alterations in the pericellular matrix (PCM) (Vincent, 2013). Although the exact function of PCM is not known but the evidence suggests that PCM plays a significant role in controlling the immediate biochemical and mechanical microenvironment of chondrocytes (Guilak et al., 2006). The growth factors and enzymes released by chondrocytes are stored and modified in PCM (Macri et al., 2007, Echtermeyer et al., 2009). In OA, marked changes occur in the PCM and it has been reported that in OA there is over production and enhanced destruction of type VI collagen (McDevitt et al., 1988, Ronzière et al., 1990, Lee et al., 2000, Murray et al., 2010). In a recent study on human OA cartilage by using atomic force microscopy, PCM enlargement and decreased mechanical function was observed as

compared to normal cartilage (Wilusz et al., 2013). The consequences of disruption in the PCM of chondrocytes in the disease pattern are largely unknown; however the proposed mechanism is reduced cell-matrix interactions via integrin receptors (Marcelino and McDevitt, 1995, Loeser, 1997, Knudson and Loeser, 2002). In another study the importance of immediate environment of chondrocytes has been highlighted by reporting that the disturbance in PCM could influence their synthetic and proliferative activities (Alexopoulos et al., 2009). Alteration in the PCM has been linked to the metabolic activity of chondrocytes but its relationship with chondrocyte morphology attained less attention. However, in a study (Murray et al., 2010) morphologically abnormal chondrocytes in OA have been related to disturbance in pericellular Type VI collagen.

There can be several responses of chondrocytes to OA and discussed in detail. Chondrocytes either undergo apoptotic/necrotic cell death (Kim et al., 2000, Thomas et al., 2007) or proliferate and form clusters (Rothwell and Bentley, 1973, Mitchell et al., 1992). Chondrocytes increase or decrease their metabolic activities (Murray et al., 2010, Goldring et al., 2011) and their phenotype is altered based upon gene expression (Lapadula et al., 1998). A typical histological finding of osteoarthritic cartilage is presence of empty lacunae and clusters of chondrocytes (Pauli et al., 2011). Several studies have reported that in OA the proliferative activity of chondrocytes increases resulting in the formation of clusters (Lotz et al., 2010). It has also been suggested that these clusters are most numerous in the SZ of degenerating cartilage close to the fissures (Schumacher et al., 2002).

Another classical histological finding of osteoarthritic cartilage is areas of hypo-cellularity indicating increased cell death as suggested by some authors (Blanco et al., 1998, Kim et al., 2000). Cell death in OA has been attributed to necrosis (Wei et al., 2006), apoptosis (Lee et al., 2004) or a variant of apoptosis termed 'chondroptosis' (see foot note[1]) (Roach et al., 2004). Various studies were conducted to investigate the causes of cell death in degenerating cartilage and have reported mechanical injuries (Tew et al., 2000), age (Grogan and D'Lima, 2010), reactive oxygen species (Henrotin et al., 2003) and cytokines (Goldring and Goldring, 2004) to be the main contributing factors in inducing cell death in OA.

The evidence of cell death in human OA cartilage has been reported in various studies but mostly the cartilage samples were obtained from patients at the time of joint replacement surgeries suggesting that they were from patients with OA at very advanced stage. This may suggest that one of the contributing factors for the presence of dead chondrocytes in these samples was end–stage disease. However, in a study carried out on early OA human cartilage tissue relatively less cell death was present (Aigner et al., 2001). It has been suggested that chondrocytes die in OA but the extent of cell death and disease stage when it occurs is controversial and has been highlighted in a review article (Carlo and Loeser, 2008). Thus there can be several factors responsible for these controversial results on cell death in OA such as the method of assessment of cell death, age of the patient and disease stage. Chondrocyte death is crucial for proper functioning of the cartilage as it leaves a greater burden on

---

Chondroptosis is a variant of apoptotic cell death in chondrocytes undergoing apoptosis in a non-classical manner with increase in endoplasmic reticulum (ER) and golgi apparatus. The ER membranes segment and provide compartments for digestion of cytoplasm and organelles leading to self-destruction of chondrocyte.

the remaining chondrocytes to maintain tissue integrity thus leading to cartilage failure (Sharif et al., 2004).

Chondrocytes have the ability to synthesize and degrade ECM with their synthetic (anabolic) and resorptive (catabolic) activities. In a healthy cartilage there exists a balance between these two metabolic activities and steady state equilibrium is maintained by chondrocytes (Wang et al., 2003). During degeneration, this equilibrium is disturbed and chondrocytes become hyperactive initially attempting to repair ("repair" see footnote[1]) cartilage (Aigner et al., 1992). However, eventually the catabolic activities override the anabolic activities and this imbalance in the metabolic processes leads to cartilage degeneration and ultimately loss of cartilage structure and function (Aigner and Dudhia, 1997).

There can be various factors involved in the destruction of cartilage matrix and are ascribed to age-related changes, excessive joint mechanical loading and the dysregulation of cytokines. These factors are related to changes in matrix metabolism causing more catabolism than anabolism and thus predisposition to OA. Excessive joint loading has been observed to be a causative factor in development of OA (Buckwalter et al., 2013). Cytokines are molecules which either enter the cell or act on the surface, can be categorised into inflammatory and anti-inflammatory cytokines (Goldring and Goldring, 2004). The interplay between these catabolic and anti-catabolic cytokines is one of the factors responsible for cartilage remodelling

---

Cartilage repair implies to the regeneration of damaged cartilage by synthesis of mechanically functional matrix. However, repair here suggests the response of chondrocytes towards damage in an effort to heal the defect and does not imply to the restoration of the normal mechanical properties of cartilage.

and the imbalance leads to cartilage destruction (Mueller and Tuan, 2011). There are many members of inflammatory cytokine group but the important ones involved in OA disease process are IL-1ß, TNFα, IL-6, IL-15, IL-17 and IL-18 (Westacott and Sharif, 1996, Martel-Pelletier et al., 1999, Goldring, 2000a, Wojdasiewicz et al., 2014).

The second group including anti-inflammatory cytokines consists of IL-4, IL-10 and IL-13 with the antagonist effect to the inflammatory cytokines. The inflammatory cytokines and most importantly IL-1ß and TNFα are the key players responsible for the destructive processes within cartilage leading to an imbalance in tissue homeostasis (Martel-Pelletier et al., 1999, Wojdasiewicz et al., 2014). The main catabolic effects produced by these inflammatory cytokines are induction of apoptosis, decreased synthesis of major components of ECM, enhanced release of proteolytic enzymes and increased synthesis of other inflammatory cytokines by chondrocytes (Fernandes et al., 2002). In contrast, anti-inflammatory cytokines act by antagonising these catabolic effects of inflammatory cytokines (Wojdasiewicz et al., 2014). Therefore, in OA an excess of inflammatory cytokines is one of the many factors responsible for cartilage degeneration (Melchiorri et al., 1998). Although OA is generally considered a non-inflammatory disease but the role of synovial inflammation cannot be denied in its pathogenesis and has been reviewed in detail (de Lange-Brokaar et al., 2012). In healthy cartilage several growth factors such as transforming growth factor ß (TGFß) play a critical role in regulating the metabolic activities of chondrocytes apart from cytokines and assist chondrocytes in maintaining normal homeostasis. Low levels of TGFß have been suggested to be involved in the development of OA (Shen et al., 2013).

Phenotypic changes (de-differentiation) in chondrocytes are another prominent feature of OA (Tesche and Miosge, 2005). The chondrocyte phenotype ("phenotype" see foot note[1]) is regulated through the cytoskeletal elements via morphogens and cytokines (Vinall et al., 2002). A specific chondrocytic phenotype with rounded morphology and the expression of type II collagen and aggrecan is required to maintain the normal architecture and functioning of articular cartilage (Eyre, 2002, Dudhia, 2005). In OA, chondrocytes dedifferentiate phenotypically and do not express cartilage specific genes thereby, leading to the anabolic failure of cartilage (Tchetina et al., 2005, Yagi et al., 2005). Phenotypic changes to chondrocytes were observed in human OA cartilage in several studies (Stockwell, 1978, Kouri et al., 1996a, Kouri et al., 1996b, Kouri et al., 1998, Lee and Loeser, 1998, Goldring, 2002, Kouri and Abbud-Lozoya, 2002, Yagi et al., 2005, Kouri and Lavalle, 2006). These phenotypic changes included several shape changes such as presence of filopodia, irregular cells, fibroblast-like shapes of chondrocytes and altered metabolism in OA. In these studies although heterogeneity to chondrocyte morphology was reported but fine details were not comprehensively studied. However, abnormal chondrocyte morphology with the presence of cytoplasmic processes was first reported in a study on degenerate and non-degenerate cartilage which stated that in human tibia plateaus ~40% chondrocytes had cytoplasmic processes of variable lengths emanating from their cell bodies (Bush and Hall, 2003). The presence of these cytoplasmic processes even in the non-degenerate cartilage raised the possibility that cytoplasmic processes might be an early event in degeneration of cartilage.

Phenotype implies to appearance of cell shapes and their metabolism

A sub-population of abnormal cells with long cytoplasmic processes was observed in a study done on human OA femoral heads with pannus (Holloway et al., 2004). Morphology is an important component of phenotype it has been reported that morphologically abnormal chondrocytes (with cytoplasmic processes) caused disruption to collagen type VI and increased levels of IL-1ß (Murray et al., 2010). In summary, various studies have been conducted to investigate the alterations in mechanical and biochemical properties of chondrocytes during cartilage degeneration but the morphology of chondrocytes does not appear to be comprehensively probed.

This study utilised CLSM to determine the morphological characteristics of chondrocytes in non-degenerate and mildly-degenerate human femoral head articular cartilage. This work has extended the previous work by Bush and co-workers in several aspects. Firstly, the samples under investigation in this work are obtained from a different joint i.e. hip joint (human femoral head) as compared to the earlier study performed on tibial plateau cartilage. As the biomechanics of hip and knee joints are different (Kirkwood et al., 2007) it is therefore possible that the morphology of chondrocytes will be different in the two joints. Comparison of the morphologies of chondrocytes in the hip and knee joint AC will provide further information on whether cytoplasmic processes are a unique property of knee cartilage alone. Secondly, the samples studied here have been obtained from healthy cartilage with no known degenerative disease of the cartilage as compared to the earlier study where cartilage originated from patients undergoing knee surgery due to OA. The importance of having samples from healthy cartilage in this study will enhance our knowledge regarding the presence of these cytoplasmic processes and

whether they are present on healthy cartilage also or they are only the characteristic feature of a joint failing due to OA.

CLSM rendered it possible to study the fine 3D morphological details of *in situ* living chondrocytes in an unperturbed cartilage environment. In this study the grade-0 and grade-1 cartilage samples were obtained from the same human femoral heads thereby, providing accurate control samples for comparison. There were eight human femoral heads obtained for this work, five of them had the whole sample with grade-0 cartilage whereas three samples had some areas of grade-1 also. Moreover, in this study morphological details of chondrocytes in normal and in early stages of degeneration were studied in various zones of human femoral head articular cartilage.

3.3 HYPOTHESIS

In grade-0 human femoral head AC, chondrocytes show morphological changes (cytoplasmic processes) which are exacerbated in grade-1 cartilage.

3.4 MATERIALS AND METHODS

3.4.1 Human femoral articular cartilage explants

Human articular cartilage explants from femoral heads of eight patients of which six were females and two males with an age of 79±3.5 yrs. (Mean±S.E.M; age range 65-89 yrs.) were prepared as rectangular blocks and the technique for preparing these explants is outlined below.

3.4.2 Source of human tissue

During hip replacement surgeries, the femoral heads are normally resected out as a whole and are discarded later after the procedure. These femoral heads were obtained by courtesy of Dr. Anish Amin (Consultant orthopaedic surgeon) from the Edinburgh Royal Infirmary (ERI) with the ethical approval of Local Research Ethics Committee. Additionally, an informed consent for the use of material for experimental purposes was taken by Dr. Anish Amin from 8 patients undergoing hip replacement surgery due to fracture of the hip joint. The femoral heads were immediately transferred to sterile plastic jars containing standard-DMEM (section 2.1.1) and were transported safely to the laboratory. The samples were dissected and osteochondral explants were obtained and prepared for CLSM within 6-8 hours following surgery. Additionally, after obtaining informed patient consent and ethical approval from the ethical committee five samples of patients with various clinical conditions were also obtained and the particulars of patients with clinical conditions were summarised in Table 3.1.

ID.	Age (yrs.)	Sex	Sample origin	Sample composition	Diagnosis	Duration of symptoms
1.	18	Male	Knee joint	Osteochondral fragment	Osteochondritis Dissecans (OCD)	months
2.	30	Male	Ankle joint	Osteochondral fragment of talus	OCD	months
3.	26	Female	Ankle joint	Osteochondral fragment of talus	OCD	months
4.	36	Female	Hip joint	Femoral head	Avascular necrosis (AVN)	months
5.	55	Male	Subtalar joint	Osteochondral fragment of calcaneus	fracture	days

Table 3.1: Particulars of human cartilage samples.
Details of patients and human cartilage explants obtained from various joints in different clinical conditions.

3.4.3 Removal of osteochondral explants

Most of the cartilage in the 8 human femoral heads obtained from patients undergoing hip replacement was normal and macroscopically graded by Dr. Anish Amin as grade-0 cartilage. However, in 3 of the samples it was possible to also obtain some cartilage that showed mild degeneration (grade-1). The grade-0 and grade-1 cartilage areas were both present on the same human femoral head. Macroscopically grade-1 cartilage areas were roughened, discoloured and showed splitting and pitting of cartilage (Fig. 3.4b). The samples were initially graded by Dr. Anish and then re-confirmed by the author. The grading methodology applied to differentiate between grade-0 and grade-1 cartilage samples comprised of earlier macroscopic examination and later on microscopic confirmation as summarised in Table 3.2. based on already described grading system (Pritzker et al., 2006). Osteochondral explants comprising full thickness of the cartilage with some underlying subchondral bone were harvested with scalpel # 24 from these graded

areas. The explants were then trimmed measuring approximately 4 mm x 4 mm and stored in standard culture medium (Fig. 3.1).

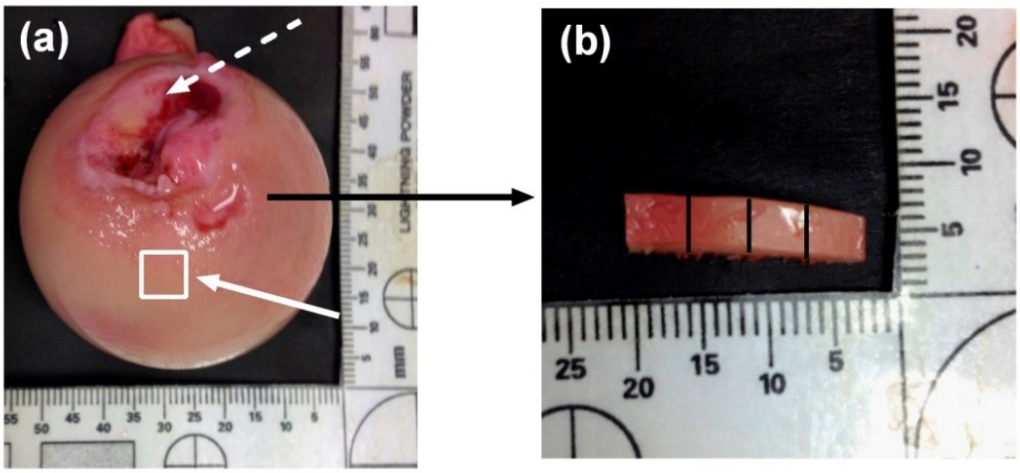

Figure 3.1: Preparation of human femoral osteochondral explants.
(a) Human femoral head indicating area (white outlined box) where explants were harvested, (b) rectangular osteochondral strip dissected into osteochondral explants by scalpel with measurements 4 mm x 4 mm (grade-0 cartilage). The broken arrow indicates the fovea. Photographs (a) and (b) kindly provided by Mr. Scott I Paterson, Centre for Integrative Physiology, University of Edinburgh.

3.4.4 Staining, fixation and preparation of human osteochondral explants for CLSM

The human femoral osteochondral explants were incubated with CMFDA and PI with final concentrations of 12.5 and 10µM respectively for 2 hours in dark on the rocking table to label the living and dead cells respectively. The explants were then washed in PBS to remove excess of dye and fixed in 4% PFA overnight at 4°C. The

samples were washed in PBS twice and mounted in the culture wells for microscopy and stored as described for the bovine explants until used (section 6.4.1.2).

3.4.5 CLSM of human cartilage explants

A Zeiss Axioskop LSM 510 upright CLSM was used with an Ar laser with excitation wavelength (EX_λ) of 488nm and HeNe laser with EX_λ 543 to excite the fluorophores CMFDA and PI respectively. The precise details of confocal settings utilised to image human femoral osteochondral explants were similar to those for the bovine cartilage explants in both axial and coronal planes and given in detail (section 6.4.1.3). The images were obtained by utilising both low (Fig. 3.2) and high power (Fig. 3.3) magnification objectives in both the planes. The CLSM axial and coronal reconstructions were created using the Volocity^{TM} software as described for the bovine cartilage (section 6.4.1.3).

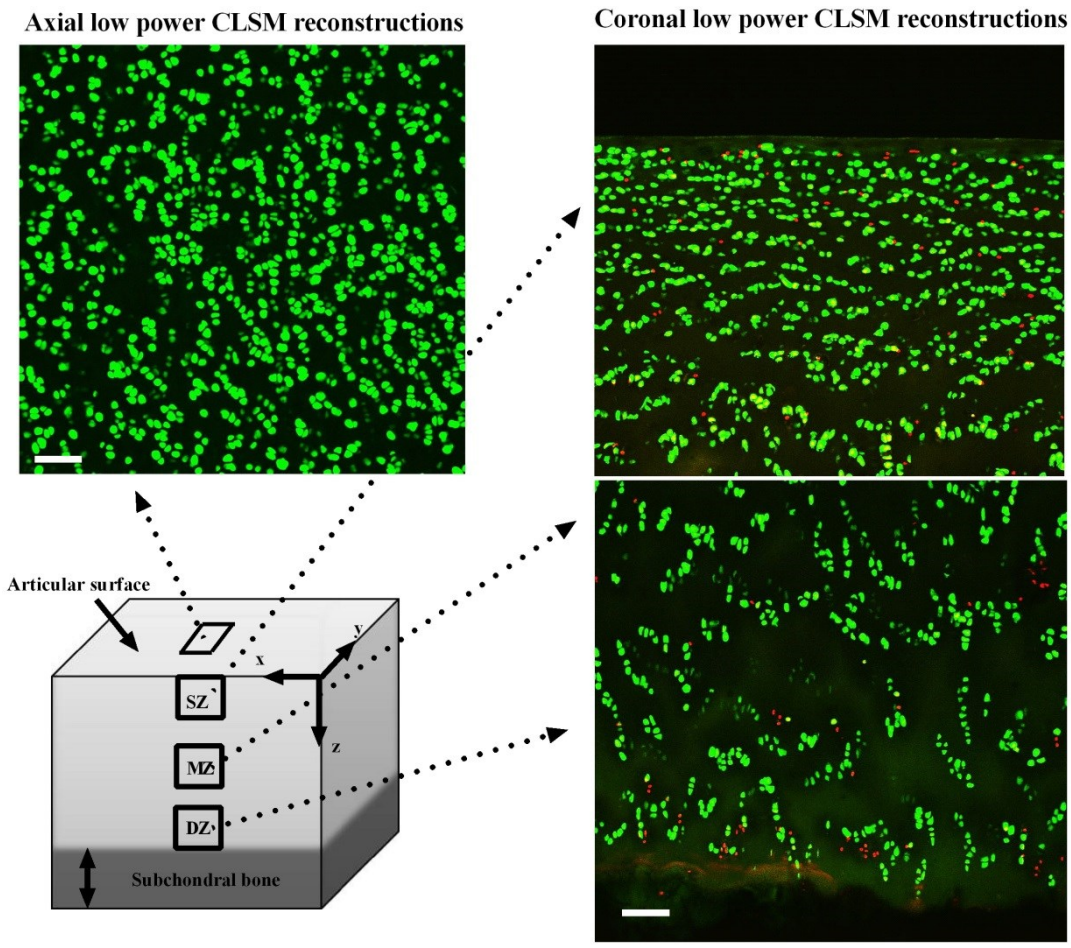

Figure 3.2: Axial and coronal CLSM for human femoral articular cartilage explants imaged with low power (x10) objective.

The x, y and z axes labelled on the diagram of the explant. (Left panel) Axial optical sections of the articular cartilage imaged top-down and the series of optical sections reconstructed in the axial plane, (Right panel) Coronal optical sections of cartilage imaged the full thickness of the cartilage and the series of optical sections reconstructed in the coronal plane. Chondrocytes labelled with CMFDA and PI for living and dead cells respectively. Scale bar = 100µm for both axial and coronal reconstructed images.

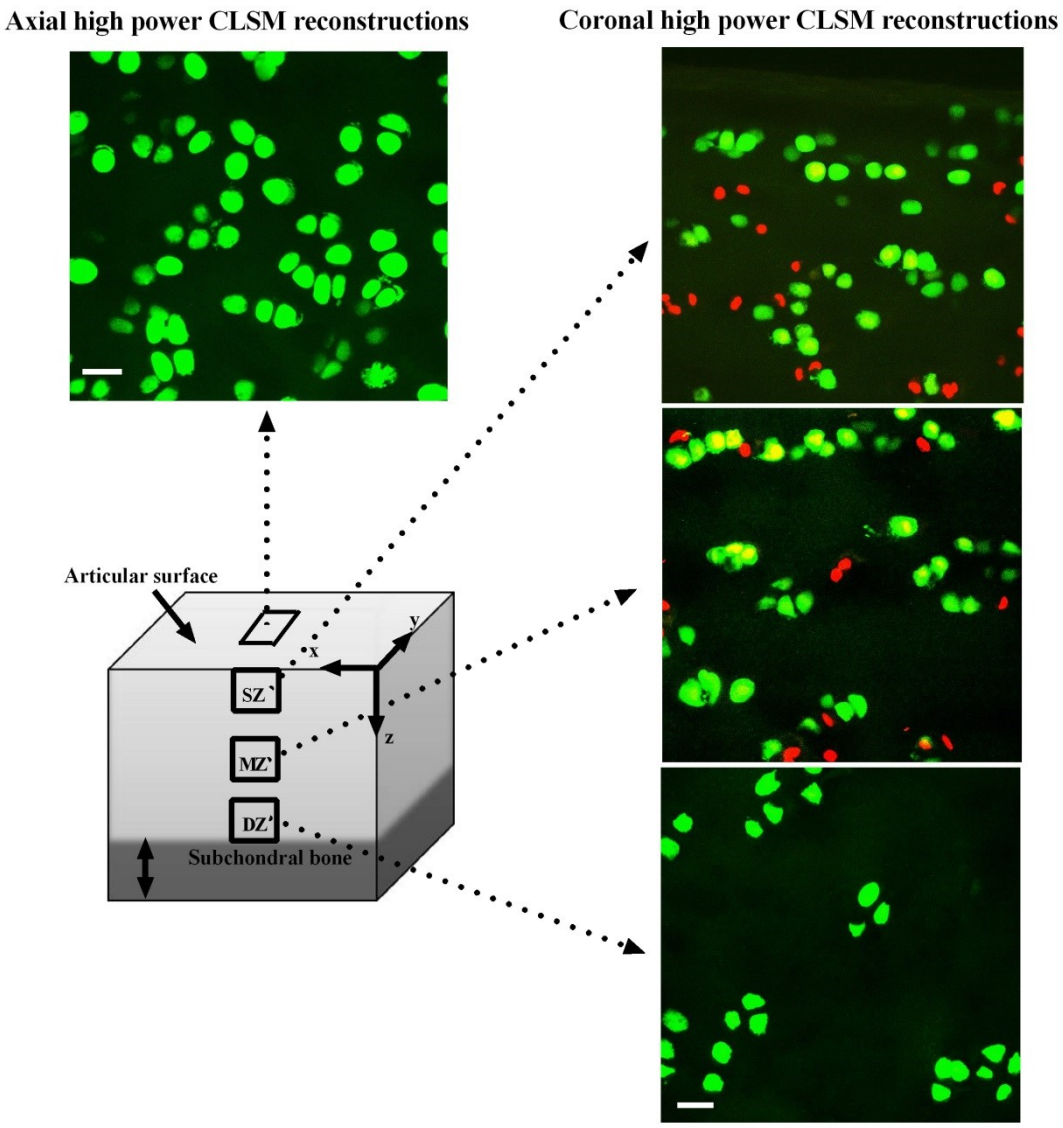

Figure 3.3: Axial and coronal CLSM for human femoral articular cartilage explants imaged with high power (x40DW) objective.

The x, y and z axes labelled on the diagram of the explant. (Left panel) Axial optical sections of the articular cartilage imaged top-down and the series of optical sections reconstructed in the axial plane, (Right panel) Coronal optical sections of grade-0 cartilage imaged the full thickness of the cartilage and the series of optical sections reconstructed in the coronal plane. The yellow-coloured cells are possibly dying cells where PI could penetrate because the membrane is compromised but the cells could take up some CMFDA also as all the cytoplasm has not disintegrated yet. Scale bar = 25µm for both axial and coronal reconstructed images.

3.4.6 Volume and morphological analysis of *in situ* human chondrocytes

The volume and morphology of chondrocytes was determined in the three zones (zones defined in section 3.5.1.1) of cartilage using the high power (x40 DW) magnification images taken in the coronal plane. The volume measurement technique on Volocity™ software was identical to the chondrocytes cultured in agarose gels and the same correction factor was also applied to obtain corrected measurements (sections 4.4.1.7.1. & 4.4.1.7.2).

Various characteristics of chondrocyte clusters present in the human explants were determined by using the same methodology as described in the cultured chondrocytes in gels (section 4.4.1.7.1). The morphology of chondrocytes was categorised by modifying the classification method used for bovine chondrocytes to take account of wide range of shapes observed in human chondrocytes. The length of cytoplasmic processes was measured in 3D following the protocol mentioned in the methods section of cultured chondrocytes (4.4.1.7.3). However, the cells with processes were further categorised into 4 groups [length (L) 1-4; where $L1<5\mu m$, $5<L2\leq10\mu m$, $10<L3\leq15\mu m$ and $L4>15\mu m$) with respect to the length of processes. This categorisation was important as it allowed a detailed analysis of data obtained on the length of processes. The range of lengths of processes observed in human cartilage was categorised in a different way as compared to length of processes observed within chondrocytes cultured in agarose gels because of the differences in minimum and maximum lengths observed. The percentages of cells having cytoplasmic processes of specific length categories were determined with the formula 100 ×

(number of cells with specific length category/total number of cells with processes) %.

3.5 RESULTS

3.5.1 Morphological characteristics of chondrocytes within grade-0 and grade-1 human femoral articular cartilage

The axial and coronal CLSM images of fluorescently-labelled chondrocytes were visualised to compare the morphology of chondrocytes in grade-0 and grade-1 human femoral head cartilage. A detailed analysis of quantitative data regarding chondrocyte morphology in the various zones of cartilage was performed on the coronal images.

3.5.1.1 *Cartilage grading and demarcation of various zones*

As a first step, cartilage of the whole joint surface was graded macroscopically (Pritzker et al., 2006) and then explants from selected graded areas were obtained for grade-0 and grade-1 cartilage. The cartilage grade was assessed by visualisation (Table 3.2) where most of the cartilage was non-degenerate however it was also possible to obtain some mildly degenerate cartilage explants from the same joint which permitted a comparison. Photographs of femoral heads (Fig. 3.4 a & b) and CLSM reconstructed images of the coronal views of cartilage explants (Fig. 3.5 a & b) represent examples of grade-0 and grade-1 cartilage regarding their macroscopic and microscopic appearances respectively. The detailed results were presented in the later sections.

The second step was to define various zones of cartilage depending upon its cellular composition. CLSM low power images were used to delineate the zones of cartilage depending upon the criteria already described which defined SZ as first 100µm of the tissue (10% of cartilage thickness), MZ from 200µm to 400µm from surface (60% of tissue) and DZ as 300µm inward from tide mark (30% of tissue) (Humbree et al., 2007). Average overall thickness of grade-0 cartilage was 1250±22µm (mean±SEM for n=5), the SZ was defined as the first 125µm which constituted approximately the top 10% of the articular cartilage containing cells mostly flattened in shape. The MZ was outlined as between 125-875µm from the surface of the cartilage which consisted of approximately 60% of the cartilage with cells mostly spheroidal in appearance. Finally the DZ was defined as 375µm upwards from the tide mark and this comprised of approximately 30% of the cartilage thickness (Fig. 3.5). Thickness of the cartilage varied between the samples therefore the zones were defined by measuring in micro-meters the thickness of each zone.

The low power (x10) coronal images showed relatively less PI-labelled chondrocytes in the grade-0 as compared to grade-1 cartilage. In addition, chondrocyte clustering was obvious in the grade-1 as compared to grade-0 (Fig. 3.5). The quantitative data regarding detailed analysis of morphological characteristics of chondrocytes in grade-0 and grade-1 human femoral cartilage were presented in later sections of this chapter.

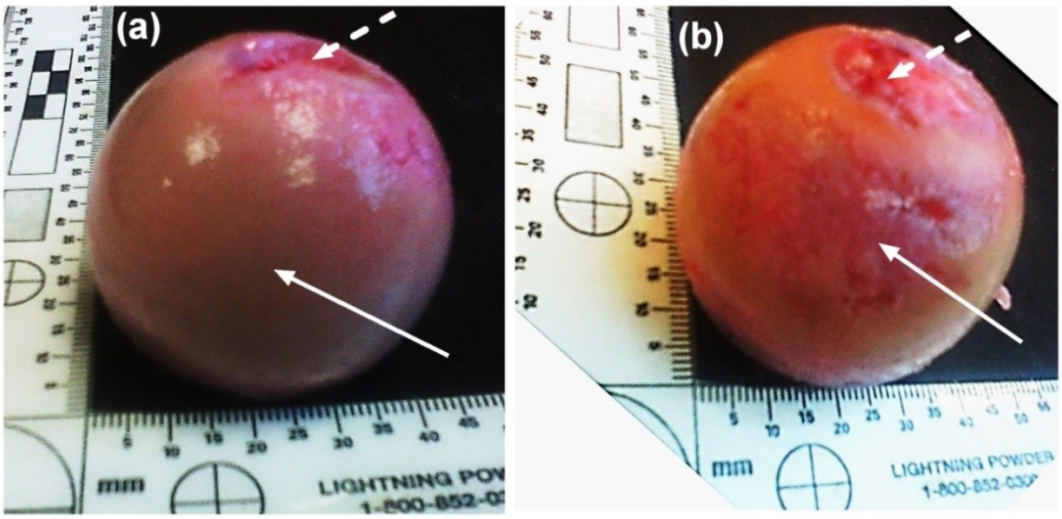

Figure 3.4: The appearance of grade-0 and grade-1 human femoral heads.
In these representative photographs, examples of (a) Grade-0 and (b) Grade-1 human femoral articular cartilage are shown. The gross appearance of cartilage (identified by solid arrows) was used for grading the cartilage samples. The broken arrows indicate the fovea.

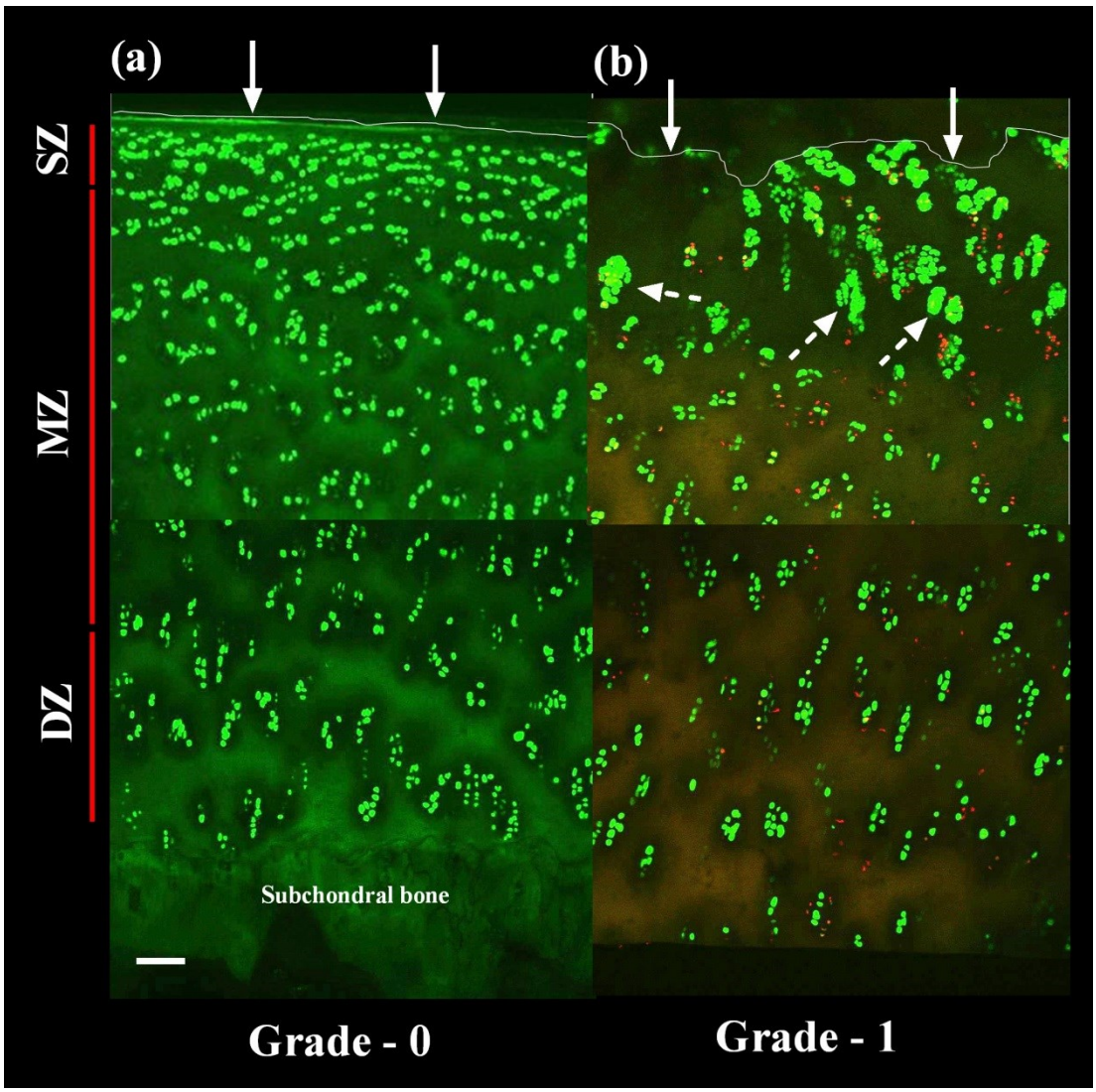

Figure 3.5: An overview of chondrocyte arrangement in the grade-0 and grade-1 human femoral head articular cartilage.

Representative CLSM coronal low power (x10) reconstructed images of CMFDA and PI-labelled chondrocytes showing (a) Grade-0 and (b) Grade-1 cartilage. Grade-0 cartilage showed smooth regular surface with minimal morphological changes to chondrocytes, whereas grade-1 displayed obvious surface roughness and erosions with clustering. Solid arrows indicate smooth and rough surfaces of grade-0 and grade-1 cartilage respectively and broken arrows indicate examples of chondrocyte clusters present in grade-1 cartilage. Scale bar for all panels = 100µm.

3.5.1.2 *Morphology of chondrocytes in grade-0 and grade-1 human femoral articular cartilage (Axial view)*

Although axial and coronal both CLSM images were obtained for grade-0 and grade-1 human cartilage the quantitative analysis of chondrocytes was performed on the coronal images in order to determine chondrocyte morphology in all the zones of cartilage. The axial CLSM images of low and high power magnification were visualised and an initial overview of the cartilage was given in this section. Marked changes to chondrocyte morphology and large areas of hypo-cellularity were clearly evident in the grade-1 (axial view) as compared to grade-0 cartilage explants even at low magnification. There were hardly any PI-labelled cells observed in the grade-0 and grade-1 cartilage samples (Fig. 3.6).

When chondrocytes were viewed with a high power magnification objective (x40DW) marked heterogeneity to chondrocyte morphology (processes/clusters) was observed in the grade-1 cartilage. In grade-0 cartilage, chondrocytes were mostly relatively normal (spheroidal/elliptical) in shape and only few cells had fine cytoplasmic processes (Fig. 3.7a). In grade-0 cartilage occasionally abnormal cells with fine cytoplasmic processes were present but there were far more abnormal cells with long cytoplasmic processes in grade-1 cartilage (Fig. 3.7b). Moreover, chondrocyte density appeared to be less in the degenerate as compared to non-degenerate cartilage, but it appeared to be compensated for by clustering.

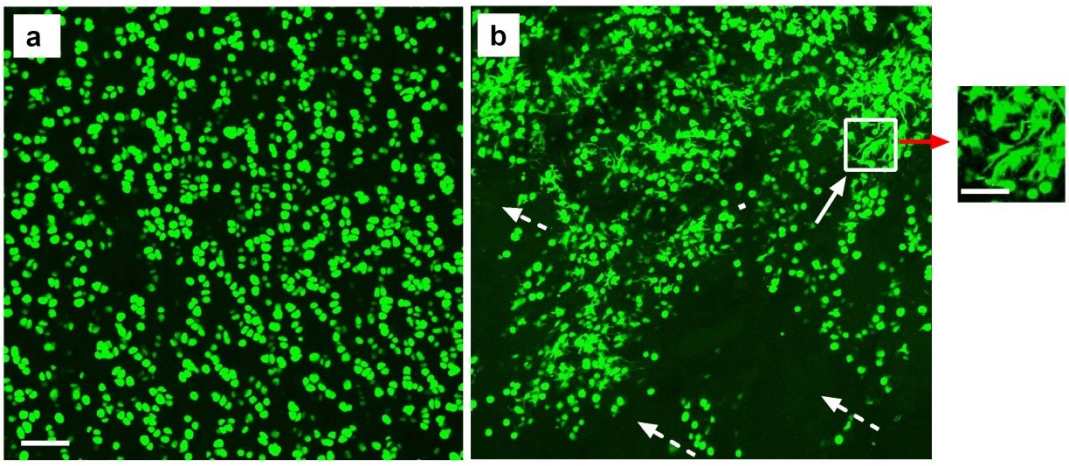

Figure 3.6: Axial CLSM reconstructed images of chondrocytes within human femoral head articular cartilage.

CLSM reconstructions of low magnification (x10) images of CMFDA and PI-labelled chondrocytes (live and dead cells respectively) in human (a) Grade-0 and (b) Grade-1 articular cartilage explants. In these representative examples [*N*=8 & *N*=5] for grade-0 and grade-1 femoral heads respectively, chondrocytes within grade-0 and grade-1 cartilage are shown, which exhibit normal morphology in grade-0 and abnormal morphology in grade-1 (indicated by solid arrow) and areas of hypo-cellularity (indicated by broken arrows). There were no PI-labelled chondrocytes detected in these images although this fluorescent indicator has been added. Scale bar for both panels and for the inset image = 100µm & 50µm respectively.

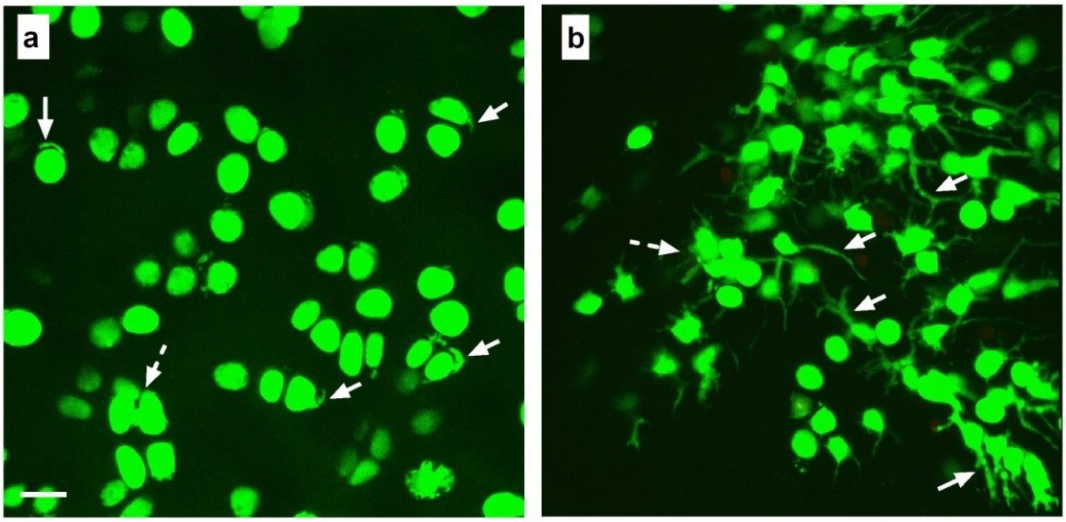

Figure 3.7: Axial CLSM reconstructed images of fluorescently-labelled human chondrocytes in femoral head articular cartilage.
CLSM reconstructed images at high magnification (x40DW) of CMFDA and PI-labelled chondrocytes (live and dead cells respectively) within (a) Grade-0 and (b) Grade-1 human femoral articular cartilage. The solid arrows indicate examples of cytoplasmic processes and the broken arrows the examples of clusters present in these representative images. There were no PI-labelled chondrocytes detected in these images although this fluorescent indicator has been added. Scale bar for both panels = 25μm.

3.5.1.3 *Volume of chondrocytes in grade-0 cartilage*

Chondrocytes survive in a unique environment with tight volume regulation and it has been suggested that loss of this control plays a role in their viability and progression of OA (Bush and Hall, 2003, Bush et al., 2005). The volume of chondrocytes in SZ, MZ and DZ of cartilage was measured with the baseline threshold method (sections 4.4.1.7.1. & 4.4.1.7.2) and frequency distribution calculated (% of total number of cells studied in the particular zone). The frequency of chondrocyte's volume in all the three zones of cartilage (Fig. 3.8d) displayed a

wide range. The cell volumes were ranked in the groups with a difference of 99μm^3 and the number of cells in each group was expressed as a percentage of the total number of cells in the specified ROI typically to a depth of 50μm through the z-axis. In the SZ, MZ and DZ the volume of chondrocytes ranged from 254 to 2079 μm^3, 272 to 2686 μm^3 and 255 to 2080 μm^3 respectively (Figs. 3.8a-c). The median volume of cells in the SZ, MZ and DZ was 875, 1035 and 839 μm^3 respectively. The cell volume varied hugely in all the three zones and there was an obvious overlap of the values in the three zones (Fig. 3.8d) suggesting that cell volume might not be a clear distinguishing characteristic for the cells in a specific zone. The average volume of chondrocytes in the MZ was significantly greater than in SZ and the DZ (P<0.001 and P<0.01 respectively; ANOVA; Fig. 3.8e). However, no difference in average volume was apparent between cells in SZ and DZ.

These results indicated that in the grade-0 cartilage there was marked heterogeneity in chondrocyte volume across all the zones.

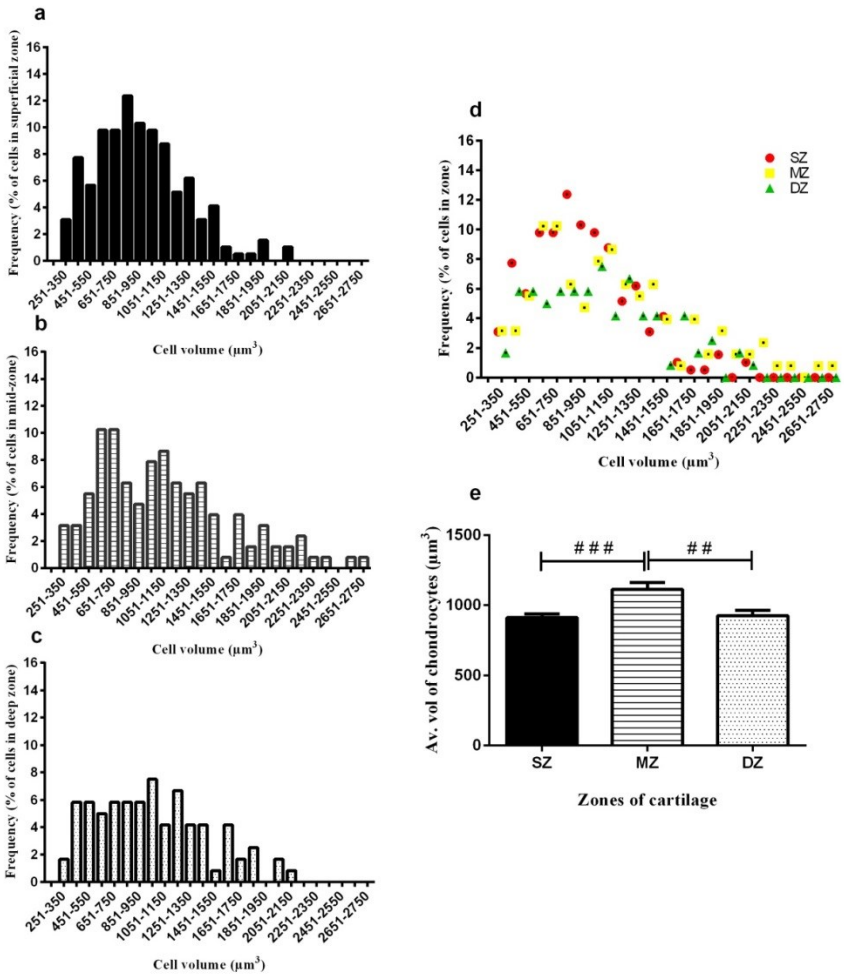

Figure 3.8: Volumes of chondrocytes in SZ, MZ and DZ in grade-0 human cartilage.

Chondrocyte volume was ranked in bands of 99µm^3, graphs in left panels show frequency distribution of volume of chondrocytes in (a) SZ (b) MZ and (c) DZ of cartilage. In the right panel graphs display (d) volume of cells in all the zones and (e) average volume of cells in the three zones of human femoral articular cartilage. Data were from [*N(n')*=8(194, 127 and 120) for the SZ, MZ and DZ respectively]. # indicated a significant difference according to one-way ANOVA followed by Tukey's multiple comparison post-hoc test. The single, double and triple symbols showed the level of significance for P<0.05, 0.01 and 0.001 respectively**.**

3.5.1.4 *Morphological characteristics of chondrocytes in grade-0 and grade-1 human femoral articular cartilage (coronal view)*

In the earlier sections (3.5.1.1. and 3.5.1.2.) there were indications that the morphology of chondrocytes was different between grade-0 and grade-1 cartilage

explants and in this section a more detailed quantitative analysis was presented. Chondrocyte morphology was compared in the various zones of grade-0 and grade-1 human cartilage explants.

In the low power (x10) magnification coronal view of grade-0 cartilage explants, there was a pattern of distribution of chondrocytes in the various zones of cartilage as described already in the tibia plateau (Bush and Hall, 2003). There were flattened chondrocytes in the superficial zone oriented parallel to the surface of cartilage (Fig. 3.9a). The cells beneath these were relatively spheroidal in shapes as compared to SZ chondrocytes and would represent primarily the MZ, and the chondrocytes with more rounded appearance, arranged mostly in vertical columns were considered to be the cells in the DZ (Fig. 3.9a, c). However, chondrocytes within the grade-1 cartilage had lost their normal distribution pattern in all the zones and their orientation was disorganised (Fig. 3.9b, d). Within the zones of cartilage particularly in the SZ and MZ, areas of hypo-cellularity were observed and were common in all the samples. The cells in the SZ and MZ were abnormal in morphology with cytoplasmic processes emanating from cell bodies and chondrocyte clustering was also present. However, in the DZ, chondrocytes were spheroidal in morphology (Fig. 3.9b, d). Chondrocyte density appeared to be less in the grade-1 as compared to grade-0 cartilage. In grade-0 cartilage more PI-labelled chondrocytes were present in the SZ and DZ as compared to the MZ (Fig. 3.9a, c). In grade-1 cartilage more PI-labelled cells were present in the SZ compared to the cells in MZ and DZ (Fig. 3.9b, d).

The high power magnification images of the coronal views of grade-0 and grade-1 cartilage were analysed and quantitative data regarding the morphological characteristics of chondrocytes were obtained. Marked heterogeneity of chondrocyte

morphology (clusters/processes) was observed in grade-1 as compared to grade-0 cartilage. The results were presented as related to changes in chondrocyte clustering and abnormal chondrocyte morphology as described in the following two sections.

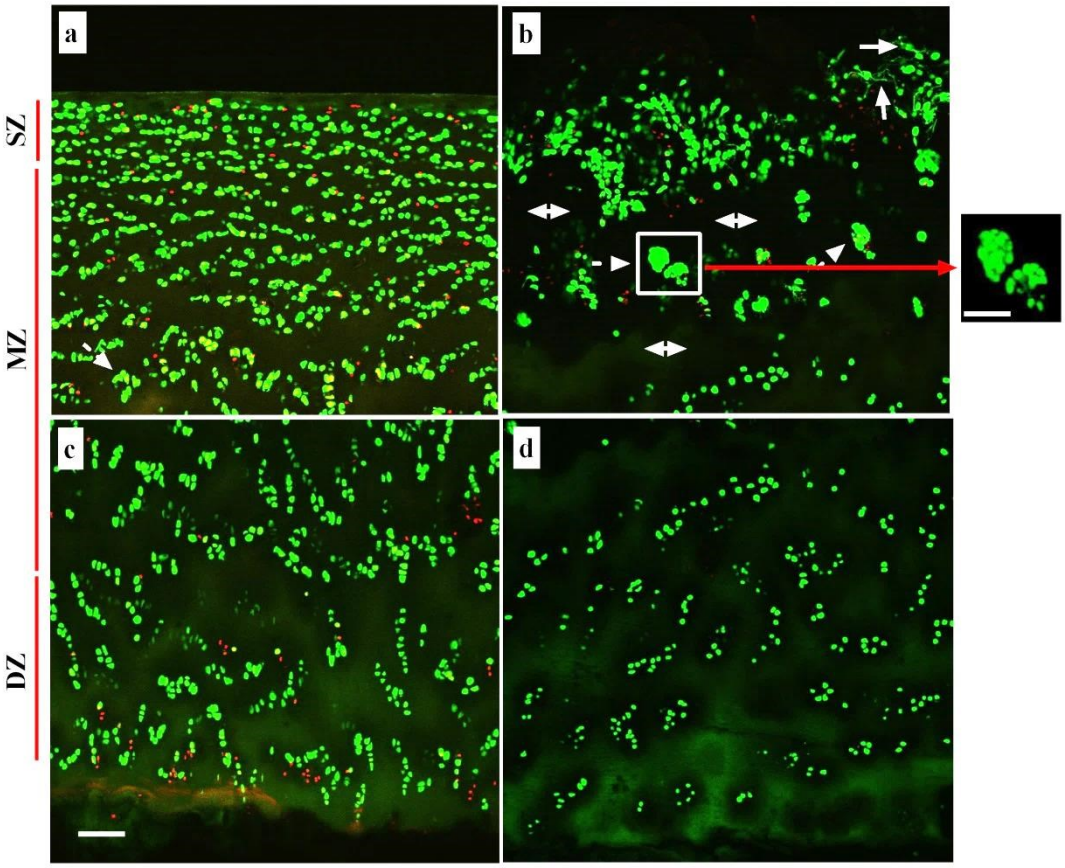

Figure 3.9: Coronal CLSM reconstructed images of human femoral articular cartilage.

Low magnification (x10) reconstructed CLSM images of CMFDA and PI-labelled chondrocytes (live and dead cells respectively) in the SZ, MZ and DZ of (a, c) grade-0 and (b, d) grade-1 human cartilage. Solid arrows indicate examples of abnormal cells with processes; broken arrows show examples of clusters formed and two-headed arrows indicate the areas of hypo-cellularity in grade-1 cartilage. Scale bar for all panels and for the inset image = 100µm & 50µm respectively.

3.5.1.4.1 Chondrocyte cluster formation in the various zones of grade-0 and grade-1 human femoral articular cartilage

Quantitative data regarding morphology of chondrocytes was obtained from the coronal CLSM images in order to determine morphology of chondrocytes in all the zones of cartilage. The images presented here are the 2D images obtained by reconstruction of series of 3D optical images and might show presence of clusters when projections were made because cells come closer. However, the analysis was performed on 3D images with the Volocity^{TM} software which accounted for the presence of cells in 3D and therefore the actual clusters present were analysed. A characteristic feature routinely observed in grade-1 cartilage was the presence of chondrocyte clusters (Fig. 3.10). In order to quantify this so that non-degenerate and degenerate cartilage explants could be compared, various parameters of clusters were analysed (see Figs. 3.11 & 3.12). As a first step clusters were defined (section 4.2.1.6.1) and then quantitative data in terms of number of clusters, number of cells/cluster, percentage of cells involved, volume of clusters and volume of individual cells in a cluster were obtained and compared in the three zones of grade-0 and grade-1 cartilage. The zones of cartilage were defined as demonstrated in section 3.4.1.1.

3.5.1.4.1.1 Number of clusters

In grade-0 cartilage, very few clusters were present in all the zones of cartilage. The average number of clusters was significantly higher in SZ than the DZ (P<0.01; ANOVA; Fig. 3.11a). Similarly, in grade-1 cartilage also the number of clusters present in the SZ was significantly greater in comparison to DZ (P<0.05; ANOVA;

Fig. 3.12a). The average number of clusters in the SZ of grade-1 cartilage was greater than that in the SZ of grade-0 cartilage but the difference was not statistically significant. This suggested an increasing number of clusters were formed in the SZ and MZ of grade-1 as compared to grade-0 cartilage.

3.5.1.4.1.2 Number of cells per cluster

The number of cells per cluster in grade-0 explants was significantly higher in the SZ and MZ as compared to the DZ ($P<0.001$; ANOVA for the three zones; Fig. 3.11b). In grade-1 cartilage, the number of cells per cluster was significantly higher in the SZ as compared to the DZ ($P<0.05$; ANOVA). The number of cells per cluster in the SZ and MZ of grade-1 cartilage (7.36±1.5 and 8.25±3.3 cells) were significantly higher than those in the SZ and MZ of grade-0 cartilage (3±0.3 and 3±0.1; $P=0.009$ and $P=0.04$; Student's t-test respectively; Fig. 3.12b).

3.5.1.4.1.3 Percentage of chondrocytes forming clusters

The percentage of chondrocytes forming clusters was significantly higher in the SZ as compared to the DZ in both grade-0 and grade-1 cartilage explants ($P<0.05$; ANOVA both conditions; Figs. 3.11c & 3.12c). However, a comparison of grade-0 and grade-1 osteochondral explants revealed that a significantly higher percentage of chondrocytes formed clusters in the SZ of grade-1 cartilage (43.3±16.04%) as compared to the SZ cells of grade-0 cartilage (11±3.3%; $P=0.008$; Fig. 3.12c), possibly because the number of cells per cluster increased involving more cells for cluster formation. In the MZ also a very high percentage of chondrocytes formed clusters in grade-1 (27.8±22.08%) as compared to grade-0 cartilage (9.2±3.9%) but the difference was not statistically significant. In the DZ, no clusters were detected in

grade-0 and grade-1 cartilage explants (Figs. 3.11c & 3.12c). This suggested that with cartilage degeneration, the percentage of chondrocytes within clusters increased in the SZ and MZ having more cells per cluster rather than an increase in the number of clusters however, no clusters were observed in the DZ.

3.5.1.4.1.4 Volume of clusters

In grade-0 cartilage explants, the average volume of clusters in the SZ and MZ were not statistically significantly different (Fig. 3.11d). Similarly, in grade-1 cartilage the volume of clusters was not significantly different between the SZ and MZ. However, the volume of clusters was significantly higher in the SZ in grade-1 cartilage as compared to grade-0 cartilage (P=0.005; Student's t-test; Fig. 3.12d). This suggested that with degeneration, cluster volume increased in the SZ due to increasing number of cells per cluster and also because the volume of individual cells in the cluster increased.

3.5.1.4.1.5 Volume of individual cells in a cluster

The volume of individual cells in a cluster was calculated (see Materials and Methods) and compared between grade-0 and grade-1 cartilage explants. In grade-0 and grade-1 cartilage the average volume of individual cells in a cluster was not significantly different in the SZ and MZ (Figs. 3.11e, 3.12e). However, the volume of individual cells in a cluster was significantly higher in the SZ of grade-1 cartilage as compared to grade-0 cartilage (P=0.02; Student's t-test; Fig. 3.12e).

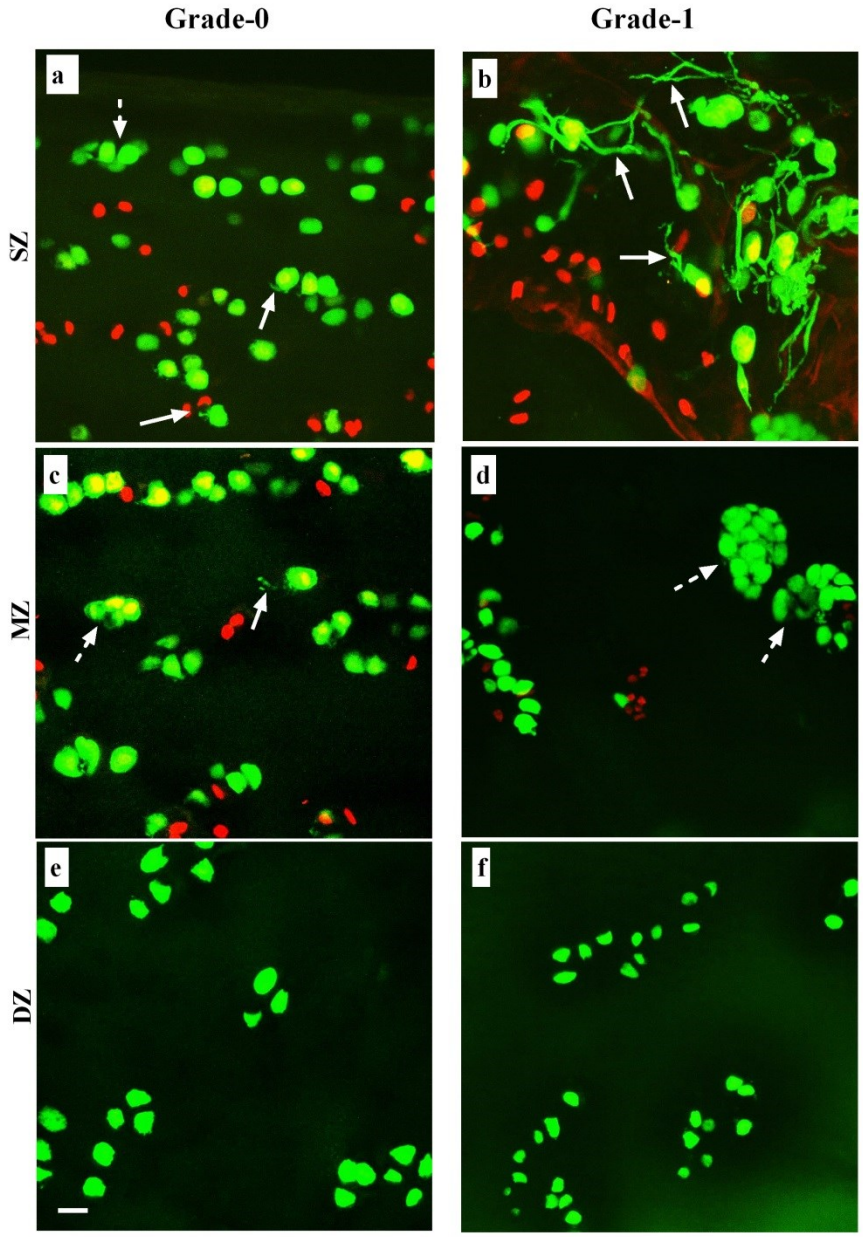

Figure 3.10: Coronal CLSM reconstructed images of chondrocytes within grade-0 and grade-1 human femoral articular cartilage.

High power (x40DW) coronal CLSM reconstructed images of fluorescently-labelled chondrocytes (CMFDA and PI for live and dead cells respectively) were imaged in SZ, MZ and DZ of the (a, c, e) grade-0 and (b, d, f) grade-1 cartilage. The cells in the DZ appear to be smaller than the cells in SZ and MZ of cartilage in grade-1 cartilage. The solid arrows show examples of cells with cytoplasmic processes and the broken arrows indicate examples of clusters present in various zones of cartilage. Scale bar for all panels = 25µm.

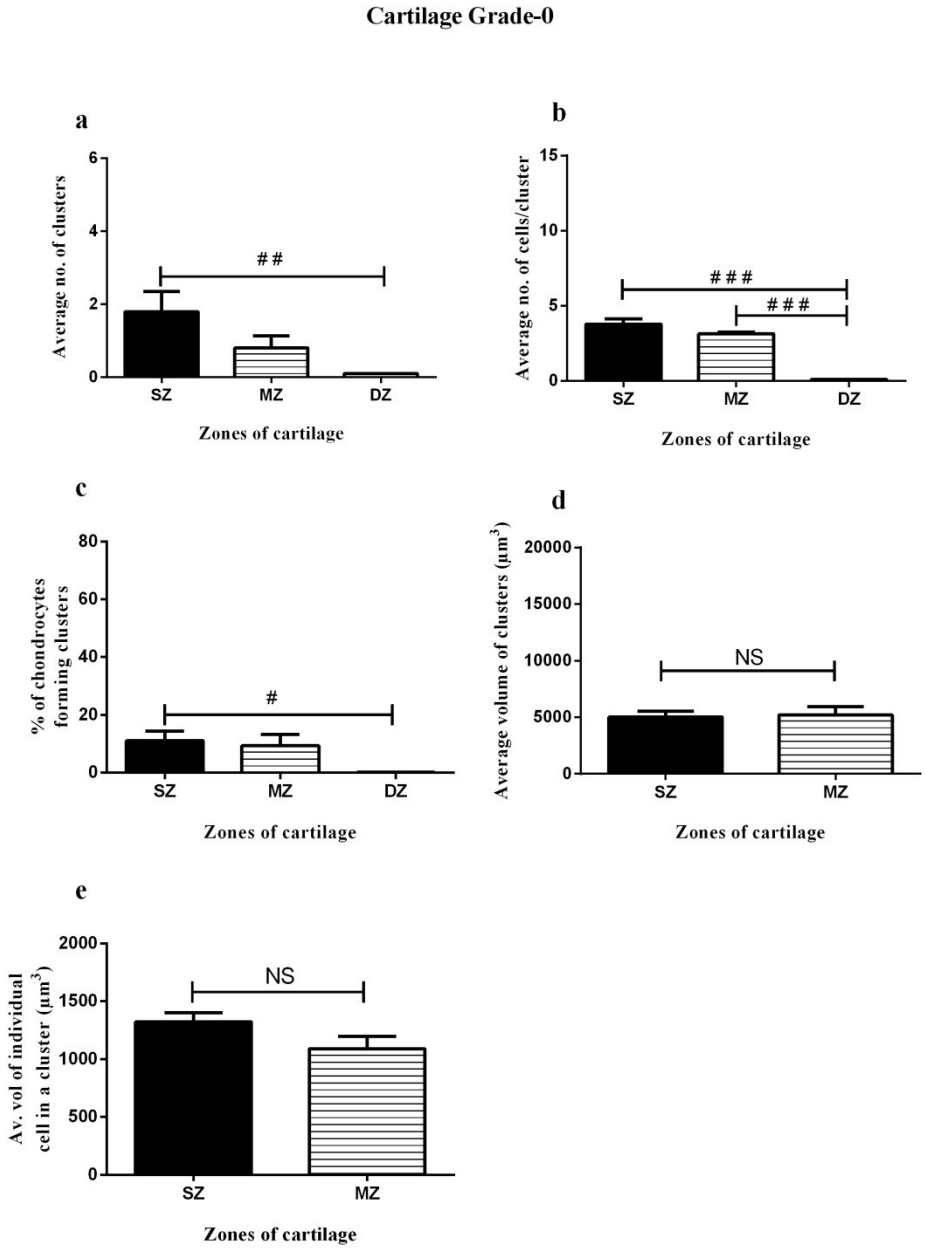

Figure 3.11: Analysis of chondrocyte clusters formed in the human femoral grade-0 articular cartilage.

Graphs show pooled data for (a) average number of clusters, (b) average number of cells per cluster, (c) percentage of cells present in clusters, (d) average volume of clusters (μm^3) and (e) average volume of individual cell in a cluster (μm^3) in grade-0 explants. Data were from [*N(n')*=8(1154)] for grade-0 cartilage explants. # indicated a significant difference according to one-way ANOVA followed by Tukey's multiple comparison post-hoc test. The single, double and triple symbols showed the level of significance for $P<0.05$, 0.01 and 0.001 respectively.

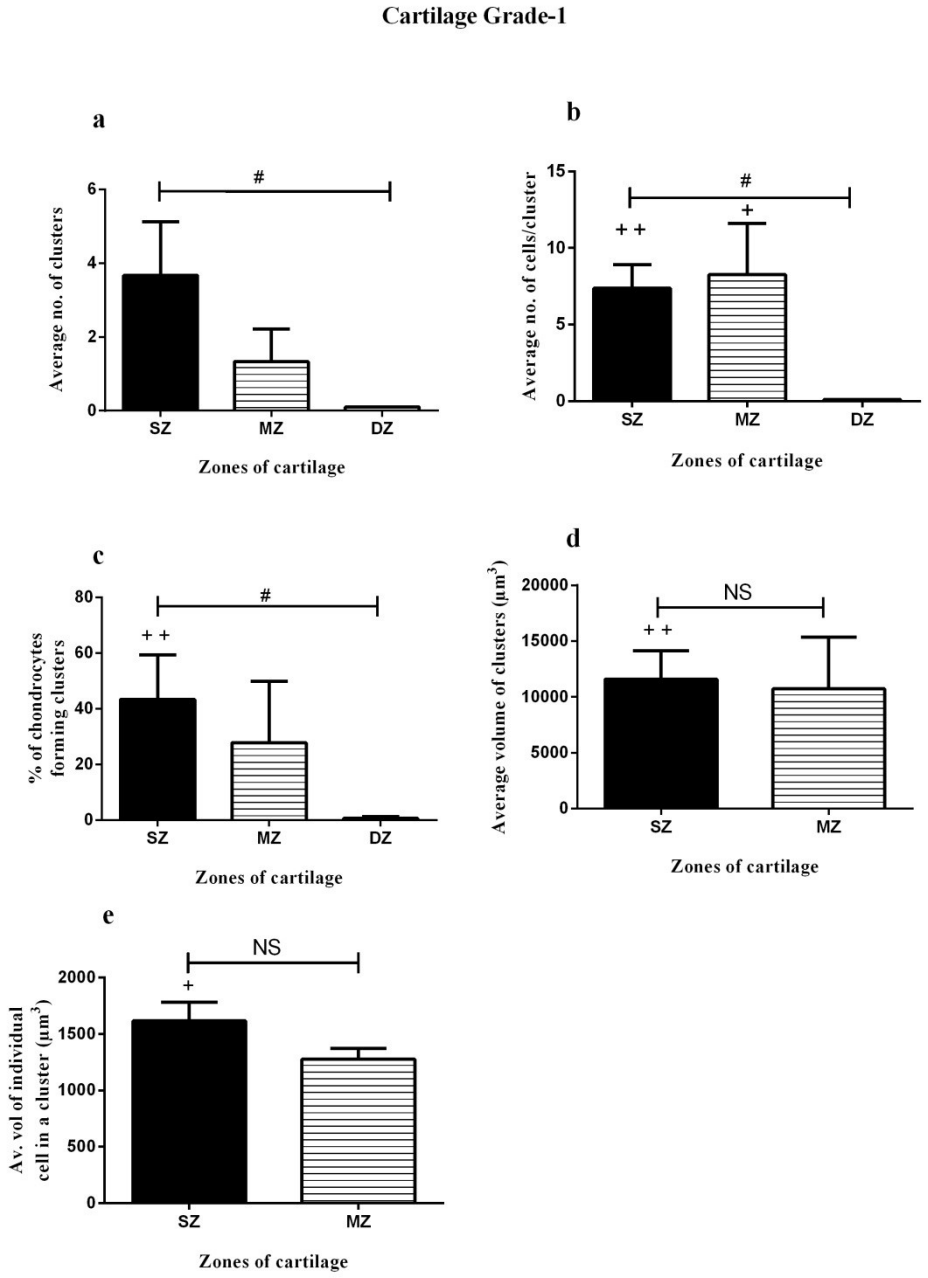

Figure 3.12: Analysis of chondrocyte clusters formed in the human femoral grade-1 articular cartilage.

Graphs show pooled data for (a) average number of clusters, (b) average number of cells per cluster, (c) percentage of cells present in clusters, (d) average volume of clusters (μm^3) and (e) average volume of individual cell in a cluster (μm^3) in grade-1 explants. Data were from [*N(n')*=3(360)] for grade-1 cartilage explants. # indicated a significant difference according to one-way ANOVA followed by Tukey's multiple comparison post-hoc test. + showed a significant difference between grade-0 and grade-1 cartilage explants according to Student's t-test. The single, double and triple symbols showed the level of significance for $P<0.05$, 0.01 and 0.001 respectively.

To summarise this section, clustering was observed only in the SZ and MZ of grade-0 and grade-1 human cartilage explants with none detected in the DZ. In grade-0 cartilage, only few chondrocytes were present in clusters. In grade-1 cartilage, chondrocytes were present in large clusters with a greater number of cells per cluster. Clustering was more pronounced in the SZ of grade-1 as compared to grade-0 cartilage. These results suggested that in grade-1 cartilage, numerous large clusters were present as compared to grade-0 cartilage where few small sized clusters were observed.

3.5.1.4.2 Abnormal morphology of *in situ* chondrocytes

Chondrocytes displayed marked shape changes in grade-1 as compared to grade-0 cartilage (Fig. 3.10). In this section the morphological characteristics of chondrocytes were quantified in more detail, by determining the percentage of chondrocytes with processes, number of processes per cell and the length of cytoplasmic processes in all the three zones (in coronal views) and compared in grade-0 and grade-1 cartilage explants.

3.5.1.4.2.1 Chondrocytes with cytoplasmic processes

In grade-0 cartilage, overall in all the zones of cartilage, 17±2% chondrocytes exhibited cytoplasmic processes and no significant difference existed between the percentages of chondrocytes with processes between the three zones of cartilage (Fig. 3.13a). However, in grade-1 cartilage throughout the whole thickness of cartilage, a significantly higher percentage of chondrocytes had cytoplasmic processes (35±5%) as compared to grade-0 cartilage (P=0.0007; Fig. 3.13b). The zone-wise analysis of chondrocyte morphology revealed that in the SZ of grade-1 cartilage, a significantly higher percentage of chondrocytes had cytoplasmic

processes (47±11%) as compared to grade-0 cartilage (17±4%; *P*=0.004; Fig. 3.13b). In the MZ and DZ no significant difference existed between the percentages of chondrocytes having processes (Fig. 3.13b).

3.5.1.4.2.2 Number of processes per cell

The number of processes per cell varied considerably across the various zones of grade-0 and grade-1 cartilage. In grade-0 cartilage the number of processes per cell was not significantly different in the three zones ranging from one (commonly) to four (rarely) processes per cell (Fig. 3.13c). However, in the grade-1 cartilage the number of processes per cell was significantly higher in the SZ as compared to MZ and DZ chondrocytes (*P*<0.01 and 0.05; ANOVA for the three zones; Fig. 3.13d). Additionally, the number of processes per cell was significantly higher in the SZ, ranging from one (commonly) to seven (rarely) processes per cell in grade-1 cartilage as compared to grade-0 cartilage (*P*=0.008; Fig. 3.13d).

3.5.1.4.2.3 Average length of cytoplasmic processes

The length of the cytoplasmic processes was quite variable within various zones of cartilage. In grade-0 cartilage the average length of cytoplasmic processes in the SZ and MZ was 5±0.2 μm [*N(n')*=8(89) and 8(79) for SZ and MZ respectively] and was significantly greater than the average length of cytoplasmic processes in the DZ [3±0.2 μm; *N(n')*=8(28); *P*<0.001 for both; ANOVA for the three zones; Fig. 3.13e]. In grade-1 cartilage the average length of processes in the SZ was (15.6±2 μm) significantly longer than length of processes in MZ (6±0.5 μm) and DZ (4±0.5 μm; *P*<0.01 for both; ANOVA for the three zones; Fig. 3.13f). Moreover, the average length of the cytoplasmic processes was significantly longer in the SZ, MZ and DZ

of grade-1 cartilage as compared to these three zones of grade-0 cartilage ($P<0.0001$; $P=0.01$ and $P=0.03$ for the SZ, MZ and DZ respectively; Fig. 3.13f). These results suggested that the length of cytoplasmic processes increased in the various zones with cartilage degeneration.

3.5.1.4.2.4 Percentage of chondrocytes with processes of various lengths

The length of the cytoplasmic process was fairly variable and the range was extensive. Keeping in mind the complex nature of these results, the cells with processes were further categorised into 4 groups with length (L) 1-4 (length categories). Based on the length of the processes these groups were defined as L1<5µm, 5<L2≤10µm, 10<L3≤15µm and L4>15µm. The percentage of cells having cytoplasmic processes of specific length category was determined (section 3.4.6) and compared in grade-0 and grade-1 cartilage explants.

In grade-0 cartilage, throughout the whole thickness of cartilage, a significantly higher percentage of chondrocytes had cytoplasmic processes within L1 category as compared to L2, L3 and L4 categories ($P<0.001$; ANOVA; Fig. 3.14a). However, in grade-1 cartilage, chondrocytes had processes ranging from L1-L4 categories in length and no difference existed between the percentages of chondrocytes having cytoplasmic processes with L1-L4 categories. In grade-0 and grade-1 cartilage there was no significant difference between processes within L1 category. However, processes within L2, L3 and L4 categories were significantly higher in grade-1 cartilage as compared to grade-0 cartilage ($P=0.001$, $P=0.004$ and $P=0.04$ respectively; Student's t-test; Fig. 3.14b).

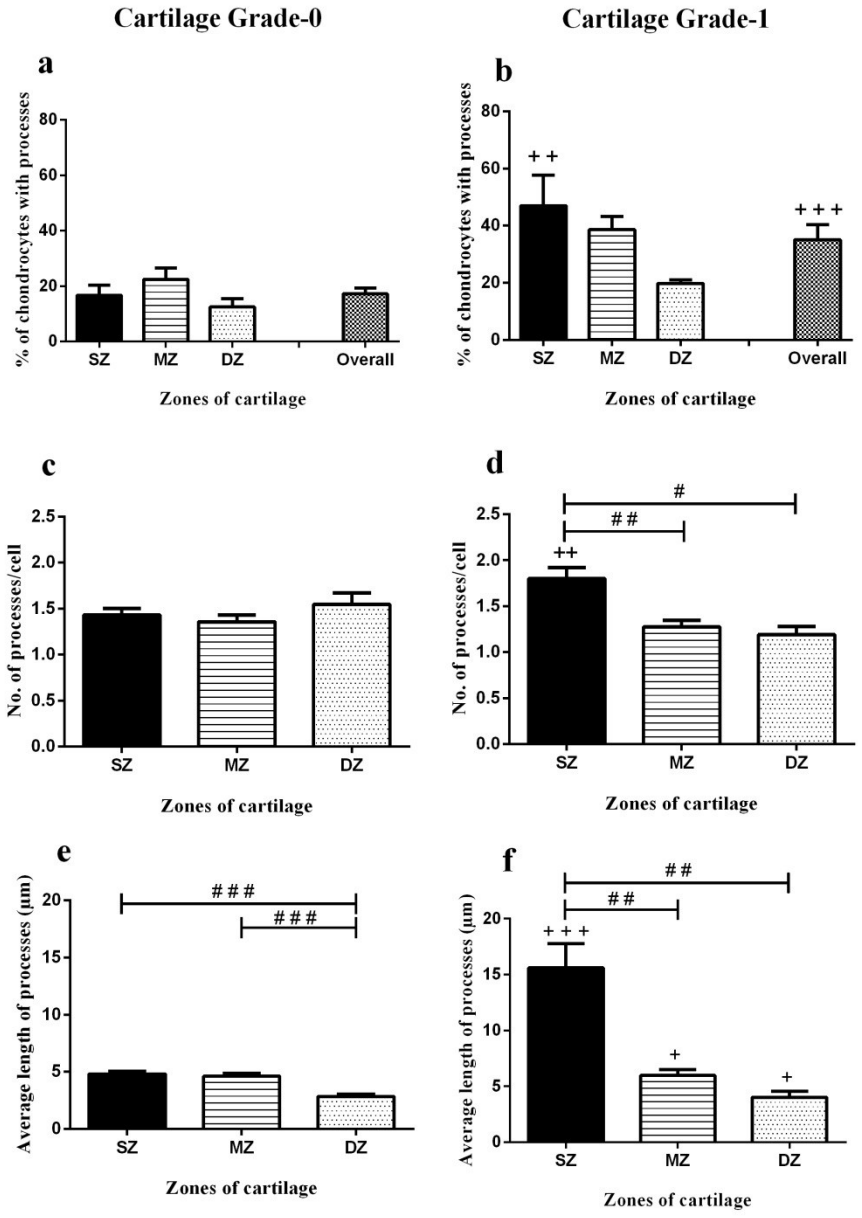

Figure 3.13: Morphological characteristics of chondrocytes in grade-0 and grade-1 human femoral head articular cartilage.

Graphs show pooled data regarding (a, b) percentage of cells with cytoplasmic processes, (c, d) number of processes per cell and (e, f) average length of cytoplasmic processes (µm) in grade-0 and grade-1 cartilage respectively. Data were from [*N(n')*=8(1154) and 3(360)] for grade-0 and grade-1 cartilage explants respectively. # indicated a significant difference according to one-way ANOVA followed by Tukey's multiple comparison post-hoc test. + showed a significant difference between grade-0 and grade-1 cartilage explants according to Student's t-test. The single, double and triple symbols showed the level of significance for $P<0.05$, 0.01 and 0.001 respectively.

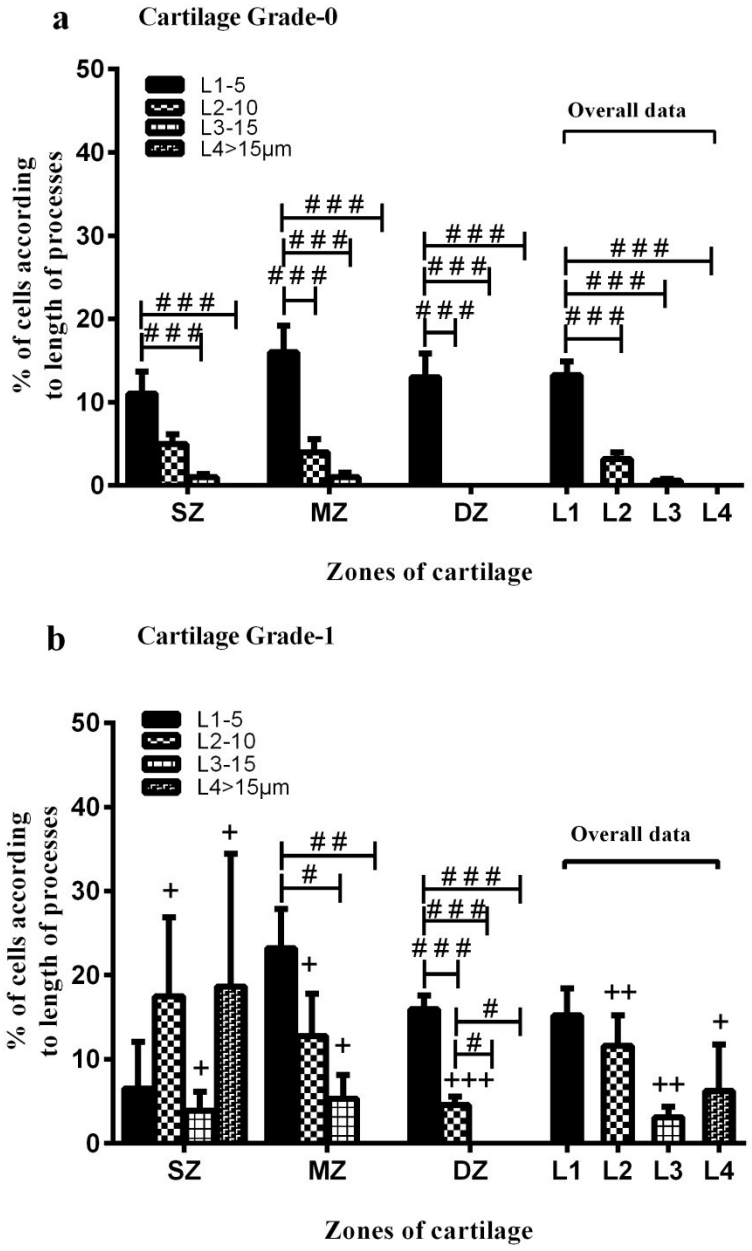

Figure 3.14: Percentages of chondrocytes with processes within various zones of cartilage.

Graphs show pooled data for the percentage of chondrocytes with cytoplasmic processes of various lengths in (a) grade-0 and (b) grade-1 human femoral head articular cartilage. Data were from [*N(n')*=8(1154) and 3(360)] for grade-0 and garde-1 cartilage explants respectively. # indicated a significant difference according to one-way ANOVA followed by Tukey's multiple comparison post-hoc test. + showed a significant difference between grade-0 and grade-1 cartilage explants according to Student's t-test. The single, double and triple symbols showed the level of significance for $P<0.05$, 0.01 and 0.001 respectively.

3.5.1.4.2.4.1 Superficial Zone

In grade-0 cartilage in the SZ, a significantly higher percentage of chondrocytes had processes in L1 category (11±3%) as compared to L3 category (1±0.3%; $P<0.001$; Fig. 3.14a), 5±1% cells had processes in L2 category which were not significantly different from the percentage of cells with L1 category and no cell had processes in the L4 category. In grade-1 cartilage in the SZ, chondrocytes had processes belonging to all the four length categories (L1-L4) and statistically no difference existed in the percentage of chondrocytes having processes of different length categories ($P>0.05$). However, when the SZ chondrocytes of grade-0 and grade-1 cartilage explants were compared, a significantly higher percentage of chondrocytes had processes of length categories L2, L3 and L4 in grade-1 cartilage as compared to grade-0 cartilage ($P=0.03$, $P=0.02$ and $P=0.03$ respectively; Fig. 3.14a & b). Moreover, no difference was found between the percentages of chondrocytes having processes with L1 length category. In summary, in the SZ the percentage of chondrocytes with cytoplasmic processes having L2-L4 length categories, increased in grade-1 as compared to grade-0 cartilage.

3.5.1.4.2.4.2 Mid-zone

In the MZ of grade-0 and grade-1 cartilage, the length of cytoplasmic processes varied between L1 and L3 categories and no processes within L4 category were found. In the MZ of grade-0 cartilage a significantly higher percentage of chondrocytes had processes with L1 length category as compared to L2, L3 and L4 categories ($P<0.001$; ANOVA; Fig. 3.14a). In the MZ of grade-1 cartilage the length of processes ranged between L1-L3 categories and no processes with L4 category were present. There was statistically no difference between the percentages of

chondrocytes having processes with L1 and L2 length categories (P>0.05). However, a significantly higher percentage of chondrocytes had L1 length category processes as compared to those with L3 and L4 categories (P<0.05 and P<0.01 respectively; Fig. 3.14b). When grade-0 and grade-1 cartilage explants were compared, it was observed that in the MZ no difference existed between percentages of cells with processes in L1 length category. Additionally, a significantly higher percentage of chondrocytes had processes with L2 and L3 categories in grade-1 cartilage as compared to grade-0 cartilage (P=0.04 and P=0.03 respectively; Fig. 3.14b). In summary, in the MZ the percentage of chondrocytes with cytoplasmic processes having L2 and L3 categories increased in grade-1 as compared to grade-0 cartilage.

3.5.1.4.2.4.3 Deep Zone

In grade-0 cartilage within the DZ, chondrocytes had processes only L1 in length category and processes with length ranging from L2-L4 categories were not observed (Fig. 3.14a). In grade-1 cartilage in the DZ, chondrocytes had processes with L1 and L2 length categories but L3 and L4 categories were absent. In grade-1 cartilage a significantly higher percentage of chondrocytes had processes with L1 category as compared to L2 (P<0.001; ANOVA; Fig. 3.14b). When the DZ of grade-0 and grade-1 cartilage was compared, there was no significant difference between the percentages of chondrocytes with processes in L1 length category (P>0.05). However, a significantly higher percentage of chondrocytes had processes with L2 category in grade-1 as compared to grade-0 cartilage (P<0.0001; Student's t-test; Fig. 3.14b). In summary, in the DZ the percentage of chondrocytes having processes within L2 length category increased in grade-1 as compared to grade-0 cartilage.

To summarise this section on the abnormal morphology of chondrocytes, in grade-0 as compared to grade-1 cartilage fewer, fine cytoplasmic processes with an average length of 5µm were present within cells of all zones. However, in grade-1 cartilage numerous chondrocytes had cytoplasmic processes of variable lengths. There existed a general trend regarding the presence of cells with processes, in relation to depth of the cartilage which suggested that they were seen mostly in the SZ, less in the MZ and least in the DZ. Moreover, the number of processes per cell and the length of these cytoplasmic processes also decreased with increasing depth of cartilage.

3.5.2 Viability and morphology of chondrocytes in human articular cartilage obtained from various clinical conditions

Marked changes to chondrocyte morphology were observed in osteochondral explants obtained from patients with different clinical conditions. Five human cartilage samples from various joints under different clinical conditions were obtained and cell viability and morphology of fluorescently-labelled chondrocytes was visualised by CLSM. Four of these samples were small fragments of cartilage and bone whereas only one was a complete femoral head, all obtained post-operatively. Three osteochondral fragments were obtained from patients suffering from osteochondritis dissecans (OCD) and fourth one from a patient having fracture of the ankle joint. The osteochondral explants from femoral head were obtained after dissection with the similar protocol as that performed for the explants in the earlier section of this chapter. However, the osteochondral fragments were simply trimmed and rectangular pieces were obtained for CLSM. The samples were incubated with CMFDA and PI (live and dead chondrocytes respectively) and prepared for CLSM. The samples were imaged at low and high magnification for axial view (all samples)

and coronal views (where possible). The details of the methodology for cartilage preparation and imaging can be viewed in the Materials and Methods (sections 3.4.3 and 3.4.4).

3.5.2.1 *Human osteochondral fragment (knee joint) (OCD)*

An osteochondral fragment of the knee joint with the dimensions of 1.3 cm x 0.5 cm (Fig. 3.15) was obtained from 18 yrs. old male diagnosed as suffering from the OCD and consisted of cartilage with some underlying bone. Chondrocytes were labelled with CMFDA and PI (for live and dead cells respectively) and imaged with CLSM. The areas of hypo-cellularity were present and chondrocyte morphology was typical of grade-1 cartilage (Figs. 3.6b & 3.7b). Chondrocytes were present in clusters and had multiple cytoplasmic processes (Fig. 3.16). There were no PI-labelled chondrocytes observed although this fluorescent dye was used for labelling these explants.

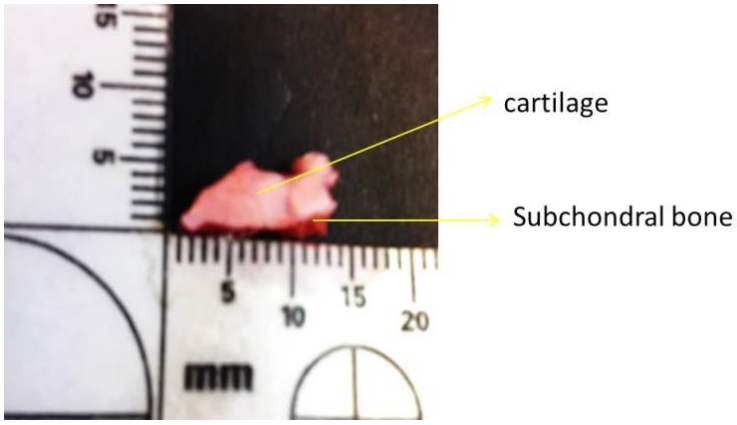

Figure 3.15: Photograph of osteochondral fragment of knee joint.

Arrows indicate cartilage and subchondral bone.

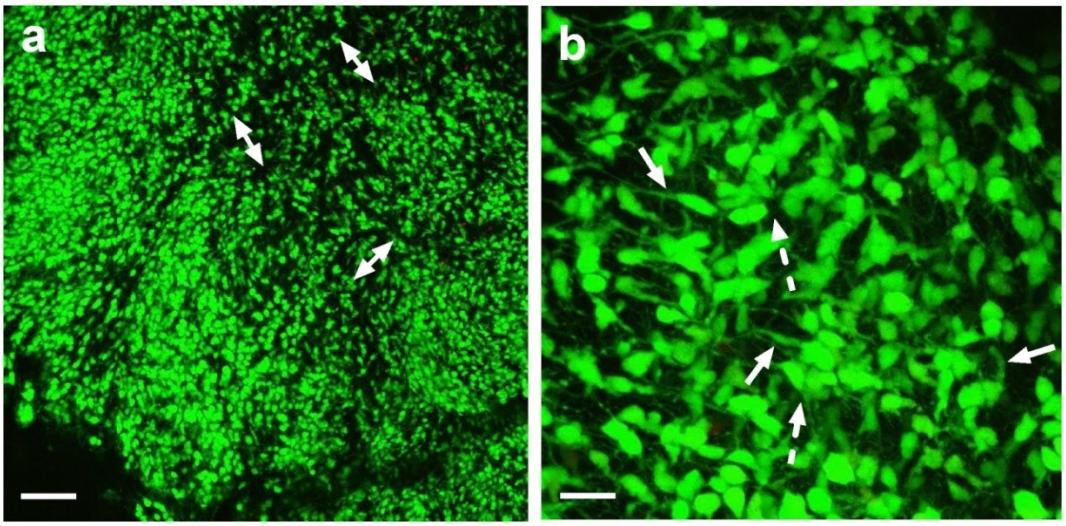

Figure 3.16: Axial CLSM reconstructed images of chondrocytes of human knee articular cartilage of a patient suffering from OCD.
CLSM reconstructions of (a) low (x10) and (b) high (x40 DW) magnification images of CMFDA and PI labelled chondrocytes (live and dead cells respectively). The solid arrows indicated examples of cytoplasmic processes, broken arrows indicated examples of clusters present and two headed arrows indicated areas of hypo-cellularity. Scale bar for left and right panels = 100µm and 25µm respectively.

3.5.2.2 *Human osteochondral fragment of talus (ankle joint) (OCD)*

An osteochondral fragment from talus bone of ankle joint was obtained after surgery from a 30 yrs. old male patient suffering from OCD. The dimensions of the sample were 1cm x 1cm and it comprised of thin cartilage with some underlying bone (Fig. 3.17). The low and high power CLSM images showed presence of numerous PI-labelled chondrocytes in the axial and coronal views of the cartilage sample as compared to the OCD knee joint sample (Fig. 3.16). Chondrocyte morphology displayed marked heterogeneity and areas of hypo-cellularity were present. Morphology of chondrocytes was altered in terms of cell proliferation and shape of cells. Chondrocytes were no more spheroidal in morphology, were present in clusters

and had multiple cytoplasmic processes emanating from their cell bodies (Figs. 3.18 & 3.19).

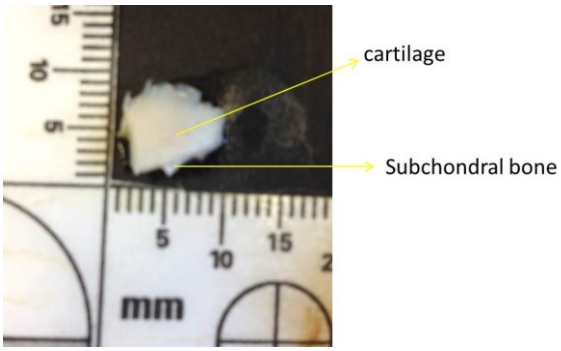

Figure 3.17: Photograph of osteochondral fragment of talus from human ankle joint.
Arrows indicate cartilage and subchondral bone.

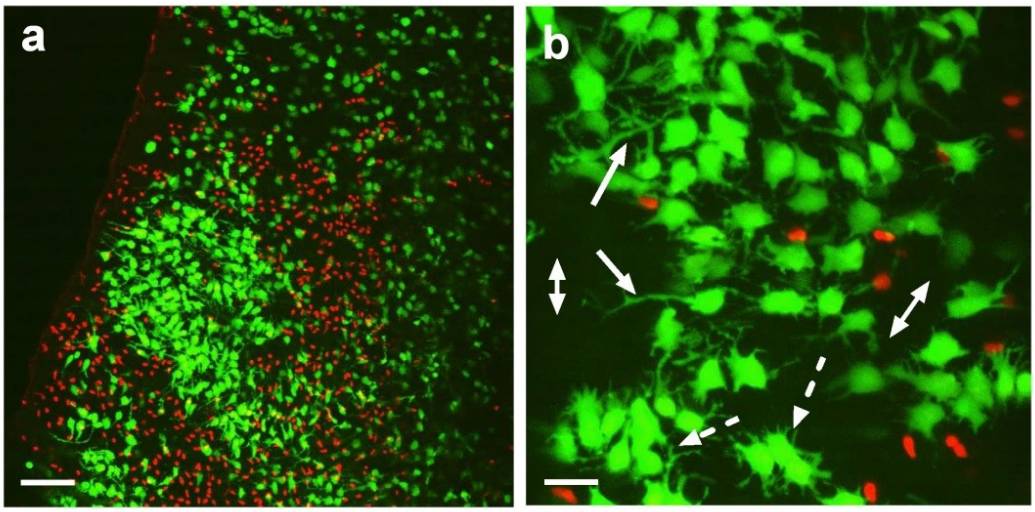

Figure 3.18: Axial CLSM reconstructed images of human ankle joint cartilage of a patient suffering from OCD.
CLSM reconstructions of (a) low (x10) and (b) high (x40 DW) magnification images of CMFDA and PI-labelled chondrocytes (live and dead cells respectively) in human cartilage from talus bone (ankle joint). The solid arrows indicated examples of cytoplasmic processes, broken arrows indicated examples of clusters and two headed arrows indicated areas of hypo-cellularity. Scale bar for left and right panels = 100µm and 25µm respectively.

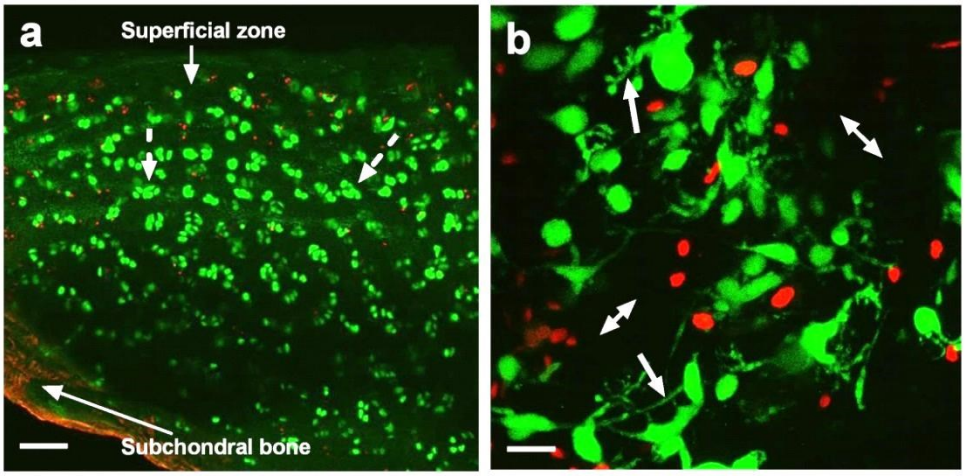

Figure 3.19: Coronal CLSM reconstructed images of human ankle joint cartilage of a patient suffering from OCD.
CLSM reconstructions of (a) low (x10) and (b) high (x40 DW) magnification images of CMFDA and PI labelled chondrocytes (live and dead cells respectively) in human cartilage from talus bone (ankle joint). The solid arrows indicated examples of cytoplasmic processes, broken arrows indicated examples of clusters present and two headed arrows indicated areas of hypo-cellularity. The subchondral bone has been labelled with PI. Scale bar for left and right panels = 100µm and 25µm respectively.

3.5.2.3 *Human osteochondral fragment of talus (ankle joint) (OCD)*

The sample was acquired from talus bone of ankle joint of 26 yrs. old female patient diagnosed as OCD since months. The dimensions of the osteochondral fragment obtained were 1cm x 0.5cm and comprised of cartilage from talus bone with some underlying bone (Fig. 3.20). When the cartilage was viewed with the low and high power magnification objectives, some PI-labelled chondrocytes and areas of hypo cellularity were seen. Moreover, chondrocytes showed marked heterogeneity in morphology characterised by the presence of clusters and multiple long cytoplasmic processes (Fig. 3.21). The cartilage was examined in the coronal view and both low and high magnification images displayed areas of hypo-cellularity and the PI-labelled chondrocytes were numerous in the SZ as compared to MZ and DZ.

Chondrocytes in the SZ and MZ displayed morphological changes with the presence of multiple cytoplasmic processes. However, in the DZ chondrocytes were relatively spheroidal in morphology as compared to SZ and MZ chondrocytes (Fig. 3.22).

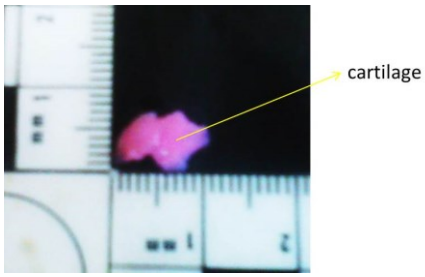

Figure 3.20: Photograph of osteochondral fragment of talus from human ankle joint.

Arrow indicates the cartilage but the underlying bone is not visible in the photograph.

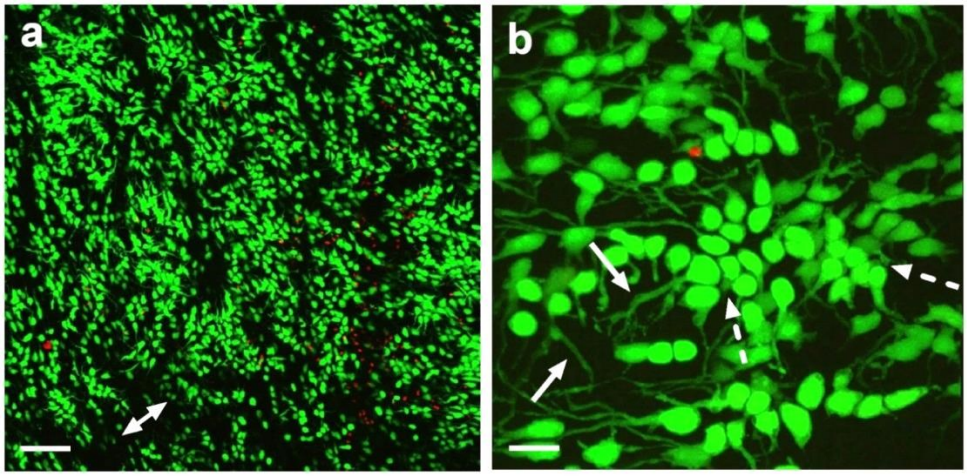

Figure 3.21: Axial CLSM reconstructed images of human ankle joint cartilage. CLSM reconstructions of (a) low (x10) and (b) high (x40 DW) magnification images of CMFDA and PI labelled chondrocytes (live and dead cells respectively) in human cartilage from the talus bone (ankle joint). The solid arrows indicated examples of cytoplasmic processes, broken arrows indicated examples of clusters and two headed arrows indicated areas of hypo-cellularity. Scale bar for left and right panels = 100µm and 25µm respectively.

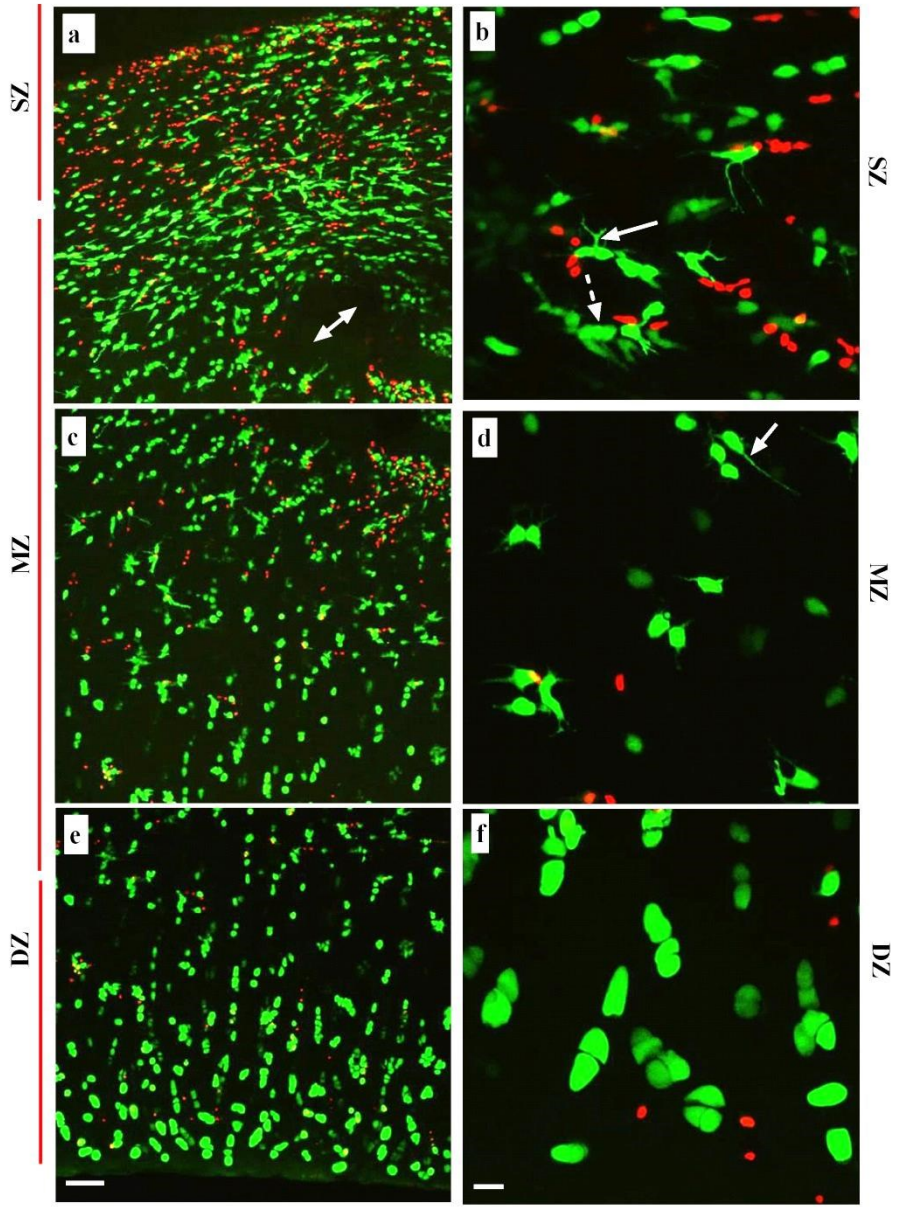

Figure 3.22: Coronal CLSM reconstructed images of human ankle joint cartilage.

CLSM reconstructions of (a, c, e) low (x10) and (b, d, f) high (x40 DW) magnification images of CMFDA and PI labelled chondrocytes (live and dead cells respectively) in human cartilage from talus bone (ankle joint) within the various zones of cartilage. The solid arrows indicated examples of cytoplasmic processes, broken arrows indicated examples of clusters present and two headed arrows indicated areas of hypo-cellularity. Scale bar for left and right panels = 100µm and 25µm respectively.

3.5.2.4 *Human femoral head articular cartilage (hip joint) (AVN)*

Human femoral head was obtained from 36 yrs. old female patient suffering from AVN since months. When the femoral head was viewed for its general appearance it was grossly abnormal. The femoral head was shrunken and its shape was non-spheroidal with several raised and depressed areas of cartilage (Fig. 3.23). The osteochondral explants were obtained from the femoral head from the area indicated on the photograph (Fig. 3.23).

The low and high power axial images of the fluorescently-labelled chondrocytes showed irregular cartilage surface and extensive cell death as indicated by the presence of PI-labelled chondrocytes. Marked areas of hypo cellularity were obvious and chondrocyte morphology was strikingly abnormal. Chondrocytes were flattened in shape and were present in clusters and had multiple cytoplasmic processes (Fig. 3.24). In the low and high power coronal images of the cartilage the morphologically abnormal chondrocytes were present in the SZ and MZ. However, chondrocytes in the DZ were relatively normal (spheroidal) in morphology (Fig. 3.25).

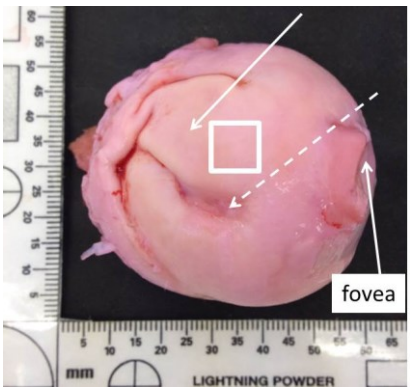

Figure 3.23: Photograph of human femoral head of a patient suffering from avascular necrosis.
The solid arrow indicated raised areas and the broken arrow indicated depressed areas of cartilage still attached to the underlying subchondral bone. The white box showed the area from where sample was obtained. The fovea is labelled on the photograph.

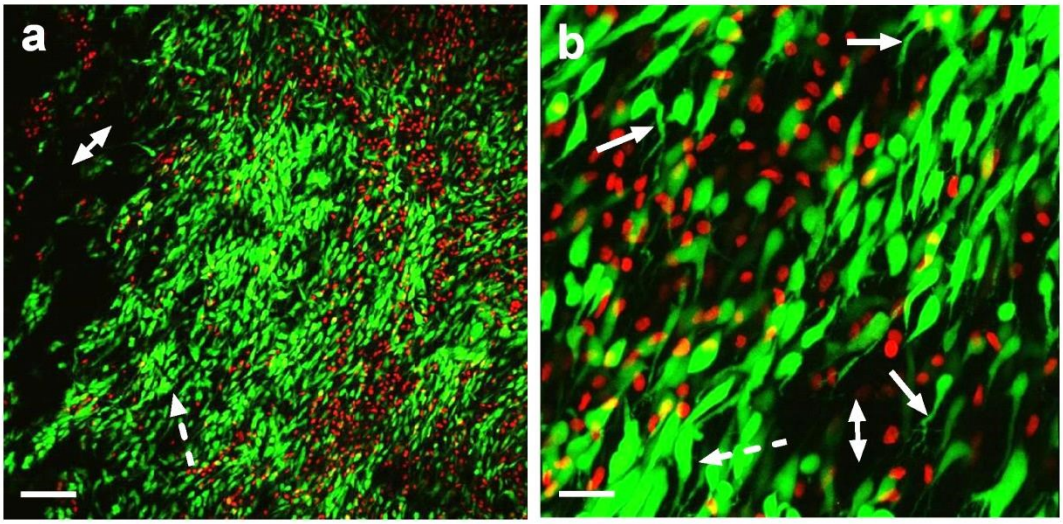

Figure 3.24: Axial CLSM reconstructed images of human femoral head cartilage of a patient suffering from avascular necrosis.
CLSM reconstructions of (a) low (x10) and (b) high (x40 DW) magnification images of CMFDA and PI labelled chondrocytes (live and dead cells respectively) in human femoral head cartilage. The solid arrows indicated examples of cytoplasmic processes, broken arrows indicated examples of clusters and two headed arrows indicated areas of hypo-cellularity. Scale bar for left and right panels = 100µm and 25µm respectively.

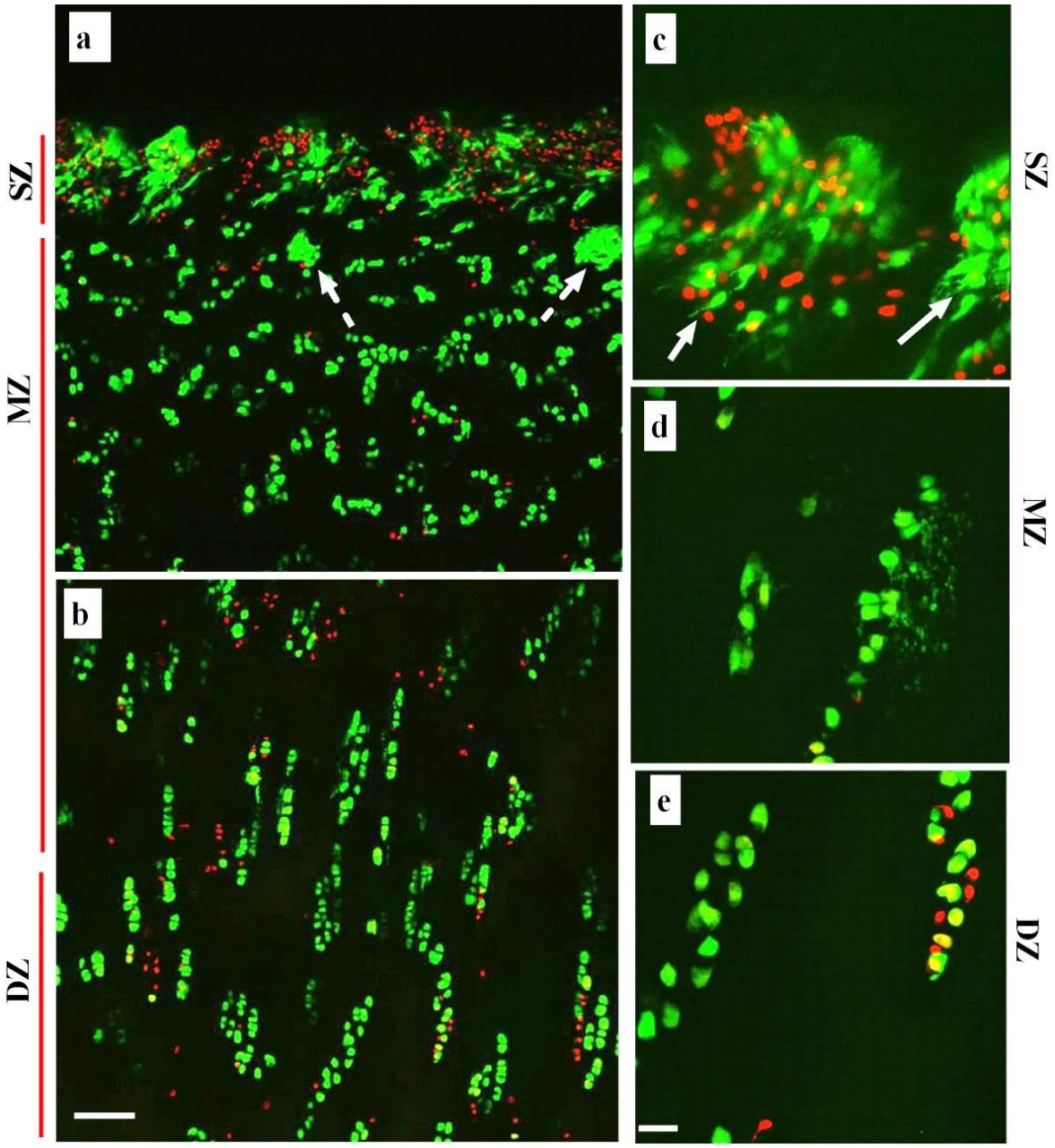

Figure 3.25: Coronal CLSM reconstructed images of human femoral head cartilage from a patient of avascular necrosis.

CLSM reconstructions of (a, b) low (x10) and (c, d & e) high (x40 DW) magnification images of CMFDA and PI labelled chondrocytes (live and dead cells respectively) within various zones in human femoral head cartilage. The solid arrows indicated examples of cytoplasmic processes; broken arrows indicated examples of clusters present. Scale bar for left and right panels = 100µm and 25µm respectively.

3.5.2.5 *Osteochondral fragment of calcaneus bone (subtalar joint)*

This sample was obtained from the calcaneus bone of a 55 yrs. old male who had suffered from acute trauma with fracture dislocation of subtalar joint a few days before the sample was obtained. The sample was 1.3 cm x 1 cm in dimensions and consisted of the cartilage grade-0 and underlying bone (Fig. 3.26). Fluorescently-labelled chondrocytes were imaged and both low and high power axial images showed no chondrocyte death in the sample. Additionally, chondrocytes were normal (elliptical/spheroidal) in morphology and there was no clustering present (Fig. 3.27). In the low and high power coronal images, the cartilage surface was regular and only few dead chondrocytes were present in the SZ as compared to MZ and DZ. The morphology of chondrocytes was normal (elliptical/spheroidal in shape with no cytoplasmic processes) throughout the whole thickness of cartilage. In addition to this chondrocytes were not present in the form of clusters in any of the zones of cartilage (Fig. 3.28).

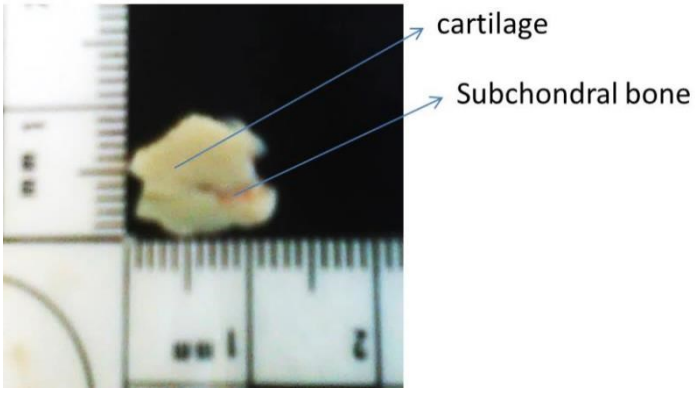

Figure 3.26: Photograph of osteochondral fragment of calcaneus from human subtalar joint.
The arrows indicate cartilage and subchondral bone.

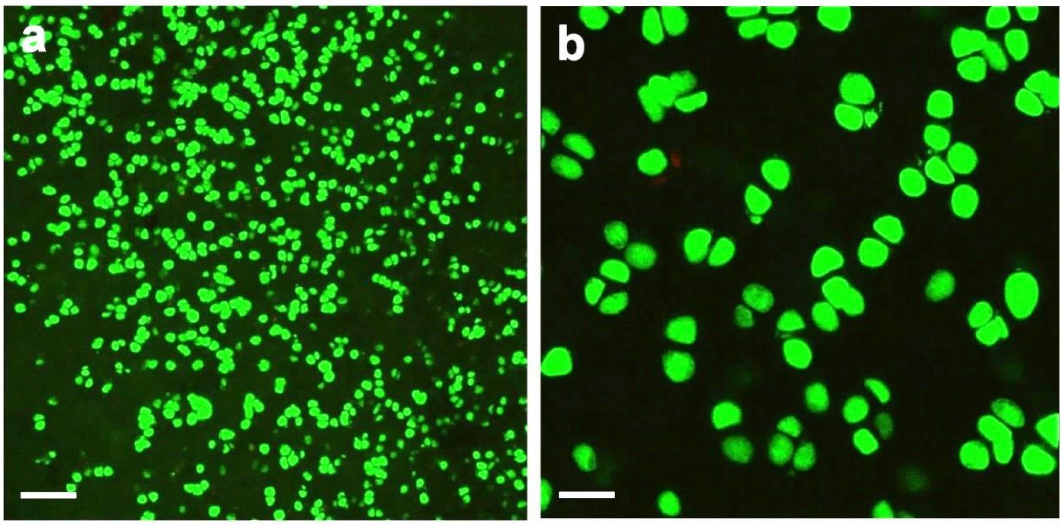

Figure 3.27: Axial CLSM reconstructed images of human subtalar joint cartilage.

CLSM reconstructions of (a) low (x10) and (b) high (x40 DW) magnification images of CMFDA and PI-labelled chondrocytes (live and dead cells respectively) in human cartilage from the calcaneus bone (subtalar joint). Scale bar for left and right panels = 100µm and 25µm respectively.

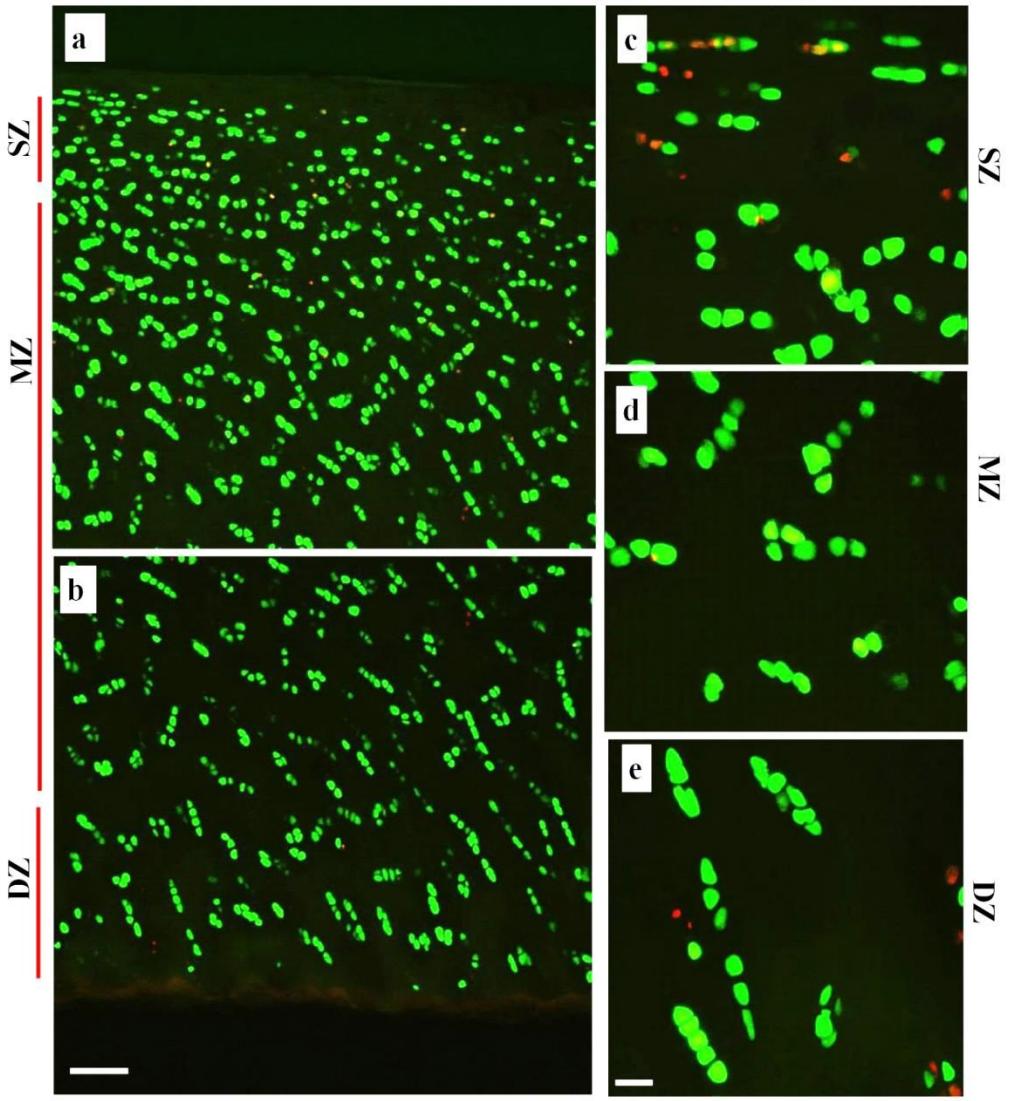

Figure 3.28: Coronal CLSM reconstructed images of human subtalar joint cartilage.
CLSM reconstructions of (a, b) low (x10) and (c, d, e) high (x40 DW) magnification images of CMFDA and PI-labelled chondrocytes (live and dead cells respectively) in human cartilage obtained from calcaneus bone (subtalar joint) within the various zones of cartilage. Scale bar for left and right panels = 100µm and 25µm respectively.

To summarise this section, in the cartilage of patients suffering from two clinical conditions namely OCD and AVN certain features of cartilage degeneration were present. The surface of the cartilage was irregular and chondrocyte morphology was strikingly altered. These abnormal chondrocytes had elongated cell bodies with

multiple cytoplasmic processes and chondrocyte clusters were also present. These morphological changes (clusters/processes) appeared to be present mostly in the SZ extending into the MZ. However, DZ chondrocytes were mostly normal in morphology.

3.6 DISCUSSION

This study utilised fluorescent-mode CLSM to visualise *in situ* chondrocyte morphology in grade-0 and grade-1 human femoral articular cartilage and cartilage obtained from various clinical conditions. The main aims of this work were to study human femoral head cartilage samples obtained from patients after hip replacement surgery to determine morphology of chondrocytes in non-OA cartilage and to compare the morphological characteristics of human femoral articular chondrocytes with other human cartilage samples studied. These human femoral head articular cartilage samples were a valuable biological material to study chondrocyte morphology and the CLSM technique used in this study was a suitable method to determine the morphological characteristics of chondrocytes due to several reasons: **Firstly,** the human femoral heads were obtained from patients undergoing surgery for fracture and had no known diseases of the joints which assured that grade-0 cartilage was healthy and was an appropriate control for the study. **Secondly,** grade-1 cartilage was obtained from the same joint from which grade-0 cartilage was obtained and the importance of this was twofold (a) chondrocyte morphology of non-degenerated and mildly-degenerated cartilage could be fairly compared and (b) early morphological changes in cartilage degeneration could be studied. **Thirdly,** the results from these human samples were directly applicable to the human disease OA because of similar mechanical and biochemical environment. **Fourthly,** the

volume/morphological data obtained from femoral articular cartilage could be directly compared with already available data on volume/morphology of chondrocytes from other joints such as knee joint. **Lastly,** the changes to morphology of chondrocytes in grade-1 human cartilage could be compared with morphological changes observed in bovine chondrocytes cultured in weak gels (chapter 4) to determine similarities and differences.

However, the concerns with the use of these samples and CLSM technique were (a) possibly the dissection of samples could induce morphological changes but the chances were less. If shape changes were the cutting artefact then the presence of heterogeneous chondrocytes in the axial sections was not possible (b) the removal of explants from the femoral heads might lead to cartilage swelling (Maroudas and Venn, 1977). This was minimised by dissecting explants along with underlying bone because the lack of bone leads to cartilage swelling due to imbibition of fluid (Maroudas, 1990) and (c) these samples were rarely obtained and therefore, data could be obtained from a very limited number of samples.

In this study the volume/morphology of chondrocytes *in situ* in grade-0 grade-1 were studied in human femoral cartilage and in various clinical conditions. The cartilage was obtained from patients undergoing hip replacement surgery for fracture neck of femur and graded according to the macroscopic and microscopic characteristics of author's own criteria given in Table 3.2. Although 3 samples of grade-0 human cartilage were obtained from the femoral heads which contained areas of grade-1 cartilage also, the results indicated that there was no significant difference between these cartilage samples and the grade-0 samples obtained from heads containing no

grade-1 areas, therefore, the data obtained were grouped together. The grading criteria used in this study is comparable for the macroscopic appearance of cartilage with the previously published grading system (Pritzker et al., 2006). However, microscopic changes presented here cannot be directly compared with the previously published grading system for degenerating cartilage such as (Pritzker et al., 2006) because in the present study the grading has been done on the basis of CLSM microscopic examination of chondrocyte morphology but in previous study histology was performed. Several features to be considered between previous grading systems and our criteria were (a) macroscopically cartilage was intact in grades-0/1 according to previous grading system and observed to be intact in grade-0 and roughened in grade-1 cartilage samples in this study (b) the tissue is uninvolved in grade-0 according to the previous grading system but slight morphological changes were observed in grade-0 cartilage in this study in terms of presence of few small clusters and few fine cytoplasmic processes (c) the tissue changes included cluster formation in grade-1 cartilage in both previously reported and grading criteria used in this study (d) in the previous grading system there is sub-grading also which states that the grades of cartilage can be like 1.5, 2.5, & 3.5 and so on in between 1, 2, 3 & 4. Therefore, comparison of the two grading methodologies suggested that macroscopically grade-0 in the present study is equivalent to grade-0 or between 0 and 1 according to the previous grading system. Microscopic examination revealed presence of some morphological changes in grade-0 cartilage in the present study suggesting the possibility of these morphological changes as the very initial events in degenerating cartilage. The grade-1 in the present study appears to be between grade-1 and grade-2 according to the previous system based upon the macroscopic and

microscopic features. The additional morphological feature reported in the present study which can possibly become an important additional feature of grading system is the presence of cytoplasmic processes. Therefore the fine morphological details of grade-0 and grade-1 cartilage presented in this study provided new insights into the grading system already available.

Cartilage grade	**Macroscopic examination (surface properties)**	**CLSM examination (chondrocyte morphology)**
Grade-0	• No visible changes • Smooth surface • Glistening appearance of cartilage • Pale in colour	• Smooth and even surface • Chondrocytes present in a pattern within the various zones of cartilage • Few chondrocytes present in the form of small clusters • 85% chondrocytes were normal • 17±2% chondrocytes had cytoplasmic processes • The average length of cytoplasmic processes was ≤5µm
Grade-1	• Uneven surface • Rough surface • Discolouration of cartilage • Splitting and pitting of cartilage	• Rough/eroded surface • Chondrocyte orientation pattern was disturbed • Large clusters present with greater number of cells per cluster • 65% chondrocytes were normal • 35±5% chondrocytes had cytoplasmic processes • The percentage of abnormal cells, number of processes per cell and length of processes followed a trend throughout cartilage depth, having greatest values in SZ, lesser in MZ and least in the DZ.

Table 3.2: Characteristics of grade-0 and grade-1 human femoral head articular cartilage.
The surface properties of cartilage and chondrocyte morphology taken into consideration to grade the cartilage explants.

Chondrocyte cell death is common feature of cartilage degeneration in OA (Kim et al., 2000); in this chapter PI-labelled chondrocytes were hardly visible in the axial low and high power CLSM images of grade-0 and grade-1 human femoral cartilage (Figs. 3.6 & 3.7). In the coronal CLSM images of grade-0 and grade-1 cartilage PI-labelled chondrocytes were present (Figs. 3.9 & 3.10). The possible explanation could be that the DNA degrading enzymes in synovial fluid similar to FCS could have digested the DNA of dead cells thus rendering PI-labelling impossible in axial images (Zhou et al., 2011). In the coronal sections the cut edges were imaged and the cell death was a result of cartilage trimming during preparation of osteochondral explants as reported by others (Amin et al., 2008a).

CLSM with fluorescent-mode is a powerful technique which rendered the determination of three-dimensional living *in situ* chondrocyte volume possible in relatively unperturbed ECM (Errington et al., 1997, Bush and Hall, 2001a, Bush and Hall, 2001b). The details of the volume measurement protocol by using 3D image analysis software and the correction factor applied have been discussed in detail in Materials and Methods section of chapter 4 in this thesis. The correction factor utilised for calculation of volume of chondrocytes in human and bovine chondrocytes was identical. The results showed variable but reproducible values of chondrocyte volume in the various zones of human femoral cartilage. In the SZ, MZ and DZ the volume of chondrocytes ranged from 254 to 2079 μm^3, from 272 to 2686 μm^3 and from 255 to 2080 μm^3 respectively (Figs. 3.8a-c). The mean and ranges of volumes of chondrocytes in various zones in human tibia plateau and human femoral head cartilage were compared (Table 3.3). The values were different from the volume of cells from tibia plateau cartilage ranging from 193 to 903 μm^3 in SZ, from 135 to

2093 μm^3 and from 273 to 1703 μm^3 for MZ and DZ, respectively as reported already (Bush and Hall, 2003). There was marked heterogeneity in the volumes of chondrocytes in each zone both in tibia plateau and human femoral head cartilage with the greatest in MZ. In the tibia plateau cartilage the mean volume of chondrocytes was greatest in the DZ but was greatest in the MZ in femoral head cartilage in this study. These differences in the volumes of chondrocytes in different joints were possibly due to (a) differences in experimental techniques used in the present and previous study (b) differences in loading patterns and biomechanics of knee and hip joints.

Source of cartilage	**Volume of chondrocytes (μm^3) Mean and range**		
	SZ	**MZ**	**DZ**
Tibia plateau	396 193 to 903	522 135 to 2093	590 273 to 1703
Femoral head	912 254 to 2079	1113 272 to 2686	927 255 to 2080

Table 3.3: Comparison of chondrocyte volume in various zones of grade-0 human tibia plateau (Bush and Hall, 2003) and femoral head articular cartilage (author's results).
Values are given as mean and the range of volume in SZ, MZ and DZ of cartilage.

The results in this chapter showed that in the grade-0 and grade-1 human femoral cartilage there were two key findings regarding the morphology of chondrocytes. **Firstly,** in grade-1 cartilage numerous large clusters were present as compared to grade-0 where few small sized clusters were observed. Additionally, clustering was more pronounced in SZ of grade-1 cartilage as compared to grade-0 (Fig. 3.12). **Secondly,** in grade-0 cartilage fewer, short cytoplasmic processes were present

within chondrocytes of all zones. In grade-1 cartilage these cytoplasmic processes were present mostly in the SZ, less in the MZ and least in the DZ. The number of processes per cell and the length of processes followed similar trend (Fig. 3.13).

Chondrocyte clustering was routinely seen in the grade-1 cartilage as described by others as a hallmark of degeneration in OA (Mitchell et al., 1992, Lotz et al., 2010) but was evident in the SZ (Fig. 3.9). The occurrence of clusters in the SZ might be due to the enhanced access of proliferative/growth factors from synovial fluid to these cells due to loosening of matrix (Meachim and Collins, 1962). Additionally, the compromised integrity of the collagen matrix in the SZ might lead to the enhanced proliferative activity of chondrocytes in degenerate cartilage (Hollander et al., 1995).

Another key finding was the presence of cytoplasmic processes emanating from chondrocyte cell bodies within both non-degenerate and mildly degenerate cartilage explants. CLSM technique used here rendered it possible to visualise these fine morphological structures and by using the 3D software Volocity^{TM} these processes were traced in 3D and measured accurately. It is unlikely that these cytoplasmic processes were a cutting artefact as they were clearly visible in the axial images also. The possibility that the cytoplasmic processes were dye labelling or imaging artefacts was negligible because CMFDA labels the cytoplasm of living cells specifically and CLSM causes minimal disturbances to tissue architecture (Brakenhoff et al., 1990). The presence of these processes in the non-degenerate cartilage raised the possibility of having these processes as an early change in chondrocyte morphology during degeneration. Moreover, the cartilage samples used in this study were from elderly patients suggesting that these cytoplasmic processes might be the result of normal

aging process. Another evidence to support this theory is the absence of these processes in a single human cartilage sample obtained from a relatively younger patient in this study (Fig. 3.26). The age of the patient was 55 yrs. operated for acute fracture of subtalar joint. The chondrocyte morphology was normal with no cytoplasmic processes present both in the axial and CLSM views of sample (Figs. 3.27 & 3.28). This theory can be further supported by stating that bovine chondrocytes showed no evidence of presence of these processes and were obtained from 3 yr. old cows (Chapter 6). It is also possible that the grading system employed in this study was slightly different, due to which the cartilage categorized as grade-0 might not be grade-0 strictly and can be grade-0.5 instead. This can possibly explain the presence of cytoplasmic processes in non-degenerate cartilage.

There is existing evidence that in several previous studies presence of cytoplasmic processes was observed but they were not comprehensively studied (Stockwell, 1978, Kouri et al., 1996b, Lee and Loeser, 1998, Kouri and Abbud-Lozoya, 2002). In the study by Kouri and co-workers these cytoplasmic extensions were named as filopodia and they suggested that these structures have a possible role in cell migration and grouping to form clusters. One possible reason why these cytoplasmic processes were not studied extensively in the previous studies could be the limitations of the techniques utilised. In most of these studies histological techniques were applied and it is possible that dehydration and fixation steps involved in histology caused cell shrinkage and thus obscured these fine morphological details. The presence of these cytoplasmic processes was first reported in a study done on tibia plateau cartilage by using fluorescent-mode CLSM and reported that even in non-degenerate cartilage 40% of chondrocytes had these cytoplasmic processes

(Bush and Hall, 2003). In this previous study the authors also suggested two possible theories i.e. active and passive theories for the production of these processes. These tibia plateau cartilage samples were obtained from patients undergoing total knee replacement (TKR) therefore it is difficult to obtain non-degenerate cartilage from an OA failing joint. In comparison to these samples the human femoral head samples used in the present study were obtained from patients undergoing hip replacement surgery without known degenerative disease of joint. Therefore grade-0 cartilage samples utilised in this study are more likely to be actually non-degenerate. This may also possibly explain the presence of these cytoplasmic processes on 17% chondrocytes as compared to 40% reported in the previous study.

In the present study several findings regarding the existence of these cytoplasmic processes potentially added to already existing knowledge about this morphological structure. **Firstly,** presence of cytoplasmic processes in human femoral non-degenerate cartilage, **secondly**, with cartilage degeneration number and length of the processes increased and **lastly**, these processes were most numerous in the SZ of cartilage. The possible explanation for the existence of these processes in cartilage degeneration could be attributed to the damage to the PCM either due to loss of PGs or due to disruption of collagen Type VI. This weakened immediate micro-environment of chondrocytes could allow cytoplasm to protrude out and form processes. PCM plays a vital role in transducing chemical and mechanical signals in articular cartilage (Guilak et al., 2006) and therefore regulates structure and functions of chondrocytes. These abnormal chondrocytes will possibly produce altered matrix causing further destruction of ECM. However, the exact mechanism for initiating this process is unknown. The possible explanation for the presence of greatest

heterogeneity of chondrocyte morphology in the SZ could be due to greater access of proliferative/growth factors to these chondrocytes caused by cartilage loosening (Hollander et al., 1995).

The samples from five different patients were also obtained suffering from other clinical conditions, such that three samples were from OCD patients, one from AVN and one from an acute fracture trauma. The grading of the cartilage samples suffering from OCD was not possible because they were small samples but grossly the cartilage surface was intact which suggested they were macroscopically normal (Figs. 3.15, 3.17 & 3.20). In the AVN sample the whole femoral head was abnormal in shape and there were raised and depressed areas but the cartilage did not show any surface fibrillations (Fig. 3.23). The cartilage sample obtained from the fractured subtalar joint was very small and grading of cartilage was difficult but cartilage surface appeared to be intact and healthy (Fig. 3.26). These clinical samples belonged to younger patients as compared to the femoral head grade-0 and grade-1 discussed earlier in this study. The patients were suffering from OCD and AVN for few months before these samples were obtained but the one obtained from fractured subtalar joint was obtained within days after fracture. The results showed that in the cartilage samples obtained from patients who suffered from OCD and AVN chondrocytes displayed obvious morphological changes (clusters/processes). However, the sample obtained after fracture showed that chondrocytes in all the zones of cartilage had normal morphology with no evidence of clusters/cytoplasmic processes (Figs. 3.27 & 3.28). Moreover, the clusters and processes were present mostly within SZ and MZ but the cells in the DZ were relatively normal in morphology. The possible explanation for the presence of cytoplasmic processes in

OCD could be due to absence of weight bearing on these loose bodies. These fragments were possibly detached and floating in the joint space for months without weight bearing which may lead to the cartilage destruction and appearance of cytoplasmic processes. In AVN the presence of morphologically abnormal chondrocytes is possibly related to cartilage degeneration due to decreased blood supply/nutrition and necrosis of the bone. The presence of cytoplasmic processes in OCD and AVN samples and in human femoral head grade-0 cartilage suggested that this may be a key morphological feature of cartilage degeneration. In a previous study the histological evaluation of OCD samples revealed the presence of bone necrosis and cartilage degeneration (Yonetani et al., 2010). In this previous study irregularity and fibrosis in the superficial layers and normal deep layers were reported. In the present study chondrocytes in the deep layers of OCD cartilage were normal and this is in agreement with the previous study. However, in the present study the fine details of chondrocyte morphology have been presented in the CLSM axial and coronal images thereby increasing our knowledge regarding the irregularity in superficial layers mentioned in the previous study. Our findings regarding the presence of cytoplasmic processes is in agreement with a previous morphological and molecular study conducted on OCD fragments where cytoplasmic extensions of chondrocytes were observed (Skagen et al., 2011). However, in the previous study the morphological analysis was performed on the histological sections whereas, in the present study fluorescent-mode CLSM has been performed to obtain 3D images of chondrocyte morphology in OCD.

Further, investigations are required in order to explore the role of cytoplasmic processes in cartilage degeneration.

CHAPTER 4: RESULTS

THE EFFECTS OF VARYING GEL STRENGTH AND FCS CONCENTRATION ON THE MORPHOLOGICAL CHARACTERISTICS OF BOVINE CHONDROCYTES CULTURED IN 3D AGAROSE GELS

4.1 CHAPTER SUMMARY

Chondrocyte morphology has a strong influence on the metabolism of extracellular matrix (ECM). As a first step towards understanding this relationship a 3D agarose gel model was utilised to study changes in chondrocyte morphology. Chondrocyte shape can be altered by using strong/weak gels and this is a model to study the effect of gel strength and increasing concentrations of FCS on chondrocyte properties. Chondrocytes were isolated from bovine metacarpal-phalangeal joints using collagenase. Gels were prepared with variable agarose concentration as strong or weak (2% or 0.2% (v/v) to determine the effect of gel strength on chondrocyte morphology and cultured for 14 days in DMEM (380mOsm; with added NaCl, 10% FCS and 50µg/ml ascorbic acid) at 37^{o}C; 5%CO_2; pH 7.4. In some of the experiments varying concentrations of FCS 1-10% were added to the culture medium and cells were cultured for 7 days. Chondrocytes were fluorescently-labelled with CMFDA and PI (for live and dead cells at day 1 of culture), with CMFDA and DRAQ5 (at days 3 and 7) and volume/morphology examined by confocal microscopy at distinct time points and data were presented as Mean±S.E.M. After one week of culture, chondrocyte density in strong gels remained unaffected and chondrocytes were mostly spheroidal; 18.5±1% chondrocytes exhibited fine processes and 42.5±0.1% of the chondrocytes in defined region of interest formed small clusters with average number of 3.9±0.2 cells/cluster. However, in weak gels, chondrocyte density increased significantly as compared to strong gels (P=0.03), and 66.9±1.3% (P=0.006) of chondrocytes had processes with lengths 7-63µm and 76±5% of the cell population (P=0.001) were present in large clusters with average number of 6.3±0.5 cells/cluster (P=0.002). In the weak gel after seven days,

increasing FCS concentration markedly elevated the %age of chondrocytes in clusters from 31.1±0.2% in 1% FCS, to 87.3±0.23% in 10% FCS (P<0.05). Additionally, the percentage of chondrocytes with processes increased with increasing concentration of FCS from 14.4±0.2% in 1% FCS, to 88.7±1.6% in 10% FCS (P<0.001). In summary chondrocytes cultured in weak 3D gels and with high concentrations of FCS displayed morphological changes (clusters/processes) as compared to those in the strong gels and with low concentrations of FCS. Chondrocyte morphology changed in the weak agarose gels, suggesting that these morphological changes might play a role in changes to matrix metabolism.

4.2 INTRODUCTION

In OA, the chondrocytes produce changes in matrix metabolism leading to cartilage degeneration (Aigner et al., 2007). Various biomechanical, biochemical and genetic factors lead to an imbalance in the normal turnover of articular cartilage by disrupting cell-matrix associations (Goldring, 2000a). As a generally accepted view in OA these disturbances include loss of proteoglycans and disorganization/loosening of collagen network which begins near the surface of the cartilage (Desrochers et al., 2012). The loosening of collagen network leads to softening and swelling of the cartilage (Aigner and McKenna, 2002). The disease process is generally thought to occur in two phases: (a) biosynthetic phase in which the chondrocytes attempt to repair the damaged cartilage and (b) degenerative phase during which the enzymes produced from these cells destroy the matrix. These changes reduce the load bearing capacity of cartilage thus making it mechanically fragile and resulting in its progressive loss (Howell, 1986).

In early OA, chondrocytes attempt to restore the damaged cartilage by enhanced synthesis of aggrecans and collagen type II in response to these biochemical changes in the matrix properties (Lippiello et al., 1977, Eyre et al., 1980, Aigner et al., 1992). Various growth factors play a significant role in the cartilage repair by stimulating synthetic activity of chondrocytes (Fortier et al., 2011). The reaction pattern of chondrocytes includes rapid proliferation, increased synthesis of collagens and proteoglycans and enhanced production of matrix degrading enzymes (Goldring, 2000a). Various studies conducted to study the osteoarthritic changes in human articular cartilage reported that the chondrocytes making an inappropriate and mechanically weak cartilage became hyperactive and proliferated forming clusters of cells, a hallmark of OA (Weiss and Mirow, 1972, Rothwell and Bentley, 1973, Mitchell et al., 1992, Kouri et al., 1996b, Pfander et al., 2001). It has been suggested that this cluster formation could be due to an enhanced access to the growth and proliferative factors from the synovial fluid due to loosening of the cartilage matrix (Meachim and Collins, 1962).

Although changes in the biochemical environment of the cartilage in OA have been studied in detail the biosynthetic response of chondrocytes to these degenerative changes associated with morphology of these cells has not been comprehensively studied. In several studies conducted on OA cartilage the morphologically abnormal chondrocytes were observed but they were not studied comprehensively in association with the cartilage degeneration (Stockwell, 1978, Lee and Loeser, 1998, Tesche and Miosge, 2004). The possible reason could be the histological techniques used in these studies resulted in the cell shrinkage and masking of these cytoplasmic processes. As an example in a previous study conducted on bacteria the scientists

noticed considerable cell shrinkage due to dehydration during histological procedure (Woldringh et al., 1977). Therefore, the conventional histological methods rendered it impossible to study chondrocytes without alteration in their morphology. However, in this work fluorescent-mode CLSM was utilised to study the morphological properties of chondrocytes in thick gel moulds (Brakenhoff et al., 1990) in a relatively unperturbed environment. Additionally, by using CLSM 3D morphology of chondrocytes has been determined in this study as compared to the previous studies with 2D image analysis of chondrocyte morphology. Therefore, CLSM rendered it possible to study fine morphological details of chondrocytes in 3D (cytoplasmic processes) thereby providing new insights into changes to chondrocyte morphology.

Few studies conducted on chondrocyte volume and morphology in OA demonstrated abnormal chondrocyte morphology in this disorder (Kouri et al., 1998, Bush and Hall, 2003). When the morphology of chondrocytes was studied using vital fluorescent stains and CLSM imaging technique in both normal and degenerate cartilage, 40% cells had cytoplasmic processes as shown in Figure 4.1 (Bush and Hall, 2003). In this previous study morphologically abnormal superficial zone chondrocytes were even observed in macroscopically normal cartilage suggesting a paradox that even the cartilage was macroscopically normal but microscopically there were signs of early OA. Another possibility for the presence of these abnormal cells in macroscopically normal cartilage could be that the occurrence of processes on cells is a result of normal aging process. An evidence to support this theory is that in bovine chondrocytes (obtained from young 3 yr. old cows) these cytoplasmic processes were never observed. In osteoarthritic femoral head cartilage with pannus

cells with multiple elongated cytoplasmic processes were observed (Holloway et al., 2004). Furthermore, there exists a relationship between chondrocyte morphology and its biosynthetic activity. It was reported in a study that the abnormal chondrocytes in OA led to the disruption of collagen type VI and increased levels of IL-1ß (Murray et al., 2010).

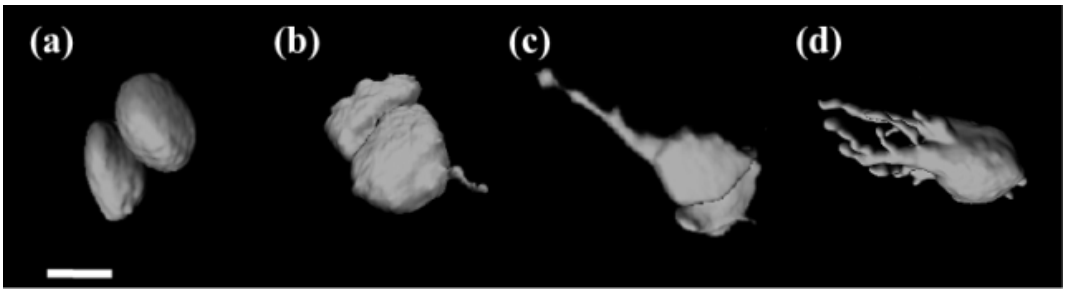

Figure 4.1: Examples of morphologically abnormal human articular mid zone chondrocytes.
This figure illustrates features that were used to describe in situ mid zone chondrocytes with varying morphologies. The chondrocytes in this zone were (a) 'morphologically normal' and spheroidal with a relatively smooth surface. Some cells as illustrated in (b), had a single small (<8 μm) cytoplasmic processes, whereas in others as shown in (c), the single process from one chondrocyte extended by more than 8 μm. Occasionally, as shown in the example in (d), a single chondrocyte had multiple processes, some of which were greater than 8 μm. (Adapted from Bush and Hall, 2003). Scale bar = 10μm.

In order to study chondrocyte morphology, cell isolation and *in vitro* culture techniques give a wide range of flexibility for altering the culture conditions and also changes in morphology can be studied over a time course by keeping the cells alive for several weeks. It has been reported previously that chondrocytes de-differentiate (flattened fibroblast-like shape) when cultured in 2D and also accompanied by altered expression of the ECM (type I collagen) because of the phenotypic changes (Mark et al., 1977, Marlovits et al., 2004). However, these de-differentiated cells could be differentiated (rounded shape) back to their normal phenotype with the re-

expression of functional matrix (type II collagen) when cultured back in 0.5% 3D agarose gels (Benya and Shaffer, 1982). The cellular morphology and cell-matrix interactions differed in 2D and 3D environments significantly (Cukierman et al., 2001). Therefore, providing a 3D environment for chondrocyte culture may enable the cells to overcome the phenotypic problems associated with 2D cultures as 3D system mimics the *in vivo* conditions (Schuh et al., 2012a). Moreover, chondrocytes cultured in 3D agarose cultures produce mechanically functional ECM (Buschmann et al., 1992).

In the present study 3D agarose gels with two different gel strengths (strong and weak) were used to culture chondrocytes to study their morphology. The strong gels were used as a control to compare intact cartilage and weak gels as experimental condition to compare weakened matrix in cartilage degeneration. The purpose of using these gel strengths was to use gel stiffness as a tool to control chondrocyte shape. The agarose gels were considered a suitable model to culture chondrocytes because they can maintain their phenotype in agarose gels during long term culture (Benya and Shaffer, 1982, An et al., 2001) and also because chondrocytes produce mechanically functional matrix when cultured in 2% agarose gels (Buschmann et al., 1992).

Gel stiffness influences chondrocyte proliferation and rate of production of ECM as reported previously (Schuh et al., 2012b). Chondrocytes when cultured in weak gels (0.75%) as compared to stiff gels (1.5%) had a greater cell density and amount of ECM after two weeks (Schuh et al., 2012b). Although effect of gel stiffness on chondrocyte biosynthetic properties was studied the effect of gel strength on chondrocyte morphology was not studied in detail previously.

The increasing concentration of agarose decreases penetration of serum factors (Johnson et al., 1996) and the response of bovine chondrocytes to growth factors has been studied to be affected by the culture conditions (van Susante et al., 2000). Therefore, in the present study FCS concentration was varied to determine its effect on chondrocyte morphology. Cell tracker green (CMFDA) fluorescent molecular and DRAQ5-DNA dyes were used to label the cytoplasm and nuclei respectively, when imaged by CLSM provided 3D information about the morphology and density of cells.

The main aims of this chapter were (a) to develop a model to determine at what stage of culture chondrocytes change shape (b) to study the effect of gel strength on chondrocyte morphology and (c) to study the effect of increasing concentrations of FCS on chondrocyte morphology.

4.3 HYPOTHESES

4.3.1 Primary hypothesis

Bovine chondrocytes cultured in weak 3D agarose gels show increased volume and abnormal morphology (clusters/cytoplasmic processes) as compared to strong gels.

4.3.2 Secondary hypothesis

Increasing concentrations of FCS accelerate changes in the volume and morphology of bovine chondrocytes cultured in weak 3D agarose gels.

4.4 MATERIALS AND METHODS

4.4.1 3D agarose gel model to culture isolated bovine chondrocytes

4.4.1.1 *Isolated bovine chondrocytes*

4.4.1.2 *Bovine joint dissection and cartilage removal*

Bovine metacarpal-phalangeal joints of 3 yr. old cows were obtained from a local abattoir and washed to remove mud and faeces. The skin and hoof were removed using a number 24 scalpel blade. The joint was then sprayed with 70% (v/v) alcohol and under aseptic conditions dissected in a class 1-flow hood by using a number 24 blade to cut open the joint. The joint was examined carefully to ensure the joint capsule had not been punctured and whether cartilage was non-degenerate or degenerate in appearance. Non-degenerate joints had healthy cartilage with smooth surface and without fissures whereas, joints with irregular cartilage surface and discoloration were considered degenerated/unhealthy. The macroscopic appearance of joints for healthy and degenerate was assessed in this study according to the criteria mentioned in a study performed on human knee joints (Musumeci et al., 2013). The degenerate and punctured joints were discarded and only non-degenerate un-punctured joints were included in the study. Healthy full depth (FD) explants of cartilage down to and including small sections of subchondral bone were removed carefully with a number 11 scalpel blade from load-bearing areas of this hinge joint (Fig. 4.2). The cartilage explants (approximately 0.35 g) obtained from one joint were washed twice with DMEM 380mOsm (section 2.1.1) to remove synovial fluid and then transferred to 380mOsm DMEM (20ml) and cultured at 37˚C, 5% CO_2 (pH 7.4) until required.

Figure 4.2: Bovine joint dissection and cartilage removal.
Bovine feet (a) washed, (b) skin and hoofs removed, (c) metacarpophalangeal joint dissected out and cartilage removed. Scale bar for all panels = 10cm. Photographs kindly provided by Dr. Innes D M Smith, Centre for Integrative Physiology, University of Edinburgh.

4.4.1.3 *Isolation of chondrocytes from bovine articular cartilage*

The cartilage obtained was incubated with collagenase (0.8mg/ml) for approximately 18 hrs at 37˚C, 5% CO_2 (pH 7.4) for the enzyme to weaken the ECM of the cartilage samples, thus releasing the chondrocytes (Kuettner et al., 1982). The flask was then gently mixed to loosen undigested cartilage. Under strict aseptic conditions in the flow hood, the sample was filtered initially through a tea strainer and flushed through with excess 380mOsm DMEM. Later the filtrate was again filtered through a nylon cloth filter (Monodur®) with a pore of 200µm. The filtrate was topped up with 380mOsm DMEM to 50 ml and centrifuged (Hettich Zentrifugen Universal 32 R) at 21˚C, 1500 RPM for 10 min with an accelerating and decelerating setting of 9. The supernatant was pipetted off carefully and the remaining cell pellet gently re-suspended in 380mOsm DMEM. This was repeated once again until a clear pellet was obtained and was then re-suspended in approximately 2ml of DMEM. A 1:1 preparation of the chondrocyte solution with 1% trypan blue stain (Thermo Fisher Scientific, UK) was prepared by mixing 5µl of each. A haemocytometer was charged

with this cell suspension and the cells were counted. There were few dead cells and the cell viability was ~99%. The samples with cell viability below 95% were discarded. Samples with a count of approximately 30 x 10^6 cells /ml were used and the final cell density in the gels was approximately 15 x 10^6 cells /ml for culture similar to seeding densities previously utilised (Buschmann et al., 1995, Mauck et al., 2002). Isolated chondrocytes in 380mOsm DMEM were kept at 37˚C in the water bath inside the flow hood until required.

4.4.1.4 *Chondrocyte culture in strong and weak agarose gels*

Gels were prepared 4% w/v by mixing 4g low melting point (LMP) agarose thoroughly in 100 ml of PBS and heated in the microwave (180°C) for about 30 seconds. The small volume of PBS evaporated during heating was restored and stirred thoroughly. The agarose solution was incubated in a water bath to bring the temperature to 37˚C before being poured in the rectangular gel cast (124mm x 88mm) and 7mm deep (Fig. 4.3a). The gel cast was placed on ice in a box to cause rapid cooling of the agarose solution to set the gel promptly. After about 15 min, the gel mixture was poured in the cast while still on the ice. A Perspex sheet with 5mm long rods was placed on the cast and kept at approx. 8°C for 15 min to obtain properly formed wells in the gel mould (Fig. 4.3b). The chondrocyte cell suspension was divided into equal parts in order to culture them in the gels of two different strengths of 0.2% and 2% w/v agarose solutions (section 4.2), prepared by mixing 0.04 and 0.4 g of agarose powder in 10 ml of PBS respectively. Some pilot experiments were performed using three different concentrations of agarose (2%, 0.5% and 0.2% w/v) in order to determine appropriate concentrations of agarose for strong and weak gels. Based upon the results of these pilot experiments it was

observed that after 1 week chondrocytes cultured in 0.5% gels displayed less shape changes as compared to 0.2% gels. Therefore, 2% and 0.2% w/v agarose concentrations were used as strong and weak gels in this study. The agarose was mixed thoroughly in PBS by heating in the microwave and the volume kept at 10ml for each solution, then incubated for 15min (37˚C). The agarose solutions were mixed in the chondrocyte cell suspensions 1:1, mixed thoroughly but gently and pipetted into pre-formed wells in the gel by using pre-warmed pipette tips throughout. The gel cast was placed on the ice box to cause the rapid cooling of the chondrocyte-gel solutions especially for the weak gels. Each solution was pipetted with fresh pipette tips in the wells of the gel cast. The gel was placed in the fridge for 2hr to set. Blocks of gel were then cut with a sterile scalpel blade and placed in 6 well culture plates with 9 ml of DMEM 380mOsm pipetted in each well and incubated at 37˚C with 5% CO_2 (pH 7.4) until required (Fig. 4.3c). The culture medium was changed with freshly prepared culture medium on alternate days during the culture period.

In the experiments where the effect of gel strength on chondrocyte morphology was studied, the culture medium contained the same concentration of FCS (10%). However, in experiments performed to investigate the effect of increasing concentrations of FCS on chondrocyte morphology, the composition of the culture medium was altered, by culturing these chondrocytes in different concentrations of FCS (1%, 2%, 5% and 10%) both for strong (2%) and weak (0.2%) gels. The solutions with 1%, 2%, 5% and 10% FCS were prepared by adding 5ml, 10ml, 25ml and 50ml respectively to 500ml of culture medium and then pipetted into the culture

plates. Apart from the concentration of FCS in the serum the remaining methodology of these experiments was same as already described.

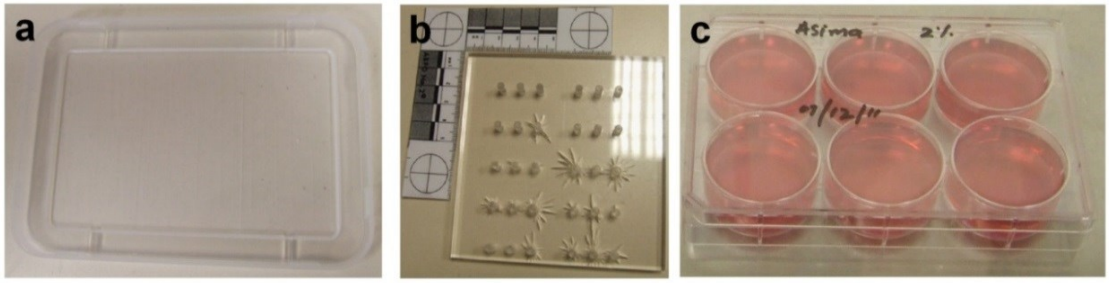

Figure 4.3: Chondrocyte culture in 3D agarose gels.
The gel mould prepared in (a) the rectangular gel cast with dimensions L=124mm, B=88mm and depth=7mm, (b) Perspex sheet with 5mm long rods to make wells in the gel mould and (c) 6-well culture plate for keeping the gels in culture in the incubator.

4.4.1.5 *Preparation of cultured chondrocytes for microscopy*

Isolated bovine chondrocytes were cultured in strong and weak agarose gels and kept in the incubator under controlled conditions up to 7 days. During the course of culture chondrocytes were viewed by CLSM at three time points. At day 1 chondrocytes were incubated with CMFDA (12.5µM) and PI (5 µM) and at days 3 and 7 with CMFDA (12.5µM) and DRAQ5 (18 µM) as final concentrations in the well during the last hour of incubation, to label the cytoplasm (green) and nuclei (red) respectively. DRAQ5 is a far-red fluorescent DNA dye which stained the nuclei of chondrocytes (Martin et al., 2005) and rendered counting of the cells possible in the clusters (section 2.1.2). The gels were then washed in PBS to remove excess of dye, fixed in 4% formaldehyde for 30mins and mounted in small cell culture dishes (Cellstar®; 35x10mm) with Super Glue gel (Loctite). A pin-head size drop of glue

was applied to the base of the dish and one of the edges of the gel block was gently placed on it and allowed to attach. The chondrocytes cultured in wells were considerably distant from the point of attachment of gel and were imaged within ~30 min by confocal laser scanning microscopy (CLSM) and the samples were stored in PBS at 4°C (in dark) prior to imaging.

4.4.1.6 *Acquisition of images of chondrocytes cultured in 3D agarose gel by CLSM*

The fluorescent images of the chondrocytes cultured in different gel concentrations were obtained using a Zeiss Askioskop LMS510 confocal microscope with x10 (dry), or x40 Dipping Water (DW) and x63 DW lenses having numerical apertures (NA) of 0.3, 0.8 and 0.95 respectively. Argon/2 laser with the excitation wavelength (EX_λ) of 488 nm and HeNe2 laser with EX_λ = 633 nm or 543nm were used to excite the fluorophores CMFDA and DRAQ5 or PI respectively and the emission then measured through a band pass filter of 505-530 nm and a long pass filter of 650 nm respectively. The images were optimized by adjusting detector gain and offset slider to minimise pixel saturation and background intensity respectively. The Z stack images acquired were 5.8µm steps typically 100µm deep for the x10, 1µm steps typically 100µm deep for the x40 DW and 1µm steps typically 50µm deep for x63 DW objectives respectively, with a frame size of 1024 x 1024 pixels. The scanning speed for the images was 9 frames/sec with 8-bit (data depth) having a pinhole setting of 1 Airy unit.

4.4.1.7 *Analysis of images using Volocity™ 3D image analysis software*

The 3D images obtained from CLSM by x40 DW objective were then analysed by Volocity™ software version 5.4.1 (Improvision, Coventry, UK). The three dimensional information acquired from CLSM images was visualised and analysed using Volocity™ software to obtain quantitative data. A 3D region of interest (ROI) was applied to the images with the dimensions of x, y, z 230, 230 and 100µm respectively and the number of cells were counted in these specified ROIs. Cell density was calculated as number of cells/mm^3x10^3 by the formula (total no. of CMFDA and DRAD5 labelled cells/ volume of gel imaged).

4.4.1.7.1. Volume measurement protocol by Volocity™

A measurement protocol was developed on Volocity™ to determine the volume of individual, pairs and clusters of chondrocytes in the high power magnification (x40 DW) images. In order to determine the volume accurately, it was essential to determine the edge of the cell precisely and this was achieved by using the threshold segmentation method. By this approach the edge between the cell and the matrix was defined and volume calculated by using the Volocity™ measurement protocol. This measuring protocol determined single cells as separate items but the clusters were identified as a whole unit. The volume of the clusters was measured by the same methodology as explained for individual cells thus by measuring the whole unit as a cluster. This was because the threshold of intensity was similar for all the cells in the cluster and the segmentation of individual cells in the cluster was not possible (Fig. 4.4). The number of cells in the clusters was therefore counted by eye on Volocity™

by counting the DRAQ5 labelled nuclei. The volume of individual cells in a cluster was determined by the formula (total volume of cluster in μm^3/total number of cells in cluster). The percentage of chondrocytes forming clusters was calculated with the formula 100 × (number of cells forming clusters/total number of cells) %. Chondrocytes exist typically as pairs in healthy bovine cartilage (Sasazaki et al., 2008) termed as chondron ("chondron" see foot note[1]), possibly can be isolated as pair during cell isolation step and therefore were not considered clusters in this study. A cluster was defined as a group of more than two cells together in this study.

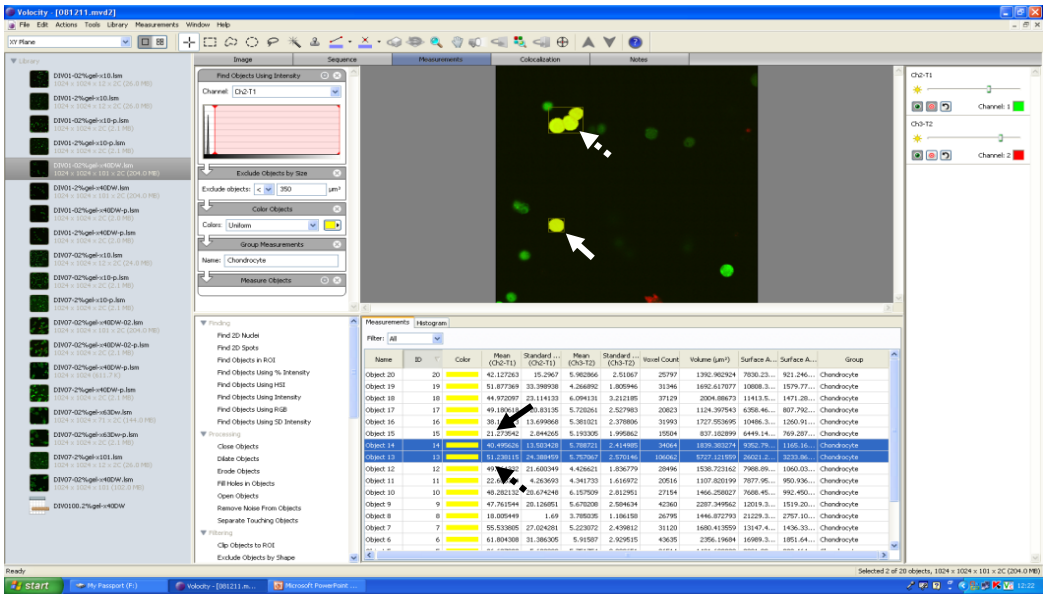

Figure 4.4: Volocity™ measurement protocol.
Examples of confocal microscopy x40 (DW) image of CMFDA labelled chondrocytes. A chondrocyte (solid white arrow) and a cluster (broken white arrow) segmented by Volocity™ measurement protocol identifying objects by intensity and calculating their volumes (μm^3) as indicated by black solid and broken arrows respectively.

"A chondron is defined as the chondrocyte and its pericellular microenvironment" and can exist in single, double or linear column arrangement (Poole, 1997).

4.4.1.7.2. Calibration of Volume measurement protocol

The measurement protocol was calibrated by the fluorescent latex beads. Fluoresbrite™ (Polyscience Inc., Warrington) of known diameter (10.16 μm) and volume (549 μm^3) were imaged under conditions identical to those used for bovine chondrocytes. The diameter of the calibration beads was checked in both planar and axial axes to confirm spherical geometry. The baseline threshold was adjusted to identify edges of the beads and then volume measured. The volumes of the beads both in the strong and weak gels were determined and the values obtained (mean ± SEM) were 762.25 ± 8.21 μm^3 (n=12) and 763.6 ± 15.05 μm^3 (n=8) as shown in Figs. 4.5a & b. There was slight overestimation of volume by this protocol due to diffraction of light and thus the correction factor of 0.72 was determined. The volume measured for chondrocytes were multiplied by this factor to determine the corrected volume and this was in good agreement with a correction factor of 0.7 which was applied by Bush & Hall (2001). The method used to acquire quantitative data from 3D CLSM images is summarised (Fig. 4.6).

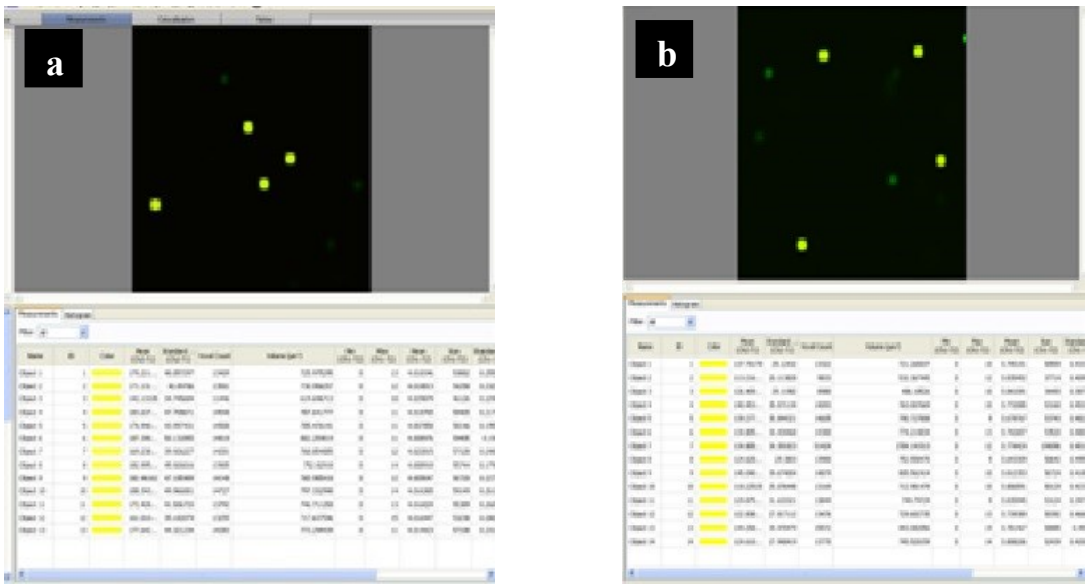

Figure 4.5: Volume measurement of fluorescent latex beads.
CLSM images of fluorescently labelled beads with x40 (DW) objective in (a) 2% and (b) 0.2% gel strengths.

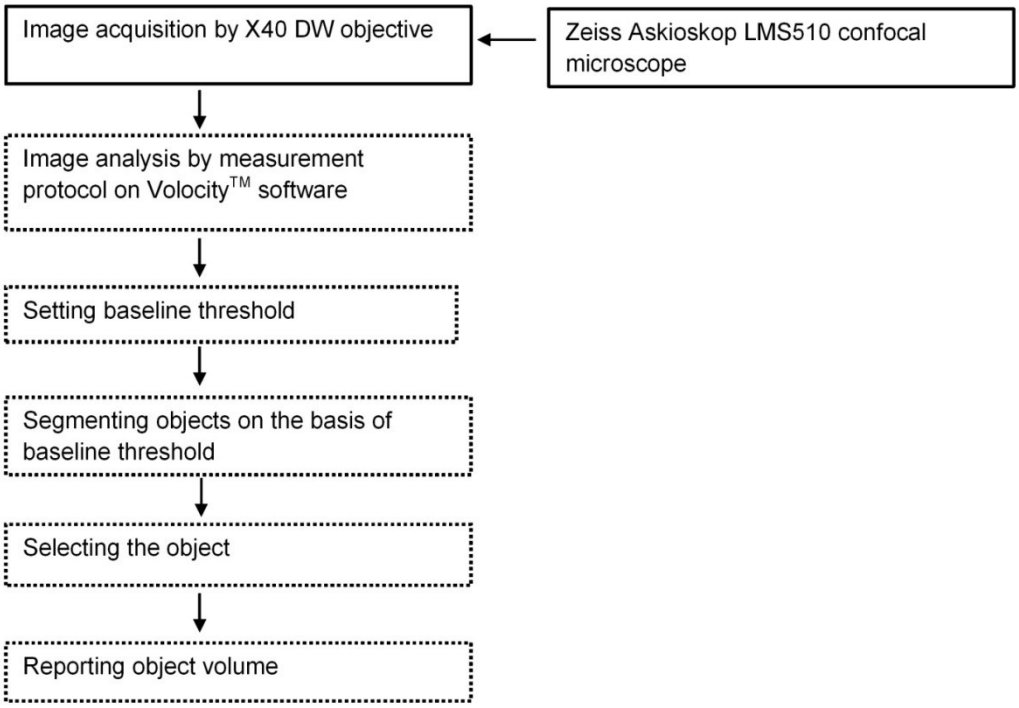

Figure 4.6: A flow diagram demonstrating analysis of images.
The key steps concerned in the analysis of 3D images acquired by CLSM using Volocity™ software shown in the boxes outlined with broken lines.

4.4.1.7.3. Measurement of length of cytoplasmic processes in 3D by Volocity™

The length of the cytoplasmic processes in the images was determined by using Volocity™ software as it enabled the measurement of the length in 3D by tracing the process in the z direction. The methodology utilised is shown in the example of an image with cell having processes (Fig. 4.7). The measurement of the cytoplasmic process was started at its origin from the cell body and then traced throughout its whole length until termination (Fig. 4.7). The length of cytoplasmic processes was categorised into three groups as small (0-29.9 µm), medium (30-59.9 µm) and large (≥60 µm) taking into consideration the minimum and maximum length of cytoplasmic processes in these experiments. The percentage of abnormal chondrocytes was calculated with the formula 100 × (number of abnormal cells/total number of all normal and abnormal cells) %.

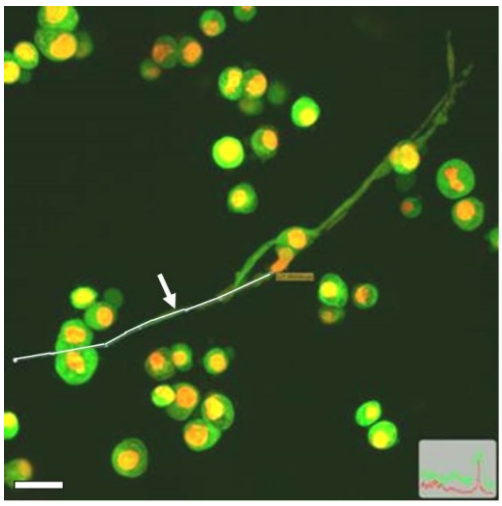

Figure 4.7: Length measurement of a cytoplasmic process in 3D using Volocity™ software.
Example of a x40 (DW) CLSM image of CMFDA and DRAQ5 labelled chondrocyte with cytoplasmic processes demonstrating the methodology to measure the length of the process (as indicated by arrow) in 3D by tracking the process in z direction. (Scale bar=25µm).

4.5 RESULTS

4.5.1 Effect of agarose gel strength on bovine chondrocyte density and morphology cultured in 3D agarose gels with 10% FCS

In the strong gels chondrocyte density remained unaffected and few morphological changes were observed. However, chondrocyte density and morphology changed markedly in the weak strength of agarose gels during the progression of the culture and complex changes were observed (Fig. 4.20). Freshly isolated bovine articular chondrocytes were cultured in strong or weak gel strengths over 14 days and images were obtained by CLSM to visualise morphology of cells at various time points on 1st, 3rd, 7th and 14th day *in vitro*. PI was used to label nuclei of dead cells at day1 and DRAQ5 was used to label the nuclei of live cells (at days 3 and 7) to count the cells involved in forming the clusters (section 4.4.1.5). PI was used at day 1 to assess chondrocyte viability at the beginning of culture and DRAQ5 at later time points because clusters were not present at day 1 and developed later on during culture. Nuclei of the live cells were counted in the specified ROI which enabled measurement of cell density. Quantitative analysis of the cell density, volume and morphology of chondrocytes was performed as described (section 4.4.1.7). The results at distinct time points were presented in the following sections.

4.5.1.1 *Changes to chondrocyte density during 7 days of culture in strong and weak agarose gels*

Quantitative data regarding chondrocyte density were obtained from high power (x40) CLSM images at different time points on 1st, 3rd and 7th day of culture in both strong and weak gel strengths (Figs. 4.10, 4.14 & 4.21). Cell density was unaffected during the course of culture in the strong gel cultures (Fig. 4.8). However, cell

density increased significantly in the weak gels as compared to strong gels by day 7 (14.2±2 and 8.6±0.6 cells/mm^{3}x10^3 [*N(n')*=6(525) and 6(313) respectively]; *P*=0.03; Fig. 4.8). Moreover, the cell density increased significantly in the weak gels by day 7 in comparison with day 1 and day 3 in the same gel strength (*P*<0.05 and *P*<0.001 respectively; Fig. 4.8).

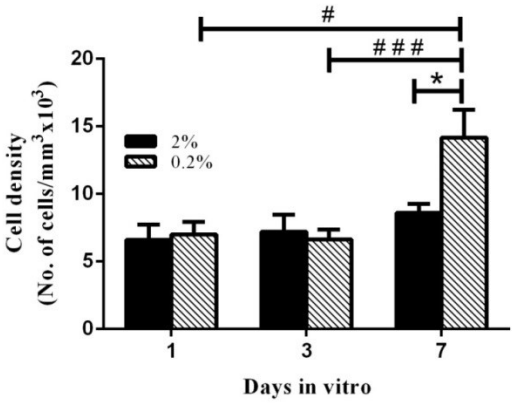

Figure 4.8: Chondrocyte density in the strong and weak gels over 7 days of culture.
Graph shows pooled data on cell density at various time points in strong and weak gels respectively. Data were from [N(n′)=6(175, 228, 313) in strong gels and 6(111, 491, 525) in the weak gels at days 1, 3 and 7 respectively. * indicated a significant difference according to unpaired student's t-test. # indicated a significant difference according to one-way ANOVA followed by Tukey's multiple comparison post-hoc test. The single, double and triple symbols showed the level of significance for *P*<0.05, 0.01 and 0.001 respectively.

4.5.1.2 *Changes to chondrocyte volume at day 1*

The volume of chondrocytes changed considerably when cultured in two agarose gel strengths but chondrocyte morphology remained unaffected and very few cytoplasmic processes were observed. The low (x10) and high (x40) power images of chondrocytes on day 1 showed relatively normal spheroidal morphology of chondrocytes with heterogeneity in cell size in both concentrations of agarose (Figs. 4.9 & 4.10).

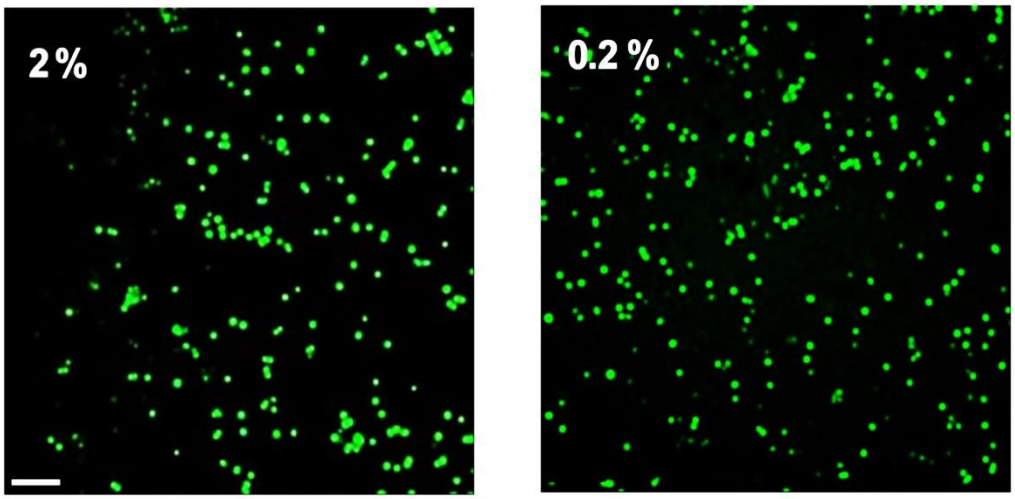

Figure 4.9: Axial CLSM reconstructions of isolated chondrocytes cultured in 3D strong and weak gel cultures.
Confocal microscope low power (x10 objective) images of chondrocytes incubated with CMFDA and PI from day 1 of culture in strong and weak gel strengths. Scale bar = 100µm.

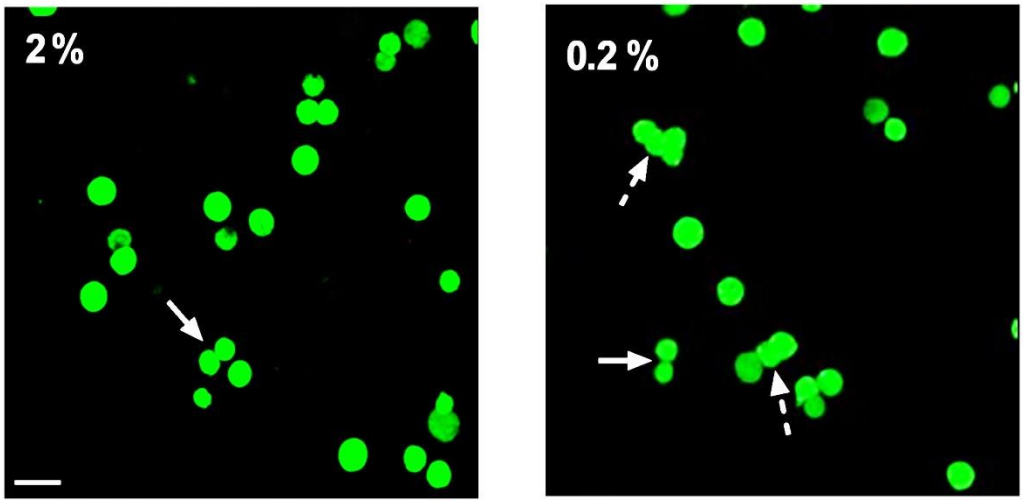

Figure 4.10: Axial CLSM reconstructions of isolated chondrocytes cultured in 3D strong and weak gel cultures.
Confocal microscope high power (x40 DW objective) images of chondrocytes incubated with CMFDA and PI from day 1 of culture in strong and weak gel strengths. Solid arrows indicate examples of pairs of cells and broken arrows indicate examples of clusters. Scale bar = 25µm.

Data regarding the distribution of volume measurements of chondrocytes on day 1 of culture in strong and weak gels were shown in Fig. 4.11. The range for volume of chondrocytes in strong gels was from 262.6 μm^3 to 2412.9 μm^3 and in weak gels from 330.5 μm^3 to 3547.2 μm^3. The highest frequency of chondrocytes in the strong gels had volumes in the range of 700-800 μm^3 whereas in the weak gels the majority of cells had volume in the range of 900-1100 μm^3. The volume of isolated chondrocytes increased significantly on day 1 when cultured in weak gels as compared to the strong gels (P=0.005; Fig. 4.12) suggesting that volume changed after one day of culture.

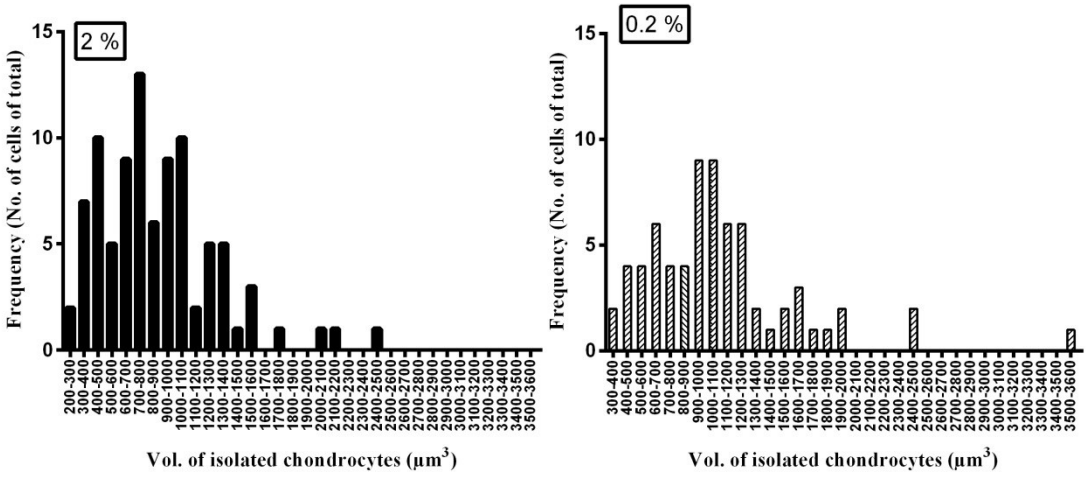

Figure 4.11: Frequency distribution of chondrocyte volume (μm^3) in different gel strengths on day 1 of culture.
Cells were ranked into 100 (μm^3) bands and the values obtained from [*N(n')*=6(91) and 6(69)] samples in the strong and weak gels respectively.

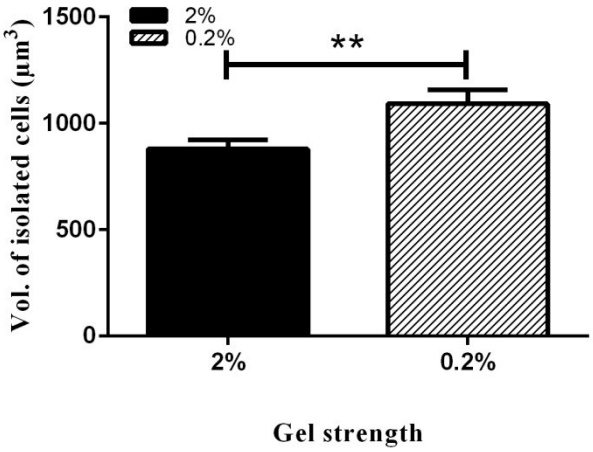

Figure 4.12: Chondrocyte volume increased in the weak gel cultures at day 1. Pooled data regarding the volume of isolated chondrocytes (μm^3) cultured in strong and weak gel strengths at day 1. Values obtained from [*N(n')*=6(91) and 6(69)] samples in strong and weak gels respectively. * indicated a significant difference according to unpaired student's t-test. The single, double and triple symbols showed the level of significance for $P<0.05$, 0.01 and 0.001 respectively.

However, cluster formation and presence of cytoplasmic processes studied in these cultured chondrocytes were not found to be significantly different between both the concentrations of gel (Tables 4.1 & 4.2) at day 1. Very few chondrocytes were present in small sized clusters with an average of 3 cells/cluster. There existed no significant difference between various parameters of clusters present in strong and weak gels at day 1 (Table 4.1). Only 1-2% of the cells had a single fine small cytoplasmic process cultured in both concentrations of gel. One finding worth mentioning is that at day 1 the average length of the processes in weak gels was greater than in strong gel but the difference at this early stage of culture was not statistically significant (Table 4.2). This suggested that although the volume of chondrocytes increased in the weak gels after day 1 of culture, the morphology of the

cells remained virtually unchanged and very few abnormal cells with cytoplasmic processes were present.

Characteristics of clusters formed	Strong (2%) gel	Weak (0.2%) gel	*P* value*
No. of clusters per field of view	2.6 ± 0.5	1.3 ± 0.3	0.1
No. of cells/cluster	3.4 ± 0.3	3.7 ± 0.3	0.5
Av. Volume of clusters (μm^3)	2726.1 ± 357.1	2785.3 ± 666.5	0.9
Av. Volume of individual cell in cluster (μm^3)	795.7 ± 80	803.9 ± 217.3	0.9
% of chondrocytes forming clusters	17.8 ± 6.3	13.6 ± 3.9	0.6

Table 4.1: Characteristics of clusters present in strong and weak gel strengths at day 1 of culture.
Data were presented regarding the number of clusters, number of cells/cluster, volume of clusters, volume of individual cell in a cluster and % of chondrocytes present in clusters on day 1 in strong and weak gels. Data shown as mean ± standard error, ***** indicated probability value result from un-paired Student's t-test with $P<0.05$.

Characteristics of chondrocytes with processes		Strong (2%) gel	Weak (0.2%) gel	*P* value*
% of chondrocytes with processes		1.7 ± 0.4	2.7 ± 0.4	0.4
No. of processes / cell		1.5 ± 0.5	1.5 ± 0.5	0.9
Av. Length of processes (µm)	Small	4.2 ± 0.1	19.5 ± 4.5	0.07
	Medium	0	0	0
	Long	0	0	0
% of chondrocytes with processes according to length categories	Small	1.7 ± 0.4	2.7 ± 0.4	0.4
	Medium	0	0	0
	Long	0	0	0

Table 4.2: Chondrocytes with cytoplasmic processes present in strong and weak gels at day 1 of culture.
Data were presented regarding the % of chondrocytes with processes, number of processes/cell, length of processes and the % of chondrocytes with processes according to length categories on day 1 in strong and weak gels. Data shown as mean ± standard error, * indicated probability value result from un-paired Student's t-test with $P<0.05$.

4.5.1.3 *Development of abnormal chondrocyte morphology by day 3*

Chondrocytes cultured in weak gels displayed marked changes in morphology by day 3 and had cytoplasmic processes emanating from the cell body as compared to the chondrocytes in strong gels (Fig. 4.14). The mean volume of isolated cells cultured in weak gels was significantly 13% greater ($P=0.03$) than those in the strong gels (Fig. 4.15). However, the volume of chondrocytes in weak gels at day 3 when

compared to the volume at day 1 showed no significant difference (P>0.05), suggesting that the chondrocytes by day 3 did not change volume significantly but started producing cytoplasmic processes. The volume measurements of abnormal chondrocytes with processes did not include the volume of processes because when the threshold was applied the processes were not segmented along with the cells. However, the volume of processes appeared to be very small and did not affect the volume measurements of individual cells.

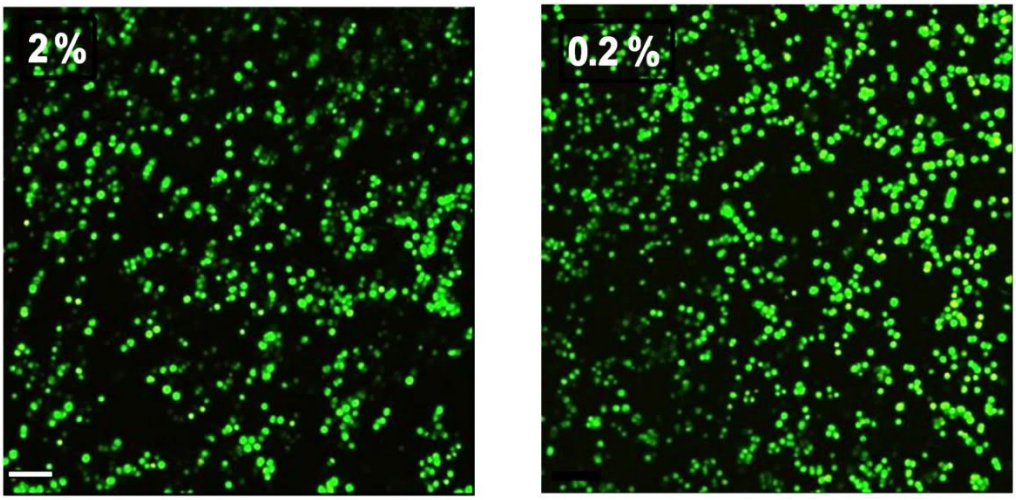

Figure 4.13: Axial CLSM reconstructions of isolated chondrocytes cultured in 3D strong and weak gel cultures.
Confocal microscope low power (x10 objective) images of chondrocytes incubated with CMFDA and DRAQ5 from day 3 of culture in strong and weak gel strengths. Scale bar = 100μm.

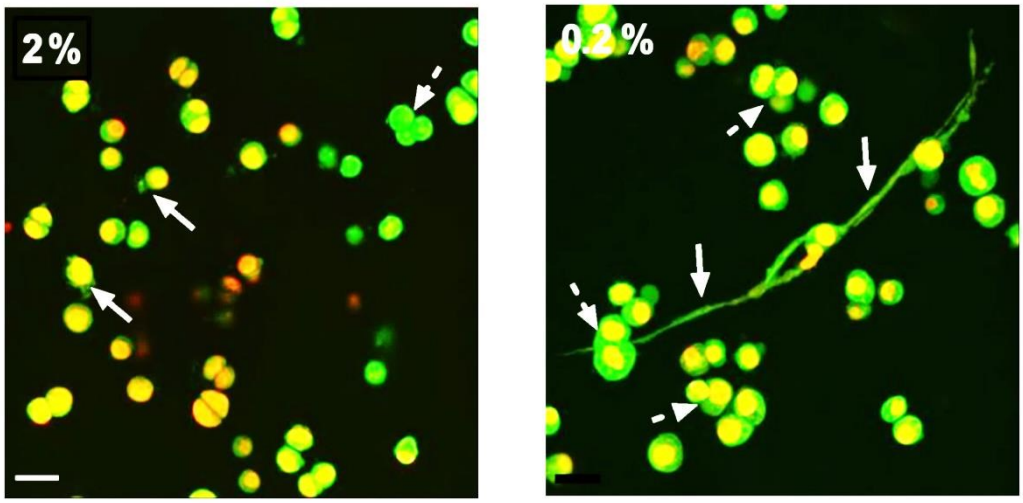

Figure 4.14: Axial CLSM reconstructions of isolated chondrocytes cultured in 3D strong and weak gel cultures.
Confocal microscope high power (x40 DW objective) images of chondrocytes labelled with CMFDA and DRAQ5 from day 3 of culture in strong and weak gel strengths. Solid arrows point to the examples of cells with cytoplasmic processes and the broken arrows indicate examples of cell clusters. Few red cells in 2% gel indicate dead cells. Scale bar = 25μm.

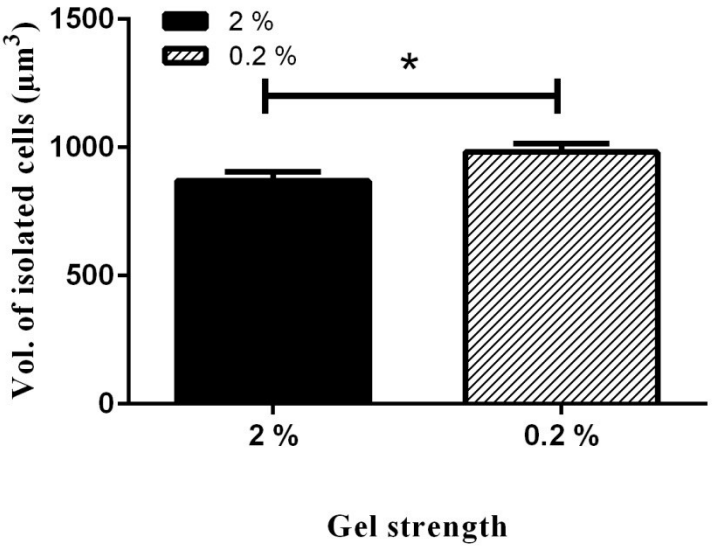

Figure 4.15: Chondrocyte volume increased in the weak gel cultures at day 3.
Pooled data regarding the volume of isolated chondrocytes (μm^3) cultured in strong and weak gel strengths at day 3. Values obtained from [*N(n')*=6(84) and 6(169)] samples in strong and weak gels respectively. * indicated a significant difference according to unpaired student's t-test. The single, double and triple symbols showed the level of significance for $P<0.05$, 0.01 and 0.001 respectively.

At day 1, chondrocyte morphology remained unaffected in strong and weak gels. By day 3, a significantly higher % age of chondrocytes cultured in the weak gels produced cytoplasmic processes in comparison to those in strong gels (P=0.015; Fig. 4.16) where cells were mostly rounded in shape. The average number of processes per chondrocyte was greater in weak concentration of agarose but the difference from strong gels was not statistically significant (P=0.2; Fig. 4.17). Some of the chondrocytes cultured in weak gels developed single or multiple cytoplasmic processes of smaller, medium and longer lengths (section 4.4.1.7.3. for length categories) as compared to the chondrocytes in strong gels which demonstrated only small and medium sized processes (Fig. 4.18).

The average length of small and medium sized processes did not differ in both strong and weak gels but a significantly higher percentage of chondrocytes showed the presence of small, medium and long processes in the weak gels as compared to strong gels (P=0.02; P=0.04 and P=0.03 respectively; Fig. 4.19). Moreover, in the weak gels, the percentage of chondrocytes having smaller processes was significantly higher than the cells with medium and long processes (P=0.001; P=0.01 respectively).

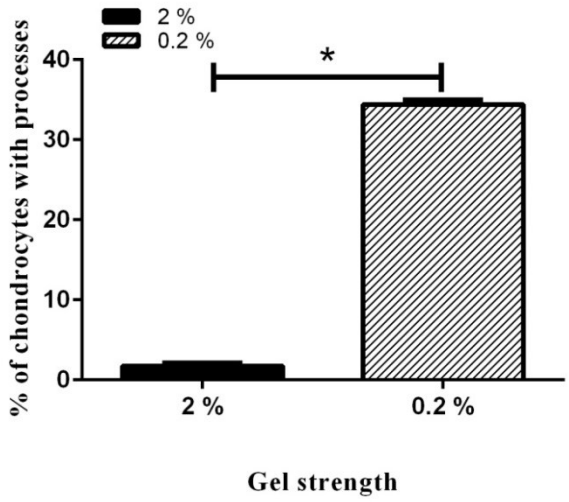

Figure 4.16: Percentage of chondrocytes with cytoplasmic processes increased in weak gel cultures as compared to strong gels at day 3.
Values obtained from [*N(n')*=6(228) and 6(491)] samples in strong and weak gels respectively. * indicated a significant difference according to unpaired student's t-test. The single, double and triple symbols showed the level of significance for *P*<0.05, 0.01 and 0.001 respectively.

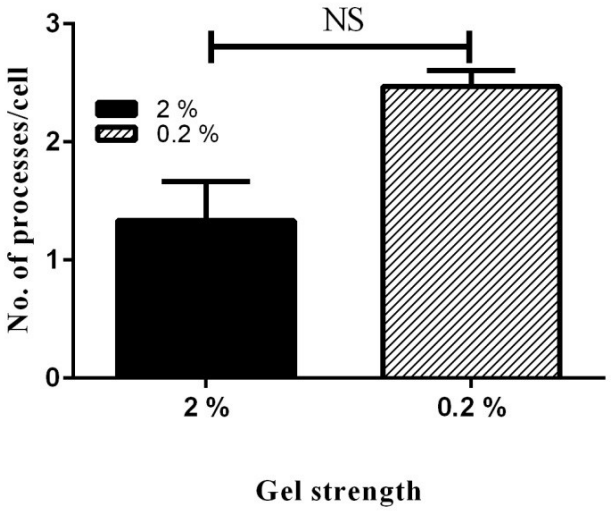

Figure 4.17: Number of processes per chondrocyte in weak gel cultures as compared to strong gels at day 3.
The difference between the number of processes/cell was statistically not significant between the strong and weak gel cultures. Values obtained from [*N(n')*=6(228) and 6(491)] samples in strong and weak gels respectively.

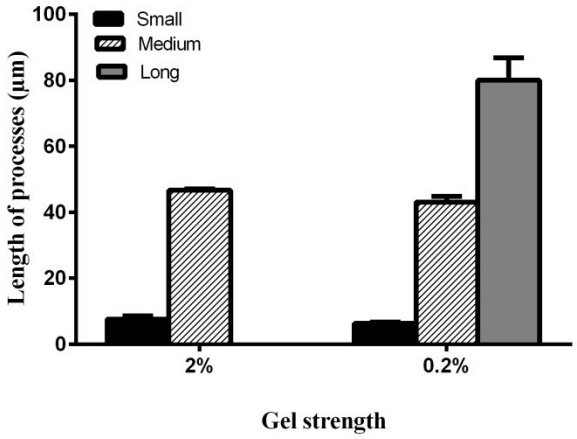

Figure 4.18: Various categories of length of processes in strong and weak gel cultures.

Chondrocytes cultured in weak gels displayed small, medium and long processes as compared to strong gels where only small and medium sized processes were present at day 3. Values were from [*N(n')*=6(228) and 6(491)] in strong and weak gels respectively.

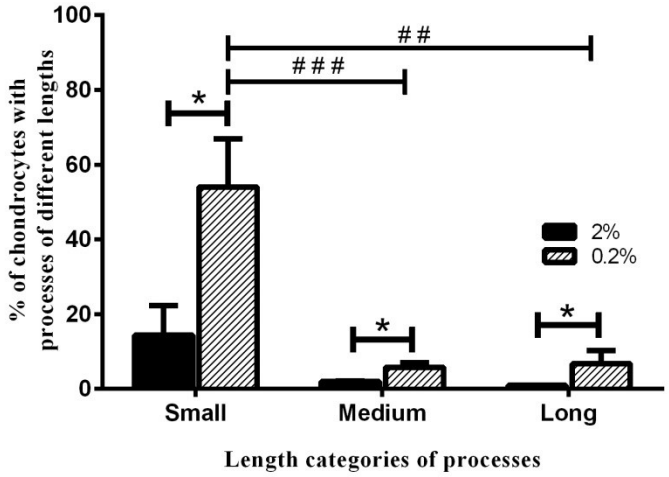

Figure 4.19: The percentage of chondrocytes with various lengths of cytoplasmic processes increased in the weak gels.

The percentage of chondrocytes with small, medium and long processes was higher in the weak gels as compared to the strong gels at day 3 of culture. Values displayed for a sample size [*N(n')*=6(228) and 6(491)] in strong and weak gels respectively. * indicated a significant difference according to unpaired student's t-test. # indicated a significant difference according to one-way ANOVA followed by Tukey's multiple comparison post-hoc test. The single, double and triple symbols showed the level of significance for $P<0.05$, 0.01 and 0.001 respectively.

At day 3, there was no effect on cultured chondrocytes in terms of cluster formation and various characteristics of clusters did not differ significantly in both the gel strengths (Table 4.3). This suggested that cytoplasmic processes developed before chondrocyte cluster formation.

Characteristics of clusters formed	Strong (2%) gel	Weak (0.2%) gel	*P* value*
No. of clusters per field of view	2.5 ± 1	2.6 ± 0.6	0.9
No. of cells/cluster	4 ± 0.2	4 ± 0.2	0.6
Av. Volume of clusters (μm^3)	3746.6 ± 466.7	3789.9 ± 312.1	0.9
Av. Volume of individual cell in cluster (μm^3)	966.8 ± 70.1	969.1 ± 59.1	0.9
% of chondrocytes forming clusters	20.7 ± 6.6	24.1 ± 5.5	0.7

Table 4.3: Characteristics of clusters present in strong and weak gel strengths at day 3 of culture.
There existed no significant difference between various parameters of clusters present in strong and weak gels at day 3. Data were presented regarding the number of clusters, number of cells/cluster, volume of clusters, volume of individual cell in cluster and % of chondrocytes forming clusters on day 3 in strong and weak gels. Data shown as mean ± standard error, ***** indicated probability value result from un-paired Student's t-test with $P<0.05$.

To summarise the results of this section by day 3 of culture the chondrocytes were larger in volume and showed higher percentage of cytoplasmic processes when cultured in weak agarose gels compared with strong gels. There was no significant

difference between any of the characteristics of the clusters formed in strong and weak gels by day 3.

4.5.1.4 *Chondrocyte cluster formation and development of abnormal morphology by day 7 of culture in weak gels*

Cultured chondrocytes displayed striking changes in the cell morphology within weak agarose gels after 7 days even in the images obtained by using low power (x10 dry) objective (Fig. 4.20). In the weak agarose gels, chondrocytes showed dramatic changes to morphology characterised by cluster formation and development of cytoplasmic processes (Fig. 4.21 & 4.22). The volume of isolated chondrocytes was significantly higher in weak gels as compared to the cells cultured in strong gels (P=0.02; Fig. 4.23).

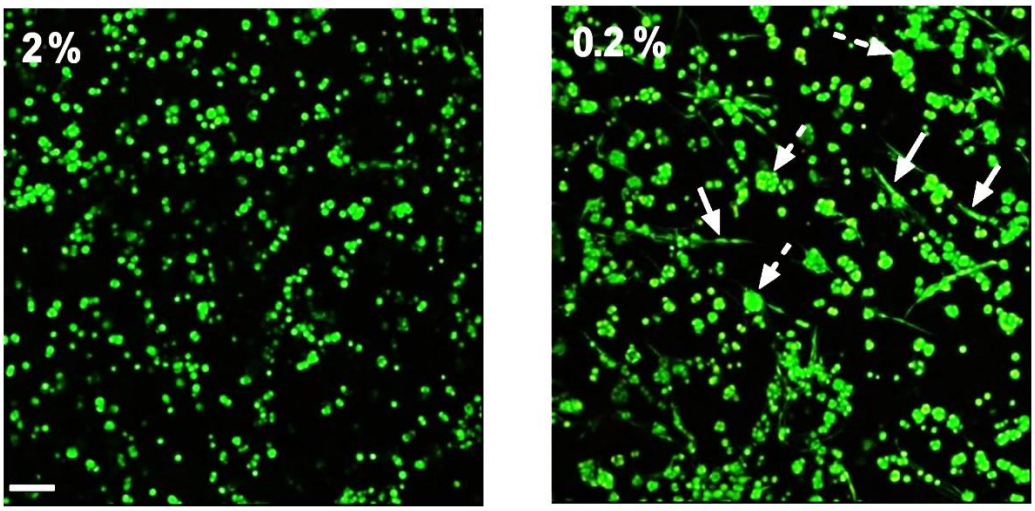

Figure 4.20: Axial CLSM reconstructions of low power images showing cluster formation and development of cytoplasmic processes in the weak gels.
Confocal microscope x10 objective images of isolated chondrocytes incubated with CMFDA and DRAQ5 at day 7 of culture in strong and weak gel strengths. Solid arrows identify examples of cells developing cytoplasmic processes and examples of clusters of cells indicated with broken line arrows. Scale bar = 100µm.

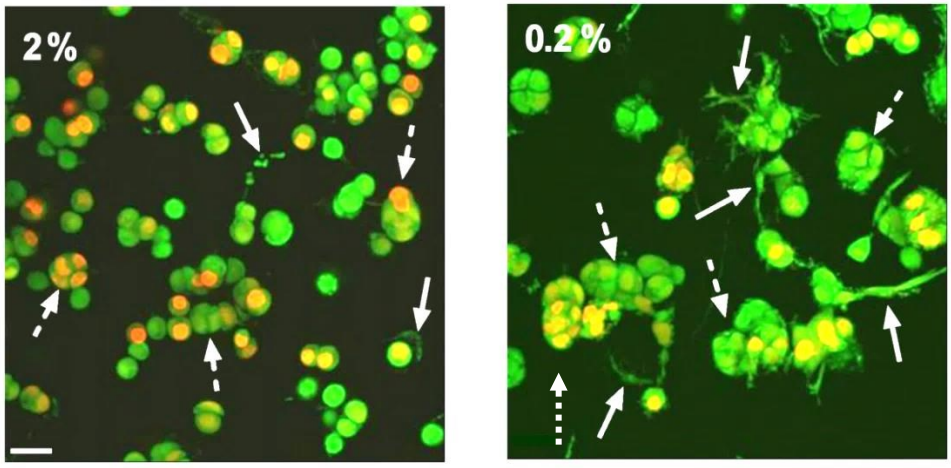

Figure 4.21: Axial CLSM reconstructions of high power images indicating cluster formation and development of cytoplasmic processes in the weak gels.
Examples of confocal microscope x40 objective images of isolated chondrocytes incubated with CMFDA and DRAQ5 at day 7 of culture in strong and weak gel strengths. Chondrocytes in weak gels developed abnormal morphology by day 7 and those in the strong gels remained unaffected. Solid arrows indicate examples of cells developing cytoplasmic processes and the examples of cell clusters indicated with broken line arrows. Scale bar = 25µm.

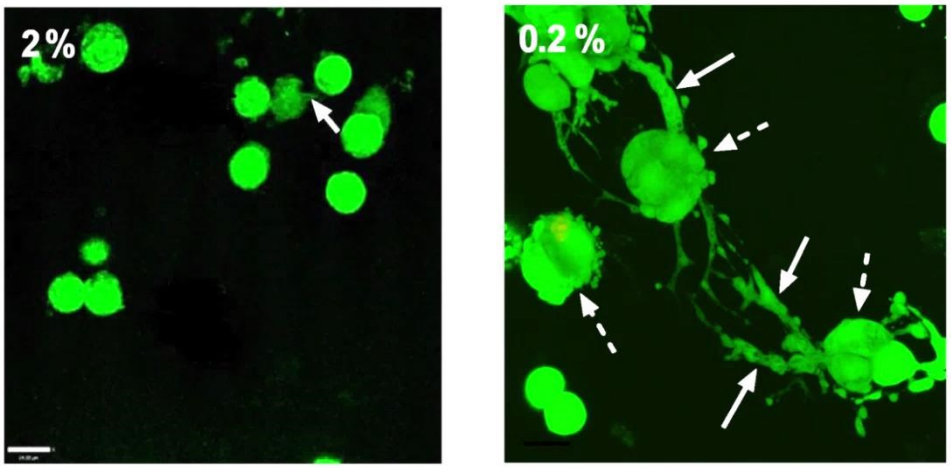

Figure 4.22: Axial CLSM reconstructions of high power images demonstrating abnormal morphology of chondrocytes in weak gels.
Confocal microscope x63DW objective images of fluorescently-labelled isolated chondrocytes at day 7 of culture in strong and weak gel strengths. Solid arrows point to the examples of cells demonstrating cytoplasmic processes and the broken arrows indicate cell clusters. Scale bar = 14µm.

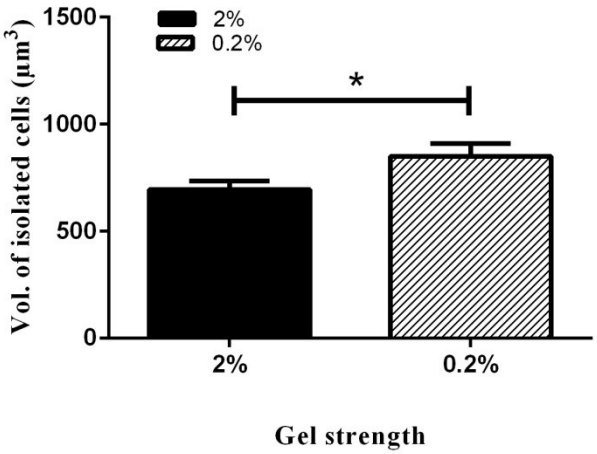

Figure 4.23: Chondrocyte volume increased in the weak gel cultures.
The volume of isolated chondrocytes (μm^3) cultured in strong and weak gels at day 7 displayed in the graph were from [N(n′)=6(66) and 6(41)] chondrocytes cultured in strong and weak gels respectively. * indicated a significant difference according to unpaired student's t-test. The single, double and triple symbols showed the level of significance for $P<0.05$, 0.01 and 0.001 respectively.

4.5.1.4.1 Chondrocyte clustering

An obvious morphological feature of chondrocytes observed routinely when cultured in weak gels was the formation of clusters. Quantitative data regarding the number of clusters, number of cells/cluster, percentage of cells forming clusters, the volume of clusters and volume of individual cells in a cluster was obtained at day 7 of culture (section 4.4.1.7.1). The number of clusters and number of cells per cluster in the weak gels were significantly higher as compared to those in strong gels ($P<0.05$ and $P=0.002$ respectively; Figs. 4.24a & b). In the weak gel cultures a significantly higher percentage of chondrocytes formed clusters (76±5% [*N(n')*]=[6(525)]) as compared to those in strong gels (41±5% [*N(n')*]=[6(313); $P=0.001$; Fig. 4.24c]). At day 7 of culture chondrocytes in weak gels formed large clusters having on the average 6-7 cells per cluster ($P=0.0007$) as compared to strong gels comprising of average 3-4 cells per cluster (Fig. 4.24d). The volume of individual chondrocytes in a

cluster showed no significant difference after 7 days of culture in both the gel strengths (Fig. 4.24e). Moreover, the volume of isolated chondrocytes and of the individual chondrocytes in the culture appeared to be similar in both gel strengths.

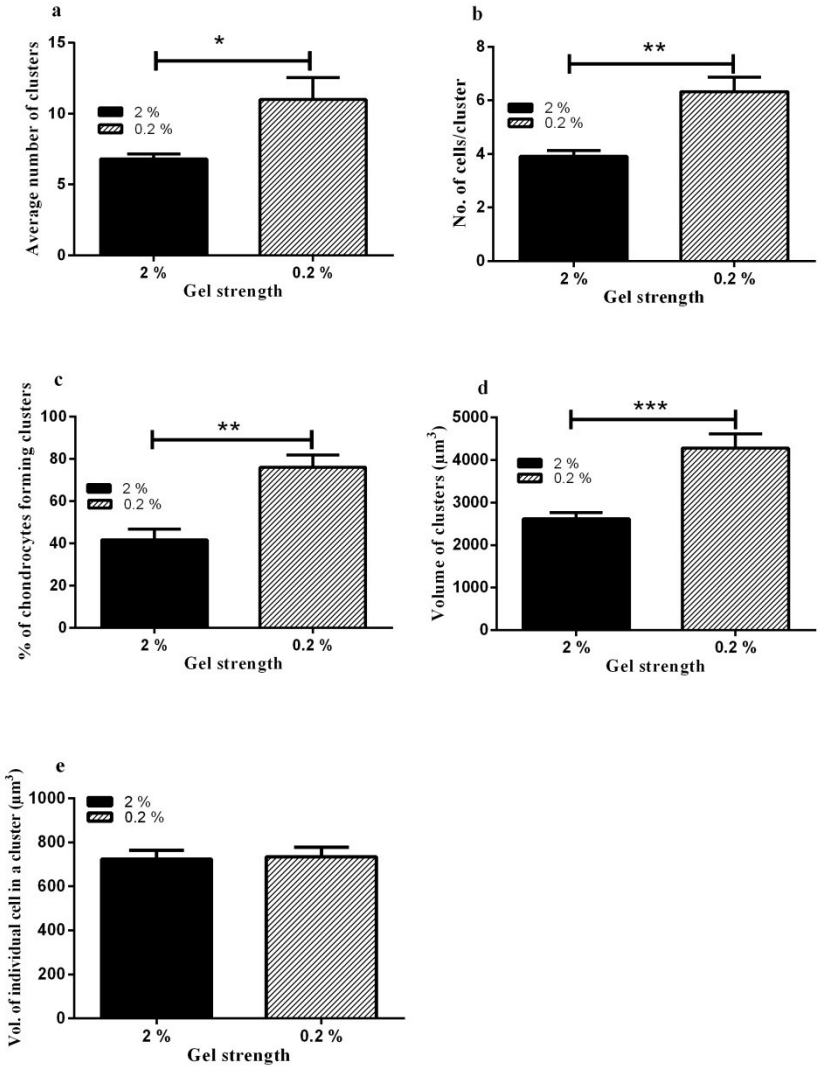

Figure 4.24: Characteristics of chondrocyte clusters present in strong and weak gels at day 7.

Values displayed for (a) average number of clusters formed (b) average number of cells/cluster (c) % of chondrocytes present in clusters (d) average volume of the clusters (μm^3) and (e) average volume of individual chondrocyte in a cluster (μm^3). Data obtained from [*N(n')*]=[6(313) and 6(525)] in strong and weak gels respectively. * indicated a significant difference according to unpaired student's t-test. The single, double and triple symbols showed the level of significance for $P<0.05$, 0.01 and 0.001 respectively.

4.5.1.4.2 Chondrocyte morphology

Chondrocytes cultured in weak gels displayed marked shape changes by day 7 characterised by the appearance of cytoplasmic processes (Figs. 4.21 & 4.22). A significantly higher percentage of chondrocytes, (67±1%; [*N(n')*]=[6(525)]; section 4.4.1.7.3.) in weak gel cultures had cytoplasmic processes emanating from their cell bodies after 7 days of *in vitro* culture as compared to 18±1% [*N(n')*]=[6(313)] cells in strong gels (Fig. 4.25; P=0.006). The number of processes/cell was also significantly higher in the weak gels as compared to strong gels (Fig. 4.26; P=0.0002). The analysis of the length categories of processes (section 4.4.1.7.3.) revealed the presence of small, medium and long processes emanating from the chondrocytes in weak gels and only small and medium sized processes present at the chondrocytes in the strong gel. Chondrocytes cultured in weak gels displayed long processes as compared to strong gels where no long processes were observed (Fig. 4.27). A significantly higher percentage of chondrocytes had small, medium and long processes in the weak gels as compared to strong gels (P<0.0001; P=0.0009 and P=0.03 respectively; Fig. 4.28). Moreover, a higher percentage of chondrocytes had smaller processes (0-29.9 μm) as compared to medium (30-59.9 μm) and long (≥60 μm) processes in the weak gels (P<0.001 for all conditions). Additionally, the % of chondrocytes having medium processes were more numerous than the ones with long processes in the weak gels *(*P<0.001).

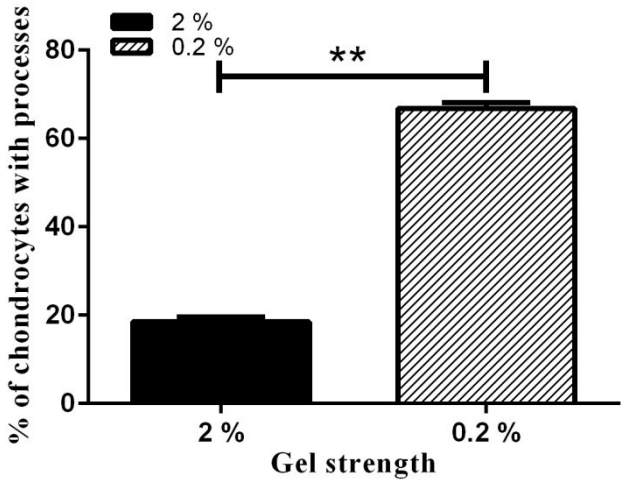

Figure 4.25: A higher percentage of chondrocytes had cytoplasmic processes in the weak gels at day 7.

The percentage of chondrocytes producing cytoplasmic processes increased significantly in the weak gels as compared to the strong gels at day 7. Pooled data obtained from [*N(n')*=6(313) and 6(525)] samples in strong and weak gels respectively. * indicated a significant difference according to unpaired student's t-test. The single, double and triple symbols showed the level of significance for *P*<0.05, 0.01 and 0.001 respectively.

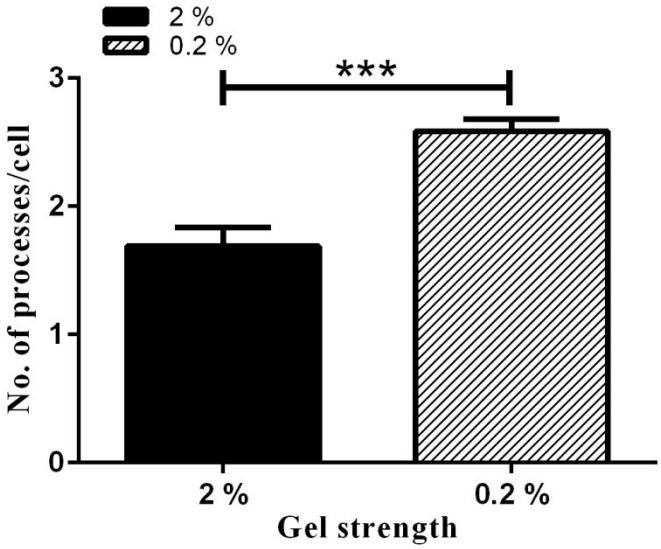

Figure 4.26: Number of processes per cell increased in the weak gels at day 7.

Chondrocytes cultured in weak gels had a higher number of processes per cell as compared to the strong gels. Values obtained from [*N(n')*=6(313) and 6(525)] samples in strong and weak gels respectively. * indicated a significant difference according to unpaired student's t-test. The single, double and triple symbols showed the level of significance for *P*<0.05, 0.01 and 0.001 respectively.

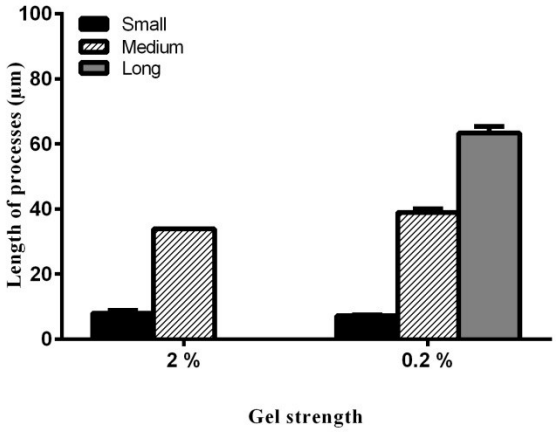

Figure 4.27: Various categories of length of processes in strong and weak gel cultures.

Chondrocytes cultured in weak gels displayed small, medium and long processes as compared to strong gels where only small and medium sized processes were present at day 7. Values regarding the average length of these processes was displayed with sample size [*N(n')*=6(313) and 6(525)] in strong and weak gels respectively.

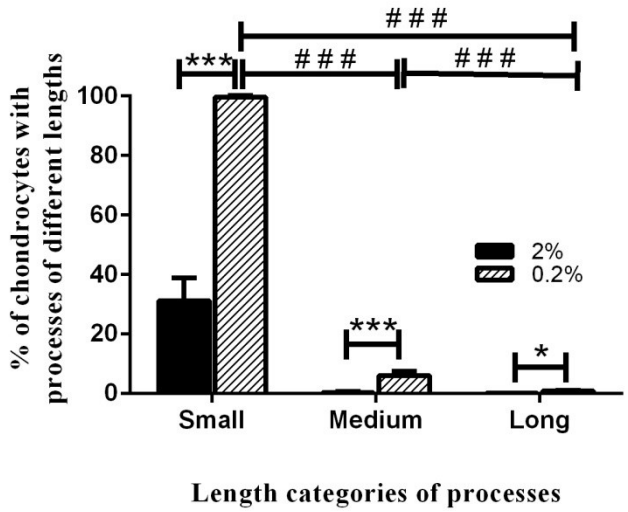

Figure 4.28: The percentage of chondrocytes with various lengths of cytoplasmic processes increased in the weak gels.

The percentage of chondrocytes with small, medium and long processes was higher in the weak gels as compared to the strong gels at day 7 of culture**.** Values displayed for a sample size [*N(n')*=6(313) and 6(525)] in strong and weak gels respectively. * indicated a significant difference according to unpaired student's t-test. # indicated a significant difference according to one-way ANOVA followed by Tukey's multiple comparison post-hoc test. The single, double and triple symbols showed the level of significance for $P<0.05$, 0.01 and 0.001 respectively.

To summarise the results, the differences in the development of morphological changes in both strengths of agarose gels were strikingly obvious. By day 7 of culture bovine chondrocytes cultured in weak agarose gels demonstrated marked heterogeneity of chondrocyte morphology in terms of enlargement of cells, cluster formation and development of cytoplasmic processes. Chondrocytes cultured in strong agarose gels displayed similar type of morphological changes as seen in the weak gels but statistically less in quantity.

4.5.1.5 *Images of chondrocytes cultured in 3D gels with different strengths of agarose after 14 days of culture*

Chondrocytes isolated from bovine cartilage were kept in culture for 14 days in strong and weak gels and imaged with low (x10) and high (x40 DW) power objectives to observe any changes to the morphology of chondrocytes. The images obtained (Figs. 4.29 & 4.30) displayed complex morphological changes in the weak gels with the production of large-sized clusters and numerous cytoplasmic processes. However, chondrocytes cultured in the strong gels maintained their morphology relatively unchanged even after 14 days of *in vitro* culture. A very detailed analysis of chondrocyte morphological changes observed in strong and weak gels was performed in this study by day 7 of culture. However, by day 14 the morphology of chondrocytes became complicated and huge clusters of abnormal cells were formed. Volume of single cell within strong gels could be determined but in the weak gels there were no single cells present (Fig. 4.30) therefore, data analysis was not possible. Thus it was almost impossible to analyse volume/morphology of cells at day 14, to illustrate the changes only the images have been presented.

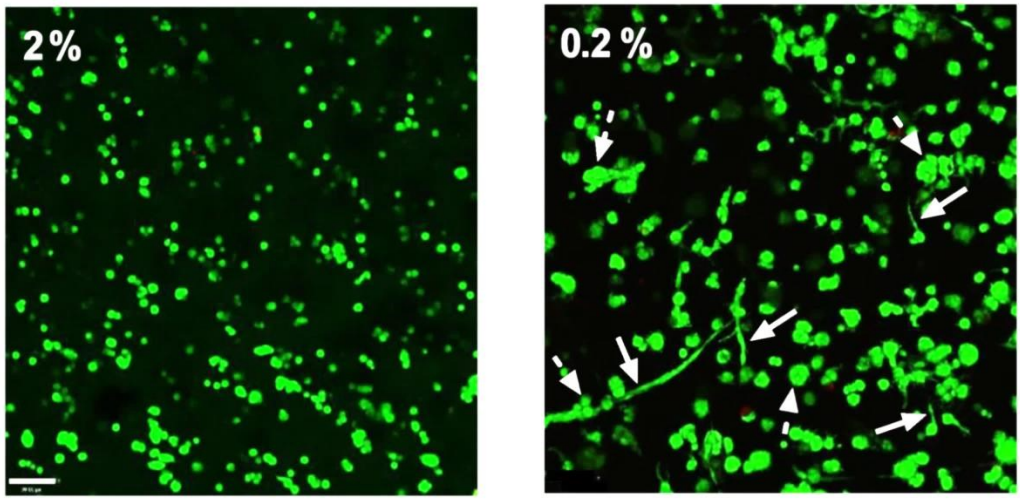

Figure 4.29: Axial CLSM reconstructions of low power images showing cluster formation and development of cytoplasmic processes in the weak gels.
Confocal microscope x10 objective images of isolated chondrocytes incubated with CMFDA and PI at day 14 of culture in strong and weak gel strengths. Solid arrows indicate the examples of cells developing cytoplasmic processes and the examples of cell clusters indicated with broken line arrows. Scale bar = 100µm.

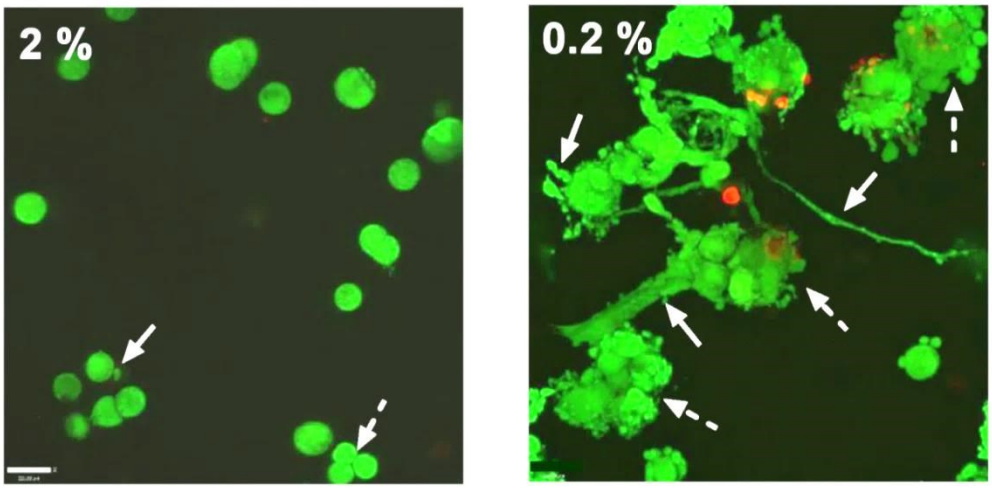

Figure 4.30: Axial CLSM reconstructions of isolated chondrocytes cultured in 3D strong and weak gel cultures.
Confocal microscope high power (x40 DW objective) images of chondrocytes labelled with CMFDA and PI from day 14 of culture in strong and weak gel strengths. Solid arrows point to the examples of cells developing cytoplasmic processes and the broken arrows indicate examples of cell clusters. Scale bar = 25µm.

To summarise this section, chondrocytes cultured in weak agarose gels showed an increase in volume and marked changes in morphology in terms of cluster formation and abnormal shapes with cytoplasmic processes as compared to strong gels. However, the changes in volume and morphology were also seen in the chondrocytes cultured in strong gels but these developed more slowly as compared to those in the weak gels. The results suggested that the changes were basically similar between strong and weak gels but were simply more rapid in the weak gels.

4.5.2 Effect of increasing concentrations of FCS on the morphology of bovine chondrocytes cultured in strong and weak 3D agarose gels

In the previous section in this chapter, regarding the effect of gel strength on chondrocyte morphology 10% FCS was used in the culture medium. It was possible that the morphological changes observed in the weak gels were due to increased penetration of FCS into the gels. To investigate this effect, in the present section varying concentrations of FCS were used (1%-10%). However, in these experiments serum-free/0% FCS was not utilised as a culture condition because FCS-supplemented medium is required for the chondrocyte growth and maintenance of phenotype in cultures as reported already (Glaser and Conrad, 1984). Freshly isolated bovine chondrocytes were cultured over 7 days in strong and weak gels with FCS present at 1%, 2%, 5% or 10%. The morphology of cells was analysed at the 1st and 7th day of culture by obtaining low and high power CLSM images and quantitative data obtained by using 3D image analysis software (sections 4.4.1.7.1. & 4.4.1.7.3).

4.5.2.1 *Changes to chondrocyte volume at day 1*

The volume of chondrocytes increased in the weak gel strengths with the increasing concentrations of FCS but no abnormal chondrocytes with processes were present. When visualised on day 1 of culture with x10 objective, chondrocyte density appeared to be broadly similar and there was little evidence of clustering in either strong or weak gels in the four different concentrations of FCS (Fig. 4.31). Chondrocytes cultured in either strong or weak agarose gels in the four different concentrations of FCS imaged with x40 objective, were spheroidal in shape (Fig. 4.32). Occasionally, pairs of chondrocytes could be seen in both the gel strengths (examples shown in Fig. 4.32). Heterogeneity in cell sizes was discernible but no obvious morphological changes (cytoplasmic processes/clusters) were present in either gel strengths cultured with 1%, 2%, 5% or 10% FCS (Fig. 4.32). The cell density was calculated from x40 magnification images of chondrocytes in strong and weak gels at day 1 as previously described (section 4.4.1.7). Cell density was not markedly different in strong and weak agarose gels with 1%, 2%, 5% or 10% FCS (4.9, 5.67, 7.18, 7.56; in strong and 8.69, 7.93, 9.45, 9.45/mm^3x10^3 in weak gels respectively; data obtained from a single experiment). It was noticed that cell density in strong gels cultured with 1% FCS was only 4.9 /mm^3x10^3 which suggested that possibly a certain level of FCS is required for chondrocyte culture. However, in the weak gels with 1% FCS this was not observed because the penetrability of serum in weak gels was more as compared to strong gels (Johnson et al., 1996).

The volume of isolated chondrocytes in weak gels was higher as compared to the volume of chondrocytes in strong gels cultured in 2%, 5% and 10% FCS ($P<0.05$ for the three higher concentrations of FCS) but not with very low (1%) concentration of FCS as shown in Fig. 4.33. Chondrocytes cultured in both gel strengths with increasing concentrations of FCS showed no cytoplasmic processes by day 1 of culture. Rarely (1-2) small clusters involving 3-4 cells per cluster were observed in both gel strengths with 1%, 2%, 5% and 10% FCS concentrations on day 1 of culture (Table 4.4; data obtained from a single experiment). The average volume of clusters and the volume of individual cells in a cluster appeared to be unaffected in both gel strengths with all the four concentrations of FCS (Table 4.4). These results suggested that the volume of chondrocytes increased in the weak gel cultures with higher concentrations of FCS after 1 day but the morphology of cells was unaffected by gel strength and FCS concentration.

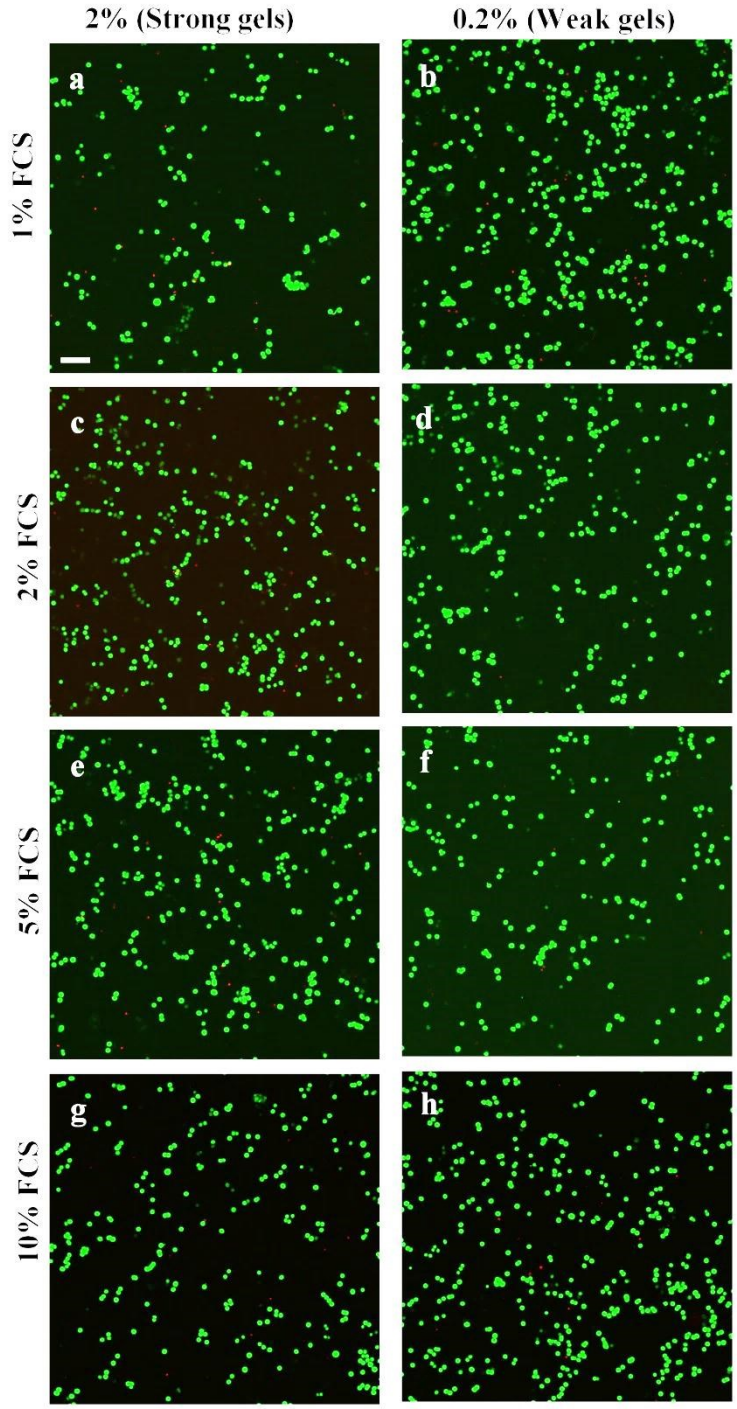

Figure 4.31: Axial CLSM reconstructions of isolated chondrocytes cultured in strong and weak gels with varying concentrations of FCS.

Confocal microscope low power (x10 objective) magnification images of chondrocytes incubated with CMFDA and PI from day 1 of culture in (a, c, e, g) strong and (b, d, f, h) weak gel strengths with (a, b) 1%, (c, d) 2%, (e, f) 5% and (g, h) 10% concentrations of FCS. Scale bar for all panels = 100μm.

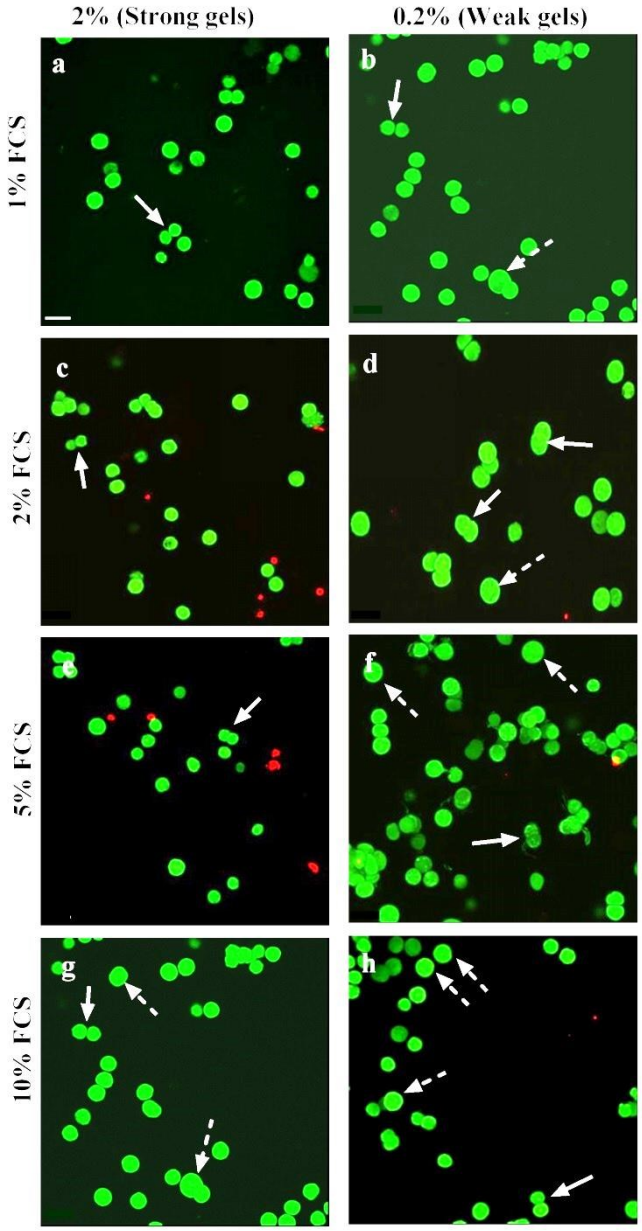

Figure 4.32: Axial CLSM reconstructions of images of isolated chondrocytes in strong and weak gels cultured with varying concentrations of FCS.
Confocal microscope high power (x40 objective) magnification images of chondrocytes incubated with CMFDA and PI from day 1 of culture in (a, c, e, g) strong and (b, d, f, h) weak gel strengths with (a, b) 1%, (c, d) 2%, (e, f) 5% and (g, h) 10% concentrations of FCS. The solid arrows indicate examples of chondrocyte pairs and broken arrows indicate examples of swollen chondrocytes displaying heterogeneity in cell sizes. In the weak gels numerous swollen cells present and in strong gels only in 10% FCS few swollen chondrocytes observed. Scale bar for all panels = 25μm.

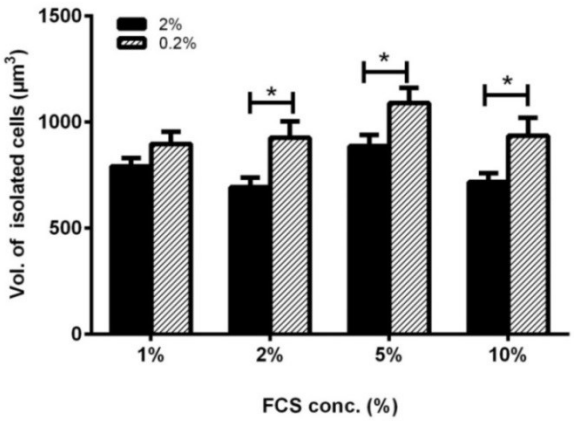

Figure 4.33: Chondrocyte volume increased in the weak gels as compared to strong gels at higher concentrations (2%, 5% and 10%) of FCS.
Data regarding the volume of isolated chondrocytes (μm^3) cultured in strong and weak gel strengths at day 1 with increasing concentrations of FCS. Values obtained from [*N(n')*= 2(10, 6, 11, 4) in strong gels and 2(16, 12, 5, 18)] in weak gels cultured with 1%, 2%, 5% and 10% FCS concentrations respectively. * indicated a significant difference according to unpaired student's t-test. The single, double and triple symbols showed the level of significance for *P*<0.05, 0.01 and 0.001 respectively.

FCS conc. (%)	**1%**		**2%**		**5%**		**10%**	
Gel strength	2%	0.2%	2%	0.2%	2%	0.2%	2%	0.2%
No. of clusters	1	1	2	1	1	0	1	1
No. of cells/cluster	3	4	4.5	3	4	0	3	3
Vol. of cluster (μm^3)	1828.5	3168.4	2147.5	3096.9	2899.9	0	3043.4	1424.5
Vol. of ind. cell in a cluster (μm^3)	609.5	633.6	536.8	1032.3	724.9	0	1014.5	474.8

Table 4.4: Characteristics of clusters present in strong and weak gel strengths in different concentrations of FCS at day 1 of culture.
Data were presented regarding the number of clusters, number of cells/cluster, volume of clusters and volume of individual cell in a cluster on day 1 in strong and weak gels. Data were shown from a single experiment. 0 values in the table indicated no cluster present.

4.5.2.2 *Changes to chondrocyte density during 7 days of culture in strong and weak agarose gel cultures*

Chondrocyte density was determined by analysing the CLSM images obtained by using high power magnification (x40DW) objective. Fluorescently-labelled nuclei of cells were counted and the cell density determined by the formula detailed previously (section 4.4.1.7). After 7 days of *in vitro* culture cell density remained unaffected in the strong gel cultures with increasing concentrations of FCS (Fig. 4.34; $P>0.05$; ANOVA). In the weak gel cultures, chondrocyte density increased significantly in the presence of 10% FCS as compared to 1% and 2% FCS (Fig. 4.34; $P<0.05$; ANOVA for both conditions). These results suggested proliferation of cells in the clusters in the weak gels with increasing concentrations of FCS.

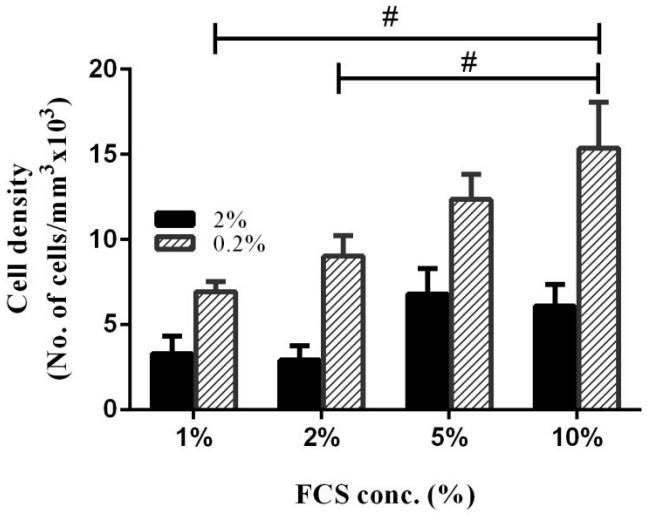

Figure 4.34: Chondrocyte density increased in the weak gels over 7 days of culture with higher concentrations of FCS.
Graph shows pooled data on cell density at day 7 in the weak gels as compared to strong gels. Values were from [*N(n')*=6(35, 34, 180, 98) in strong gels and 6(222, 334, 389, 569) in the weak gels with 1%, 2%, 5% and 10% FCS respectively]. # indicated a significant difference according to one-way ANOVA followed by Tukey's multiple comparison post-hoc test. The single, double and triple symbols showed the level of significance for $P<0.05$, 0.01 and 0.001 respectively.

4.5.2.3 *Formation of clusters and development of abnormal chondrocyte morphology in weak gels compared to strong gels in the presence of higher concentrations of FCS by day 7*

Chondrocytes cultured in weak gels showed marked changes in morphology compared to those in strong gels. Moreover, the morphological changes observed in weak gels which were characterised by cluster formation and presence of cytoplasmic processes appeared to be intensified with increasing concentrations of FCS (Fig. 4.35). The CLSM images acquired on day 7 by x40 objective of chondrocytes cultured in strong and weak gels with different concentrations of FCS (Fig. 4.36) were analysed for chondrocyte morphology. Quantitative data regarding morphology of chondrocytes (volume/clusters/processes) were obtained and presented in the following sections.

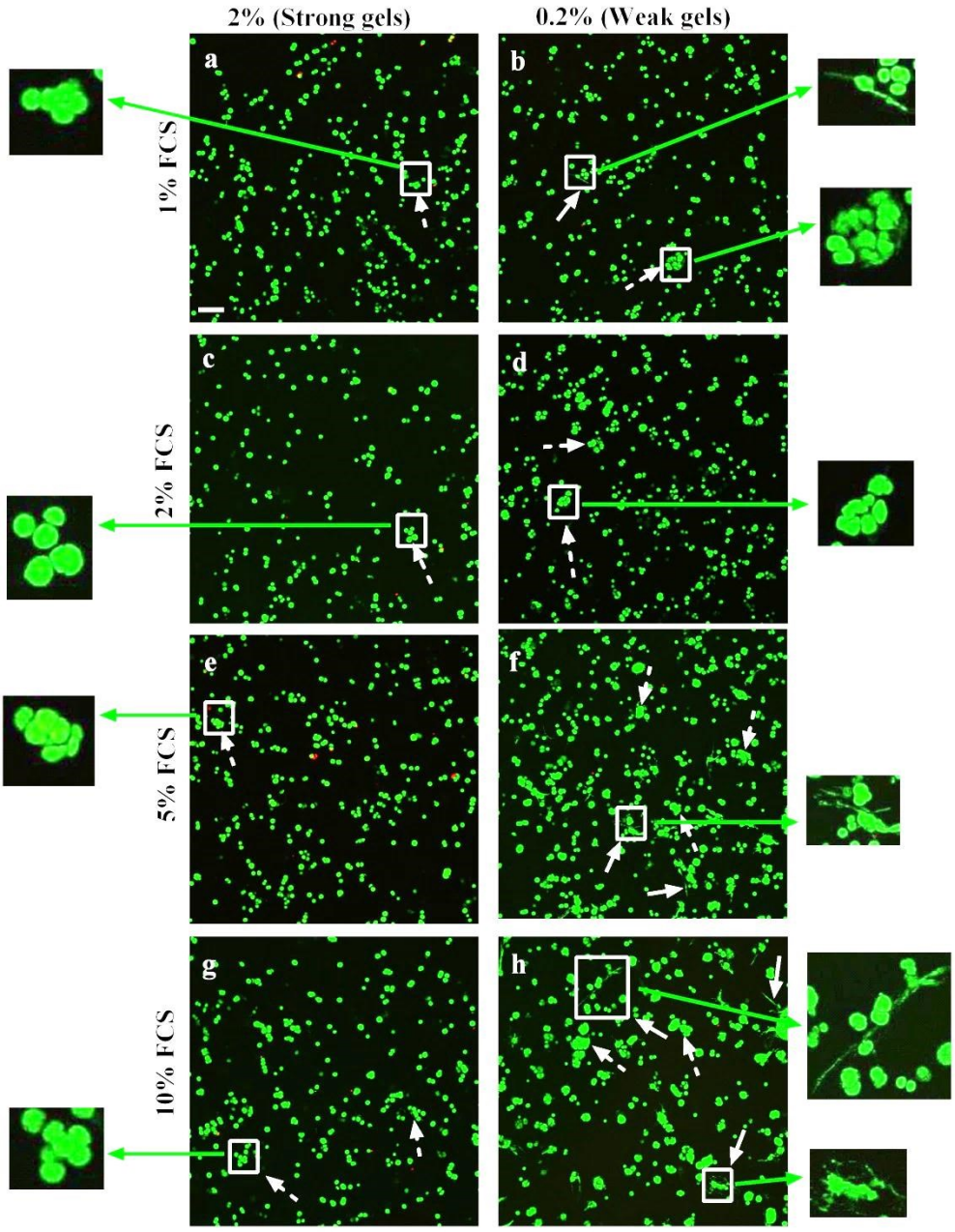

Figure 4.35: Axial CLSM reconstructions of isolated chondrocytes showing evidence of abnormal chondrocyte morphology (clusters/processes) in the weak gels with high concentrations of FCS.

Confocal microscope low power magnification images of chondrocytes incubated with CMFDA and DRAQ5 from day 7 of culture in (a, c, e, g) strong and (b, d, f, h) weak gel strengths with (a, b) 1%, (c, d) 2%, (e, f) 5% and (g, h) 10% concentrations of FCS. The solid arrows indicate examples of chondrocytes with processes and broken arrows indicate examples of clusters formed. Inset images show three times zoomed in areas with examples of clusters/processes. Scale bar for all panels = 100μm.

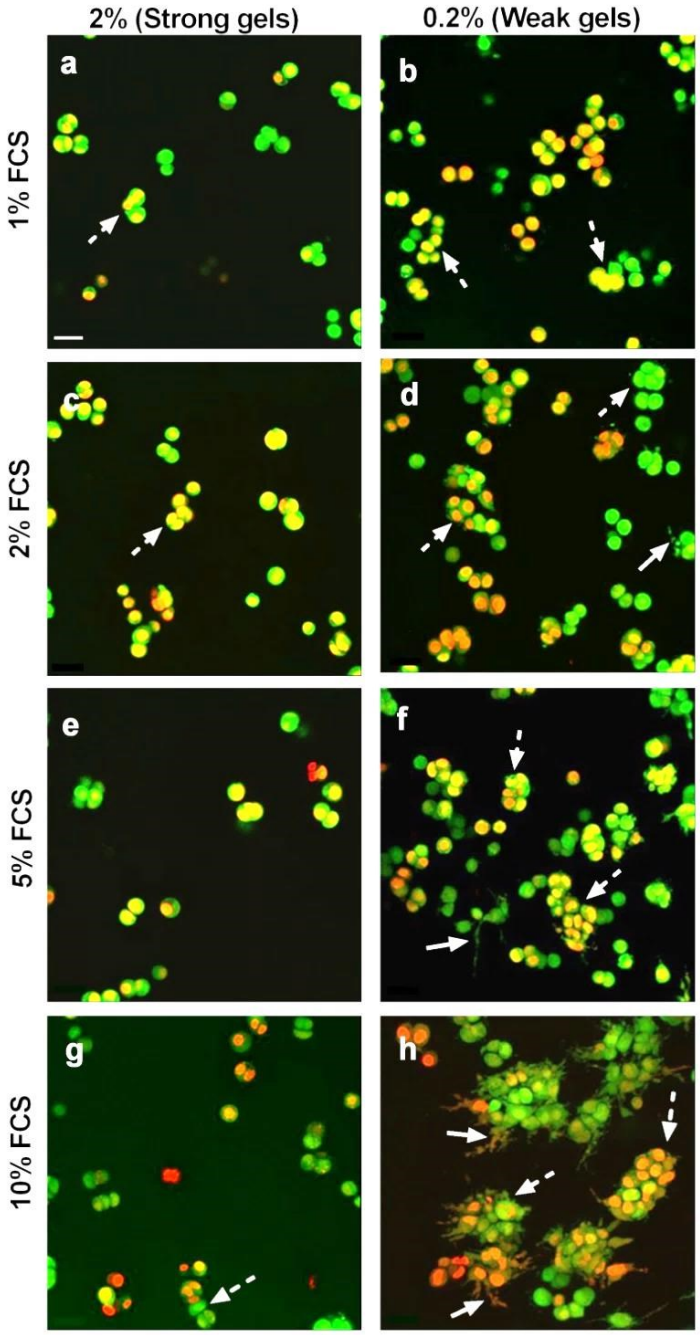

Figure 4.36: Axial CLSM reconstructions of isolated chondrocytes showing increasing evidence of clusters and abnormal chondrocyte morphology with processes in weak gels with high concentrations of FCS.

Confocal microscope high power magnification images of chondrocytes incubated with CMFDA and DRAQ5 from day 7 of culture in (a, c, e, g) 2% and (b, d, f, h) 0.2% gel strengths with (a, b) 1%, (c, d) 2%, (e, f) 5% and (g, h) 10% concentrations of FCS. The solid arrows indicate examples of cytoplasmic processes and broken arrows indicate examples of cell clusters. Scale bar for all panels = 25µm.

The volume of chondrocytes cultured in strong and weak gels was not affected with higher (5% and 10%) concentrations of FCS by day 7 but the volume was significantly higher in weak gels cultured in the presence of 1% and 2% FCS concentrations (*P*=0.02 in both conditions; Fig. 4.37). This suggested that basically the reduced chondrocyte volume in the strong gels could be overcome by raising the FCS concentration.

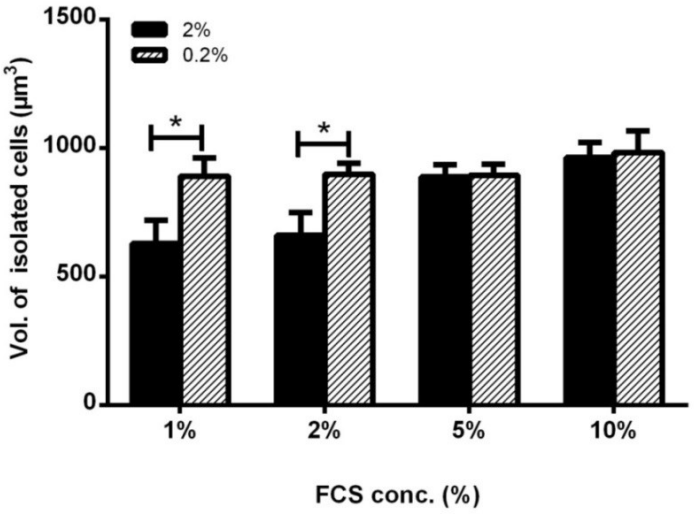

Figure 4.37: Chondrocyte volume was higher in the weak gels as compared to strong gels in the lower concentrations of FCS by day 7.
Data regarding the volume of isolated chondrocytes (μm^3) cultured in strong and weak gel strengths at day 7 in increasing concentrations of FCS. Values obtained from [*N(n')*=6(8, 12, 21, 21)] in strong gels and 6(66, 60, 43, 19)] in weak gels cultured with 1%, 2%, 5% and 10% FCS concentrations respectively. * indicated a significant difference according to unpaired student's t-test. The single, double and triple symbols showed the level of significance for *P*<0.05, 0.01 and 0.001 respectively.

4.5.2.3.1 Chondrocyte clustering

A significantly higher number of clusters/field of view was seen in chondrocytes cultured in weak gels with higher concentrations (5% and 10%) of FCS as compared to those in strong gels (*P*=0.04 in both conditions). However, the number of clusters

formed in the presence of lower concentrations (1% and 2%) of FCS remained unaffected in both gel strengths. Additionally, a significantly higher number of clusters was formed in the weak gels in the presence of 5% and 10% as compared to the cells in weak gels with 1% FCS ($P<0.01$ for both conditions; Fig. 4.38a). There was no significant difference regarding the number of clusters formed in the strong gels with all the four concentrations of FCS ($P>0.05$; ANOVA).

The number of cells per cluster was significantly higher in the weak gels as compared to strong gels cultured with 10% FCS ($P=0.01$; Fig. 4.38b). Chondrocytes cultured in weak gel strengths with highest concentration (10%) of FCS displayed a higher number of cells per cluster as compared to the lower concentrations (1%, 2% and 5%) of FCS in the same gel strength ($P<0.05$, $P<0.001$ and $P<0.01$ respectively; Fig. 4.38b). However, no significant difference existed regarding the number of cells per cluster amongst the chondrocytes cultured in strong gels with all the four concentrations of FCS ($P>0.05$; ANOVA).

The percentage of chondrocytes present in clusters increased significantly by day 7 in the weak gels as compared to strong gels with 10% FCS ($P=0.01$). In the weak gels, a very high percentage of cells were present in clusters as compared to those in strong gels [80±7%; 53±11; $N(n')$=6(98) and 6(569) for strong and weak gels respectively]. Moreover, in the weak gels a significantly higher percentage of chondrocytes were present in clusters in the presence of 5% and 10% FCS as compared to chondrocytes cultured in the presence of 1% FCS in the same gel strength ($P<0.05$ and $P<0.001$ respectively; Fig. 4.38c). Additionally, a higher percentage of chondrocytes were present in clusters in weak gels with 10% FCS as

compared to those in 2% FCS in the same gel strength (P<0.01). However, the percentage of cells present in clusters remained unaffected in the strong gels with all the four concentrations of FCS (P>0.05; ANOVA).

The volume of clusters present in the weak gels with 10% FCS was significantly higher than the volume of clusters present in 1% and 2% FCS in the same strength of gel (P<0.05 and P<0.01 respectively). When the volume of clusters present in both the gel strengths was compared (Fig. 4.38d) significantly higher values were observed in the cells cultured in the weak gels with 10% FCS (P=0.009) and no difference was observed in the lower concentrations of FCS (1%, 2% and 5%). Moreover, the volume of clusters present in strong gels showed no significant difference in all concentrations of FCS (Fig. 4.38d; P>0.05; ANOVA). The mean volume of individual cells present in the cluster was found to be approximately the same in all the culture conditions (Fig. 4.38e).

These results strongly suggested that the cell density increased significantly possibly due to cell proliferation in the weak gels with increasing concentrations of FCS. A very high percentage of chondrocytes in weak gels in the presence of 10% FCS formed clusters as compared to strong gels with the same concentration of FCS. Moreover, these clusters in weak gels were large-sized with many cells per cluster as compared to those in strong gels. The results suggested that increasing the concentrations of FCS accelerated formation of clusters in the weak gels but not in the strong gels.

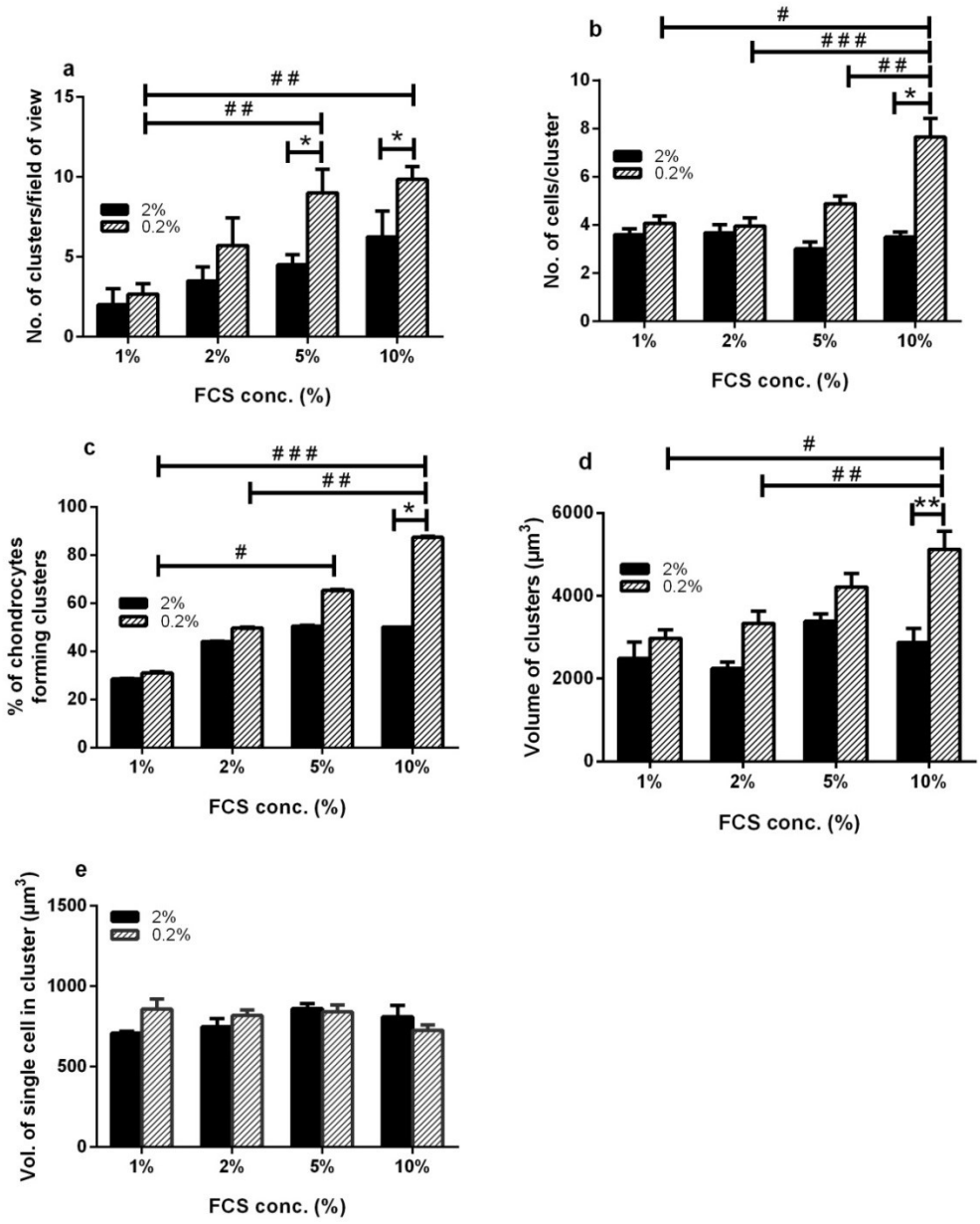

Figure 4.38: Characteristics of clusters present in the strong and weak gels with varying concentrations of FCS at day 7.

Values displayed for (a) average number of clusters present, (b) average number of cells/cluster, (c) % of chondrocytes present in clusters, (d) average volume of the clusters (μm^3) and (e) average volume of individual chondrocyte in a cluster (μm^3). Data obtained from [*N(n')*=6(35, 34, 180, 98) in strong gels and 6(222, 334, 389, 569)] in weak gels cultured with 1%, 2%, 5% and 10% concentrations of FCS respectively. * indicated a significant difference according to unpaired student's t-test. # indicated a significant difference according to one-way ANOVA followed by Tukey's multiple comparison post-hoc test. The single, double and triple symbols showed the level of significance for $P<0.05$, 0.01 and 0.001 respectively.

4.5.2.3.2 Chondrocyte morphology

Chondrocytes cultured in weak gels after 7 days demonstrated a significantly higher percentage of chondrocytes with cytoplasmic processes in the presence of higher concentrations of FCS (5 and 10%) as compared to those in strong gels (P=0.0006 and P<0.0001 respectively; Fig. 4.39). In the weak gels, chondrocytes cultured with 2% and 5% of FCS had a significantly higher percentage of cells with processes as compared to those with 1% FCS in the same gel strength (P<0.01 and P<0.05 respectively). Moreover, chondrocytes cultured in the weak gels with 10% FCS had a significantly higher percentage of these abnormal cells with processes as compared to all the three lower concentrations (1%, 2% and 5%) of FCS (P<0.001; for all the conditions). However, the percentage of chondrocytes with cytoplasmic processes was not affected with increasing the concentrations of FCS for the cells cultured in strong gels. Thus, these results suggested that FCS and gel strength were related factors and the penetration of FCS into the gels was controlled by gel strength. Both these factors appeared to work in a similar manner and altered the same characteristics (volume/morphology) of chondrocytes.

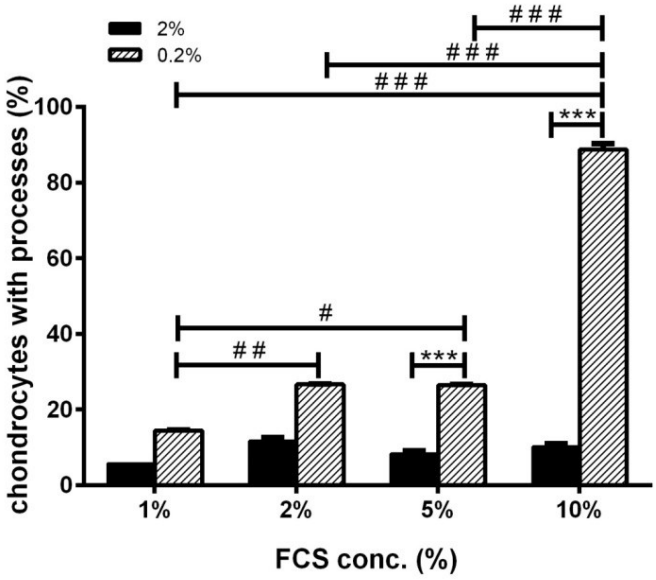

Figure 4.39: A higher percentage of chondrocytes had cytoplasmic processes in the weak gels with higher concentrations of FCS at day 7.
Pooled data obtained from [*N(n')*=6(35, 34, 180, 98) in strong gels and 6(222, 334, 389, 569)] in weak gels cultured with 1%, 2%, 5% and 10% concentrations of FCS respectively. * indicated a significant difference according to unpaired student's t-test. # indicated a significant difference according to one-way ANOVA followed by Tukey's multiple comparison post-hoc test. The single, double and triple symbols showed the level of significance for $P<0.05$, 0.01 and 0.001 respectively.

The number of processes per cell was significantly higher in chondrocytes cultured in weak gels in the presence of higher concentrations (5% and 10%) of FCS as compared to those in strong gels ($P<0.0001$ and $P=0.0002$ respectively). In the weak gels, a significantly higher number of processes per cell were seen in the presence of 10% FCS as compared to those in 1%, 2% and 5% FCS ($P<0.001$, $P<0.001$ and $P<0.01$ respectively) at the same gel strength. Moreover, chondrocytes cultured in weak gels with 5% FCS had higher numbers of processes per cell as compared to those cultured in the presence of 1% and 2% FCS in the same gel strength ($P<0.001$ for both conditions; Fig. 4.40). However, the number of cytoplasmic processes per

cell remained unaffected by increasing the concentrations of FCS in the strong gels after 7 days of *in vitro* culture.

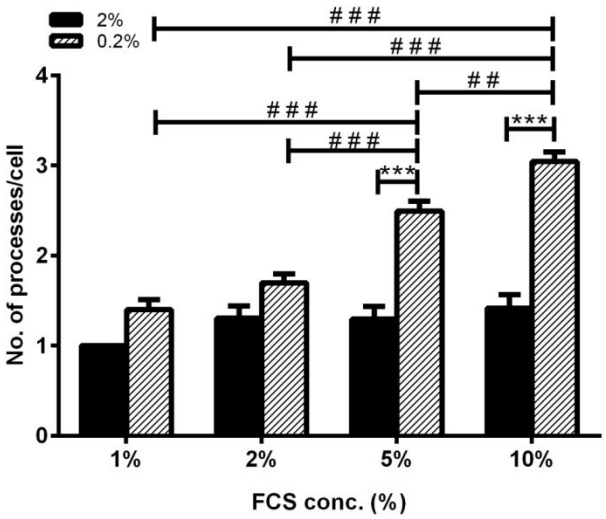

Figure 4.40: Number of processes per cell increased in the weak gels with higher concentrations of FCS at day 7.
Pooled data obtained from [*N(n')*=6(35, 34, 180, 98) in strong gels and 6(222, 334, 389, 569) in weak gels cultured with 1%, 2%, 5% and 10% concentrations of FCS respectively. * indicated a significant difference according to unpaired student's t-test. # indicated a significant difference according to one-way ANOVA followed by Tukey's multiple comparison post-hoc test. The single, double and triple symbols showed the level of significance for $P<0.05$, 0.01 and 0.001 respectively.

To summarise this section, when bovine chondrocytes were cultured in weak agarose gels with high concentrations of FCS cell density increased and displayed marked changes in morphology characterised by cluster formation and production of cytoplasmic processes as compared to cells cultured in strong gels. Moreover, increasing the concentration of FCS accelerated these morphological changes in weak gels but had no effect in strong gels. These results suggested that the factors present in FCS augmented cell proliferation and the morphological changes (clusters/cytoplasmic processes). Therefore, quantitatively both FCS and strength of

gels had the same effect on characteristics of chondrocytes and they appeared to be related in controlling chondrocyte morphology. The penetration of FCS was regulated by gel strength.

4.6 DISCUSSION

This study aimed at developing a reproducible *in vitro* 3D agarose gel culture model to study the morphological and volume changes in chondrocytes. The results supported the hypotheses such that chondrocytes cultured in weak agarose gels and with high concentrations of FCS displayed striking changes in volume and morphology (clusters/cytoplasmic processes) as compared to strong gels and with low concentrations of FCS. An obvious striking increase in density, volume and production of abnormal morphology (clusters/processes) was observed in the cells cultured in weak compared to the strong agarose gels (Figs. 4.21 & 4.22). Similar morphological changes were also observed in strong gels but the effect was mild. In other words strong gels appeared to slow down the changes to chondrocyte morphology. Additionally, chondrocytes cultured in weak gels over one week with high concentration of FCS displayed marked increase in chondrocyte density and altered morphology (clusters/processes) as compared to the low concentration of FCS (Fig. 4.36) where lower cell density and lesser clusters/processes were observed.

Various difficulties were encountered to establish this culture model and were minimised by taking great care and sometimes altering the methodology. The production of successful sterile cell cultures was the greatest problem and was

overcome by using rigorous aseptic experimental conditions. All the instruments used in these experiments were autoclaved, the joints were dissected under strict aseptic sterile conditions in class I-flow hood, freshly-prepared culture medium with antibiotics was used and medium changed on alternate days during the culture period. A specific type of agarose was used in these experiments, having a low melting point, was very sensitive to temperature changes therefore, 2% gel-chondrocyte suspension tended to set prematurely before getting thoroughly mixed and pipetted into the gel mould. This problem was solved by keeping the suspension warm in a water bath at 37˚C inside the flow hood and also by using pre-warmed pipette tips. The weak agarose gels took more time to set and were difficult to handle as they would often fall out of the 3D gel mould. This was overcome by cooling the gel mould to 4°C before pipetting the weak gel-chondrocyte suspension. This would let the temperature of the suspension fall quickly when pipetted in the wells causing the weak gels to set at once and firmly in the wells. The CLSM image acquisition was also problematic due to thickness of the gel blocks and it was optimized by cutting the base of the gel blocks carefully with a sharp sterile scalpel blade. However, the methodology finally used for obtaining these results was quite reproducible and allowed the successful culture of chondrocytes in different concentrations of agarose over a period of two weeks, thereby, promoting the maintenance of chondrocyte phenotype over the culture period. Use of bovine chondrocytes for orthopaedic research is well established as they can be obtained in adequate number and the cost effect is minimal and the findings from these cells may be relevant in the human condition (OA) by carrying out similar experiments on human tissue. As a general observation the changes in chondrocyte morphology were

more numerous on the gel surface and in the superficial layers of the gels but were easily seen until 100μm depth; below this point the fluorescent signals were very weak. Chondrocytes were occasionally present in pairs (Fig. 4.32) and this bichondral configuration is often present in intact bovine cartilage as previously reported by (Sasazaki et al., 2008). The chondrocyte pairs *in situ* were therefore possibly isolated as pairs following incubation with collagenase.

The volume of isolated bovine chondrocytes when cultured in weak gels increased significantly even after 1 day during *in vitro* culture as compared to the strong gels (Fig. 4.12). In a previous study it has been reported that the volume changes due to a change in medium osmolarity of *in situ* and isolated articular chondrocytes from 280mOsm to 380mOsm were similar (chondrocyte volume = 668 ± 31.7 μm^3 and 646 ± 54.6 μm^3 respectively) (Bush and Hall, 2001a). In the present experiments as DMEM with osmolarity raised to 380 mOsm (by adding NaCl) was used we believed that the isolated cells would maintain their *in situ* volume (Bush and Hall, 2001a). However, the likely explanation for increase in volume noticed in weak gels as compared to strong gels may be that chondrocytes have a tendency to swell and they can do this more easily in the weak gels as compared to strong gels.

Abnormal chondrocytes with processes developed in weak gels due to enhanced penetration of FCS therefore, both the factors appeared to be related such that FCS penetrability was enhanced in weak gel strength. Chondrocytes cultured in weak agarose gels started developing cytoplasmic processes in the early days of *in vitro* culture compared to strong gels (Fig. 4.14) and there could be several possible theories to explain these morphological changes. Since the penetrability of serum factors has been shown to decrease with increasing concentration of agarose

(Johnson et al., 1996), decreased stiffness of hydrogel could increase the availability of nutritive factors to the chondrocytes cultured in weak gels. Therefore, one possible explanation for morphological changes of these chondrocytes cultured in weak concentration of agarose gels is possibly due to increased rate of penetration of FCS into the weak gels. These serum morphogenic factors such as growth hormone, thyroid hormones T3/T4 and insulin possibly stimulated chondrocytes and promoted their synthetic activity. As a result, enhanced production of catabolic cytokines such as IL-1ß and TNFα caused destruction of the pericellular matrix of chondrocytes possibly collagen type VI and thus cytoplasmic extensions protruded out. This mechanism can be explained in the light of a study which stated that the abnormal chondrocytes with processes were associated with high levels of IL-1ß and disrupted pericellular collagen type VI (Murray et al., 2010). The previous and present studies cannot be directly compared because the previous study was performed on in situ chondrocytes and the results of present study are based on cultured chondrocytes. Although IL-1ß levels and type VI was beyond the scope of this work it can be speculated that abnormal cultured chondrocytes with processes may also produce high levels of IL-1ß thereby causing disruption of collagen type VI. Second possible explanation could be that the cells respond by sensing the stiffness of the culture material (Schuh et al., 2010). This can be well explained with a recent study highlighting the influence of substrate stiffness on mechanical properties of chondrocytes regulated by changes in actin cytoskeleton, focal adhesions and altered ECM synthesised (Chen et al., 2014). Therefore, it is possible that in the present study the ability of chondrocytes to sense the stiffness of their environment led to different morphological responses in different gel strengths. Third possibility could

be that the structural macromolecules such as PGs produced by chondrocytes in weak concentration of agarose gel were diffused through the gels possibly due to lack of an effective scaffold and enough attachment sites. However, the strong gels were dense enough to provide a scaffold for attachment and thus the ECM remained localised to the chondrocytes rather than getting diffused and assisted them in maintaining their spheroid morphology (Buschmann et al., 1992). Therefore, these reduced cell-matrix interactions in the weak gels could be a possible cause of abnormal shapes and development of processes.

In a very recent study it was reported that matrix stiffness does not influence the maintenance of chondrocytic phenotype (Schuh et al., 2012b) but increased cluster formation, enhanced expression of DNA and ECM formation by chondrocytes cultured in softer gels as compared to the stiffer gels was observed. Moreover, they measured expression of type II collagen and observed no effect of gel strength on expression of type II collagen. On the other hand the study presented here highlighted the detailed analysis of changes to chondrocyte morphology with varying gel strength. The common feature between previous and present study was chondrocyte cluster formation in weak/soft gels as compared to strong/stiff gels. There can be several reasons why morphological changes were not observed by Schuh and co-workers but the few main ones will be discussed here. One possibility is the difference in culture conditions as the minimum concentration of agarose used in their experiments was 0.75% and in the present study very weak gel strength (0.2%) was used and this might be the cause of altered morphology. However, an interesting future experiment could be culturing chondrocytes in 0.75% gel strength and studying their morphology as this can give a better insight as to whether

chondrocytes change shape at 0.75% gel strength or not. The other likely possibility is that in the previous study, immunohistochemistry (IHC) was used to study expression of collagen types I and II whereas in the present study chondrocytes were labelled with CMFDA. It was unlikely to visualise chondrocyte shape changes with the fluorescent markers labelling matrix in the previous study whereas labelling chondrocytes with CMFDA rendered it possible to visualise cytoplasmic processes as it labelled the cytoplasm.

We have also frequently observed cluster formation later during *in vitro* culture. Large sized clusters having more number of cells/cluster were present in weak gels as compared to strong gels (Fig. 4.21) and the number of clusters formed was significantly higher in weak gels with higher concentration of FCS as compared to the lesser concentrations of FCS (Fig. 4.36). An explanation could be the greater access of growth and proliferative factors present in the serum to the chondrocytes cultured in weak gels and to those within weak gels with higher concentrations of FCS. These growth factors might have stimulated the cells leading to proliferation and clusters were formed (van Susante et al., 2000). However, the chondrocytes cultured in strong gels with lower levels of penetration of FCS displayed low proliferative activity and lesser cluster formation (Johnson et al., 1996). Previous studies done on the degenerated osteoarthritic human cartilage (Weiss and Mirow, 1972, Bush and Hall, 2003) also observed cluster formation. Cluster formation is considered the hallmark of OA and the weak gels used in this study as an *in vitro* model for OA also displayed this change in cultured bovine chondrocytes (Figs. 4.24 & 4.38). Furthermore, the occurrence of chondrocyte clusters in the degenerate/weakened matrix in the superficial layers of cartilage have been related to

the enhanced access of growth factors present in synovial fluid (Meachim and Collins, 1962). The detailed quantitative analysis of data regarding cluster formation revealed that the volume of individual chondrocytes in the clusters remained unaffected but the total volume of clusters and number of cells per cluster increased significantly (Fig. 4.24). These findings suggested that in the weak gels under the effect of certain proliferative factors such as growth hormone present in FCS chondrocyte proliferation was triggered in forming clusters rather than increasing in volume.

This study has provided new insights regarding the effect of gel strength and morphogenic factors present in serum on chondrocyte morphology. In conclusion, both factors i.e. FCS and gel strength appeared to be related in controlling chondrocyte morphology as penetrability of FCS increased due to weak gel strength. In contrast, in the strong gels the penetration of FCS was reduced. Whether 3D agarose gel model developed in this study can be utilised to study chondrocyte morphological changes in OA has been discussed further later in the thesis (chapter 9).

CHAPTER 5: RESULTS

EVALUATION OF MATRIX PRODUCED BY CHONDROCYTES CULTURED IN STRONG OR WEAK AGAROSE GELS

5.1 CHAPTER SUMMARY

Chondrocyte morphology strongly influences the metabolism of ECM. This chapter aimed to assess the matrix produced by isolated bovine chondrocytes cultured in strong (2%) or weak (0.2%) agarose gel concentrations at days 1, 3 and 7 of culture. Haematoxylin and eosin (H&E), Alcian blue and Masson's trichrome stainings were performed by histology for chondrocyte morphology, proteoglycans (PGs) and collagen respectively. The H&E staining showed presence of chondrocyte clusters in weak gels by days 3 and 7 of culture as compared to strong gel strength. By days 3 and 7 of culture the percentage of Alcian blue staining was significantly higher in the cryosections of strong gels as compared to weak gels ($P<0.001$). However, Masson's trichrome staining results were inconclusive in these strong or weak gel sections. The abnormal chondrocytes in weak agarose gels produced altered matrix.

5.2 INTRODUCTION

In articular cartilage, chondrocytes are responsible for the production of matrix macromolecules thereby maintaining the normal tissue architecture and providing load-bearing properties to cartilage for its normal functioning. The major components of cartilage matrix are PGs (mainly aggrecan) and collagens (McDevitt, 1973). Matrix synthesis and breakdown are controlled by the anabolic and catabolic activities of chondrocytes thereby, maintained at a steady state level (Pearle et al., 2005). In OA, this balance is disturbed and chondrocyte catabolic activities exceed anabolic activities leading to cartilage degeneration (Goldring and Goldring, 2004). Therefore, in the pathophysiology of OA, altered chondrocyte metabolism is one of the mechanisms involved in cartilage degeneration. This altered chondrocyte

metabolism leads to loss of PGs and loosening of matrix as early events of OA (Malemud, 1991). The loss of PGs leads to matrix weakening, increased permeability and swelling of the cartilage (Wang et al., 2013a) thereby reducing stiffness (Maroudas, 1976) and mechanical resilience of the tissue. This weakened matrix increases access of proliferative factors from the synovial fluid to the chondrocytes thus stimulating them and producing clusters especially in the superficial layers of cartilage (Schumacher et al., 2002, Lotz et al., 2010).

Cell metabolism has already been associated to changes in cell shape and volume in several other types of cells (D'Anselmi et al., 2011). Few studies conducted on the morphology of chondrocytes in OA have reported abnormal chondrocyte morphology in this disorder (Kouri et al., 1998, Bush and Hall, 2003). There exists a strong relationship between chondrocyte morphology and the biosynthetic activity as reported in a study where fibroblast-like chondrocytes were seen in late stages of OA and were associated with the expression of abnormal matrix rich in type I collagen and small molecular weight PGs (Tesche and Miosge, 2005). Additionally, in a recent study, abnormal chondrocyte morphology has been related to increased levels of IL-1ß and decreased pericellular type VI collagen levels (Murray et al., 2010). To determine the effect of abnormal chondrocyte morphology on matrix metabolism 3D agarose gel model has been utilised in this study.

As explained in the previous chapter (chapter 4) a 3D agarose gel model was developed and utilised as a tool to control chondrocyte shape, therefore, strong and weak gels were used as control and experimental conditions. The strong gels were used to compare healthy intact matrix whereas, weak gels to compare damaged/weakened matrix. The importance of using agarose gel cultures could be

due to two main reasons: **Firstly,** chondrocytes when isolated from their native environment by cell isolation technique using enzymatic digestion of ECM and cultured in 3D agarose gels have shown to maintain their phenotype during long-term culture (Benya and Shaffer, 1982). **Secondly,** chondrocytes synthesize mechanically functional proteoglycan-collagen matrix when cultured in agarose gels (Buschmann et al., 1992) and have been reported most suitable for chondrocyte culture (Schuh et al., 2012a).

In the preliminary work presented in this thesis by using fluorescent-mode CLSM chondrocytes displayed marked changes to morphology (clusters/processes) when cultured in weak gels as compared to strong gels (section 4.6). Whether these chondrocytes with abnormal morphology produced altered matrix in comparison to morphologically normal chondrocytes, histological examination was performed and results presented in this chapter.

5.3 HYPOTHESIS

The abnormal chondrocytes with cytoplasmic processes in weak agarose gels produced altered matrix in comparison to normal chondrocytes cultured in strong gels.

5.4 MATERIALS AND METHODS

5.4.1 Tissue processing for histology of isolated chondrocytes cultured in 3D agarose gel moulds

Freshly isolated bovine chondrocytes were cultured in two different gel strengths (2% and 0.2%) i.e. strong and weak according to the methodology already described

(section 4.4). At three time points (days 1, 3 and 7) the strong and weak gels containing cultured bovine chondrocytes were snap frozen and sectioned to prepare for the histological staining.

5.4.2 Snap freezing and sectioning of gels

A beaker containing hexane was placed in dry ice one hour prior to snap freezing to cool hexane to approx. -70°C. The strong and weak gels were placed in aluminium foil boats and immersed in the pre-cooled hexane to snap freeze. Snap freezing is a technique for rapid cooling of samples to maintain tissue integrity at molecular level as much as possible by avoiding dehydration of samples. In a previous study it has been reported that rapid cooling caused very little damage to the cartilage matrix (Guan et al., 2006). After freezing, the gel blocks were wrapped in aluminium foil separately, labelled and stored at -80°C until required. The gels were taken out from -80° freezers and kept in -20° freezers a night before cutting in order to equilibrate them to the cutting temperature. A few drops of OCT (optimal cutting temperature, Bright Instrument Company, UK) were poured on the chuck of the cryostat (Leica CM3050S, Leica Microsystems Ltd., UK) and the gel blocks were submerged almost one-third in the OCT in such a way that it covered the base of the gel block and just lower one-third of the sides of block. The gel block was left in OCT for 5 min until it was frozen and the gel was fixed properly to the chuck. The chuck was placed in the cutting position and oriented at an angle to cut the block symmetrically. The samples were then sectioned (10 µm thick) by adjusting temperature between -23°C and -26°C. The sections were cut slowly and cautiously to avoid any wrinkling of the tissue and collected onto Superfrost microscopy slides (Thermo Scientific, UK).

Slides were labelled, individually wrapped in aluminium foil, kept in boxes and stored at -80°C until used. The slides were left at room temperature before being unwrapped and used for histology.

5.4.3 Histological staining

The sections were stained with H&E, Alcian blue and Masson's trichrome staining techniques in a single large-batch in order to limit artefact introduced discrepancies in the staining intensity. The details of histological staining steps were given in following sections.

5.4.3.1 *H&E staining of frozen sections*

The H&E staining was performed to visualise the morphology of chondrocytes cultured in strong and weak gels at three time points during the culture. The frozen sections were fixed in 4% PFA for 20 min at room temperature, rinsed gently in tap water. The slides were then placed in jars containing filtered Harris' haematoxylin (Avwioro, 2011) composed of 1 g haematoxylin, 10 ml absolute alcohol, 20 g potassium alum, 200 ml distilled water (D/W), 0.5 g mercuric oxide and 8 ml glacial acetic acid added once solution is cooled (Sigma-Aldrich, Poole, U.K.) for 5 min, and then washed in running water. The slides were placed in STWS (Scott's tap water substitute) composed of 20 g magnesium sulphate, 3.5 g sodium bicarbonate (Sigma-Aldrich Co. Ltd., Poole, UK) and 1 L D/W as this blues the haematoxylin; for 3 min and then washed in water for 3 min. The staining was checked under the microscope and the slides were placed in 1% water based filtered eosin composed of 1 g eosin in 100 ml (Sigma-Aldrich, Poole, U.K.) for 2 min. The slides were rinsed briefly in water and placed in 5% Potassium alum composed of 5 g potassium

aluminium sulphate in 100 ml of D/W, for 2 min and rinsed in water again. The slides were placed on racks and left to air dry overnight inside the flow hood and the flow hood was left on. The next day, slides were mounted directly in organic solvent soluble DPX mounting medium distyrene plasticizer xylene (DPX, Sigma-Aldrich Co. Ltd., Poole, UK) a mixture of distyrene, plasticizer and xylene, cover slipped and left in the flow hood overnight. After drying, the slides were placed in slide boxes and stored at room temperature until used.

5.4.3.2 *Alcian blue staining of frozen sections*

Proteoglycans (PGs) are composed of glycosaminoglycans (GAGs) covalently attached to the core protein. These highly sulphated negatively charged PGs in the cultured chondrocytes were stained with 1% Alcian blue 8GX (Sigma-Aldrich, Poole, U.K.); pH1.0. 1 g of Alcian blue 8GX dissolved thoroughly on a magnetic stirrer in 100 ml of 0.1M HCl at room temperature; solution filtered and stored at room temperature. The sections were fixed with 4% PFA, washed with PBS (x3) and then stained in filtered Alcian blue solution overnight. The slides were rinsed once with 0.1M HCl (0.36 ml of HCl was dissolved in 100 ml of D/W to prepare 0.1M HCl), then with PBS (x2) and then with water. The sections were counterstained in Nuclear fast red solution composed of 12.5 g of aluminium sulphate dissolved in 250 ml of D/W; 0.25 g of nuclear fast red was added and slowly heated to boil and cool; solution filtered and a grain of thymol (Sigma-Aldrich, Poole, U.K.) was added as a preservative, for 5 min to stain the nuclei pink and washed in running tap water for 1 min and finally rinsed in D/W once for 2 min. The slides were then dehydrated in ascending grades of ethanol (70%, 95% and 100% for 2 min each), cleared in xylene

(5 min), mounted and cover-slipped in DPX and stored as previously described (section 5.4.3.1).

5.4.3.3 *Masson's trichrome staining of frozen sections*

To stain the collagen amongst the cultured chondrocytes in strong and weak gels, the frozen sections were stained with a Masson's trichrome staining technique (Suvik and Effendy, 2012). Masson's trichrome does not selectively stain any particular type of collagen rather collectively stains the overall collagen present within the tissue. In a recent study the histological evaluation of overall cartilage repair was performed by Masson's trichrome and type II collagen was detected by immunohistochemistry (Chung et al., 2014). The sections were fixed with 4% PFA, washed in D/W and stained in Weigert's iron Hematoxylin working solution (Stock solution A: 1g Hematoxylin was dissolved in 100 ml of 95% alcohol; Stock solution B: 4 ml of 29% ferric chloride and 1 ml of concentrated HCl was added to 95 ml of D/W; equal parts of stock solution A and B were mixed) for 5 min. The slides were then rinsed in running warm tap water for 10 min and then washed in D/W. The slides were then placed in jars containing Biebrich scarlet-acid fuchsin solution (90 ml of 1% aqueous Biebrich scarlet, 10 ml of 1% aqueous acid fuchsin and 1 ml of glacial acetic acid were dissolved) for 10 min and then washed in D/W. The sections were then differentiated in phosphomolybdic-phosphotungstic acid solution (25 ml of 5% phosphomolybdic acid solution was added to 25 ml of 5% phosphotungstic acid solution) for 15 min. The sections were transferred directly (without rinse) to Aniline blue solution (2.5 g aniline blue was dissolved in 2 ml of glacial acetic acid and 100 ml of D/W) and stained for 15 min, rinsed briefly in D/W and differentiated in 1%

acetic acid solution (1 ml of glacial acetic acid was added to 99 ml of D/W) for 3 min and finally washed in D/W. The slides were dehydrated very quickly through absolute ethyl alcohol, cleared in xylene, mounted, dried and stored as previously described.

5.4.4 Acquisition of photomicrographs of stained sections of cultured bovine chondrocytes

The photomicrographs of the stained sections of chondrocytes cultured in different gel concentrations were obtained using Leica DMRE 35578 upright microscope (Leica Microsystems GmbH, Wetzlar, Germany) with 12V 100W halogen bulb for bright field (BF) illumination and during imaging the condenser disc was adjusted for bright field position. The images were obtained with x10 PL Fluotar or x20 PL Apo/oil lenses with NA of 0.30 and 0.70 respectively and captured with mounted digital QImaging Retiga 2000R-monochrome cooled CCD camera (Photometrics, Tucson, U.S.A.). An RGB (red green blue) filter placed in front of the camera allowed capture of colour images. The coloured images were then viewed and captured by using QCapture Pro v6.0 software (Photometrics, Tucson, U.S.A.) after adjusting the appropriate light intensity. On all the slides various sections were imaged randomly and in one session with similar microscopic adjustments in order to avoid discrepancies in the measurement of intensity of staining colour due to variability in the intensity of light.

5.4.5 Analysis of images by using ImageJ analysis software

The photomicrographs of stained histological sections were then analysed by Java-based image processing software ImageJ version 1.46h (ImageJ, NIH, Bethesda, MD,

U.S.A.). The images acquired provided information regarding the staining intensity which was visualised and analysed to obtain quantitative data. H&E stained photomicrographs were visualised to compare the density and morphology of cultured chondrocytes in the strong and weak gels.

The high power (x20 oil immersion) magnification images were used for determination of staining pattern of the cultured chondrocytes at days 1, 3 and 7 of culture and compared in both concentrations of agarose gel. A specified ROI was applied with dimensions of x, y, z 178, 192 and 10 μm respectively around the cells/clusters and not taking into account the background staining of gels. Firstly, after applying the ROI the image was cropped and the area of the whole ROI was measured. Secondly, colour threshold was adjusted and blue stained area around cell/cluster was measured. Lastly, a percentage of Alcian blue staining was determined with the formula 100 x (Blue stained area around cell/cluster/total area of ROI applied) %. It was possible to determine percentage of Alcian blue staining between single cells. However, in order to determine percentage staining of individual chondrocytes within a cluster, the staining of the cluster was determined initially. This was because the threshold of intensity of blue colour was similar for all the cells in the cluster and the segmentation of staining around individual cells in the cluster was not possible (Fig. 5.1). The number of cells in the clusters was counted by eye on ImageJ by counting the nuclei stained with Nuclear fast red dye. Therefore, the average Alcian blue staining around individual cells in a cluster was determined with the formula (percentage of Alcian blue staining in cluster (%)/total number of cells in cluster).

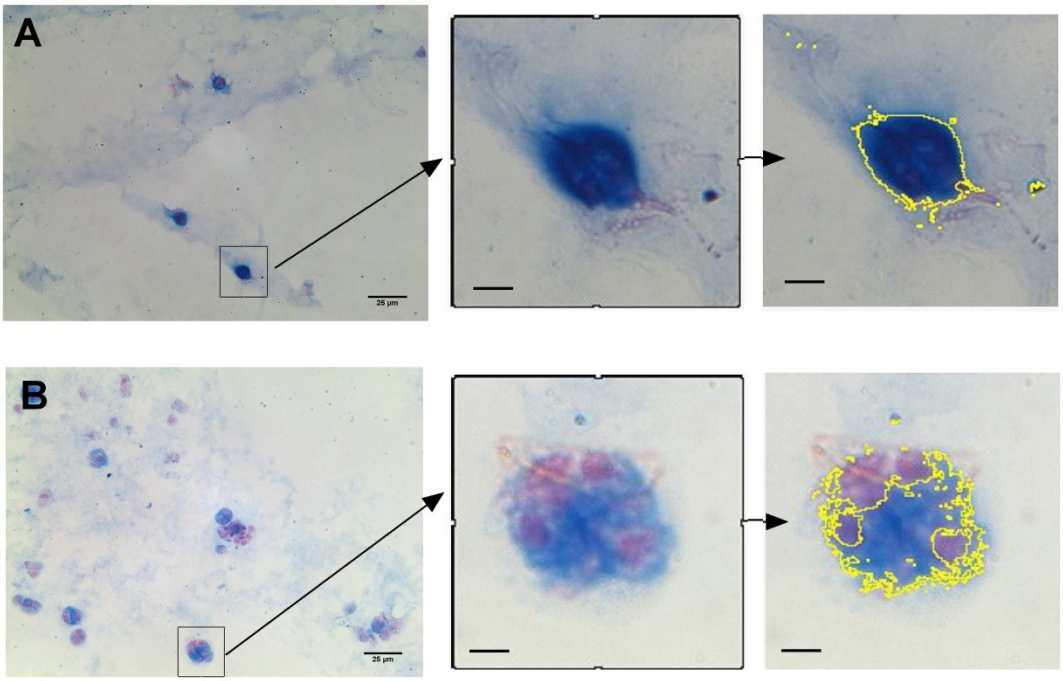

Figure 5.1: Determination of staining intensity of images by ImageJ analysis software.
Examples of determination of Alcian blue stained area for (A) single cell in the strong gel and (B) cluster in the weak gel. The left panel shows full image with the application of specified ROI, centre panel contains cropped images within ROI and right panel comprises of images outlining the blue area determined after adjusting for colour threshold. Scale bar for all panels and for inset images = 25µm & 3.5µm respectively.

5.5 RESULTS

5.5.1 Histological evaluation of matrix produced by isolated bovine chondrocytes cultured in strong or weak agarose gels

In order to investigate and compare the differences in matrix produced by chondrocytes with altered morphology (clusters/cytoplasmic processes) and morphologically normal chondrocytes, histology was performed. As a first step, it was observed that the strong gels had higher intensity of background staining with

Alcian blue caused by the staining of agarose gel molecules as compared to weak gels throughout the culture (Fig. 5.2; $P<0.002$). Therefore, a region of interest (ROI) was determined to encompass the staining intensity around individual cells/clusters rather than taking into account the whole image in order to avoid the discrepancies produced due to background staining. Therefore, this background staining had no impact on the results. An alternative method could have been to subtract the background staining value in both strong and weak gels. However, to be more accurate chondrocytes and clusters were analysed individually.

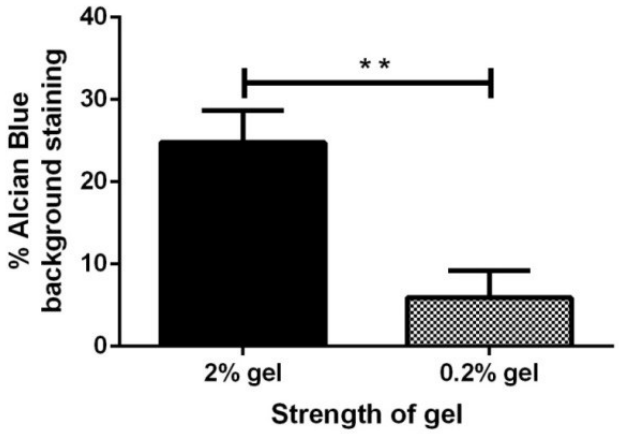

Figure 5.2: Percentage intensity of background staining of Alcian blue in strong and weak gels.
Graph shows pooled data with a significantly less background staining of Alcian blue in weak gels as compared to strong gels. Data were from [*N(n)* = 3(8)]. * indicated a significant difference according to unpaired student's t-test. The single, double and triple symbols showed the level of significance for $P<0.05$, 0.01 and 0.001 respectively.

5.5.1.1 *Alcian blue staining*

The histology sections of isolated chondrocytes cultured in strong and weak gels were stained with Alcian blue to stain PGs present at three time points. The specified

ROI (section 5.4.5) was selected and applied to all the images and in both strengths of agarose gels. The percentage staining was calculated by applying the specified ROI to all the images without any alteration in the dimensions of ROI. The data seemed to be complicated by days 3 and 7 of culture because of the presence of clusters therefore; average percentage staining around individual cells in the cluster was calculated (section 5.4.5). At day 1, slight Alcian blue staining was observed around chondrocytes but there was background staining in the sections having chondrocytes cultured in both strengths of gel and nuclei could be seen (Figs. 5.3a, b & 5.4a, b). At days 3 and 7 of culture the Alcian blue stain was less in the chondrocytes cultured in weak as compared to strong gels (Figs. 5.3 & 5.4). The Alcian blue staining was not easily visible at low power magnification hence high power images were analysed to study the different staining pattern in both gel strengths.

The quantitative data regarding percentage of Alcian blue staining varied in the two strengths of gel. At day 1, chondrocytes cultured in strong and weak gels showed almost no staining with Alcian blue (Fig. 5.5). The chondrocytes cultured in both gel strengths showed a significant increase in the percentages of Alcian blue staining by days 3 and 7 of culture as compared to day 1 (Fig. 5.5; $P<0.001$; one-way ANOVA for the two time points and in both strengths of gel). Alcian blue staining appeared more intense and structured around chondrocytes in the strong as compared to weak gels where staining was less in intensity and diffused in appearance (Fig. 5.4e&f).

Percentages of Alcian blue staining were compared in both strengths of agarose gel and was observed that at day 3, percentage of Alcian blue staining was significantly higher in the chondrocytes cultured in strong gels (4.9±0.4%) as compared to weak

gels (2±0.1%; Fig. 5.5; $P<0.001$; student's t-test). Similarly, at day 7 the percentage of Alcian blue staining was also found to be significantly higher in the strong gels (6.5±0.4%) as compared to weak gels (1.7±0.2%; Fig. 5.5; $P<0.001$; student's t-test). Additionally, the percentage of Alcian blue staining around chondrocytes increased significantly at day 7 as compared to day 3 ($P<0.05$). However, the percentage of Alcian blue staining by day 7 remained unaffected in weak agarose gels as compared to day 3, but they appeared to stain positively for Alcian blue after day 3.

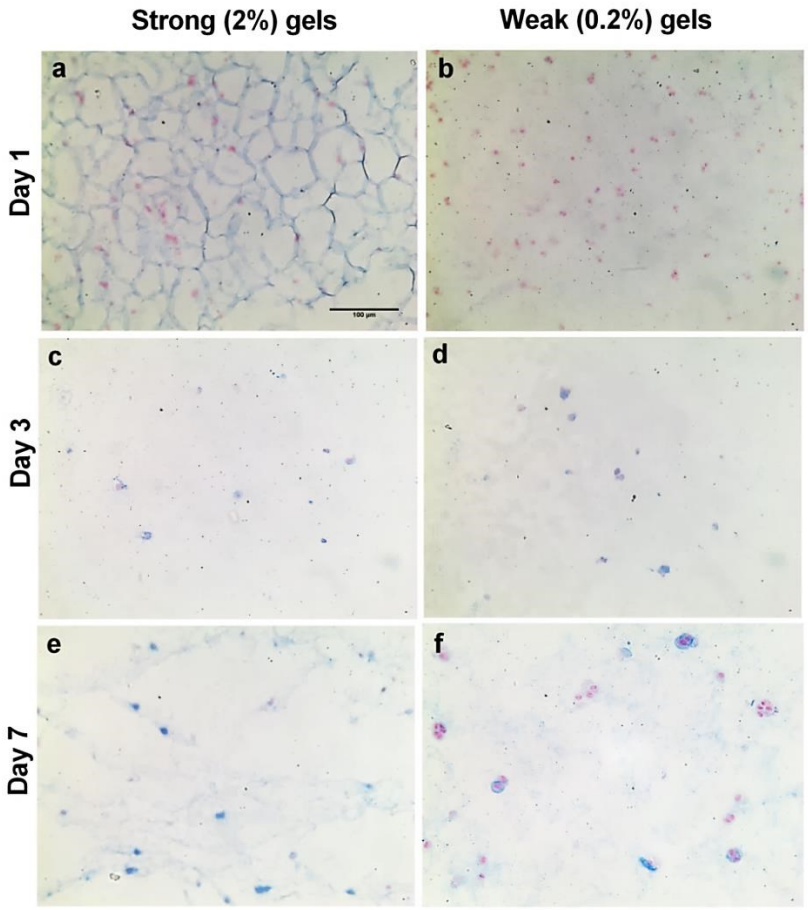

Figure 5.3: Photomicrographs of Alcian blue stained sections of chondrocytes cultured in different gel strengths at low power magnification.
The histological sections of cultured chondrocytes stained with Alcian blue and imaged at low power (x10) at (a, b) day 1, (c, d) day 3 and (e, f) day 7 of culture in strong (left panel) and weak (right panel) agarose gels. Section (a) shows artefact in labelling. Scale bar for both panels = 100µm.

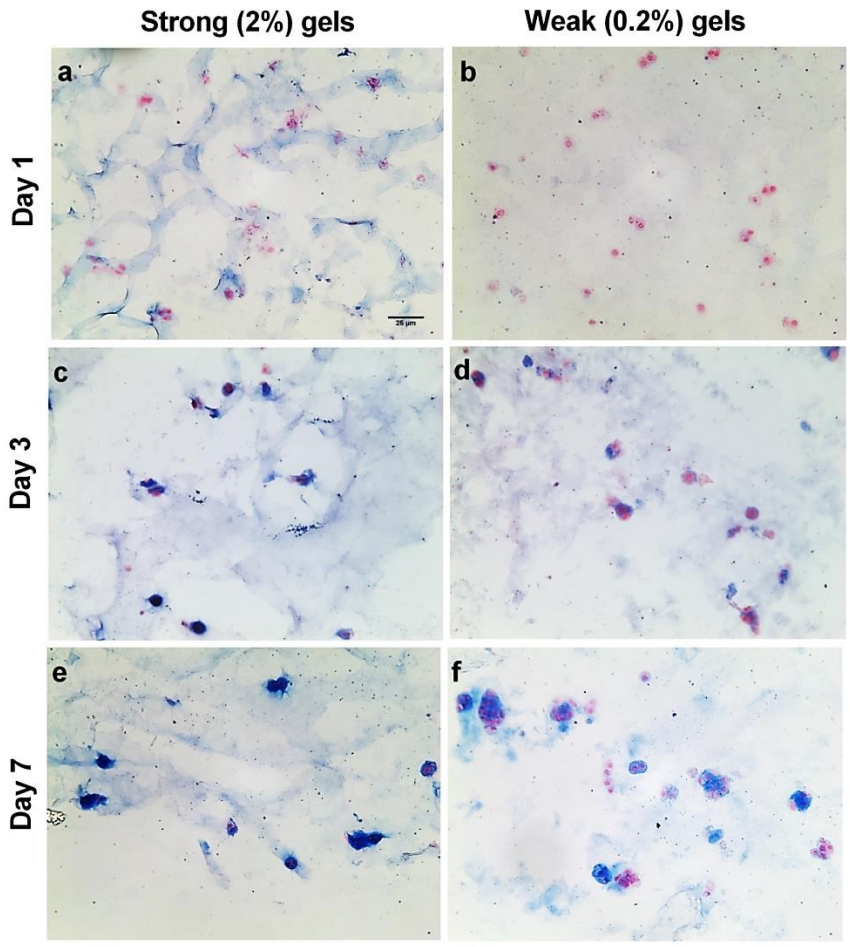

Figure 5.4: Photomicrographs of Alcian blue stained sections of chondrocytes cultured in different gel strengths at high power magnification.
The histological sections of cultured chondrocytes stained with Alcian blue and imaged at high power (x20 oil immersion) at (a, b) day 1, (c, d) day 3 and (e, f) day 7 of culture in strong (left panel) and weak (right panel) agarose gels. Scale bar for both panels = 25µm.

To summarise this section, percentage of Alcian blue staining increased progressively during the course of culture in the strong gels. In the weak gels percentage of Alcian blue staining increased significantly by day 3 but no further increase was detected by day 7. At days 3 and 7 of culture percentages of Alcian blue staining were significantly less in weak gels as compared to strong gels.

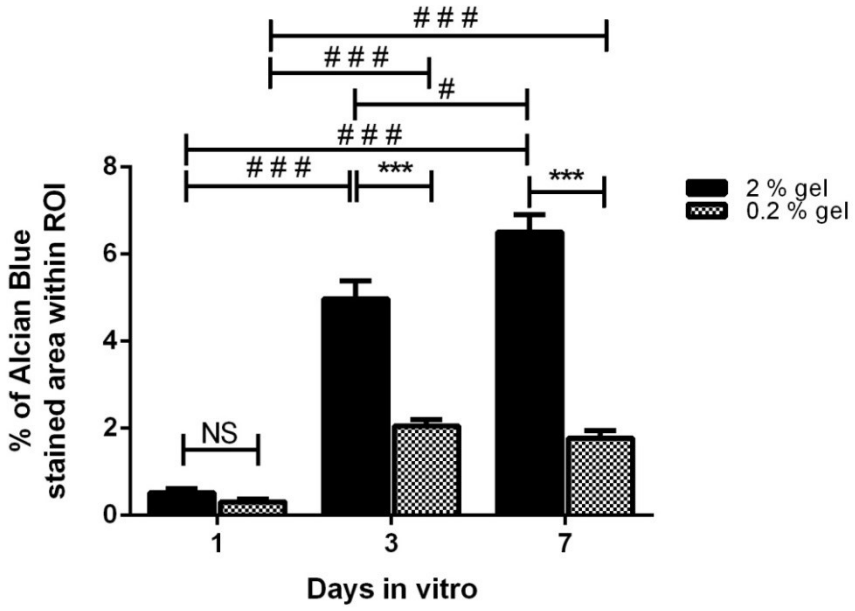

Figure 5.5: The percentage of Alcian blue staining of isolated bovine chondrocytes cultured in strong and weak gels.
Graph shows pooled data regarding percentage of Alcian blue staining of cultured chondrocytes at days 1, 3 and 7 of culture in different gel strengths. Data were from [*N(n')* = 6(10,10), (27, 42) and (43, 54) cells at days 1, 3 and 7 strong and weak gels respectively]. * indicated a significant difference according to unpaired student's t-test. # indicated a significant difference according to one-way ANOVA followed by Tukey's multiple comparison post-hoc test. The single, double and triple symbols showed the level of significance for $P<0.05$, 0.01 and 0.001 respectively.

5.5.1.2 *H&E staining*

The H&E stain the nuclei and cytoplasm of the cells as purple and pink respectively, haematoxylin is a powerful and selective nuclear stain giving sharp outline of nuclear structure (Avwioro, 2011). The low and high power images of H&E stained sections of cultured chondrocytes (Figs. 5.6 & 5.7) showed cluster formation in the weak as compared to strong gels by days 3 and 7 of culture. In the preliminary experiments,

with the use of fluorescent mode CLSM, chondrocytes cultured in weak gels showed cytoplasmic processes emanating from the cell bodies as compared to the chondrocytes cultured in strong gels (section 4.5). These results suggested that chondrocytes changed shape dramatically in the weak gels. However, it was not possible to visualise these fine morphological details by the routine histological techniques. With H&E histological staining, at day 7 of culture the cell density also appeared to increase in the weak gels as compared to strong gels (Figs. 5.6 & 5.7). Quantitative data regarding cell density could not be acquired with H&E staining because of the clusters present and it was not possible to count number of cells in a cluster in a 2D image. Moreover, the non-specific H&E staining of the background was more in the strong gels as compared to the weak gels (Figs. 5.6 & 5.7). The explanation for this background staining can be due to haematoxylin binding to the polysaccaride agarose as it has the ability to bind to carbohydrates (Avwioro, 2011).

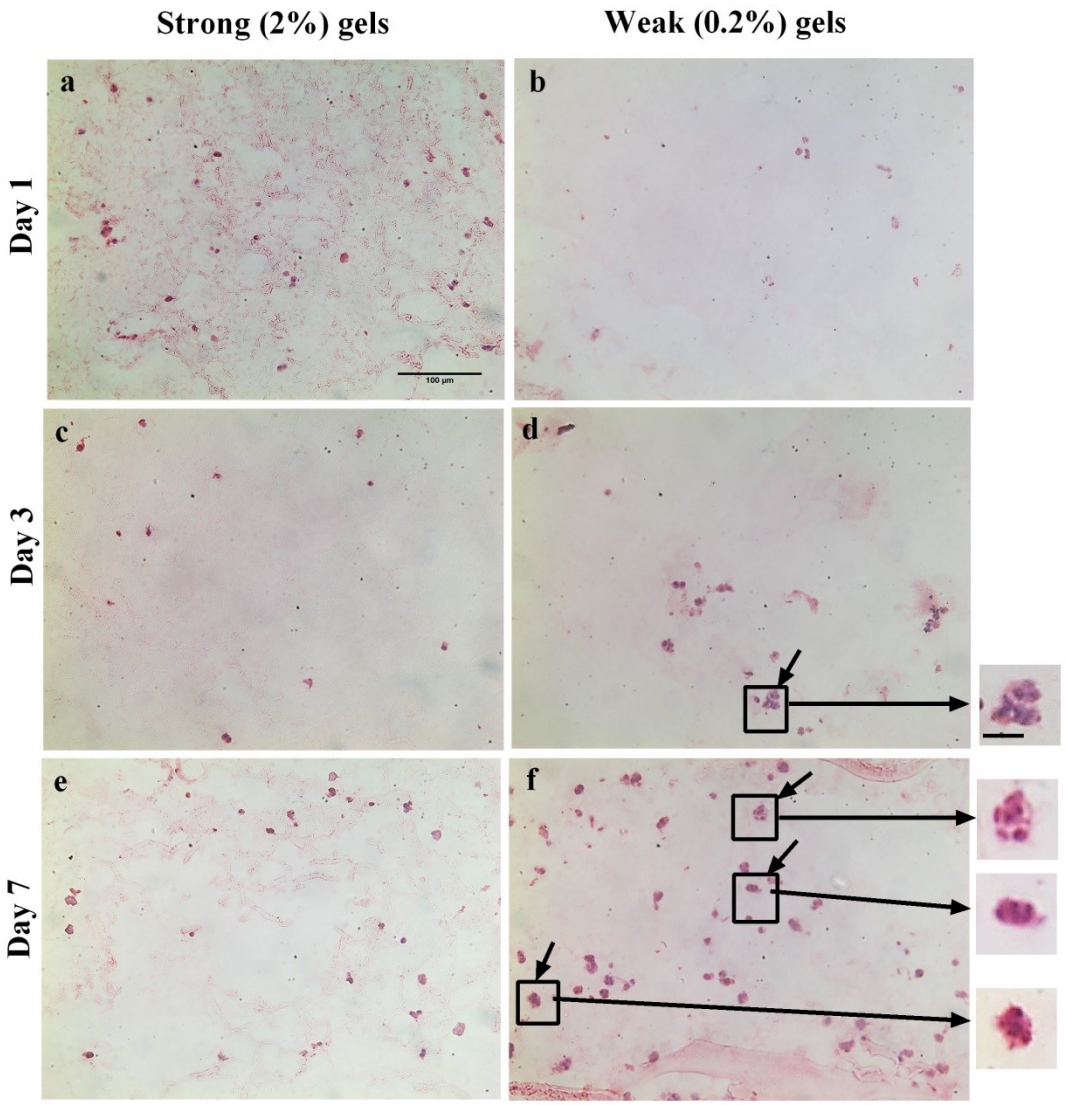

Figure 5.6: Photomicrographs of H&E stained sections of isolated chondrocytes cultured in different gel strengths at low power.

The histological images (x10) of cultured chondrocytes at (a, b) day 1, (c, d) day 3 and (e, f) day 7 of culture in strong (left panel) and weak (right panel) gels. The inset images show twice zoomed in areas and indicates to the examples of chondrocyte clusters present in the weak gels. Scale bar for all panels and for inset images = 100µm & 25µm respectively.

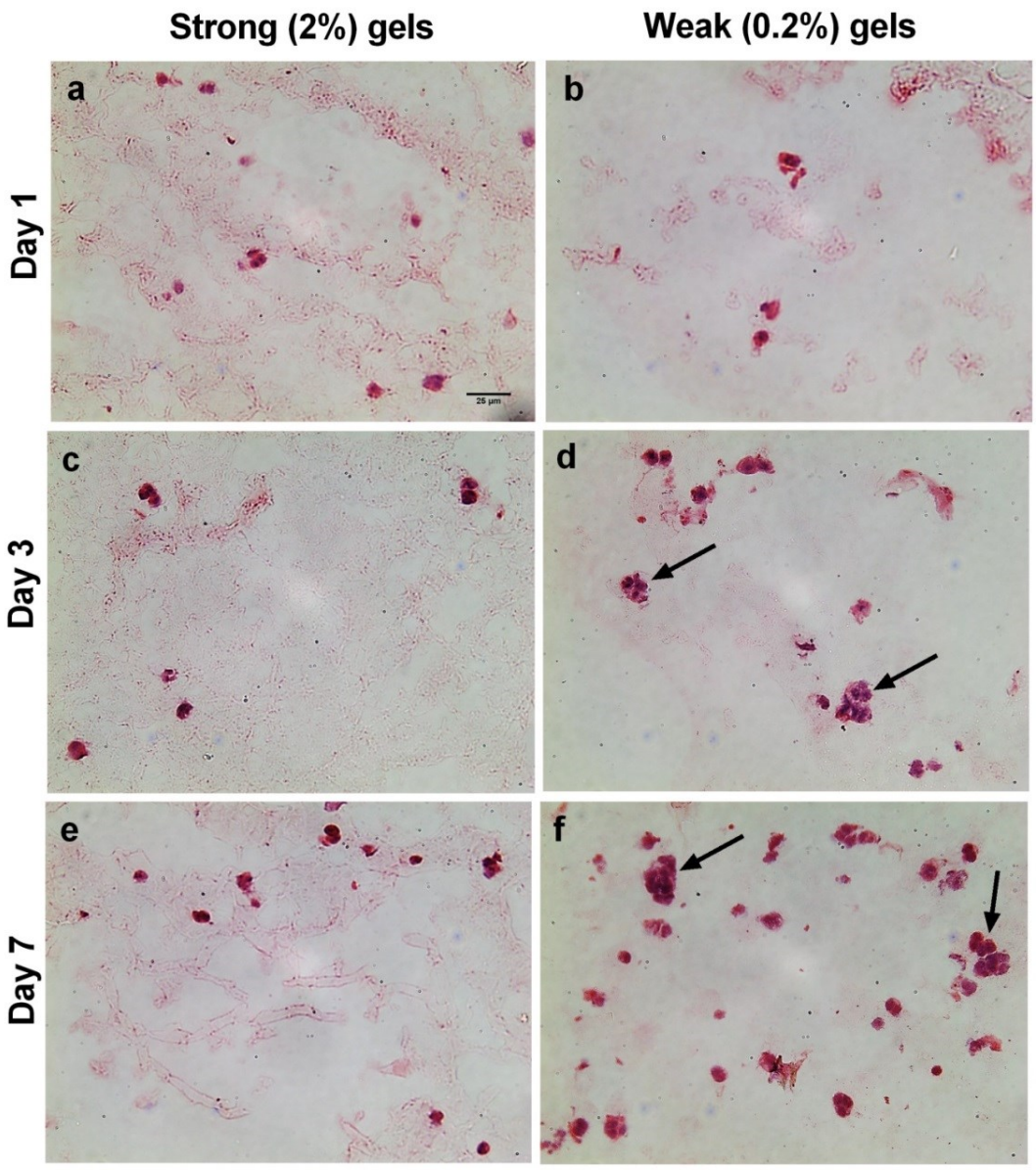

Figure 5.7: Photomicrographs of H&E stained sections of isolated chondrocytes cultured in different gel strengths at high power.

The histological images (x20 oil immersion) of cultured chondrocytes at (a, b) day 1, (c, d) day 3 and (e, f) day 7 of culture in strong (left panel) and weak (right panel) gels. Solid arrows indicate to the examples of chondrocyte clusters present in the weak gels. Scale bar for both panels = 25µm.

5.5.1.3 *Masson's trichrome staining*

The histology sections of cultured chondrocytes in strong and weak gels were stained with Masson's trichrome stain to roughly estimate the presence of collagen produced by cultured cells. This technique stains nuclei black, cytoplasm/muscle red and collagen blue (Kiernan, 2008). The Masson's trichrome staining technique stained the collagen present as shown in a representative control image of cartilage section with blue (Fig. 5.8B). The low and high power magnification images of Masson's trichrome showed weak staining (Figs. 5.8 & 5.9) during the course of culture. The positive staining in the control samples and weak staining observed in the experimental sections indicated two possibilities. The first one was that the technique was not successful for detecting collagen within chondrocytes cultured in agarose gels. Second possibility was that in such a short time no significant levels of collagen were produced by chondrocytes. In summary this staining method couldn't stain collagen if produced by these cultured chondrocytes at days 3 and 7 of culture in both the gel strengths.

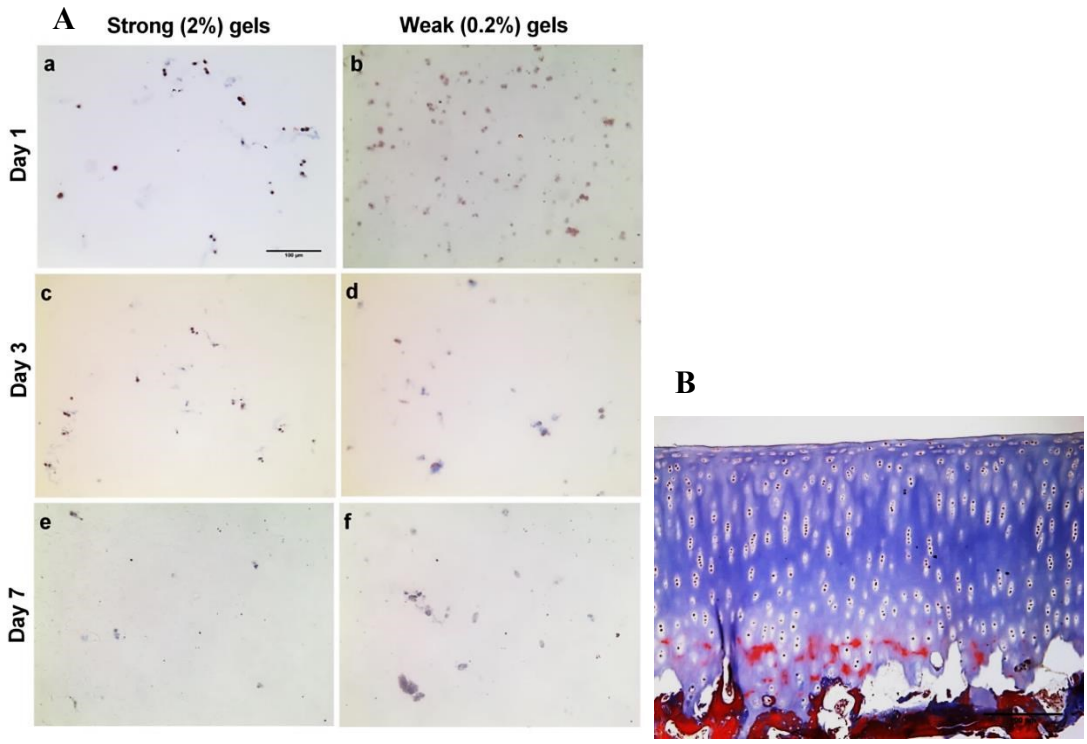

Figure 5.8: Low power photomicrographs of Masson's trichrome stained sections of chondrocytes cultured in strong and weak gels.

(A) The histological sections of cultured bovine chondrocytes stained with Masson's trichrome and imaged at low power (x10) at (a, b) day 1, (c, d) day 3 and (e, f) day 7 of culture in strong (left panel) and weak (right panel) gels. (B) The representative image of positive control for collagen staining with Masson's trichrome stain in bovine articular cartilage showing presence of collagen in all the zones of cartilage. Scale bar for all the panels = 100µm.

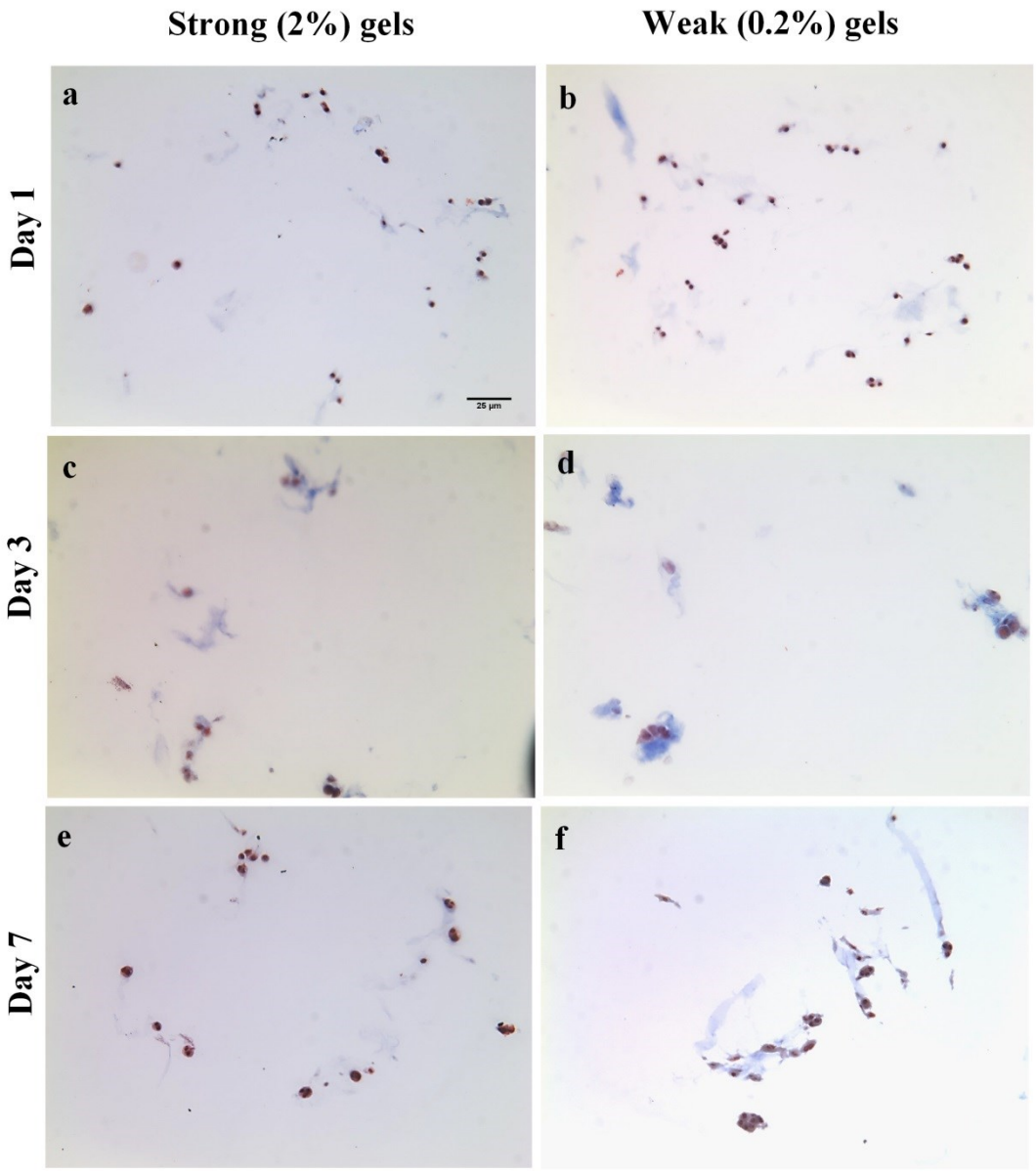

Figure 5.9: High power photomicrographs of Masson's trichrome stained sections of chondrocytes cultured in strong and weak gels.

The histological sections of cultured bovine chondrocytes stained with Masson's trichrome and imaged at high power (x20 oil immersion) at (a, b) day 1, (c, d) day 3 and (e, f) day 7 of culture in strong (left panel) and weak (right panel) gels. Scale bar for both panels = 25µm.

5.6 DISCUSSION

The results partially supported the main hypothesis of the study such that Alcian blue staining was significantly less in the chondrocytes cultured in weak gels but the results for the Masson's trichrome staining were unconvincing. The histology with H&E revealed the presence of chondrocyte clusters in the weak gels but not in strong gels (Figs. 5.6 & 5.7). The Alcian blue staining pattern might indicate higher levels of PGs in strong versus weak gels (Fig. 5.5). However, Masson's trichrome staining results were indecisive and collagen if produced by these cultured chondrocytes could not be successfully detected in strong and weak gels by day 7.

Some technical difficulties encountered during staining procedure and data acquisition were attempted to be minimised. **Firstly,** in the Alcian blue stained sections there was non-specific background staining because of binding of dye to the agarose molecules due to its ability to bind polysaccharides (Terry et al., 2000). This background staining was more intense in strong gels as compared to weak gels (Fig. 5.2). During culture this background Alcian blue staining intensity did not increase in either strengths of gel (Fig. 5.4) but the staining intensity around chondrocytes increased in the strong gels (Fig. 5.5). This suggested that may be the background staining was not due to binding of dye to the PGs rather it was due to binding to agarose molecules. **Secondly,** in the Masson's trichrome staining technique with the protocol published by others (Suvik and Effendy, 2012) showed inconclusive results (Figs. 5.8A & 5.9). Although by the same protocol cartilage samples (positive control) were stained successfully for the presence of collagen (Fig. 5.8B). These technical staining issues are now discussed in detail.

In this study the fine morphological details (cytoplasmic processes) were possibly masked because of the histological techniques performed and changes to chondrocyte morphology were not visible (Fig. 5.7). To author's knowledge there is no reported evidence of presence of cytoplasmic processes with routine histology and light microscopy. The few studies done on OA tissue reporting the presence of these cytoplasmic processes in this disorder utilised CLSM to visualise this morphological feature of chondrocytes (Kouri et al., 1998, Bush and Hall, 2003).

Cluster formation is a characteristic feature of OA (Lotz et al., 2010) and was observed routinely in H&E stained sections in this study at days 3 and 7 in the weak gels as compared to strong gels (Figs. 5.6 & 5.7). These findings are in agreement with previous studies where cluster formation was observed in chondrocytes cultured in agarose gels (Buschmann et al., 1992, Ross et al., 2006, Schuh et al., 2012b). The presence of these clusters could be possibly due to the greater access of proliferative/growth factors present in serum to the chondrocytes cultured in weak gels as compared to strong gels (Schuh et al., 2012b). This can be well explained by considering a study reporting the greater diffusive hindrance in the gels with higher concentration of agarose (Johnson et al., 1996). In this previous study it was reported that in the dilute gels with low concentration of agarose there was less hindrance to diffusion and therefore greater diffusivity. This previous study also suggested that in more concentrated gels the diffusion was hindered. Therefore, in the present study possibly growth/proliferative factors such as growth hormone and insulin present in the FCS could diffuse more in the weak gels as compared to the strong gels. These factors could possibly trigger chondrocytes to proliferate and form clusters.

Masson's trichrome staining for the cultured chondrocytes in strong and weak gels results were indecisive (Figs. 5.8 & 5.9). A possible explanation could be that these chondrocytes were cultured over a period of just 7 days and this time period was not enough to produce a quantity of collagen detectable by this histological technique. However, in a previous study production of small amounts of type II collagen by chondrocytes was detected at day 6 of culture in 2% agarose gels but the technique used was IHC to detect collagen (Bougault et al., 2008). Masson's trichrome is a very crude method for staining collagen in comparison to IHC which is quite a sensitive method of collagen staining. Therefore, possible explanation of these indecisive results can be either insufficient production of collagen by cultured chondrocytes or the insensitivity of the technique utilised.

Alcian blue staining is considered a standard histological staining method and has been successfully used to stain PGs amongst the chondrocytes cultured in agarose gels (An et al., 2001). In order to minimise the error produced by background staining, the ROI was created and applied in the vicinity of chondrocytes and the percentage staining was calculated for individual cells (section 5.4.5). In the Alcian blue stained sections at days 3 and 7, the percentage of Alcian blue staining was significantly less around chondrocytes in the weak gels as compared to strong gels (Fig. 5.5). This decreased Alcian blue staining intensity in weak gels led to the notion that chondrocytes possibly produced lesser amount of PGs as compared to strong gels and there may be several possible explanations for this observation. **Firstly,** it is possible that the chondrocytes in weak gels with altered morphology were synthesizing lesser amounts of PGs as compared to the chondrocytes with normal morphology in the strong gels. This possibility could be explained keeping in view

the previous work which suggested that loss of chondrocytic phenotype was associated with decreased synthesis of PGs (Benya and Shaffer, 1982). **Secondly,** possibly chondrocytes in weak gels were metabolically activated by the factors in the serum and this led to the destruction and loss of PGs synthesized. This can be explained on the basis of already reported enhanced synthetic/proliferative activity of chondrocytes causing destruction of PGs in OA (Sandell, 2007, Goldring et al., 2008). **Thirdly,** these abnormal chondrocytes were possibly synthesizing low molecular weight PGs rather than aggrecan which stained less intensely with Alcian blue (Tesche and Miosge, 2005). The low molecular weight PGs such as decorin and biglycan have been stated to be up regulated in the late stages of OA in human articular cartilage and exhibited reduced staining with Alcian blue (Bock et al., 2001). **Lastly,** it can be speculated that due to the absence of effective scaffold around chondrocytes in weak gels the PGs produced were possibly diffused through the gels. This may also give rise to the possibility that some of the background staining in the weak gels was due to the PGs diffusing through weak gels and stained with Alcian blue.

The results presented here also showed that chondrocytes cultured in strong gels displayed progressive increase in the Alcian blue staining throughout the course of culture (Fig. 5.5). This observation is quite obvious due to a previous study which stated increase in production of PGs with time when cultured in agarose gels (Schuh et al., 2012b). Chondrocytes cultured in weak gels showed an initial increase in Alcian blue staining by day 3 but then no further increase was present at the later time point (Fig. 5.5). Therefore, it is possible that chondrocytes cultured in weak gels

in this study underwent morphological changes, thereby, producing catabolic cytokines causing enhanced destruction of PGs.

In conclusion, the histological examination of chondrocytes cultured in weak gels showed cluster formation with H&E, reduced Alcian blue staining and inconclusive results with Masson's trichrome staining. Therefore, this study provided some new insights into the relationship of chondrocyte morphology with their metabolism.

CHAPTER 6: RESULTS

MORPHOLOGICAL CHARACTERISTICS OF CHONDROCYTES IN INJURED CARTILAGE CULTURED UNDER VARIOUS CONDITIONS

6.1 CHAPTER SUMMARY

In degenerate cartilage, chondrocytes often exhibit increased volume, abnormal morphology, enhanced proliferation/cluster formation and loss of viability. These changes may lead to abnormal matrix production/poor repair, enhancing susceptibility to secondary osteoarthritis (OA). This chapter aimed to develop an *in vitro* model of mechanically-injured cartilage, to study changes in chondrocyte viability and morphology at the injured site. Full-depth cartilage explants obtained from bovine metacarpal-phalangeal joints were divided into four experimental groups. **Group 1**: Osteochondral explants with partial-thickness injury i.e. did not breach the subchondral bone with a single standardised scalpel cut and viewed axially, **Group 2**: Osteochondral explants viewed coronally at the cut edge, **Group 3**: Cartilage explants without subchondral bone injured and viewed axially and **Group 4**: Cartilage explants with the superficial zone removed, injured and viewed axially. These explants were then cultured over 14d in (a) standard-DMEM, (b) 10% FCS-DMEM or (c) 10% SF-DMEM (37^{o}C, pH 7.4). At various time points, chondrocytes were fluorescently-labelled with CMFDA and PI to identify living and dead cells respectively, examined by confocal microscopy and analysed by Volocity^{TM} software. In **group 1**, at day 0, at the injury 18±0.5% chondrocytes were PI-labelled; the volume of chondrocytes was 711±24μm^3 and morphology was relatively normal. The % PI-labelled chondrocytes decreased ~80-90% in SF-DMEM and FCS-DMEM in comparison with standard-DMEM throughout the culture period. At day 3, chondrocyte volume at the injury increased in SF-DMEM and FCS-DMEM by ~55% as compared to standard-DMEM (P<0.0001 for both). At day 7, at the injury large chondrocyte clusters were formed in SF-DMEM (cluster volume,

4309±478μm^3) and FCS-DMEM (3839±190μm^3) as compared to standard-DMEM (2802±96μm^3; P<0.0001; P=0.0003 respectively). At day 14, chondrocytes at the injury in standard-DMEM were mostly spheroidal. However, 15±3% cells in SF-DMEM and 31±5% cells in FCS-DMEM showed significant morphological changes (P=0.0013; P<0.0001 respectively) which included cellular enlargement, elongation of cell body and formation of cytoplasmic processes restricted to the superficial layers of cartilage. In the injured explants from **group 2**, chondrocytes changed morphology in the presence of SF-DMEM and FCS-DMEM as compared to standard-DMEM and the changes started in the deeper layers of cartilage extending upwards progressively. In **group 3,** the sequence of changes regarding the width of injury, chondrocyte viability, volume and morphology (clusters/processes) in the presence of SF-DMEM and FCS-DMEM as compared to standard-DMEM was similar to explants in group 1. In **group 4**, at day 0, 53±5% chondrocytes were PI-labelled, chondrocytes were relatively normal in morphology with a volume of 1117.8±82.9 μm^3. During culture PI-labelled chondrocytes decreased by 96% in the presence of FCS as compared to standard-DMEM. At day 7, the volume of chondrocytes remained unaffected in both culture conditions. However, chondrocytes were present in large clusters in the presence of FCS-DMEM as compared to standard-DMEM and the volume of clusters in both conditions was significantly different (P=0.01). At day 14, chondrocytes at, and distant from, the injury in standard-DMEM were mostly spheroidal. The percentage of abnormal chondrocytes at and distant from the injury was higher in the FCS-DMEM as compared to standard-DMEM (P=0.0002; P<0.0001 respectively). These results suggested that the factors present in SF/FCS and strength/damage to matrix are

related factors such that the strength of matrix controls penetration of SF/FCS. Chondrocyte morphology markedly changed at the injury, suggesting that these morphological changes play a role in changes to matrix metabolism.

6.2 INTRODUCTION

Mechanical partial thickness injuries which don't penetrate the subchondral bone may lead to post-traumatic Osteoarthritis (PTOA), due to poor regenerative/repair capacity of chondrocytes (Campbell, 1969, Buckwalter, 1998, Newman, 1998, Hunziker, 2001). However, in full-thickness osteochondral defects where injury penetrates the subchondral bone the repair consists of formation of fibro-cartilage at the injured site. The mesenchymal stem cells in the bone marrow have the ability to differentiate into various cell types such as chondrocytes, osteocytes, fibroblasts etc. These stem cells play a vital role in repairing the full-thickness defects of articular cartilage (Shapiro et al., 1993). PTOA is secondary OA occurring as a consequence of trauma/injury and chiefly characterised by pain and disability (Brown et al., 2006). However, the mechanisms underlying this condition are partially understood so far. Loss of chondrocyte viability following injury as an early event is believed to be involved in the development of PTOA (Kramer et al., 2011). Chondrocytes' death associated with the trauma has been categorised as necrosis in the acute phase followed by apoptosis at later stages which leads to widespread degeneration of cartilage (Tew et al., 2000, D'Lima et al., 2001a, Otsuki et al., 2008). Necrotic cell death associated with trauma has been recently reported to produce chemotactic factors which attract the chondrogenic progenitor cells to the site of damage for regeneration and repair of the damaged tissue (Seol et al., 2012). Moreover, the

extracellular matrix (ECM) disruption as a result of trauma leads to the loss of proteoglycans (Quinn et al., 1998, Kurz et al., 2001, Patwari et al., 2003) and production of degrading enzymes (Kurz et al., 2005), this imbalance in ECM metabolism causes degeneration of the cartilage thereby, increasing susceptibility to PTOA (Lee et al., 2005).

The response of chondrocytes in the pathogenesis of PTOA is crucial. Under normal circumstances chondrocytes are spheroidal/ellipsoidal in shape, surrounded by PCM, do not migrate and hardly exhibit any mitotic activity (Mankin, 1982). Adjacent to the zone of dead necrotic tissue, in response to injury chondrocytes become hyperactive and try to 'repair' the defect. It has been suggested that in an attempt to 'repair' the cartilage, chondrocytes undergo proliferation/cluster formation and an over-production of ECM (Redman et al., 2004). However, it is thought that the role of chondrocytes in the repair of partial thickness defects is not effective and ultimately leads to improper wound healing. Recently, in injured cartilage in response to injury, chondrocytes have been reported to produce cytoplasmic processes (Lyman et al., 2012). In two recent studies the emerging role of chondrogenic progenitor cells in cartilage 'repair' has been studied (Seol et al., 2012, Seol et al., 2014) suggesting potential of chondrocytes to 'repair' the cartilage. How the present work builds up on the current knowledge of response of chondrocytes to injury has been discussed in the later part of this chapter (section 6.6).

In articular cartilage the ECM creates a unique environment for the chondrocytes and regulates their structure and functions via cell-matrix interactions (Gao et al., 2014). Therefore, it is crucial to study chondrocyte morphology in the relatively intact ECM environment to avoid any perturbations. CLSM is a relatively novel methodology

which has rendered the morphological analysis of chondrocytes in a relatively undisturbed and complicated ECM environment possible. This technique allows multiple optical sections to be obtained and thus the three-dimensional morphology and volume of *in situ* chondrocytes can be determined (Jones et al., 2005). Moreover, by the use of confocal microscope, minute details about morphology as e.g. cytoplasmic processes emanating from cell bodies can be visualised in 3-D as this delicate morphological feature may get masked due to shrinkage effect with the fixation techniques used for histology as reported in a study on bacteria (Woldringh et al., 1977).

Several *in vitro* studies have been done in the past using different methods to produce trauma to the cartilage (Quinn et al., 1998, Tew et al., 2000, D'Lima et al., 2001b, Kurz et al., 2005) and study its consequences. In the present study partial-thickness scalpel injured osteochondral explants were utilised to develop an *in vitro* injured cartilage model to determine chondrocyte reaction at injury. Osteochondral explants served an excellent model to study chondrocyte response in cartilage because (a) it is a relatively reproducible model (b) partial thickness injuries could be produced with ease because of intact bone (c) there was possibility although remote of synovial cells to interfere in results (d) in the uninjured areas of explants the chondrocytes remained alive (e) culture conditions could be altered and modified according to the experimental demands (f) in 'off the bone' injured explants, any interference of osteocytes and bone factors in the response of cells to injury could be ruled out (g) in explants without superficial layers response of deeper cells to injury could also be studied.

Most of the previous studies performed on traumatised cartilage utilised blunt trauma and injurious compression injuries, and thus was difficult to precisely define the extent of injury and ultimately the damage produced was widespread (Clements et al., 2004). The sharp mechanical trauma model used in this work has been utilised successfully in the past to study the chondroprotective effects of various solutions (Amin et al., 2008a, Amin et al., 2008b). This model was a preferable method to study cell viability and morphology of chondrocytes in response to injury due to various reasons: **Firstly**, the sharp scalpel cut applied in the single plane of cartilage avoided the variability in death and extent of matrix damage ascribed to the anisotropic property of cartilage structure (Jeffery et al., 1991). **Secondly**, standardization of the injury was ensured by (a) producing it with a 'push-through mode' as this enabled the application of constant amount of force on the scalpel at the site of injury which avoided variations in the percentage cell death (PCD), because the amount of cell death would be expected to vary with the extent of injurious force applied (Huntley et al., 2005) (b) applying specified ROIs at the site of injury and distant from the injury on all the images to determine PCD. **Thirdly**, sharp trauma led to less chondrocyte death as compared to blunt trauma (Redman et al., 2004) and this would cause less disruption of matrix components (Tew et al., 2000, D'Lima et al., 2001b, Quinn et al., 2001) and less release of intracellular components (Kuhn et al., 2004). **Fourthly**, this model allowed a wide range of experiments (a) to study the effect of presence or absence of subchondral bone on chondrocyte morphology in response to injury (b) to investigate whether the superficial cells alone are responsible for changes to morphology or the deep layered calls also respond similarly. **Lastly**, this was a reasonable model to study sharp

scalpel induced mechanical injury and then to compare with the cartilage distant from the injury as the changes would be confined to the site of injury (Redman et al., 2004). These injured cartilage explants had an uninjured control area outside the region of interest (ROI) i.e. distant from the injury. It allows a direct comparison of injured and uninjured cartilage areas in the same explant and this comparison is not possible with the blunt trauma and injurious compression injuries. Therefore, this *in vitro* model of sharp mechanical injury is a highly reliable, controlled and reproducible one.

Various studies conducted in the past on degenerate cartilage found chondrocytes to change phenotype thereby leading to alterations in their biosynthetic activity (Kouri et al., 1996a, Darling and Athanasiou, 2005, Tesche and Miosge, 2005, Yagi et al., 2005, Murray et al., 2010). Furthermore, several studies have investigated the biochemical changes produced by chondrocytes in the damaged/traumatised cartilage and cartilage remodelling as a consequence of trauma (Grodzinsky et al., 2000, Patwari et al., 2001, Milentijevic et al., 2005). Although biochemical response of chondrocytes to trauma has been studied extensively but morphology of chondrocytes in response to injury was not comprehensively studied. Therefore, in the present study, cartilage was injured as a mechanism to increase the likelihood that factors present in synovial fluid (SF)/foetal calf serum (FCS) could interact with the *in situ* chondrocytes and thus morphology of chondrocytes in response to injury under the effect of these factors could be studied.

6.3 HYPOTHESES

6.3.1 Primary hypothesis

Chondrocytes near injury produce morphological changes in response to some factors present in SF and FCS.

6.3.2 Secondary hypothesis

Chondrocytes throughout cartilage are susceptible to morphological changes in response to injury in the presence of SF and FCS.

6.3.3 Tertiary hypothesis

Chondrocytes produce morphological changes in the presence of SF and FCS even in the absence of subchondral bone.

6.4 MATERIALS AND METHODS

6.4.1 *In vitro* partial thickness injured bovine articular cartilage model

6.4.1.1 *Full depth bovine osteochondral explants*

6.4.1.1.1 Cartilage preparation and application of scalpel injury

Metacarpophalangeal joints of 3yr old cows obtained from local abattoir were washed, skinned, sprayed with 70% (v/v) alcohol (Fig. 6.1a) and dissected in a class 1-flow hood under strict aseptic conditions within 12hrs of slaughter (Fig. 6.1b). Osteochondral strips comprising full depth cartilage with subchondral bone attached were harvested from the articular surface between the condylar ridges of each joint

(Fig. 6.1c) and trimmed approximately into rectangular blocks with 5x6x1mm size (Fig. 6.1e). The articular surface of each cartilage explant was then injured with fresh scalpel No. 11 in a 'push through mode' along the long axis of the explant as previously described (Amin et al., 2008b). The injury was always produced in the same direction, avoiding any additional movements of scalpel, cutting carefully through the thickness of cartilage without touching the bone and using fresh scalpel blade for each explant (Fig. 6.1c). In some experiments, partial-thickness injury was not produced rather a full-thickness injury was applied involving the subchondral bone and the osteochondral explants were cut into two halves and left in culture to study the response of injured chondrocytes to various culture media in various layers of cartilage in the coronal view (Fig. 6.1d).

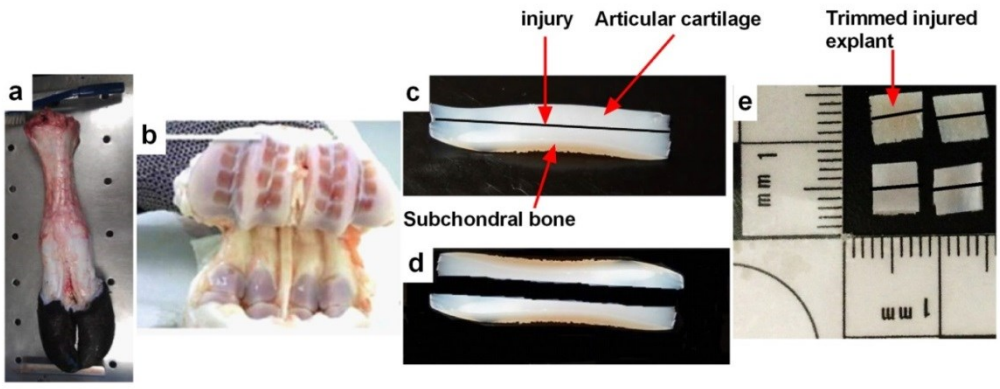

Figure 6.1: Preparation of injured bovine osteochondral explants.
(a) Bovine feet obtained from local abattoir, washed and prepared for dissection (b) metacarpophalangeal joint dissected out and cartilage explants harvested from articular surface between condylar ridges (c) an osteochondral strip comprising of full thickness of cartilage and substantial amount of underlying subchondral bone, injured along the long axis (d) osteochondral explant cut into two halves for coronal images of injured cartilage (e) trimmed injured explants for axial images of bovine cartilage. Photographs (a, b, c) kindly provided by Dr. Innes D M Smith and (e) by Mr. Scott I Paterson, Centre for Integrative Physiology, University of Edinburgh.

6.4.1.2 *Preparation of cartilage explants for microscopy*

At appropriate time points, injured explants from the culture were incubated with CMFDA and PI with final concentrations of 12.5 and 5µM respectively, during the last hour of incubation at ambient temperature to label living and dead cells respectively. The explants were then washed in PBS, fixed in 4% formaldehyde for 30mins and mounted in small cell culture dishes (Cellstar®; 35x10mm) with Super Glue gel (Loctite). For the axial images, a pin-head size drop of glue was applied to the base of the dish and one of the explant edges was gently placed on it and allowed to attach. The cells distant from the point of attachment were imaged within ~30 minutes by confocal microscopy to avoid any interference of the glue while imaging (Fig. 6.2A). For the coronal images, two tiny pieces of blue tack® (Bostik; UK) adhesive were applied in the culture dish and osteochondral explant was oriented in the lateral view without touching the coronal cut side of the explant (Fig. 6.2B). The samples were then stored in PBS at 4°C (in dark) prior to imaging.

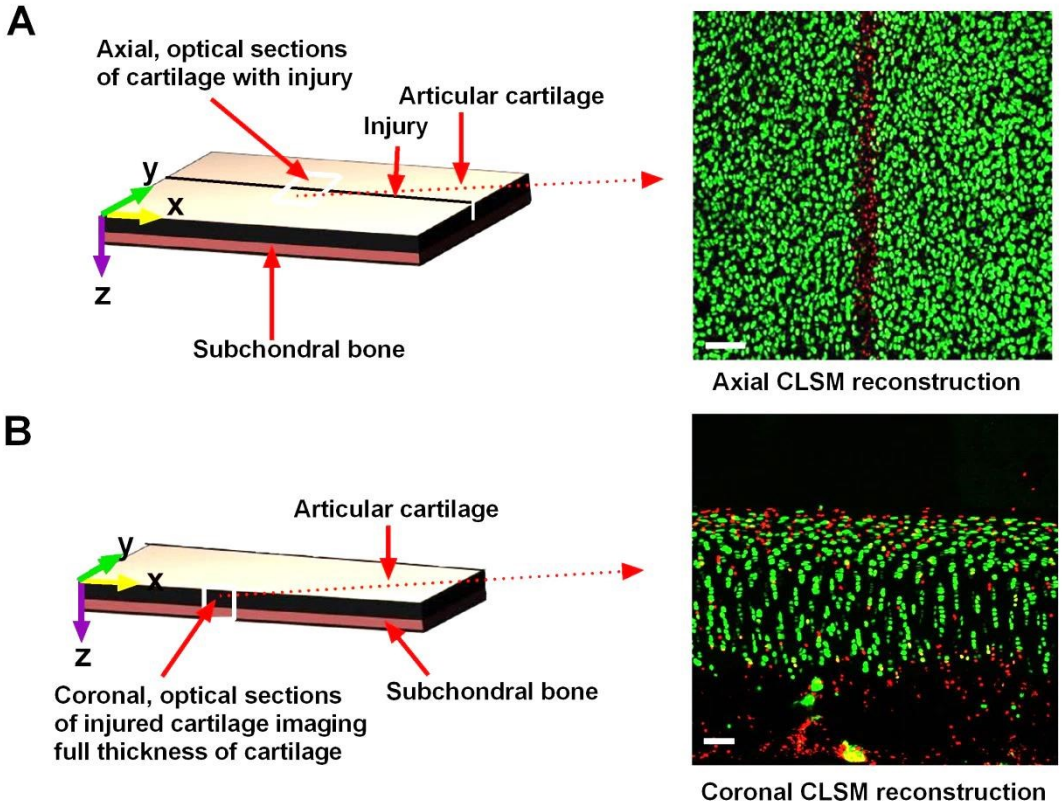

Figure 6.2: Axial and coronal CLSM for injured bovine articular cartilage explants imaged with low power (x10) objective.
The x, y and z axes labelled on the diagram of the explant. (A) Axial optical sections of the articular cartilage with injury imaged top-down and the series of optical sections reconstructed in the axial plane, (B) Coronal optical sections of injured cartilage imaged the full thickness of the cartilage and the series of optical sections reconstructed in the coronal plane. Scale bar = 100µm for both axial and coronal reconstructed images.

6.4.1.3 *CLSM in the axial and coronal planes of injured cartilage explants*

A Zeiss Axioskop LSM 510 upright CLSM was used with an Ar/2 laser with excitation wavelength (EX_λ) of 488nm and HeNe laser with EX_λ 543 to excite the fluorophores CMFDA and PI respectively. The emission light was then measured through a band pass filter of 505-530nm and a long pass filter of 650nm respectively.

The fluorescently-labelled chondrocytes *in situ* were imaged in the **axial plane** at the site of injury and ~400µm either side to observe cells distant from the injury. The viability of chondrocytes was assessed by images obtained using a low power (x10 dry; NA 0.3) objective with a standard protocol (Amin et al., 2008b) and chondrocyte morphology was studied by using x40 (NA 0.8) dipping water (DW) lens. The z stack images comprising single confocal sections through the z-axis of the tissue, typically to a depth of 50µm for high and 100µm for low power objective magnification measurements were collected at an interval of 1µm and 10µm respectively. The fluorescently-labelled chondrocytes *in situ* were imaged in the **coronal plane** at the injured site to observe cells in all the layers of cartilage both with low power and high power lenses. The z stack images comprising single confocal sections through the z-axis of the tissue, typically to a depth of 60µm for high and ~100-150µm for low power objective magnification measurements were collected at an interval of 1.1µm and 5.2µm respectively. The scanning speed was 9 frames/sec, with a pinhole setting of 1 Airy unit and a frame size of 1024x1024 pixels. The optical sections obtained by CLSM were converted into three-dimensional reconstructions/projections using Volocity™ version 5.4.1 image analysis software (Amin et al., 2008a).

6.4.1.4 *Quantification of CMFDA and PI-labelled chondrocytes*

The green and red staining pattern of CMFDA and PI-labelled (live and dead) chondrocytes was used for counting following a standard protocol published previously (Amin et al., 2008b). Briefly, the low power axial extended focus

confocal images were analysed on Volocity™ for quantifying the percentage of PI-labelled chondrocytes or percentage cell death (PCD). A 3D ROI was created and applied on the injured site with the dimensions of x, y, z 400, 913 and 100µm respectively (Fig. 6.3a). Cell death distant from the injury was determined by applying ROIs with dimensions of x, y and z 200, 913 and 100µm respectively on both sides of the injury and the average calculated (Fig. 6.3b). The counting protocol was run on the images which identified objects (individual cells) as green (live) and red (dead) on the basis of percentage threshold intensity in two channels. The mean number of live and dead cells in each ROI was calculated and % PI-labelled cells/PCD determined with the formula 100 × (number of dead cells/number of dead and live cells) %. The high power (x40 DW) axial extended focus confocal images were analysed to measure the width of the injury by Volocity™ software and determined by drawing two straight lines on either sides of injury enclosing the area containing no cells and measuring the distance between the lines (Fig. 6.3c).

6.4.1.4.1 Quantification of PCD at, and distant from the injury

PI-labelled chondrocytes at and distant from the injury were quantified by image analysis (section 6.4.1.4) and ROIs selected and applied as shown in Fig. 6.3. Quantification of PCD distant from the injury and its comparison with PCD at the injury was important as it gave an indication of whether there was any cell death due to mishandling of the explants.

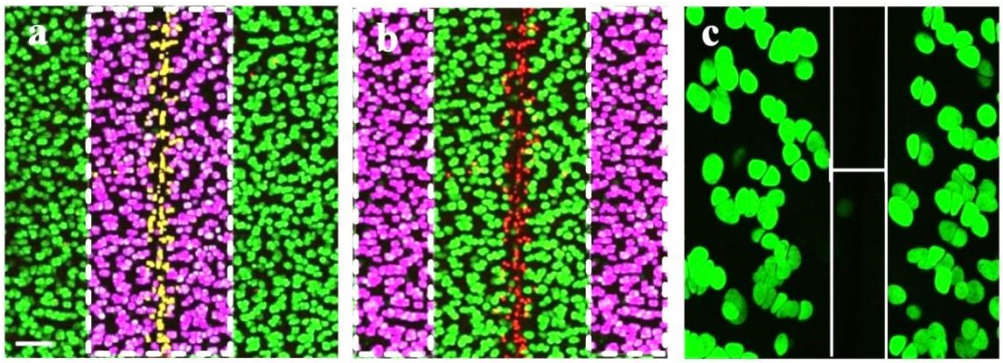

Figure 6.3: Method for quantification of PI-labelled chondrocytes at and distant from the injury and measurement of the width of injury.
Dashed white lines indicate the ROIs applied and solid white lines indicate the measurement of width of the injury. (a) Identification and counting of CMFDA and PI-labelled chondrocytes in an ROI at the injury. A projected low magnification image obtained by CLSM with an ROI applied to encompass the site of injury and PCD calculated (see Materials and Methods) (b) Chondrocyte death distant from the injury was determined by applying an ROI 200µm away from the injury both on left and right sides of image, and the average calculated. (c) A projected high magnification image showing the method for measurement of the width of injury by Volocity™. Scale bar for all panels = 100µm.

6.4.1.5 *Volume and morphological analysis of in situ chondrocytes*

The methodology applied to determine chondrocyte volume/morphology was similar to the methods utilised for cultured chondrocytes in agarose gels (section 4.4.1.7.1). The quantitative data regarding volume and 3D morphological analysis of *in situ* chondrocytes were obtained from the CLSM (x40 DW objective) images by using a measurement protocol on Volocity™. The calibration technique and correction factor applied were also similar to those applied for cultured chondrocytes in agarose gels (section 4.4.1.7.2).

The definition of a cluster formed and methodology employed for quantitative analysis of clusters was similar to the one applied for the cultured chondrocytes in agarose gels (section 4.4.1.7.1). For measurements of cell morphology the cell body

of individual chondrocytes was measured along the longest (y-axis) of the cell in 3D by using the same software. The chondrocytes which were elliptical/spheroidal in shape with no cytoplasmic processes were considered relatively 'normal' in morphology. However, cells with elongated and non-spheroidal shapes, with cytoplasmic processes emanating from cell bodies were considered 'abnormal' in morphology (Bush and Hall, 2003). These abnormal chondrocytes had a variety of characteristics based on (a) shape of cells (b) presence or absence of cytoplasmic processes (c) presence of single or multiple processes and examples are illustrated in Results. The percentage of abnormal chondrocytes was calculated with the formula 100 × (number of abnormal cells/total number of all normal and abnormal cells) %.

6.5 RESULTS

6.5.1 Standardisation of the injury

The first step was to standardise the application of the injury to ensure that the amount of cell death along the length of injury was relatively constant and it required considerable practice. This was attained by keeping the force on the scalpel constant and the percentage cell death (PCD) within a set ROI was determined and compared at various positions along the length of injury. There was no significant difference in the PCD throughout the length of the injury (Fig. 6.4) indicating that the PCD was constant.

The injured explants were incubated in (1) standard-DMEM (2) SF-DMEM or (3) FCS-DMEM for up to 14 days and media changed on alternate days. The injured explants from the various culture conditions at different time points (day 0, 3, 7 and 14) of culture were then prepared for microscopy.

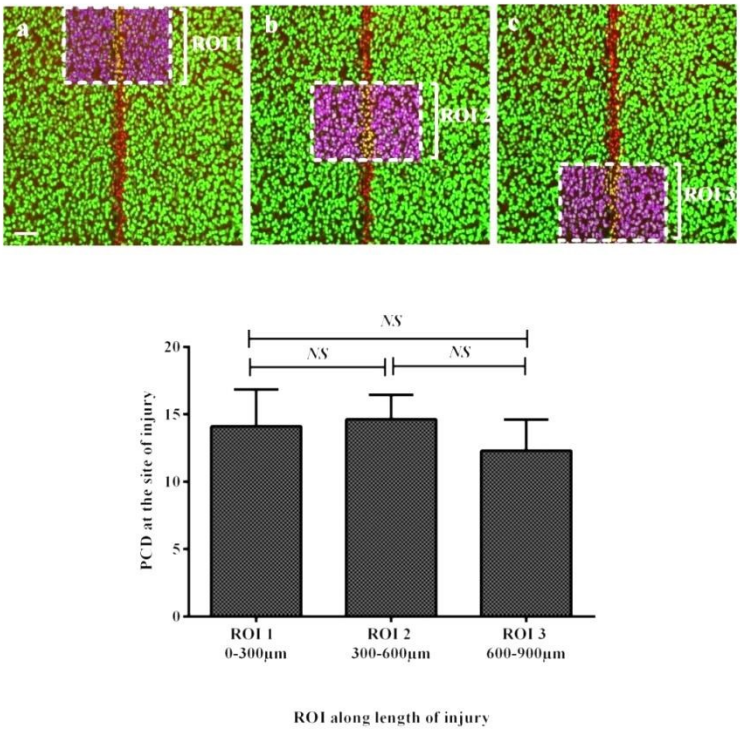

Figure 6.4: Standardisation of the scalpel injury applied along the long axis of the bovine cartilage explants.

Dashed white lines indicate the ROIs applied. Top, CLSM projected images of injured cartilage illustrating the three different ROIs along the length of injury ranging from (a) 0-300µm (ROI 1), (b) 300-600µm (ROI 2) and (c) 600-900µm (ROI 3). Individual chondrocytes within the ROI were identified on the basis of voxel intensity, CMFDA-labelled (living) and PI-labelled (dead) cells identified using purple and yellow respectively (colour codes given to identify cells separately) and the PCD calculated. Also shown is a comparison between % PI-labelled cells calculated after applying ROIs at the three different sites along the length of injury. Scale bar for all panels = 100µm. Data were for [$N(n)$] = [6(9)].

6.5.2 Morphological characteristics of chondrocytes in injured cartilage cultured under various conditions (axial view)

Osteochondral explants were injured and kept in culture with either (a) standard-DMEM (b) SF-DMEM or (c) FCS-DMEM up to 14 days (section 2.1.1). The injured explants incubated in various culture conditions were fluorescently labelled at different time points (Days 0, 3, 7 and 14), prepared for confocal microscopy and imaged **AXIALLY** with low and high power magnification objectives.

6.5.2.1 *Changes to the width of the injury following in vitro culture under various conditions*

It was a reproducible standard injury (Fig. 6.4) and width of the injury was measured as shown in Fig 6.3c. At day 0, the width of the injury was same for all culture conditions. The nature of the culture medium strikingly affected width of the injury during the course of culture. In standard-DMEM the width of the injury remained almost unaffected during the first week of culture. However, injury width increased significantly by day 14 compared to the earlier time points of culture in standard-DMEM ($P<0.05$; ANOVA over the 4 days; Fig. 6.5). The explants cultured in the presence of SF-DMEM or FCS-DMEM exhibited no change in width at day 3 but the width increased significantly in FCS-DMEM at day 7 in comparison with those in standard-DMEM ($P<0.01$; ANOVA). However, by day 14 the width of the injury decreased significantly in both of these conditions compared with day 7 ($P<0.05$; $P<0.001$ respectively) and also in comparison with the explants in the presence of standard-DMEM (Fig. 6.5; $P<0.001$; $P<0.01$ respectively). These data suggested that in explants cultured with standard-DMEM during the culture period the width of the injury remained unchanged by day 7 but increased significantly by day 14. However, in contrast in the presence of SF-DMEM and FCS-DMEM the width of the injury increased initially by day 7 but decreased markedly by day 14 of culture. This suggested the proliferation of chondrocytes at the injury possibly in response to the factors present in FCS/SF-rich media.

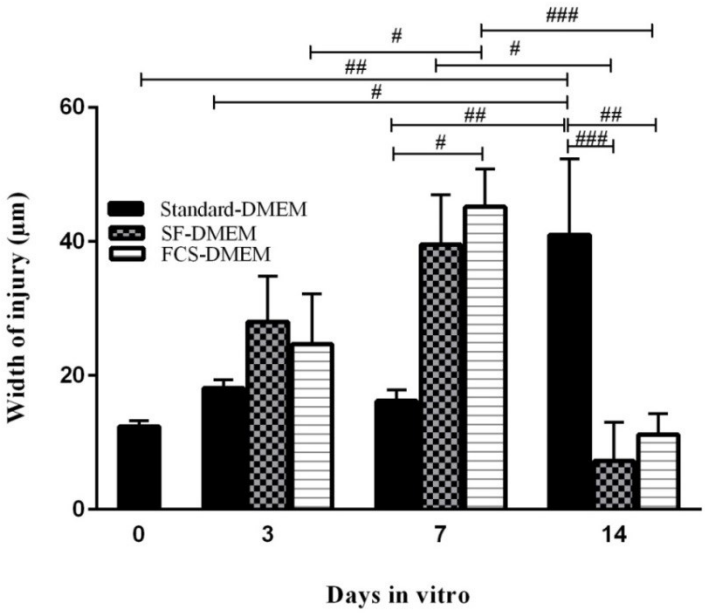

Figure 6.5: Changes in the width of the injury following culture under various conditions.
The measurements of injury width were determined as described in Materials and Methods. Data are from [*N*(*n*)]=[9(43)]. # indicated a significant difference according to one-way ANOVA followed by Tukey's multiple comparison post-hoc test. The single, double and triple symbols showed the level of significance for $P<0.05$, 0.01 and 0.001 respectively.

6.5.2.2 *Loss of PI-labelled cells at the site and distant from the injury*

The percentage of PI-labelled chondrocytes within the ROI (section 6.4.1.4) depended strongly on the various culture conditions used (Fig. 6.6a-j). The low power (x10) CLSM reconstructions as shown in Fig. 6.6, demonstrated the decrease in PI-labelled chondrocytes in the presence of SF-DMEM and FCS-DMEM even at day 3 of culture but this decrease in PI-labelled chondrocytes was not seen in the presence of standard-DMEM.

There was no significant difference between the % PI-labelled cells at the injury in explants cultured with standard-DMEM even after 14 days of culture (Fig. 6.7a;

P>0.05; one-way ANOVA). In marked contrast, the % PI-labelled cells at the injury in explants cultured in the presence of SF-DMEM or FCS-DMEM decreased significantly (Fig. 6.7a; *P*<0.01; *P*<0.001 respectively; ANOVA) at day 3. However, the loss of PI-labelled cells in FCS-DMEM compared with SF-DMEM showed no difference (Fig. 6.7a). Similarly, at day 7 and 14 of culture the % PI-labelled chondrocytes decreased significantly in SF-DMEM and FCS-DMEM compared to injured explants cultured in standard-DMEM (Fig. 6.7a; *P*<0.01; *P*<0.001 respectively at day 7; *P*<0.001 for both conditions at day 14; ANOVA). As expected the % PI-labelled chondrocytes at the injury were significantly higher under all culture conditions as compared to those distant from the injury at all the time points (Fig. 6.7b), only by day 7 the difference was not significant in the explants cultured with SF-DMEM (*P*<0.0001 at day 0, *P*<0.0001; *P*=0.0054; *P*<0.002 at day 3; *P*=0.0005; *P*>0.05; *P*=0.04 at day 7 and *P*<0.0001; *P*=0.0012; *P*=0.005 at day 14; for standard-DMEM, SF-DMEM and FCS-DMEM respectively). These results suggested that in the presence of SF-DMEM and FCS-DMEM, the % PI-labelled chondrocytes decreased dramatically by approximately 80-90% in comparison with standard-DMEM throughout the culture period which showed no significant change.

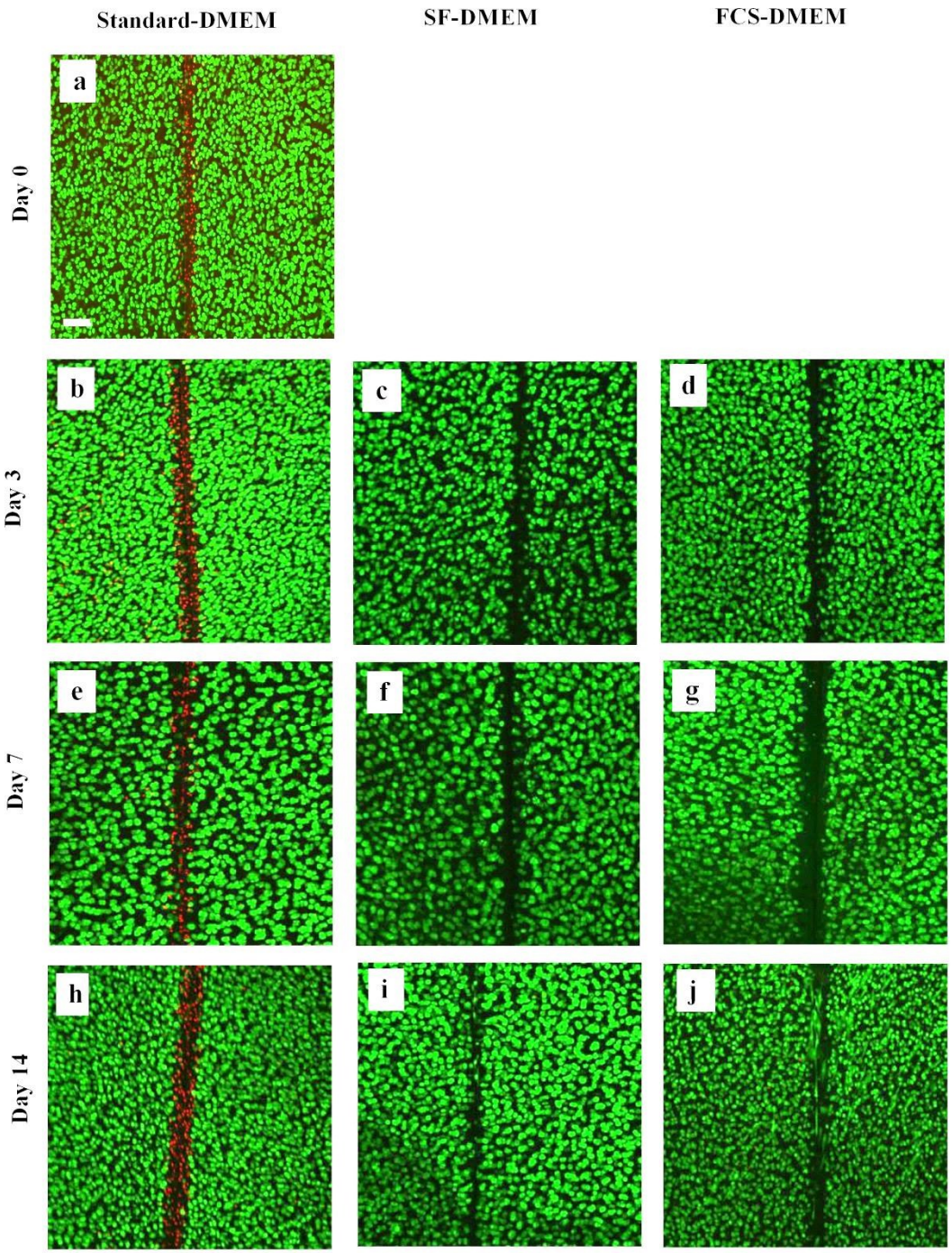

Figure 6.6: Axial CLSM reconstructions of injured cartilage explants cultured in various conditions showing the loss of PI-labelled chondrocytes in SF-DMEM and FCS-DMEM as compared to standard-DMEM.

CLSM reconstructions of low magnification (x10) images, typically to a depth of 100µm collected at an interval of 10µm of CMFDA and PI-labelled chondrocytes (live/dead, respectively) in injured explants at (a) day 0, (b,c,d) day 3, (e,f,g) day 7 and (h,I,j) day 14 cultured in standard-DMEM, SF-DMEM and FCS-DMEM respectively. Scale bar for all panels = 100µm.

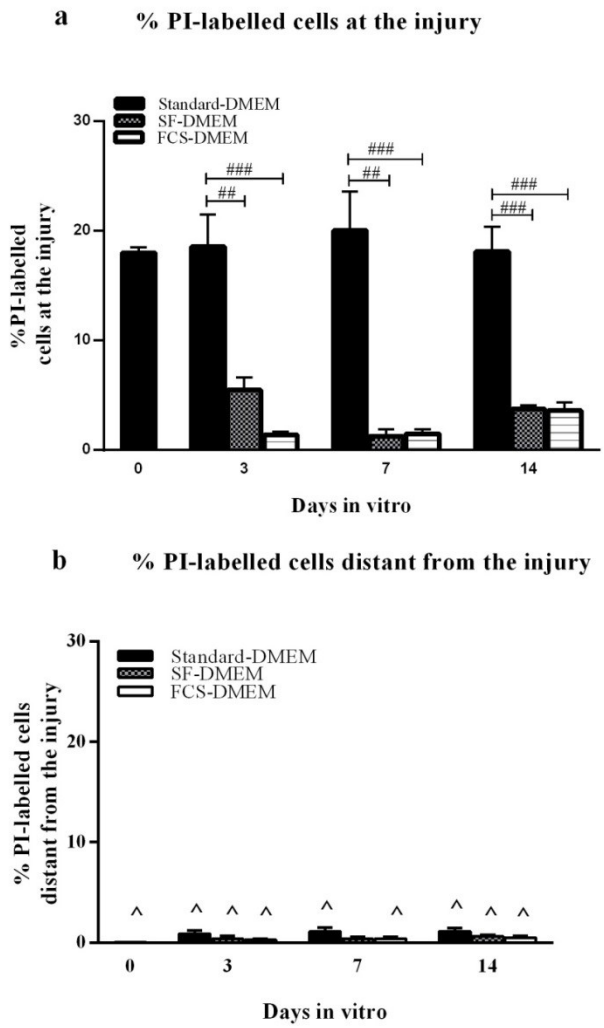

Figure 6.7: The percentage of PI-labelled cells at and distant from the injury in cartilage cultured under various conditions.

Graphs show a comparison between the % PI-labelled cells (a) at the injury and (b) distant from the injury under the three culture conditions. Data were from [*N*(*n*)=18(52)]. # indicated a significant difference between different culture conditions at one time point according to one-way ANOVA followed by Tukey's multiple comparison post-hoc test. ^ indicated a significant difference between the values at and distant from the injury according to unpaired student's t-test. The single, double and triple symbols showed the level of significance for $P<0.05$, 0.01 and 0.001 respectively.

6.5.2.3 *Morphological characteristics of chondrocytes in response to various culture media*

During the course of culture, chondrocyte morphology changed dramatically in the presence of the different culture media following what appeared to be a complex sequence of events. In order to understand aspects of these changes, the results were presented at distinct time points as related to changes in (A) chondrocyte volume, (B) chondrocyte clustering and (C) abnormal chondrocyte morphology and are now described in the following 3 sections.

6.5.2.3.1 Changes to the volume of chondrocytes at and distant from the injury at day 3

At day 3, the volume of chondrocytes changed considerably under the influence of different culture media. The high power (x40DW) images showed the increase in volume and abnormal morphology of chondrocytes at the injury in the presence of SF-DMEM and FCS-DMEM (Fig. 6.8a-j).

The volume of chondrocytes **at the injury** at day 0 was 711±25μm^3, and this did not change significantly by day 3 when explants were cultured in standard-DMEM (Fig. 6.9a). The volume of chondrocytes within explants cultured with SF-DMEM and FCS-DMEM increased approximately by 55% at day 3 as compared to standard-DMEM (P<0.0001 for both SF-DMEM and FCS-DMEM) and approximately 70% in comparison with the volume at day 0 (P<0.0001 for both SF-DMEM and FCS-DMEM) at the injury (Fig. 6.9a). Moreover, chondrocyte volume at the injury at day 3 increased approximately 32% in the presence of SF-DMEM and 13% in the presence of FCS-DMEM as compared to that **distant from the injury** (Fig. 6.9b; P<0.0001; P=0.0002 for SF-DMEM and FCS-DMEM respectively). However, in

standard-DMEM no difference in volume was observed at and distant from the injury (Fig. 6.9b).

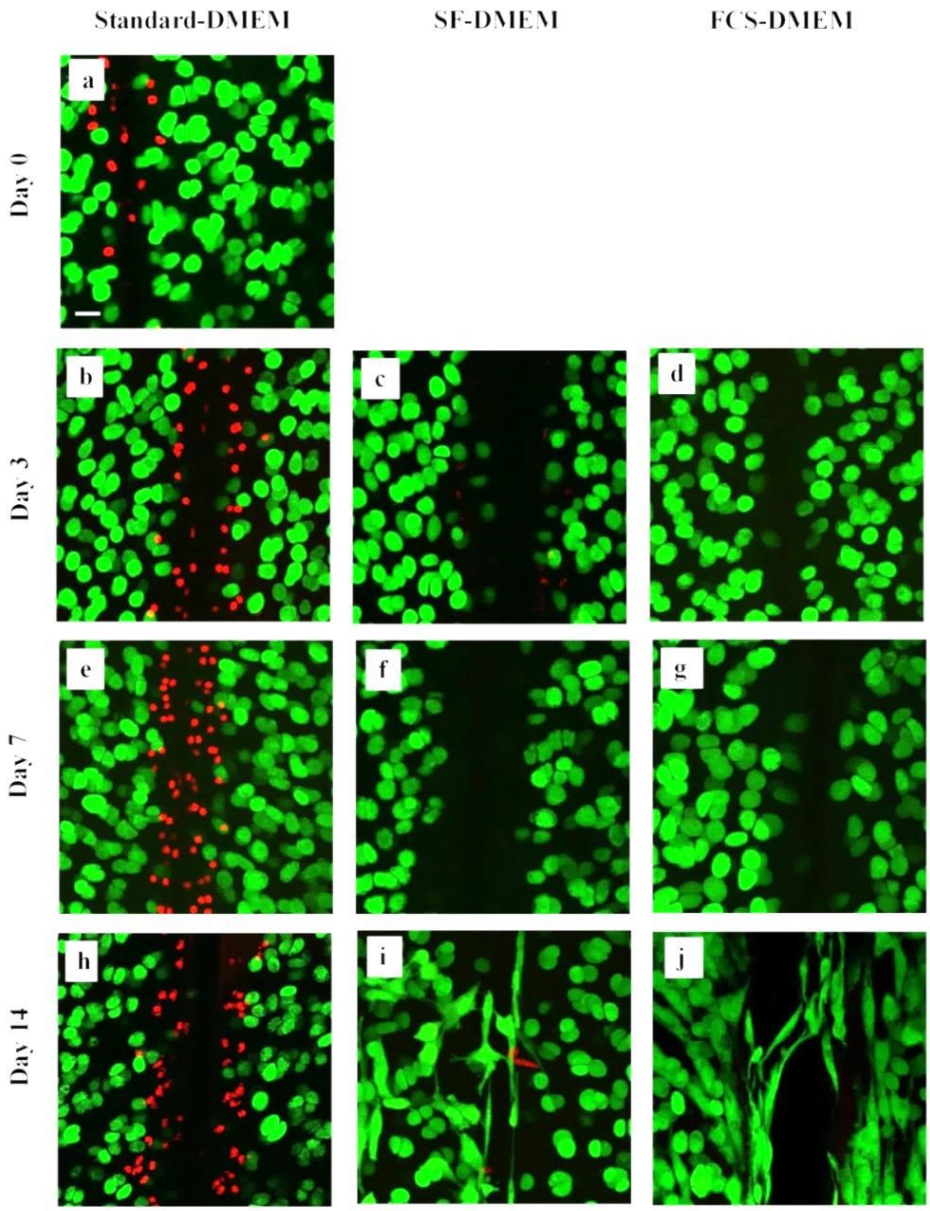

Figure 6.8: Axial CLSM reconstructions of injured cartilage cultured in various culture media showing morphological changes to chondrocytes at injury in the presence of SF-DMEM and FCS-DMEM as compared to standard-DMEM.
CLSM reconstructions of images obtained by x40(DW) objective typically to a depth of 50µm at an interval of 1µm through the z-axis of the tissue. These images were of CMFDA and PI-labelled chondrocytes (live/dead respectively) in injured explants at (a) day 0, (b,c,d) day 3, (e,f,g) day 7 and (h,i,j) day 14 cultured in standard-DMEM, SF-DMEM and FCS-DMEM respectively. Scale bar for all panels = 25µm.

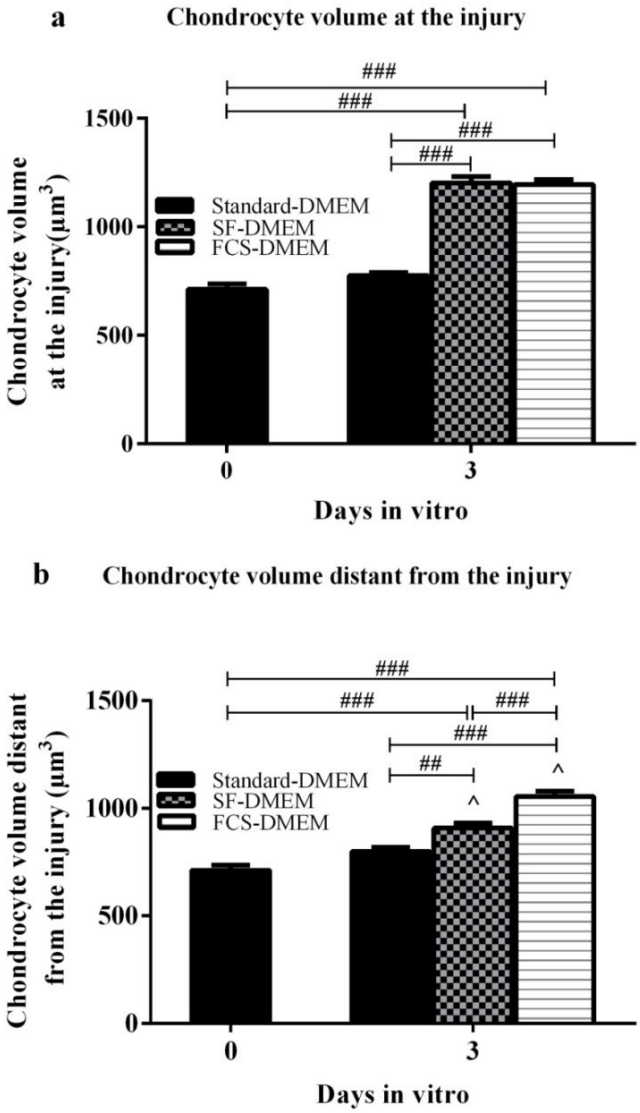

Figure 6.9: Changes to chondrocyte volume at and distant from the injury at day 3 in response to various culture conditions.

Graphs summarise the pooled data for the volume of chondrocytes at days 0 and 3 demonstrating significant changes in chondrocyte volume (a) at and (b) distant from the injury. Data were from [$N(n')$=18(55,55) at day 0, 18(289,134) for standard-DMEM, (112,108) for SF-DMEM and (253,111) for FCS-DMEM, at the injury and distant from the injury respectively]. # indicated a significant difference between different culture conditions and at two time points according to one-way ANOVA followed by Tukey's multiple comparison post-hoc test. ^ indicated a significant difference between the values at and distant from the injury according to unpaired student's t-test. The single, double and triple symbols showed the level of significance for P<0.05, 0.01 and 0.001 respectively.

These results indicated that chondrocyte volume at the injury increased in the presence of SF-DMEM and FCS-DMEM as compared to standard-DMEM. Additionally, at day 3 the volume of chondrocytes at the injury was higher as compared to those distant from the injury in both the culture conditions.

6.5.2.3.2 Chondrocyte cluster formation at day 7

An obvious morphological feature of chondrocytes at the injury which was observed routinely was the formation of clusters in response to some of the culture media (Fig. 6.8f,g). In order to quantify this so that various culture conditions could be compared, different parameters of clusters were analysed at day 0 and 7 at and distant from the injury (Figs. 6.10A & B). Clusters were defined and quantitative data regarding their number, number of cells/cluster, percentage of cells involved, volume of clusters and the volume of individual cells in a cluster (section 4.4.1.7.1) were obtained. At day 0 in the normal fresh osteochondral explants chondrocytes were typically present in pairs and only 3±1% chondrocytes within the specified ROI formed approx. 3-4 clusters with no more than 3 cells per cluster.

The pooled data regarding average number of clusters formed at the injury exhibited an increasing trend in the presence of SF-DMEM and FCS-DMEM as compared to the explants cultured in standard-DMEM (Fig. 6.10Aa). The number of clusters formed in the presence of FCS-DMEM was significantly higher as compared to day 0 ($P<0.05$) and standard-DMEM at day 7 ($P<0.01$) but the difference between SF-DMEM and standard-DMEM was not significant at both time points (Fig. 6.10Aa). Moreover, at day 7 the number of clusters formed in the presence of FCS-DMEM were significantly higher than SF-DMEM ($P<0.05$; Fig. 6.10Aa). The number of clusters formed at the injury were significantly higher as compared to distant from

the injury in the explants cultured in the presence of FCS-DMEM (P=0.03) but the difference at and distant from the injury was not significantly different in the presence of SF-DMEM (Fig. 6.10Ba). These data indicated that the effect of FCS-DMEM on chondrocyte clustering appeared to more potent than SF-DMEM.

The number of cells per cluster at the injury was significantly higher in the explants cultured in the presence of FCS-DMEM by day 7 as compared to day 0 (Fig. 6.10Ab; P<0.0001). At day 7, significantly greater number of cells per cluster were found at the injury in the presence of FCS-DMEM as compared to standard-DMEM (Fig. 6.10Ab; P<0.0001). Number of cells per cluster was significantly greater in FCS-DMEM as compared to SF-DMEM (Fig. 6.10Ab; P<0.05) Additionally, the average number of cells in a cluster was significantly greater at the injury as compared to distant from the injury in the presence of FCS-DMEM (Fig. 6.10Bb; P=0.02).

At the site of injury, the percentage of chondrocytes forming clusters increased by day 7 in the presence of SF-DMEM and FCS-DMEM as compared to standard-DMEM (Fig. 6.10Ac). In the explants cultured with FCS-DMEM, a significantly higher percentage of chondrocytes formed clusters (27±4%) as compared to those in standard-DMEM (7±3%; P<0.05) and percentage of chondrocytes forming clusters at day 0 (3±1%; P<0.05). However, in the presence of SF-DMEM, 11±4% chondrocytes formed clusters but the difference from standard-DMEM was not statistically significant. Moreover, a significantly higher percentage of chondrocytes formed clusters at the site of injury as compared to distant from the injury in the explants cultured in the presence of FCS-DMEM (Fig. 6.10Bc; P=0.01).

At day 7 of culture, the volumes of clusters close to and distant from the injury showed no significant change in injured explants in the presence of standard-DMEM (Figs. 6.10Ad and 6.10Bd). However, chondrocytes at the injury in the presence of SF-DMEM and FCS-DMEM formed large clusters having on the average 4-5 cells per cluster ($P<0.01$; $P<0.001$ respectively) as compared to standard-DMEM comprising of average 3 cells per cluster and also in comparison with the volume of clusters at day 0 containing 3 cells per cluster (Fig. 6.10Ad; $P<0.01$ for both conditions). Additionally, although a similar trend of volume increase was observed distant from the injury yet significantly large sized clusters were formed at the injury as compared to those distant from the injury both in SF-DMEM and FCS-DMEM (Fig. 6.10Bd; $P=0.0005$; $P=0.01$ respectively) and no significant change observed in standard-DMEM.

The volume of individual chondrocytes in a cluster was calculated (section 4.4.1.7.1) and compared in different culture conditions at and distant from the injury. At day 7 the volume of individual chondrocytes in a cluster increased significantly in the presence of SF-DMEM as compared to standard-DMEM (Fig. 6.10Ae; $P<0.01$). The volume of individual chondrocytes in a cluster increased significantly in the presence of SF-DMEM and FCS-DMEM as compared to volume at day 0 ($P<0.001$ for both SF-DMEM and FCS-DMEM). Moreover, in the explants cultured in the presence of SF-DMEM and FCS-DMEM, the volume of individual chondrocytes in a cluster was significantly higher than those distant from the injury (Fig. 6.10Be; $P=0.03$; $P=0.008$ respectively).

Total number of chondrocytes in specified ROI did not show any significant change at day 7 in the three culture conditions (158±14 in standard-DMEM, 133±21 in SF-DMEM and 137±12 in FCS-DMEM) and also in comparison with day 0 (168±28).

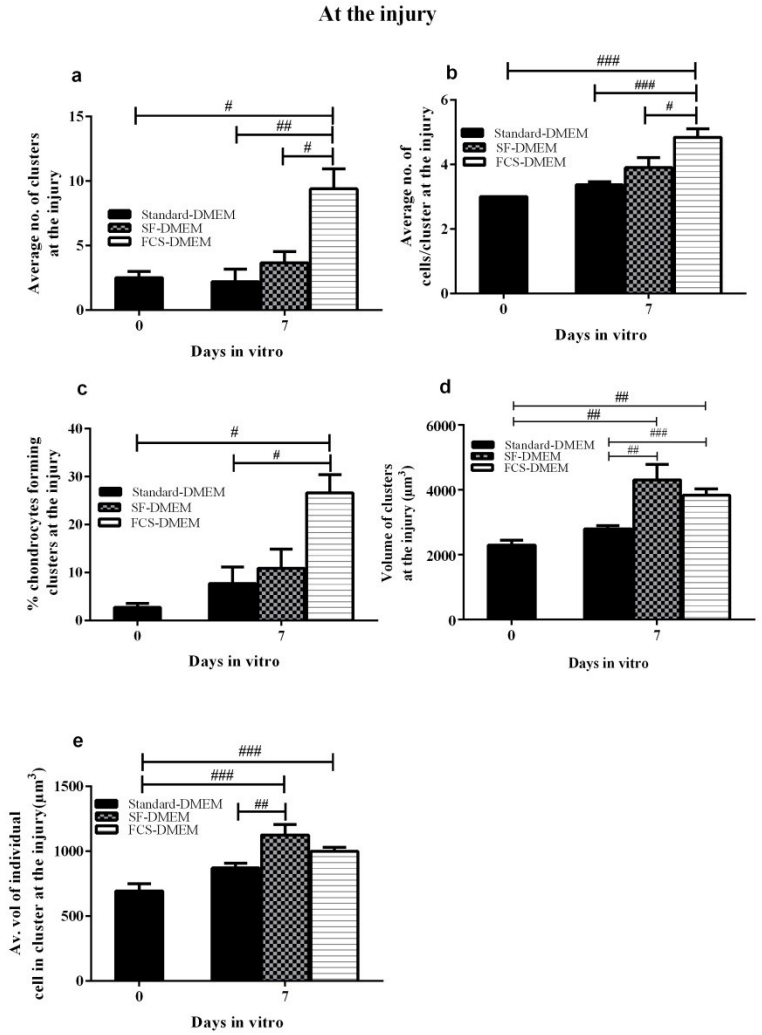

Figure 6.10A: Analysis of chondrocyte clusters formed at day 7 in response to various culture conditions at the injury.

Graphs show pooled data for (a) average number of clusters formed (b) average number of cells in a cluster (c) % of cells involved in forming clusters (d) average volume of clusters (μm^3) of chondrocytes formed (e) average volume of individual cell in a cluster (μm^3) at the injury. Data were from [$N(n)$=18(19)]. # indicated a significant difference between different culture conditions and at two time points according to one-way ANOVA followed by Tukey's multiple comparison post-hoc test. The single, double and triple symbols showed the level of significance for P<0.05, 0.01 and 0.001 respectively.

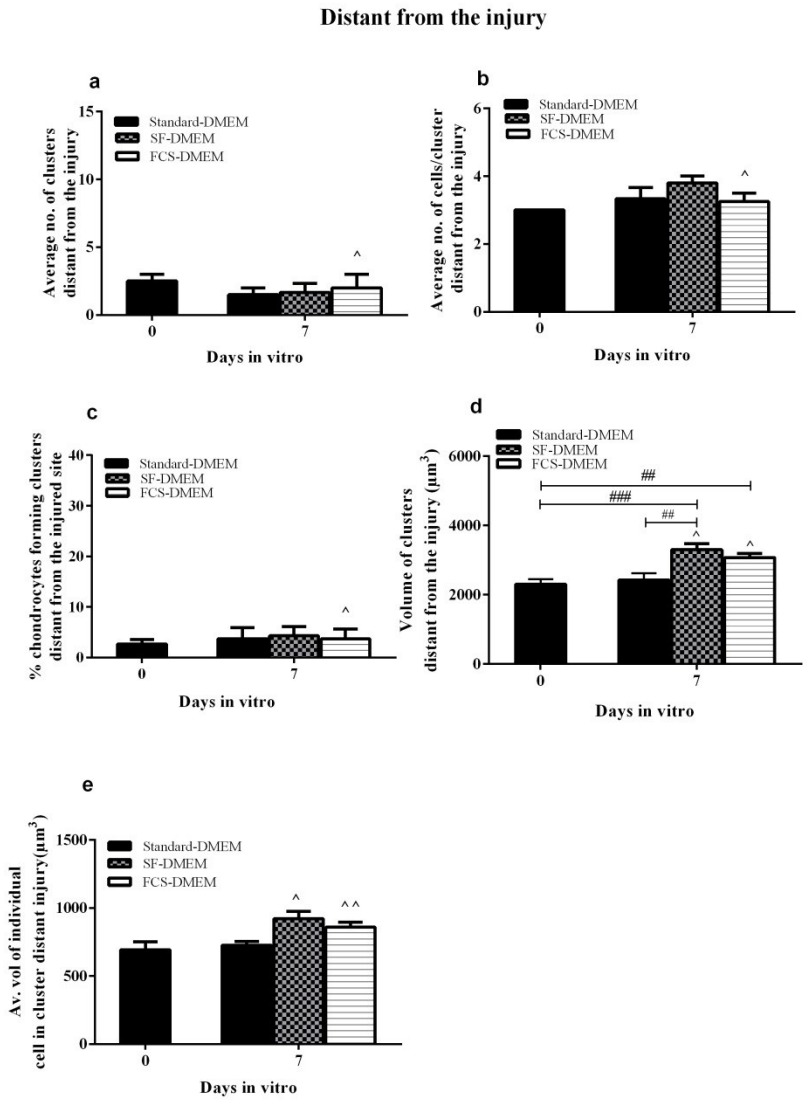

Figure 6.10B: Analysis of chondrocyte clusters formed at day 7 in response to various culture conditions distant from the injury.

Graphs show pooled data for (a) average number of clusters formed (b) average number of cells in a cluster (c) % of cells involved in forming clusters (d) average volume of clusters (μm^3) of chondrocytes formed (e) average volume of individual cell in a cluster (μm^3) distant from the injury. Data were from [$N(n)$=18(19)]. # indicated a significant difference between different culture conditions and at two time points according to one-way ANOVA followed by Tukey's multiple comparison post-hoc test. ^ indicated a significant difference between the values at and distant from the injury according to unpaired student's t-test. The single, double and triple symbols showed the level of significance for P<0.05, 0.01 and 0.001 respectively.

To summarise this section, at day 0, only few chondrocytes were present in clusters. At day 7, at the injury, chondrocytes were present in large clusters in the presence of SF-DMEM and FCS-DMEM as compared to standard-DMEM. Chondrocyte clustering was observed to be stimulated to a greater extent in the presence of FCS-DMEM compared to SF-DMEM. This suggested that although the trends between SF and FCS were similar, subtle differences existed between their effects possibly because of differences in their chemical composition. Therefore, FCS seemed to be more potent in triggering chondrocyte clustering as compared to SF. Distant from the injury, in the presence of SF-DMEM and FCS-DMEM only few chondrocytes formed small sized clusters and the difference at the site and distant from the injury was significant but no difference was observed in the presence of standard-DMEM.

6.5.2.3.3 Development of abnormal chondrocyte morphology/volume by day 14

Chondrocytes in the superficial layers at the injury displayed marked shape changes by day 14 in the presence of SF-DMEM and FCS-DMEM (Fig. 6.11b,c) but not in standard-DMEM. Chondrocyte morphology was relatively 'normal' (elliptical/spheroidal in shape with no cytoplasmic processes) at days 0, 3 and 7 under all culture conditions. The chondrocytes cultured in standard-DMEM exhibited normal morphology after 14 days both in the superficial and deeper regions of cartilage (Fig. 6.11a,d). However, at day 14 of culture in the presence of SF-DMEM and FCS-DMEM chondrocytes showed a dramatic change to 'abnormal' forms characterised by cell enlargement, elongation of the cell body and production of cytoplasmic processes (Fig. 6.12b-f) at the injury.

The changes to chondrocyte morphology occurred in the presence of SF-DMEM and FCS-DMEM and not in standard-DMEM in the superficial layers of cartilage (Fig. 6.11b,c). These abnormal chondrocytes were restricted to the superficial 30µm of the cartilage and the chondrocytes residing deeper than 30µm of cartilage (Fig. 6.11e,f) demonstrated relatively normal volume and morphology.

Morphological characteristics of chondrocytes were quantified (section 6.4.1.5.) and the data compared at day 0 and day 14 in various culture conditions. After 14 days of culture, 15±3% [*N(n)*]=[18(23)] cells in SF-DMEM and 31±5% [*N(n)*]=[18(23)] cells in FCS-DMEM showed significant morphological changes as compared to chondrocytes at the injury in standard-DMEM (Fig. 6.12a; P=0.0013; P<0.0001 respectively) and chondrocytes at day 0 (P<0.01; P<0.001 respectively) which were all 'normal' in morphology. However, the abnormal cells were greater in number in the presence of FCS-DMEM as compared to SF-DMEM (P<0.01). Distant from the injury in relatively normal cartilage chondrocytes with abnormal morphology were occasionally observed (Fig. 6.12b). However, the percentage of abnormal cells was significantly greater at the injury as compared to distant from the injury in the injured explants cultured with SF-DMEM and FCS-DMEM (Fig. 6.12b; P<0.05 for SF-DMEM and FCS-DMEM). Additionally, in the presence of standard-DMEM, chondrocyte morphology remained unaffected at or distant from the injury (Fig. 6.12b).

Chondrocyte volume was measured at and distant from the injury in addition to the volume measurements at day 3, were compared between the three different culture conditions. There was an overall three-fold increase in the volume of chondrocytes at the injury in the presence of SF-DMEM and FCS-DMEM as compared to standard-

DMEM. The average volume of individual abnormal chondrocytes at the injury by day 14 was 2965±438μm^3 [*N(n)*=18(23)] following culture in the presence of SF-DMEM. Chondrocyte volume measured 2197±185μm^3 [*N(n)*=18(23)] in FCS-DMEM and 790±17μm^3 [*N(n)*=18(23)] following culture in standard-DMEM. Volume was significantly higher in SF-DMEM and FCS-DMEM as compared to standard-DMEM (Fig. 6.12c; $P<0.0001$ for both SF-DMEM and FCS-DMEM). Additionally, the volume of chondrocytes at the injury after 14 days of culture in SF-DMEM and FCS-DMEM was significantly greater than the volume of chondrocytes at day 0 (711±25μm^3) [*N*(*n*)=18(23)] ($P<0.0001$ for both SF-DMEM and FCS-DMEM). However, distant from the injury in the presence of SF-DMEM and FCS-DMEM, the volume of chondrocytes was significantly lower than those at the injury (Fig. 6.12d; $P<0.0001$ for both SF-DMEM and FCS-DMEM). In the presence of standard-DMEM, the volume of chondrocytes showed no significant changes at the site or distant from the injury.

The average length of the cell body of individual abnormal cells at the injury increased by approx. x4 in the presence of SF-DMEM and FCS-DMEM as compared to standard-DMEM (Fig. 6.12e; $P<0.0001$ for both SF-DMEM and FCS-DMEM) and also in comparison with the length of cell body at day 0 ($P<0.0001$ for both SF-DMEM and FCS-DMEM). The length of cell bodies at the injury was found to be significantly greater as compared to those distant from the injury in the explants cultured in the presence of SF-DMEM and FCS-DMEM (Fig. 6.12f; $P<0.0001$ for both SF-DMEM and FCS-DMEM). In the presence of standard-DMEM there was no significant change observed in the length of cell bodies at or distant from the injury.

These results demonstrated the marked heterogeneity of chondrocyte morphology by day 14 of culture in SF-DMEM and FCS-DMEM, which was not present following culture in standard-DMEM. However distant from the injury, changes in chondrocyte morphology were also occasionally observed but these changes were significantly less as compared to those at the injury (Fig. 6.12b). Additionally, the effect of FCS was significantly more potent in producing changes to chondrocyte morphology and volume as compared to SF (Fig. 6.12a; $P<0.05$).

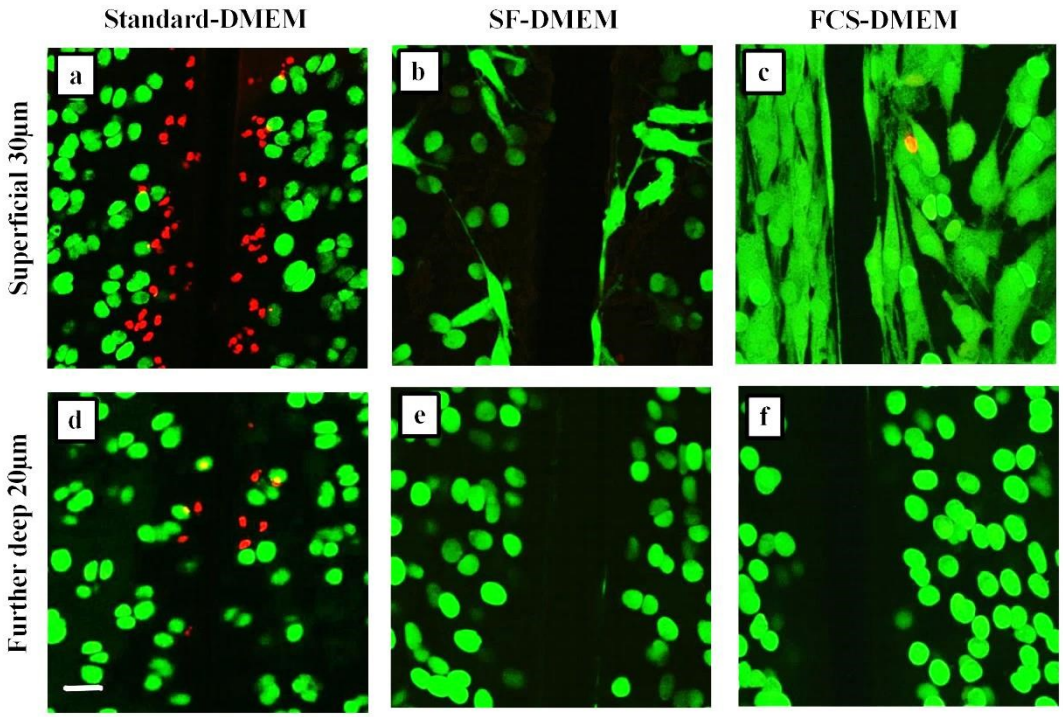

Figure 6.11: Heterogeneity of chondrocyte morphology at day 14 at the injury in response to different culture media.
High magnification axial CLSM reconstructions of fluorescently-labelled chondrocytes at day 14, (a, b, c) superficial 30µm and (d, e, f) a further deep 20µm of the cartilage, cultured in standard-DMEM, SF-DMEM and FCS-DMEM respectively. Scale bar for all panels = 25 µm.

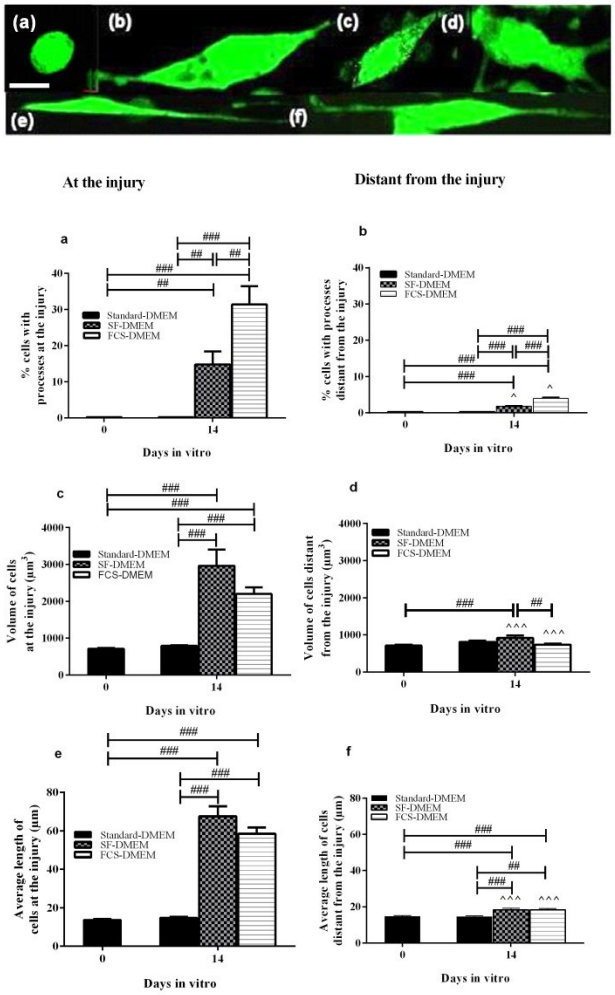

Figure 6.12: Examples and characteristics of the heterogeneous nature of chondrocyte morphology.

Top panel shows examples of 'abnormal' chondrocytes in response to injury in the presence of SF-DMEM and FCS-DMEM at day 14 of culture. The varieties of chondrocytes observed were (a) relatively 'normal' with spheroidal shape (b) 'abnormal chondrocyte' with flattened, elongated cell body. 'Abnormal' chondrocytes as illustrated in (c,d,e,f), had elongated body and single/multiple cytoplasmic processes emanating from the cell body. High magnification CLSM images and scale bar for all panels = 10µm. Graphs show pooled data for (a, b) % abnormal cells at and distant from the injury, (c, d) average volume of cells (μm^3) at and distant from the injury and (e, f) average length of cells (µm) at and distant from the injury. Data were for [$N(n)$]=[18(23)]. # indicated a significant difference between different culture conditions and at two time points according to one-way ANOVA followed by Tukey's multiple comparison post-hoc test. ^ indicated a significant difference between the values at and distant from the injury according to unpaired student's t-test. The single, double and triple symbols showed the level of significance for P<0.05, 0.01 and 0.001 respectively.

6.5.3 Morphology of chondrocytes in injured cartilage cultured under various conditions (coronal view)

Injured osteochondral explants for coronal imaging were prepared and imaged as described earlier (sections 6.4.1.1.1. & 6.4.1.2). The explants were imaged coronally to study the morphological characteristics of chondrocytes in the various zones. Full-depth osteochondral explants comprising of full thickness of the cartilage and subchondral bone were trimmed approximately into 6x5x1mm size and kept in various culture conditions for 14 days. The various culture conditions used in these experiments were (a) standard-DMEM, (b) SF-DMEM (10%) or (c) FCS-DMEM (10%). These explants were not injured axially and the cut edges of the explants were the injured coronal areas focussed at in these experiments. The chondrocytes were fluorescently-labelled and imaged for the **CORONAL** view at different time points (Days 0, 3, 7 and 14) to study the effect of culture media on chondrocyte morphology in superficial, mid and deep zones of cartilage (SZ, MZ, DZ). The CLSM images were obtained at low (x10dry) and high power (x40DW) magnification.

Chondrocyte morphology remained unaffected in all the layers of cartilage in the explants cultured in the presence of standard-DMEM (Fig. 6.13b,e&h). The cartilage explants cultured in the presence of SF-DMDM and FCS-DMEM showed changes to chondrocyte morphology during the course of culture. By day 3 of culture chondrocytes in the deeper layers of cartilage changed morphology in the presence of SF-DMEM (Fig. 6.13c) and FCS-DMEM (Fig. 6.13d). By day 7, chondrocytes in the middle layers also showed morphological changes in the explants cultured in the presence of SF-DMEM and FCS-DMEM (Fig. 6.13f,g). By day 14, of culture the

abnormal chondrocytes were present throughout the thickness of the cartilage involving the superficial layers also in the explants cultured in the presence of SF-DMEM and FCS-DMEM (Fig. 6.13i,j).

The morphology of chondrocytes remained relatively normal in the superficial and middle layers of cartilage cultured in standard-DMEM even after 14 days of culture (Fig. 6.14a,b,e&h). The chondrocytes in the middle zone of cartilage showed marked heterogeneity in terms of morphology in explants cultured in the presence of SF-DMEM and FCS-DMEM by day 7 (Fig. 6.14f,g). By day 14 of culture these abnormal chondrocytes could be seen even in the superficial layers of cartilage explants cultured with SF-DMEM and FCS-DMEM (Fig. 6.14i,j). The abnormal chondrocytes were enlarged, flattened and had cytoplasmic processes emanating from their cell bodies.

The coronal images of cartilage explants suggested that the composition of culture media had affected the morphology of chondrocytes. Chondrocytes changed morphology in the presence of SF-DMEM and FCS-DMEM as compared to standard-DMEM and the changes started in the deeper layers of cartilage extending upwards progressively. This suggested that chondrocytes in deep layers had greater access to factors present in SF-DMEM and FCS-DMEM and therefore changed morphology earlier as compared to the cells in upper layers of cartilage.

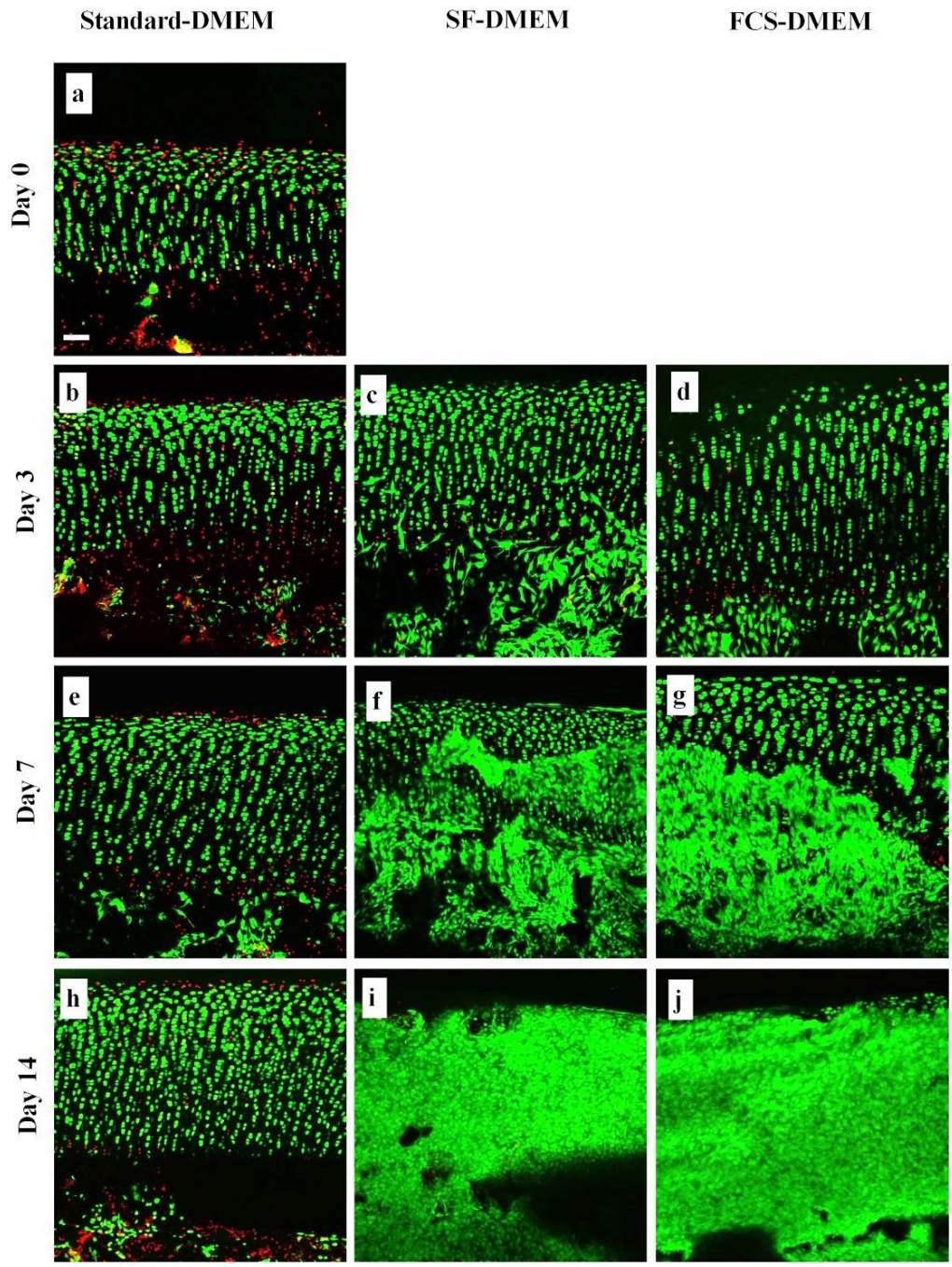

Figure 6.13: Coronal CLSM reconstructions of injured cartilage explant showing progressive changes to chondrocyte morphology.

Coronal CLSM reconstructions of low power (x10) magnification images, typically taken to a depth of ~100-150µm in the z axis of the cartilage (see Materials and Methods) collected at an interval of 5.2µm z stacks. Cartilage explants labelled with CMFDA and PI (live/dead cells respectively) imaged at (a) day 0, (b,c,d) day 3, (e,f,g) day 7 and (h,i,j) day 14 cultured in standard-DMEM, SF-DMEM and FCS-DMEM respectively. Scale bar for all panels = 100µm.

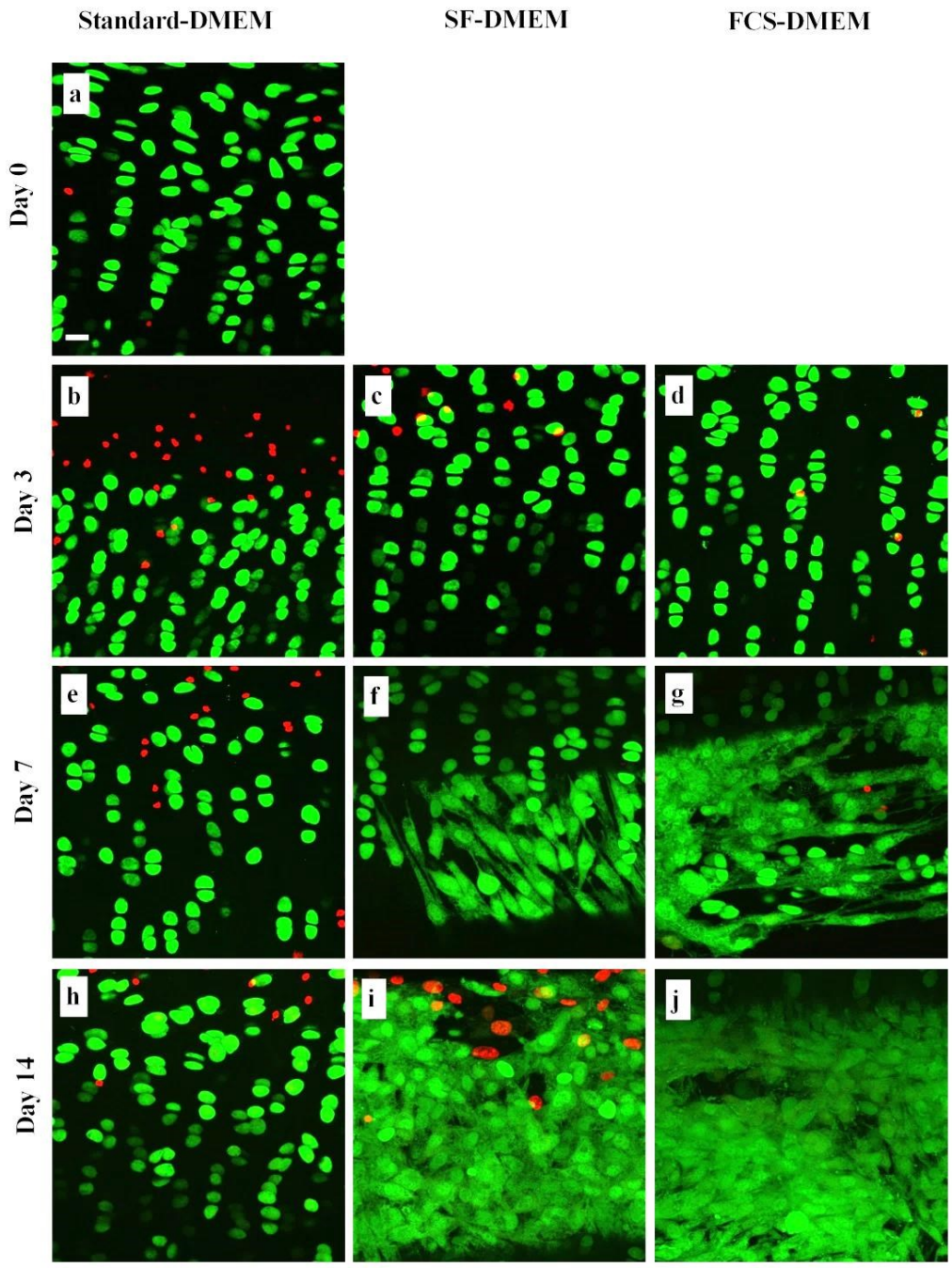

Figure 6.14: Coronal CLSM reconstructions of mid to deep zones of injured cartilage explants cultured in various culture conditions.

Coronal CLSM reconstructions of high power (x40DW) magnification images, typically taken to a depth of ~60µm in the z axis of the cartilage collected at an interval of 1.1µm z stacks. Cartilage explants labelled with CMFDA and PI (live/dead cells respectively) imaged at (a) day 0, (b,c,d) day 3, (e,f,g) day 7 and (h,i,j) day 14 cultured in standard-DMEM, SF-DMEM and FCS-DMEM respectively. Scale bar for all panels = 25µm.

6.5.4 Morphological characteristics of chondrocytes in injured cartilage without subchondral bone cultured under various conditions

It was possible that some of the cells observed originated from the bone component of the osteochondral explants. Accordingly, injured cartilage explants without subchondral bone were cultured under various conditions to rule out any possibility of contamination of injury with bone cells and to exclude the effect of any factors released from the exposed bone parts. Explants comprising of the full thickness of cartilage without subchondral bone were injured and kept in various culture conditions for 14 days. The full depth cartilage explants without subchondral bone were obtained with careful dissection (example shown in Fig. 6.15) and injured with the standardised injury protocol (section 6.4.1.1.1). The various culture media used for these experiments were (a) standard-DMEM (b) SF-DMEM or (c) FCS-DMEM. Explants were labelled for the live and dead chondrocytes with CMFDA and PI respectively. These fluorescently-labelled chondrocytes were imaged at days 0, 3, 7 and 14 by CLSM and both low and high power magnification images were obtained. The images were analysed for various features regarding PCD, volume of chondrocytes, cluster formation and presence of cytoplasmic processes by 3D image analysis software.

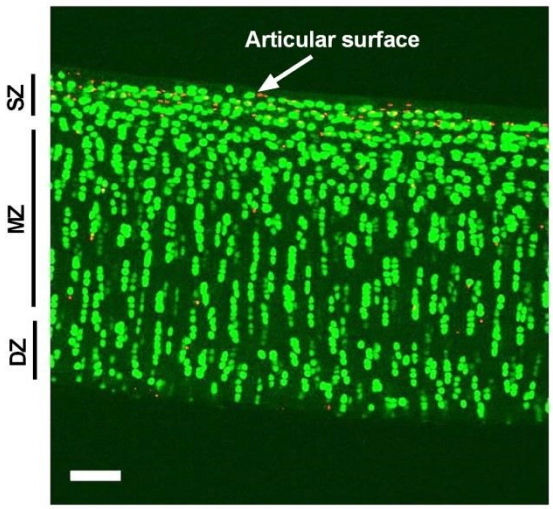

Figure 6.15: Coronal CLSM reconstructed image of full depth cartilage without subchondral bone.
An example of CMFDA and PI labelled (for live and dead cells respectively) coronal image taken at low power magnification (x10) of full depth cartilage without bone at day 0 of culture showing SZ, MZ and DZ. Scale bar = 100μm.

6.5.4.1 *Changes to the width of injury in explants without bone following culture in various culture media*

The width of the injury was measured (Fig. 6.3) to assess the reaction of the injured area to varying culture media. The width of injury remained unaffected in cartilage explants without subchondral bone cultured in standard-DMEM during first 7 days of culture (Fig. 6.16; $P>0.05$ according to ANOVA). By day 14 the width of injury increased significantly in explants cultured with standard-DMEM as compared to all the three earlier time points (Fig. 6.16; $P<0.001$ for days 0, 3 and 7 of culture). The width of injury increased significantly in the explants cultured in the presence of SF-DMEM and FCS-DMEM as compared to standard-DMEM (Fig. 6.16; $P<0.0001$ for both conditions) at day 3 and (Fig. 6.16; $P<0.0001$ for both conditions) at day 7 of

culture. However, by day 14 of culture the width of injury decreased significantly in the presence of SF-DMEM and FCS-DMEM as compared to standard-DMEM (Fig. 6.16; $P<0.0001$ for both conditions). During the initial 7 days of culture, the width of injury increased in SF-DMEM and FCS-DMEM but decreased dramatically during the last 7 days of culture. These results proposed that during the course of culture in explants cultured in SF-DMEM and FCS-DMEM the width of injury was reduced as compared to standard-DMEM.

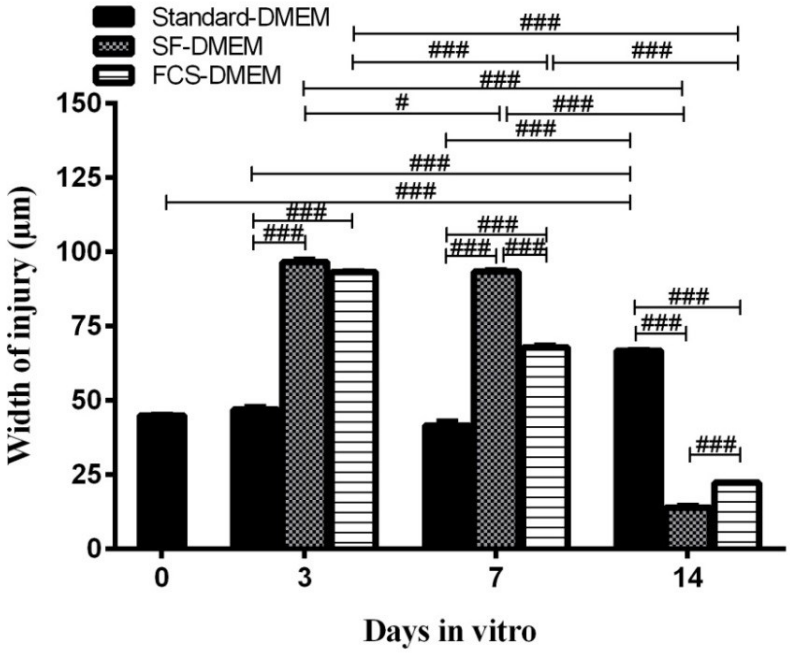

Figure 6.16: Variations in the width of injury (explants without bone) following culture under various conditions.
Graph shows pooled data regarding width of the injury at days 0, 3, 7 and 14 of culture in three different culture conditions. Data were from [$N(n)$]=[6(25)]. # indicated a significant difference between different culture conditions and at various time points according to one-way ANOVA followed by Tukey's multiple comparison post-hoc test. The single, double and triple symbols showed the level of significance for $P<0.05$, 0.01 and 0.001 respectively.

6.5.4.2 *Loss of PI-labelled cells at and distant from the injury*

In a previous section (section 6.5.2.2) the loss of PI-labelled chondrocytes at the injury in axially imaged osteochondral explants was determined in various culture conditions. Likewise, % of PI-labelled chondrocytes was determined within specified ROIs at and distant from the injury (section 6.4.1.4) in the injured cartilage explants without subchondral bone to determine the effect of varying culture media. The composition of the culture medium markedly affected the % of PI-labelled chondrocytes (Fig. 6.17a-j). In the explants cultured with SF-DMEM and FCS-DMEM the PI-labelled cells reduced dramatically even at day 3 of culture (Fig. 6.17c&d) as compared to standard-DMEM (Fig. 6.17b).

In the injured explants without bone the percentage of PI-labelled chondrocytes **at the injury** remained unaffected throughout the culture period in the explants cultured with standard-DMEM (Fig. 6.18a; $P>0.05$; one-way ANOVA). There was a significant decrease in the % of PI-labelled chondrocytes in the explants cultured with SF-DMEM and FCS-DMEM as compared to standard-DMEM (Fig. 6.18a; $P<0.001$; $P<0.0001$) at day 3, (Fig. 6.18a; $P<0.001$; $P<0.0001$) at day 7 and (Fig. 6.18a; $P<0.0001$ for both conditions) at day 14 of culture. The loss of PI-labelled chondrocytes was significantly higher in the explants cultured with FCS-DMEM as compared to SF-DMEM at day 3 and 7 of culture (Fig. 6.18a; $P<0.001$ and $P<0.05$ respectively).

The percentage of PI-labelled chondrocytes was significantly higher at the injury as compared to **distant from the injury** throughout the culture period in the explants cultured with standard-DMEM (Fig. 6.18b; $P=0.002$; $P=0.0009$; $P=0.0001$ and

P=0.0001) at days 0, 3, 7 and 14 respectively. In the explants cultured with SF-DMEM the % of PI-labelled chondrocytes was higher at the injury as compared to distant from the injury at days 3 and 7 of culture (Fig. 6.18b; *P*=0.007 and *P*=0.001 respectively. However, by day 14 no difference existed in the % of PI-labelled cells at and distant from the injury in the explants cultured with SF-DMEM. Moreover, it was found that there existed no significant difference at days 3, 7 and 14 in the % of PI-labelled chondrocytes at and distant from the injury in the explants cultured with FCS-DMEM (Fig. 6.18b; *P*>0.05 for all conditions).

These results suggested that the % of PI-labelled chondrocytes decreased markedly in the explants without subchondral bone cultured in the presence of SF-DMEM and FCS-DMEM as compared to standard-DMEM throughout the culture. In general, the effect of FCS-DMEM appeared to be more potent as compared to SF-DMEM. In summary the pattern of loss of PI-labelled chondrocytes in the injured explants without bone appeared to be the same as for osteochondral explants.

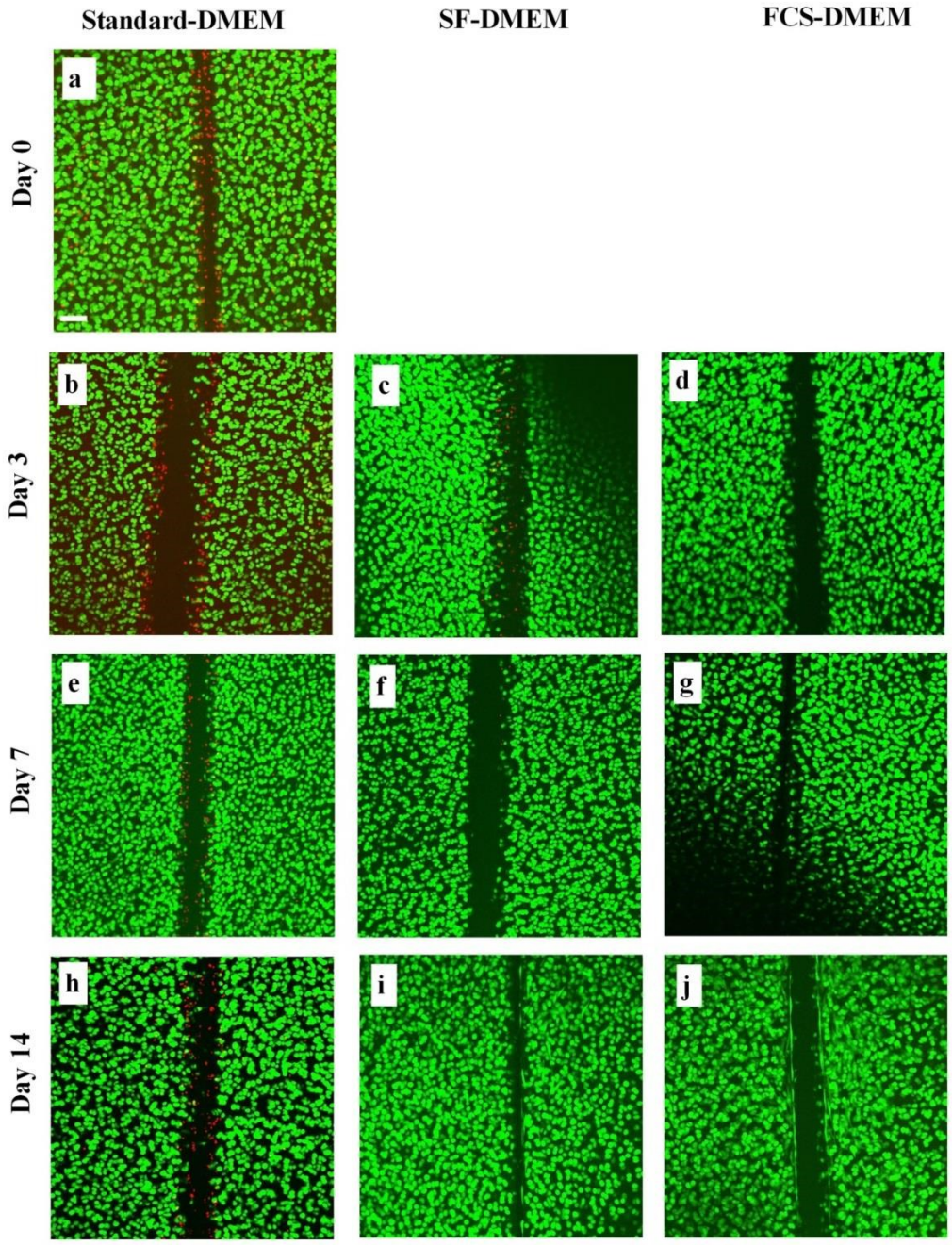

Figure 6.17: Axial CLSM reconstructions of injured cartilage explants without subchondral bone in various culture conditions.

CLSM reconstructions of low magnification (x10) images, typically to a depth of 100µm collected at an interval of 10µm of CMFDA and PI-labelled chondrocytes (live/dead, respectively) in injured explants at (a) day 0, (b,c,d) day 3, (e,f,g) day 7 and (h,I,j) day 14 cultured in standard-DMEM, SF-DMEM and FCS-DMEM respectively. Scale bar for all panels = 100µm.

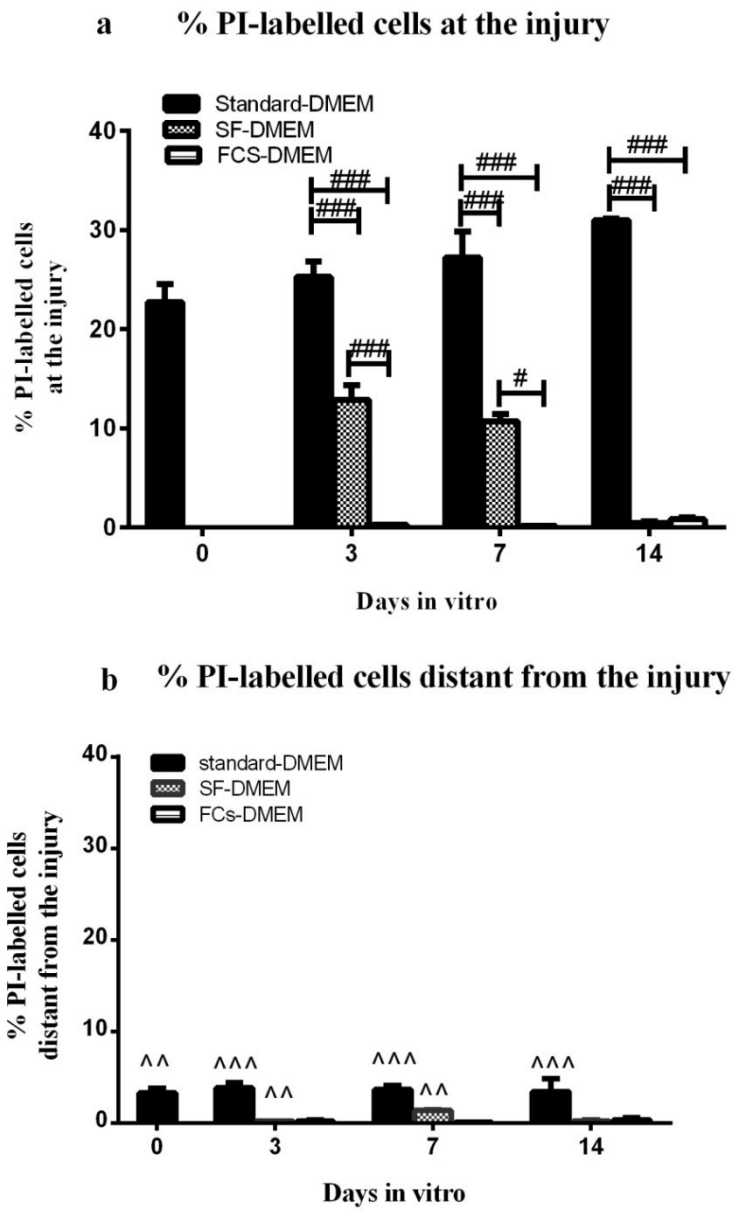

Figure 6.18: The percentage of PI-labelled cells at and distant from the injury in cartilage without bone cultured under various conditions.

Graphs show a comparison between the % PI-labelled cells (a) at the injury and (b) distant from the injury under the three culture conditions. Data were from [$N(n)$=6(25)]. # indicated a significant difference between different culture conditions at various time points according to one-way ANOVA followed by Tukey's multiple comparison post-hoc test. ^ indicated a significant difference between the values at and distant from the injury according to unpaired student's t-test. The single, double and triple symbols showed the level of significance for P<0.05, 0.01 and 0.001 respectively.

6.5.4.3 *Changes to chondrocyte volume by day 3 of culture*

Considerable changes to chondrocyte volume and morphology were seen at the injury in the cartilage explants (without bone) cultured in SF-DMEM and FCS-DMEM as compared to standard-DMEM as shown in high power (x40) magnification CLSM images (Fig. 6.19a-j).

The volume of chondrocytes at day 0 at the injury was 888±33μm^3, and did not change by day 3 for the explants cultured in standard-DMEM (Fig. 6.20; P>0.05; one-way ANOVA). Chondrocyte volume at the injury increased significantly in the explants cultured with SF-DMEM and FCS-DMEM as compared to standard-DMEM by day 3 of culture (Fig. 6.20; P<0.0001 and P<0.01 respectively). Additionally, the volume of chondrocytes increased in the presence of SF-DMEM and FCS-DMEM by day 3 in comparison with the volume of chondrocytes at day 0 (Fig. 6.20; P<0.001 for both the conditions according to ANOVA).

These results suggested that by day 3 of culture chondrocyte volume increased at the injury in the presence of SF-DMEM and FCS-DMEM as compared to standard-DMEM. Chondrocyte volume remained unaffected in the presence of standard-DMEM.

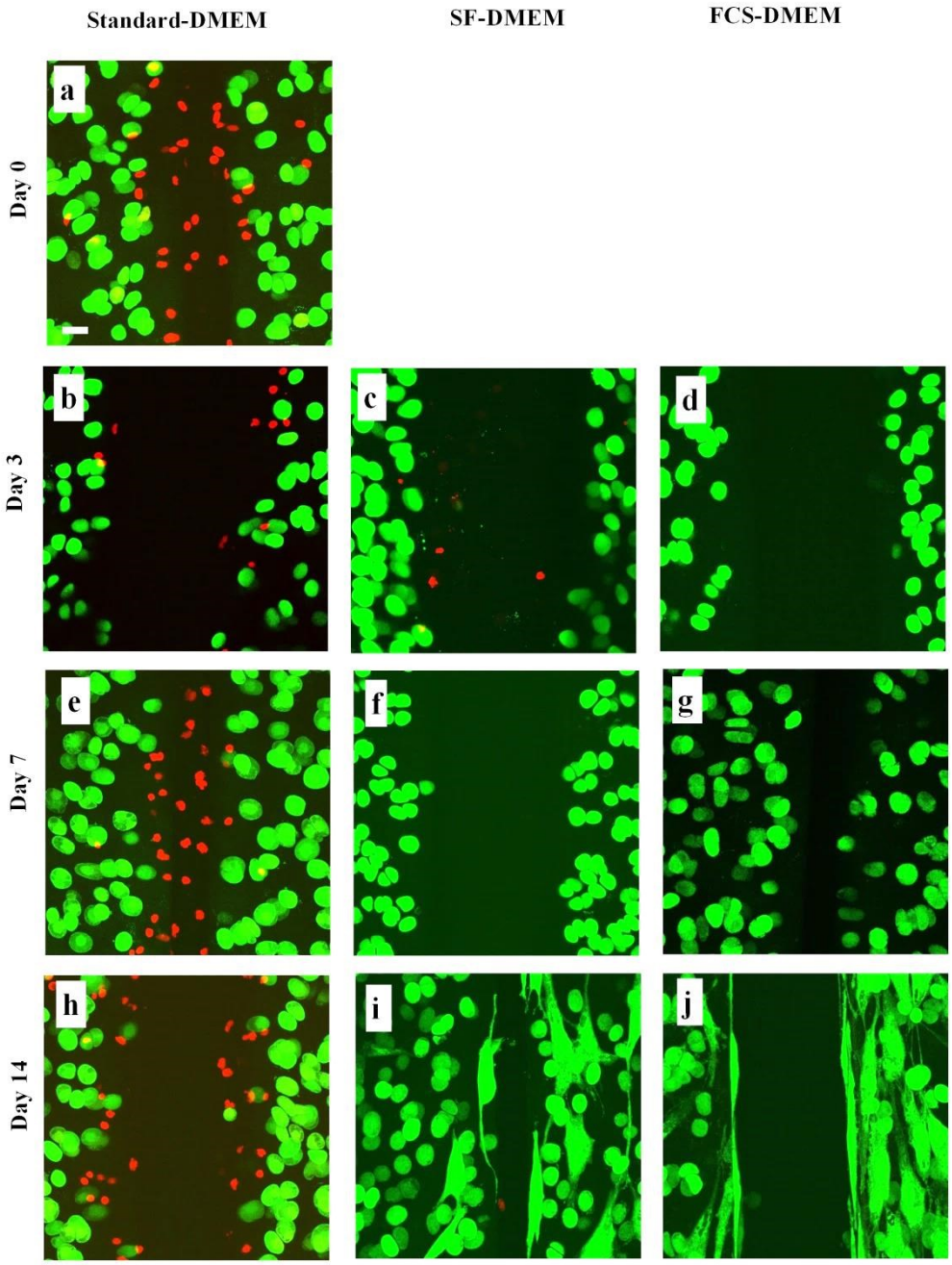

Figure 6.19: Axial CLSM reconstructions of injured cartilage without bone cultured in various conditions showing morphological changes to chondrocytes at the injury.

Images obtained by x40(DW) objective typically to a depth of 50µm at an interval of 1µm through the z-axis of the tissue. Chondrocytes were incubated with CMFDA and PI (live/dead respectively) in injured explants without bone at (a) day 0, (b,c,d) day 3, (e,f,g) day 7 and (h,i,j) day 14 cultured in standard-DMEM, SF-DMEM and FCS-DMEM respectively. Scale bar for all panels = 25µm.

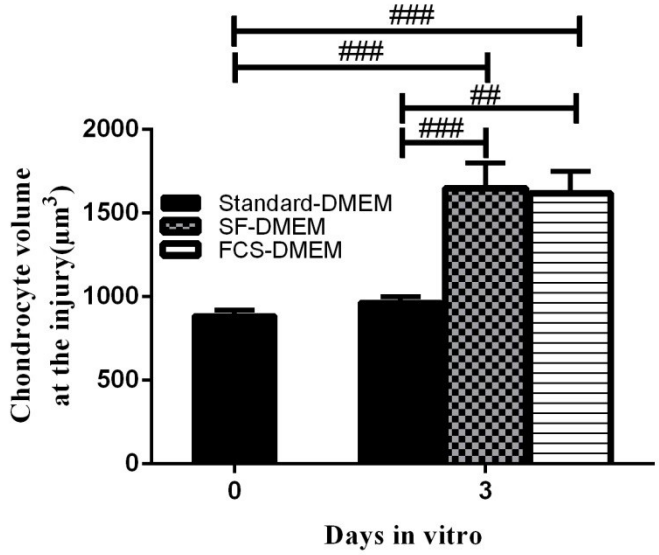

Figure 6.20: Changes to chondrocyte volume at the injury (explants without bone) in response to various culture conditions.
Graph shows pooled data on volume of chondrocytes at the injury indicating changes in response to various culture media by day 3 of culture. Data were from [*N*(*n'*)=6(38)]. # indicated a significant difference between different culture conditions and at two time points according to one-way ANOVA followed by Tukey's multiple comparison post-hoc test. The single, double and triple symbols showed the level of significance for $P<0.05$, 0.01 and 0.001 respectively.

6.5.4.4 *Chondrocyte clustering by day 7 of culture*

Cluster formation, being a characteristic feature of chondrocytes was observed routinely. The clusters were defined and various characteristics of clusters were analysed (section 4.4.1.7.1) in different culture conditions and displayed (Fig. 6.21a-e). Chondrocytes formed a significantly higher number of clusters at the injury in the explants cultured in the presence of FCS-DMEM as compared to standard-DMEM by day 7 of culture (Fig. 6.21a; $P<0.05$). The number of clusters formed in the presence of FCS-DMEM increased by day 7 as compared to the number of clusters at day 0 (Fig. 6.21a; $P<0.05$; ANOVA). However, the number of clusters formed in SF-

DMEM by day 7 did not differ significantly from those in standard-DMEM and from day 0 (Fig. 6.21a; $P>0.05$; ANOVA).

At day 7, the number of cells per cluster increased in the presence of FCS-DMEM as compared to standard-DMEM but the difference was not statistically significant (Fig. 6.21b; $P>0.05$) however, increased significantly in comparison to the number of cells per cluster at day 0 of culture (Fig. 6.21b; $P<0.05$; ANOVA). However, at day 7 the number of cells per cluster remained unaffected in the presence of SF-DMEM as compared to standard-DMEM and also in comparison to day 0 (Fig. 6.21b).

The volume of clusters formed at day 7 in the injured explants cultured in SF-DMEM and FCS-DMEM was significantly greater than the volume of clusters formed in standard-DMEM (Fig. 6.21c; $P<0.01$ and $P<0.05$ respectively). The volume of clusters formed at day 7 in the presence of SF-DMEM and FCS-DMEM was also significantly higher than the volume of clusters present at day 0 (Fig. 6.21c; $P<0.01$ and $P<0.05$ respectively; ANOVA). The volume of individual cell in a cluster was significantly higher in the explants cultured with SF-DMEM as compared to standard-DMEM by day 7 (Fig. 6.21d; $P=0.04$).

At the injury, at day 7 of culture, the percentage of chondrocytes forming clusters increased in the presence of SF-DMEM and FCS-DMEM as compared to standard-DMEM (Fig. 6.21e). At day 7, in the presence of SF-DMEM and FCS-DMEM, a significantly higher percentage of chondrocytes (17±2% and 18±2% respectively) formed clusters as compared to standard-DMEM (8±0.2%; $P<0.05$ for both conditions). Additionally, a significantly higher percentage of chondrocytes formed

clusters in the presence of SF-DMEM and FCS-DMEM by day 7 of culture as compared to day 0 (P<0.05 for both conditions; ANOVA).

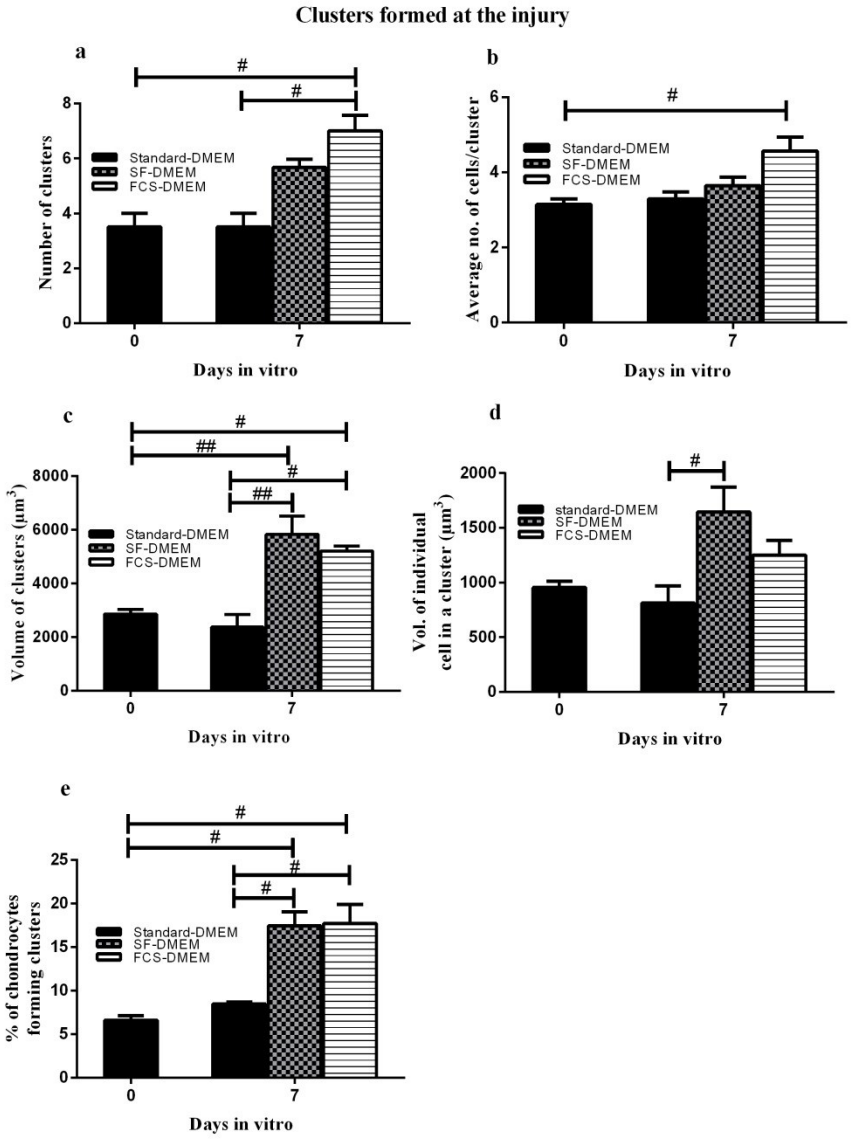

Figure 6.21: Various characteristics of clusters formed at injury in the explants (without bone) cultured in various culture conditions.

Graphs show pooled data for (a) number of clusters, (b) number of cells per cluster, (c) volume of clusters (µm^3), (d) volume of individual cell in cluster (µm^3) and (e) % of chondrocytes forming clusters. Data were for [*N(n)*=6(10)]. # indicated a significant difference between different culture conditions and at two time points according to one-way ANOVA followed by Tukey's multiple comparison post-hoc test. The single, double and triple symbols showed the level of significance for P<0.05, 0.01 and 0.001 respectively.

To summarise this section, at day 0 very few chondrocytes were present in clusters. By day 7 of culture, chondrocytes were present in large clusters at the injury in the explants cultured with SF-DMEM and FCS-DMEM as compared to standard-DMEM. The effects of SF and FCS appeared to be almost similar but clustering was triggered more in the presence of FCS as compared to SF.

6.5.4.5 *Abnormal chondrocyte morphology by day 14 of culture*

The nature of some of the culture media led to marked heterogeneity in chondrocyte morphology at the injury. In the presence of standard-DMEM chondrocyte morphology at the injury remained unaffected throughout the culture period (Fig. 6.19a,b,e,h). However, chondrocytes at the injury in the presence of SF-DMEM and FCS-DMEM showed dramatic changes in terms of morphology (Fig. 6.19c,f,i & 6d,g,j respectively). The morphology of chondrocytes changed from normal spheroidal shape to abnormal shapes characterised by cell enlargement, flattening/elongation of cell bodies and production of cytoplasmic processes emanating from the cell bodies (examples shown in Fig. 6.22). These morphological changes were seen in the explants cultured in the presence of SF-DMEM and FCS-DMEM and not in standard-DMEM and were restricted to the superficial 30µm of the cartilage (Fig. 6.23b,c). The chondrocytes in the deeper layers beyond 30µm depth were found to be relatively normal and spheroidal in shape (Fig. 6.23e,f).

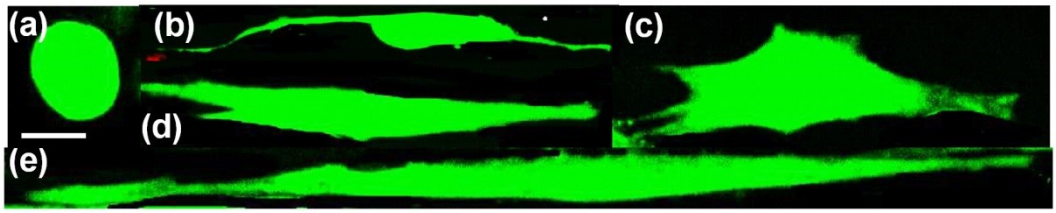

Figure 6.22: Altered morphology of chondrocytes in various culture conditions by day 14.

Examples of abnormal chondrocytes at the injury in the explants cultured in the presence of SF-DMEM and FCS-DMEM at day 14. Varieties of shape changes were seen at high power magnification (a) relatively normal chondrocyte with spheroidal shape. Abnormal chondrocytes (b, c, d and e) showing enlarged, flattened cells with multiple cytoplasmic processes emanating from cell bodies. Scale bar = 10µm.

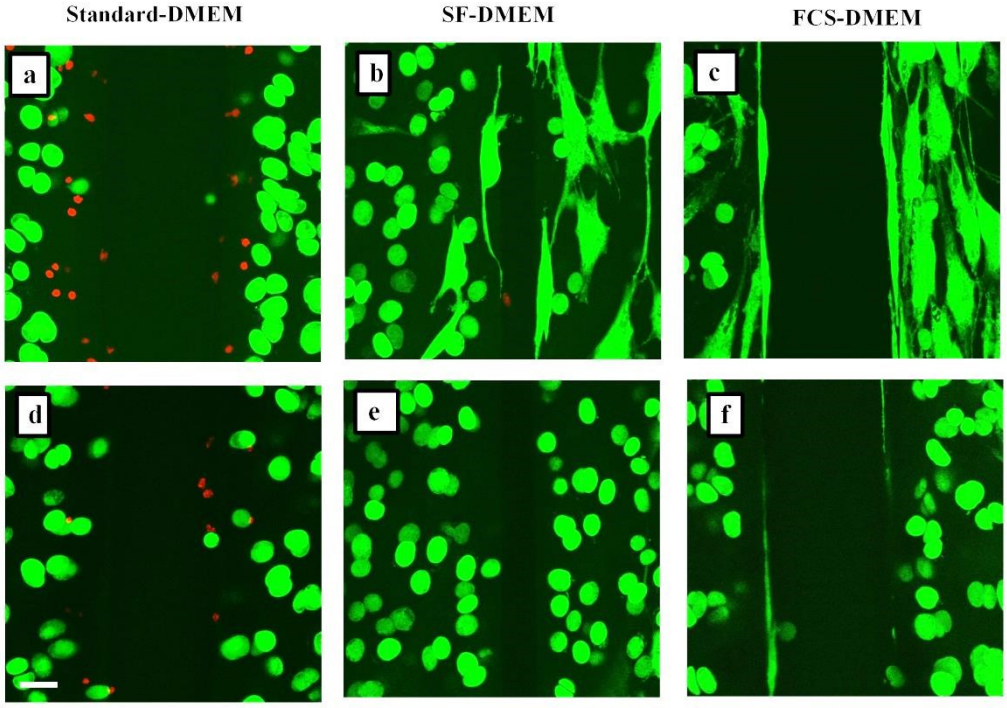

Figure 6.23: Heterogeneity in chondrocyte morphology at the injury in the presence of various culture media at day 14.

Axial CLSM reconstructions of high power magnification images of fluorescently labelled chondrocytes at the injury by day 14, (a, b, c) superficial 30µm and (d, e and f) a further 20µm deep of the cartilage cultured in standard-DMEM (a, d), SF-DMEM (b, e) and FCS-DMEM (c, f). Scale bar = 25µm.

Quantitative data regarding various characteristics of chondrocyte morphology at the injury were obtained by the 3D image analysis software (section 6.4.1.5) and compared for day 0 and 14 of culture in various conditions. At the injury, 17±5% and 25±3% chondrocytes were morphologically abnormal [*N(n)*=6(10); in SF-DMEM and FCS-DMEM respectively] as compared to standard-DMEM at day 14 ($P<0.0001$ for both conditions) and also in comparison to day 0 (Fig. 6.24a; $P<0.0001$ for both conditions) where chondrocytes were relatively normal in shape.

There was an overall three-fold increase in the volume of chondrocytes at the injury following culture in SF-DMEM and FCS-DMEM as compared to standard-DMEM. The average volume of individual abnormal chondrocytes at injury by day 14 of culture was significantly higher in SF-DMEM and FCS-DMEM as compared to standard-DMEM (Fig. 6.24b; $P<0.0001$ for both conditions) and also in comparison to day 0 ($P<0.0001$ for both conditions).

There was an approximate x4 increase in the length of cell bodies of individual abnormal chondrocytes at the injury cultured in the presence of SF-DMEM and FCS-DMEM as compared to standard-DMEM by day 14 of culture (Fig. 6.24c; $P<0.0001$ for both conditions) and also in comparison to day 0 ($P<0.0001$ for both conditions). Moreover, the length of cell bodies at injury was significantly greater in FCS-DMEM as compared to SF-DMEM (Fig. 6.24c; $P<0.001$).

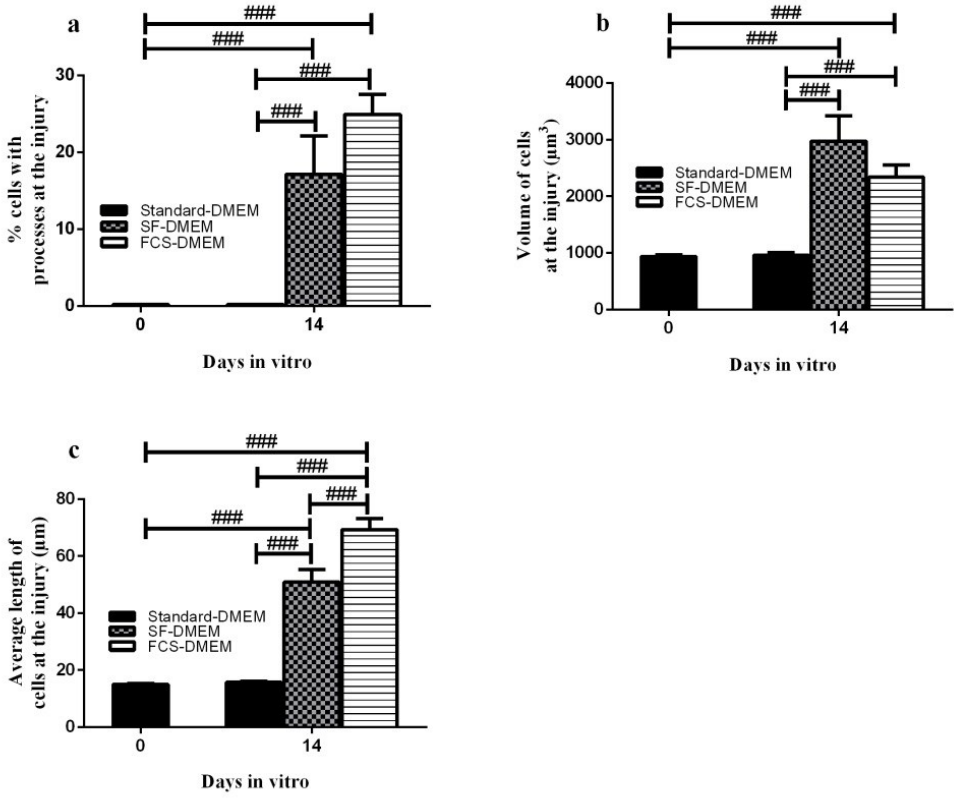

Figure 6.24: Morphological characteristics of chondrocytes at the injury in various culture conditions at day 14.
Graphs show pooled data regarding (a) percentage of abnormal cells with cytoplasmic processes at injury (b) average volume of cells at the injury (μm^3) and (c) average length of cell bodies of chondrocytes (µm) at the injury in the presence of standard-DMEM, SF-DMEM and FCS-DMEM at day 0 and 14 of culture. Data were from [*N(n)*=6(10)]. # indicated a significant difference between different culture conditions and at two time points according to one-way ANOVA followed by Tukey's multiple comparison post-hoc test. The single, double and triple symbols showed the level of significance for $P<0.05$, 0.01 and 0.001 respectively.

To summarise the results of this section, there was marked heterogeneity in chondrocyte morphology at the injury in the cartilage explants (without subchondral bone) cultured with SF-DMEM and FCS-DMEM and not in the presence of standard-DMEM. Moreover, the effect of FCS appeared to be more potent as compared to SF. Therefore, these results suggested that the morphological changes

observed in chondrocytes at the injury were similar to those in the explants with subchondral bone.

6.5.5 Morphological characteristics of chondrocytes in injured cartilage without superficial layers cultured under various conditions

It is possible that the chondrocytes which changed shape at the injury in response to factors present in FCS/SF are limited to the superficial zone alone and the chondrocytes residing deep in the cartilage do not possess this property. In view of investigating this, cartilage explants containing the deeper layers of chondrocytes with a substantial amount of subchondral bone were injured with the standardised injury method. The superficial layers of cells with the thickness of 431±42μm (n=4; Fig. 6.25a) were removed with careful dissection and the deep layers of cartilage with the thickness of 314.9±23μm (n=6; Fig. 6.25b) along with the underlying subchondral bone were injured and kept in culture for 14 days. The culture media used in these experiments were either (a) standard-DMEM or (b) FCS-DMEM and in these experiments SF was not used.

These injured explants without the superficial layers of cells were labelled with CMFDA and PI (live and dead cells respectively) at days 0, 7 and 14. The fluorescently labelled chondrocytes were imaged with CLSM with both low and high power magnification objectives. Quantitative data regarding PCD (% of PI-labelled chondrocytes), volume, cluster formation and abnormal morphology of cells in the middle and deep layers of cartilage were obtained by analysing the images.

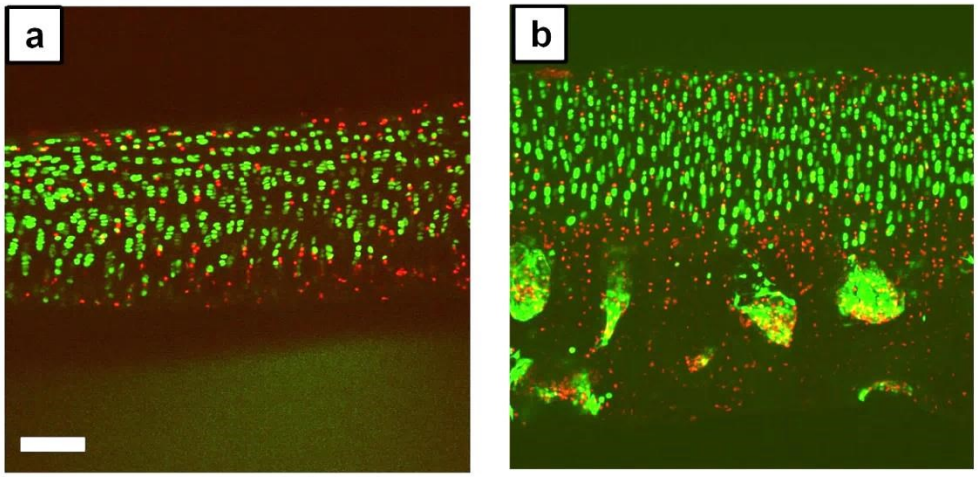

Figure 6.25: Coronal CLSM reconstructions of superficial and deep layers of cartilage.
Examples of coronal view of CMFDA and PI (live and dead cells respectively) labelled chondrocytes imaged at low power magnification (x10 dry) showing (a) superficial layers of cartilage (b) deep layers of cartilage with the underlying subchondral bone. Explants shown in panel b were used in these experiments. Scale bar = 100µm.

6.5.5.1 *PI-labelled cells at and distant from the injury*

In the previous sections the loss of PI-labelled chondrocytes at the injury in osteochondral explants and explants without subchondral bone in the presence of some of the culture media has been detailed (sections 6.7 & 6.18 respectively). Likewise, the percentage of PI-labelled chondrocytes changed considerably in the presence of FCS-DMEM as compared to standard-DMEM (Fig. 6.26b,d). Quantitative data regarding the % of PI-labelled chondrocytes was obtained at and distant from the injury in the cartilage explants without superficial layers cultured in standard-DMEM and FCS-DMEM. The PI-labelled chondrocytes decreased in the explants cultured in the presence of FCS-DMEM even by day 7 of culture as shown

in low power magnification images (Fig. 6.26d) but no such effect was seen in standard-DMEM (Fig. 6.26b). By day 14, in the explants cultured in serum-rich medium, chondrocyte morphology changed dramatically on the whole surface of the cartilage irrespective of at and distant from the injury (Fig. 6.26e). The % of PI-labelled chondrocytes was similar at and distant from the injury due to the fact that in addition to the experimental scalpel injury applied to these explants, they were also injured while dissecting out the superficial layers of cartilage (Fig. 6.26a).

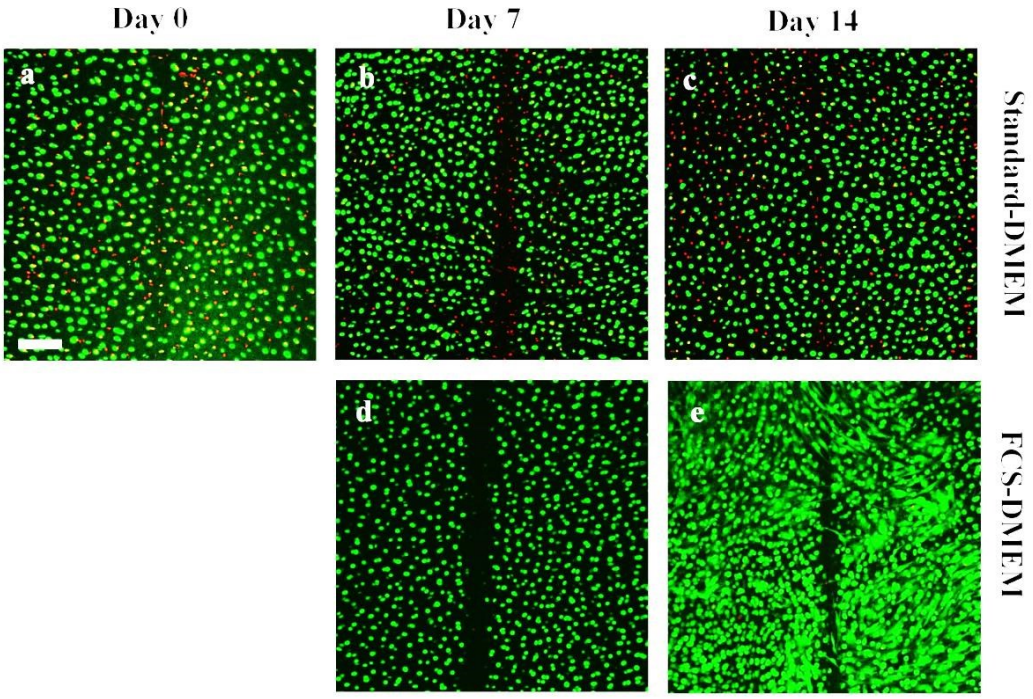

Figure 6.26: Axial CLSM reconstructions of injured cartilage explants without the superficial layers showing abnormal chondrocyte morphology by day 14 in FCS-DMEM.

Low magnification (x10) reconstructed images of CMFDA and PI labelled (live and dead cells respectively) chondrocytes of the injured cartilage explants without superficial layers at (a) days 0, (b, d) 7 and (c, e) 14 of culture in standard-DMEM and FCS-DMEM respectively. Scale bar for all panels = 100µm.

The % of PI-labelled chondrocytes **at the injury** remained unaffected in the explants cultured with standard-DMEM throughout the culture period at days 0, 7 and 14 of culture (Fig. 6.27a; $P>0.05$; ANOVA for the three time points). In the injured explants without superficial layers cultured in FCS-DMEM the % of PI-labelled chondrocytes decreased significantly as compared to standard-DMEM at days 7 and 14 of culture (Fig. 6.27a; $P<0.0001$ for both time points).

The % of PI-labelled chondrocytes **distant from the injury** remained unaffected in the explants cultured with standard-DMEM during the course of culture at days 0, 7 and 14 (Fig. 6.27b; $P>0.05$; ANOVA for the three time points). As expected in the presence of FCS-DMEM, there was a significant reduction in the % of PI-labelled chondrocytes as compared to standard-DMEM at days 7 and 14 of culture (Fig. 6.27b; $P<0.0001$ for both the days). Additionally, no difference was found between the % of PI-labelled chondrocytes at or distant from the injury in the explants cultured with either standard-DMEM or FCS-DMEM throughout the culture (Fig. 6.27a,b; $P>0.05$).

These results suggested that under the effect of FCS there was ~96% decrease in the % of PI-labelled chondrocytes at the injury as compared to standard-DMEM similar to the data from experiments where SZ was intact.

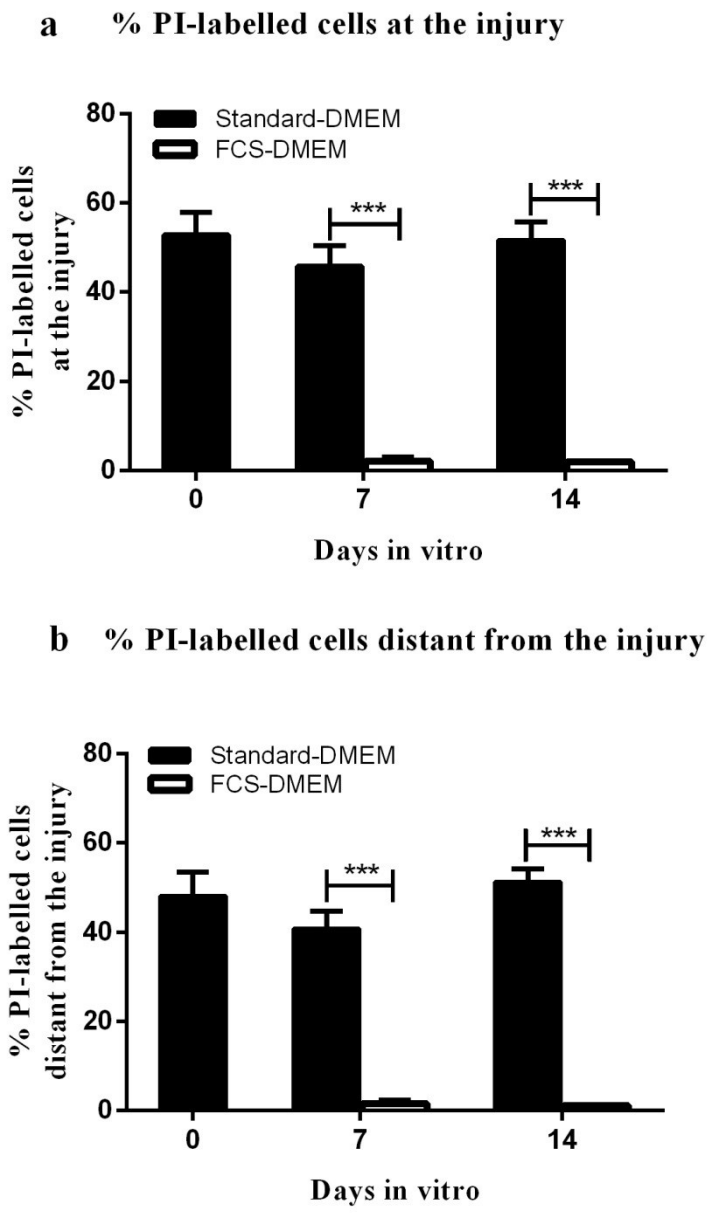

Figure 6.27: Decreased percentage of PI-labelled chondrocytes at and distant from the injury in the explants without SZ cultured in the presence of FCS-DMEM.

The graphs show pooled data regarding the percentage of PI-labelled chondrocytes (a) at the injury and (b) distant from the injury in the explants (without superficial layers) cultured in various conditions throughout the culture period. Data were from [$N(n)$=6(25)]. * indicated a significant difference between two culture conditions at one time point according to t-test. The single, double and triple symbols showed the level of significance for P<0.05, 0.01 and 0.001 respectively.

6.5.5.2 *Morphology of deep zone chondrocytes in response to various culture conditions*

This study aimed at investigating whether the DZ chondrocytes in the presence of serum-rich medium change morphology or this is exclusively the property of chondrocytes in the SZ. The data showed that the morphology of chondrocytes changed markedly during the course of culture in the presence of FCS-DMEM. These morphological changes were analysed in terms of volume, cluster formation and abnormal morphology of chondrocytes and the results were presented at different time points (Days 0, 7 and 14).

6.5.5.2.1 Volume/cluster formation of deep layer chondrocytes at and distant from the injury by day 7

In these experiments, the superficial layers of cartilage were removed, therefore the majority of cells studied here were from middle and deep layers of cartilage. The morphology of chondrocytes in the deep zone of cartilage changed markedly in the explants cultured in the presence of FCS-DMEM as compared to standard-DMEM (Fig. 6.28).

At day 7, volume of chondrocytes appeared to be slightly elevated at the injury in the explants cultured in FCS-DMEM (1491.9±155.8μm^3) than the volume of those cultured in the presence of standard-DMEM (1351.4±105μm^3) and also in comparison to day 0 (1117.8±82.9μm^3) but the difference was not statistically

significant (Fig. 6.29a; $P>0.05$). The volume of chondrocytes in the DZ of healthy cartilage at day 0 was higher than the volume of chondrocytes in the SZ of cartilage as measured in the earlier experiments mentioned in this chapter ($711\pm25\mu m^3$). Additionally, the volume of chondrocytes in both the culture conditions was similar at and distant from the injury (Fig. 6.29b; $P>0.05$).

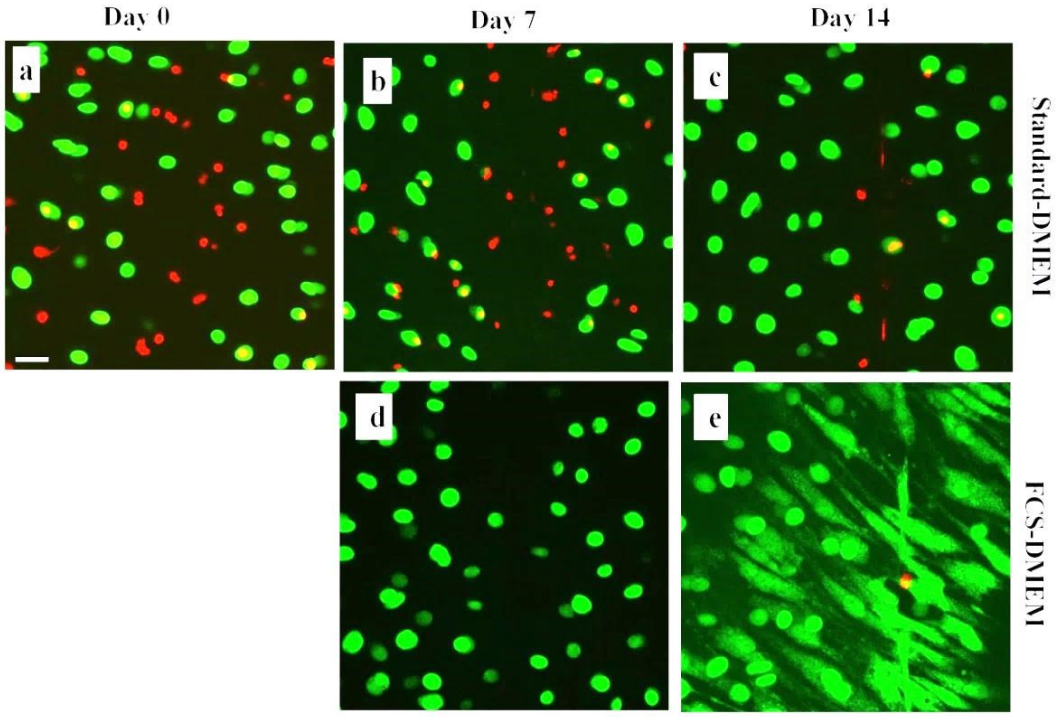

Figure 6.28: Axial CLSM reconstructions of injured cartilage without SZ cells showing changes to chondrocyte morphology by day 14 of culture in FCS-DMEM as compared to standard-DMEM.
High power magnification (x40DW) reconstructed images taken at a depth of 50µm with an interval of 1µm through the z-axis of the tissue. Chondrocytes were incubated with CMFDA and PI (to identify live and dead cells respectively) in the injured explants without superficial layers and imaged at days (a) 0, (b, d) 7 and (c, e) 14 of culture in standard-DMEM and FCS-DMEM respectively. Scale bar for all panels = 25µm.

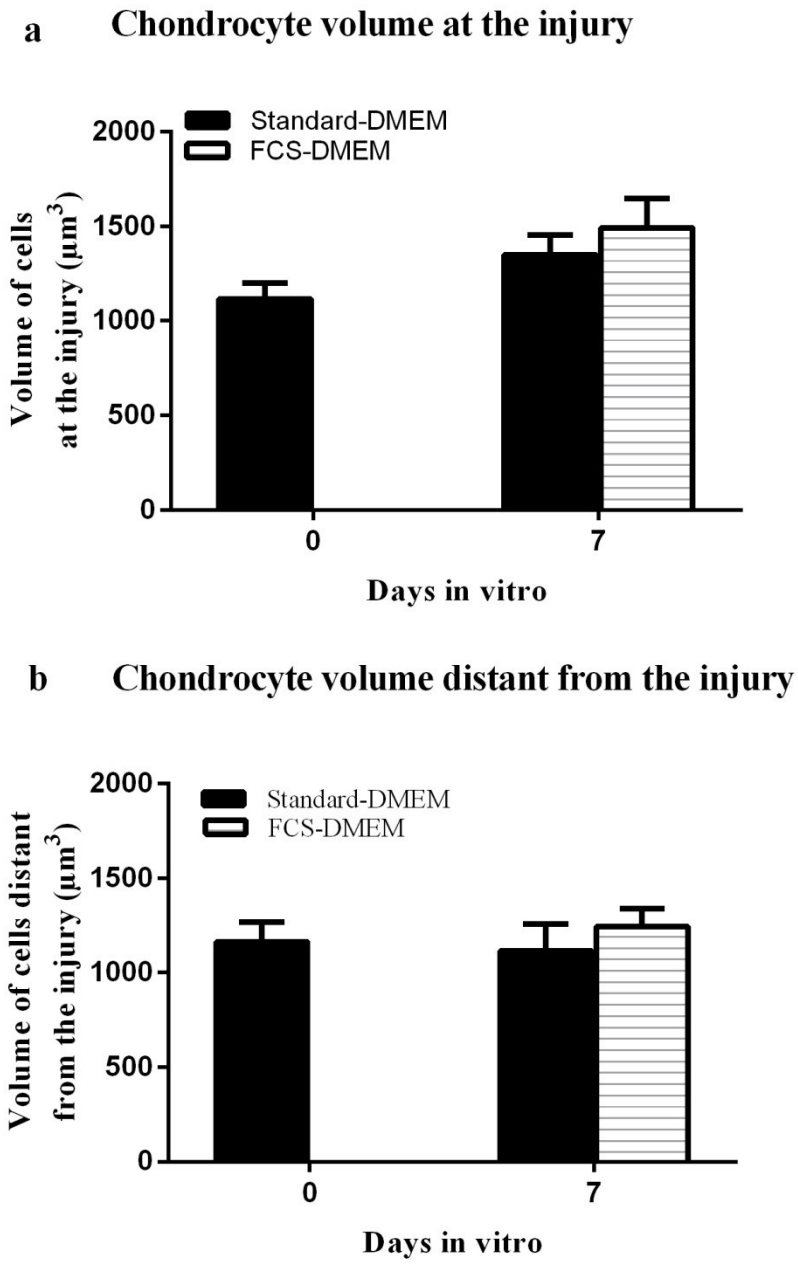

Figure 6.29: Volume of chondrocytes at and distant from the injury in the injured explants (without superficial layers) by day 7.

Graphs summarise pooled data regarding the volume of chondrocytes in standard-DMEM and FCS-DMEM showing no volume changes (a) at the injury and (b) distant from the injury. Data were from [$N(n')$=6(11,8) at day 0, (19,52) in standard-DMEM, (20,20) in FCS-DMEM at day 7, at and distant from the injury respectively. The differences between the volume of chondrocytes at and distance from the injury at days 0 and 7 were not statistically significant.

In the injured explants without superficial layers chondrocyte clustering was observed and was affected by the nature of the culture medium. At day 7, the number of clusters formed at and distant from the injury in the explants cultured with FCS-DMEM were significantly higher than those found in standard-DMEM (Figs. 6.30Aa and 6.30Ba; $P<0.05$ for both at and distant from the injury; ANOVA) and also in comparison to those at day 0 (Fig. 6.30Aa and 6.30Ba; $P<0.05$ for both conditions; ANOVA). However, the number of clusters formed at the injury and distant from the injury in both the culture conditions was not different. The number of cells/cluster was found to be similar in both the culture conditions at and distant from the injury (Figs. 6.30Ab and 6.30Bb; $P>0.05$ for all the conditions).

A higher percentage of chondrocytes formed clusters by day 7 of culture in the explants cultured in the presence of FCS-DMEM as compared to standard-DMEM at and distant from the injury (Figs. 6.30Ac and 6.30Bc). In the injured explants (without superficial layers) cultured in the presence of FCS-DMEM at the injury a significantly higher percentage (20±3%) of chondrocytes formed clusters comapred to those in standard-DMEM (7±1%; $P<0.05$) and percentage of chondrocytes forming clusters at day 0 (5±1%; $P<0.05$). Similarly, distant from the injury, a higher percentage of chondrocytes formed clusters in the presence of FCS-DMEM (23±1%) as compared to those in standard-DMEM (5±1%; $P<0.01$) and also in comparison to day 0 (5±1%; $P<0.01$). However, no difference was found between the percentages of chondrocytes forming clusters at and distant from the injury in both the culture conditions (Figs. 6.30Ac and 6.30Bc; $P>0.05$).

At day 7 of culture, the volumes of clusters formed at and distant from the injury in the presence of FCS-DMEM were significantly greater as compared to those in standard-DMEM (Figs. 6.30Ad and 6.30Bd; $P<0.05$ for both conditions) and also in comparison to day 0 ($P<0.05$ for both conditions). However, no difference was found between the volumes of clusters formed at and distant from the injury in both the culture conditions ($P>0.05$).

The volume of individual cells in a cluster was calculated (section 4.4.1.7.1) and compared in both the culture conditions at days 0 and 7. The volume of individual cells in a cluster at and distant from the injury increased significantly by day 7 for the explants cultured in FCS-DMEM as compared to standard-DMEM (Figs. 6.30Ae and 6.30Be; $P<0.001$ and $P<0.01$ respectively) and also in comparison to day 0 ($P<0.001$ and $P<0.05$ respectively). However, no difference was found between the volumes of individual cells in a cluster at and distant from the injury in both the culture conditions ($P>0.05$).

To summarise the results of this section, the volume of chondrocytes at and distant from the injury in both the culture conditions remained unaffected by day 7 of culture. At day 0 only few chondrocytes formed small sized clusters. At day 7, numerous chondrocytes formed large clusters at and distant from the injury in the injured explants (without superficial layers of cells) cultured in the presence of FCS-DMEM as comapred to standard-DMEM. Moreover, there was no difference between clusters formed at and distant from the injury in both the culture conditions.

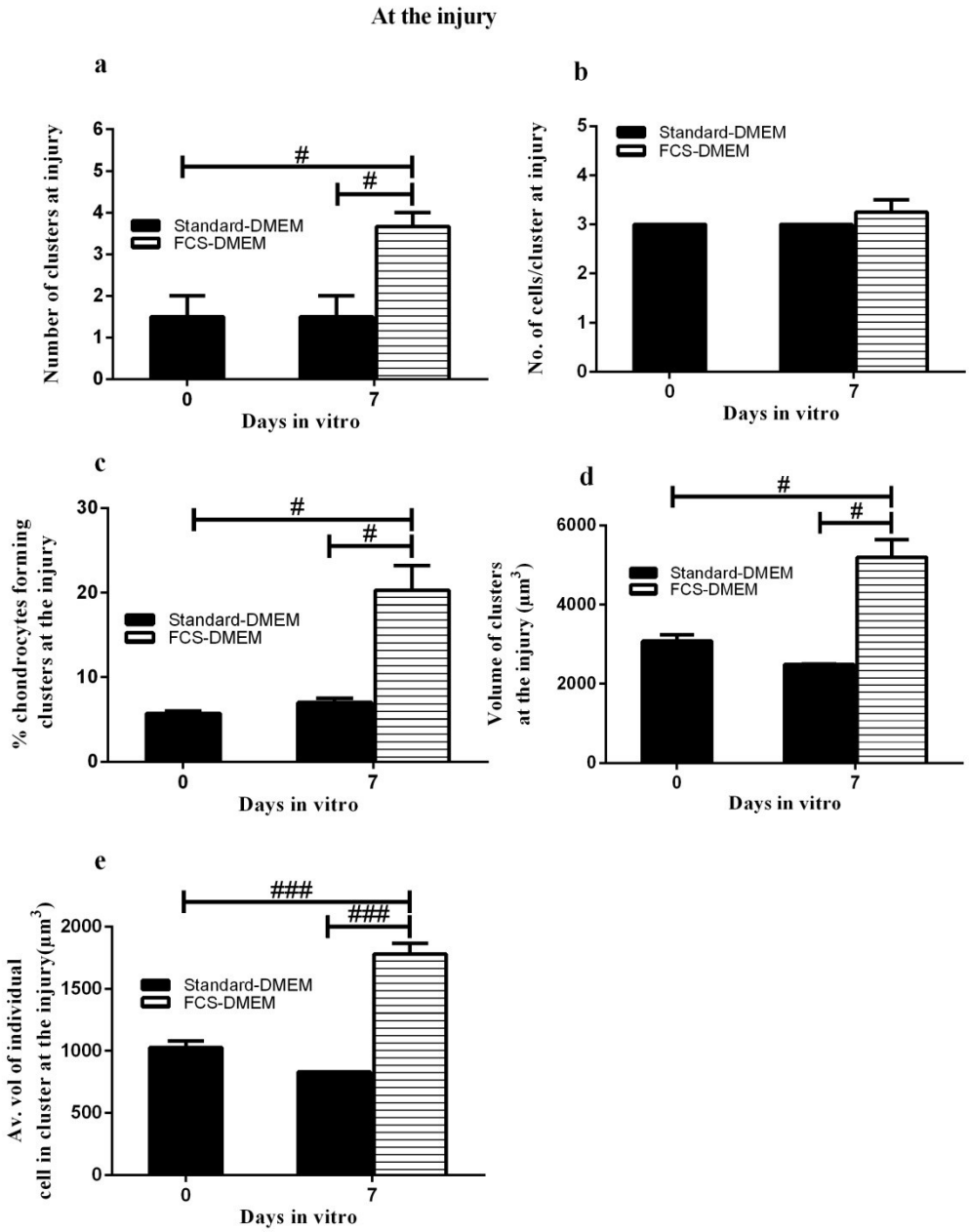

Figure 6.30A: Characteristics of clusters formed in injured explants without superficial layers at the injury cultured in various culture conditions.

Graphs show pooled data for (a) average number of clusters formed (b) average number of cells in a cluster (c) % of cells involved in forming clusters (d) average volume of clusters (μm^3) of chondrocytes formed and (e) average volume of individual cell in a cluster (μm^3) at the injury. Data were from [$N(n)$=6(12)]. # indicated a significant difference between different culture conditions and at two time points according to one-way ANOVA followed by Tukey's multiple comparison post-hoc test. The single, double and triple symbols showed the level of significance for P<0.05, 0.01 and 0.001 respectively.

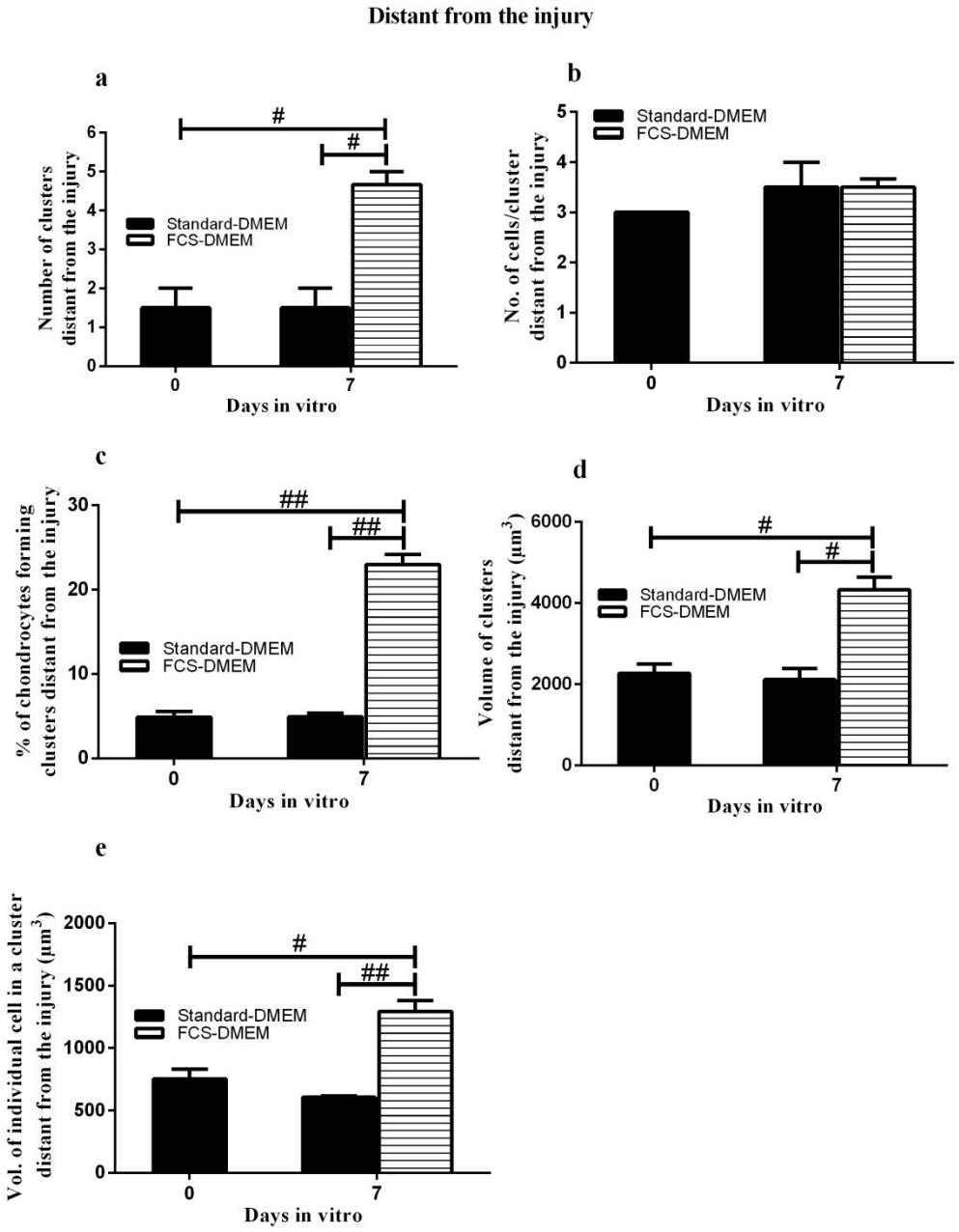

Figure 6.30B: Characteristics of clusters formed in injured explants without superficial layers distant from the injury cultured in various culture conditions. Graphs show pooled data for (a) average number of clusters formed (b) average number of cells in a cluster (c) % of cells involved in forming clusters (d) average volume of clusters (μm^3) of chondrocytes formed and (e) average volume of individual cell in a cluster (μm^3) distant from the injury. Data were from [$N(n)$=6(12)]. # indicated a significant difference between different culture conditions and at two time points according to one-way ANOVA followed by Tukey's multiple comparison post-hoc test. The single, double and triple symbols showed the level of significance for P<0.05, 0.01 and 0.001 respectively.

6.5.5.2.2 Development of abnormal morphology of deep layer chondrocytes at and distant from the injury by day 14

The morphology of chondrocytes remained unaffected in the injured explants (without superficial layers) cultured in the presence of standard-DMEM and cells were relatively normal in morphology characterised by spheroidal shape (Fig. 6.31a,c). However, presence of FCS in the culture medium markedly affected chondrocyte morphology by day 14. The morphological changes observed were associated with cell enlargement, flattening, lengthening and production of cytoplasmic processes from the cell bodies. Therefore abnormal chondrocytes were not restricted to the upper layers of the injured explants but the abnormal cells were also present in the deeper layers of cartilage (Fig. 6.31b,d).

Quantitative data regarding various morphological properties of chondrocytes at and distant from the injury was obtained by the use of 3D image analysis software and compared for days 0 and 14 of culture in the presence of standard-DMEM and FCS-DMEM.

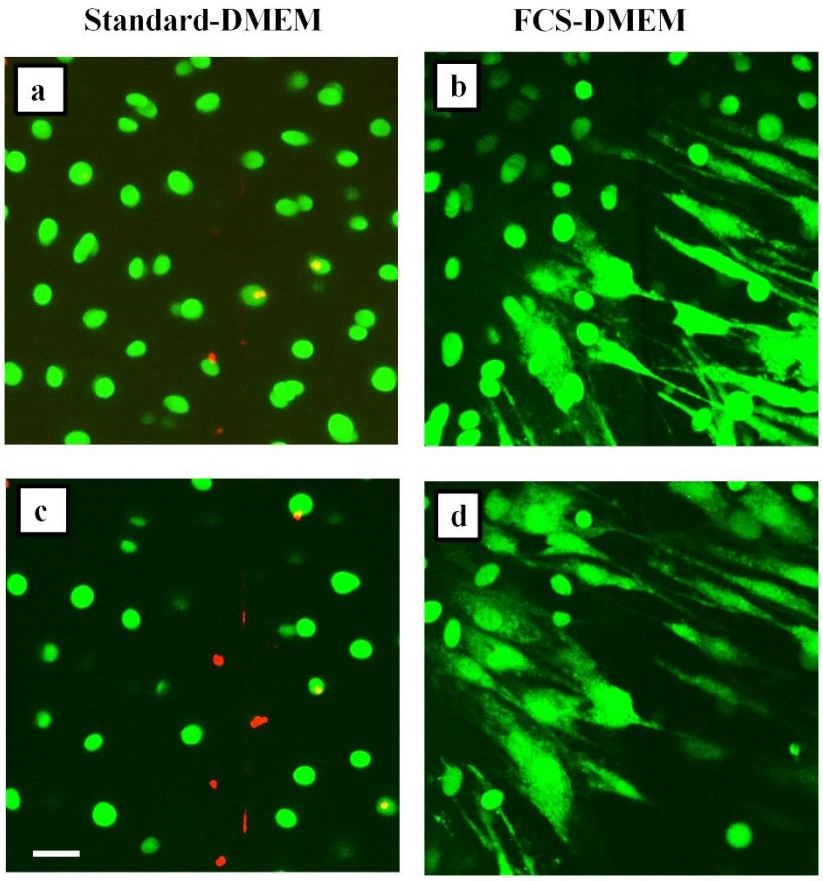

Figure 6.31: Heterogeneity of chondrocyte morphology by day 14 in the injured explants (without superficial layers) cultured in various culture conditions.
Axial CLSM reconstructions of high power magnification images of CMFDA and PI labelled chondrocytes (live and dead cells respectively) at the injury by day 14 (a,b) superficial 30µm (c,d) a further deep 20µm in the cartilage cultured in standard-DMEM and FCS-DMEM respectively. Scale bar for all panels=25µm.

At day 14, the percentage of abnormal chondrocytes with processes at and distant from the injury was significantly higher in the explants cultured in the presence of FCS-DMEM as compared to standard-DMEM (Fig. 6.32a,b; $P<0.0001$ for both conditions) and also in comparison to day 0 (Fig. 6.32a,b; $P<0.0001$ for both conditions) where cells were relatively normal. However, there existed no difference

(P>0.05) between the percentages of abnormal chondrocytes cultured in the presence of FCS-DMEM at and distant from the injury by day 14.

The volume of these abnormal chondrocytes increased overall approximately x2 at and distant from the injury in the presence of FCS-DMEM as compared to the volume of chondrocytes in standard-DMEM (Fig. 6.32c,d; P<0.0001 for both conditions) and also in comparison to day 0 (P<0.001 for both conditions). Additionally, there was no difference between the volume of chondrocytes at and distant from the injury in the presence of FCS-DMEM by day 14 (Fig. 6.32c,d; P>0.05).

The length of cell bodies increased approximately x5 at and distant from the injury by day 14 in the explants cultured with FCS-DMEM as compared to standard-DMEM (Fig. 6.32e,f; P<0.0001 for both conditions) and also in comparison to day 0 (P<0.001 for both conditions). Moreover, there was no difference between the average length of cell bodies of these abnormal chondrocytes at and distant from the injury in the presence of FCS-DMEM by day 14 (Fig. 6.32e,f; P>0.05).

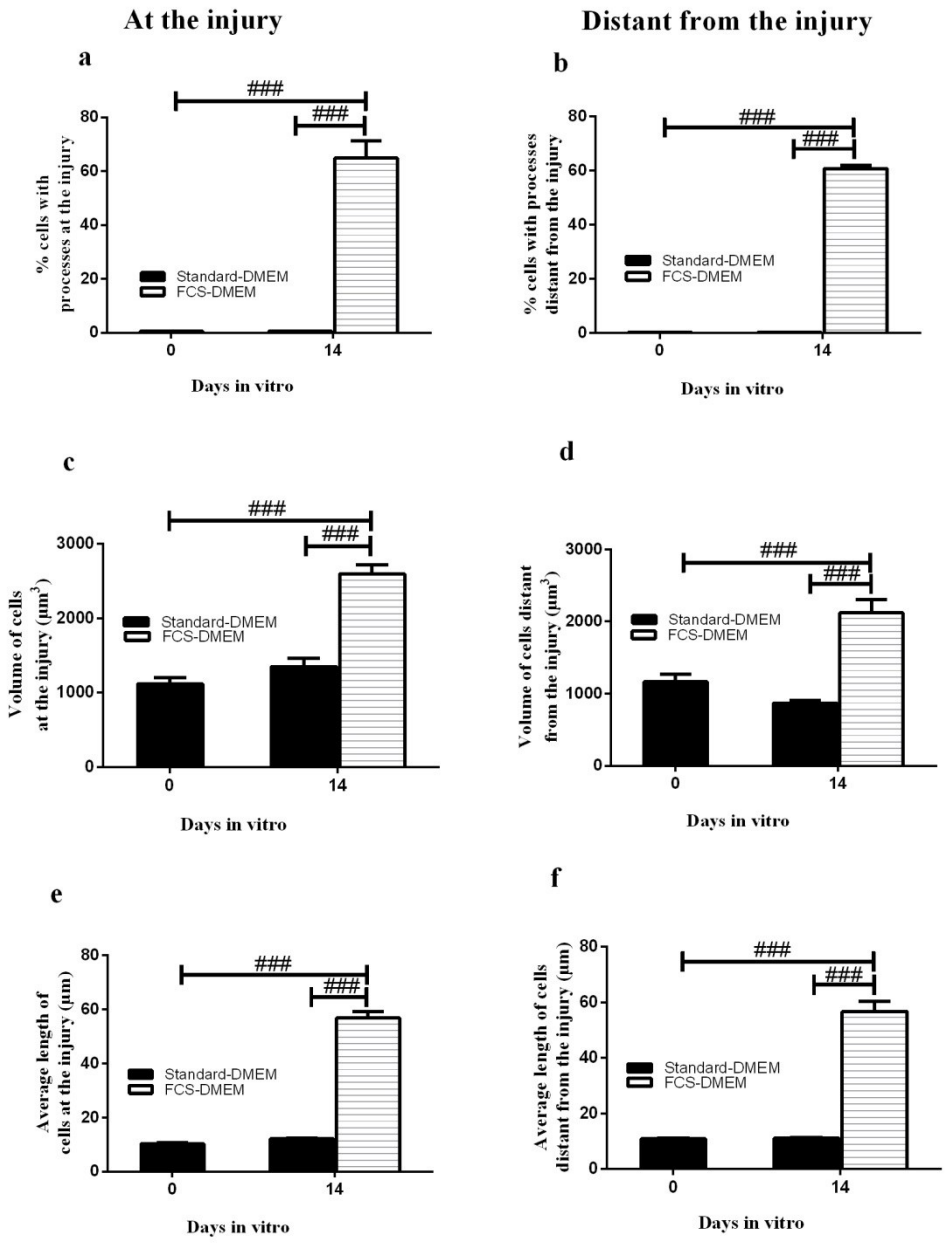

Figure 6.32: Heterogeneous morphology of chondrocytes at and distant from the injury cultured in various culture media.

Graphs show pooled data regarding the (a,b) percentage of abnormal chondrocytes, (c,d) average volume of chondrocytes (µm^3) and (e,f) average length of cell bodies of chondrocytes (µm), at and distant from the injury respectively in the presence of standard-DMEM and FCS-DMEM at day 0 and 14 of culture. Data were from [*N(n)*=6(17)]. # indicated a significant difference between different culture conditions and at two time points according to one-way ANOVA followed by Tukey's multiple comparison post-hoc test. The single, double and triple symbols showed the level of significance for *P*<0.05, 0.01 and 0.001 respectively.

To summarise the results of this section, chondrocytes displayed marked heterogeneity in terms of morphological characteristics in the cartilage explants (without superficial layers) cultured in the presence of FCS-DMEM as compared to standard-DMEM where the morphology remained unaffected. Additionally, in the presence of FCS the characteristics and extent of these morphological changes was similar at and distant from the injury.

In this study, in the injured osteochondral explants chondrocytes at the injury in response to factors present in FCS/SF displayed morphological changes restricted to the superficial layers of cartilage. However, in the injured explants without superficial layers chondrocytes at and distant from the injury displayed morphological changes in the presence of serum-rich medium. These results suggested that the triggering factor for these shape changes could possibly be the morphogenic factors present in the serum and more the accessibility of these factors more marked the shape changes will be.

6.6 DISCUSSION

This study aimed to develop and utilise an *in vitro* model of injured bovine articular cartilage to study the response of chondrocytes to sharp injury in the presence of varying culture media. The results strongly supported the primary hypothesis of the study that chondrocytes in the superficial layers at the injury displayed marked shape changes in response to the factors present in SF and FCS as compared to standard-DMEM. In the present work the results also supported the secondary hypothesis that the chondrocytes throughout the cartilage were vulnerable to shape changes under the effect of factors present in SF and FCS. Additionally, the results also supported

the tertiary hypothesis that chondrocytes at the injury produced morphological changes in the presence of SF and FCS even in the absence of subchondral bone.

The concerns with the use of this model were (a) production of a standardized injury required practice and several attempts (b) it did not resemble the *in vivo* mechanical and biochemical environment and (c) the explants when removed from the bone underwent a generalised swelling of the cartilage. The advantages of utilising this model have been explained in detail (section 6.2) which clearly suggested it to be a reproducible and a highly controlled model to study chondrocyte response to injury.

In this study the changes to *in situ* chondrocyte viability and morphology near scalpel induced mechanical injury in full depth osteochondral explants in response to varied culture media over a period of 14 days by utilising CLSM both in the axial and coronal planes have been investigated. In addition to this, we also studied similar parameters in cartilage explants without subchondral bone and without superficial zone. The results showed that width of the injury decreased significantly in the explants cultured in the presence of SF/FCS-DMEM and increased significantly with standard-DMEM. In the presence of SF and FCS there was a significant loss of PI-labelled chondrocytes near injury as compared to standard-DMEM. At the site of injury, volume of chondrocytes significantly increased, formed large sized clusters by day 7 and exhibited marked heterogeneity in morphology by day 14 in the explants cultured with SF/FCS as compared to standard-DMEM. Moreover, these changes in chondrocyte viability and morphology were found to be significantly obvious at the site of injury and only in the superficial zone, as compared to the control uninjured cartilage distant from the injury, in the injured explants with and without subchondral bone. In contrast to this, in the injured explants without

superficial zone these changes to viability and morphology of chondrocytes showed no difference between at and distant from the injury and were not restricted to the superficial layers. These results will now be discussed in detail.

There were marked changes at the injury in the presence of different types of culture media. Initially at the beginning of the experiments width of the injury created was same in all the explants (Fig. 6.5). The width of injury increased significantly in the presence of standard-DMEM as compared to SF and FCS (Figs. 6.5 & 6.16) and could be attributed to collagen damage due to injury leading to invariable increase in water content and tissue swelling (Maroudas, 1976) and loss of GAGs (Torzilli and Grigiene, 1998). There exists a paradox that although the tissue is swelling but there is loss of GAGs. In contrast, the width of injury decreased in explants cultured in the presence of SF-DMEM and FCS-DMEM. The underlying mechanism for this decrease in width of injury is not known however, a simple explanation could possibly be the cytoplasmic extensions protruded by chondrocytes at the injured site under the effect of serum led to the reduction in the width of injury. Additionally, it is possible that chondrocytes get metabolically stimulated by the factors present in SF and FCS and the new matrix formed at the injury led to the decrease in width of injury in these culture conditions.

Chondrocyte death following tissue trauma leading to reduction in the cellularity and malfunctioning of chondrocytes has been suggested to predispose the cartilage to the development of PTOA (Simon et al., 1976, Blanco et al., 1998). Cell death is a common feature of mechanical trauma (Tew et al., 2000, Bush et al., 2005) here we have used low power (x10 dry) images of CLSM with CMFDA/PI labelling for the quantification of living/dead chondrocytes respectively (Amin et al., 2008a) and

PCD (Fig. 6.6a-j, 6.17a-j & 6.26a-e). The use of fluorescent probes as indicators of viability of chondrocytes serves as a valuable tool in the cartilage research. In this work PI-labelled chondrocytes were lost significantly in the explants cultured in the presence of SF/FCS as compared to DMEM (Fig. 6.7a, 6.18a & 6.27a). Moreover, the % PI-labelled chondrocytes were significantly higher at the site of injury as compared to those distant from the injury in the presence of SF-DMEM and FCS-DMEM in the explants with and without bone (Fig. 6.7b, 6.18b). However, in the injured explants without the superficial zone there existed no difference between the % of PI-labelled chondrocytes at and distant from the injury (Fig. 6.27b) possibly because the explants were additionally injured while dissecting out the superficial layers of cartilage. Although use of PI labelling for assessing amount of cell death is a widely used method (Bush and Hall, 2001a, Chen et al., 2003) it has recently been reported that it might be misleading especially with the use of FCS in the tissue cultures (Zhou et al., 2011). Data were presented suggesting that most likely DNase I (Gaipl et al., 2006) and heat stable nucleases (von Kockritz-Blickwede et al., 2009) present in serum degraded the DNA of dead cells and thus PI, the DNA binding dye could not detect dead cells accurately. However, they compared the effects of serum and serum-free media but not considered the effect of SF on the PI-labelling of dead chondrocytes despite of the fact that SF is also used in tissue cultures (Lee et al., 1997) and it more closely approximates the *in vivo* environment. The results of present experiments augmented these observations suggesting that SF seems to have the same effect but less potent than FCS which possibly prevented labelling of dead chondrocytes. Moreover, the loss of PI-labelled chondrocytes was reduced in the presence of SF as compared to FCS, indicating the possibility that DNA degrading

enzyme(s) were present at higher concentrations in FCS as compared to SF, although they were both diluted to the same extent (10%) in the culture media. The differences in the cartilage ECM metabolism by the use of FCS and SF supplemented culture media had already been established (Martin et al., 2002) indicating that FCS was more potent than SF.

At day 0, in fresh cartilage the volume of DZ chondrocytes was higher than the volume of chondrocytes in the SZ (section 6.5.5.2.1), these observations are in agreement with already reported volume of chondrocytes in different zones of bovine cartilage (Bush and Hall, 2001a). Chondrocyte volume in injured explants with and without subchondral bone near injury increased significantly in the presence of SF and FCS as compared to standard-DMEM and those distant from the injury. Initial volumes of chondrocytes at the beginning of culture were 711±25μm^3 and 888±33μm^3 respectively which were found to be within the range of the volume of superficial zone chondrocytes (252 to 836 μm^3) in intact bovine articular cartilage (Bush and Hall, 2001a). There was a significant increase in the volume of chondrocytes near injury in the presence of SF and FCS (55% for both) as compared to the volume of cells in standard-DMEM (Figs. 6.9 & 6.20). These findings may be similar to the increased chondrocyte volume changes observed in degenerative osteoarthritic cartilage where enhanced access of growth factors due to weakened matrix are thought to stimulate hypertrophic changes in chondrocytes (Dreier, 2010, van der Krann and van den Berg, 2012, Turunen et al., 2013). However, in the injured cartilage explants without superficial zone the volume of chondrocytes at the beginning of culture was 1117.8±82.9μm^3 which was within the volume range of mid and deep zone (266 to 1149 μm^3 and 372 to 1377 μm^3 respectively) intact bovine

cartilage (Bush and Hall, 2001a). Additionally, the volume of these chondrocytes increased but not significantly following culture in FCS-DMEM which is also in agreement with the previously reported findings (Bush and Hall, 2001a). Therefore possibly serum factors caused volume increase in chondrocytes at the injury.

Chondrocyte cluster formation was another key morphological feature observed in the experimental model and is also a hallmark of OA (Pfander et al., 2001). In fresh healthy cartilage, chondrocytes typically occur in pairs (Sasazaki et al., 2008). Therefore, in this study 3 or more cells together were considered as a cluster and it was also noticed that in healthy control cartilage rarely chondrocytes were present as a cluster (with no more than 3 cells). In a previous study the clusters have been defined to contain 2-6 cells in bovine OA cartilage model (McGlashan et al., 2008). In the presence of standard-DMEM, chondrocytes formed few clusters at the injured site. However, under the effect of SF-DMEM and FCS-DMEM increased number and size of chondrocyte clusters were formed at the injury (Figs. 6.10A, 6.21 & 6.30A), suggesting the presence of growth factors in SF and FCS (Martin et al., 2002, Khan et al., 2010). Moreover, the morphological changes observed were almost similar in the presence of SF/FCS but faster in FCS due to the fact that FCS would appear to be a more potent chondrocyte stimulator than SF (Figs. 6.10, 6.12, 6.21, 6.24 & 6.30) as reported already (Martin et al., 2002). Chondrocytes distant from the injury also exhibited some cluster formation under the effect of SF and FCS. The factors present in SF and FCS influenced chondrocytes distant from the injury but the effect was less marked possibly because the matrix distant from the injury was intact thereby hindering diffusion of these factors. The average total number of chondrocytes in the specified ROI did not change significantly during the

course of culture in various culture conditions (section 6.5.2.3.2.). This suggested the possibility that the chondrocytes can move toward one another within the matrix and form clusters. This phenomenon was suggested in a previous study (Kouri et al., 1996b) carried out on human OA and non-OA cartilage. Findings in this previous study discovered the presence of clusters in fibrillated areas but the total number of cells in the fibrillated and non-fibrillated areas of cartilage was not different. Therefore, the phenomenon that chondrocytes actually migrate and form clusters can be considered.

The 'abnormal' chondrocyte morphology observed in the explants cultured in the presence of SF and FCS but not present in standard-DMEM (Figs. 6.12, 6.13, 6.24 & 6.32) might indicate a potential role of growth factors in cartilage injuries. The role of specific growth factors and combinations of growth factors in cartilage regeneration has been extensively reviewed (Fortier et al., 2011). There were significant morphological changes which included cellular enlargement, elongation of the cell body and formation of cytoplasmic processes (Figs. 6.12a-f, 6.14a-j, 6.22a-e & 6.28a-e). These abnormal chondrocytes were present in the superficial layers of cartilage near injury (Figs. 6.11 & 6.23). However, the cells in the deeper layers were spheroidal and relatively 'normal' in the injured explants with and without subchondral bone. These findings might be taken to indicate enhanced penetration and activity of factors from SF and FCS on these cells. However, in the injured explants (coronal view) and the ones without superficial zone, these abnormal chondrocytes were not restricted to a specific zone (Figs. 6.13 & 6.31 respectively) which suggested that greater the access of these growth factors the more the shape changes. These results thus suggested that chondrocytes irrespective

of the zone are capable of showing morphological changes and this is not the property of chondrocytes in the superficial layers alone rather it is due to the extent of penetration of the 'factors' into the matrix.

There are some interesting parallels of this heterogeneous population of cells with the chondrogenic progenitor cells in the superficial layers of cartilage (Dowthwaite et al., 2004). It has been reported in a study that in an adult human articular cartilage chondrogenic progenitor cells constitute 7.5% of the total cell population (Alsalameh et al., 2004). Additionally these progenitor cells are localised mostly to the superficial layers of cartilage (Alsalameh et al., 2004, Dowthwaite et al., 2004). It is unlikely that the morphologically heterogeneous population of chondrocytes in this work are progenitor cells because of two reasons. **Firstly,** the percentage of progenitor cells in adult articular cartilage is far less than the percentage of morphologically heterogeneous chondrocytes seen in the study presented here. **Secondly,** progenitor cells are mostly present in the superficial layers of cartilage whereas, in this work the morphologically heterogeneous chondrocytes could be observed irrespective of the cartilage zone. In a recent study it has also been proposed that chondrogenic progenitor cells migrate to the site of injury in response to the chemotactic factors to repopulate the injured site (Seol et al., 2012). In this study the triggering element for shape changes is less likely to be the chemotactic factors because of three possible reasons: **(a)** in this study the chemotactic factors produced from injured explants (from dead cells) were thought to be minimal as most of the PI-labelled chondrocytes were lost under the effect of SF and FCS **(b)** the amount of cell death in this injured cartilage model was minimal due to sharp injury whereas in the previous work blunt trauma was applied producing greater cell death

(Redman et al., 2004) and therefore, possibly the quantity of chemotactic factors produced in the present study was less compared to the previous work **(c)** if chemotactic factors alone would have the ability to stimulate these cells then in our control explants cultured in standard-DMEM chondrocytes with abnormal morphologies would have been seen (Fig. 6.8). Therefore, it might be possible that either the growth factors alone excited these cells or the growth factors triggered the chemotactic factors to stimulate chondrocytes. As already mentioned the possibility of having chemotactic factors as stimulators for chondrocytes is minimal in the experiments detailed in this study therefore, morphogenic factors present in FCS/SF are the possible regulators of chondrocyte morphology.

In the present study, chondrocytes produced cytoplasmic processes at the injury in the presence of FCS/SF in the culture media and these processes were aligned along the edge of the injury (Fig. 6.8). These results are in agreement with a recent study where it was reported that in the presence of FCS the chondrocytes produced cytoplasmic processes and these tend to move and align along the edge of the defect produced in cartilage (Lyman et al., 2012). However, the present work builds upon the already reported observations regarding the response of chondrocytes to mechanical injury in the previous study in several ways. **Firstly,** the modes of injury in the present and previous study were different. In the previous study drill-bit was used and in the present study scalpel cut was produced to mechanically injure cartilage. The advantages of utilising sharp injury model as compared to other forms of trauma have already been discussed (section 6.2). **Secondly,** in the previous study the production of cytoplasmic processes in the presence of FCS has been reported but in the present study their existence in the presence of SF and absence in standard-

DMEM were novel findings. **Thirdly,** in the previous study the injured explants with subchondral bone were studied as injury model. However, in the present study chondrocytes in the injured cartilage explants without subchondral bone were also studied and displayed marked shape changes thus ruling out any possibility of interference of injured site with osteocytes or bone factors. Whether these cells are progenitor cells and they are migratory in nature has not been addressed in the present study. However, in author's opinion in response to injury chondrocytes residing in any zone of cartilage have the ability to change shape in the presence of serum morphogenic factors.

The existence of chondrocyte cytoplasmic processes in non-degenerate and degenerate human tibial plateau cartilage and the possible theories for their appearance have been described already (Bush and Hall, 2003). There are some parallels between these already reported abnormal chondrocytes in the previous study and the abnormal chondrocytes at injury observed in the present study. However, direct comparison is hard because in the study presented here bovine cartilage was used as the experimental material whereas this previously reported study was conducted on human cartilage. The common morphological feature observed between bovine chondrocytes in this work and human chondrocytes in previous study was the presence of single or multiple cytoplasmic processes emanating from cell bodies. However, the main difference existed was the shape of the cell body. In the bovine cartilage in this work majority of these abnormal chondrocytes had flattened and elongated cell bodies. In contrast in the previous study on human cartilage the cell bodies of these abnormal chondrocytes with processes were neither elongated nor flattened rather they had irregular shapes.

There was a possibility that some factors released from exposed bone parts and also bone cells released in culture medium could migrate at the site of injury. This seems unlikely because these possibilities have been ruled out fully as detailed in the results section on the injured cartilage explants without subchondral bone. In the absence of subchondral bone the response of chondrocytes to injury was similar to those with subchondral bone.

It had already been established that chemical composition of the culture medium greatly affected the properties of cartilage and chondrocytes in culture (Bian et al., 2008). FCS (McQuillan et al., 1986, van Susante et al., 2000) and SF (Nuver-Zwart et al., 1988, Lee et al., 1997) had been widely used in cartilage research to study mechanical and biochemical properties of chondrocytes with the aim to provide chondrocytes all the nutrients needed for survival whereas, in several other studies serum-free media had been utilized (Glaser and Conrad, 1984). The use of serum/SF-rich and serum/SF-free media was based upon requirements for tissue culture of these studies and the basic focus had been to demonstrate the metabolism of chondrocytes in terms of production of ECM assuming that morphology of chondrocytes remained normal. However, the results of our study strongly suggested that the morphological characteristics of chondrocytes were strikingly altered in the serum and SF supplemented culture media. It is therefore possible that these changes in morphology reported here would reflect altered phenotype of these chondrocytes, resulting in altered ECM production (Sandell and Aigner, 2001, Tesche and Miosge, 2005). It has been reported previously that presence of FCS in the culture medium also potentially directly affects the matrix by reduction in GAG content and loss of mechanical properties of the cartilage (Bian et al., 2008). Based upon our results we

suggested that great care should be taken with the use of FCS and SF in long-term cartilage and chondrocyte culture experiments. There may also be a marked difference between the actions of FCS and SF present in the culture medium as shown in the data suggesting FCS to be more potent in its actions as compared to SF (Figs. 6.10 & 6.12) therefore; chondrocyte phenotype when cultured in the presence of FCS/SF should be monitored.

The morphological alterations observed in chondrocytes near the injured site in the presence of SF and FCS resembled some of the key changes in terms of hypertrophy-like changes (Dreier, 2010), cluster formation (Kouri et al., 1998) and abnormal morphology with cytoplasmic processes (Bush and Hall, 2003) seen in early OA. It is tempting to speculate that there are similarities between the changes occurring in OA and those observed in the injury model with SF/FCS. By identifying the factors present in SF and FCS that stimulated chondrocytes leading to morphological changes in injured/weakened cartilage, treatment strategies may be developed or modified in order to prevent these changes with the aim to avoid cartilage degeneration and ultimately progression of OA.

CHAPTER 7: RESULTS

EVALUATION OF EXTRACELLULAR MATRIX PRODUCED BY CHONDROCYTES IN RESPONSE TO INJURY CULTURED UNDER VARIOUS CONDITIONS

7.1 CHAPTER SUMMARY

This chapter aimed to assess the extracellular matrix (ECM) produced by chondrocytes at the injury in the presence of various culture media. The histological and immunohistochemical (IHC) examination of chondrocyte morphology and ECM produced by them in response to injury was performed with various dyes. The quantification of staining intensity was performed with image J analysis software. The haematoxylin and eosin (H&E) staining showed presence of chondrocyte clusters within superficial layers in the explants cultured in the presence of SF-DMEM and FCS-DMEM as compared to standard-DMEM. By day 14, percentage of Alcian blue stained area around chondrocytes was significantly less in the explants cultured with SF-DMEM and FCS-DMEM as compared to standard-DMEM (P<0.001). Masson's trichrome staining technique stained collagen blue and revealed no difference in the percentage stained area after 14 days of culture in either of the culture conditions. IHC staining of the coronal sections of these injured explants showed no difference in staining pattern of collagen types I & II in the explants cultured in various culture conditions. Therefore, chondrocytes at the injury in the presence of FCS produced an altered matrix as compared to standard-DMEM.

7.2 INTRODUCTION

Several studies performed in the past have shown that in degenerate/damaged cartilage, chondrocytes frequently show decreased viability, increased volume, cluster formation and phenotypic changes (Anderson et al., 2011, Kramer et al., 2011). These changes may lead to abnormal matrix production, poor repair and thus enhanced predisposition to secondary/post traumatic osteoarthritis (PTOA). In this

work as detailed in chapter 6, a mechanical injury cartilage model has been developed in a defined way to determine the morphological response of chondrocytes in the presence and absence of synovial fluid (SF) and foetal calf serum (FCS).

Chondrocytes regulate the ECM architecture of articular cartilage and is dependent upon the presence of large quantities of PGs entangled within a frame-work of predominantly type II collagen fibres (McDevitt, 1973). In healthy cartilage there normally exists a balance between the anabolic and catabolic activities of chondrocytes thereby steady state equilibrium exists in their metabolic activities responsible for maintenance of normal homeostasis of the cartilage matrix (Pearle et al., 2005).

Mechanical partial thickness injuries lead to chondrocyte death (Tew et al., 2000) and damage to the cartilage matrix (Milentijevic et al., 2005). As a result of mechanical trauma the cartilage healing process is ineffective and this may lead to the development of PTOA (Buckwalter and Brown, 2004). Apart from chondrocyte death another main feature of PTOA is cartilage degeneration due to an imbalance in the metabolic activities of chondrocytes (Guilak et al., 2004). This imbalance occurs when the catabolic activities override anabolic activities (Goldring and Goldring, 2004). The inflammatory cytokines such as IL-1, IL-6 and TNFα are most likely contributors to the enhanced catabolic activities in the pathophysiology of cartilage degeneration and their levels increase after joint injury (Melchiorri et al., 1998, Lee et al., 2009).

During degeneration of cartilage, chondrocytes change their phenotype (Tesche and Miosge, 2005). However, strong interactions between chondrocyte phenotype and

functions impact cartilage in such a way that it is difficult to know where and when pathological changes begin. The cell phenotype comprises of its morphology, biochemistry and behaviour. One aspect of chondrocyte differentiated phenotype is spheroidal/ellipsoidal shape and has been associated with the expression of large aggregating PGs (aggrecan) and collagen type II in healthy cartilage. However, chondrocyte phenotype is unstable (Darling and Athanasiou, 2005) and during cartilage degeneration, chondrocytes change their phenotype and are de-differentiated (Sandell and Aigner, 2001). The de-differentiated phenotype has been associated with the expression of type I collagen (Glowacki et al., 1983) and altered pattern of production of PGs with predominant production of small molecular weight PGs (Tesche and Miosge, 2005).

In a recent study it has been reported that in response to trauma to the cartilage several changes occur in chondrocyte morphology such as cell flattening and extension of filopodia towards the injured site (Lyman et al., 2012). In another recent study the response of chondrocytes to injury has been studied which stated the emergence and repopulation of injured site by chondrogenic progenitor cells via the chemokines synthesised by dead chondrocytes (Seol et al., 2012). In the present thesis in the preliminary work by using fluorescent-mode CLSM marked chondrocyte shape changes were observed at the injury in the presence of SF/FCS in the culture media (Chapter 6). There exists a close relationship between chondrocyte metabolic activities and cell morphology (Glowacki et al., 1983). The key question addressed in this study is whether morphologically abnormal chondrocytes at the injury in the presence of SF/FCS produced altered matrix in comparison to relatively normal chondrocytes in standard-DMEM. This work was therefore performed to

study the effect of chondrocyte shape on the matrix produced. Although with the histological techniques it is not possible to study changes to chondrocyte morphology but the aim of applying these techniques on the injured cartilage samples was (a) to develop standard histological methods for investigating ECM produced by chondrocytes at the injury and (b) to evaluate the expression of matrix produced by them.

7.3 HYPOTHESIS

The abnormal chondrocytes at the injury in the presence of FCS-DMEM and SF-DMEM produced altered ECM in comparison to normal chondrocytes in standard-DMEM.

7.4 MATERIALS AND METHODS

7.4.1 Tissue processing for histology and IHC of injured bovine cartilage explants

7.4.1.1 *Fixation and decalcification*

The injured bovine osteochondral explants at separate time points (day 0 and 14) cultured in various culture media were fixed in 4% PFA (v/v in water) overnight at 4°C and then washed in PBS. The explants were viewed under a dissection microscope and with scalpel No. 24 cut through the injured site along with the underlying bone in order to obtain the coronal sections of the cartilage at the site of injury. The samples were decalcified in 10% EDTA; 20 g of EDTA was dissolved in 80 g of distilled water (D/W) and pH adjusted by using NaOH to pH 8.0; diluted to

prepare 10% EDTA and stored at room temperature) over a rolling plate for two weeks, at room temperature with changing the solution every three days.

7.4.1.2 *Paraffin embedding*

After fixation and decalcification, the sections were washed in PBS, fitted in the embedding cassettes and processed in the Sakura Tissue-Tek VIP tissue processor (Sakura Finetek Ltd, UK) following a standard protocol as given below:

1. 70% alcohol, 1 hour.
2. 90% alcohol, 1 hour.
3. 95% alcohol, 1 hour.
4. Industrial methylated spirit (IMS) 99, 1 hour.
5. IMS 99, 1 hour.
6. IMS 99, 1 and half hour.
7. 100% alcohol, 2 hours.
8. Xylene, 1 hour.
9. Xylene, 2 hours.
10. Xylene, 2 hours.
11. Paraffin wax, 4 hours.

Finally, the samples were placed on a cold plate after embedding in paraffin blocks to set for at least 2 hours. The explants were embedded with the coronal side facing down so that after cutting the sections would contain the whole thickness of cartilage along with the underlying bone. The paraffin embedded cartilage samples were stored in boxes, labelled and stored at room temperature until used.

7.4.1.3 *Sample sectioning*

The paraffin embedded coronal sections of injured cartilage were placed on ice before cutting. The samples were then sectioned (5µm thick) serially on wax microtome Leica RM2245 (Leica Microsystems Ltd., UK). The sections were then floated in a water bath at 40°C to straighten them out and picked up carefully onto Superfrost microscope slides. The slides were kept overnight in the oven set at 37°C to dry. After overnight drying, the slides were kept in boxes at room temperature until used.

7.4.2 Histological and histochemical stainings

7.4.2.1 *H&E staining of wax embedded sections*

H&E are extensively used dyes in histology to label the nuclei and cytoplasm of cells as purple and pink respectively to study the gross morphology and topographical arrangement of cells (Avwioro, 2011). However, with this technique it is impossible to study the fine details of chondrocyte morphology (cytoplasmic processes). The microscopic structure of the injured cartilage kept in various culture conditions was viewed by H&E staining performed according to the standard protocol (Avwioro, 2011). The sections were stained with H&E as previously described for frozen sections (section 5.4.3.1) with only differences in first and last steps. As a first step they were dewaxed in xylene for 25 min and then rehydrated gradually through descending grades of alcohols (absolute, 90% and 70% alcohols for 5 min each). As a last step they were dehydrated through ascending grades of alcohol (70%, 90%, 95%, absolute alcohol 1 & 2) for 5 min each and cleared in mounting xylene. The slides were then mounted and stored as previously described (section 5.4.3.1).

7.4.2.2 *Alcian blue staining of wax embedded sections*

Alcian blue staining was performed on the coronal sections of the injured bovine cartilage cultured under various culture conditions to stain the negatively charged GAGs present in the cartilage tissue. The sections were deparaffinised and rehydrated as previously described (section 7.4.2.1). The sections were incubated in 3% (v/v) acetic acid (3 ml of glacial acetic acid were added to 97 ml of D/W) for 3 min and then stained in Alcian blue solution 8GX; pH 2.5 (1 g of Alcian blue 8GX was dissolved in 100 ml of 3% acetic acid; mixed well and pH adjusted to 2.5 using acetic acid; filtered and stored at room temperature) for 45 min. The slides were washed in running tap water for 2 min, counterstained in Nuclear fast red solution (prepared as described in section 5.4.3.2) for 3 min and washed again in running tap water for 1 min. Finally, the slides were rinsed in D/W for 2 min, dehydrated in series of ascending alcohols and cleared in xylene. The slides were then mounted and stored as previously described (section 5.4.3.1).

7.4.2.3 *Masson's trichrome staining of wax embedded sections*

This technique stains nuclei black, cytoplasm/muscle red and collagen blue (Kiernan, 2008). The collagen present in the cartilaginous tissue was stained blue with Masson's trichrome staining (Figs. 7.7 and 7.8). As a first step the sections were deparaffinised and rehydrated as already described (section 7.4.2.1). The sections were then stained with the same protocol (section 5.4.3.3) regarding the staining of collagen around cultured chondrocytes in agarose gels with the exception of the first and last steps. Lastly, the slides were dehydrated in series of ascending alcohols,

cleared in xylene, cover slipped with DPX mounting medium, dried and stored as previously described.

7.4.2.4 *IHC for collagen type I and II*

The wax embedded cartilage sections were deparaffinised by incubating slides in xylene for 25 min. The sections were then rehydrated gradually through descending grades of alcohols (absolute, 90% and 70% alcohols for 5 min each). The sections were circled with DAKO pen (DakoCytomation, UK), post fixed in 4% PFA at room temperature for 5 min and washed thoroughly in PBS for 5 min on the rocking table. For antigen retrieval, sections were equilibrated for 10 min in 0.02% HCl pre-warmed at 37°C and then digested in 6 mg/ml of pepsin (Sigma-Aldrich, UK) in 0.02% HCl for 45 min at 37°C (Ward et al., 2006). After antigen retrieval, the slides were dipped first in PBS and then in water and air dried at room temperature. The sections were post fixed in 4% PFA for 10 min at room temperature and washed in PBS for 5 min on rocking table. In order to avoid non-specific staining with DAB substrate (Streefkerk, 1972), endogenous peroxidase activity was quenched by incubating the slides twice with 3% H_2O_2 (6ml H_2O_2 in 54ml of D/W) for 10 min each at room temperature. The slides were then washed in PBS on the rocking table (5 min each washing). The sections were blocked first in Avidin and then in Biotin blocking solution (DakoCytomation, UK) for 10 min each by incubating slides in humid chamber. The slides were washed in PBS for 5 min on rocking table. The sections were blocked in serum free protein blocking solution (DakoCytomation, UK) for 45 min at room temperature in the humid chamber. The sections were blotted to draw out all the extra fluid and incubated overnight with the primary

antibody (anti collagen type I or type II) diluted in the antibody diluent (DakoCytomation, UK) at 4°C in a humid chamber. The dilutions used were 1:200 for anti-collagen I mouse monoclonal antibody, species reactivity with rat, rabbit, cow, human, pig and deer (ab90395, Abcam, UK) and 1:50 for anti-collagen II mouse antibody, species reactivity with human, bovine, chick, rat, mouse, xenopus and ovine (CIICI, Developmental Studies Hybridoma Bank, Iowa). The sections were washed x3 in PBS (5 min each on the rocking table) and incubated for 30 min with EnVision®+Dual Link system-HRP (containing goat anti-mouse and anti-rabbit immunoglobulins conjugated to peroxidase-labelled polymer; DakoCytomation, UK) at room temperature and washed x3 in PBS (5 min each on the rocking table). The sections were then incubated with liquid DAB substrate chromogen system (DakoCytomation, UK) and staining checked under the microscope. Lastly, the slides were washed in PBS and mounted directly with Mowiol (Polysciences, Germany).

Pilot experiments were carried out (data not shown) to determine the optimum working dilutions (1:200 for type I & 1:50 for type II) for the primary antibodies used to detect collagen type I and II. In the negative control slides the sections were treated with PBS instead of primary antibodies.

Images of histological and IHC stained sections of bovine injured cartilage were captured using Leica DMRE 35578 upright microscope with mounted digital QImaging Retiga 2000R-monochrome cooled CCD camera.

7.4.2.5 *Analysis of images by using ImageJ analysis software*

The low power (x10) magnification images were analysed using ImageJ software and quantitative data were acquired and compared regarding stained area in the injured

explants cultured with various culture media. Data from Alcian blue, Masson's trichrome, collagen type I and II were acquired to determine matrix remodelling associated with response of cartilage to injury. In the preliminary experiments with CLSM, heterogeneity of chondrocyte morphology was observed at the injury in the superficial layers of explants cultured in presence of some of the culture media. Therefore, a ROI with the dimensions of x, y, z 542, 106 and 5µm respectively was selected (Fig. 7.1a) aiming at the analysis of matrix present around chondrocytes in the superficial layers of cartilage. Firstly, after applying the ROI the image was cropped and the area of the whole ROI was measured by the software (Fig. 7.1b). Secondly, colour threshold was adjusted manually and stained area around cells was measured by the software (Fig. 7.1c). Lastly, a percentage of stained area was determined with the formula 100 x (stained area around cells/total area of ROI applied) %. In order to standardise our technique of adjusting colour threshold firstly control images from day 0 of healthy uninjured cartilage were utilised to measure the intensity of threshold and then it was applied to all the images from experimental conditions with minor individual adjustments per image.

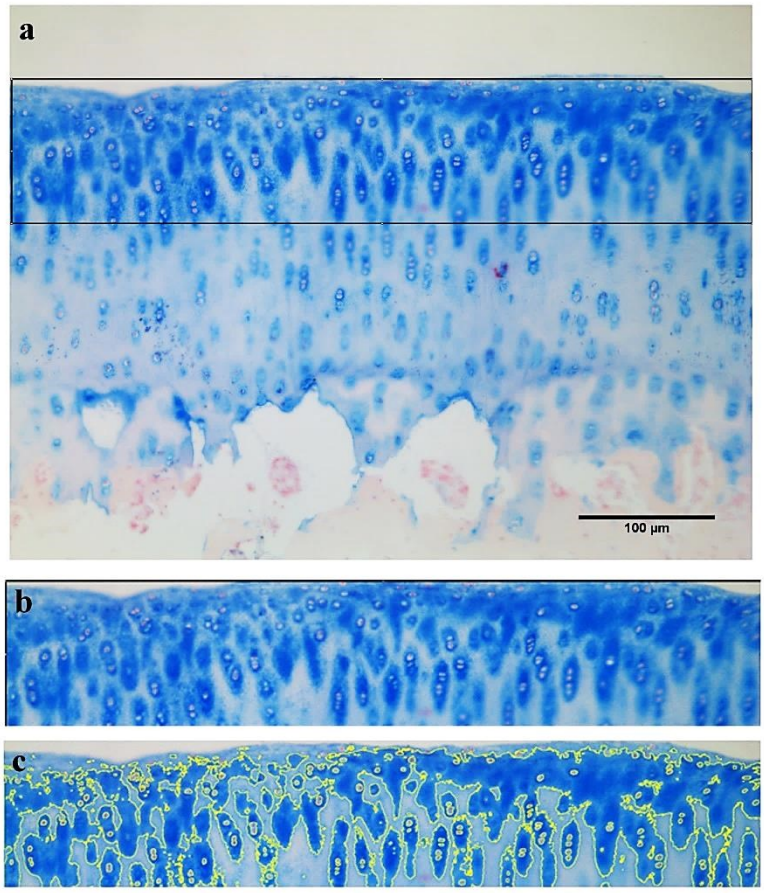

Figure 7.1: Determination of stained area of images by Image J analysis software.
Example of determination of Alcian blue stained area for the superficial layers of cells (a) application of specified ROI (b) cropped image within ROI and (c) comprises of image outlining the blue area determined after adjusting for colour threshold. Scale bar = 100µm.

7.5 RESULTS

7.5.1 Histological and IHC evaluation of ECM in the injured cartilage explants cultured under various conditions

In the preliminary set of experiments by using fluorescent-mode CLSM (chapter 6) the results showed marked heterogeneity to chondrocyte morphology in response to injury in the presence of FCS and SF as compared to standard-DMEM in the culture

media. In order to investigate whether chondrocytes at the site of injury with cytoplasmic processes produced altered ECM in comparison to normal chondrocytes, the histology and immunohistochemistry was performed and the results presented in the following sections. The techniques used for the histological preparation of the samples may introduce artefacts and have been discussed later (section 7.6).

The injured explants in various culture conditions were processed for histology and IHC (section 7.4.2) at day 0 and 14 of culture. The sections were stained with H&E, Alcian blue or Masson's trichrome for histological evaluation and the presence of type I and type II collagen was analysed by IHC. The stained coronal sections were imaged with both low (x10) and high (x20 oil immersion) power magnification objectives. Results regarding the histological and IHC evaluation of matrix components around chondrocytes in response to injury following culture under various conditions were given in the following sections.

7.5.1.1 *H&E staining*

Low power images of coronal view of the injured cartilage site (section 7.4.1.1) stained with H&E cultured under various conditions at day 0 and 14 of culture (Fig. 7.2). At day 14, the staining intensity appeared to be less in the explants cultured in the presence of SF-DMEM as compared to FCS-DMEM and standard-DMEM (Figs. 7.2c & 7.3c). At high power magnification by day 14, chondrocyte clusters were observed at the injury in the superficial layers of cartilage in explants cultured in the presence of SF-DMEM and FCS-DMEM as compared to standard-DMEM and also in comparison to day 0 (Fig. 7.3). It was not possible to visualise the fine morphological details (cytoplasmic processes) with H&E staining technique even at

high power magnification (Fig. 7.3). Therefore, with H&E staining chondrocyte abnormalities in cell shape could not be studied but the clusters were visible.

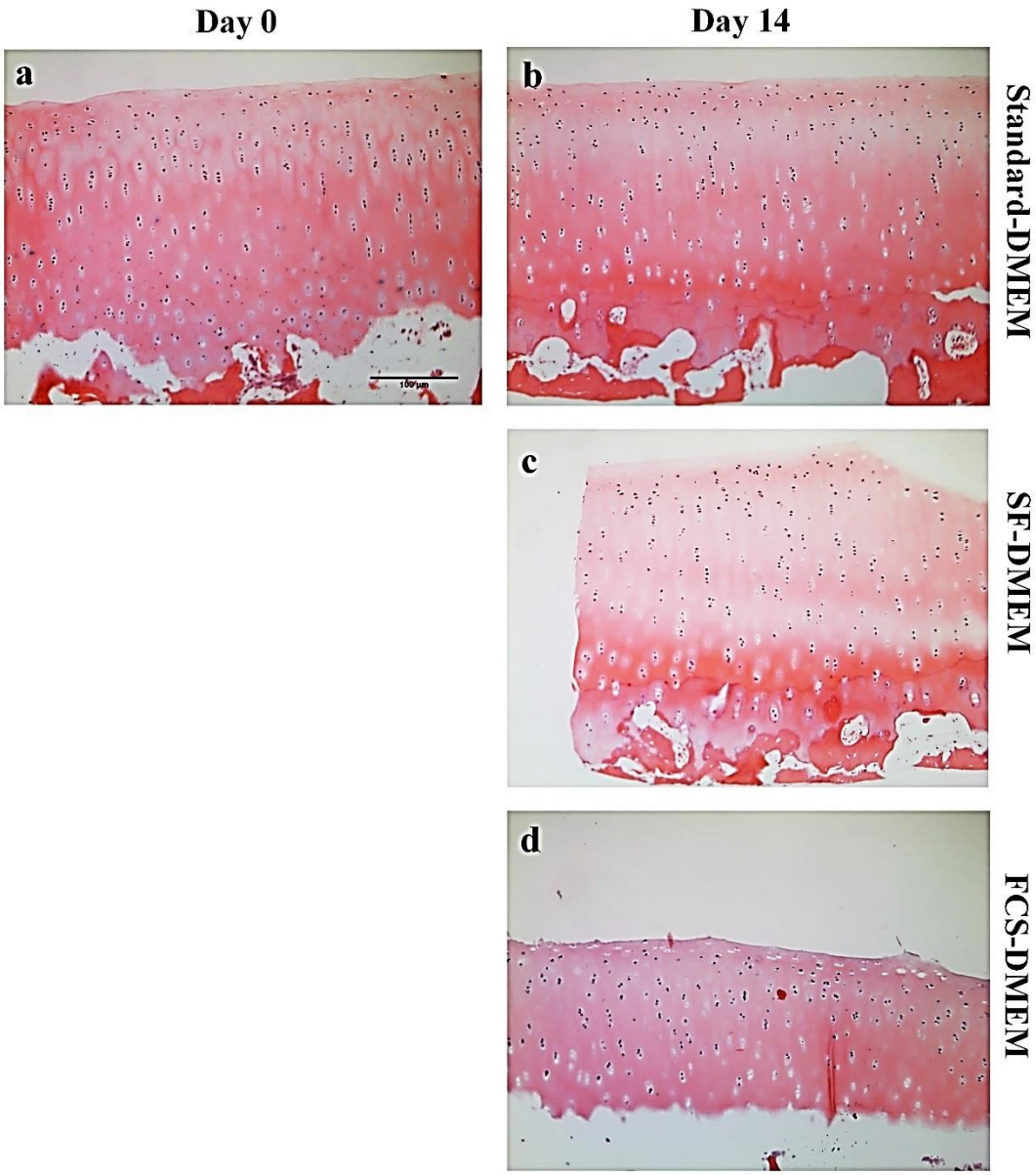

Figure 7.2: Typical photomicrographs of H&E stained coronal sections at the injury at low power magnification.

The histological sections of injured cartilage stained with H&E and imaged (x10) at (a) day 0 and (b, c, d) day 14 following culture in standard-DMEM, SF-DMEM and FCS-DMEM respectively. The results obtained from at least three independent experiments. Photomicrograph (a) represents the H&E staining in uninjured cartilage. Scale bar = 100µm.

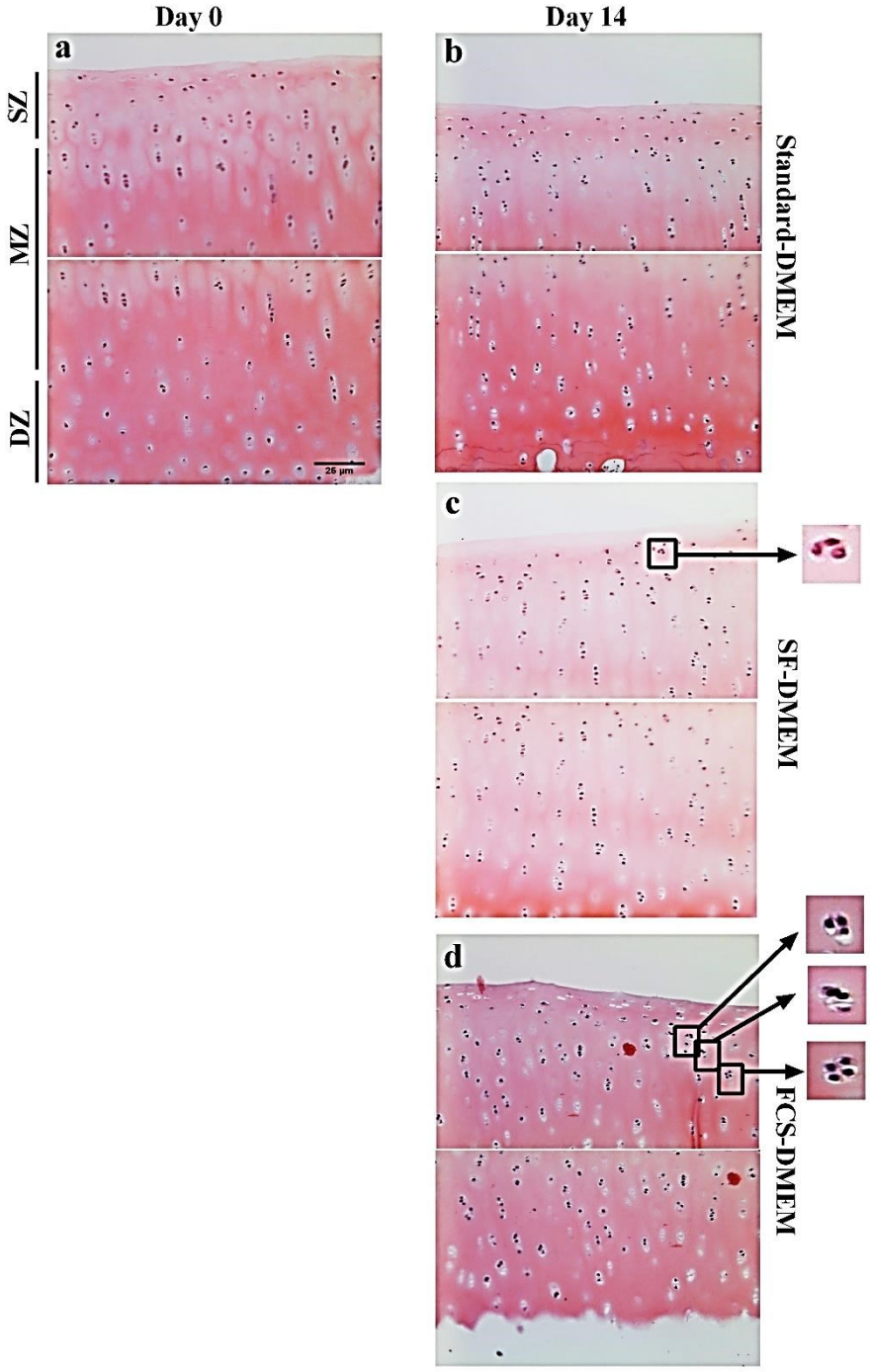

Figure 7.3: Typical photomicrographs of H&E stained coronal sections from site of injury at high power magnification.

The histological sections of injured cartilage stained with H&E and imaged (x20oil immersion) at (a) day 0 and (b, c, d) day 14 following culture in standard-DMEM, SF-DMEM and FCS-DMEM respectively. The examples of chondrocyte clusters shown in twice as zoomed inset images. The results obtained from at least three independent experiments. Photomicrograph (a) represents the H&E staining in uninjured cartilage. Scale bar = 25µm.

7.5.1.2 *Alcian Blue staining*

The coronal sections at the injured site were stained with Alcian blue to detect the presence of GAGs (within specified ROI) by chondrocytes in response to injury following culture under various media. At day 14 of culture, Alcian blue staining appeared to be less in the explants cultured in the presence of SF-DMEM and FCS-DMEM as compared to standard-DMEM and also in comparison to day 0 (Figs. 7.4 & 7.5).

The percentage of Alcian blue stained area within the ROI (Fig. 7.1a) varied under the different culture conditions. There was no significant difference between the percentage of Alcian blue stained area at the injury in the explants cultured with standard-DMEM even after 14 days of culture (Fig. 7.6; $P>0.05$; one-way ANOVA). In contrast, by day 14 the percentage of Alcian blue stained area was significantly less in explants cultured in the presence of SF-DMEM (15±1.4%) and FCS-DMEM (21±3%) as compared to standard-DMEM (56±1%; $P<0.001$; ANOVA for both the conditions) and also in comparison to day 0 (59±2.5%; Fig. 7.6; $P<0.001$; ANOVA for both the conditions). Additionally, by day 14 no significant difference existed between the % of Alcian blue stained area in the explants cultured in the presence of SF-DMEM and FCS-DMEM (Fig. 7.6; $P>0.05$; one-way ANOVA).

To summarise the results of this section, in the presence of SF-DMEM and FCS-DMEM chondrocytes at the injury showed the presence of less GAGs as compared to standard-DMEM. These coronal sections have been obtained from the site of injury by cutting through the full-depth of the cartilage. The images were analysed by

applying a specified ROI already explained (section 7.4.2.5) to ensure that the ECM evaluation was performed around the chondrocytes at the injury.

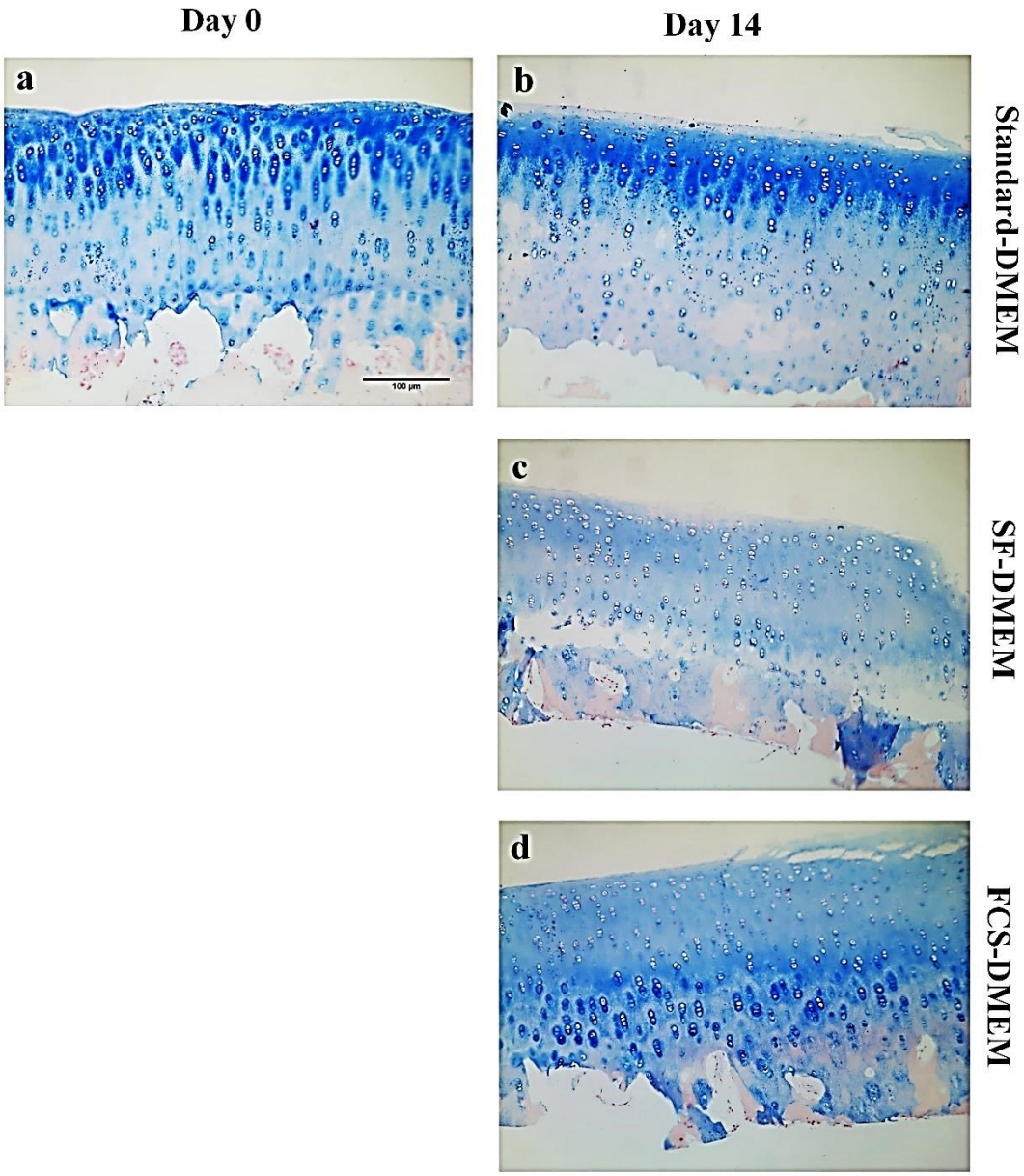

Figure 7.4: Typical photomicrographs of Alcian blue stained coronal sections from the site of injury at low power magnification.
The histological sections of injured cartilage stained with Alcian blue and imaged (x10) at (a) day 0 and (b, c, d) day 14 following culture in standard-DMEM, SF-DMEM and FCS-DMEM respectively. The results obtained from at least three independent experiments. Photomicrograph (a) represents the Alcian blue staining in uninjured cartilage. Scale bar = 100µm.

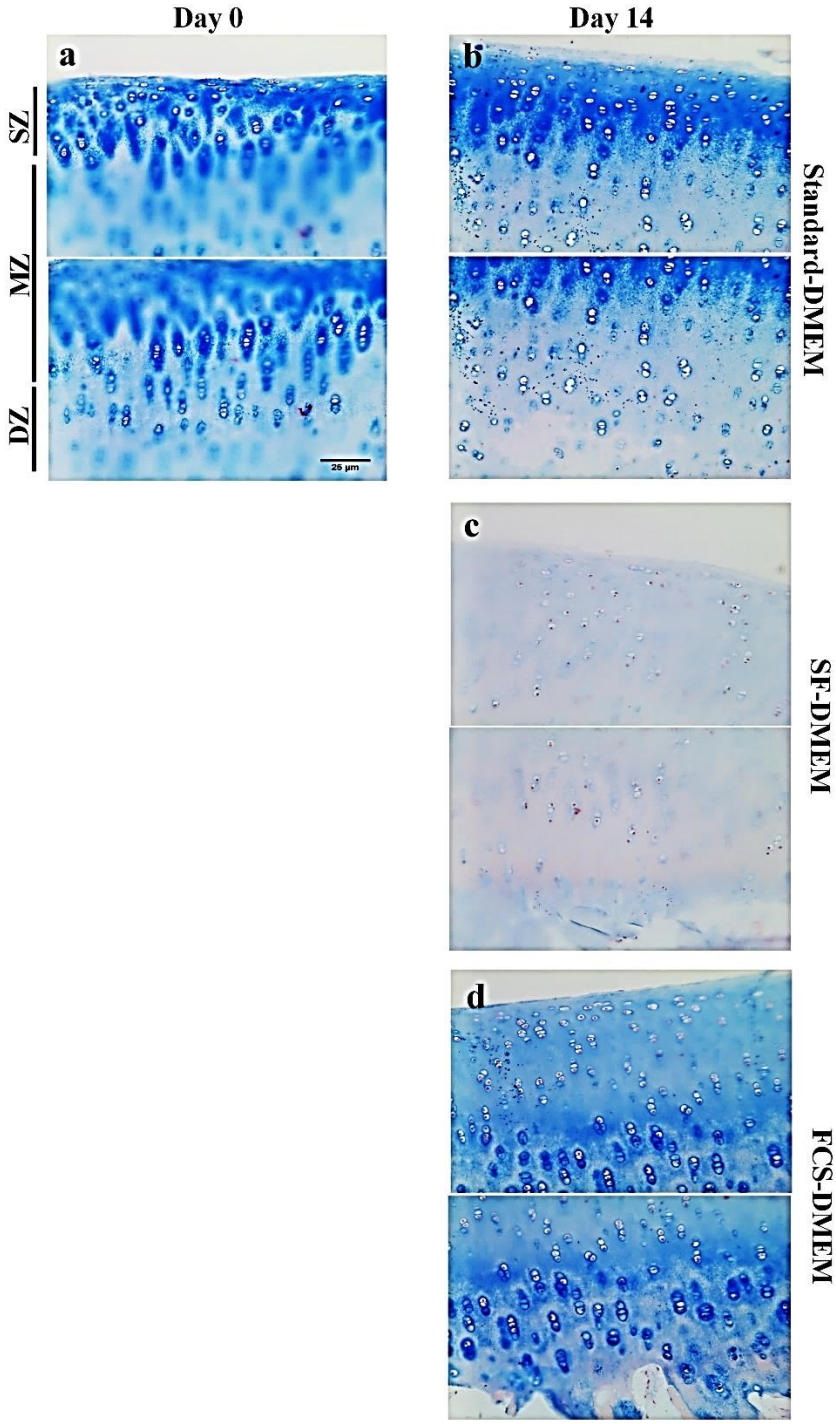

Figure 7.5: Typical photomicrographs of Alcian blue stained coronal sections from the site of injury at high power magnification.

The histological sections of injured cartilage stained with Alcian blue and imaged (x20 oil immersion) at (a) day 0 and (b, c, d) day 14 following culture in standard-DMEM, SF-DMEM and FCS-DMEM respectively. The results obtained from at least three independent experiments. Photomicrograph (a) represents the Alcian blue staining in uninjured cartilage. Scale bar = 25µm.

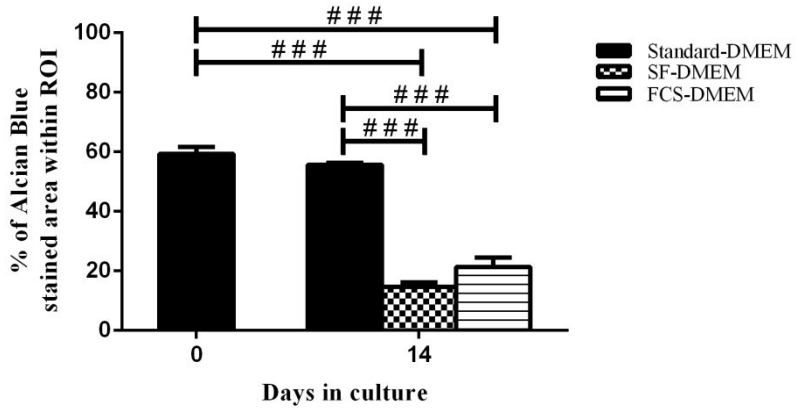

Figure 7.6: The percentage of Alcian blue stained area at the injury in cartilage explants cultured under various conditions.
Graphs show pooled data regarding percentage of Alcian blue stained area at day 0 and 14 of culture under three culture conditions. Data were from [*N(n)* = 9(16)]; ANOVA. # indicated a significant difference between different culture conditions and at two time points according to one-way ANOVA followed by Tukey's multiple comparison post-hoc test. The single, double and triple symbols showed the level of significance for $P<0.05$, 0.01 and 0.001 respectively.

7.5.1.3 *Masson's trichrome staining*

The coronal histological sections of injured cartilage at two time points (day 0 and 14) during the course of culture were stained with Masson's trichrome staining to determine the presence of collagen in response to injury cultured under various conditions. The low and high power magnification images of cartilage sections revealed relatively similar Masson's trichrome stained area in all the culture conditions (Figs. 7.7 & 7.8). At day 14 the percentage of Masson's trichrome stained area (within ROI) was unaffected by the nature of culture media and no significant difference existed between the explants cultured under various conditions and also in comparison to day 0 (Fig. 7.9; $P>0.05$; one-way ANOVA).

To summarise the results of this section, presence of collagen around chondrocytes in response to injury following cultured under various conditions remained unaffected after 14 days of culture.

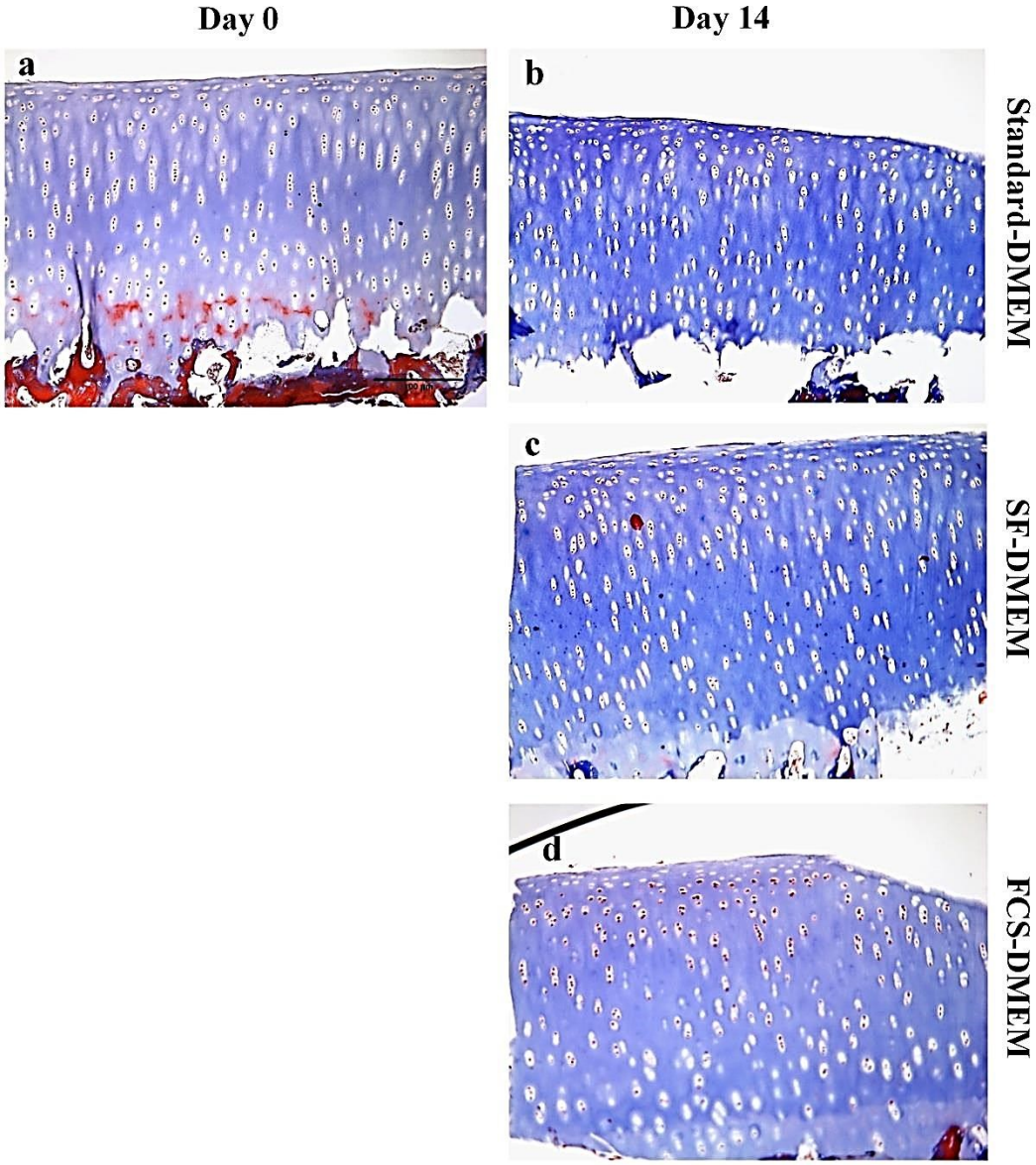

Figure 7.7: Typical photomicrographs of Masson's trichrome stained coronal sections of injured cartilage at low power magnification.
The histological sections of injured cartilage stained with Masson's trichrome and imaged (x10) at (a) day 0 and (b, c, d) day 14 following culture in standard-DMEM, SF-DMEM and FCS-DMEM respectively. The results obtained from at least three independent experiments. Photomicrograph (a) represents the Masson's trichrome staining in uninjured cartilage. Scale bar = 100µm.

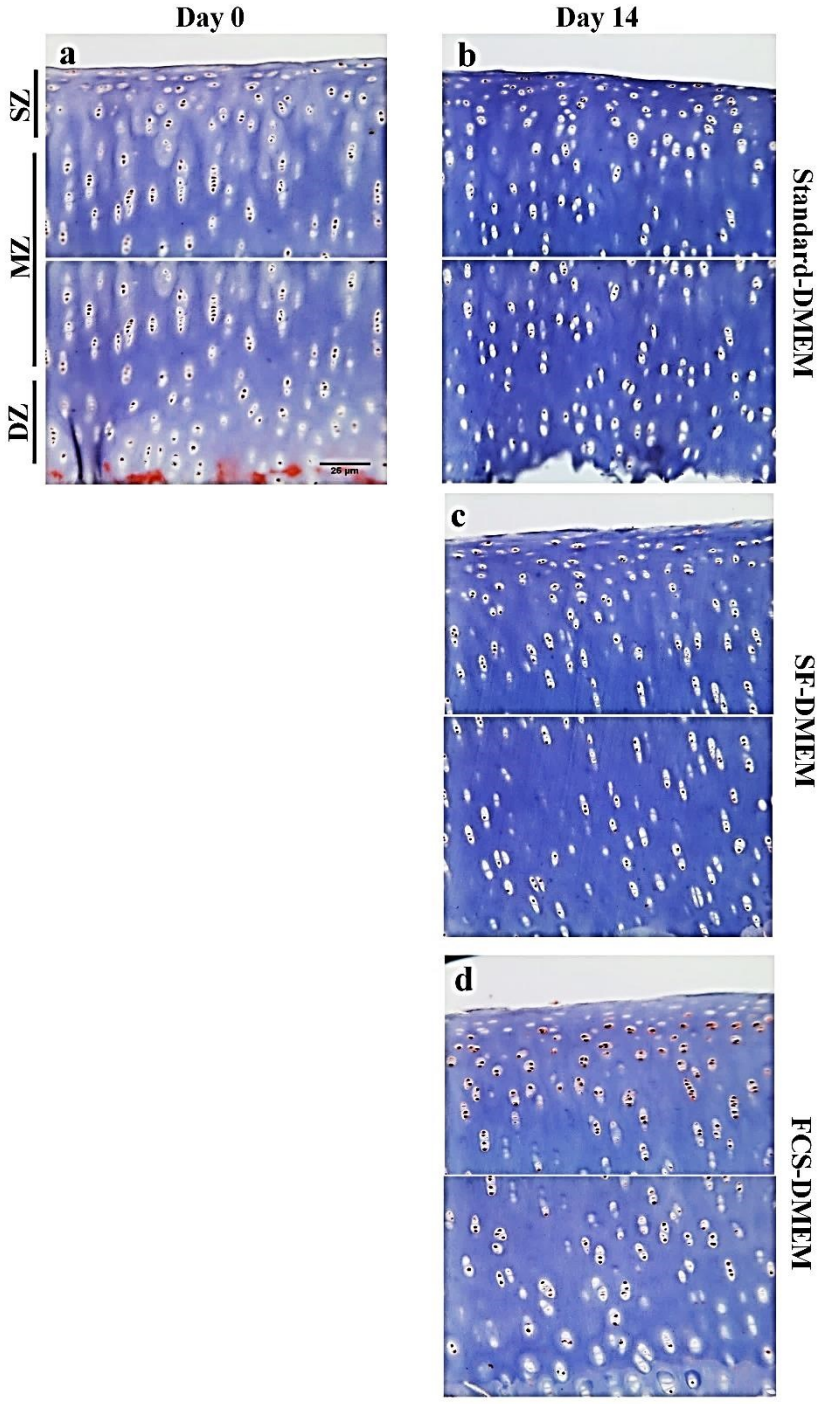

Figure 7.8: Typical photomicrographs of Masson's trichrome stained coronal sections of injured cartilage at high power magnification.

The histological sections of injured cartilage stained with Masson's trichrome and imaged (x20 oil immersion) at (a) day 0 and (b, c, d) day 14 following culture in standard-DMEM, SF-DMEM and FCS-DMEM respectively. The results obtained from at least three independent experiments. Photomicrograph (a) represents the Masson's trichrome staining in uninjured cartilage. Scale bar = 25µm.

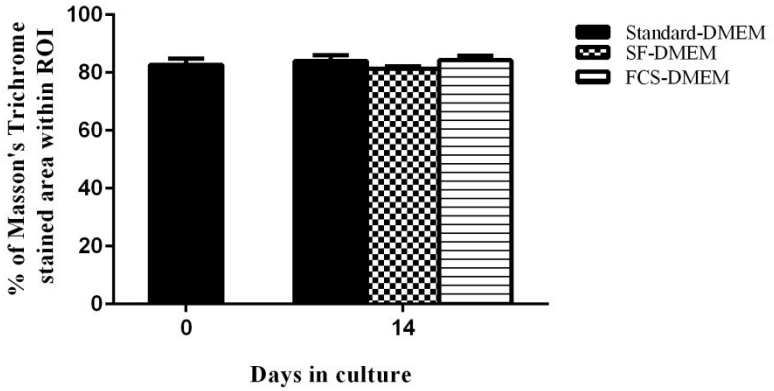

Figure 7.9: Percentage of Masson's trichrome stained area at the injury in cartilage explants cultured under various conditions.
Graphs show pooled data regarding percentage of Masson's trichrome stained area at day 0 and 14 of culture under three culture conditions. Data were from [N(n) = 9(16)]. There was no significant difference between the percentages of Masson's trichrome stained area at day 0 and 14 in various culture conditions.

7.5.1.4 *Type II collagen*

IHC is a powerful technique for the identification of proteins in a tissue and its specificity depends on how efficiently the antibody (known) binds to the antigen (unknown). The specificity can be determined by the use of positive control labelling the cells already known to have the protein and negative controls by substituting the primary antibody with serum (Burry, 2000). In this study the positive and negative controls for type II collagen were sections of articular cartilage with the subchondral bone (Fig. 7.10B) as type II collagen is present in abundance in the cartilage matrix (Eyre, 2002) and absent in the bone. IHC staining of the coronal sections of injured cartilage was done to determine the presence of type II collagen around chondrocytes at the injury following culture under various conditions (Figs. 7.10 & 7.11).

At day 0, 49±3% of the area (within ROI) exhibited collagen type II staining. There was no difference between the percentage of type II collagen staining in the explants cultured in the presence of various culture media at day 14 and also in comparison to day 0 (Fig. 7.12; *P*>0.05; one-way ANOVA).

These results suggested that the presence of type II collagen around chondrocytes in response to injury remained unaffected following culture in various media.

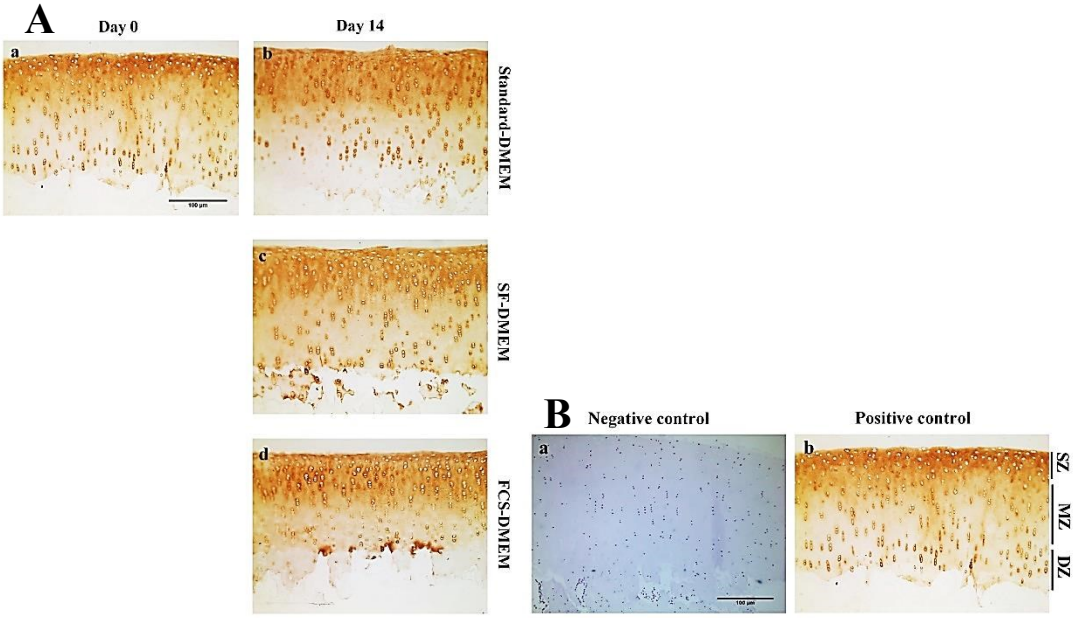

Figure 7.10: Representative images of IHC staining for type II collagen of injured cartilage explants.
(A) Low power magnification (x10) photomicrographs of type II collagen staining of cartilage at (a) day 0 and (b, c, d) day 14 cultured in standard-DMEM, SF-DMEM and FCS-DMEM respectively. (B) The representative images of (a) negative and (b) positive controls for type II collagen IHC in bovine articular cartilage showing the presence of type II collagen in all the zones of cartilage. The results obtained from at least three independent experiments. Photomicrograph A (a) represents collagen type II staining in uninjured cartilage. Scale bar for all the panels = 100µm.

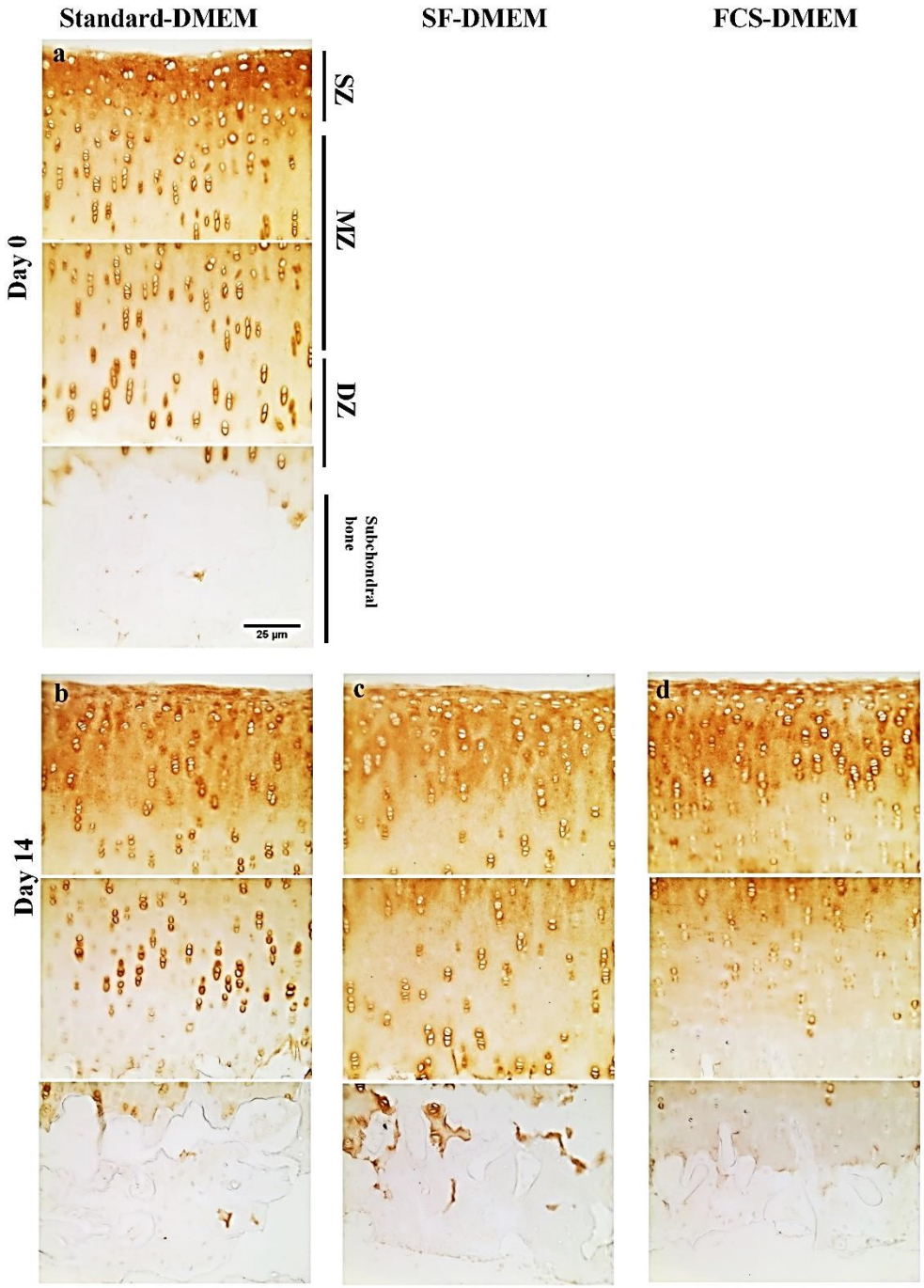

Figure 7.11: Representative photomicrographs of IHC of type II collagen in injured cartilage.

High power (x20 oil immersion) photomicrographs of type II collagen stained cartilage at (a) day 0 and (b, c, d) day 14 of culture in standard-DMEM, SF-DMEM and FCS-DMEM respectively. The results obtained from at least three independent experiments. Photomicrograph (a) represents collagen type II staining in uninjured cartilage. Scale bar for all panels = 25µm.

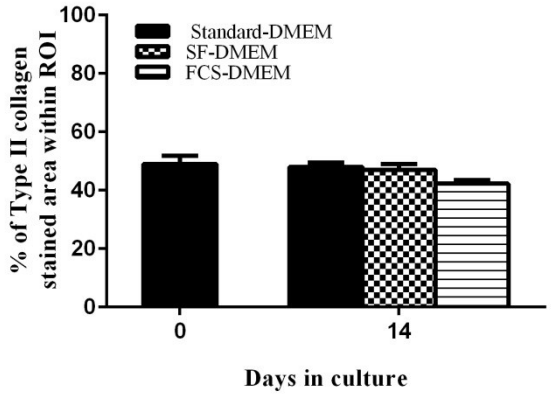

Figure 7.12: Percentage of type II collagen stained area in the injured cartilage. Graphs show pooled data regarding percentage of type II collagen stained area at day 0 and 14 of culture under three culture conditions. Data were from [N(n) = 9(16)]. There was statistically no significant difference between percentages of type II stained areas at day 0 and 14 of culture in various culture conditions.

7.5.1.5 *Type I collagen*

IHC for type I collagen was performed to determine the presence of type I collagen around chondrocytes in response to injury following culture under various culture conditions. The low and high power IHC photomicrographs of injured cartilage stained for type I collagen showed no difference in the presence of type I collagen by chondrocytes at the injury cultured in the presence of various culture media (Fig. 7.13 & 7.14).

At day 0, in the control explants 0.8±0.1% (within ROI) of type I collagen stained area was observed. Type I collagen remained unaffected in the explants cultured in the presence of various culture media after 14 days of culture. There was no increase in the percentage of type I collagen stained area in the explants cultured in the presence of SF-DMEM/FCS-DMEM (Fig. 7.15). To summarise the results of this

section, in the injured explants cultured in various culture media chondrocytes at the injury showed no alterations in expression of collagen type I.

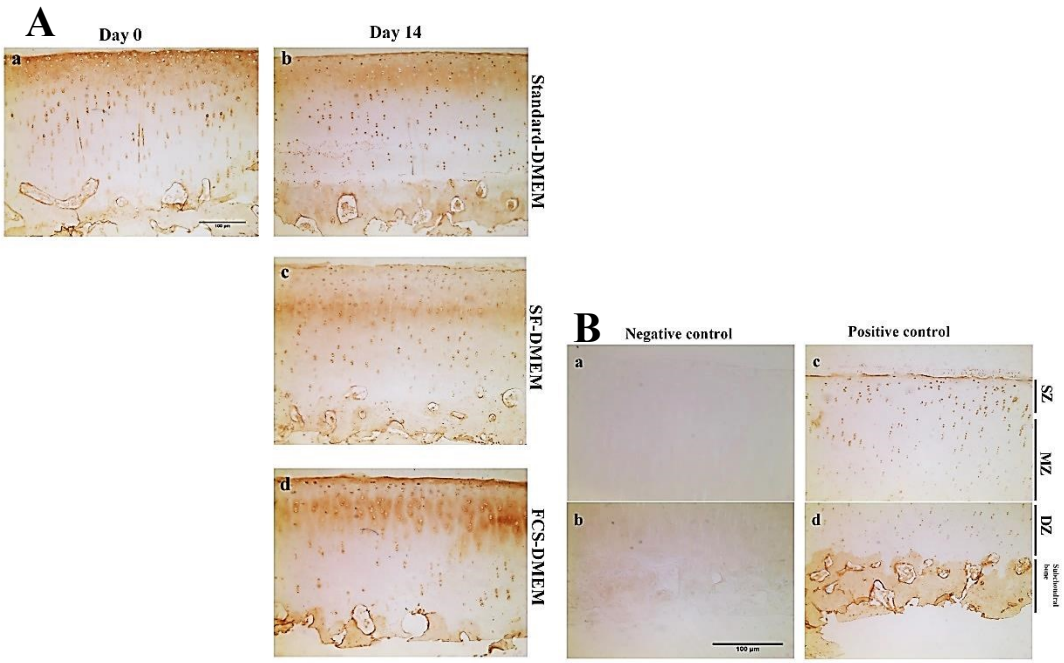

Figure 7.13: Representative images of immunohistochemical staining for type I collagen of injured cartilage explants.

(A) Low power magnification (x10) photomicrographs of type I collagen staining of cartilage at (a) day 0 and (b, c, d) day 14 cultured in standard-DMEM, SF-DMEM and FCS-DMEM respectively. (B) The representative images of (a, b) negative and (c, d) positive controls for type I collagen IHC in bovine articular cartilage showing the absence of type I collagen in all the zones of cartilage and present in the subchondral bone. The results obtained from at least three independent experiments. Photomicrograph A (a) represents collagen type I staining in uninjured cartilage. Scale bar for all the panels = 100µm.

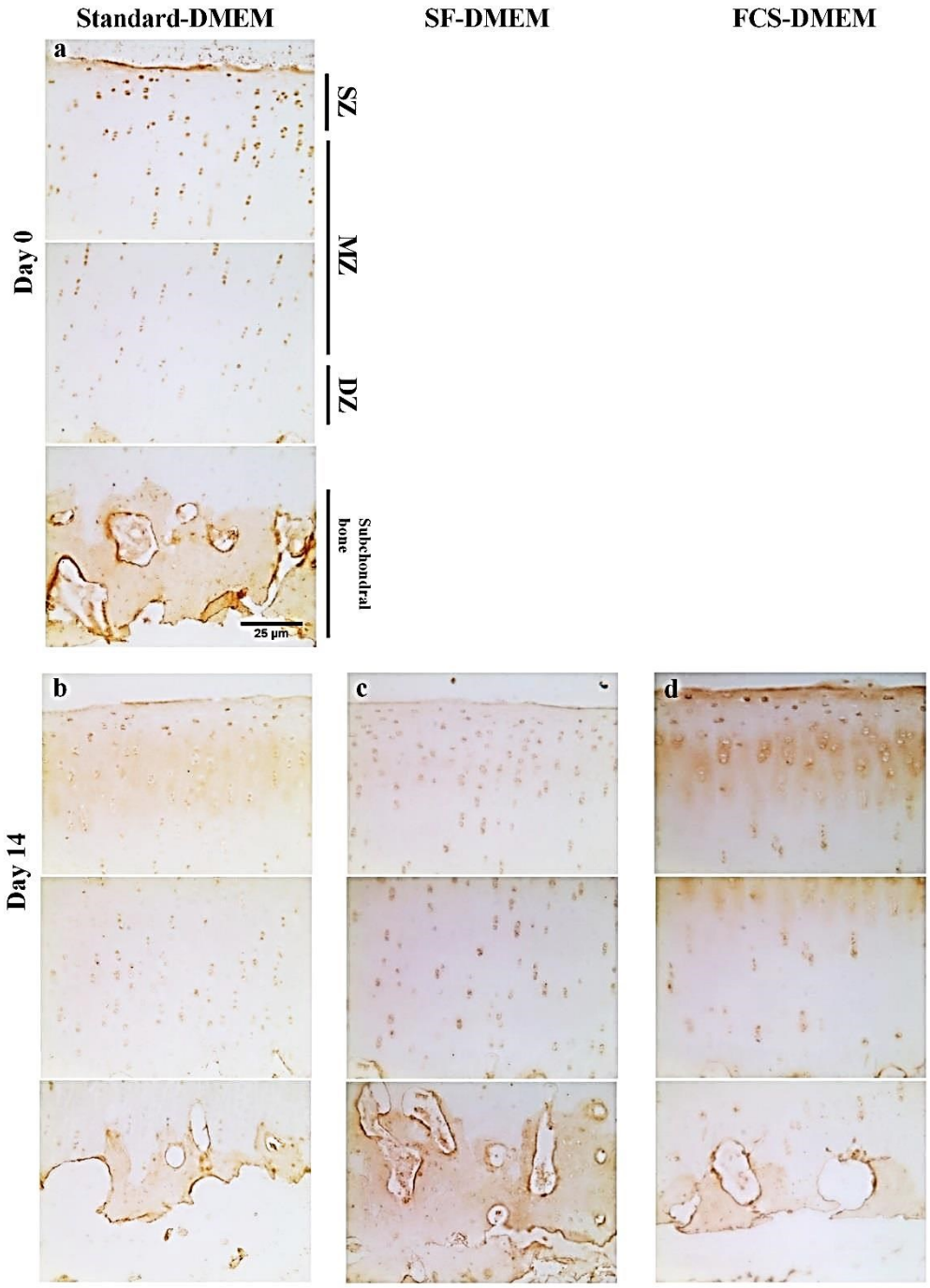

Figure 7.14: Representative photomicrographs of IHC of type I collagen in injured cartilage.

High power (x20 oil immersion) photomicrographs of type I collagen stained cartilage at (a) day 0 and (b, c, d) day 14 of culture in standard-DMEM, SF-DMEM and FCS-DMEM respectively. The results obtained from at least three independent experiments. Photomicrograph (a) represents collagen type I staining in uninjured cartilage. Scale bar for all panels = 25µm.

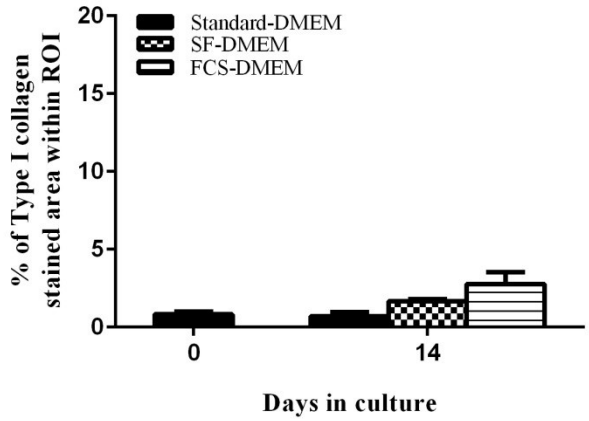

Figure 7.15: Percentage of type I collagen stained area in the injured cartilage. Pooled data regarding percentage of type I collagen stained area at day 0 and 14 of culture under three culture conditions. Data were from [N(n) = 9(16)]. There was no significant difference between percentages of type I collagen stained areas at day 0 and 14 cultured in the presence of varying culture media.

In summary, in response to injury, GAGs and collagen type II remained unaffected in the explants cultured in the presence of standard-DMEM even after 14 days in comparison to day 0, also type I collagen was not present. Chondrocytes at the injury showed significant reduction in GAGs in the explants cultured in the presence of SF-DMEM and FCS-DMEM. However, there was no change in the expression of collagen types I & II by chondrocytes in response to injury in the explants cultured in the presence of SF-DMEM and FCS-DMEM.

7.6 DISCUSSION

There were two basic aims of the study firstly, to develop methods to study ECM produced by chondrocytes at the injury in the presence of various culture media and secondly to evaluate whether matrix produced by abnormal chondrocytes at the injury in the presence of SF/FCS was altered as compared to the matrix produced by

relatively normal chondrocytes at the injury in the presence of standard-DMEM. The results obtained supported the hypothesis to an extent that in the explants cultured in the presence of SF-DMEM and FCS-DMEM the Alcian blue staining was significantly less, Masson's trichrome staining and IHC of collagen types I & II remained unaffected as compared to standard-DMEM.

There were certain technical issues related to the development of histological and IHC techniques used here to study the matrix produced and will be discussed in detail. In the preliminary experiments with CLSM (chapter 6) chondrocytes in response to injury in the presence of SF and FCS displayed marked heterogeneity to chondrocyte morphology with the presence of cytoplasmic processes after 14 days of culture. In the H&E stained sections the technique involved in the histological procedure obscured the fine morphological details of these abnormal chondrocytes and the cytoplasmic processes were not visible, but clusters were still observed even with routine histology. In the Alcian blue stained histological sections the staining intensity was strikingly reduced in explants cultured in the presence of SF/FCS as compared to standard-DMEM. When injured cartilage explant sections were stained with Masson's trichrome staining which is a crude method of estimation of presence of collagens (Chung et al., 2014) revealed no significant difference between different culture conditions. Similarly, IHC of collagen types I & II showed no difference around chondrocytes at the injury in explants cultured in different conditions. The results obtained and the technical issues regarding the methods involved will now be discussed in detail.

The technical problems encountered while obtaining sections and with staining procedures were attempted to be minimised. **First** difficulty was to obtain sections of

cartilage explants at the site of injury. Several attempts were made but it was impossible to obtain axial sections on cutting from paraffin-embedded tissue because the surface of the cartilage was irregular. Next, it was attempted to cut the tissue in the coronal view. Although sectioning was possible but while cutting with microtome the tissue often split apart at the site of injury. The last attempt was successful where under the dissection microscope the cartilage explants were split into two at the site of already produced injury and marked for the injured site. With the microtome from the marked injured site coronal sections of the injured site of tissue were obtained. **Second** problem was with the H&E staining fine details of morphology (cytoplasmic processes) were not visible but the clusters could be observed. This technical issue has already been discussed (section 5.6).

In this study with H&E staining chondrocyte clusters were present at the injury in the explants cultured in the presence of SF/FCS (Fig. 7.3). These results are in agreement with previously reported work on rat articular cartilage where a greater number of chondrocyte clusters was observed after traumatic loading and culturing cartilage in the presence of FCS (Henson and Vincent, 2008). The cluster formation in articular cartilage after trauma can possibly be explained to be stimulated by the growth/proliferative factors especially in the superficial layers of cartilage (Schumacher et al., 2002, Lotz et al., 2010). Several growth factors are known to stimulate cluster formation in chondrocytes and fibroblast growth factor-2 (FGF-2) is thought to be the principal/potent factor to stimulate clustering (Khan et al., 2010). Therefore, it is likely that chondrocytes at the injury in the presence of SF/FCS formed clusters due to enhanced access to factors.

In this study, Alcian blue staining decreased considerably in the injured explants cultured in the presence of SF-DMEM and FCS-DMEM as compared to standard-DMEM (Fig. 7.6). Alcian blue staining reflects an estimate of PGs present in the tissue and there can be four possible explanations for this staining pattern. **First** possibility could be reduction in PGs due to breakdown by the action of factors in SF/FCS. This is unlikely because FCS used in explant cultures is known to stimulate PG synthesis by chondrocytes through insulin-like growth factor-1 present in it (McQuillan et al., 1986). **Second** possibility could be that the PGs were lost in the culture medium by diffusion through the injured site. This is unlikely to occur because if this would also have happened then in the control samples of this study cultured in the presence of standard-DMEM there would have been less staining with Alcian blue (Fig. 7.6). However, there was no statistically significant difference between the percentages of Alcian blue staining at day 0 and day14 in standard-DMEM suggesting no loss of PGs by diffusion during the culture period. The loss of PGs in culture can be determined by quantitative analysis of culture media for presence of PGs. **Third** possibility could be the loss of PGs under the effect of enhanced catabolic activity of morphologically abnormal chondrocytes at injury in the presence of SF/FCS. In the initial experiments on injured cartilage, chondrocytes at the injury changed shape (flattened, elongated and with cytoplasmic processes) in the presence of SF-DMEM and FCS-DMEM (Results chapter 6) as compared to standard-DMEM. In the Alcian blue stained sections less staining was observed in the explants cultured with SF-DMEM and FCS-DMEM. Therefore, this suggested that morphologically heterogeneous chondrocytes at the injury under the effect of SF/FCS showed loss of PGs. These results can be explained by previous work which

suggested loss of PGs following trauma to bovine and human cartilage augmented by the catabolic cytokines (Sui et al., 2009). This previous study and the results of present study cannot be directly compared because the time course of experiments in the previous study was different from the present work. However, the findings from the previous work can be used to explain the results in the present work. **Fourth** possibility could be the production of low molecular weight PGs such as decorin and biglycan by abnormal chondrocytes at the injury cultured in the presence of SF/FCS-DMEM which stain less intensely with Alcian blue (Bock et al., 2001, Tesche and Miosge, 2004). In author's opinion the third and fourth possibilities are the most likely causes of differences in Alcian blue stained area in injured cartilage samples cultured in various conditions.

The results of the Masson's trichrome staining in this work showed no difference in the overall collagen stained area in various culture conditions (Fig. 7.9). This staining technique is just a rough estimate of the overall collagen content in the cartilage (Chung et al., 2014) therefore; results are indecisive. Type I and II collagen were detected by performing IHC and the standardisation of the technique was performed by using positive and negative control samples (Figs. 7.10 & 7.13). IHC of the injured cartilage sections cultured under various conditions revealed no difference in collagen type II (Fig. 7.12) and type I staining (Fig. 7.15) around chondrocytes in the injured explants cultured in the presence of various culture conditions. This can be possibly explained by considering the low turnover rate of collagen type II in the cartilage tissue (Lippiello et al., 1977). Collagens in the normal adult human cartilage have a half-life of 117 yrs. (Verzijl et al., 2000). The results in this study also showed

slight staining of type I collagen at day 0 (Fig. 7.15). The possible explanation for this can be non-specific staining of type I collagen antibodies.

A limitation of this study was that direct relationship between chondrocyte morphology and matrix components could not be established. Here overall matrix of the cartilage was being analysed and not being matched precisely to the individual chondrocytes with altered morphology. The techniques utilised in this study rendered it impossible to visualise the fine details of chondrocyte morphology (cytoplasmic processes) in these histological sections. An interesting future experiment will be to fluorescently label chondrocytes and matrix components to visualise morphology and matrix on the same tissue sections.

In summary, the results have supported the hypothesis that morphologically abnormal chondrocytes at injury in the presence of SF/FCS-DMEM produced altered matrix as compared to normal chondrocytes in the presence of standard-DMEM.

CHAPTER 8: RESULTS

EFFECTS OF VARIOUS CULTURE CONDITIONS ON THE SHORT- AND LONG-TERM MORPHOLOGY OF CHONDROCYTES IN INJURED CARTILAGE

8.1 CHAPTER SUMMARY

In this study it was hypothesised that chondrocytes at the injury in hyperosmolar serum-rich medium do not produce morphological changes as compared to standard serum-rich culture medium. The aim of this chapter was to assess *in situ* chondrocyte viability and morphological characteristics at the scalpel injury in response to varying culture media. Osteochondral explants were exposed initially to the altered osmolarities (320 and 615 mOsm) then injured with standardised scalpel injury and then again exposed to the two osmolarities. The injured explants were divided into two experimental groups to determine short- and long-term response of chondrocytes to varying culture media after 14 days of culture in **Group 1:** either (a) standard-DMEM or (b) standard-FCS **Group 2:** (a) standard-DMEM (b) standard-FCS (c) hyperosmolar-DMEM and (d) hyperosmolar-FCS. Chondrocytes were examined by fluorescent-mode confocal microscopy and analysed by Volocity^{TM} software. At day 0, the width of injury, percentage of PI-labelled chondrocytes and the volume of chondrocytes at the injury was significantly less in the explants exposed to 615 mOsm as compared to 320 mOsm (P<0.0001); all the cells were with normal morphology. In **group 1**, the percentage of PI-labelled chondrocytes decreased ~96% in the presence of standard-FCS throughout the culture period irrespective of osmolarities. At day 7, the volume of chondrocytes increased in explants exposed to 615 mOsm and kept in culture with either standard-DMEM or standard-FCS and in explants exposed to 320 mOsm and cultured with standard-FCS. Chondrocyte clustering was stimulated in the presence of FCS irrespective of the osmolarities. At day 14, chondrocytes at the injury in standard-DMEM were mostly spheroidal.

However, at the injury 17±3% and 13±1% chondrocytes exposed to 320 and 615 mOsm (P=0.0003 and P<0.0001; respectively) and cultured in standard-FCS displayed marked shape changes. In **group 2**, width of the injury remained unaffected in hyperosmolar-DMEM, increased in standard-DMEM and decreased markedly in the presence of FCS (both osmolarities). Throughout the culture period percentage of PI-labelled chondrocytes decreased in the presence of FCS irrespective of the osmolarities. At day 7, the volume of chondrocytes and cluster formation increased significantly in the presence of FCS in both the osmolarities, the effect was more pronounced in standard-FCS as compared to hyperosmolar-FCS. At day 14, at the injury the morphology of chondrocytes changed strikingly in the presence of standard-FCS alone. In contrast, morphology of chondrocytes remained unaffected in standard-DMEM, hyperosmolar-DMEM and hyperosmolar-FCS. In summary, medium osmolarity significantly affected viability and morphology of chondrocytes at the injury. Therefore, medium osmolarity would appear to be a more powerful regulator of chondrocyte morphology than the growth factors in serum.

8.2 INTRODUCTION

Mechanical injuries to articular cartilage heal poorly, producing a functionally and structurally inferior tissue because of poor regenerative capacity of the cartilage (Buckwalter, 1998). It is suggested that these injuries lead to chondrocyte death and damage to matrix (Tew et al., 2000) and may play a role in causing cartilage degeneration and ultimately development of PTOA (Hunziker, 2001). As a consequence of mechanical injury, the collagen network is disrupted and PGs are lost (D'Lima et al., 2001b, Quinn et al., 2001, Redman et al., 2004). PGs are negatively

charged and are responsible for maintaining the hydration status of cartilage by creating osmotic pressure within cartilage via Gibbs-Donnan equilibrium conditions (Urban, 1994, Hopewell and Urban, 2003). This high extracellular osmolarity of the cartilage (350-450 mOsm) as compared to synovial fluid or plasma increases the tendency of fluid movement into the cartilage which is restricted by the intact collagen network (Maroudas, 1976, Lai et al., 1991, Urban, 1994). This explains the high tendency of the cartilage swelling and when in injury the matrix is damaged there is loss of PGs and the water content of the cartilage is increased (Maroudas, 1976, Maroudas and Venn, 1977, McArthur and Gardner, 1992, Wheaton et al., 2004).

Chondrocytes are very sensitive to changes in extracellular osmolarity of the cartilage and behave as osmometers over a certain range of osmotic pressure (Bush and Hall, 2001a). In response to hypotonic challenge, chondrocytes swell up by taking up water and this swelling is opposed by efflux of ions (K^+ and Cl^-) and taurine (to decrease intracellular osmolarity) facilitating osmotic efflux of water and this mechanism is termed regulatory volume decrease (RVD) (Lang et al., 1998, Bush and Hall, 2001b, Hoffmann et al., 2009). In contrast, following exposure to hypertonic challenge chondrocytes shrink and then they recover their volume through the mechanism of regulatory volume increase (RVI) involving activation of Na^+ -K^+ -2Cl^- co-transport, Na^+/H^+ exchange and Na^+ channels (Hall et al., 1996a, Kerrigan et al., 2006, Hoffmann et al., 2009). These membrane electrolyte transporters get activated and charged ions including Na^+ ,K^+ and Cl^- are transported into the cell to balance the intracellular ionic concentration and extracellular ionic concentration thereby, limiting volume change (Hall et al., 1996b, Cheung and Ko,

2013). The volume regulatory mechanisms in chondrocytes have been studied extensively (Bush and Hall, 2001a, Bush and Hall, 2005, Lewis et al., 2011). In response to the hypotonic challenge, the over distended cells become highly sensitive and are more prone to injury (Bush et al., 2005) and this explains that chondrocyte viability following mechanical injury is inversely related to the extracellular osmolarity (Amin et al., 2008b). Chondroprotective effect of hyperosmolarity on injured articular cartilage has been reported previously where cell death was markedly reduced in hyperosmolar environment (480 mOsm) as compared to 0 mOsm (Amin et al., 2008b). Additionally it has been reported recently that hyperosmolarity enhances cartilage repair (Eltawil et al., 2014, Huang et al., 2015). The studies regarding chondroprotective effects of hyperosmolarity on injured cartilage suggested that the onset of PTOA could possibly be delayed by using strategies to reduce chondrocyte morbidity due to trauma. In addition to chondrocyte volume alterations in extracellular osmolarity may influence protein synthesis (Urban et al., 1993, Hopewell and Urban, 2003) and cytoskeletal organisation (Chao et al., 2006).

Hyperosmotic conditions (550 mOsm) in human articular chondrocytes are known to up- and down- regulate 88 and 51 genes respectively at the post transcription levels, thereby controlling chondrocyte functions (Tew et al., 2011). SOX9 is an essential transcription factor required for the ECM synthesis and regulates expression of collagen type II (Bell et al., 1997) and aggrecan (Bi et al., 1999), two very important ECM macromolecules. Additionally, SOX9 regulates chondrocyte phenotype as shown in a previous study where osteoarthritic human chondrocytes regained chondrocytic properties when transduced with SOX9 gene (Tew et al., 2005). In turn,

SOX9 is regulated by hyperosmotic conditions (Tew et al., 2009) and its expression is enhanced by hyperosmolar loading of chondrocytes (Peffers et al., 2010). Various studies have reported hyperosmotic extracellular environment to be chondroprotective in nature and more suitable for phenotypic stability of human articular chondrocytes (Tew and Hardingham, 2006, Tew et al., 2009). These studies suggested that hyperosmolar environment may play role in controlling chondrocyte phenotype via SOX9 regulation at the post transcriptional level. The phenotype comprises cell morphology and metabolism and there exists a close relationship between chondrocyte morphology and metabolism. Several studies conducted on degenerate cartilage in the past reported changes to chondrocyte phenotype and their biosynthetic activity (Kouri et al., 1996a, Darling and Athanasiou, 2005, Tesche and Miosge, 2005, Yagi et al., 2005, Murray et al., 2010). Therefore, it is suggested that hyperosmotic environment regulates chondrocyte phenotype and may play role in controlling matrix metabolism.

The chondroprotective role of hyperosmolarity in injured cartilage in terms of viability has already been established therefore studying morphological response of chondrocytes in injured cartilage to the hyperosmolar conditions will enhance knowledge regarding the chondroprotective role of hyperosmolarity to trauma. The osmolarities used in these experiments are based upon previous experiments where 380 mOsm was used as a control being very similar to that experienced by chondrocytes *in situ* and 550 mOsm as a hyperosmolar condition (Palmer et al., 2001, Hopewell and Urban, 2003, Tew et al., 2009). The objective was to use our full-depth osteochondral explant with scalpel induced injury model to study the effect of osmolarity on the chondrocyte morphology at the injury.

8.3 HYPOTHESIS

Chondrocytes at the injury do not produce morphological changes in response to hyperosmolar serum-rich medium compared with exposure to standard serum-rich culture medium.

8.4 MATERIALS AND METHODS

8.4.1 Culture media with varying osmolarity

The culture media with varying osmolarities utilised in these experiments were prepared as detailed earlier (section 2.1.1.1). The two groups of injured cartilage explants were kept in culture under four experimental conditions (a) standard-DMEM; 343±2.6 mOsm; mean±S.E.M.; N=3 (DMEM-343) (b) standard-FCS; 339±2.6 mOsm; mean±S.E.M.; N=3 (FCS-339) (c) hyperosmolar-DMEM; 609±1.4 mOsm (DMEM-609) and (d) hyperosmolar-FCS; 606±0.8 mOsm (FCS-606). Therefore, for simplicity the two types of culture media used in short-term exposure experiments have been abbreviated as (a) standard-DMEM and (b) standard-FCS. The four types of culture media used for the long-term exposure experiments have been abbreviated formally as (a) standard-DMEM (b) standard-FCS (c) hyperosmolar-DMEM and (d) hyperosmolar-FCS.

8.4.2 *In vitro* partial thickness injured bovine articular cartilage model

The partial thickness injury model described in chapter 6 was utilised here to study the effect of various culture conditions on short- and long-term morphology of chondrocytes. Full-depth osteochondral bovine cartilage explants were obtained from

bovine metacarpophalangeal joints following the methodology explained earlier (section 6.4). For experiments on **short-term** exposure to hyperosmolarity osteochondral explants were divided into two groups and exposed to either (a) 320±1.5 mOsm (mean±S.E.M.; N=3) or (b) 615±1.6 mOsm (mean±S.E.M.; N=3) for 5 min. The explants were then injured with the standardised protocol (section 6.4.1.1.1) and exposed post-injury to the two osmolarities for another 5 min. The injured explants were then kept in freshly prepared culture media with either (a) standard-DMEM or (b) standard-FCS up to 14 days.

The experiments on **long-term** exposure to hyper-osmolarity composed exposure of injured explants for 14 days in culture with media of varying osmolarities. Osteochondral explants were divided into two groups and exposed to either (a) 320±1.5 mOsm (mean±S.E.M.; N=3) or (b) 615±1.6 mOsm (mean±S.E.M.; N=3) for 5 min. The explants were then injured with the standardised injury protocol and again exposed to the two osmolarities for 5 min post-injury. These injured cartilage explants were then kept in culture under four experimental conditions (a) standard-DMEM (b) standard-FCS (c) hyperosmolar-DMEM and (d) hyperosmolar-FCS.

8.4.3 Preparation of cartilage explants for microscopy

During culture period, for short- and long-term exposure to hyperosmolarity experiments chondrocytes in the explants were fluorescently-labelled at three time points i.e. days 0, 7 and 14 (section 6.4.1.2), prepared for CLSM and imaged axially with low and high power magnification objectives (section 6.4.1.3).

8.4.4 Quantification of chondrocyte viability and morphology

The CLSM low and high power magnification images were analysed by Volocity™ software. Quantitative data regarding the width of injury, percentage cell death (PCD), volume of chondrocytes, cluster formation and morphology of chondrocytes was determined by the similar methodology as applied for the experiments in chapter 6 (sections 6.4.1.4 & 6.4.1.5).

8.5 RESULTS

8.5.1 Morphological characteristics of chondrocytes in injured cartilage after short-term exposure to varying osmolarities cultured under various conditions

Hyperosmolarity markedly alters the response of chondrocytes to injury. Injured osteochondral explants were exposed to two different osmolarities pre- and post-injury and then cultured in either (a) standard-DMEM or (b) standard-FCS to study the short-term response of chondrocyte morphology. The low power (x10) magnification images of CMFDA and PI-labelled chondrocytes showed markedly reduced cell death at the injury after exposure to hyperosmolar solution at day 0 (Fig. 8.1a & b). The width of injury seemed to be less in explants exposed to 615mOsm solution as compared to 320mOsm at day 0. At day 14, chondrocytes cultured in standard-FCS displayed marked shape changes irrespective of exposure to two osmolarities.

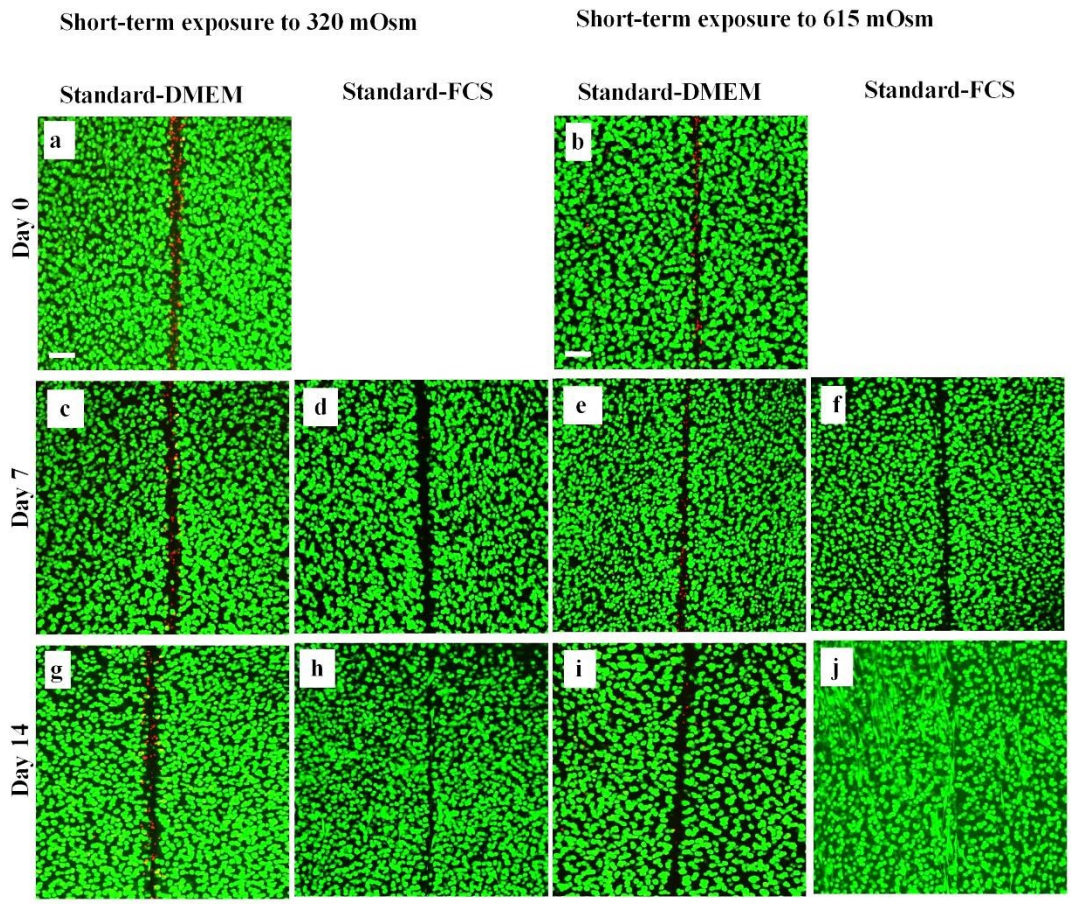

Figure 8.1: Axial CLSM reconstructions of injured cartilage explants exposed to different osmolarities for short-term following culture in various conditions.
CLSM reconstructions of low power (x10) magnification images of injured cartilage, CMFDA and PI labelled chondrocytes (live/dead cells respectively). The left panel shows images of injured cartilage after short-term exposure to 320 mOsm and right panel contains images after exposure to 615 mOsm at (a,b) day 0, (c,d,e,f) day 7 and (g,h,i,j) day 14 cultured in standard-DMEM and standard-FCS respectively. Scale bar for all panels = 100 μm.

8.5.1.1 *Changes to the width of injury after short-term exposure to varying osmolarities following in vitro culture under various conditions*

The width of injury was measured (section 6.4.1.4) to assess the response of cartilage to the trauma after short-term exposure to varying osmolarities and culture in various conditions (Fig. 8.1). In the presence of FCS by day 14, the width of injury was decreased and the gap was filled with morphologically abnormal chondrocytes and matrix (Fig. 8.1).

In the explants exposed to **320 mOsm** pre- and post-injury, the width of injury remained unaffected in the presence of standard-DMEM during the first week of culture. However, it increased significantly by day 14 of culture in standard-DMEM compared to earlier time points ($P<0.05$; ANOVA over the three days; Fig. 8.2a). In the injured explants exposed to 320 mOsm and cultured in standard-FCS the width of injury appeared to increase during the first week of culture in comparison to standard-DMEM but the difference was not statistically significant ($P>0.05$). However, by day 14 the width of injury decreased significantly compared to earlier time points of culture ($P<0.001$; ANOVA over the three days; Fig. 8.2a) and also in comparison with the explants cultured in standard-DMEM ($P<0.0001$; Fig. 8.2a).

After short-term exposure to **615 mOsm,** the width of injury remained unaffected in explants cultured with standard-DMEM during the first week of culture. However, the width of injury decreased significantly by day 14 of culture in standard-DMEM as compared to day 7 ($P<0.01$; ANOVA; Fig. 8.2b). In the injured explants exposed to 615 mOsm and then cultured in the presence of standard-FCS, the width of injury remained unaffected during first week of culture. However, the width of injury

decreased significantly by day 14 in these explants in comparison to earlier time points of culture (P<0.001; ANOVA over the three days; Fig. 8.2b) and also in comparison to standard-DMEM (P<0.0001; Fig 8.2b).

The width of injury was significantly less in the explants exposed to 615 mOsm as compared to 320 mOsm at all the time points and in both the culture conditions (Fig. 8.2b), only by day 14 no difference existed between the explants cultured in the presence of standard-FCS (P<0.0001 at day 0; P=0.0003; P=0.001 at day 7 and P<0.0001; P>0.05 at day 14; for standard-DMEM and standard-FCS respectively). These data suggested that at day 0, the width of injury was significantly less in the explants exposed to 615 mOsm as compared to 320 mOsm. Moreover, in the explants exposed to 320 mOsm and cultured with standard-DMEM the width of injury increased significantly by day 14. In contrast, in the explants exposed to 615 mOsm and kept in culture with standard-DMEM the width of injury decreased significantly by day 14. However, in the presence of standard-FCS, the width of injury decreased markedly by day 14 of culture in the explants exposed to both 320 mOsm and 615 mOsm osmolarities and the injury gap was almost completely filled with chondrocytes of varying morphology (Fig. 8.4h,j).

To summarise this section, by day 14 of culture the morphology of chondrocytes at the injury in the serum-rich culture media was markedly altered irrespective of short-term exposure to the two osmolarities and these enlarged, elongated chondrocytes with cytoplasmic processes filled in the injury gap.

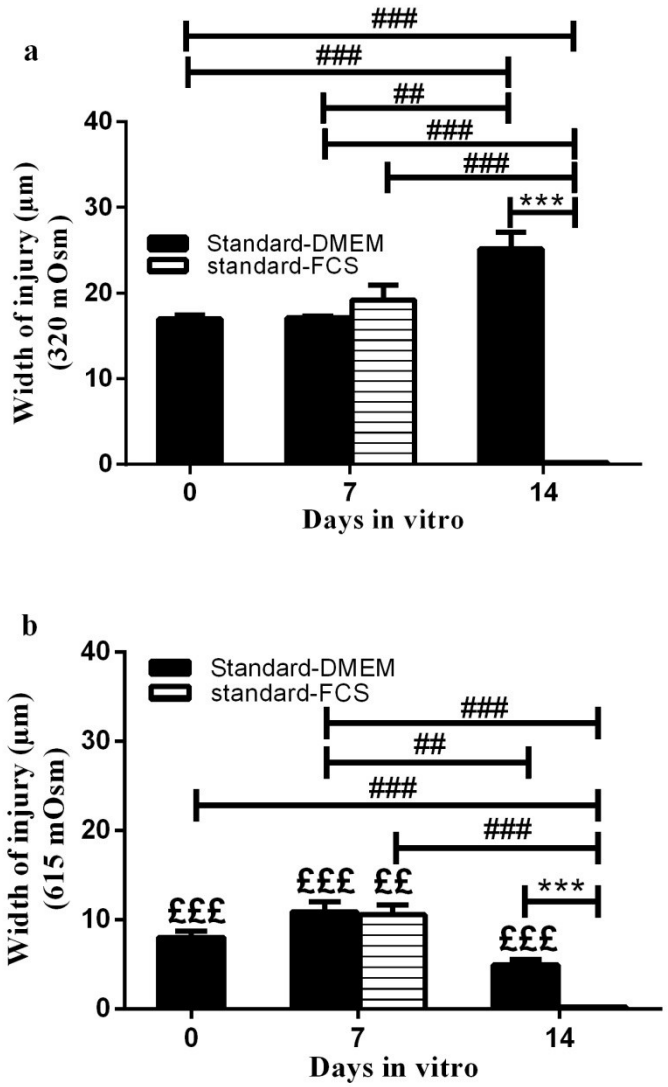

Figure 8.2: Variations in the width of injury after exposure to varying osmolarities following culture under various conditions.

Graphs summarise data regarding the width of injury after short-term exposure to (a) 320 mOsm and (b) 615 mOsm following culture in standard-DMEM and standard-FCS. Data given as [*N(n)*=8(30)]. * indicated a significant difference between two culture conditions at one time point according to t-test. # indicated a significant difference between different culture conditions at two time points according to one-way ANOVA followed by Tukey's multiple comparison post-hoc test. £ indicated significant difference between the two osmolarities. The single, double and triple symbols showed the level of significance for $P<0.05$, 0.01 and 0.001 respectively.

8.5.1.2 *Loss of PI-labelled cells at and distant from the injury after short-term exposure to varied osmolarities following culture in various conditions*

The objective was to determine the effect of varied osmolarities on the percentage of PI-labelled cells at and distant from the injury. Specified ROIs were created and applied (section 6.4.1.4) at and distant from the injury on the low power magnification CLSM images of the injured cartilage exposed to 320 mOsm and 615 mOsm at three time points during culture (Days 0, 7 and 14). The percentage of PI-labelled chondrocytes was determined at and distant from the injury to determine the effect of short-term exposure to varying culture media. The short-term exposure to various osmolarities and the composition of the culture medium markedly affected the percentage of PI-labelled chondrocytes (Fig. 8.1a-j).

The percentage of PI-labelled chondrocytes **at injury** in the explants exposed to 320 mOsm and 615 mOsm remained unaffected throughout the culture period in the presence of standard-DMEM ($P>0.05$; ANOVA over the three days for both conditions; Fig. 8.3a,c). The percentage of PI-labelled chondrocytes decreased significantly in the explants exposed to 320 mOsm and 615 mOsm and then cultured in the presence of standard-FCS as compared to standard-DMEM at day 7 and 14 of culture ($P<0.0001$; for both time points and both conditions; Fig. 8.3a,c) and also in comparison to day 0 ($P<0.001$; for both time points and both conditions; Fig. 8.3a,c).

The percentage of PI-labelled chondrocytes was significantly higher at the injury as compared to **distant from the injury** throughout the culture period in the explants cultured in the presence of standard-DMEM after short-term exposure to 320 mOsm ($P<0.0001$; for all the three time points; Fig. 8.3b) and 615 mOsm ($P<0.0001$;

P=0.0006 and *P*=0.005; for day 0, 7 and 14 respectively; Fig. 8.3d). However, at day 7 and 14 of culture no significant difference existed in the percentage of PI-labelled chondrocytes at and distant from the injury in the explants exposed to both 320 mOsm and 615 mOsm and then cultured in the presence of standard-FCS (Fig. 8.3b, d).

The percentage of PI-labelled chondrocytes was significantly less in the explants exposed to 615 mOsm as compared to 320 mOsm at all the time points in the explants cultured in the presence of standard-DMEM ($P<0.0001$; for all the three time points; Fig. 8.3c). However, at day 7 and 14 no difference existed in the percentage of PI-labelled chondrocytes in the explants exposed to 320 mOsm and 615 mOsm and kept in culture with standard-FCS (Fig. 8.3c).

These results suggested that the percentage of PI-labelled chondrocytes was significantly less in the explants exposed to 615 mOsm as compared to 320 mOsm throughout the culture period in the explants cultured in the presence of standard-DMEM. Moreover, the percentage of PI-labelled chondrocytes decreased significantly in the explants cultured in the presence of standard-FCS as compared to standard-DMEM throughout the culture period irrespective of the short-term exposure to varied osmolarities.

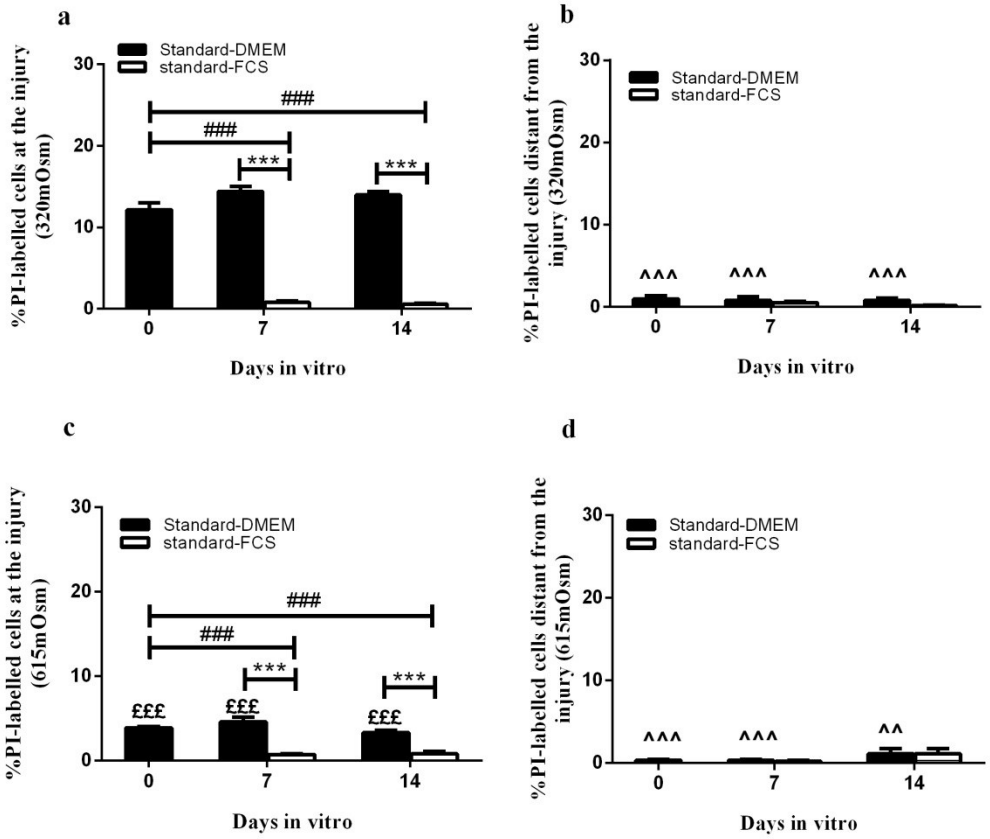

Figure 8.3: The percentage of PI-labelled chondrocytes at and distant from the injury after short-term exposure to different osmolarities following culture in various conditions.

Graphs in the top panel show pooled data to compare the percentage of PI-labelled chondrocytes after short-term exposure to 320 mOsm (a) at the injury and (b) distant from the injury, bottom panel graphs show a comparison between the percentage of PI-labelled chondrocytes after short-term exposure to 615 mOsm (c) at the injury and (d) distant from the injury under the two culture conditions. Data were from [*N(n)*=8(30)]. * indicated a significant difference between two culture conditions at one time point according to t-test. # indicated a significant difference between different culture conditions at various time points according to one-way ANOVA followed by Tukey's multiple comparison post-hoc test. £ indicated significant difference between the two osmolarities. ^ indicated a significant difference between at the injury and distant from the injury. The single, double and triple symbols showed the level of significance for $P<0.05$, 0.01 and 0.001 respectively.

8.5.1.3 *Volume/morphology of chondrocytes at the injury in response to short-term exposure to different osmolarities following culture in various conditions*

During the course of culture, chondrocyte volume/morphology at injury changed strikingly in response to the presence of FCS in the culture medium irrespective of exposure to varied osmolarities. These morphological changes were analysed by determining quantitative data regarding volume, cluster formation and heterogeneity to chondrocyte morphology. The results were acquired at different time points (Days 0, 7 and 14) and given in the following two sections.

8.5.1.3.1 Volume of chondrocytes at the injury by day 7

At day 0, chondrocytes were normal (elliptical/spheroidal) in morphology at the injury in the explants exposed to varied osmolarities (Fig. 8.4). During the course of culture, marked changes to the morphology of chondrocytes were seen at the injury in the explants exposed to 320 mOsm and 615 mOsm and kept in culture in the presence of standard-FCS as compared to standard-DMEM. The high power CLSM images displayed the development of abnormal chondrocyte morphology at the injury in the presence of standard-FCS (Fig. 8.4h,j).

At day 0, the volume of chondrocytes at the injury was found to be significantly higher in the explants exposed to 320 mOsm (1064.8±18μm^3) as compared to 615 mOsm (861.8±14.5μm^3; P<0.0001; Fig. 8.5a,b). At day 7, the volume of chondrocytes at the injury increased significantly in the explants exposed to **320 mOsm** and cultured in the presence of standard-FCS (1160±41μm^3) as compared to

standard-DMEM (1035.9±34.5μm^3; P=0.02) and also in comparison to day 0 (1064.8±18μm^3; P<0.05; Fig. 8.5a). It is worth noticing that increase in chondrocyte volume in the presence of standard-FCS was small but significantly different statistically.

At day 7, the volume of chondrocytes at the injury increased significantly in the explants exposed to **615 mOsm** and kept in culture in the presence of standard-DMEM (1068.2±65.8μm^3) as compared to day 0 (861.8±14.5μm^3; P<0.001; Fig. 8.5b). Moreover, at day 7 the volume of chondrocytes increased significantly (the difference was less) in the explants exposed to 615 mOsm and kept in culture in the presence of standard-FCS (1219±40.8μm^3) as compared to standard-DMEM (1068.2±65.8μm^3; P=0.04) and also in comparison to day 0 (861.8±14.5μm^3; P<0.001; Fig. 8.5b). Therefore, the presence of FCS in the culture medium stimulated a slight increase (statistically significant) in cell volume compared to standard-DMEM irrespective of exposure to two different osmolarities. However, at day 7 there existed no difference between the volumes of chondrocytes cultured in either standard-DMEM or standard-FCS after exposure to both the osmolarities (Fig. 8.5).

These results indicated that at day 0 the chondrocytes in 615 mOsm were shrunken (Fig. 8.5b). At day 7, the volume increased significantly in the explants exposed to 615 mOsm and kept in culture with standard-DMEM. Additionally, at day 7 the volume of chondrocytes at the injury increased significantly in the explants cultured in the presence of standard-FCS as compared to standard-DMEM regardless of the short-term exposure to varied osmolarities.

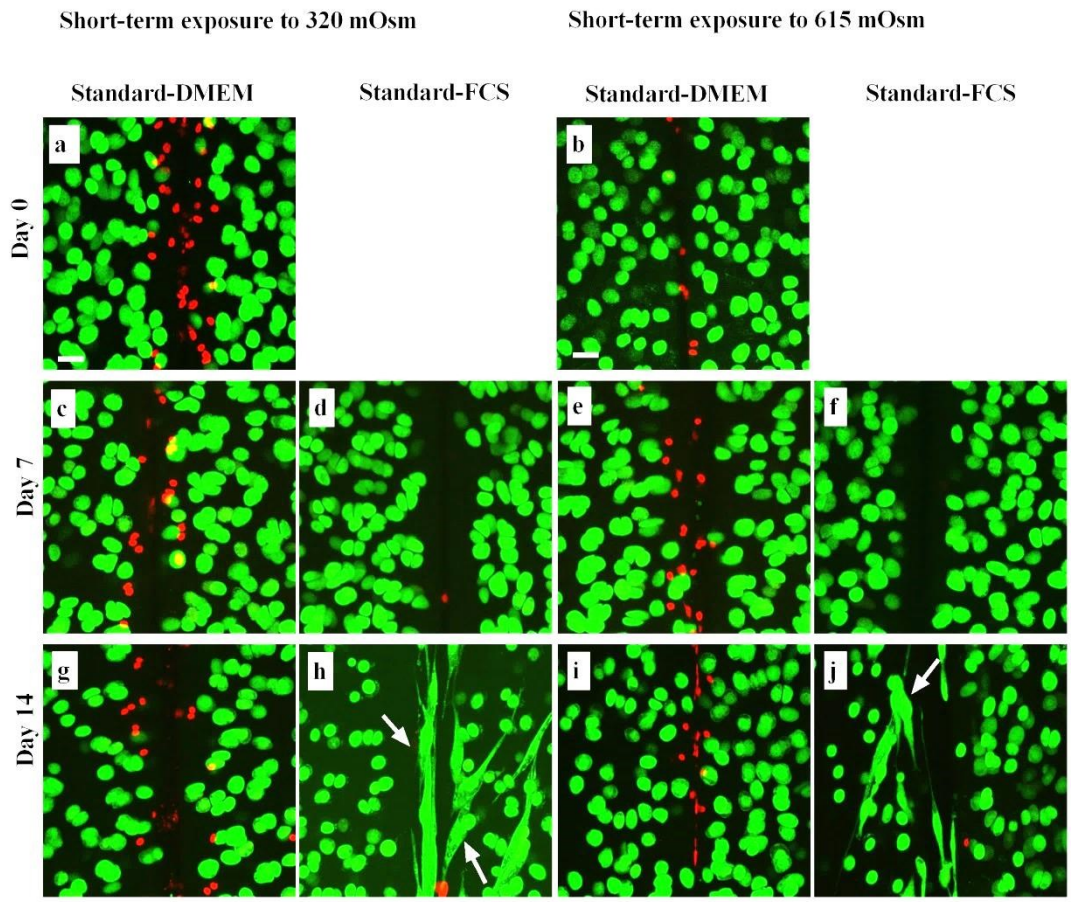

Figure 8.4: Axial CLSM reconstructions of injured cartilage explants exposed to different osmolarities for short-term showing changes to chondrocyte morphology following culture in various conditions.

CLSM reconstructions of high power (x40DW) magnification images of injured cartilage of CMFDA and PI labelled chondrocytes (live/dead cells respectively). The left panel shows images of injured cartilage after short-term exposure to 320 mOsm and right panel contains images after short-term exposure to 615 mOsm at (a,b) day 0, (c,d,e,f) day 7 and (g,h,i,j) day 14 cultured in standard-DMEM and standard-FCS respectively. Solid arrows indicate examples of chondrocytes with altered morphology (processes) at the injury. Scale bar for all panels = 25 μm.

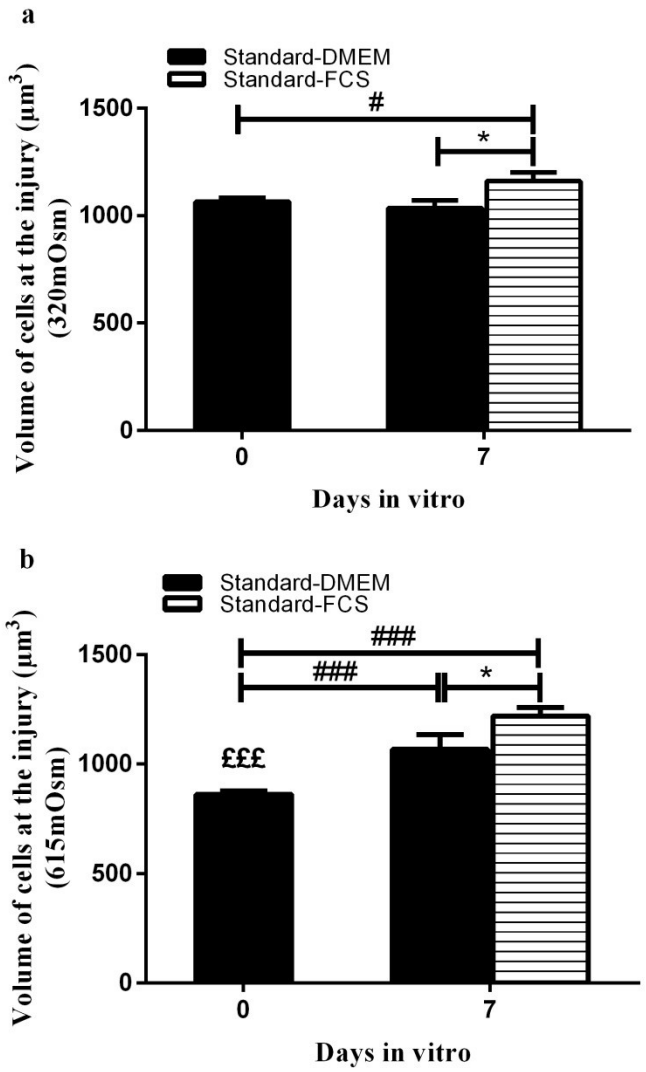

Figure 8.5: Changes to chondrocyte volume at the injury after short-term exposure to different osmolarities following culture in various conditions.
Graphs show pooled data regarding the volume of chondrocytes at the injury demonstrating comparison between short-term exposure to (a) 320 mOsm and (b) 615 mOsm following culture in the presence of standard-DMEM and standard-FCS. Data were from [*N(n')*=8(98) at day 0, 8(37) and 8(44) at day 7 in standard-DMEM and standard-FCS respectively after exposure to 320 mOsm] and [*N(n')*=8(116) at day 0, 8(36) and 8(57) at day 7 in standard-DMEM and standard-FCS respectively after exposure to 615 mOsm]. * indicated a significant difference between two culture conditions at one time point according to t-test. # indicated a significant difference between different culture conditions at two time points according to one-way ANOVA followed by Tukey's multiple comparison post-hoc test. £ indicated significant difference between the two osmolarities. The single, double and triple symbols showed the level of significance for $P<0.05$, 0.01 and 0.001 respectively.

8.5.1.3.2 Chondrocyte cluster formation at the injury by day 7

8.5.1.3.2.1 Number of clusters formed

At day 0, the average number of clusters formed at the injury in the explants exposed to 320 mOsm (3.4±0.2) were significantly higher than those formed in 615 mOsm (1.6±0.2; P=0.0004; Figs. 8.6Aa and 8.6Ba). The presence of clusters (although few) in healthy cartilage is unlikely and possibly suggested an artefact of the software (discussed in section 8.6). Moreover, the clusters present at day 0 involved on an average no more than 3 cells per cluster. During the course of culture, at day 7 in the explants exposed to **320 mOsm** and kept in culture with standard-FCS, the number of clusters increased significantly as compared to standard-DMEM (P=0.0008) and also in comparison to day 0 (P<0.001; Fig. 8.6Aa). At day 7, in the explants exposed to **615 mOsm** and kept in culture with standard-FCS, the number of clusters increased as compared to standard-DMEM but the difference was not statistically significant (P>0.05; Fig. 8.6Ba). However, in comparison to day 0, a significantly higher number of clusters were formed in explants exposed to 615 mOsm and cultured in standard-FCS (P<0.01; Fig. 8.6Ba). Additionally, at day 7, the number of clusters formed at the injury after exposure to 320 mOsm was significantly higher than 615 mOsm when cultured in the presence of standard-FCS (P=0.0005; Fig. 8.6Ba). There were more clusters formed in the presence of standard-FCS following exposure to 320 mOsm as compared to 615 mOsm. This suggested that by raising the osmolarity of medium to 615 mOsm with FCS, cluster formation was inhibited.

8.5.1.3.2.2 Number of cells/cluster

At day 7, the number of cells/cluster increased significantly in the explants exposed to 320 mOsm and cultured with standard-FCS as compared to standard-DMEM (P=0.04) and also in comparison to day 0 (P<0.01; Fig. 8.6Ab). The number of cells/cluster remained unchanged in both culture conditions in the explants exposed to 615 mOsm (P>0.05; Fig. 8.6Bb). The number of cells/cluster after exposure to 320 mOsm were significantly higher than 615 mOsm when explants were cultured in the presence of standard-FCS (P=0.03; Fig. 8.6Bb).

8.5.1.3.2.3 Percentage of chondrocytes forming clusters

The percentage of chondrocytes which formed clusters was calculated to determine chondrocyte proliferation for cluster formation. At day 0, a significantly higher percentage of chondrocytes formed clusters at the injury in the explants exposed to 320 mOsm (7±0.7%) as compared to 615 mOsm (4±0.5%; P=0.006; Figs. 8.6Ac and 8.6Bc). At day 7, in injured explants exposed to 320 mOsm and cultured in standard-FCS, a significantly higher percentage of chondrocytes (39±4%) formed clusters as compared to standard-DMEM (11.3±0.2%; P=0.003) and percentage of chondrocytes forming clusters at day 0 (7±0.7%; P<0.001; Fig. 8.6Ac). At day 7, in the injured explants exposed to 615 mOsm and cultured in the presence of standard-DMEM the percentage of chondrocytes forming clusters increased significantly as compared to day 0 (P<0.05; Fig. 8.6Bc). Additionally, the percentage of chondrocytes forming clusters increased significantly by day 7, in the explants exposed to 615 mOsm and kept in culture with standard-FCS (13.5±2%) as compared to standard-DMEM (8±1%; P=0.04) and also in comparison to day 0 (4±0.4%; P<0.01; Fig. 8.6Bc).

Moreover, at day 7 a significantly higher percentage of chondrocytes formed clusters in explants exposed to 320 mOsm as compared to 615 mOsm and cultured in the presence of standard-DMEM and standard-FCS (P=0.04 and P=0.005; for both conditions respectively; Figs. 8.6Ac and 8.6Bc). This suggested that cluster formation was inhibited by raising the osmolarity.

8.5.1.3.2.4 Volume of clusters

At day 0, clusters with a slightly higher volume were formed at the injury in the explants exposed to 320 mOsm as compared to 615 mOsm (P=0.03; Figs. 8.6Ad and 8.6Bd). However, the P value only 0.03 indicated the difference was less but statistically significant. These measurements take into account the number of cells/cluster considered later. At day 7, the volume of clusters at the injury in the explants exposed to 320 mOsm and cultured in standard-FCS increased significantly as compared to standard-DMEM (P=0.02) and also in comparison to the volume of clusters at day 0 (P<0.01; Fig. 8.6Ad). At day 7, the volume of clusters at the injury increased significantly in the explants exposed to 615 mOsm and kept in culture with standard-FCS (P<0.01; Fig. 8.6Bd). Additionally, the volume of clusters was significantly greater in the explants exposed to 320 mOsm as compared to 615 mOsm and kept in culture with standard-FCS (P=0.04; Fig. 8.6Bd). These results suggested that volume of clusters increased in the presence of standard-FCS (irrespective of exposure to two osmolarities). Additionally, when the osmolarity was raised to 615 mOsm, small sized clusters were formed as compared to 320 mOsm.

8.5.1.3.2.5 Volume of individual cells in a cluster

This was determined to assess whether in the presence of FCS the cluster formation was either a result of cell proliferation or simply the cell volume increased or due the involvement of both the mechanisms. The volume of individual cells in a cluster was calculated and compared after exposure to 320 mOsm and 615 mOsm following culture in both conditions at day 0 and 7. At day 0, the volume of individual cells in a cluster at the injury was significantly greater in the explants exposed to 320 mOsm as compared to 615 mOsm (P=0.04; Figs. 8.6Ae and Be). After a week, the volume of individual cells in a cluster remained unaffected after exposure to 320 mOsm and kept in culture with standard-DMEM. However, the volume of individual cells in a cluster increased in the explants exposed to 320 mOsm and kept in culture with standard-FCS as compared to standard-DMEM but the difference was not statistically significant (P>0.05; Fig. 8.6Ae). At day 7, the volume of individual cells in a cluster increased significantly in the explants exposed to 615 mOsm and kept in culture with standard-FCS as compared to day 0 (P<0.05; Fig. 8.6Be).

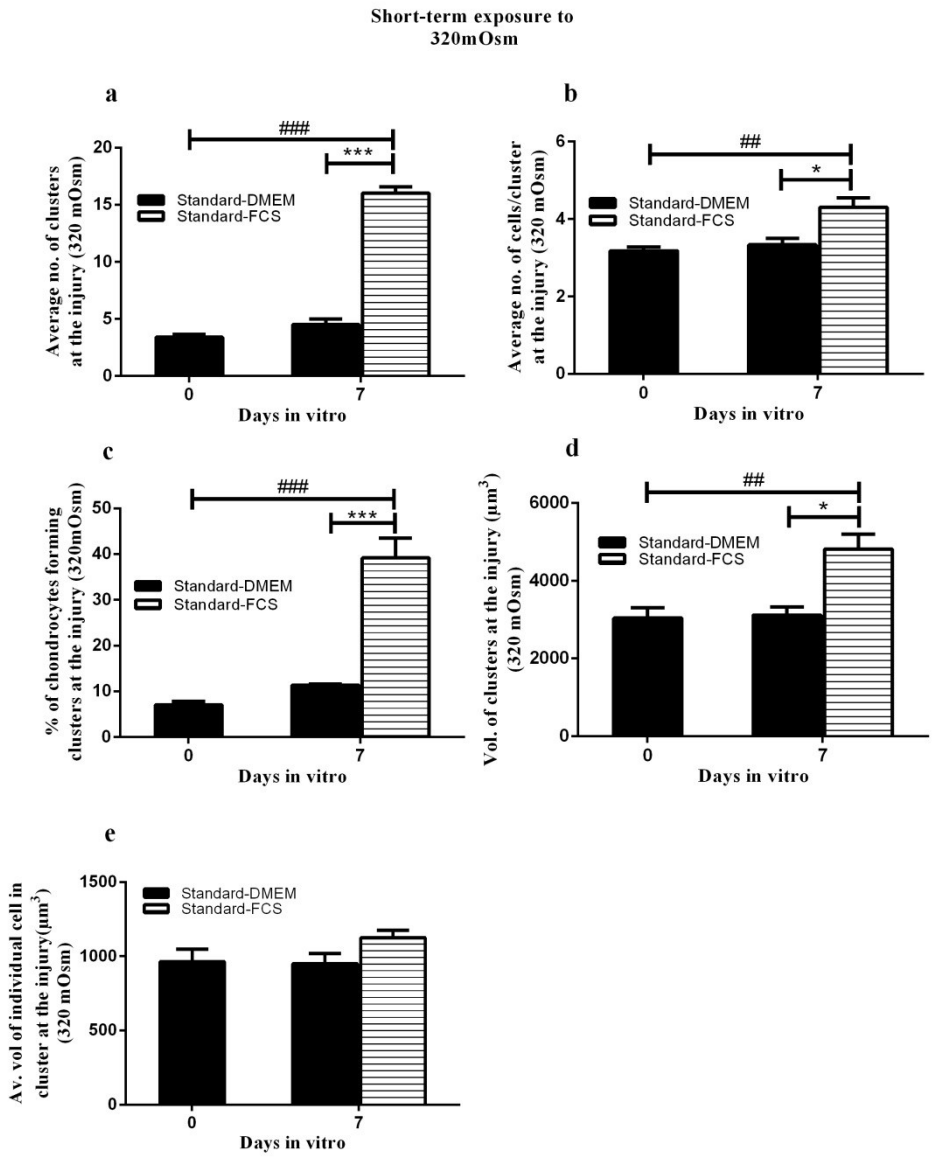

Figure 8.6A: Characteristics of chondrocyte clusters formed at the injury after short-term exposure to 320 mOsm following culture under various conditions.
Graphs represent pooled data for (a) average number of clusters formed (b) average number of cells in a cluster (c) percentage of cells involved in forming clusters (d) average volume of chondrocyte clusters (μm^3) and (e) average volume of individual cell in a cluster (μm^3) after exposure to 320 mOsm cultured in standard-DMEM and standard-FCS. Data were from [*N(n)*=8(24)]. * indicated a significant difference between two culture conditions at one time point according to t-test. # indicated a significant difference between different culture conditions at two time points according to one-way ANOVA followed by Tukey's multiple comparison post-hoc test. The single, double and triple symbols showed the level of significance for $P<0.05$, 0.01 and 0.001 respectively.

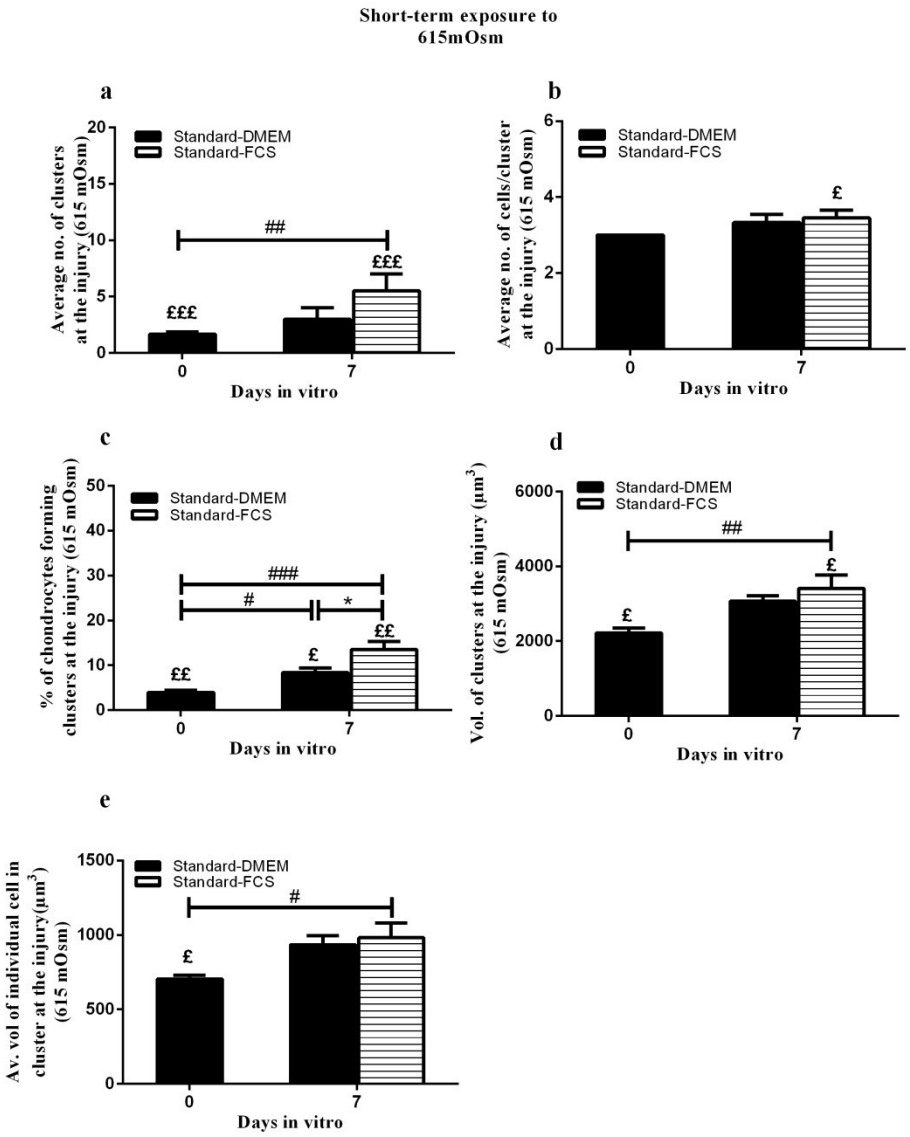

Figure 8.6B: Characteristics of chondrocyte clusters formed at the injury after short-term exposure to 615 mOsm following culture under various conditions.
Graphs represent pooled data for (a) average number of clusters formed (b) average number of cells in a cluster (c) percentage of cells involved in forming clusters (d) average volume of chondrocyte clusters (μm^3) and (e) average volume of individual cell in a cluster (μm^3) after exposure to 615 mOsm cultured in standard-DMEM and standard-FCS. Data were from [*N(n)*=8(24)]. * indicated a significant difference between two culture conditions at one time point according to t-test. # indicated a significant difference between different culture conditions at two time points according to one-way ANOVA followed by Tukey's multiple comparison post-hoc test. £ indicated significant difference between the two osmolarities. The single, double and triple symbols showed the level of significance for P<0.05, 0.01 and 0.001 respectively.

To summarise this section at day 0, in the explants exposed to 615 mOsm very few small sized clusters were formed as compared to 320 mOsm. During the course of culture, clustering was stimulated in the presence of FCS with fewer clusters after exposure to 615 mOsm as compared to 320 mOsm. After exposure to 320 mOsm the number of cells/cluster increased but the volume of individual cell in cluster remained unaffected. In contrast, after exposure to hyperosmolar solution the number of cells/cluster remained unaffected and the volume of individual cell in cluster increased significantly. The effects of FCS in terms of cluster formation appeared to be similar and more potent in the injured explants exposed to 320 mOsm as compared to 615 mOsm.

8.5.1.3.3 Development of abnormal chondrocyte morphology/volume by day 14

Chondrocytes exhibited marked shape changes at the injury by day 14 in the presence of FCS-DMEM but not in standard-DMEM. However, during the first week of culture chondrocyte morphology was relatively 'normal' under all culture conditions (Fig. 8.4c,d,e,f). Chondrocyte morphology at the injury remained unaffected and relatively 'normal' throughout the culture period in the injured explants exposed to 320 mOsm and 615 mOsm and cultured in standard-DMEM (Fig. 8.4g,i). However, marked changes to chondrocyte morphology/volume were seen in the explants exposed to both 320 mOsm and 615 mOsm and cultured in standard-FCS (Fig. 8.4h,j). The dramatic changes to chondrocyte morphology seen at the injury in the presence of FCS were characterised by cell flattening, elongation, enlargement and production of cytoplasmic processes.

Quantitative data regarding various parameters of morphology of chondrocytes were obtained (section 6.4.1.5) and compared at day 0 and 14 in various culture conditions. By day 14, at the injury 17±3% and 13±1% chondrocytes after short-term exposure to 320 mOsm and 615 mOsm respectively, showed significant morphological changes in standard-FCS as compared to chondrocytes in standard-DMEM (P=0.0003 and P<0.0001; respectively) and also in comparison to cells at day 0 (P<0.001; for both the conditions; Fig. 8.7a,b) where all the cells were relatively 'normal' in morphology. Additionally, at day 14 the percentage of abnormal chondrocytes at the injury in the presence of standard-FCS was significantly higher in the explants exposed to 320 mOsm as compared to 615 mOsm (P=0.04; Fig. 8.7b).

At day 14, chondrocyte volume was measured for all the four experimental conditions and compared with day 0. At day 0, the volume of chondrocytes at the injury was significantly higher in the explants exposed to 320 mOsm as compared to 615 mOsm (P<0.0001). The average volume of individual abnormal chondrocytes at the injury in the presence of standard-FCS at day 14 was significantly higher as compared to standard-DMEM (P<0.0001) and also in comparison to day 0 (P<0.001; Fig. 8.7c). The morphology of chondrocytes remained unaffected (spheroidal) but the volume of cells at the injury increased significantly by day 14 in the explants exposed to 615 mOsm and kept in culture with standard-DMEM (P<0.001). At day 14, the average volume of abnormal chondrocytes at the injury in the explants exposed to 615 mOsm and cultured in the presence of standard-FCS increased significantly as compared to standard-DMEM (P<0.0001) and also in comparison to day 0 (P<0.001; Fig. 8.7d). These results suggested that chondrocyte volume

increased after exposure to both the osmolarities and cultured in standard-FCS as compared to standard-DMEM. Moreover, by the end of culture period chondrocytes exposed to 615 mOsm and cultured in standard-DMEM displayed an increase in volume as compared to 320 mOsm and cultured in standard-DMEM.

At day 0, the average length of cell body of chondrocytes at the injury was significantly greater in the explants exposed to 320 mOsm as compared to 615 mOsm (P=0.02). By day 14 of culture, in the explants exposed to both the osmolarities (320 mOsm and 615 mOsm) the average length of cell bodies of individual abnormal cells at the injury in the presence of standard-FCS increased by approx. x5 as compared to standard-DMEM (P<0.0001; for both the conditions) and also in comparison to day 0 (P<0.001; for both the conditions; Fig. 8.7e,f). However, by day 14 the length of cell bodies of chondrocytes at the injury remained unaffected after exposure to both the osmolarities when the explants were cultured in standard-DMEM.

To summarise this section, marked heterogeneity of chondrocyte morphology was observed at the injury by day 14 in the presence of standard-FCS after exposure to both osmolarities and not in the presence of standard-DMEM. However, the effect of FCS appeared to be more pronounced on the morphology of chondrocytes which were exposed to 320 mOsm in comparison to 615 mOsm. Higher osmolarity helped to maintain normal chondrocyte morphology in the presence of FCS.

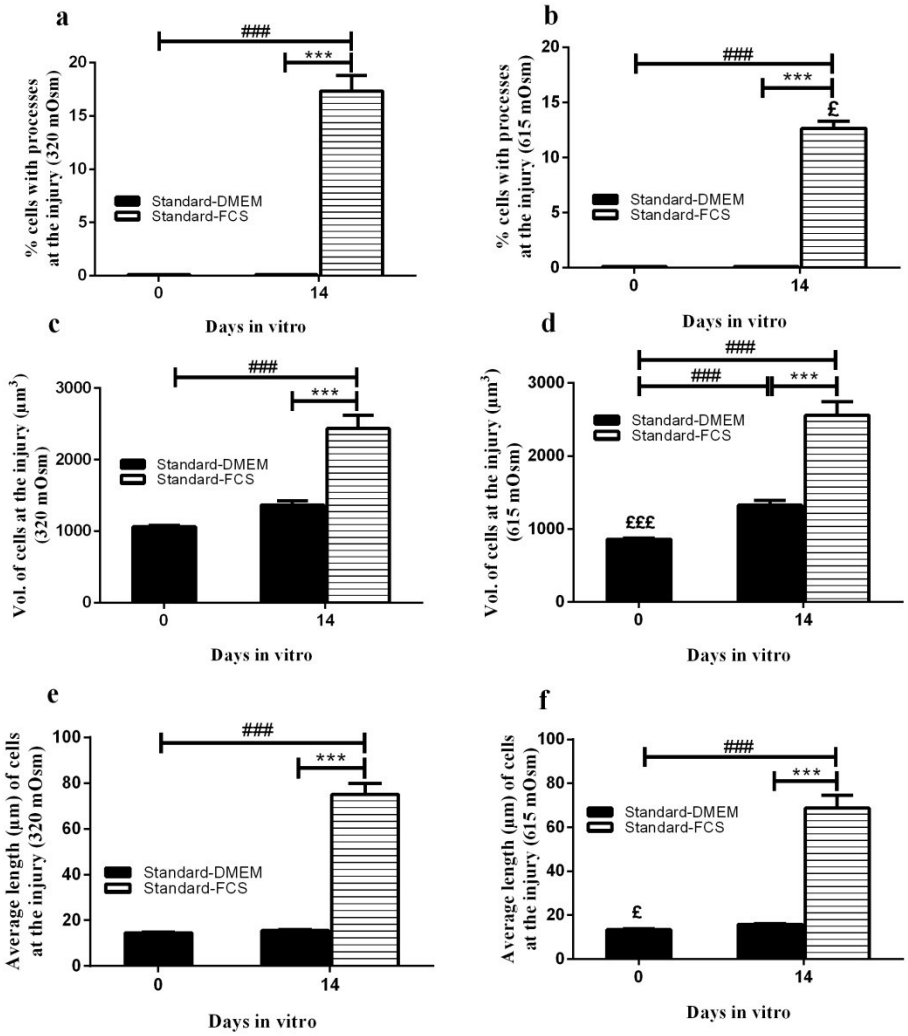

Figure 8.7: Characteristics of the heterogeneous nature of chondrocyte morphology at the injury by day 14 of culture in various conditions after short-term exposure to different osmolarities.

Graphs show pooled data regarding (a, b) percentage of abnormal cells at the injury after exposure to 320 mOsm and 615 mOsm, (c, d) average volume of cells at the injury (μm^3) after exposure to 320 mOsm and 615 mOsm and (e, f) average length of cell bodies (µm) of chondrocytes at the injury after exposure to 320 mOsm and 615 mOsm following culture in standard-DMEM and standard-FCS respectively. Data were from [*N(n)*=8(24)]. * indicated a significant difference between two culture conditions at one time point according to t-test. # indicated a significant difference between different culture conditions at two time points according to one-way ANOVA followed by Tukey's multiple comparison post-hoc test. £ indicated significant difference between the two osmolarities. The single, double and triple symbols showed the level of significance for $P<0.05$, 0.01 and 0.001 respectively.

8.5.2 Morphological characteristics of chondrocytes in injured cartilage after long-term exposure to culture media with varying osmolarities

Osmolarity and composition of the culture medium markedly affected chondrocyte viability, proliferation and morphology at the injury. Injured explants were exposed to two different osmolarities pre- and post-injury and then cultured in four different culture conditions (a) standard-DMEM (b) standard-FCS (c) hyperosmolar-DMEM and (d) hyperosmolar-FCS to assess the response of chondrocytes at the injury. Quantitative data regarding the width of injury, % of PI-labelled chondrocytes, volume, cluster formation and morphology of chondrocytes was obtained and described in the following sections.

8.5.2.1 *Changes to the width of injury after long-term exposure to varied osmolarities under various culture conditions*

The width of the injury was measured to determine the response of injured cartilage to the long-term exposure to various osmolarities and also to the nature of the culture media used. During two weeks of culture, different osmolarities and the nature of the culture media strikingly affected the width of the injury.

During the first week of culture, the width of the injury remained unaffected in the injured explants cultured in the presence of standard-DMEM. However, by day 14 the width of injury increased significantly in the presence of standard-DMEM as compared to earlier time points ($P<0.001$; Fig. 8.8a). In the injured explants cultured with standard-FCS, the width of the injury remained unaffected by day 3 of culture, increased significantly by day 7 as compared to standard-DMEM ($P<0.0001$) and also in comparison to earlier time points ($P<0.001$). However, by day 14 the width of injury decreased significantly in the presence of standard-FCS as compared to

standard-DMEM (P<0.0001) and also in comparison to all the earlier time points (P<0.05; Fig. 8.8a). In the injured explants cultured in the presence of hyperosmolar-DMEM, the width of the injury remained unaffected throughout the culture period (P>0.05; Fig. 8.8b). In the explants cultured in the presence of hyperosmolar-FCS, the width of the injury increased significantly by day 3 as compared to hyperosmolar-DMEM (P=0.0001) and also in comparison to day 0 (P<0.01). By day 7, the width of the injury in these explants was greater than hyperosmolar-DMEM *(P*=0.0002). However, by day 14 the width of injury decreased significantly in these explants as compared to the earlier time points (Days 3 and 7) of culture (P<0.01; Fig. 8.8b).

The width of the injury was also compared in the explants kept in culture following long-term exposure to standard and hyperosmolar DMEM and FCS. The width of the injury was significantly less in the explants cultured in the presence of hyperosmolar-DMEM as compared to standard-DMEM throughout the culture period (P<0.001; Fig. 8.8b). Moreover, the width of injury was significantly less in the explants cultured with hyperosmolar-FCS as compared to standard-FCS (P=0.0002) at day 7 and no difference existed between the two culture conditions at day 3 and 14 of culture.

To summarise, during the course of culture, the width of injury increased significantly in the presence of standard-DMEM by day 14. However, in the presence of hyperosmolar-DMEM the width of injury remained unaffected throughout the culture period. In the presence of standard-FCS, the width of injury increased initially by day 7 but decreased markedly by day 14 of culture. However,

in hyperosmolar-FCS the width of injury increased initially by day 3 and decreased strikingly by day 14 of culture.

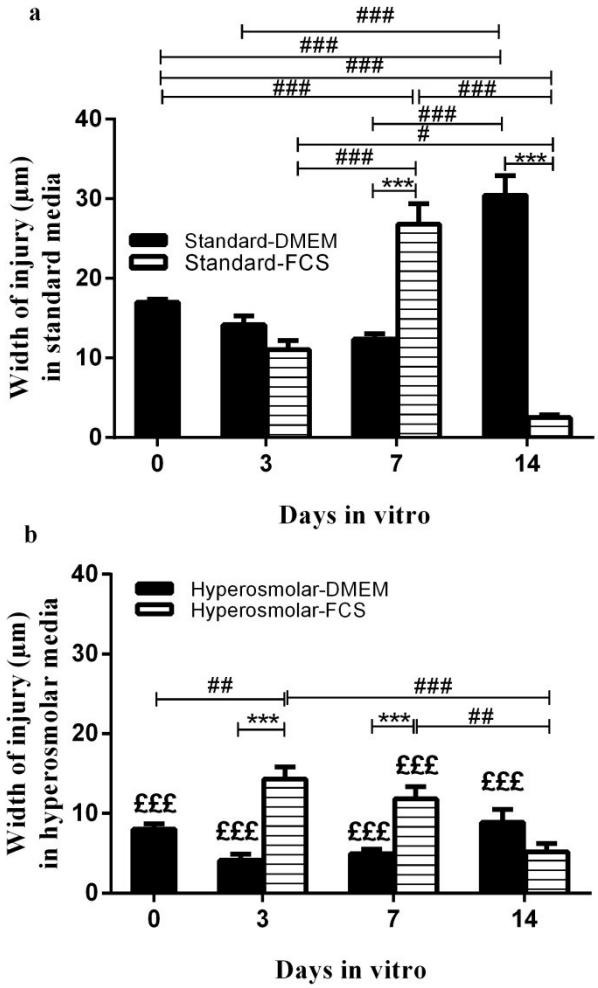

Figure 8.8: Changes to the width of injury after long-term exposure to varied osmolarities.

Graphs display pooled data giving a comparison between the long-term exposure to (a) 320 mOsm, cultured in either standard-DMEM or standard-FCS and (b) 615 mOsm, cultured in either hyperosmolar-DMEM or hyperosmolar-FCS. Data were from [*N(n)*=8(42)]. * indicated a significant difference between two culture conditions at one time point according to t-test. # indicated a significant difference between different culture conditions at various time points according to one-way ANOVA followed by Tukey's multiple comparison post-hoc test. £ indicated significant difference between the two osmolarities. The single, double and triple symbols showed the level of significance for $P<0.05$, 0.01 and 0.001 respectively.

8.5.2.2 *Loss of PI-labelled chondrocytes at the injury after long-term exposure to varied osmolarities*

The percentage of PI-labelled chondrocytes was measured within the specified ROIs applied at the injury on the low magnification CLSM images of injured cartilage following culture in media of different osmolarities. The values of percentage of PI-labelled cells were obtained at various time points (Days 0, 3, 7 and 14) during the course of culture and compared to assess the effect of long-term exposure of varied osmolarities and the nature of the culture medium used on the percentage of PI-labelled chondrocytes at the injury. Different osmolarities and the nature of the culture media used strikingly affected the percentage of PI-labelled chondrocytes at the injury (Fig. 8.9. a-n).

Throughout the culture, the percentage of PI-labelled chondrocytes at the injury remained unaffected in the explants cultured in the presence of standard- and hyperosmolar-DMEM ($P>0.05$; Fig. 8.10b). However, the percentage of PI-labelled chondrocytes decreased significantly at the injury in the presence of standard- and hyperosmolar-FCS as compared to standard- and hyperosmolar-DMEM respectively at days 3, 7 and 14 of culture ($P\leq0.001$; Fig. 8.10a, b) and also in comparison to day 0 ($P<0.001$).

The percentage of PI-labelled chondrocytes was also compared between the explants cultured in standard and hyperosmolar media. The percentage of PI-labelled

chondrocytes was significantly less in the explants cultured in the presence of hyperosmolar-DMEM as compared to standard-DMEM throughout the culture period ($P<0.0001$, $P<0.0001$, $P=0.0004$, $P<0.0001$; for days 0, 3, 7 and 14 respectively; Fig. 8.10b). However, in the presence of FCS no difference existed between the standard- and hyperosmolar-FCS at days 7 and 14 of culture. Only at day 3, the percentage of PI-labelled chondrocytes was significantly less in the presence of hyperosmolar-FCS as compared to standard-FCS ($P=0.001$; Fig. 8.10a,b).

These results suggested that the percentage of PI-labelled chondrocytes at the injury was significantly less in the explants cultured in the presence of hyperosmolar-DMEM as compared to standard-DMEM throughout the culture period. Additionally, there was a significant reduction in the percentage of PI-labelled chondrocytes in the explants cultured in the presence of FCS as compared to DMEM irrespective of the osmolarities of culture media throughout the culture period.

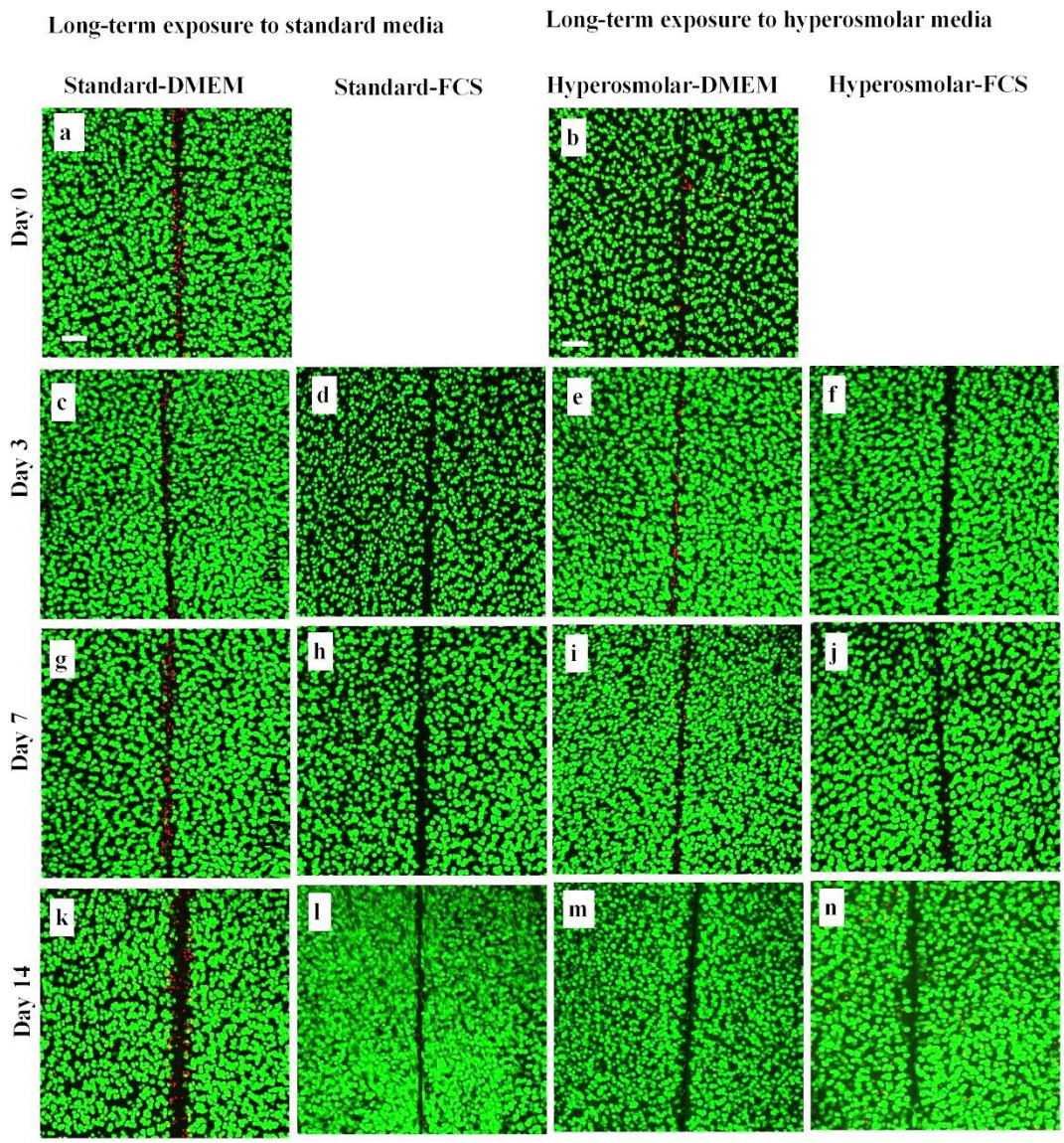

Figure 8.9: Axial CLSM reconstructions of injured cartilage explants after long-term exposure to varied osmolarities.

CLSM reconstructions of low power (x10) magnification images of injured cartilage of CMFDA and PI labelled chondrocytes (live/dead cells respectively). The two left panels show images of injured cartilage after long-term exposure to standard media and two right panels contain images after long-term exposure to hyperosmolar media at (a,b) day 0, (c,d,e,f) day 3, (g,h,i,j) day 7 and (k,l,m,n) day 14 cultured in DMEM and FCS respectively. Scale bar for all panels = 100 μm.

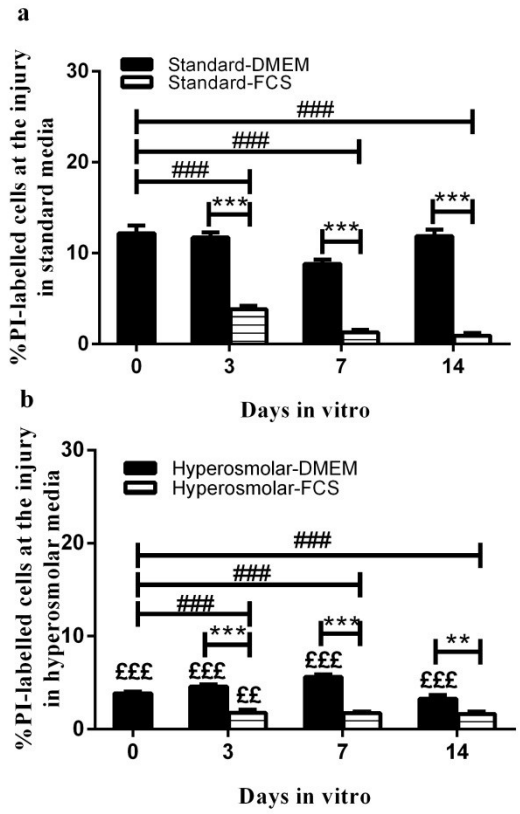

Figure 8.10: The percentage of PI-labelled chondrocytes at the injury after long-term exposure to different osmolarities in various culture conditions.
Graphs show pooled data to compare the percentage of PI-labelled chondrocytes at the injury after long-term exposure to (a) standard media and (b) hyperosmolar media cultured in DMEM and FCS. Data were from [*N(n)*=8(58)]. * indicated a significant difference between two culture conditions at one time point according to t-test. # indicated a significant difference between different culture conditions at various time points according to one-way ANOVA followed by Tukey's multiple comparison post-hoc test. £ indicated significant difference between the two osmolarities. The single, double and triple symbols showed the level of significance for $P<0.05$, 0.01 and 0.001 respectively.

8.5.2.3 *Changes to the volume/morphology of chondrocytes at the injury after long-term exposure to two osmolarities in standard-DMEM and FCS-DMEM*

Long-term exposure to two different osmolarities and the nature of the culture medium had a pronounced effect on the volume/morphology of chondrocytes at the

injury. Quantitative data regarding volume, cluster formation and heterogeneous nature of chondrocyte morphology following culture in different culture conditions was obtained at various time points and compared. The results acquired are given in the following sections.

8.5.2.3.1 Changes to volume/cluster formation of chondrocytes at the injury by day 7

The morphology of chondrocytes was markedly altered in the explants cultured in the presence of standard-FCS as compared to hyperosmolar-FCS and also in comparison to standard-DMEM and hyperosmolar-DMEM (Fig. 8.11) where chondrocyte morphology remained unaffected (spheroidal).

8.5.2.3.1.1 Chondrocyte volume

Following culture, by day 7 the volume of chondrocytes at the injury increased significantly in the explants exposed to 615 mOsm and cultured in the presence of hyperosmolar-DMEM ($P<0.001$). However, at day 7, the volume of chondrocytes exposed to 615 mOsm and cultured in the presence of hyperosmolar-FCS increased significantly as compared to hyperosmolar-DMEM ($P=0.0019$) and also in comparison to day 0 ($P<0.001$; Fig. 8.12b), but was found to be significantly less than those in standard-FCS ($P=0.01$).

These results suggested that by day 7, the volume of chondrocytes in standard-DMEM remained unaffected but increased significantly in the presence of hyperosmolar-DMEM. Moreover, the volume of chondrocytes increased significantly in the presence of FCS as compared to DMEM in both the osmolarities,

but the effect was more pronounced in the presence of standard-FCS as compared to hyperosmolar-FCS.

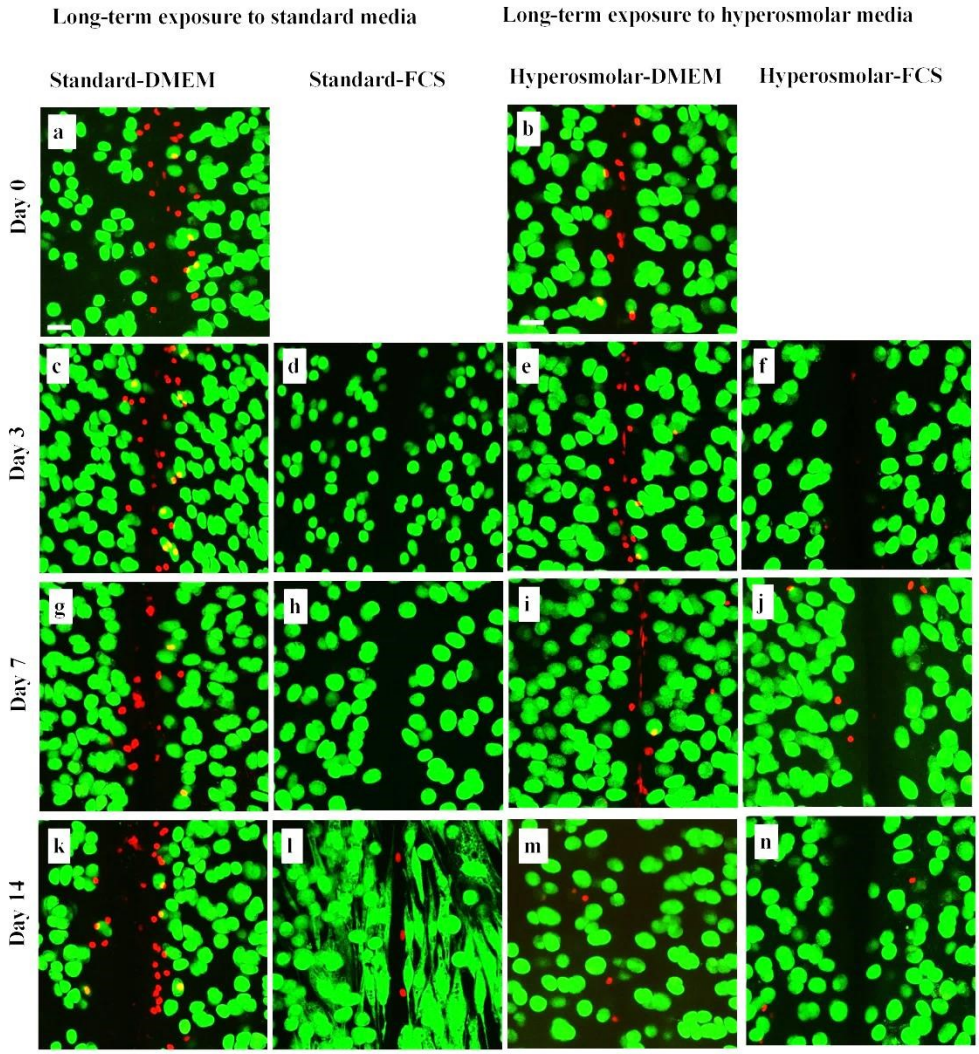

Figure 8.11: Axial CLSM reconstructions of injured cartilage explants cultured for long-term in various osmolarities with DMEM and FCS.
CLSM reconstructions of high power (x40DW) magnification images of CMFDA/PI labelled chondrocytes (Live and dead cells respectively). The two left panels contain images of explants exposed to 320 mOsm (a) at day 0, (c, d) at day 3, (g, h) at day 7 and (k, l) at day 14 of culture in the presence of standard-DMEM and standard-FCS respectively. The two right panels contain images of explants exposed to 615 mOsm (b) at day 0, (e, f) at day 3, (i, j) at day 7 and (m, n) at day 14 of culture in the presence of hyperosmolar-DMEM and hyperosmolar-FCS respectively. Scale bar for all panels = 25 μm.

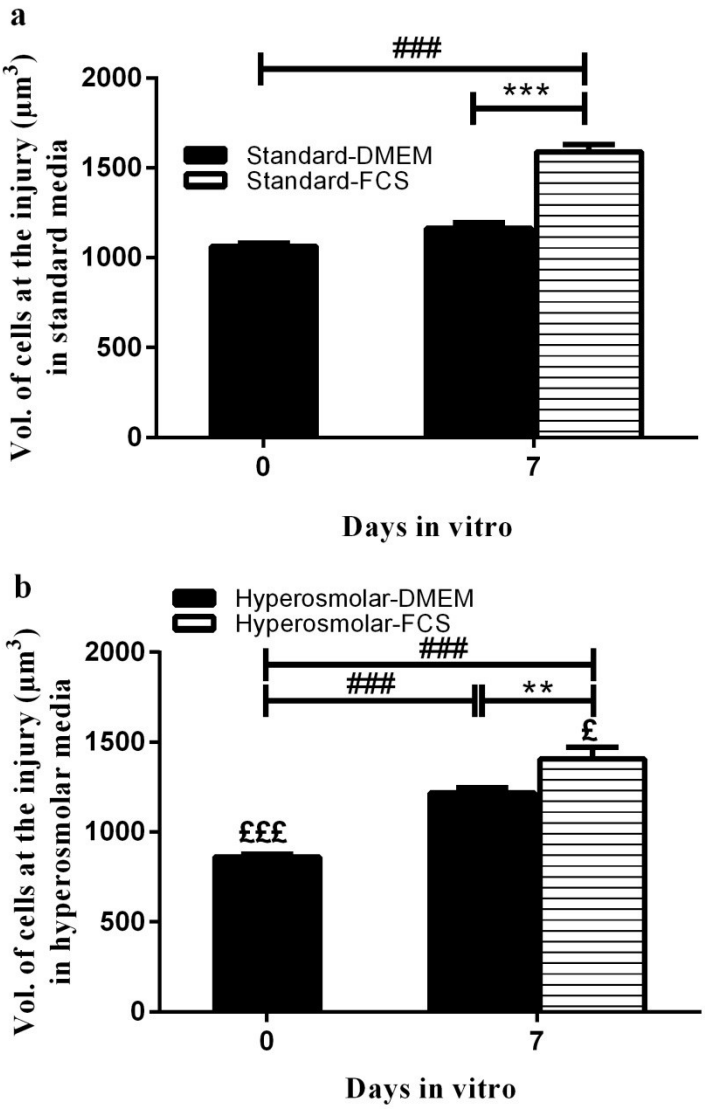

Figure 8.12: Changes to chondrocyte volume at the injury after long-term exposure to various osmolarities.

Graphs contain pooled data to compare the volume of chondrocytes at the injury following culture in (a) standard-DMEM/FCS and (b) hyperosmolar-DMEM/FCS. Data were from [*N(n')*=8(98) at day 0, 8(83) and 8(81) at day 7 in standard-DMEM and standard-FCS respectively] and [*N(n')*=8(116) at day 0, 8(93) and 8(42) at day 7 in hyperosmolar-DMEM and hyperosmolar-FCS respectively]. * indicated a significant difference between two culture conditions at one time point according to t-test. # indicated a significant difference between different culture conditions at two time points according to one-way ANOVA followed by Tukey's multiple comparison post-hoc test. £ indicated significant difference between the two osmolarities. The single, double and triple symbols showed the level of significance for $P<0.05$, 0.01 and 0.001 respectively.

8.5.2.3.1.2 Chondrocyte clusters

8.5.2.3.1.2.1 Number of clusters

At day 7, in the presence of standard-FCS the number of clusters at the injury increased significantly as compared to standard-DMEM (P=0.02) and also in comparison to day 0 (P<0.01; Fig. 8.13Aa). At day 7, the number of clusters increased significantly in the presence of hyperosmolar-FCS as compared to day 0 (P<0.05; Fig. 8.13Ba). Moreover, by day 7, the average number of clusters remained significantly lower in the presence of hyperosmolar-DMEM and hyperosmolar-FCS as compared to standard-DMEM and standard-FCS respectively (P=0.04; for both the conditions; Fig. 8.13Ba). These results suggested that hyperosmolarity inhibits cluster formation.

8.5.2.3.1.2.2 Number of cells per cluster

At day 7, the number of cells per cluster increased significantly in the presence of standard-FCS as compared to day 0 (P<0.05; Fig. 8.13Ab) and remained unaffected in all the other culture conditions (P>0.05; Figs. 8.13Ab and 8.13Bb).

8.5.2.3.1.2.3 Percentage of chondrocytes forming clusters

At day 7, in the injured explants exposed to 320 mOsm and cultured in the presence of standard-FCS a significantly higher percentage of chondrocytes formed clusters (24±3%) as compared to standard-DMEM (11±1%; P=0.01) and also in comparison to day 0 (7±1%; P<0.001; Fig. 8.13Ac). Similarly, in the injured explants exposed to

615 mOsm and cultured in hyperosmolar-FCS a significantly higher percentage of chondrocytes formed clusters (14±0.5%) as compared to hyperosmolar-DMEM (5±1%; P=0.006) and also in comparison to day 0 (4±0.5%; P<0.001; Fig. 8.13Bc). However, by day 7 in the explants exposed to 615 mOsm a significantly less percentage of chondrocytes formed clusters in hyperosmolar-DMEM and hyperosmolar-FCS as compared to standard-DMEM and standard-FCS respectively (P=0.03 & P=0.04 respectively).

8.5.2.3.1.2.4 Volume of clusters

At day 7, the volume of clusters remained unaffected in the explants cultured in standard-DMEM but increased significantly in the presence of hyperosmolar-DMEM as compared to day 0 (P<0.05). At day 7, in the explants exposed to 320 mOsm and 615 mOsm and cultured in the presence of standard- and hyperosmolar-FCS respectively, the volume of clusters increased significantly as compared to standard- and hyperosmolar-DMEM respectively (P=0.03 and P=0.04 respectively) and also in comparison to day 0 (P<0.001; for both the conditions; Figs. 8.13Ad and 8.13Bd).

8.5.2.3.1.2.5 Volume of individual cells in a cluster

The volume of individual cells in a cluster was calculated and compared in all the four culture conditions at day 0 and 7. At day 7, in the explants exposed to 320 mOsm and cultured with standard-FCS the average volume of individual cells in a cluster increased significantly in comparison to day 0 (P<0.001; Fig. 8.13Ae). At day 7, in the injured explants exposed to 615 mOsm and kept in culture with hyperosmolar-DMEM and hyperosmolar-FCS, the volume of individual cells in a

cluster increased significantly in comparison to day 0 (P<0.05 and P<0.001 respectively; Fig. 8.13Be).

To summarise this section in the presence of standard- and hyperosmolar-FCS clustering was triggered resulting in the formation of numerous, large-sized clusters as compared to standard- and hyperosmolar-DMEM. However, the effects of standard-FCS were significantly more marked as compared to hyperosmolar-FCS. Therefore, hyperosmolarity inhibited cluster formation at the injury even in the presence of FCS, suggesting the antagonising action of raised osmolarity on the proliferative effects of factors present in serum.

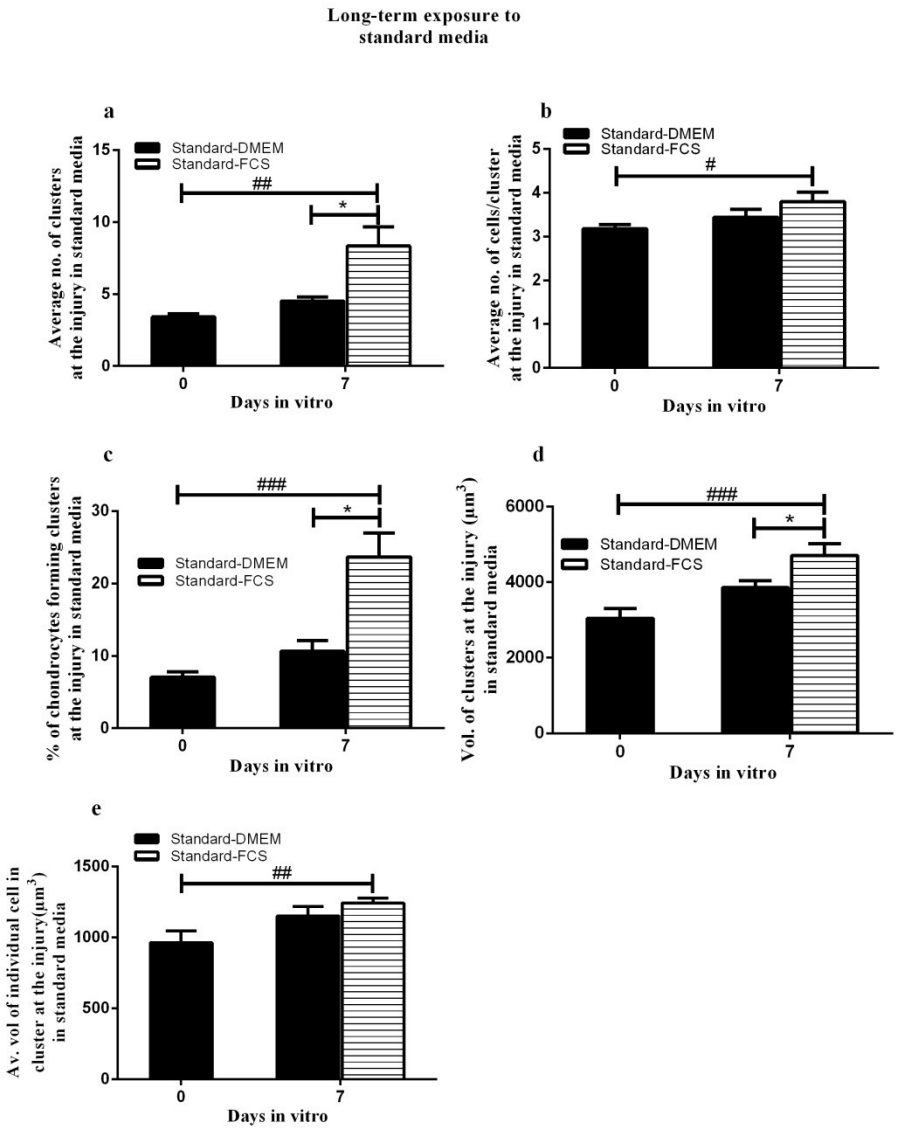

Figure 8.13A: Characteristics of clusters formed at the injury in the injured explants after long-term exposure to standard culture media.

The graphs contain pooled data regarding (a) average number of clusters formed (b) average number of cells in a cluster (c) percentage of cells involved in forming clusters (d) average volume of chondrocyte clusters (μm^3) and (e) average volume of individual cells in a cluster (μm^3) after exposure to 320 mOsm, cultured in standard-DMEM/FCS. Data were from [*N(n)*=8(26)]. * indicated a significant difference between two culture conditions at one time point according to t-test. # indicated a significant difference between different culture conditions at two time points according to one-way ANOVA followed by Tukey's multiple comparison post-hoc test. The single, double and triple symbols showed the level of significance for $P<0.05$, 0.01 and 0.001 respectively.

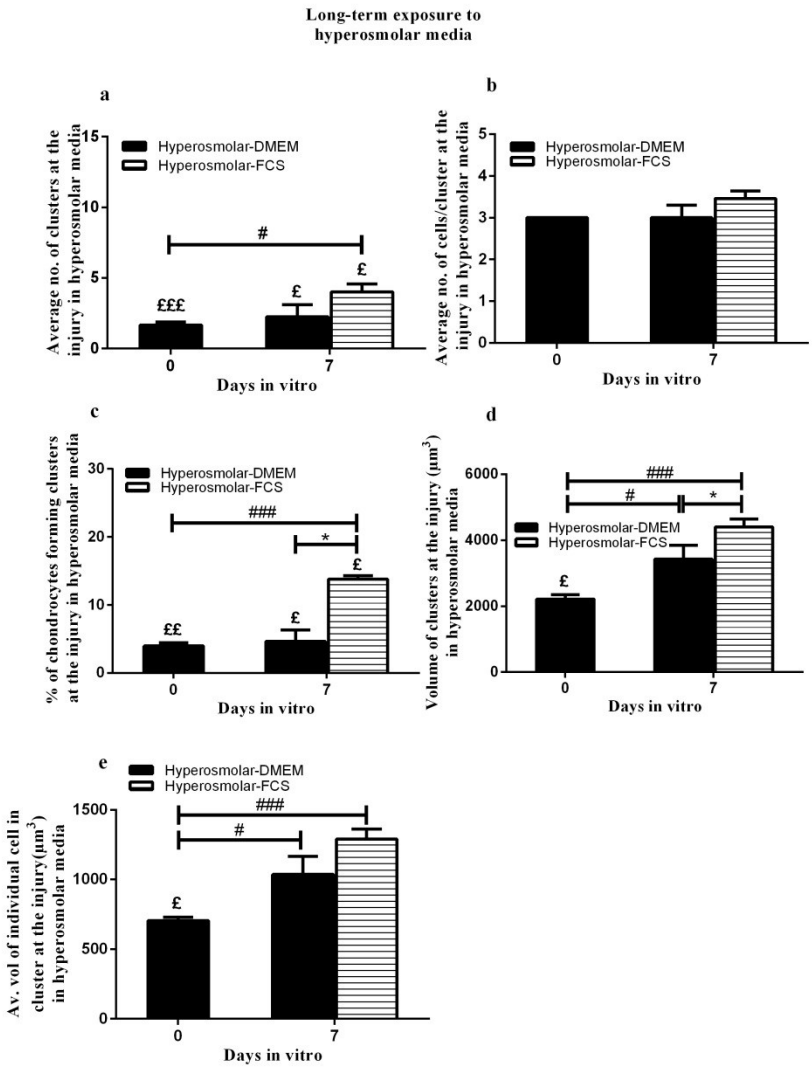

Figure 8.13B: Characteristics of clusters formed at the injury in the injured explants after long-term exposure to hyperosmolar culture media.

The graphs contain pooled data regarding (a) average number of clusters formed (b) average number of cells in a cluster (c) percentage of cells involved in forming clusters (d) average volume of chondrocyte clusters (μm^3) and (e) average volume of individual cells in a cluster (μm^3) after exposure to 615 mOsm, cultured in hyperosmolar-DMEM/FCS. Data were from [*N(n)*=8(26)]. * indicated a significant difference between two culture conditions at one time point according to t-test. # indicated a significant difference between different culture conditions at two time points according to one-way ANOVA followed by Tukey's multiple comparison post-hoc test. £ indicated significant difference between the two osmolarities. The single, double and triple symbols showed the level of significance for $P<0.05$, 0.01 and 0.001 respectively.

8.5.2.3.2 Development of abnormal chondrocyte volume/morphology at the injury after long-term exposure to varied osmolarities by day 14

Marked heterogeneity to chondrocyte morphology was observed at the injury in the explants exposed to 320 mOsm and kept in culture in the presence of standard-FCS by day 14 (Fig. 8.11l). The morphology of chondrocytes remained unaffected and relatively 'normal' at days 0, 3 and 7 of culture. However, at day 14 only in the explants cultured with standard-FCS chondrocytes displayed marked shape changes in terms of elongation of cell bodies, cell enlargement, flattening and production of cytoplasmic processes from cell bodies. Chondrocyte morphology was unaffected following culture in standard-DMEM, hyperosmolar-DMEM and hyperosmolar-FCS (Fig. 8.11k,m&n respectively). Quantitative data regarding volume, length of cell bodies and percentage of abnormal chondrocytes with processes was obtained and compared in all the four culture conditions at days 0 and 14 of culture.

8.5.2.3.2.1 Chondrocyte morphology

At day 0, the morphology of chondrocytes was spheroidal and relatively normal in the injured explants exposed to 320 mOsm and 615 mOsm. At day 14, the percentage of abnormal chondrocytes at the injury was significantly higher in the explants cultured in standard-FCS as compared to standard-DMEM (P=0.006), in comparison to day 0 (P<0.01; Fig. 8.14a) and also in comparison to hyperosmolar-FCS (P=0.006; Fig. 8.14b) where all the cells were relatively 'normal'. In addition, the explants exposed to 615 mOsm and cultured with hyperosmolar-DMEM also displayed no morphological changes to chondrocytes at the injury.

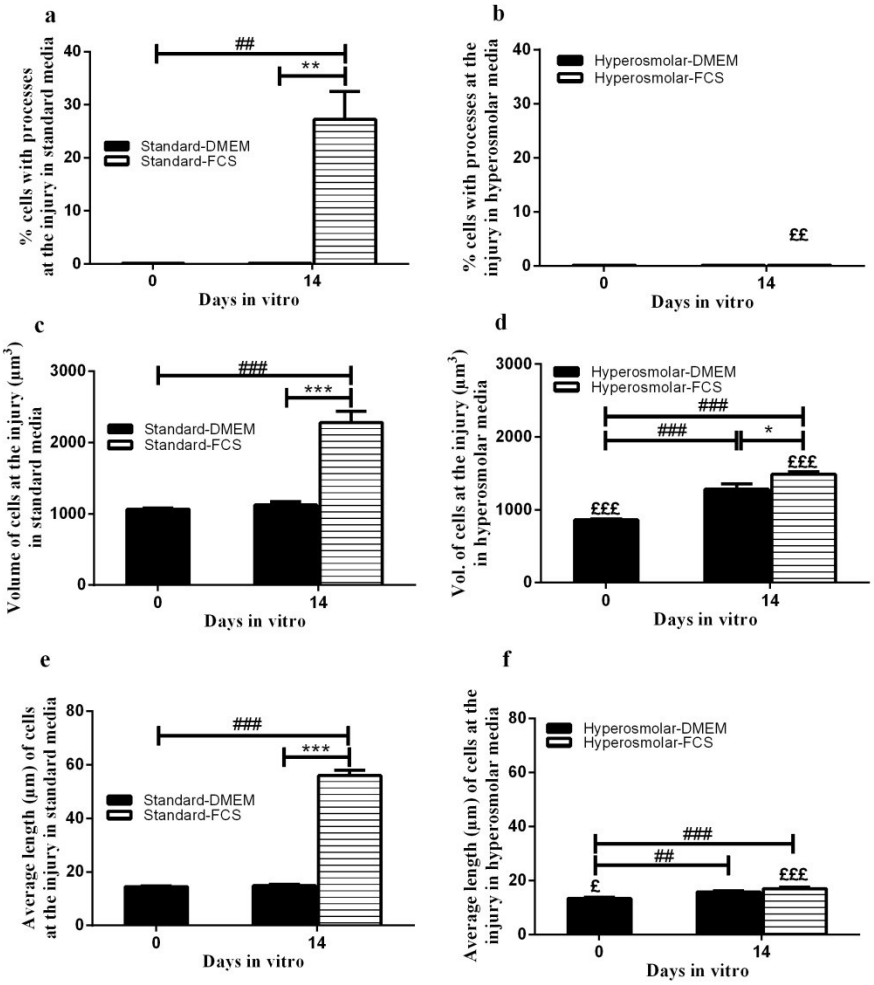

Figure 8.14: Characteristics of heterogeneous nature of chondrocyte morphology at the injury following long-term exposure to varied osmolarities in different culture conditions.

Graphs in the left panels display pooled data for (a) % of abnormal cells (c) average volume of cells (μm^3) and (e) average length of cell bodies (µm) at the injury in the presence of standard-DMEM/FCS. The right panels contain graph which show pooled data for (b) % of abnormal cells (d) average volume of cells (μm^3) and (f) average length of cell bodies (µm) at the injury in the presence of hyperosmolar-DMEM/FCS. Data were from [*N(n)*=8(24)]. * indicated a significant difference between two culture conditions at one time point according to t-test. # indicated a significant difference between different culture conditions at two time points according to one-way ANOVA followed by Tukey's multiple comparison post-hoc test. £ indicated significant difference between the two osmolarities. The single, double and triple symbols showed the level of significance for $P<0.05$, 0.01 and 0.001 respectively.

8.5.2.3.2.2 Chondrocyte volume

At day 14, the average volume of individual abnormal chondrocytes following culture in standard-FCS was significantly greater than standard-DMEM (P<0.0001) and also in comparison to day 0 (P<0.001; Fig. 8.14c) where all the cells were relatively 'normal'. However, in the explants exposed to 615 mOsm and cultured in the presence of hyperosmolar-DMEM and hyperosmolar-FCS the morphology of chondrocytes remained unaffected (spheroidal) but the volume increased significantly as compared to day 0 (P<0.001; for both the conditions; Fig. 8.14d). However, the volume of chondrocytes at day 14, in hyperosmolar-FCS was significantly greater than hyperosmolar-DMEM (P=0.01; Fig. 8.14d). Moreover, the average volume of relatively 'normal' chondrocytes at the injury in hyperosmolar-FCS was significantly less than the volume of individual abnormal cells at injury in standard-FCS (P<0.0001; Fig. 8.14d).

8.5.2.3.2.3 Length of cell bodies of chondrocytes

At day 0 the average length of cell bodies of chondrocytes was significantly greater in the explants exposed to 320 mOsm (14.5±0.3µm) as compared to 615 mOsm (13.4±0.4µm; P=0.02; Fig. 8.14f). At day 14, in the injured explants exposed to 320 mOsm and cultured in the presence of standard-FCS the average length of individual abnormal cells at the injury (56±2µm) increased approx. x4 as compared to standard-DMEM (15±4µm) and also in comparison to day 0 (14.5±0.3µm; P<0.001 for both the conditions; Fig. 8.14e). At day 14, the length of cell bodies of chondrocytes increased significantly in the explants exposed to 615 mOsm and cultured in

hyperosmolar-DMEM (16±0.4μm) and hyperosmolar-FCS (17±0.4μm) as compared to day 0 (13.4±0.4μm; $P<0.01$ and $P<0.001$ respectively; Fig. 8.14f). Additionally the average length of cell bodies of abnormal chondrocytes at the injury in the presence of standard-FCS was approx. x3 greater than the average length of relatively 'normal' chondrocytes in hyperosmolar-FCS ($P<0.0001$; Fig. 8.14f).

To summarise this section, chondrocyte volume/morphology changed strikingly at the injury in the explants cultured in the presence of standard-FCS. However, the morphology of chondrocytes remained unaffected (spheroidal) in the injured explants cultured in the presence of standard-DMEM, hyperosmolar-DMEM and hyperosmolar-FCS.

8.6 DISCUSSION

The hypothesis was that chondrocytes at the injury do not produce morphological changes in response to hyperosmolar serum-rich medium compared with exposure to standard serum-rich culture medium. The experiments described in this study were performed on two groups where in group I the effect of short-term exposure of hyperosmolarity on chondrocyte morphology was determined. The results suggested that after exposure to hyperosmolar solution, cell proliferation and cluster formation was inhibited. Although, at the site of injury marked changes to morphology were observed in the presence of FCS, but the effect was less pronounced after exposure to hyperosmolar solution. In group 2 the effect of long-term exposure of hyperosmolarity was studied. The results suggested that by increasing the osmolarity of serum-rich culture medium the clustering was inhibited and chondrocytes

maintained their normal (spheroidal) morphology at the injury. In other words hyperosmolarity reversed the effects of FCS.

The scalpel injured bovine cartilage model utilised in this study was a reproducible and controlled model (section 6.5.1). However, when the cartilage explants were exposed to 320 mOsm and 615 mOsm and then injured following the standardised injury protocol, it was observed that the explants exposed to hyperosmolar solution 'felt' tougher to produce injury. The quantitative data at day 0, regarding the width of injury also showed that the width of injury was markedly less in the explants exposed to hyperosmolar solution (Fig. 8.2). In a very recent *in vivo* study on injured rat cartilage no difference in width of injury was reported after exposure to hyperosmolar saline (600 mOsm) in comparison to normal saline (300 mOsm) (Eltawil et al., 2014). This dissimilarity in results regarding width of injury after exposure to hyperosmolar solution can be attributed to the differences in the tissue architecture/composition of rat and bovine cartilage samples. In order to explain the results from the present study one possible explanation could be that exposure of cartilage to hyperosmolar environment caused water withdrawal from the tissue rendering the matrix more resilient and difficult to produce the same injury as that experienced in lower osmolarity. The width of the injury remained unaffected after short-term exposure to 615 mOsm following culture in standard-DMEM (Fig. 8.2). Similarly the width of the injury remained unaffected in the explants after long-term exposure to hyperosmolar-DMEM (Fig. 8.8). The possible explanation could be that by providing hyperosmolar environment to cartilage, chondrocytes at the injury functioned normally because several processes within chondrocytes are known to be regulated by hyperosmotic environment (Tew et al., 2011). Thus possibly the normal

biosynthetic functions of chondrocytes led to less catabolism and the matrix was not destroyed further and width of the injury remained unaffected. In comparison to this in the injured explants cultured in the presence of hyperosmolar-FCS, during long-term exposure to raised osmolarity there was an initial increase in the width of injury by day 3 and later on by day 14 it decreased markedly (Fig. 8.8). One possible explanation for these changes in the width of injury could be that in the earlier days of culture due to injury there was collagen loss and increased tissue hydration leading to swelling of tissue and increase in the width of injury (Maroudas, 1976). The decrease in the width of injury during later stages of culture in the hyperosmolar environment could possibly be explained by the previously reported findings where ECM synthesis was seen to be regulated by SOX9 (Bell et al., 1997, Bi et al., 1999) and expression of SOX9 was increased by hyperosmotic environment (Tew et al., 2009). Therefore, by raising the osmolarity of the culture medium chondrocytes at the injury possibly expressed high levels of SOX9 thereby enhancing ECM synthesis leading to decrease in the width of injury.

The percentage of PI-labelled chondrocytes at day 0 was significantly less in the explants exposed to 615 mOsm (hyperosmolar) solutions as compared to 320 mOsm and this in agreement with the previous work stating the chondroprotective effect of hyperosmolar solution on injured cartilage (Amin et al., 2008b, Eltawil et al., 2014). At day 0, by raising the osmolarity initially chondrocytes at the injury were shrunken (Figs. 8.5 & 8.12). During the course of culture by day 7, following short- and long-term exposure to hyperosmolarity volume of chondrocytes increased and chondrocytes restored their original volume when cultured in standard-DMEM (Figs. 8.5b & 8.12b). This phenomenon can be well explained by considering the RVI by

chondrocytes to restore their volume (Hall et al., 1996a, Kerrigan et al., 2006). The volume of chondrocytes increased markedly in the presence of FCS as compared to DMEM irrespective of short- and long-term exposure to both osmolarities (Figs. 8.5 & 8.12). However, this stimulatory effect of FCS on chondrocyte volume was considerably less effective in the explants exposed to hyperosmolar environment for long-term thereby, suggesting that osmolarity is a more powerful regulator of chondrocyte volume or morphology. In other words the effects of FCS can be reversed by raising the medium osmolarity.

In this injured bovine articular cartilage model, cluster formation was routinely observed in some of the culture conditions. Typically in healthy bovine superficial zone of cartilage, chondrocytes are arranged as pairs (Sasazaki et al., 2008). Apart from chondrocytes occurring in pairs few small sized clusters with no more than three cells per cluster were also observed in healthy cartilage. These small sized clusters were more frequent in the explants exposed to 320 mOsm as compared to 615 mOsm (Figs. 8.6Aa,8.6Ba & 8.13Aa,8.13Ba). One possible explanation for these findings is that when cartilage was exposed to 320 and 615 mOsm the chondrocytes were swollen and shrunken respectively. The swollen cells in lower osmolarity possibly appeared to be closer together and were segmented as clusters by the Volocity^{TM} software. This could be considered as an artefact of the software and excluded from the data but in this thesis we have considered 3 cells together a cluster and included in data analysis. The definition of cluster utilised in the present study is based upon a previous definition of cluster (McGlashan et al., 2008). This explanation possibly justifies the presence of clusters on day 0 after exposure to 320 mOsm. In the presence of FCS clustering was stimulated and numerous large sized

clusters having 3-8 cells per cluster were formed as compared to standard-DMEM which could be well explained as a consequence of the stimulatory effect of growth factors present in serum (Khan et al., 2010).

A very interesting finding in this study was the inhibitory effect of hyperosmolarity on the chondrocyte cluster formation following short- and long-term exposure to two osmolarities (Figs. 8.6A,B & 8.13A,B). These findings are in agreement with the previously reported study where chondrocyte proliferation rate decreased at 550 mOsm as compared to 280 mOsm (Xu et al., 2010). In summary, hyperosmolarity inhibited several effects of FCS as listed below:

- Hyperosmolarity inhibited increase in the width of injury by day 7 of culture
- Hyperosmolarity inhibited increase in the volume of chondrocytes at injury
- Hyperosmolarity inhibited cluster formation at the injury
- Hyperosmolarity prevented morphological changes to chondrocytes at injury

These results suggested that by raising the osmolarity of the culture medium most of the effects of FCS can possibly be inhibited or reversed.

The osmosensitive nature of chondrocytes regarding volume changes in healthy and degenerate cartilage (Bush and Hall, 2001a, Bush and Hall, 2005) and matrix production is already known (Urban et al., 1993, Negoro et al., 2008). However, the results of present study build up on the previous knowledge by reporting that effects of FCS on chondrocyte morphology can possibly be reversed by hyperosmolarity. The results presented in this chapter have highlighted two key findings regarding morphological changes of chondrocytes. The first finding was that when explants were exposed for short-term to hyperosmolar solution (615 mOsm) and cultured in

the presence of standard-FCS, by day 14 significantly less percentage of chondrocytes (13±1%) at the injury displayed morphological changes as compared to 320 mOsm (17±3%; *P*=0.04; Fig. 8.7a,b). The second key finding was that when explants were exposed for long-term to hyperosmolar-FCS culture medium, even after two weeks of culture chondrocytes maintained their normal morphology and were spheroidal in shape (Fig. 8.14). This suggested two possibilities that either hyperosmolarity itself or through inhibition of morphogenic factors in serum regulated chondrocyte morphology. Therefore, by raising the osmolarity of the culture medium morphological changes to chondrocytes in the presence of serum could be prevented. One explanation could be that chondrocyte phenotype is known to be regulated by SOX9 transcription factor (Tew et al., 2005) and this factor in turn is controlled by hyperosmolarity (Tew et al., 2009). Therefore, it is possible that in the present study under the effect of hyperosmolar culture environment the expression of SOX9 may be enhanced thereby maintaining normal chondrocyte phenotype with normal (spheroidal/ellipsoidal) morphology.

In a later study it has been reported that chondrocytes close to the injury produced cytoplasmic processes in the presence of serum-rich medium (Lyman et al., 2012). However, the study presented here has added to the previous work by Lyman and co-workers in two ways. Firstly, by short-term exposure to hyperosmolar solution the proliferative and morphogenic effects of FCS can be reduced, Secondly, by raising the osmolarity of the culture medium for long-term the effects of FCS on the morphology of chondrocytes can be inhibited. Thus this study has provided new insights into the chondroprotective effect of hyperosmolar environment especially in terms of maintaining normal morphology.

In conclusion, FCS stimulates a morphological change in chondrocyte morphology at the injury which can be prevented by raising the osmolarity of the culture medium.

CHAPTER 9: GENERAL DISCUSSION

The common underlying theme of the whole thesis was to study changes to chondrocyte morphology. This question was addressed by studying morphology of human and bovine chondrocytes in a range of different conditions (a) non-degenerate and mildly degenerate human cartilage (b) bovine chondrocytes cultured in strong and weak agarose gels (c) *in situ* chondrocytes in bovine injured cartilage explants cultured under various conditions and (d) *in situ* chondrocytes in bovine injured cartilage explants cultured in hyperosmolar conditions. Bovine chondrocytes were utilised in these experiments as bovine cartilage is non-degenerate and the chondrocytes have 'normal' morphology. However, if human cartilage have been used instead then there was possibility of having chondrocytes of mixed shapes i.e. both 'normal' and 'abnormal' cells. The basic aims of the studies conducted in this thesis were to determine changes to chondrocyte morphology in human cartilage, to utilise agarose gels and injured cartilage explants as *in vitro* models to introduce morphological changes to chondrocytes in various conditions and to compare morphological changes observed in these models to human cartilage. Therefore, in this work morphological changes to chondrocytes were introduced experimentally to determine whether these changes resemble those observed in human cartilage and ultimately to determine how morphological changes influence matrix metabolism.

The main hypotheses of this work are summarised as following:

1. In grade-0 human femoral head AC, chondrocytes show mild perturbation in morphology which exacerbates in grade-1 cartilage.
2. Bovine chondrocytes cultured in weak 3D agarose gel moulds show volume and morphological changes which accelerate with the increasing concentrations of FCS.

3. Chondrocytes at the injury produce morphological changes in response to some factors present in FCS/SF, not restricted to the superficial layers of cartilage and produced even in the absence of subchondral bone.
4. Chondrocytes at the injury do not produce morphological changes in response to hyperosmolar serum-rich medium.

This chapter aimed at discussing the two experimental *in vitro* culture models (a) weak 3D agarose gel model and (b) partial thickness mechanically injured bovine cartilage model, utilised in this thesis to increase the current knowledge of changes to chondrocyte morphology in various experimental conditions. The techniques involved in designing and benefits of utilising 3D agarose gel and injured cartilage explant models have been discussed in Chapters 4 and 6 respectively. Here the key features of chondrocyte morphology in weak 3D agarose gel model and partial thickness injured cartilage model are discussed in comparison to human Grade-1 cartilage. Additionally the effect of hyperosmolarity on the morphological changes in injured cartilage explants has been discussed.

9.1 Comparisons between morphology of chondrocytes in weak 3D agarose gel and mechanically injured bovine articular cartilage models utilised and human grade-1 cartilage

The morphology of chondrocytes in the two *in vitro* models utilised in the thesis and human grade-1 cartilage are compared and discussed. It is possible that the morphological changes observed in agarose gel and injured cartilage models have certain similarities/differences with those observed in human grade-1 cartilage therefore initially summarised in Table 9.1. and then discussed in detail. The main purpose of this comparison between chondrocyte morphology in different conditions

was to determine whether these shape changes are related or independent of each other.

Chondrocyte morphology		Human femoral head Grade-1 (mildly-degenerate) cartilage SZ	Isolated bovine chondrocytes cultured in Weak 3D Agarose gels	Partial thickness mechanically injured bovine cartilage in serum-rich medium	Mechanically injured bovine cartilage in hyperosmolar serum-rich medium
Examples of Images showing morphology of chondrocytes				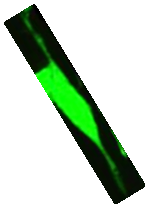	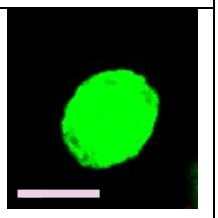
Volume of chondrocytes		No data	↑	↑↑	↓
Characteristics of chondrocyte clusters formed	% of chondrocytes forming clusters	↑↑	↑↑↑	↑	↓↓
	No. of clusters	↑	↑↑↑	↑↑	↓↓
	No. of cells/cluster	↑↑↑	↑↑	↑	No difference
	Volume of clusters	↑↑	↑↑↑	↑↑↑	No difference
	Volume of individual cells in cluster	↑	No difference	↑↑	No difference
Presence of cytoplasmic processes	% of chondrocytes with processes	↑↑	↑↑	↑↑↑	None
	No. of processes/cell	↑↑	↑↑↑	No data	No data
	Average length of processes	↑↑↑	↑↑↑	No data	No data

Table 9.1: Comparison of key morphological characteristics of chondrocytes in various clinical and experimental conditions in comparison to their respective control groups.
The control groups for grade-1 cartilage, weak agarose gels, injured cartilage in serum-rich media and injured cartilage in hyperosmolar serum-rich media were grade-0 cartilage, strong agarose gels, injured cartilage in serum-free media and injured cartilage in standard serum-rich media respectively. Scale bar for all images = 10μm. ↑ and ↓ arrows indicate relative increase and decrease, the more arrows the greater the effect.

In degenerate cartilage, chondrocytes exhibit increase in volume (Bush and Hall, 2003) therefore, chondrocyte volume in weak agarose gel and in injured cartilage models was determined. The volume of chondrocytes increased significantly in the weak gels (Fig. 4.12) and at the injury in injured cartilage (Fig. 6.9) and this is in agreement with the volume changes observed in human degenerate cartilage (Bush and Hall, 2003). In weak gels and in injured cartilage models, a higher percentage of chondrocytes formed large clusters involving numerous cells per cluster in a pattern similar to those observed in human grade-1 cartilage (Table 9.1). Additionally, chondrocytes produced cytoplasmic processes following culture in weak gels and in response to injury in serum-rich medium similar to those observed in human grade-1 cartilage (Table 9.1). Percentages of chondrocytes with cytoplasmic processes in the weak agarose gels, in injured cartilage in the presence of FCS and in grade-1 human cartilage were 67±1% [*N(n')*]=[6(525)], 31±5% [*N(n)*]=[18(23)] and 35±5% [*N(n')*=3(360)] respectively. The length of processes and number of processes per cell was comparable between cultured chondrocytes and those present in human grade-1 cartilage. The average length of cytoplasmic processes within cultured chondrocytes in weak gels and human grade-1 cartilage was 8.5±0.3 μm and 15.6±2 μm respectively. Chondrocytes cultured in weak gels and in grade-1 human cartilage displayed number of processes per cell ranging from one (commonly) to twelve (rarely) and from one (commonly) to seven (rarely) respectively.

In summary, there were various similarities and few differences between morphological changes observed within *in vitro* models to those present in grade-1 cartilage. The volume changes and cluster formation observed in weak agarose and injured cartilage models were similar to those observed in grade-1 cartilage.

Cytoplasmic processes were exhibited by chondrocytes in all three conditions but there were subtle differences regarding the occurrence of these processes in terms of percentages of chondrocytes with processes, length and number of processes per cell. However, the main difference observed was in the shape of chondrocyte cell bodies. They were irregular in the weak agarose gels and in human grade-1 cartilage but flattened and elongated at the injury in injured cartilage (see examples in Table 9.1). This suggested that morphological changes observed in the two models were quite similar to those in the human grade-1 cartilage.

It is well known that during progression of OA degenerative processes lead to several mechanical and physical changes in the cartilage matrix in terms of (a) loosening (Aigner and McKenna, 2002) (b) increased permeability (c) swelling (Wang et al., 2013a) and (c) decreased rigidity (Maroudas, 1976). In an attempt to develop an *in vitro* model where chondrocytes could possibly be cultured in an environment resembling the weakened and less rigid matrix as observed in OA, weak gel moulds with very low concentration of agarose (0.2%) were used. A model of weakened matrix was also prepared by applying the sharp scalpel cut to bovine cartilage explants with a push-through mode which would possibly enhance the permeation of factors present in FCS. Therefore, two possible common features between weak 3D agarose gel and injured cartilage models in comparison to human grade-1 cartilage were (a) weakened matrix and (b) enhanced penetration of the factors and both the features may be inter-related. It has been reported previously that decreased concentration of agarose in gels leads to increased diffusivity (Johnson et al., 1996) and damage to the cartilage leads to enhanced penetration of nutritive/proliferative factors (Schumacher et al., 2002). Strength of the matrix and rate of penetration of

factors were not measured directly in this work and was beyond the scope of this work therefore can be considered a limitation of the study. However, based upon the observations of previous studies mentioned above weak agarose gels and injured cartilage were considered comparable to the weakened matrix in OA and therefore utilised as models in the present work.

The results presented in Chapters 4 and 6, suggested that both weakened matrix and enhanced access to factors present in the culture media were responsible for the morphological changes in chondrocytes. In a separate set of experiments cultured chondrocytes in weak gels also exhibited accelerated shape changes with increasing FCS concentration. This suggested that gel strength and penetration of factors could be a related phenomenon such that increasing the gel strength may lead to decreased penetration of factors (see Results section 4.5.2).

It is not possible to fully explain the basis of production of these cytoplasmic processes from the data presented in this work. However, possible mechanisms based upon the similarities between the two *in vitro* models and human grade-1 cartilage can be suggested as the key players leading to the production of cytoplasmic processes. A possible mechanism for the development of these cytoplasmic processes could be the defects in the immediate microenvironment of the chondrocytes due to loss of PGs. The narrow tissue region immediately surrounding the chondrocytes is called PCM. It is a highly organised matrix composed of collagen fibres with embedded PGs such that these macromolecules provide resilience to structure and help chondrocytes maintain their architecture. The PGs especially biglycans and decorins small leucine-rich PGs (SLRP) are concentrated in the PCM and interact with type VI collagen (Heinegard, 2009) present in the immediate vicinity of

chondrocytes (Guilak et al., 2006). Type VI collagen is present in the PCM of chondrocytes in the form of a network which is regulated by SLRPs in the cartilage (Wiberg et al., 2002). It has been reported that cartilage degeneration in OA is associated with loss of PGs (Pearle et al., 2005) and in this work also, chondrocytes in weak gels and injured explants cultured in the presence of serum showed decreased PGs (Figs. 5.5 and 7.6). Therefore, it is possible that the sites from where PGs are lost lead to disruption of collagen type VI and the cytoplasmic extensions protrude out through these potentially disrupted places in PCM. Based upon this theory it is possible that in strong agarose gels, chondrocytes in culture synthesised a stable and compact PCM around them thereby assisting them to maintain their morphology.

The production of cytoplasmic processes may also possibly be due to increased metabolic activities of chondrocytes in relation to the enhanced penetration of morphogenic factors present in FCS. There are several hormones/proteins present in FCS which may serve as morphogenic factors stimulating growth/proliferation of chondrocytes such as growth hormone, thyroid hormones (T3 & T4), insulin etc. In a study it has been reported that the penetration of morphogenic factors to chondrocytes increases in cartilage degeneration with the formation of fissures (Meachim and Collins, 1962). This explains the possibility of greater access of FCS to chondrocytes cultured in weak gels. The growth factors play a pivotal role in cartilage healing and treatment of early OA as they are known to stimulate chondrocytes thereby enhancing their synthetic and metabolic activities (Fortier et al., 2011, Civinini et al., 2013). The metabolic activities constitute both anabolic and catabolic activities of chondrocytes. Some growth factors such as fibroblast growth

factor-2 (FGF-2) are also known to induce catabolic activities in human articular chondrocytes (Yan et al., 2011). FGF-2 is also thought to be a principal stimulating factor for cluster formation (Khan et al., 2010). In a previous study these abnormal chondrocytes with long processes were proposed to be associated with breakdown of PCM (Holloway et al., 2004). Additionally, it was reported in a study that the abnormal chondrocytes with processes were associated with high levels of intracellular IL1ß and disrupted type VI collagen in the PCM as compared to chondrocytes of normal (rounded) morphology (Murray et al., 2010). The increased production of degradative enzymes and catabolic cytokines in turn may degrade the matrix surrounding chondrocytes leading to production of cytoplasmic processes. This might lead to the establishment of a vicious circle with abnormal chondrocytes causing matrix damage and in turn weakened matrix leading to more abnormal chondrocytes due to enhanced penetration of morphogenic factors through weak matrix. The weak agarose gel model contains very low concentration of agarose thereby providing chondrocytes an environment which resembles the damaged matrix and greater penetration of morphogenic factors from the serum possibly leading to production of processes.

In the injured cartilage explants, cells at the injury in response to SF/FCS showed marked changes to chondrocyte morphology comprised of cell enlargement, flattening and production of cytoplasmic processes (Figs. 6.8, 6.19 and 6.28). This heterogeneous population of cells has some interesting parallels with chondrogenic progenitor cells (CPCs) but whether these are chondrocytes or CPCs is not known. At the site of injury these heterogeneous cells produced cytoplasmic processes observed to be in the direction of injury while producing scalpel cut i.e. along the

damaged cartilage. These cytoplasmic processes appear to align at the injury (Fig. 6.8). There are at least two possible sources for the appearance of this heterogeneous population of cells at the injury (a) migrating CPCs or (b) chondrocytes at the injury changed shape. It has been reported that chondrogenic progenitor cells in response to injury guided by 'alarmins' migrate to the site of injury (Seol et al., 2012). However, it is unlikely that in our experiments these were progenitor cells because possibility of presence of alarmins is less as the dead chondrocytes were lost in the serum-rich medium. The possible explanation for the loss of dead cells in serum would be the digestion of dead cell nuclei in the culture by DNase present in the serum (Zhou et al., 2011). This suggested that presence of alarmins was less likely to attract chondrogenic progenitor cells in the injured cartilage experiments in present study. Therefore, chondrocytes at the injury possibly produced cytoplasmic processes due to enhanced access to factors as a consequence of cartilage weakening produced by scalpel injury.

In another recent study by Lyman and co-workers the production of cytoplasmic processes has been reported in response to cartilage injury (Lyman et al., 2012). This is an informative study and there are several similarities and differences between the work reported by Lyman et al and the study presented in this thesis. (a) In the previous study the production of cytoplasmic processes in the presence of serum-rich culture medium was reported similar to the findings in the present study. In the previous study no data were given for the response of chondrocytes in the absence of serum, however the present work gives a detailed comparison of response of chondrocytes to injury in the serum-rich and serum-free media. (b) In the previous study there were no data regarding volume and shape of these heterogeneous cells

with processes, however in the present study a detailed account of viability, volume and other morphological details of chondrocytes have been reported in response to injury. The results of the present study are in agreement with this previous study regarding the reaction of chondrocytes at injury to produce cytoplasmic processes in the presence of FCS. However, several additional findings in the present work build upon the previous knowledge regarding response of chondrocytes to injury.

The injured cartilage explants were exposed to hyperosmolar serum rich medium for short- and long-term. The data displayed an inhibiting effect of raised osmolarity on the action of morphogenic factors present in serum. Chondrocyte proliferation/cluster formation at the injury was inhibited in the presence of hyperosmolar culture medium (Figs. 8.6A,B and 8.13A,B). Moreover, chondrocyte morphology remained unaffected (spheroidal) and no abnormal cells (with processes) were observed even after 14 days of *in vitro* culture in hyperosmolar serum-rich and serum-free culture media (Figs. 8.11 and 8.14). These findings suggested the protective action of hyperosmolarity on chondrocyte morphology. One possible underlying mechanism for these findings could be that hyperosmolarity causes the chondrocytes to shrink and possibly maintain their spheroidal shape. The explanation for this effect could be through the regulatory action of SOX9 transcription factor on chondrocyte morphology. SOX9 is a key controller of chondrocyte phenotype and its expression is known to be increased by hyperosmolarity (Tew et al., 2005, Tew et al., 2009). Therefore, it is possible that when injured cartilage was cultured in the presence of raised osmolarity SOX9 was overexpressed and thus prevented morphological changes in chondrocytes. Secondly, another possibility is that the morphogenic

factors in FCS can only stimulate chondrocytes at a control osmolarity and hyperosmolarity inactivates them.

9.2 Model

The fine morphological details of *in situ* and *in vitro* articular chondrocytes have been studied in a range of conditions. In this section an attempt has been made to bring all these results together so as to formulate a relatively simple working model (Fig. 9.1).

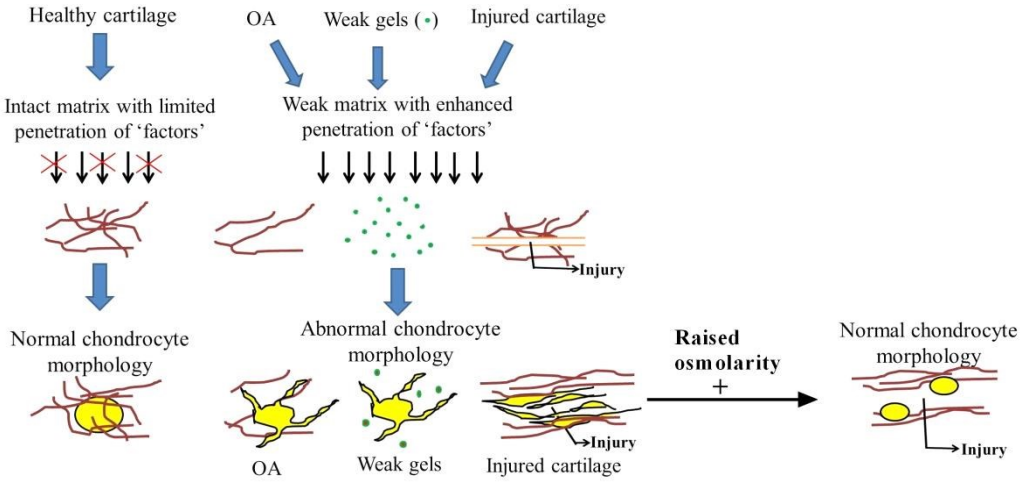

Figure 9.1: A simplified model to account for the variations in chondrocyte morphology observed under various experimental conditions.
Chondrocytes cultured in weak agarose gels/injured cartilage explants display morphological changes (production of cytoplasmic processes) possibly due to enhanced penetration of factors in serum. Raised medium osmolarity inhibited the effect of factors in serum; thereby appeared to prevent alterations to chondrocyte morphology in injured cartilage. The red crosses in the figure indicated less penetration of factors.

9.3 Importance in experimental and clinical research

The findings of this work have translational significance in future experimental and clinical research in cartilage degeneration and cartilage injury. Some of these implications are discussed in the following sections.

9.3.1 Pathogenesis of cartilage degeneration in OA and other joint disorders

The presence of cytoplasmic processes in grade-0 human cartilage and increase in their production with cartilage degeneration (Figs. 3.7 and 3.9) suggests this characteristic to be an earlier event in degeneration. Whether these abnormal chondrocytes play a role in cartilage degeneration or cartilage degeneration leads to the production of these cytoplasmic processes is not known. However, the samples were from patients within an age range of 65-89 yrs. which means the donors were old aged and this can possibly be a contributing factor for the development of cytoplasmic processes due to chondrocyte senescence. In a previous study it has been reported that with aging chondrocytes show phenotypic changes contributing to cartilage progression OA (Price et al., 2002). It is unknown whether cytoplasmic processes are a characteristic of chondrocytes in old age and needs to be investigated. The abnormal morphology of chondrocytes (cytoplasmic processes) is not a good sign as this indicates possibly deterioration in chondrocyte synthetic activity and ultimately cartilage damage (Kouri et al., 1996a, Darling and Athanasiou, 2005, Tesche and Miosge, 2005, Yagi et al., 2005, Murray et al., 2010). Therefore, if chondrocyte morphology proves to be an earlier component of degenerative joint diseases, it may become a potential therapeutic target for slowing disease progression such as formulating drugs which can possibly assist chondrocytes to maintain their

normal morphology. Chondrocytes cultured in weak agarose gels displayed some morphological changes similar to the early OA changes but proposing weak agarose gel model as a method to study OA *in vitro* at this stage would be too early. Further studies are needed to investigate the levels of degradative enzymes produced by these morphologically abnormal chondrocytes in agarose gels.

In addition to grade-1 human AC, morphological changes to chondrocytes have also been observed in other clinical conditions as OCD and AVN (Figs. 3.16, 3.18, 3.19, 3.21, 3.22, 3.24 and 3.25). This may suggest that in addition to OA, morphology of chondrocytes is an important feature in other joint disorders. However, it is unclear whether weakened matrix leads to these morphologically abnormal chondrocytes or the shape changes are an earlier event and lead to matrix degradation and weakening.

9.3.2 Cartilage injury and response of chondrocytes

Cartilage trauma is associated with chondrocyte death and determination of extent of cell death is important to estimate the severity of injury as sharp trauma led to less cell death as compared to blunt trauma (Redman et al., 2004). PI is a membrane impermeable DNA dye which cannot cross intact membrane and therefore labels nuclei of dead cells as red. As discussed in chapter 6, in the presence of FCS and SF PI-labelled chondrocytes were lost, thus overestimating chondrocyte viability with the use of DNA-binding dyes such as PI. Therefore, for cell density measurements in cartilage research especially in culture experiments with serum-rich medium instead of using fluorescent dyes, trypan blue staining may be used to detect dead cells (Zhou et al., 2011). The cytoplasmic processes produced by chondrocytes at the injury in the presence of serum attempted to fill in the injured area suggesting the

potential of chondrocytes for an active mechanism in response to injury. However the evaluation of ECM produced by these abnormal chondrocytes showed decreased PGs (Fig. 7.6) and unaffected collagen types II & I (Figs. 7.12 & 7.15 respectively). These findings suggest that may be the matrix produced by these cells is mechanically an inferior quality matrix unable to withstand compressive forces. However, further investigations are required to determine the quantitative and qualitative assessment of the matrix produced by these abnormal cells.

By raising osmolarity of medium for short-term, cell death due to injury was significantly reduced and for long-term chondrocyte morphology remained unaffected in serum-rich medium even after 14 days and they maintained their normal spheroidal shape. This suggested the protective role of hyperosmolarity on chondrocyte viability and morphology in response to injury. Raising the osmolarity of joint irrigation solutions during orthopaedic surgical procedures may have a chondroprotective role and has been reported already (Amin et al., 2010). However, the results presented in this work suggest the positive effects of hyperosmolarity on chondrocyte morphology also and this may be therapeutically beneficial. By devising strategies to increase the osmolarity of synovial fluid, chondrocytes can possibly be forced to retain their normal (spheroidal) morphology. As a strong relationship exists between chondrocyte morphology and matrix synthesis, therefore this intervention may be helpful in maintenance of normal turnover of matrix thereby preventing cartilage degeneration.

By identifying the factors present in SF and FCS that stimulated chondrocytes leading to morphological changes in injured/weakened cartilage, treatment strategies may be developed or modified to prevent these changes. The stimulatory effect of

these specific factors can possibly be inhibited by formulating antagonist drugs against the factors.

9.4 Implications

The work presented in this thesis has implications in the following areas:

9.4.1 Pathogenesis of OA

The results from this work show that chondrocytes change shape due to factors present in serum. By using separation techniques these factors can be identified and possibly used as a diagnostic test in monitoring the progression of cartilage degeneration in OA. Additionally, by limiting the access of these factors e.g. FGF-2, IGF-1 etc. to the damaged/weakened cartilage matrix progression of degeneration can possibly be delayed or prevented.

9.4.2 Treatment of OA

The morphologically abnormal chondrocytes observed in this work need to be investigated further to identify signalling pathways involved and to identify chondrocytic markers associated with these abnormal cells. The possible future experiments can be to use techniques such as laser micro dissection to dissect out individual cells of interest (cells with processes) and study the RNA expression levels of various markers by these cells. These investigations will have implications in devising treatment strategies for OA disease progression.

9.4.3 Cartilage repair following injury

The observation that hyperosmolarity drives chondrocytes to normal (spheroidal) shape following trauma can prove to be useful in promoting cartilage repair after

injury. However, further investigations are needed to study the quality of matrix produced by chondrocytes following exposure to raised osmolarity. The signalling pathways involved in maintaining chondrocyte morphology in hyperosmotic environment need to be investigated e.g. expression levels of SOX9 by these chondrocytes.

9.4.4 Role of morphologically abnormal chondrocytes in OA

The presence of abnormal chondrocyte morphology in non-degenerate cartilage raises the possibility of these cells to be a result of normal aging process. Therefore, morphology of chondrocytes over wider age ranges needs to be investigated. Moreover, the quality of matrix expressed by these chondrocytes (with processes) needs to be investigated to establish the role of these cells in the progression of OA.

9.5 Future work

In order to propose weak 3D gel culture an *in vitro* model to study changes in early OA several investigations need to be done further to determine various parameters. The cell structure-function relationship has already been studied and reported that spheroidal chondrocytic phenotype is necessary to produce a functional matrix (Fedewa et al., 1998, Schnabel et al., 2002, Marlovits et al., 2004, Youngstrom et al., 2015). Therefore, the key future experiments would be to study the quantity and type of matrix produced by chondrocytes cultured in weak agarose gels associated to the shape changes. The expression of matrix macromolecules can be determined by performing PCR, western blotting and hydroxyproline incorporation methods. Furthermore, the ECM produced by the chondrocytes cultured in both gel strengths

needs to be compared in order to get an insight whether the chondrocytes with altered morphology in weak gels produce mechanically inferior matrix. Therefore, future experiments in this regard may include IHC for detection of collagen type I and II amongst the chondrocytes cultured in strong and weak gels.

In a study carried out on human osteoarthritic cartilage, increased expression of IL-Iß levels and loss of pericellular type VI collagen have already been demonstrated in abnormal cells with processes (Murray et al., 2010). IL-Iß is a pro-inflammatory cytokine produced in larger quantities in OA responsible for causing damage to the cartilage through increased levels of MMPs (Aigner et al., 2007). Collagen type VI is localised to the PCM in non-degenerate cartilage and gets disrupted in OA (Soder et al., 2002Soder et al., 2002). Fluorescence immunohistochemistry can be performed on the cultured chondrocytes in strong and weak gels to determine the expression level of IL-Iß and Collagen type VI in normal and abnormal chondrocytes. These experiments will assist in correlating these changes to chondrocyte morphology and will be additional supportive evidence that this model can be utilised successfully to study OA.

Further detailed studies are needed to investigate the role of chondrocytes (with altered morphology) in cartilage repair process at the injury. Whether these chondrocytes produce mechanically functional or an altered inferior quality matrix needs to be investigated. In this work histological staining for H&E, Alcian blue, Masson's trichrome and IHC for collagen type I & II of the injured cartilage samples was performed. However, the results obtained are preliminary and further experiments are needed to probe the properties of cells under consideration. The future challenge will be to more precisely clarify the relationship between

chondrocyte morphology and matrix metabolism (both synthesis and breakdown) by determining the type of collagen and the levels of degradative enzymes produced by these abnormal cells. Additionally, Identification of morphogenic factors stimulating chondrocytes can be determined with the use of dialysed FCS by using dialysing membranes of variable slit sizes or commercially available FCS at various molecular weight cut-offs. Moreover, thorough investigations can be carried out to determine the mechanism through which hyperosmolarity inhibited the effect of serum and chondrocyte morphology remained unaffected at the injury. In this regard analysis of various genes such as SOX9 over or under expressed by these abnormal chondrocytes in hyperosmolar condition can be determined through polymerase chain reaction (PCR).

APPENDIX

List of published abstracts, oral and poster presentations related to this work

Published abstracts

1. A. Karim and A.C. Hall. Morphological properties of chondrocytes cultured in weak 3D agarose gels. *Bone Joint J*. 2013; 95-B: Supp 13, 47.

2. A. Karim and A.C. Hall. Morphological characteristics of chondrocytes in injured cartilage cultured under various conditions. 4th joint meeting of Bone Research Society and British Orthopaedic Research Society, Oxford, 4th – 5th September 2013. (in process).

Oral presentation

A. Karim and A.C. Hall. Morphological characteristics of chondrocytes in injured cartilage cultured under various conditions. 4th joint meeting of Bone Research Society and British Orthopaedic Research Society, Oxford, 4th - 5th September 2013.

Poster presentations

1. A. Karim and A.C. Hall. Morphological properties of chondrocytes cultured in weak 3D agarose gels. Annual meeting of British Orthopaedic Research

Society (BORS), London, 24th – 25th September 2012. Runners up for prize for this poster.

2. A. Karim and A.C. Hall. Morphological properties of chondrocytes cultured in weak 3D agarose gels. 40th Scottish Microscopy Group Symposium, Edinburgh, 14th November 2012.

BIBLIOGRAPHY

AARON, R. K. & RACINE, J. 2013. Pathogenesis and Epidemiology of Osteoarthritis. *Rhode Island Medical Journal***,** 19-22.

ABRAMSON, S. B., ATTUR, M., AMIN, A. R. & CLANCY, R. 2001. Nitric oxide and inflammatory mediators in the perpetuation of osteoarthritis. *Current Rheumatology Reports,* 3**,** 535–541.

ACHARYA, C., YIK, J. H. N., KISHORE, A., DINH, V. V., DI CESARE, P. E. & HAUDENSCHILD, D. R. 2014. Cartilage oligomeric matrix protein and its binding partners in the cartilage extracellular matrix: Interaction, regulation and role in chondrogenesis. *Matrix Biology,* 37**,** 102-111.

ADAMS, J. C. & WATT, F. M. 1993. Regulation of development and differentiation by the extracellular matrix. *Development,* 117**,** 1183-1198.

ADOLPHE, M. & DEMIGNOT, S. 2000. Versatility of differentiated functions of cultured joint chondrocytes. Eventual usefulness in treatment. *Bulletin de l Academie Nationale de Medecine,* 184**,** 593-600; discussion 601-594

AHEARNE, M., YANG, Y., EL HAJ, A. J., THEN, K. Y. & LIU, K. K. 2005. Characterizing the viscoelastic properties of thin hydrogel-based constructs for tissue engineering applications. *Journal of the Royal Society Interface,* 2**,** 455-463.

AIGNER, T. & DUDHIA, J. 1997. Phenotypic modulation of chondrocytes as a potential therapeutic target in osteoarthritis:A hypothesis. *Annals of the Rheumatic Diseases,* 56**,** 287-291.

AIGNER, T., HEMMEL, M., NEUREITER, D., GEBHARD, P. M., ZEILER, G., KIRCHNER, T. & MCKENNA, L. 2001. Apoptotic cell death is not a widespread phenomenon in normal aging and osteoarthritic human articular knee cartilage:A study of proliferation, programmed cell death (apoptosis), and vability of chondrocytes in normal and osteoarthritic human knee cartilage. *Arthritis and Rheumatism,* 44**,** 1304-1312.

AIGNER, T. & MCKENNA, L. 2002. Molecular pathology and pathobiology of osteoarthritic cartilage. *Cellular and Molecular Life Sciences,* 59**,** 5-18.

AIGNER, T., SOEDER, S., GEBHARD, P. M., MCALINDEN, A. & HAAG, J. 2007. Mechanisms of disease: role of chondrocytes in the pathogenesis of osteoarthritis-structure, chaos and senescence. *Nature Reviews Rheumatology,* 3**,** 391-399.

AIGNER, T., STÖß, H., WESELOH, G., ZEILER, G. & MARK, K. V. D. 1992. Activation of collagen type II expression in osteoarthritic and rheumatoid cartilage. *Virchows Archive B: Cell Pathology Including Molecular Pathology,* 62**,** 337-345.

AIGNER, T., VORNEHM, S. I., ZEILER, G., DUDHIA, J., VON DER MARK, K. & BAYLISS, M. T. 1997. Suppression of cartilage matrix gene expression in upper zone chondrocytes of osteoarthritic cartilage. *Arthritis and Rheumatism,* 40**,** 562-569.

ALEXOPOULOS, L. G., YOUN, I., BONALDO, P. & GUILAK, F. 2009. Developmental and osteoarthritic changes in Col6a1 knockout mice: The biomechanics of collagen VI in the cartilage pericellular matrix. *Arthritis and Rheumatism,* 60**,** 771-779.

ALMONTE-BECERRIL, M., NAVARRO-GARCIA, F., GONZALEZ-ROBLES, A., VEGA-LOPEZ, M. A., LAVALLE, C. & KOURI, J. B. 2010. Cell death of chondrocytes is a combination between apoptosis and autophagy during the pathogenesis of Osteoarthritis within an experimental model. *Apoptosis* 15**,** 631–638.

ALSALAMEH, S., AMIN, R., GEMBA, T. & LOTZ, M. 2004. Identification of mesenchymal progenitor cells in normal and osteoarthritic human articular cartilage. *Arthritis and Rheumatism,* 50**,** 1522–1532.

AMIN, A. K., HUNTLEY, J. S., BUSH, P. G., SIMPSON, A. H. R. W. & HALL, A. C. 2008a. Chondrocyte death in mechanically injured articular cartilage—The influence of extracellular calcium. *Journal of Orthopaedic Research,* 27**,** 778-784.

AMIN, A. K., HUNTLEY, J. S., BUSH, P. G., SIMPSON, A. H. R. W. & HALL, A. C. 2008b. Osmolarity influences chondrocyte death in wounded articular cartilage. *The Journal of Bone and Joint Surgery,* 90**,** 1531-1542.

AMIN, A. K., HUNTLEY, J. S., PATTON, J. T., BRENKEL, I. J., SIMPSON, A. H. & HALL, A. C. 2011. Hyperosmolarity protects chondrocytes from mechanical injury in human articular cartilage: an experimental report. *Journal of Bone and Joint Surgery. British Volume,* 932**,** 277-284.

AMIN, A. K., HUNTLEY, J. S., SIMPSON, A. H. & HALL, A. C. 2010. Increasing the osmolarity of joint irrigation solutions may avoid injury to cartilage: a pilot study. *Clinical Orthopedics and Related Research,* 468**,** 875-884.

AN, Y. H., WEBB, D., GUTOWSKA, A., MIRONOV, V. A. & FRIEDMAN, R. J. 2001. Regaining chondrocyte phenotype in thermosensitive gel culture. *The Anatomical Record,* 263**,** 336-341.

ANDERSON, D. D., CHUBINSKAYA, S., GUILAK, F., MARTIN, J. A., OEGEMA, T. R. & OLSON, S. A. 2011. Post-traumatic osteoarthritis: Improved understanding and opportunities for early inter-vention. *Journal of Orthopaedic Research,* 29**,** 802-809.

ANDREW, T. A., SPIVEY, J. & LINDEBAUM, R. H. 1981. Familial osteochondritis dissecans and dwarfism. *Acta Orthopaedica Scandinavica,* 52**,** 519–523.

APOLD, H., MEYER, H. E., NORDSLETTEN, L., FURNES, O., BASTE, V. & FLUGSRUD, G. B. 2014. Risk factors for knee replacement due to primary osteoarthritis, a population based, prospective cohort study of 315,495 individuals. *Musculoskeletal Disorders,* 15**,** 2-11.

ARCHER, C. W. & FRANCIS-WEST, P. 2003. The cells in focus: The chondrocyte. *The International Journal of Biochemistry and Cell Biology,* 35**,** 401-404.

ASZODI, A., HUNZIKER, E. B., BRAKEBUSCH, C. & FASSLER, R. 2003. ß1 integrins regulate chondrocyte rotation, G1 progression, and cytokinesis. *Genes and Development,* 17**,** 2465–2479.

ATHANASIOU, K. A., ROSENWASSER, M. P., BUCKWALTER, J. A., MALININ, T. I. & MOW, V. C. 1991. Interspecies comparisons of in situ intrinsic mechanical properties of distal femoral cartilage. *Journal of Orthopaedic Research,* 9**,** 330-340.

AVWIORO, G. 2011. Histochemical uses of haematoxylin - A review. *Journal of Physics and Chemistry of Solids,* 1**,** 24-34.

AYDELOTTE, M. B., GREENHILL, R. R. & KUETTNER, K. E. 1988. Differences between sub-populations of cultured bovine articular chondrocytes. II. Proteoglycan metabolism. *Connective Tissue Research,* 18**,** 223-34.

BALGUDE, A. P., YU, X., SZYMANSKI, A. & BELLAMKONDA, R. V. 2001. Agarose gel stiffness determines rate of DRG neurite extension in 3D cultures. *Biomaterials,* 22**,** 1077-1084.

BANK, R. A., BAYLISS, M. T., LAFEBER, F. P. J. G., MAROUDAS, A. & TEKOPPELE, J. M. 1998. Ageing and zonal variation in post-translational modification of collagen in normal human articular cartilage: the age-related increase in Non-Enzymatic Glycation affects biomechanical properties of cartilage. *Biochemical Journal,* 330**,** 345–351.

BANK, R. A., SOUDRY, M., MAROUDAS, A., MIZRAHI, J. & TEKOPPELE, J. M. 2000. The increased swelling and instantaneous deformation of osteoarthritic cartilage is highly correlated with collagen degradation. *Arthritis and Rheumatism,* 43**,** 2202-2210.

BARBERO, A., PLOEGERT, S., HEBERER, M. & MARTIN, I. 2003. Plasticity of clonal populations of dedifferentiated adult human articular chondrocytes. *Arthritis and Rheumatism,* 48**,** 1315–1325.

BELL, D. M., LEUNG, K. K., WHEATLEY, S. C., NG, L. J., ZHOU, S., LING, K. W., SHAM, M. H., KOOPMAN, P., TAM, P. P. & CHEAH, K. S. 1997. SOX9 directly regulates the type-ll collagen gene. *Nature Genetics,* 16**,** 174-178.

BENYA, P. D., PADILLA, S. R. & NIMNI, M. E. 1978. Independent regulation of collagen types by chondrocytes during the loss of diierentiated function in culture. *Cell volume,* 15**,** 1313-1321.

BENYA, P. D. & SHAFFER, J. D. 1982. Dedifferentiated chondrocytes reexpress the differentiated collagen phenotype when cultured in agarose gels. *Cell,* 30**,** 215-224.

BERTRAM, K. L. & KRAWETZ, R. J. 2012. Osmolarity regulates chondrogenic differentiation potential of synovial fluid derived mesenchymal progenitor cells. *Biochemical and Biophysical Research Communications,* 422**,** 455-461.

BHALLA, A., SANKARALINGAM, S., DUNDAS, R., SWAMINATHAN, R., WOLFE, C. D. & RUDD, A. G. 2000. Influence of raised plasma osmolality on clinical outcome after acute stroke. *Stroke,* 31**,** 2043-8.

BHOSALE, A. M. & RICHARDSON, J. B. 2008. Articular cartilage: structure, injuries and review of management. *British Medical Bulletin,* 87**,** 77-95.

BI, W., DENG, J. M., ZHANG, Z., BEHRINGER, R. R. & DE CROMBRUGGHE, B. 1999. Sox9 is required for cartilage formation. *Nature Genetics,* 22**,** 85-89.

BIAN, L., LIMA, E. G., ANGIONE, S. L., NG, K. W., WILLIAMS, D. Y., XU, D., STOKER, A. M., COOK, J. L., ATESHIAN, G. A. & HUNG, C. T. 2008. Mechanical and biochemical characterization of cartilage explants in serum-free culture. *Journal of Biomechanics,* 41**,** 1153-1159.

BILLINGHURST, R. C., DAHLBERG, L., IONESCU, M., REINER, A., BOURNE, R., RORABECK, C., MITCHELL, P., HAMBOR, J., DIEKMANN, O., TSCHESCHE, H., CHEN, J., WART, H. V. & POOLE, A. R. 1997. Enhanced cleavage of Type II collagen by collagenases in osteoarthritic articular cartilage. *Journal of Clinical Investigation,* 99**,** 1534-1545.

BLANCO, F. J., GUITIAN, R., VAZQUEZ-MARTUL, E., DETORO, F. J. & GALDO, F. 1998. Osteoarthritis chondrocytes die by apoptosis. A possible pathway for osteoarthritis pathology. *Arthritis and Rheumatism,* 41**,** 284-289.

BOCK, H. C., MICHAELI, P., BODE, C., SCHULTZ, W., KRESSE, H., HERKEN, R. & MIOSGE, N. 2001. The small proteoglycans decorin and biglycan in human articular cartilage of late-stage osteoarthritis. *Osteoarthritis and Cartilage,* 9**,** 654-663.

BÖHM, B., AIGNER, T., GEHRSITZ, A., BLOBEL, C. P., KALDEN, J. R. & BURKHARDT, H. 1999. Upregulation of MDC 15 (matargidin) mRNA in human osteoarthritic cartilage. *Arthritis and Rheumatism* 42**,** 1946–1950.

BONAVENTURE, J., KADHOM, N., COHEN-SOLAL, L., NG, K. H., BOURGUIGNON, J., LASSELIN, C. & FREISINGER, P. 1994. Reexpression of cartilage-specific genes by dedifferentiated human articular chondrocytes cultured in alginate beads. *Experimental Cell Research,* 212**,** 97-104.

BOUGAULT, C., PAUMIER, A., AUBERT-FOUCHER, E. & MALLEIN-GERIN, F. 2008. Molecular analysis of chondrocytes cultured in agarose in response to dynamic compression. *BMC Biotechnology,* 8**,** 1-10.

BRAKENHOFF, G. J., BLOM, P. & BARENDS, P. J. 1979. Confocal scanning light microscopy with high aperture immersion lenses. *Journal of Microscopy,* 117**,** 219-232.

BRAKENHOFF, G. J., VAN DER VOORT, H. T. M., VAN SPRONSEN, E. A. & NANNINGA, N. 1990. Confocal Laser Scanning Microscopy: From 3-D data collection to 3D image visualization and analysis. *Science on forum: Proceedings of the second international symposium for science on forum***,** 39-46.

BROWN, T. D., JOHNSTON, R. C., SALTZMAN, C. L., MARSH, J. L. & BUCKWALTER, J. A. 2006. Posttraumatic osteoarthritis: a first estimate of incidence, prevalence, and burden of disease. *Journal of Orthopaedic Trauma,* 20**,** 739-744.

BUCKWALTER, J. A. 1998. Articular Cartilage: Injuries and potential for healing. *Journal of Orthopaedic and Sports Physical Therapy,* 28**,** 192-202.

BUCKWALTER, J. A., ANDERSON, D. D., BROWN, T. D., TOCHIGI, Y. & MARTIN, J. A. 2013. The roles of mechanical stresses in the pathogenesis of osteoarthritis: Implications for treatment of joint injuries. *Cartilage,* XX**,** 9 pages.

BUCKWALTER, J. A. & BROWN, T. D. 2004. Joint injury, repair, and remodeling: roles in post-traumatic osteoarthritis. *Clinical Orthopedics and Related Research,* 423**,** 7–16.

BUCKWALTER, J. A., HUNZIKER, E., ROSENBERG, L., COUTTS, R., ADAMS, M. & EYRE, D. 1988. Articular cartilage: composition and structure. *In:* WOO, S. L. Y. & BUCKWALTER, J. A. (eds.) *Injury and Repair of the Musculoskeletal Soft Tissues.* Park Ridge, IL: American Academy of Orthopaedic Surgeons. 405–425.

BUCKWALTER, J. A. & MANKIN, H. J. 1997a. Articular cartilage II. Degeneration and osteoarthritis, repair, regeneration and transplantation. *Journal of Bone and Joint Surgery,* 79 A**,** 612-632.

BUCKWALTER, J. A. & MANKIN, H. J. 1997b. Articular cartilage Part I : Tissue design and chondrocyte-matrix interactions. *Journal of Bone and Joint Surgery,* 79**,** 600-611.

BUCKWALTER, J. A. & MANKIN, H. J. 1998. Articular cartilage: tissue design and chondrocyte-matrix interactions. *Instructional Course Lectures,* 47**,** 477-486.

BUCKWALTER, J. A., MANKIN, H. J. & GRODZINSKY, A. J. 2005. Articular cartilage and osteoarthristis. *American Academy of Orthopaedic Surgeons. Instructional course lectures,* 54**,** 465-480.

BUCKWALTER, J. A. & MARTIN, J. A. 2006. Osteoarthritis. *Advanced Drug Delivery Reviews,* 58**,** 150–167.

BUCKWALTER, J. A., MOWER, D., UNGAR, R., SCHAEFFER, J. & GINSBERG, B. 1986. Morphometric analysis of chondrocyte hypertrophy. *Journal of Bone and Joint Surgery. American Volume,* 68**,** 243-255.

BURRY, R. W. 2000. Specificity controls for immunocytochemical methods. *The Journal of Histochemistry and Cytochemistry,* 48**,** 163-165.

BUSCHMANN, M. D., GLUZBAND, Y. A., GRODZINSKY, A. J. & HUNZIKER, E. B. 1995. Mechanical compression modulates matrix biosynthesis in chondrocyte/agarose culture. *Journal of Cell Science,* 108**,** 1497-1450.

BUSCHMANN, M. D., GLUZBAND , Y. A., GRODZINSKY, A. J., KIMURA, J. H. & HUNZIKER, E. B. 1992. Chondrocytes in agarose culture synthesize a mechanically functional extracellular matrix. *Journal of Orthopaedic Research,* 10**,** 745-758.

BUSH, P. G. & HALL, A. C. 2001a. The osmotic sensitivity of isolated and in situ bovine articular chondrocytes. *Journal of Orthopaedic Research,* 19**,** 768-778.

BUSH, P. G. & HALL, A. C. 2001b. Regulatory Volume Decrease (RVD) by isolated and in situ bovine articular chondrocytes. *Journal of Cellular Physiology,* 187**,** 304-314.

BUSH, P. G. & HALL, A. C. 2003. The volume and morphology of chondrocytes within non-degenerate and degenerate human articular cartilage. *Osteoarthritis and Cartilage,* 11**,** 242-251.

BUSH, P. G. & HALL, A. C. 2005. Passive osmotic properties of in situ human articular chondrocytes within non-degenerate and degenerate cartilage. *Journal of Cellular Physiology,* 204**,** 309-319.

BUSH, P. G., HODKINSON, P. D., HAMILTON, G. L. & HALL, A. C. 2005. Viability and volume of in situ bovine articular chondrocytes-changes following a single impact and effects of medium osmolarity. *Osteoarthritis and cartilage,* 13**,** 54-65.

CAHILL, B. R. 1995. Osteochondritis dissecans of the knee: treatment of juvenile and adult forms. *Journal of the American Academy of Orthopaedic Surgeons,* 3**,** 237–247.

CAMPBELL, C. J. 1969. The healing of cartilage defects. *Clinical Orthopaedics and Related Research,* 64**,** 45-63.

CAMPER, L., HELLMAN, U. & LUNDGREN-AKERLUND, E. 1998. Isolation, cloning, and sequence analysis of the integrin subunit α10, aβ1-associated collagen binding integrin expressed on chondrocytes. *Journal of Biological Chemistry,* 273**,** 20383–20389.

CANCEDDA, R., CANCEDDA, F. D. & CASTAGNOLA, P. 1995. Chondrocyte Differentiation. *Internationl Review of Cytology,* 159**,** 265-357.

CARACCIOLO, B. & GIAQUINTO, S. 2005. Determinants of the subjective functional outcome of total joint arthroplasty. *Archives of Gerontology and Geriatrics,* 41**,** 169-176.

CARAMES, B., TANIGUCHI, N., OTSUKI, S., BLANCO, F. J. & LOTZ, M. 2010. Autophagy is a protective mechanism in normal cartilage, and its aging-related loss is linked with cell death and osteoarthritis. *Arthritis and Rheumatism,* 62**,** 791–801.

CARLO, M. D. & LOESER, R. F. 2008. Cell death in osteoarthritis. *Current Rheumatology Reports* 10**,** 37–42.

CHAGANTI, R. K. & LANE, N. E. 2011. Risk factors for incident osteoarthritis of the hip and knee. *Current Reviews in Musculoskeletal Medicine,* 4**,** 99-104.

CHAO, P. H., WEST, A. C. & HUNG, C. T. 2006. Chondrocyte intracellular calcium, cytoskeletal organization, and gene expression responses to dynamic

osmotic loading. *American Journal of Physiology-Cell Physiology,* 291**,** C718-725.

CHEN, C., XIE, J., DENG, L. & YANG, L. 2014. Substrate stiffness together with soluble factors affects chondrocyte mechanoresponses. *ACS Applied Materials & Interfaces,* 6**,** 16106-16116.

CHEN, C. T., BHARGAVA, M., LIN, P. M. & TORZILLI, P. A. 2003. Time, stress, and location dependent chondrocyte death and collagen damage in cyclically loaded articular cartilage. *Journal of Orthopaedic Research,* 21**,** 888-898.

CHEN, C. T., BURTON-WURSTER, N., BORDEN, C., HUEFFER, K., BLOOM, S. E. & LUST, G. 2001. Chondrocyte necrosis and apoptosis in impact damaged articular cartilage. *Journal of Orthopaedic Research,* 19**,** 703-711.

CHEN, F. H., ROUSCHE, K. T. & TUAN, R. S. 2006. Technology insight: adult stem cells in cartilage regeneration and tissue engineering. *Nature Clinical Practice Rheumatology,* 2**,** 373-382.

CHEUNG, C. Y. K. & KO, B. C. B. 2013. NFAT5 in cellular adaptation to hypertonic stress - regulations and functional significance. *Journal of Molecular signalling,* 8**,** 1-9.

CHEVALIER, X. 1993. Fibronectin, cartilage, and osteoarthritis. *Seminars in Arthritis and Rheumatism,* 22**,** 307-318.

CHEVALIER, X., GROULT, N., LARGET-PIET, B., ZARDI, L. & HORNEBECK, W. 1994. Tenascin distribution in articular cartilage from normal subjects and from patients with osteoarthritis and rheumatoid arthritis. *Arthritis and Rheumatism,* 37**,** 1013-1022.

CHIROFF, R. T. & COOKE, C. P. R. 1975. Osteochondritis dissecans: a histologic and microradiographic analysis of surgically excised lesions. *Journal of Trauma,* 15**,** 689-696.

CHUBINSKAYA, S., CS-SZABÓ, G. & KUETTNER, K. E. 1998. ADAM-10 message is expressed in human articular cartilage. *Journal of Histochemistry and Cytochemistry,* 46**,** 723–729.

CHUNG, J. Y., SONG, M., HA, C. W., KIM, J. A., LEE, C. H. & PARK, Y. B. 2014. Comparison of articular cartilage repair with different hydrogel-human

umbilical cord blood-derived mesenchymal stem cell composites in a rat mode. *Stem Cell Research & Therapy,* 5**,** 1-13.

CIVININI, R., NISTRI, L., MARTINI, C., REDL, B., RISTORI, G. & INNOCENTI, M. 2013. Growth factors in the treatment of early osteoarthritis. *Clinical Cases in Mineral and Bone Metabolism,* 10**,** 26-29.

CLARK, A. L., BARCLAY, L. D., MATYAS, J. R. & HERZOG, W. 2003. In situ chondrocyte deformation with physiological compression in the feline patellofemoral joint. *Journal of Biomechanics,* 36**,** 553-568.

CLEMENTS, K. M., BURTON-WURSTER, N. & LUST, G. 2004. The spread of cell death from impact damaged cartilage: lack of evidence for the role of nitric oxide and caspases. *Osteoarthritis and Cartilage,* 12**,** 577-85.

CUKIERMAN, E., PANKOV, R., STEVENS, D. R. & YAMADA, K. M. 2001. Taking cell-matrix adhesions to the third dimension. *Science,* 294**,** 1708-1712.

D'ANSELMI, F., VALERIO, M., CUCINA, A., GALLI, L., PROIETTI, S., DINICOLA, S., PASQUALATO, A., MANETTI, C., RICCI, G., GIULIANI, A. & BIZZARRI, M. 2011. Metabolism and cell shape in cancer: a fractal analysis. *International Journal of Biochemistry and Cell Biology,* 43**,** 1052-1058.

D'LIMA, D., HASHIMOTO, S., CHEN, P., COLWELL, C. & LOTZ, M. 2001a. Human chondrocyte apoptosis in response to mechanical injury. *Osteoarthritis and Cartilage,* 9**,** 712-719.

D'LIMA, D. D., HASHIMOTO, S., CHEN, P. C., COLWELL, J., C.W. & LOTZ, M. K. 2001b. Impact of mechanical trauma on matrix and cells. *Clinical Orthopaedics and Related Reasearch,* 391S**,** S90–S99.

DANEN, E. H. & YAMADA, K. M. 2001. Fibronectin, integrins, and growth control. *Journal of Cellular Physiology,* 189**,** 1-13.

DARLING, E. M. & ATHANASIOU, K. A. 2005. Rapid phenotypic changes in passaged articular chondrocyte subpopulations. *Journal of Orthopaedic Research,* 23**,** 425-432.

DARLING, E. M., ZAUSCHER, S. & GUILAK, F. 2006. Viscoelastic properties of zonal articular chondrocytes measured by atomic force microscopy. *Osteoarthritis and Cartilage,* 14**,** 571-579.

DE CROMBRUGGHE, B., LEFEBVRE, V., BEHRINGER, R. R., BI, W., MURAKAMI, S. & HUANG, W. 2000. Transcriptional mechanisms of chondrocyte differentiation. *Matrix Biology,* 19**,** 389-394.

DE LANGE-BROKAAR, B. J. E., IOAN-FACSINAY, A., VAN OSCH, G. J. V. M., ZUURMOND, A. M., SCHOONES, J., TOES, R. E. M., HUIZINGA, T. W. J. & KLOPPENBURG, M. 2012. Synovial inflammation, immune cells and their cytokines in osteoarthritis: a review. *Osteoarthritis and Cartilage,* 20**,** 1484-1499.

DEAN, D. D., MARTEL-PELLETIER, J., PELLETIER, J. P., HOWELL, D. S. & WOESSNER, J. F. 1989. Evidence for metalloproteinase and metalloproteinase inhibitor imbalance in human osteoarthritic cartilage. *Journal of Clinical Investigation,* 84**,** 678-685.

DENNIS, J. E., COHEN, N., GOLDBERG, V. M. & CAPLAN, A. I. 2004. Targeted delivery of progenitor cells for cartilage repair. *Journal of Orthopaedic Research***,** 735-741.

DESROCHERS, J., AMREIN, M. W. & MATYAS, J. R. 2012. Viscoelasticity of the articular cartilage surface in early osteoarthritis. *Osteoarthritis and cartilage,* 20**,** 413-421.

DICESARE, P. E., MORGELIN, M., MANN, K. & PAULSSON, M. 1994. Cartilage oligomeric matrix protein and thrombospondin 1. Purification from articular cartilage, electron microscopic structure, and chondrocyte binding. *European Journal of Biochemistry,* 223**,** 927-937.

DIMICCO, M. A., PATWARI, P., SIPARSKY, P. N., KUMAR, S., PRATTA, M. A., LARK, M. W., KIM, Y. J. & GRODZINSKY, A. J. 2004. Mechanisms and kinetics of glycosaminoglycan release following in vitro cartilage injury. *Arthritis and Rheumatism,* 50**,** 840–848.

DOWTHWAITE, G. P., BISHOP, J. C., REDMAN, S. N., KHAN, I. M., ROONEY, P., EVANS, D. J., HAUGHTON, L., BAYRAM, Z., BOYER, S., THOMSON, B., WOLFE, M. S. & ARCHER, C. W. 2004. The surface of

articular cartilage contains a progenitor cell population. *Journal of Cell Science,* 117**,** 889-897.

DREIER, R. 2010. Hypertrophic differentiation of chondrocytes in osteoarthritis: the developmental aspect of degenerative joint disorder. *Arthritis Research and Therapy,* 12**,** 216-227.

DUDA, G. N., EILERS, M., LOH, L., HOFFMAN, J. E., KAAB, M. & SCHASER, K. 2001. Chondrocyte death precedes structural damage in blunt impact trauma. *Clinical Orthopedics and Related Research,* 393**,** 302-309.

DUDHIA, J. 2005. Aggrecan, aging and assembly in articular cartilage. *Cellular and Molecular Life Science,* 62**,** 2241-2256.

ECHTERMEYER, F., BERTRAND, J., DREIER, R., MEINECKE, I., NEUGEBAUER, K., FUERST, M., LEE, Y. J., SONG, Y. W., HERZOG, C., THEILMEIER, G. & PAP, T. 2009. Syndecan-4 regulates ADAMTS-5 activation and cartilage breakdown in osteoarthritis. *Nature Medicine,* 15**,** 1072-1076.

EGERBACHER, M. & HAEUSLER, G. 2003. Integrins in growth plate cartilage. *Pediatric Endocrinology Reviews,* 1**,** 2-8.

ELTAWIL, N. M., HOWIE, S. E. M., SIMPSON, A. H. R. W., AMIN, A. K. & HALL, A. C. 2014. The use of hyperosmotic saline for chondroprotection: implications for orthopaedic surgery and cartilage repair. *Osteoarthritis and Cartilage* 23**,** 469-477.

ERRINGTON, R. J., FRICKER, M. D., WOOD, J. L., HALL, A. C. & WHITE, N. S. 1997. Four-dimensional imaging of living chondrocytes in cartilage using confocal microscopy: a pragmatic approach. *American Journal of Physiology-Cell Physiology,* 272**,** C1040-C1051.

EYRE, D. 2002. Collagen of articular cartilage. *Arthritis Research,* 4**,** 30-35.

EYRE, D. R. 2004. Collagens and cartilage matrix homeostasis. *Clinical Orthopaedics and Related Research.,* 427S**,** 118-122.

EYRE, D. R., MCDEVITT, C. A., BILLINGHAM, M. E. J. & MUIR, H. 1980. Biosynthesis of collagen and other matrix proteins by articular cartilage in experimental osteoarthrosis. *Biochemical Journal,* 188**,** 823-837.

FARHAN-ALANIE, M. M. & HALL, A. C. 2014. Temperature changes and chondrocyte death during drilling in a bovine cartilage model and chondroprotection by modified irrigation solutions. *International Orthopaedics,* 38**,** 2407-2412.

FARNWORTH, L. 2000. Osteochondral defects of the knee. *Orthopedics,* 23**,** 146-157.

FEDEWA, M. M., OEGEMA, T. R. J., SCHWARTZ, M. H., MACLEOD, A. & LEWIS, J. L. 1998. Chondrocytes in culture produce a mechanically functional tissue. *Journal of Orthopaedic Research,* 16**,** 227-236.

FELL, H. B. & DINGLE, J. T. 1969. Endocytosis of sugars in embryonic skeletal tissues in organ culture. I. General introduction and histological effects. *Journal of Cell Science,* 4**,** 89-103.

FELSON, D. T., NEVITT, M. C., ZHANG, Y., ALIABADI, P., BAUMER, B., GALE, D., LI, W., YU, W. & XU, L. 2002. High prevalence of lateral knee osteoarthritis in beijing chinese compared with framingham caucasian subjects. *Arthritis and Rheumatism,* 46**,** 1217–1222.

FELSON, D. T., NIU, J., GROSS, K. D., ENGLUND, M., SHARMA, L., COOKE, T. D., GUERMAZI, A., ROEMER, F. W., SEGAL, N., GOGGINS, J. M., LEWIS, C. E., EATON, C. & NEVITT, M. C. 2013. Valgus malalignment is a risk factor for lateral knee osteoarthritis incidence and progression: findings from the multicenter osteoarthritis study and the osteoarthritis initiative. *Arthritis and Rheumatism,* 65**,** 355-362.

FERNANDES, J. C., MARTEL-PELLETIER, J. & PELLETIER, J.-P. 2002. The role of cytokines in osteoarthritis pathophysiology. *Biorheology,* 39**,** 237-246.

FICKERT, S., FIEDLER, J. & BRENNER, R. E. 2004. Identification of subpopulations with characteristics of mesenchymal progenitor cells from human osteoarthritic cartilage using triple staining for cell surface markers. *Arthritis Research & Therapy,* 6**,** R422–R432.

FORTIER, L. A., BARKER, J. U., STRAUSS, E. J., MCCARREL, T. M. & COLE, B. J. 2011. The role of growth factors in cartilage repair. *Clinical Orthopedics and Related Research,* 469**,** 2706-2715.

FOX, A. J. S., BEDI, A. & RODEO, S. A. 2009. The basic science of articular cartilage: structure, composition, and function. *Orthopaedics,* 1**,** 461-468.

FRIGAULT, M. M., LACOSTE, J., SWIFT, J. L. & BROWN, C. M. 2009. Live-cell microscopy - tips and tools. *Journal of Cell Science,* 122**,** 753-767.

FUKUI, N., IKEDA, Y., TANAKA, N., WAKE, M., YAMAGUCHI, T., MITOMI, H., ISHIDA, S., FURUKAWA, H., HAMADA, Y., MIYAMOTO, Y., SAWABE, M., TASHIRO, T., KATSURAGAWA, Y. & TOHMA, S. 2011. αvβ5 integrin promotes dedifferentiation of monolayer-cultured articular chondrocytes. *Arthritis and Rheumatism,* 63**,** 1938-1949.

GAIPL, U. S., KUHN, A., SHERIFF, A., MUNOZ, L. E., FRANZ, S., VOLL, R. E., KALDEN, J. R. & HERRMANN, M. 2006. Clearance of apoptotic cells in human SLE. *Current Directions in Autoimmunity,* 9**,** 173-187.

GALASSO, O., FAMILIARI, F., GORI, M. D. & GASPARINI, G. 2012. Recent Findings on the Role of Gelatinases (Matrix Metalloproteinase-2 and -9) in Osteoarthritis. *Advances in Orthopedics,* 2012**,** 1-7.

GAO, Y., LIU, S., HUANG, J., GUO, W., CHEN, J., ZHANG, L., ZHAO, B., PENG, J., WANG, A., WANG, Y., XU, W., LU, S., YUAN, M. & GUO, Q. 2014. The ECM-cell interaction of cartilage extracellular matrix on chondrocytes. *BioMed Research International,* 2014**,** 8 pages.

GAVRIELI, Y., SHERMAN, Y. & BEN-SASSON, S. A. 1992. Identification of programmed cell death in situ via specific labeling of nuclear DNA fragmentation. *Journal of Cell Biology,* 119**,** 493-501.

GE, Z., HU, Y., HENG, B. C., YANG, Z., OUYANG, H., LEE, E. H. & CAO, T. 2006. Osteoarthritis and therapy. *Arthritis and Rheumatism,* 55**,** 493-500.

GHADIALLY, F. N., THOMAS, I., YONG, N. & LALONDE, J.-M. A. 1978. Ultrastructure of rabbit semilunar cartilages. *Journal of Anatomy,* 125**,** 499-517.

GIANCOTTI, F. G. 2000. Complexity and specificity of integrin signalling. *Nature Cell Biology* 2**,** E13-E14.

GLASER, J. H. & CONRAD, H. E. 1984. Properties of chick embryo chondrocytes grown in serum-free medium. *Journal of Biological Chemistry,* 259**,** 6766-6772.

GLOWACKI, J., TREPMAN, E. & FOLKMAN, J. 1983. Cell shape and phenotypic expression in chondrocytes. *Proceedings of The Society for Experimental Biology and Medicine,* 172**,** 93-98.

GOLDRING, M. B. 2000a. Osteoarthritis and cartilage: The role of cytokines. *Current Rheumatology Reports,* 2**,** 459-465.

GOLDRING, M. B. 2000b. The role of the chondrocyte in osteoarthritis. *Arthritis and Rheumatism,* 43**,** 1916-1926.

GOLDRING, M. B. 2002. Molecular regulation of the chondrocyte phenotype. *Journal of Musculoskeletal & Neuronal Interactions,* 2**,** 517-520.

GOLDRING, M. B. 2012. Chondrogenesis, chondrocyte differentiation, and articular cartilage metabolism in health and osteoarthritis. *Therapeutic Advances in Musculoskeletal Disease,* 4**,** 269-285.

GOLDRING, M. B. & MARCU, K. B. 2009. Cartilage homeostasis in health and rheumatic diseases. *Arthritis Research & Therapy,* 11.

GOLDRING, M. B., OTERO, M., PLUMB, D. A., DRAGOMIR, C., FAVERO, M., EL HACHEM, K., HASHIMOTO, K., ROACH, H. I., OLIVOTTO, E., BORZÌ, R. M. & MARCU, K. B. 2011. Roles of inflammatory and anabolic cytokines in cartilage metabolism: signals and multiple effectors converge upon MMP-13 regulation in osteoarthritis. *European Cells and Materials,* 21**,** 202-220.

GOLDRING, M. B., OTERO, M., TSUCHIMOCHI, K., IJIRI, K. & LI, Y. 2008. Defining the roles of inflammatory and anabolic cytokines in cartilage metabolism. *Annals of the Rheumatic Diseases,* 67**,** 1-17.

GOLDRING, S. R. & GOLDRING, M. B. 2004. The role of cytokines in cartilage matrix degeneration in osteoarthritis. *Clinical Orthopaedics and Related Reasearch,* 427S**,** 27-36.

GOLE, M. D., POULSEN, D., MARZO, J. M. & ZIV, I. 2004. Chondrocyte viability in press-fit cryopreserved osteochondral allografts. *Journal of Orthopaedic Research,* 22**,** 781-787.

GONZALEZ, S., FRAGOSO-SORIANO, R. J. & KOURI, J. B. 2007. Chondrocytes interconnecting tracks and cytoplasmic projections observed within the superficial zone of normal human articular cartilage- A transmission electron

microscopy, atomic force microscopy, and two-photon excitation microscopy studies. *Microscopy Research and Technique,* 70**,** 1072-1078.

GRODZINSKY, A. J., LEVENSTON, M. E., JIN, M. & FRANK, E. H. 2000. Cartilage tissue remodeling in response to mechanical forces. *Annual Review of Biomedical Engineering,* 2**,** 691-713.

GROGAN, S. P. & D'LIMA, D. D. 2010. Joint aging and chondrocyte cell death. *International Journal of Clinical Rheumtology,* 5**,** 199-214.

GROGAN, S. P., MIYAKI, S., ASAHARA, H., D'LIMA, D. D. & LOTZ, M. K. 2009. Mesenchymal progenitor cell markers in human articular cartilage: normal distribution and changes in osteoarthritis. *Arthritis Research & Therapy,* 11**,** R85.

GUAN, J., URBAN, J. P. G., LI, Z. H., FERGUSON, D. J. P., GONG, C. Y. & CUI, Z. F. 2006. Effects of rapid cooling on articular cartilage. *Cryobiology,* 52**,** 430–439.

GUILAK, F., ALEXOPOULOS, L. G., UPTON, M. L., YOUN, I., CHOI, J. B., CAO, L., SETTON, L. A. & HAIDER, M. A. 2006. The pericellular matrix as a transducer of biomechanical and biochemical signals in articular cartilage. *Annals of the New York Academy of Sciences,* 1068**,** 498-512.

GUILAK, F., FERMOR, B., KEEFE, F. J., KRAUS, V. B., OLSON, S. A., PISETSKY, D. S., SETTON, L. A. & WEINBERG, J. B. 2004. The role of biomechanics and inflammation in cartilage injury and repair. *Clinical Orthopedics and Related Research,* 423**,** 17–26.

GUILAK, F., RATCLIFFE, A., LANE, N., ROSENWASSER, M. P. & MOW, V. C. 1994. Mechanical and Biochemical Changes in the Superficial Zone of Articular Cartilage in Canine Experimental Osteoarthritis. *The Journal of Bone & Joint Surgery,* 12**,** 474-484.

GUILAK, F., RATCLIFFE, A. & MOW, V. C. 1995. Chondrocyte deformation and local tissue strain in articular cartilage: a confocal microscopy study. *Journal of Orthopaedic Research,* 13**,** 410-421.

GUMBINER, B. M. 1996. Cell adhesion: the molecular basis of tissue architecture and morphogenesis. *Cell,* 84**,** 345–357.

GUO, D., DING, L. & HOMANDBERG, G. A. 2009. Telopeptides of type II collagen upregulate proteinases and damage cartilage but are less effective than highly active fibronectin fragments. *Inflammation Research,* 58**,** 161-169.

HALL, A. C., HORWITZ, E. R. & WILKINS, R. J. 1996a. The cellular Physiology of Articular cartilage. *Experimental Physiology,* 81**,** 535-545.

HALL, A. C., STARKS, I., SHOULTS, C. L. & RASHIDBIGI, S. 1996b. Pathways for K+ transport across the bovine articular chondrocyte membrane and their sensitivity to cell volume. *American Journal of Physiology,* 270**,** 1300-1310.

HE, B., WU, J. P., KIRK, T. B., CARRINO, J. A., XIANG, C. & XU, J. 2014. High-resolution measurements of the multilayer ultra-structure of articular cartilage and their translational potential. *Arthritis Research & Therapy,* 16**,** 1-16.

HEDLUND, H., BISMAR, H., MENGARELLI-WIDHILOM, S. F. P. & SVENSSON, O. 1994. Studies of the cell columns of articular cartilage using UV-confocal scanning laser microscopy and 3D image processing. *European Journal of Experimental & Musculoskel Research,* 60**,** 93-98.

HEINEGARD, D. 2009. Proteoglycans and more – from molecules to biology. *International Journal of Experimental Pathology,* 90**,** 575-586.

HENROTIN, Y. E., BRUCKNER, P. & PUJOL, J.-P. L. 2003. The role of reactive oxygen species in homeostasis and degradation of cartilage. *Osteoarthritis and Cartilage,* 11**,** 747-755.

HENSON, F. M. D. & VINCENT, T. A. 2008. Alterations in the vimentin cytoskeleton in response to single impact load in an in vitro model of cartilage damage in the rat. *BMC Musculoskeletal Disorders,* 9**,** 10 pages.

HIRAOKA, K., GROGAN, S., OLEE, T. & LOTZ, M. 2006. Mesenchymal progenitor cells in adult human articular cartilage. *Biorheology,* 43**,** 447-454.

HOFFMANN, E. K., LAMBERT, I. H. & PEDERSEN, S. F. 2009. Physiology of cell volume regulation in vertebrates. *Physiological Reviews,* 89**,** 193-277.

HOLLANDER, A. P., PIDOUX, I., REINER, A., RORABECK, C., BOUME, R. & POOLE, A. R. 1995. Damage to Type II collagen in aging and osteoarthritis starts at the articular surface, Originates around chondrocytes, and extends

into the cartilage with progressive degeneration. *Journal of Clinical Investigation,* 96**,** 2859-2869.

HOLLOWAY, I., KAYSER, M., LEE, D. A., BADER, D. L., BENTLEY, G. & KNIGHT, M. M. 2004. Increased presence of cells with multiple elongated processes in osteoarthritic femoral head cartilage. *Osteoarthritis and Cartilage,* 12**,** 17-24.

HOPEWELL, B. & URBAN, J. 2003. Adaptation of articular chondrocytes to changes in osmolality. *Biorheology,* 40**,** 73-77.

HOWELL, D. S. 1986. Pathogenesis of osteoarthritis. *The American Journal of Medicine,* 80**,** 24-28.

HUANG, Y., ZHANG, Y., DING, X., LIU, S. & SUN, T. 2015. Osmolarity influences chondrocyte repair after injury in human articular cartilage. *Journal of Orthopaedic Surgery and Research,* 10**,** 1-9.

HUBER, M., TRATTNIG, S. & LINTNER, F. 2000. Anatomy, biochemistry, and physiology of articular cartilage. *Investigative Radiology,* 35**,** 573-580.

HUGLE, T., GEURTS, J., NUESCH, C., MULLER-GERBL, M. & VALDERRABANO, V. 2012. Aging and osteoarthritis: an inevitable encounter? *Journal of Aging Research,* Article ID 950192**,** 7 pages.

HULTH, A., LINDBERG, L. & TELHAG, H. 1972. Mitosis in human articular ostoearthritic cartilage. *Clinical Orthopedics and Related Research,* 84**,** 197–199.

HUMBREE, W. C., WARD, B. D., FURMAN, B. D., ZURA, R. D., NICHOLS, L. A., GUILAK, F. & OLSON, S. A. 2007. Viability and apoptosis of human chondrocytes in osteochondral fragments following joint trauma. *Journal of Bone and Joint Surgery,* 89-B**,** 1389-1395.

HUNTLEY, J. S., BUSH, P. G., MCBIRNIE, J. M., SIMPSON, A. H. & HALL, A. C. 2005. Chondrocyte death associated with human femoral osteochondral harvest as performed for mosaicplasty. *Journal of Bone and Joint Surgery. American Volume,* 87**,** 351-360.

HUNZIKER, E. B. 2001. Articular cartilage repair: basic science and clinical progress. A review of the current status and prospects. *Osteoarthritis and Cartilage,* 10**,** 432–463.

IMAI, K., OHTA, S., MATSUMOTO, T., FUJIMOTO, N., SATO, H. & SEIKI, M. 1997. Expression of membrane-type 1 matrix metalloproteinase and activation of progelatinase A in human osteoarthritic cartilage. *American Journal of Pathology,* 151**,** 245–256.

JACKSON, A. R. & GU, W. Y. 2009. Transport properties of cartilaginous tissues. *Current Rheumatology Reviews,* 5**,** 1-18.

JAMES, C. B. & UHL, T. L. 2001. A review of articular cartilage pathology and the use of glucosamine sulfate. *Journal of Athletic Training,* 36**,** 413-419.

JANG, K. W., DING, L., SEOL, D., LIM, T. H., BUCKWALTER, J. A. & MARTIN, J. A. 2014. Low-intensity pulsed ultrasound promotes chondrogenic progenitor cell migration via focal adhesion kinase pathway. *Ultrasound in Medicine & Biology,* 40**,** 1177-1186.

JEFFERY, A. K., BLUNN, G. W., ARCHER, C. W. & BENTLEY, G. 1991. Three-Dimensional collagen architecture in bovine articular cartilage. *Journal of Bone and Joint Surgery,* 73**,** 795-801.

JEFFREY, J. E., GREGORY, D. W. & ASPDEN, R. M. 1995. Matrix damage and chondrocyte viability following a single impact load on articular cartilage. *Archives of Biochemistry and Biophysics,* 322**,** 87-96.

JIANG, Y., TONG, T., HENG, B. & OUYANG, H. 2012. Cartilage injuries: role of implantation of human stem/progenitor cells. *In:* HAYAT, M. A. (ed.) *Stem Cells and Cancer Stem Cells.* Springer, Vol. 3, 327–333.

JOHNSON, E. M., BERK, D. A., JAIN, R. K. & DEEN, W. M. 1996. Hindered diffusion in agarose gels: test of effective medium model. *Biophysical Journal,* 70**,** 1017-1026.

JONES, C. W., SMOLINSKI, D., KEOGH, A., KIRK, T. B. & ZHENG, M. H. 2005. Confocal laser scanning microscopy in orthopaedic research. *Progress in Histochemistry and Cytochemistry,* 40**,** 1-71.

JOOS, H., WILDNER, A., HOGREFE, C., REICHEL, H. & BRENNER, R. E. 2013. Interleukin-1β and tumor necrosis factor α inhibit migration activity of chondrogenic progenitor cells from non-fibrillated osteoarthritic cartilage. *Arthritis Research & Therapy,* 15**,** R119.

KERR, J. F., WYLLIE, A. H. & CURRIE, A. R. 1972. Apoptosis: a basic biological phenomenon with wide-ranging implications in tissue kinetics. *British Journal of Cancer,* 26**,** 239-257.

KERRIGAN, M. J. P., HOOK, C. S. V., QUSOUS, A. & HALL, A. C. 2006. Regulatory volume increase (RVI) by in situ and isolated bovine articular chondrocytes. *Journal of Cellular Physiology,* 209**,** 481-492.

KHAN, I. M., PALMER, E. A. & ARCHER, C. W. 2010. Fibroblast growth factor-2 induced chondrocyte cluster formation in experimentally wounded articular cartilage is blocked by soluble Jagged-1. *Osteoarthritis and Cartilage,* 18**,** 208-219.

KIERNAN, J. A. 2008. Histological and Histochemical Methods: Theory and Practice. 4th ed. Bloxham, UK: Scion.

KIM, H. A., LEE, Y. J., SEONG, S. C., CHOE, K. W. & SONG, Y. W. 2000. Apoptotic chondrocyte death in human osteoarthritis. *The Journal of Rheumatolgy,* 27**,** 455-462.

KIM, H. T., LO, M. Y. & PILLARISETTY, R. 2002. Chondrocyte apoptosis following intraarticular fracture in humans. *Osteoarthritis and Cartilage,* 10**,** 747–749.

KIM, Y. J., SAH, R. L. Y., GRODZINSKY, A. J., PLAAS, A. H. K. & SANDY, J. D. 1994. Mechanical regulation of cartilage biosynthetic behaviour: physical stimuli. *Archives of Biochemistry and Biophysics,* 311**,** 1-12.

KIRKWOOD, R. N., GOMES, H. A., SAMPAIO, R. F., CULHAM, E. & COSTIGAN, P. 2007. Biomechanical analysis of hip and knee joints during gait in elderly subjects. *Acta Ortopedica Brasileira,* 15**,** 267-271.

KLEEMANN, R. U., KROCKER, D., CEDRARO, A., TUISCHER, J. & DUDA, G. N. 2005. Altered cartilage mechanics and histology in knee osteoarthritis: relation to clinical assessment (ICRS Grade). *Osteoarthritis and Cartilage,* 13**,** 958-963.

KNUDSON, W. & LOESER, R. F. 2002. CD44 and integrin matrix receptors participate in cartilage homeostasis. *Cellular and Molecular Life Sciences,* 59**,** 36-44.

KOCH, S., KAMPEN, W. U. & LAPRELL, H. 1997. Cartilage and bone morphology in osteochondritis dissecans. *Knee Surgery, Sports Traumatolology, Arthroscopy,* 5**,** 42-45.

KOELLING, S., KRUEGEL, J., IRMER, M., PATH, J. R., SADOWSKI, B., MIRO, X. & MIOSGE, N. 2009. Migratory chondrogenic progenitor cells from repair tissue during the later stages of human osteoarthritis. *Cell Stem Cell,* 4**,** 324-335.

KOURI, J. B. & ABBUD-LOZOYA, K. A. 2002. Kinetics of the ultrastructural changes in apoptotic chondrocytes from an osteoarthrosis rat model: a window of comparison to the cellular mechanism of apoptosis in human chondrocytes. *Ultrastructural Pathology,* 26**,** 33-40.

KOURI, J. B., ARGUELLO, C., LUNA, J. & MENA, R. 1998. Use of microscopical techniques in the study of human chondrocytes from osteoarthritic cartilage: An overview. *Microscopy Research and Technique,* 40**,** 22-36.

KOURI, J. B., ARGUELLO, C., QUINTERO, M., CHICO, A. & RAMOS, M. E. 1996a. Variability in the cell phenotype of aggregates or "clones" of human osteoarthritic cartilage. A case report. *Biocell,* 20**,** 191-200.

KOURI, J. B., JIMENEZ, S. A., QUINTERO, M. & CHICO, A. 1996b. Ultrastructural study of chondrocytes from fibrillated and non-fibrillated human osteoarthritic cartilage. *Osteoarthritis and Cartilage,* 4**,** 111-125.

KOURI, J. B. & LAVALLE, C. 2006. Do chondrocytes undergo "activation" and "transdifferentiation" during the pathogenesis of OA? A review of the ultrastructural and immunohistochemical evidence. *Histology and Histopathology,* 21**,** 793-802.

KRAMER, W. C., HENDRICKS, K. J. & WANG, J. 2011. Pathogenetic mechanisms of posttraumatic osteoarthritis: opportunities for early intervention. *International Journal of Clinical and Experimental Medicine,* 4**,** 285-298.

KUETTNER, K. E., AYDELOTTE, M. B. & THONAR, E. J. 1991. Articular cartilage matrix and structure: a minireview. *The Journal of Rheumatology. Supplement,* 27**,** 46-48.

KUETTNER, K. E., PAULI, B. U., GALL, G., MEMOLI, V. A. & SCHENK, R. K. 1982. Synthesis of cartilage matrix by mammalian chondrocytes in vitro. I. Isolation, culture characteristics, and morphology. *The journal of Cell Biology,* 93**,** 743-750.

KUHN, K., D'LIMA, D. D., HASHIMOTO, S. & LOTZ, M. 2004. Cell death in cartilage. *Osteoarthritis and Cartilage,* 12**,** 1-16.

KURZ, B., JIN, M., PATWARI, P., CHENG, D. M., LARK, M. W. & GRODZINSKY, A. J. 2001. Biosynthetic response and mechanical properties of articular cartilage after injurious compression. *Journal of Orthopaedic Research,* 19**,** 1140-1116.

KURZ, B., LEMKE, A. K., FAY, J., PUFE, T., GRODZINSKY, A. J. & SCHU¨NKE, M. 2005. Pathomechanisms of cartilage destruction by mechanical injury. *Annals of Anatomy,* 187**,** 473-485.

LAI, W. M., HOU, J. S. & MOW, V. C. 1991. A triphasic theory for the swelling and deformation behaviors of articular cartilage. *Journal of Biochemical Engineering,* 113**,** 245-258.

LANG, F., BUSCH, G. L., RITTER, M., VOLKL, H., WALDEGGER, S., GULBINS, E. & HAUSSINGER, D. 1998. Functional significance of cell volume regulatory mechanisms. *Physiological Reviews,* 78**,** 247-306.

LAPADULA, G., IANNONE, F., ZUCCARO, C., GRATTAGLIANO, V., COVELLI, M., PATELLA, V., LO BIANCO, G. & PIPITONE, V. 1997. Integrin expression on chondrocytes: correlations with the degree of cartilage damage in human osteoarthritis. *Clinical and Experimental Rheumatology* 15**,** 247-254.

LAPADULA, G., IANNONE, F., ZUCCARO, C., GRATTAGLIANO, V., COVELLI, M., PATELLA, V., LO BIANCO, G. & PIPITONE, V. 1998. Chondrocyte Phenotyping in Human Osteoarthritis. *Clinical Rheumatology,* 17**,** 99-104.

LARK, M. W., BAYNE, E. K., FLANAGAN, J., HARPER, C. F., HOERRNER, L. A., HUTCHINSON, N. I., SINGER, I. I., DONATELLI, S. A., WEIDNER, J. R., WILLIAMS, H. R., MUMFORD, R. A. & LOHMANDER, L. S. 1997. Aggrecan degradation in human cartilage. Evidence for both matrix

metalloproteinase and aggrecanase activity in normal, osteoarthritic, and rheumatoid joints. *Journal of Clinical Investigation,* 100**,** 93-106.

LAVERNIA, C. J., GUZMAN, J. F. & GACHUPIN-GARCIA, A. 1997. Cost effectiveness and quality of life in knee arthroplasty. *Clinical Orthopedics and Related Research,* 345**,** 134-139.

LEE, D. A., SALIH, V., STOCKTON, E. F., STANTON, J. S. & BENTLEY, G. 1997. Effect of normal synovial fluid on the metabolism of articular chondrocytes in vitro. *Clinical Orthopedics and Related Research***,** 228-238.

LEE, G. M. & LOESER, R. F. 1998. Interactions of the chondrocyte with its pericellular matrix. *Cells and Materials,* 8**,** 135-149.

LEE, G. M., PAUL, T. A., SLABAUGH, M. & KELLEY, S. S. 2000. The incidence of enlarged chondrons in normal and osteoarthritic human cartilage and their relative matrix density. *Osteoarthritis and Cartilage,* 8**,** 44-52.

LEE, J. H., FITZGERALD, J. B., DIMICCO, M. A. & GRODZINSKY, A. J. 2005. Mechanical injury of cartilage explants causes specific time-dependent changes in chondrocyte gene expression. *Arthritis and Rheumatism,* 52**,** 2386–2395.

LEE, J. H., ORT, T., MA, K., PICHA, K., CARTON, J., MARSTERS, P. A., LOHMANDER, L. S., BARIBAUD, F., SONG, X. Y. & BLAKE, S. 2009. Resistin is elevated following traumatic joint injury and causes matrix degradation and release of inflammatory cytokines from articular cartilage in vitro. *Osteoarthritis and Cartilage,* 17**,** 613–620.

LEE, R. B. & URBAN, J. P. 1997. Evidence for a negative Pasteur effect in articular cartilage. *Biochemical Journal,* 321**,** 95–102.

LEE, S. W., LEE, H. J., CHUNG, W. T., CHOI, S. M., RHYU, S. H., KIM, D. K., KIM, K. T., KIM, J. Y., KIM, J. M. & YOO, Y. H. 2004. TRAIL induces apop-tosis of chondrocytes and influences the pathogenesis of experimentally induced rat osteoarthritis. *Arthritis and Rheumatism,* 50**,** 534-542.

LEGATE, K. R., WICKSTROM, S. A. & FASSLER, R. 2009. Genetic and cell biological analysis of integrin outside-in signaling. *Genes and Development,* 23**,** 397–418.

LEWIS, R., FEETHAM, C. H. & JOLLEY, R. B. 2011. Cell volume regulation in chondrocytes. *Cellular Physiology and Biochemistry,* 28**,** 1111-1122.

LI, Y. P., WEI, X. C., ZHOU, J. M. & WEI, L. 2013. The Age-Related Changes in Cartilage and Osteoarthritis. [Review]. *BioMed Research International. article ID 916530.***,** 12 pages.

LINDEN, B. & TELHAG, H. 1977. Osteochondritis dissecans. A histologic and autoradiographic study in man. *Acta Orthopaedica Scandinavica,* 48**,** 682-686.

LINGARD, E. A., KATZ, J. N., WRIGHT, E. A. & SLEDGE, C. B. 2004. Predicting the outcome of total knee arthroplasty. *Journal of Bone and Joint Surgery. American Volume,* 86**,** 2179-2186.

LIPPIELLO, L., HALL, D. & MANKIN, H. J. 1977. Collagen synthesis in normal and osteoarthritic human cartilage. *Journal of Clinical Investigation,* 59**,** 593-600.

LOESER, R. F. 1997. Growth factor regulation of chondrocyte integrins. *Arthritis & Rheumatism,* 40**,** 270-276.

LOESER, R. F. 2000. Chondrocyte Integrin expression and function. *Biorheology,* 37**,** 109–116.

LOESER, R. F. 2002. Integrins and cell signalling in chondrocytes. *Biorheology,* 39**,** 119-124.

LOESER, R. F. 2013. Aging processes and the development of osteoarthritis. *Current Opinion in Rheumatology,* 25**,** 108-113.

LOESER, R. F. 2014. Integrins and chondrocyte–matrix interactions in articular cartilage. *Matrix Biology,* 39**,** 11-16.

LOESER, R. F., CARLSON, C. S. & MCGEE, M. P. 1995. Expression of β1 integrins by cultured articular chondrocytes and in osteoarthritic cartilage. *Experimental Cell Research,* 217**,** 248–257.

LOHMANDER, L. S. 2000. What can we do about osteoarthritis? *Arthritis Research,* 2**,** 95-100.

LOHMANDER, L. S., NEAME, P. J. & SANDY, J. D. 1993. The structure of aggrecan fragments in human synovial fluid. Evidence that aggrecanase

mediates cartilage degradation in inflammatory joint disease, joint injury, and osteoarthritis. *Arthritis and Rheumatism,* 36**,** 1214–1222.

LOTZ, M. K. 2010. Posttraumatic osteoarthritis: pathogenesis and pharmacological treatment options. *Arthritis Research & Therapy,* 12**,** 1-9.

LOTZ, M. K., OTSUKI, S., GROGAN, S. P., SAH, R., TERKELTAUB, R. & D'LIMA, D. 2010. Cartilage cell clusters. *Arthritis and Rheumatism,* 62**,** 2206-2218.

LOUGHLIN, J. 2011. Genetics of osteoarthritis. *Current Opinion in Rheumatology,* 23**,** 479-483.

LUCAS, L., GILBERT, N., PLOTON, D. & BONNET, N. 1996. Visualisation of volume data in confocal microscopy: comparison and improvements of volume rendering methods. *Journal of Microscopy,* 181**,** 238-252.

LYMAN, J. R., CHAPPELL, J. D., MORALES, T. I., KELLEY, S. S. & LEE, G. M. 2012. Response of chondrocytes to local mechanical injury in an ex vivo model. *Cartilage,* 3**,** 58-69.

MACRI, L., SILVERSTEIN, D. & CLARK, R. A. 2007. Growth factor binding to the pericellular matrix and its importance in tissue engineering. *Advanced Drug Delivery Reviews,* 59**,** 1366-1381.

MALEMUD, C. J. 1991. Changes in proteoglycans in osteoarthritis: biochemistry, ultrastructure and biosynthetic processing. *Journal of Rheumatology Supplement,* 27**,** 60-62.

MANKIN, H. J. 1964. Mitosis in Articular Cartilage of Immature Rabbits. A histologic, stathmokinetic (colchicine) and autoradiographic study. *Clinical Orthopaedics and Related Research,* 34**,** 170-183.

MANKIN, H. J. 1982. Current Concepts Review: The Response of Articular Cartilage to Mechanical Injury. *The Journal of Bone and Joint Surgery,* 64-A**,** 460-466.

MANKIN, H. J., DORFMAN, H., LIPPIELLO, L. & ZARINS, A. 1971. Biochemical and metabolic abnormalities in articular cartilage from osteo-arthritic human hips. II. Correlation of morphology with biochemical and metabolic data. *Journal of Bone and Joint Surgery. American Volume,* 53**,** 523-537.

MANOLOPOULOS, V., WAYNE MARSHALL, K., ZHANG, H., TROGADIS, J., TREMBLAY, L. & DOHERTY, P. J. 1999. Factors affecting the efficacy of bovine chondrocyte transplantation in vitro. *Osteoarthritis and Cartilage*, 453-460.

MARCELINO, J. & MCDEVITT, C. A. 1995. Attachment of articular cartilage chondrocytes to the tissue form of type VI collagen. *Biochimica Biophysica Acta,* 1249.

MARCH, L. M. & BACHMEIER, C. J. M. 1997. Economic of osteoar-thritis: a global perspective. *Baillieres Clinical Rheumatology,* 11, 817-834.

MARK, K. V. D., GAUSS, V., MARK, H. V. D. & MULLER, P. 1977. Relationship between cell shape and type of collagen synthesized as chondrocytes lose their cartilage phenotype in culture. *Nature,* 267, 531,532.

MARLOVITS, S., HOMBAUER, M., TRUPPE, M., VECSEI, V. & SCHLEGEL, W. 2004. Changes in the ratio of type-I and type-II collagen expression during monolayer culture of human chondrocytes. *Journal of Bone and Joint Surgery,* 86-B, 286-295.

MAROUDAS, A. 1975. Biophysical chemistry of cartilaginous tissues with special reference to solute and fluid transport. *Biorheology,* 12, 233-248.

MAROUDAS, A. 1976. Balance between swelling pressure and collagen tension in normal and degenerate cartilage. *Nature,* 260, 808-809.

MAROUDAS, A. 1990. Different ways of expressing concentration of cartilage constituents. In: Maroudas A, Kuettner K, Eds. Methods in Cartilage Research. London: Academic Press 211-219.

MAROUDAS, A., EVANS, H. & ALMEDIA, L. 1973. Cartilage of the hip joint : Topographical variation of glycosaminoglycan content in normal and fibrillated tissue. *Annals of the Rheumatic Diseases,* 32, 1-9.

MAROUDAS, A. & SCHNEIDERMAN, R. 1987. "Free" and "exchangeable" or "trapped" and "non-exchangeable" water in cartilage. *Journal of Orthopaedic Research,* 5, 133-138.

MAROUDAS, A. & VENN, M. 1977. Chemical composition and swelling of normal and osteoarthrotic femoral head cartilage. *Annals of Rheumatic Diseases,* 36, 399-406.

MARSH, J. L., BUCKWALTER, J. A., GELBERMAN, R., DIRSCHL, D., OLSON, S., BROWN, T. & LLINIAS, A. 2002. Articular fractures: does an anatomic reduction really change the result? . *Journal of Bone and Joint Surgery. American Volume,* 84-A**,** 1259–1271.

MARTEL-PELLETIER, J., ALAAEDDINE, N. & PELLETIER, J.-P. 1999. Cytokines and their role in the pathophysiology of osteoarthritis. *Frontiers in Bioscience,* 4**,** 694-703.

MARTIN, J. A., WILKEY, A. L. & BRAND, R. A. 2002. Cartilage extracellular matrix metabolism differs in serum and synovial fluid. *Methods in Cell Science,* 24**,** 139-143.

MARTIN, K. R., KUH, D., HARRIS, T. B., GURALNIK, J. M., COGGON, D. & WILLS, A. K. 2013. Body mass index, occupational activity, and leisure-time physical activity: an exploration of risk factors and modifiers for knee osteoarthritis in the 1946 British birth cohort. *BMC Musculoskeletal Disorders,* 14**,** 1-11.

MARTIN, R. M., LEONHARDT, H. & CARDOSO, M. C. 2005. DNA Labeling in Living Cells. *Cytometry Part A,* 67A**,** 45–52

MATTA, C., FODOR, J., MIOSGE, N., TAKÁCS, R., JUHÁSZ, T., RYBALTOVSZKI, H., TÓTH, A., CSERNOCH, L. & ZÁKÁNY, R. 2015. Purinergic signalling is required for calcium oscillations in migratory chondrogenic progenitor cells. *European Journal of Physiology,* 467**,** 429–442.

MAUCK, R. L., SEYHAN, S. L., ATESHIAN, G. A. & HUNG, C. T. 2002. Influence of seeding density and dynamic deformational loading on the developing structure/function relationships of chondrocyte-seeded agarose hydrogels. *Annals of Biomedical Engineering,* 30**,** 1046-1056.

MAUCK, R. L., SOLTZ, M. A., WANG, C. C., WONG, D. D., CHAO, P. H., VALHMU, W. B., HUNG, C. T. & ATESHIAN, G. A. 2000. Functional tissue engineering of articular cartilage through dynamic loading of chondrocyte-seeded agarose gels. *Journal of Biomechanical Engineering,* 122**,** 252-260.

MCARTHUR, S. D. & GARDNER, D. L. 1992. Articular cartilage fibrillation and permeability to Light Green SF dye. A method for the detection of pre-microscopic disease. *Journal of Bone and Joint Surgery,* 74**,** 668-672.

MCDEVITT, C. A. 1973. Biochemistry of articular cartilage. Nature of proteoglycans and collagen of articular cartilage and their role in aging and osteoarthrosis. *Annals of Rheumatic Diseases,* 32**,** 364-378.

MCDEVITT, C. A., PAHL, J. A., AYAD, S., MILLER, R. R., URATSUJI, M. & ANDRISH, J. T. 1988. Experimental osteoarthritic articular cartilage is enriched in guanidine-soluble type VI collagen. *Biochemical and Biophysical Research Communications,* 157**,** 250-255.

MCGLASHAN, S. R., CLUETT, E. C., JENSEN, C. G. & POOLE, C. A. 2008. Primary cilia in osteoarthritic chondrocytes: from chondrons to clusters. *Developmental Dynamics,* 237**,** 2013-2020.

MCQUILLAN, D. J., HANDLEY, C. J. & ROBINSON, H. C. 1986. Control of proteoglycan biosynthesis. Further studies on the effect of serum on cultured bovine articular cartilage. *Biochemical Journal,* 237**,** 741-747.

MEACHIM, G. & COLLINS, D. H. 1962. Cell counts of normal and osteo-arthritic articular cartilage in relation to the uptake of sulphate ($^{35}SO_4$) in vitro. *Annals of Rheumatic Diseases,* 21**,** 45-50.

MELCHIORRI, C., MELICONI, R., FRIZZIERO, L., SILVESTRI, T., PULSATELLI, L., MAZZETTI, I., BORZI, R. M., UGUCCIONI, M. & FACCHINI, A. 1998. Enhanced and co-ordinated in vivo expression of inflammatory cytokines and nitric oxide synthase by chondrocytes from patients with osteoarthritis. *Arthritis and Rheumatism,* 41**,** 2165-2174.

MILENTIJEVIC, D., RUBEL, I. F., LIEW, A. S., HELFET, D. L. & TORZILLI, P. A. 2005. An in vivo rabbit model for cartilage trauma: a preliminary study of the influence of impact stress magnitude on chondrocyte death and matrix damage. *Journal of Orthopaedic Trauma,* 19**,** 466-473.

MILNER, P. I., WILKINS, R. J. & GIBSON, J. S. 2012. Cellular physiology of articular cartilage in health and disease. *In:* ROTHSCHILD, B. M. (ed.) *Principles of Osteoarthritis.* InTech, Rijeka, pp. 567-590. ISBN 978-953-51-0063-8

MINSKY, M. 1988. Memoir on inventing the confocal scanning microscope. *Scanning,* 10**,** 128-138.

MIOSGE, N., WALETZKO, K., BODE, C., QUONDAMATTEO, F., SCHULTZ, W. & HERKEN, R. 1998. Light and electron microscopic in-situ hybridization of collagen type I and type II mRNA in the fibrocartilaginous tissue of late-stage osteoarthritis. *Osteoarthritis and Cartilage,* 6**,** 278-285.

MISTRY, D., OUE, Y., CHAMBERS, M. G., KAYSER, M. V. & MASON, R. M. 2004. Chondrocyte death during murine osteoarthritis. *Osteoarthritis and Cartilage,* 12**,** 131-141.

MITCHELL, N., LEE, E. R. & SHEPARD, N. 1992. The clones of osteoarthritic cartilage. *Journal of Bone and Joint Surgery,* 74-B**,** 33-38.

MOLLENHAUER, J., BEE, J. A., LIZARBE, M. A. & VON DER MARK, K. 1984. Role of anchorin CII, a 31,000-mol-wt membrane protein, in the interaction of chondrocytes with Type II collagen. *Journal of Cell Biology,* 98**,** 1572-1579.

MORT, J. S. & BILLINGTON, C. J. 2001. Articular cartilage and changes in arthritis matrix degradation. *Arthritis Research,* 3**,** 337-341.

MUELLER, M. B. & TUAN, R. S. 2011. Anabolic/Catabolic balance in pathogenesis of osteoarthritis: identifying molecular targets. *Physical Medicine & Rehabilitation,* 3**,** S3-S11.

MUIR, H. 1995. The chondrocyte, architect of cartilage: Biomechanics, structure, function and molecular biology of cartilage matrix macromolecules. *BioEssays,* 17**,** 1039-1048.

MURPHY, L. B., SACKS, J. J., BRADY, T. J., HOOTMAN, J. M. & CHAPMAN, D. P. 2012. Anxiety and depression among US adults with arthritis: prevalence and correlates. *Arthritis Care and Research,* 64**,** 968-976.

MURRAY, C. J. L. & LOPEZ, A. D., EDITORS. 1996. The global burden of disease. A comprehensive assessment of mortality and disability from diseases, injuries, and risk factors in 1990 and projected to 2020. Cambridge (MA): Harvard School of Public Health on behalf of the World Health Organization and The World Bank.

MURRAY, D. H., BUSH, P. G., BRENKEL, I. J. & HALL, A. C. 2010. Abnormal human chondrocyte morphology is related to increased lavels of cell-associated IL-1 beta and disruption to pericellular collagen type VI. *Journal of Orthopaedic Research,* 28**,** 1507-1514.

MUSUMECI, G., CASTROGIOVANNI, P., TROVATO, F. M., DI GIUNTA, A., LORETO, C. & CASTORINA, S. 2013. Microscopic and macroscopic anatomical features in healthy and osteoarthritic knee cartilage. *OA Anatomy,* 1**,** 1-6.

NEGORO, K., KOBAYASHI, S., TAKENO, K., UCHIDA, K. & BABA, H. 2008. Effect of osmolarity on glycosaminoglycan production and cell metabolism of articular chondrocyte under three-dimensional culture system. *Clinical and Experimental Rheumatology,* 26**,** 534-541.

NEWMAN, A. P. 1998. Articular cartilage repair. *The American Journal of Sports Medicine,* 26**,** 309-324.

NISHIDA, T., KUBOTA, S., KOJIMA, S., KUBOKI, T., NAKAO, K., KUSHIBIKI, T., TABATA, Y. & TAKIGAWA, M. 2004. Regeneration of defects in articular cartilage in rat knee joints by CCN2 (connective tissue growth factor). *Journal of Bone and Mineral Research,* 19**,** 1308–1319.

NUVER-ZWART, I., SCHALKWIJK, J., JOOSTEN, L. A., VAN DEN BERG, W. B. & VAN DE PUTTE, L. B. 1988. Effects of synovial fluid and synovial fluid cells on chondrocyte metabolism in short term tissue culture. *The Journal of Rheumatology.,* 15**,** 210-216.

OHTA, S., IMAI, K., YAMASHITA, K., MATSUMOTO, T., AZUMANO, I. & OKADA, Y. 1998. Expression of matrix metalloproteinase 7 (matrilysin) in human osteoarthritic cartilage. *Laboratory Investigation,* 78**,** 79–87.

OSTERGAARD, K., SALTER, D. M., PETERSEN, J., BENDTZEN, K., HVOLRIS, J. & ANDERSEN, C. B. 1998. Expression of α and ß subunits of the integrin superfamily in articular cartilage from macroscopically normal and osteoarthritic human femoral heads. *Annals of Rheumatic Diseases,* 57**,** 303–308.

OTSUKI, S., BRINSON, D. C., CREIGHTON, L., KINOSHITA, M., SAH, R. L., D'LIMA, D. D. & LOTZ, M. K. 2008. The effect of glycosaminoglycan loss

on chondrocyte viability. A study on porcine cartilage explants. *Arthritis and Rheumatism,* 58**,** 1076–1085.

OTTE, P. 1991. Basic cell metabolism of articular cartilage. Manometric studies. *Zeitschrift für Rheumatologie,* 50**,** 304-312.

PAGET, J. 1870. On the production of some of the loose bodies in joints. *Saint Bartholomew's Hospital Reports.,* 6.

PALMER, G. D., CHAO, P.-H. G., RAIA, F., MAUCK, R. L., VALHMU, W. B. & HUNG, C. T. 2001. Time-dependent aggrecan gene expression of articular chondrocytes in response to hyperosmotic loading. *Osteoarthritis and Cartilage,* 9**,** 761–770.

PAREKH, R., LORENZO, M. K., SHIN, S. Y., POZZI, A. & CLARK, A. L. 2014. Integrin α1ß1 differentially regulates cytokine-mediated responses in chondrocytes. *Osteoarthritis and Cartilage,* 22**,** 499-508.

PASCUAL-GARRIDO, C., MCNICKLE, A. G. & COLE, B. J. 2009. Surgical Treatment Options for Osteochondritis Dissecans of the Knee. *Orthopaedics,* 1**,** 326-334.

PATWARI, P., COOK, M. N., DIMICCO, M. A., BLAKE, S. M., JAMES, I. E., KUMAR, S., COLE, A. A., LARK, M. W. & GRODZINSKY, A. J. 2003. Proteoglycan degradation after injurious compression of bovine and human articular cartilage in vitro. Interaction with exogenous cytokines. *Arthritis and Rheumatism,* 48**,** 1292–1301.

PATWARI, P., FAY, J., COOK, M. N., BADGER, A. M., KERIN, A. J., LARK, M. W. & GRODZINSKY, A. J. 2001. In vitro models for investigation of the effects of acute mechanical injury on cartilage. *Clinical Orthopaedics and Related Research,* 391S**,** S61–S71.

PAULI, C., GROGAN, S. P., PATIL, S., OTSUKI, S., HASEGAWA, A., KOZIOL, J., LOTZ, M. K. & D'LIMA, D. D. 2011. Macroscopic and histopathologic analysis of human knee menisci in aging and osteoarthritis. *Osteoarthritis and Cartilage,* 19**,** 1132-1141.

PEARLE, A. D., WARREN, R. F. & RODEO, S. A. 2005. Basic science of articular cartilage and osteoarthritis. *Clinics in Sports Medicine,* 24**,** 1-12.

PEDERSEN, D. R., GOETZ, J. E., KURRIGER, G. L. & MARTIN, J. A. 2013. Comparative digital cartilage histology for human and common osteoarthritis models. *Orthopedic Research and Reviews,* 5**,** 13-20.

PEFFERS, M. J., MILNER, P. I., TEW, S. R. & CLEGG, P. D. 2010. Regulation of SOX9 in normal and osteoarthritic equine articular chondrocytes by hyperosmotic loading. *Osteoarthritis and Cartilage,* 18**,** 1502-1508.

PFANDER, D., KORTJE, D., WESELOH, G. & SWOBODA, B. 2001. Cell proliferation in human arthrotic joint cartilage. *Zeitschrift für Orthopädie und ihre Grenzgebiete,* 139**,** 375-381.

POOLE, A. R. 1997. Articular cartilage chondrons: form, function and failure. *Journal of Anatomy,* 191**,** 1-13.

POOLE, A. R. 1999. An introduction to the pathophysiology of osteoarthritis. *Frontiers in Bioscience,* 15**,** 662-670.

POOLE, A. R., NELSON, F., DAHLBERG, L., TCHETINA, E., KOBAYASHI, M., YASUDA, T., LAVERTY, S., SQUIRES, G., KOJIMA, T., WU, W. & BILLINGHURST, R. C. 2003. Proteolysis of the collagen fibril in osteoarthritis. *Biochemical Society Symposium,* 70**,** 115-123.

POOLE, A. R., PIDOUX, I., REINER, A. & ROSENBERG, L. 1982. An Immunoelectron Microscope Study of the Organization of Proteoglycan Monomer, Link Protein, and Collagen in the Matrix of Articular Cartilage. *The Journal of Cell Biology.,* 93**,** 921-937.

POOLE, C. A., AYAD, S. & GILBERT, R. T. 1992. Chondrons from articular cartilage. Immunohistochemical evaluation of type VI collagen organisation in isolated chondrons by light, confocal and electron microscopy. *Journal of cell science,* 103**,** 1101-1110.

PRICE, J. S., WATERS, J. G., DARRAH, C., PENNINGTON, C., EDWARDS, D. R., DONELL, S. T. & CLARK, I. M. 2002. The role of chondrocyte senescence in osteoarthritis. *Aging Cell,* 1**,** 57-65.

PRITZKER, K. P. H., GAY, S., JIMENEZ, S. A., OSTERGAARD, K., PELLETIER, J.-P., REVELL, P. A., SALTER, D. & VAN DEN BERG, W. B. 2006. Osteoarthritis cartilage histopathology: grading and staging. *Osteoarthritis and Cartilage,* 14**,** 13-29.

QUINN, T. M., ALLEN, R. G., SCHALET, B. J., PERUMBULI, P. & HUNZIKER, E. B. 2001. Matrix and cell injury due to sub-impact loading of adult bovine articular cartilage explants: effects of strain rate and peak stress. *Journal of Orthopeadic Research,* 19**,** 242-249.

QUINN, T. M., GRODZINSKY, A. J., HUNZIKER, E. B. & SANDY, J. D. 1998. Effects of injurious compression on matrix turnover around individual cells in calf articular cartilage explants. *Journal of Orthopaedic Research,* 16**,** 490-499.

REDMAN, S. N., DOWTHWAITE, G. P., THOMSON, B. M. & ARCHER, C. W. 2004. The cellular responses of articular cartilage to sharp and blunt trauma. *Osteoarthritis and Cartilage,* 12**,** 106–116.

ROACH, H. I., AIGNER, T. & KOURI, J. B. 2004. Chondroptosis: a variant of apoptotic cell death in chondrocytes? *Apoptosis,* 6**,** 265-277.

RONN, K., REISCHL, N., GAUTIER, E. & JACOBI, M. 2011. Current surgical treatment of knee osteoarthritis. *Arthritis,* Article ID 454873**,** 9 pages.

RONZIÈRE, M.-C., S., R.-B., TIOLLIER, J., HARTMANN, D. J., GARRONE, R. & HERBAGE, D. 1990. Comparative analysis of collagens solubilized from human foetal, and normal and osteoarthritic adult articular cartilage, with emphasis on type VI collagen. *Biochimica et Biophysica Acta,* 1038**,** 222-230.

ROSS, J. M., SHERWIN, A. F. & POOLE, C. A. 2006. In vitro culture of enzymatically isolated chondrons: a possible model for the initiation of osteoarthritis. *Journal of Anatomy,* 209**,** 793-806.

ROTHWELL, A. G. & BENTLEY, G. 1973. Chondrocyte multiplication in osteoarthritic articular cartilage. *Journal of Bone and Joint Surgery,* 55-B**,** 588-594.

ROUGHLEY, P. J. 2001. Articular cartilage and changes in arthritis: noncollagenous proteins and proteoglycans in the extracellular matrix of cartilage. *Arthritis Research,* 3**,** 342-347.

ROUGHLEY, P. J. & LEE, E. R. 1994. Cartilage proteoglycans: structure and potential functions. *Microscopy Research and Technique,* 28**,** 385-397.

RUCKLIDGE, G. J., MILNE, G. & ROBINS, S. P. 1996. Collagen type X: A component of the surface of normal human, pig, and rat articular cartilage. *Biochemical and Biophysical Research Communiucations,* 224**,** 297-302.

SALMINEN, H., PERALA, M., LORENZO, P., SAXNE, T., HEINEGARD, D., SAAMANEN, A. M. & VUORIO, E. 2000. Up-regulation of cartilage oligomeric matrix protein at the onset of articular cartilage degeneration in a transgenic mouse model of osteoarthritis. *Arthritis and Rheumatism,* 43**,** 1742-1748.

SANDELL, L. J. 2007. Anabolic factors in degenerative joint disease. *Current Drug Targets,* 8**,** 359-365.

SANDELL, L. J. & AIGNER, T. 2001. Articular cartilage and changes in arthritis An introduction: Cell Biology of Osteoarthritis. *Arthritis Research,* 3**,** 107-113.

SASAZAKI, Y., SEEDHOM, B. B. & SHORE, R. 2008. Morphology of the bovine chondrocyte and of its cytoskeleton in isolation and *in situ*: are chondrocytes ubiquitously paired through the entire layer of cartilage? *Rheumatology,* 47**,** 1641-1646.

SCHNABEL, M., MARLOVITS, S., ECKHOFF, G., FICHTEL, I., GOTZEN, L., VÉCSEI, V. & SCHLEGEL, J. 2002. Dedifferentiation-associated changes in morphology and gene expression in primary human articular chondrocytes in cell culture. *Osteoarthritis and Cartilage,* 10**,** 62-70.

SCHUH, E., HOFMANN, S., STOK, K., NOTBOHM, H., MULLER, R. & ROTTER, N. 2012a. Chondrocyte redifferentiation in 3D: The effect of adhesion site density and substrate elasticity. *Journal of Biomedical Materials Research Part A,* 100**,** 38-47.

SCHUH, E., HOFMANN, S., STOK, K. S., NOTBOHM, H., MULLER, R. & ROTTER, N. 2012b. The influence of matrix elasticity on chondrocyte behavior in 3D. *Journal of Tissue Engineering and Regenerative Medicine,* 6**,** 31-42.

SCHUH, E., KRAMER, J., ROHWEDEL, J., NOTBOHM, H., MÜLLER, R., GUTSMANN, T. & ROTTER, N. 2010. Effect of matrix elasticity on the

maintenance of the chondrogenic phenotype. *Tissue Engineering Part A,* 16**,** 1281-1290.

SCHUMACHER, B. L., JUI-LAN, S., LINDLEY, K. M., KUETTNER, K. E. & COLE, A. A. 2002. Horizonatlly oriented clusters of multiple chondrons in the superficial zone of ankle, but not knee articular cartilage. *The Anatomical Record,* 266**,** 241-248.

SEOL, D., MCCABE, D. J., CHOE, H., ZHENG, H., YU, Y., JANG, K., WALTER, M. W., LEHMAN, A. D., DING, L., BUCKWALTER, J. A. & MARTIN, J. A. 2012. Chondrogenic progenitor cells respond to cartilage injury. *Arthritis and Rheumatism,* 64**,** 3626–3637.

SEOL, D., YU, Y., CHOE, H., JANG, K., BROUILLETTE, M. J., ZHENG, H., LIM, T. H., BUCKWALTER, J. A. & MARTIN, J. A. 2014. Effect of short-term enzymatic treatment on cell migration and cartilage regeneration:in vitro organ culture of bovine articular cartilage. *Tissue Engineering Part A,* 20**,** 1087–1014.

SHAPIRO, F., KOIDE, S. & GLIMCHER, M. J. 1993. Cell origin and differentiation in the repair of full-thickness defects of articular cartilage. *Journal of Bone and Joint Surgery. American Volume,* 75**,** 532-553.

SHARIF, M., WHITEHOUSE, A., SHARMAN, P., PERRY, M. & ADAMS, M. 2004. Increased apoptosis in human osteoarthritic cartilage corresponds to reduced cell density and expression of caspase-3. *Arthritis and Rheumatism,* 50**,** 507–515.

SHEN, J., LI, J., WANG, B., JIN, H., WANG, M., ZHANG, Y., YANG, Y., IM, H. J., O'KEEFE, R. & CHEN, D. 2013. Deletion of the Type II TGF-beta receptor gene in articular chondrocytes leads to a progressive OA-like phenotype in mice. *Arthritis and Rheumatism,* 65**,** 3107–3119.

SHLOPOV, B. V., LIE, W. R., MAINARDI, C. L., COLE, A. A., CHUBINSKAYA, S. & HASTY, K. A. 1997. Osteoarthritic lesions – involvement of three different collagenases. *Arthritis and Rheumatism,* 40**,** 2065–2074.

SICZKOWSKI, M. & WATT, F. M. 1990. Subpopulations of chondrocytes from different zones of pig articular cartilage. Isolation, growth and proteoglycan synthesis in culture. *Journal of Cell Science,* 97**,** 349-360

SIMON, W. H., RICHARDSON, S., HERMAN, W., PARSONS, J. R. & LANE, J. 1976. Long-term effects of chondrocyte death on rabbit articular cartilage in vivo. *Journal of Bone and Joint Surgery. American Volume,* 58**,** 517-526.

SKAGEN, P. S., HORN, T., KRUSE, H. A., STÆRGAARD, B., RAPPORT, M. M. & NICOLAISEN, T. 2011. Osteochondritis dissecans (OCD), an endoplasmic reticulum storage disease?: a morphological and molecular study of OCD fragments. *Scandinavian Journal of Medicine and Science in Sports,* 21**,** 17-33.

SMITH, I. D. M., WINSTANLEY, J. P., MILTO, K. M., DOHERTY, C. J., CZARNIAK, E., AMYES, S. G. B., SIMPSON, A. H. R. W. & HALL, A. C. 2013. Rapid in situ chondrocyte death induced by Staphylococcus Aureus toxins in a bovine cartilage explant model of septic arthritis. *Osteoarthritis and Cartilage,* 21**,** 1755-1765.

SODER, S., HAMBACH, L., LISSNER, R., KIRCHNER, T. & AIGNER, T. 2002. Ultrastructural localization of type VI collagen in normal adult and osteoarthritic human articular cartilage. *Osteoarthritis and Cartilage,* 10**,** 464-470.

SOFAT, N., EJINDU, V. & KIELY, P. 2011. What makes osteoarthritis painful? The evidence for local and central pain processing. *Rheumatology,* 50**,** 2157-2165.

SPECTOR, T. D., CICUTTINI, F., BAKER, J., LOUGHLIN, J. & HART, D. 1996. Genetic influences on osteoarthritis in women: a twin study. *BMJ,* 312**,** 940-943.

SRIKANTH, V. K., FRYER, J. L., ZHAI, G., WINZENBERG, T. M., HOSMER, D. & JONES, G. 2005. A meta-analysis of sex differences prevalence, incidence and severity of osteoarthritis. *Osteoarthritis and Cartilage,* 13**,** 769-781.

STOCKWELL, R. A. 1971. The interrelationship of cell density and cartilage thickness in mammalian articular cartilage. *Journal of Anatomy,* 109**,** 411-421.

STOCKWELL, R. A. 1978. Chondrocytes. *Journal of Clinical Pathology,* 31, Suppl.**,** 7-13.

STOCKWELL, R. A. 1979. Biology of cartilage cells. Cambridge: Cambridge University Press.

STOCKWELL, R. A. 1991. Cartilage failure in Osteoarthritis: Relevance of normal structure and function. A review. *Clinical Anatomy,* 4**,** 161-191.

STOCKWELL, R. A., BILLINGHAM, M. E. & MUIR, H. 1983. Ultrastructural changes in articular cartilage after experimental section of the anterior cruciate ligament of the dog knee. *Journal of Anatomy,* 136**,** 425-39.

STODDART, M. J., FURLONG, P. I., SIMPSON, A., DAVIES, C. M. & RICHARDS, R. G. 2006. A comparison of non-radioactive methods for assessing viability in ex vivo cultured cancellous bone: technical note. *European Cells and Materials,* 12**,** 16-25.

STOOP, R., BUMA, P., VAN DER KRAAN, P. M., HOLLANDER, A. P., CLARK BILLINGHURST, R., MEIJERS, T. H. M., POOLE, A. R. & VAN DEN BERG, W. B. 2001. Type II collagen degradation in articular cartilage fibrillation after anterior cruciate ligament transection in rats. *Osteoarthritis and Cartilage,* 9**,** 308–315.

STREEFKERK, J. G. 1972. Inhibition of erythrocyte pseudoperoxidase activity by treatment with hydrogen peroxide following methanol. *Journal of Histochemistry and Cytochemistry,* 20**,** 829-831.

SUI, Y., LEE, J. H., DIMICCO, M. A., VANDERPLOEG, E. J., BLAKE, S. M., HUNG, H. H., PLAAS, A. H. K., JAMES, I. E., SONG, X. Y., LARK, M. W. & GRODZINSKY, A. J. 2009. Mechanical injury potentiates proteoglycan catabolism induced by Interleukin-6 with soluble Interleukin-6 receptor and Tumor Necrosis Factor α in immature bovine and adult human articular cartilage. *Arthritis and Rheumatism,* 60**,** 2985-2996.

SUVIK, A. & EFFENDY, A. W. M. 2012. The use of Modified Masson's Trichrome staining in collagen evaluation in wound healing study. *Malaysian Journal of Veterinary Research,* 3**,** 39-47.

SZCZODRY, M., COYLE, C. H., J., K. S., SMOLINSKI, P. & CHU, C. R. 2009. Progressive chondrocyte death after impact injury indicates a need for chondroprotective therapy. *The American Journal of Sports Medicine,* 37**,** 2318–2322.

TCHETINA, E. V., KOBAYASHI, M., YASUDA, T., MEIJERS, T., PIDOUX, I. & POOLE, A. R. 2007. Chondrocyte hypertrophy can be induced by a cryptic

sequence of type II collagen and is accompanied by the induction of MMP-13 and collagenase activity: implications for development and arthritis. *Matrix Biology,* 26**,** 247–258.

TCHETINA, E. V., SQUIRES, G. & POOLE, A. R. 2005. Increased type II collagen degradation and very early focal cartilage degeneration is associated with upregulation of chondrocyte differentiation related genes in early human articular cartilage lesions. *The Journal of Rheumatology,* 32**,** 876-886.

TERRY, D. E., CHOPRA, R. K., OVENDEN, J. & ANASTASSIADES, T. P. 2000. Differential use of alcian blue and toluidine blue dyes for the quantification and isolation of anionic glycoconjugates from cell cultures: Application to proteoglycans and a high molecular weight glycoprotein synthesized by articular chondrocytes. *Analytical Biochemistry,* 285**,** 211-219.

TESCHE, F. & MIOSGE, N. 2004. Perlecan in late stages of osteoarthritis of the human knee joint. *Osteoarthritis and Cartilage,* 12**,** 852-862.

TESCHE, F. & MIOSGE, N. 2005. New aspects of pathogenesis of osteoarthritis: the role of firbroblast-like chondrocytes in late stages of the disease. *Histology and Histopathology,* 20**,** 329-337.

TEW, S. R. & HARDINGHAM, T. E. 2006. Regulation of SOX9 mRNA in Human Articular Chondrocytes Involving p38 MAPK Activation and mRNA Stabilization. *The Journal of Biological Chemistry,* 281**,** 39471-39479.

TEW, S. R., KWAN, A. P. L., HANN, A., THOMSON, B. M. & ARCHER, C. W. 2000. The reactions of articular cartilage to experimental wounding. Role of apoptosis. *Arthritis and Rheumatism,* 43**,** 215–225.

TEW, S. R., LI, Y., POTHACHAROEN, P., TWEATS, L. M., HAWKINS, R. E. & HARDINGHAM, T. E. 2005. Retroviral transduction with SOX9 enhances re-expression of the chondrocyte phenotype in passaged osteoarthritic human articular chondrocytes. *Osteoarthritis and Cartilage,* 13**,** 80-89.

TEW, S. R., PEFFERS, M. J., MCKAY, T. R., LOWE, E. T., KHAN, W. S., HARDINGHAM, T. E. & CLEGG, P. D. 2009. Hyperosmolarity regulates SOX9 mRNA posttranscriptionally in human articular chondrocytes. *American Journal of Physiology-Cell Physiology,* 297**,** C898–C906.

TEW, S. R., VASIEVA, O., PEFFERS, M. J. & CLEGG, P. D. 2011. Post-transcriptional gene regulation following exposure of osteoarthritic human articular chondrocytes to hyperosmotic conditions. *Osteoarthritis and Cartilage,* 19**,** 1036-1046.

THAMBYAH, A. 2005. A hypothesis matrix for studying biomechanical factors associated with the initiation and progression of posttraumatic osteoarthritis. *Medical Hypotheses,* 64**,** 1157–1161.

THOMAS, C. M., FULLER, C. J., WHITTLES, C. E. & SHARIF, M. 2007. Chondrocyte death by apoptosis is associated with cartilage matrix degradation. *Osteoarthritis and Cartilage,* 15**,** 27-34.

TOIVANEN, A. T., HELIOVAARA, M., IMPIVAARA, O., AROKOSKI, J. P., KNEKT, P., LAUREN, H. & KROGER, H. 2010. Obesity, physically demanding work and traumatic knee injury are major risk factors for knee osteoarthritis–a population-based study with a follow-up of 22 years. *Rheumatology (Oxford),* 49**,** 308-314.

TORZILLI, P. A. & GRIGIENE, R. 1998. Continuous cyclic load reduces proteoglycan release from articular cartilage. *Osteoarthritis and Cartilage,* 6**,** 260-268.

TORZILLI, P. A., GRIGIENE, R., BORRELLI, J. J. & HELFET, D. L. 1999. Effect of impact load on articular cartilage: cell metabolism and viability, and matrix water content. *Journal of Biomechanical Engineering,* 121**,** 433-441.

TURUNEN, S. M., LAMMI, M. J., SAARAKKALA, S., HAN, S. K., HERZOG, W., TANSKA, P. & KORHONEN, R. K. 2013. The effect of collagen degradation on chondrocyte volume and morphology in bovine articular cartilage following a hypotonic challenge. *Biomechanica and Modeling in Mechanobiology,* 12**,** 417-429.

UOZUMI, H., SUGITA, T., AIZAWA, T., TAKAHASHI, A., OHNUMA, M. & ITOI, E. 2009. Histologic findings and possible causes of osteochondritis dissecans of the knee. *The American Journal of Sports Medicine,* 37**,** 2003–2008.

URBAN, J. P. G. 1994. The chondrocyte : A cell under pressure. *British Journal of Rheumatology,* 33**,** 901-908.

URBAN, J. P. G., HALL, A. C. & GEHL, K. A. 1993. Regulation of matrix synthesis rates by the ionic and osmotic environment of articular chondrocytes. *Journal of Cellular Physiology,* 154**,** 262-270.

VAN DER KRANN, P. M. & VAN DEN BERG, W. B. 2012. Chondrocyte hypertrophy and osteoarthritis: role in initiation and progression of cartilage degeneration? *Osteoarthritis and cartilage,* 20**,** 223-232.

VAN SUSANTE, J. L., BUMA, P., VAN BEUNINGEN, H. M., VAN DEN BERG, W. B. & VETH, R. P. 2000. Responsiveness of bovine chondrocytes to growth factors in medium with different serum concentrations. *Journal of Orthopaedic Research,* 18**,** 68-77.

VERZIJL, N., DEGROOT, J., THORPE, S. R., BANK, R. A., SHAW, J. N., LYONS, T. J., BIJLSMA, J. W. J., LAFEBER, F. P. J. G., BAYNES, J. W. & TEKOPPELE, J. M. 2000. Effect of collagen turnover on the accumulation of advanced glycation end products. *The Journal of Biological Chemistry,* 275**,** 39027–39031.

VINALL, R. L., LO, S. H. & REDDI, A. H. 2002. Regulation of articular chondrocyte phenotype by bone morphogenetic protein 7, interleukin 1, and cellular context is dependent on the cytoskeleton. *Experimental Cell Research,* 272**,** 32-44.

VINCENT, T. L. 2013. Targeting mechanotransduction pathways in osteoarthritis: a focus on the pericellular matrix. *Current Opinion in Pharmacology,* 13**,** 449-454.

VON DER MARK, K., GAUSS, V., VON DER MARK, H. & MÜLLER, P. 1977. Relationship between cell shape and type of collagen synthesised as chondrocytes lose their cartilage phenotype in culture. *Nature,* 9**,** 531-532.

VON DER MARK, K., KIRSCH, T., NERLICH, A., KUSS, A., WESELOH, G., GLUCKERT, K. & STÖSS, H. 1992. Type X collagen synthesis in human osteoarthritic cartilage. Indication of chondrocyte hypertrophy. *Arthritis and Rheumatism,* 35**,** 806-811.

VON KOCKRITZ-BLICKWEDE, M., CHOW, O. A. & NIZET, V. 2009. Fetal calf serum contains heat-stable nucleases that degrade neutrophil extracellular traps. *Blood,* 114**,** 5245-5246.

WANG, J., VERDONK, P., ELEWAUT, D., VEYS, E. M. & VERBRUGGEN, G. 2003. Homeostasis of the extracellular matrix of normal and osteoarthritic human articular cartilage chondrocytes in vitro. *Osteoarthritis and Cartilage,* 11**,** 801-809.

WANG, Q., YANG, Y. Y., NIU, H. J., J., Z. W., FENG, Q. J. & CHEN, W. F. 2013a. An ultrasound study of altered hydration behaviour of proteoglycan-degraded articular cartilage. *Musculoskeletal Disorders,* 14**,** 1-7.

WANG, Q., ZHENG, Y. P. & NIU, H. J. 2010. Changes in triphasic mechanical properties of proteoglycan-depleted articular cartilage extracted from osmotic swelling behavior monitored using high-frequency ultrasound. *Molecular & Cellular Biomechanics,* 1**,** 45-58.

WANG, Y., WEI, L., ZENG, L., HE, D. & WEI, X. 2013b. Nutrition and degeneration of articular cartilage. *Knee Surgery, Sports Traumatology, Arthroscopy,* 21**,** 1751–1762.

WARD, J. M., EREXSON, C. R., FAUCETTE, L. J., FOLEY, J. F., DIJKSTRA, C. & CATTORETTI, G. 2006. Immunohistochemical markers for the rodent immune system. *Toxicologic Pathology,* 34**,** 616-630.

WEI, L., SUN, X. J., WANG, Z. & CHEN, Q. 2006. CD95-induced osteoarthritic chondrocyte apoptosis and necrosis: dependency on p38 mitogen-activated protein kinase. *Arthritis Research and Therapy,* 8**,** 10 pages.

WEISS, C. & MIROW, S. 1972. An ultrastructural study of osteoarthritic changes in the articular cartilage of human knees. *Journal of Bone and Joint surgery,* 54-A**,** 954-972.

WESTACOTT, C. I. & SHARIF, M. 1996. Cytokines in osteoarthritis: mediators or markers of joint destruction? *Seminars in Arthritis and Rheumatism,* 25**,** 254–272.

WHEATON, A. J., CASEY, F. L., GOUGOUTAS, A. J., DODGE, G. R., BORTHAKUR, A., LONNER, J. H., SCHUMACHER, H. R. & REDDY, R. 2004. Correlation of T1rho with fixed charge density in cartilage. *Journal of Magnetic Resonance Imaging,* 20**,** 519-525.

WIBERG, C., HEINEGARD, D., WENGLEN, C., TIMPL, R. & MORGELIN, M. 2002. Biglycan organizes collagen VI into hexagonal-like net-works

resembling tissue structures. *Journal of Biological Chemistry,* 277**,** 49120–49126.

WIELAND, H. A., MICHAELIS, M., KIRSCHBAUM, B. J. & RUDOLPHI, K. A. 2005. Osteoarthritis - an untreatable disease? *Nature Reviews Drug Discovery,* 4**,** 331-344.

WILUSZ, R. E., ZAUSCHER, S. & GUILAK, F. 2013. Micromechanical mapping of early osteoarthritic changes in the pericellular matrix of human articular cartilage. *Osteoarthritis and Cartilage,* 21**,** 1895-1903.

WOJDASIEWICZ, P., PONIATOWSKI, L. A. & SZUKIEWICZ, D. 2014. The role of inflammatory and anti-inflammatory cytokines in the pathogenesis of osteoarthritis. *Mediators of inflammation,* doi.org/10.1155/2014/561459.

WOLDRINGH, C. L., DE JONG, M. A., VAN DEN BERG, W. & KOPPES, L. 1977. Morphological analysis of the division cycle of two Escherichia Coli substrains during slow growth. *Journal of Bacteriology,* 131**,** 270-279.

WOLFENSON, H., LAVELIN, I. & GEIGER, B. 2013. Dynamic regulation of the structure and functions of integrin adhesions. *Developmental Cell,* 24**,** 447–458.

WONG, M., WUETHRICH, P., EGGLI, P. & HUNZIKER, E. 1996 Zone-specific cell biosynthetic activity in mature bovine articular cartilage: a new method using confocal microscopic stereology and quantitative autoradiography. *Journal of Orthopaedic Research,* 14**,** 424-432.

WOOLF, A. D. & PFLEGER, B. 2003. Burden of major musculoskeletal conditions. *Buletin of World Health Organization,* 81**,** 646-656.

WU, J., KIRK, T. & ZHENG, M. 2004. Assessment of three-dimensional architecture of collagen fibres in the superficial zone of bovine articular cartilage. *Journal of Musculoskeletal Research,* 8**,** 167-179.

XU, X., URBAN, J. P. G., TIRLAPUR, U. K. & CUI, Z. 2010. Osmolarity effects on bovine articular chondrocytes during three-dimensional culture in alginate beads. *Osteoarthritis and Cartilage,* 18**,** 433-439.

YAGI, R., MCBURNEY, D., LAVERTY, D., WEINER, S. & HORTON JR., W. E. 2005. Intrajoint comparisons of gene expression patterns in human

osteoarthritis suggest a change in chondrocyte phenotype. *Journal of Orthopaedic Research,* 23**,** 1128-1138.

YAN, D., CHEN, D., COOL, S. M., VAN WIJNEN, A. J., MIKECZ, K., MURPHY, G. & IM, H. J. 2011. Fibroblast growth factor receptor 1 is principally responsible for fibroblast growth factor 2-induced catabolic activities in human articular chondrocytes. *Arthritis Research & Therapy,* 13**,** 1-13.

YONETANI, Y., MATSUO, T., NAKAMURA, N., NATSUUME, T., TANAKA, Y., SHIOZAKI, Y., WAKITANI, S. & HORIBE, S. 2010. Fixation of detached osteo-chondritis dissecans lesions with bioabsorbable pins: clinical and histologic evaluation. *Arthroscopy,* 26**,** 782–789.

YOSHIHARA, Y., NAKAMURA, H., OBATA, K., YAMADA, H., HAYAKAWA, T., FUJIKAWA, K. & OKADA, Y. 2000. Matrix metalloproteinases and tissue inhibitors of metalloproteinases in synovial fluids from patients with rheumatoid arthritis or osteoarthritis. *Annals of the Rheumatic Diseases,* 59**,** 455-461.

YOUNGSTROM, D. W., CAKSTINA, I. & JAKOBSONS, E. 2015. Cartilage-derived extracellular matrix extract promotes chondrocytic phenotype in three-dimensional tissue culture. *Artificial Cells Nanomedicine and Biotechnology,* 24**,** 1-8.

ZAMLI, Z., ADAMS, M. A., TARLTON, J. F. & SHARIF, M. 2013. Increased chondrocyte apoptosis is associated with progression of osteoarthritis in spontaneous guinea pig models of the disease. *International Journal of Molecular Sciences,* 14**,** 17729-17743.

ZHOU, S., CUI, Z. & URBAN, J. 2011. Dead cell counts during serum cultivation are underestimated by the fluorescent live/dead assay. *Biotechnology Journal,* 6**,** 513-518.